Investigating the molecular pathways driving the sumoylation/desumoylation balance in rat hippocampal synapses

Lenka Schorova

UNIVERSITÉ CÔTE D'AZUR

ÉCOLE DOCTORALE SCIENCES DE LA VIE ET DE LA SANTÉ

AGENCE NATIONALE DE LA RECHERCHE ANR

THÈSE DE DOCTORAT

Etude des mécanismes de régulation synaptique de la balance sumoylation/désumoylation

Lenka SCHOROVA

Equipe : Implication physiologique et pathophysiologique de la sumoylation neuronale

Présentée en vue de l'obtention du grade de docteur en Interactions Moléculaires et Cellulaire **d'**Université Côte d'Azur
Dirigée par : Stéphane Martin
Soutenue le : 28 Mars 2018

Devant le jury, composé de :
Guillaume Bossis, Dr, Rapporteur
Jeremy Henley, Prof, Rapporteur
Jacques Noel, Prof, Président du Jury

SIGNALIFE

ipmc

Etude des mécanismes de régulation synaptique de la balance sumoylation/désumoylation

Jury :

Président du jury

Jacques Noël, Prof, UCA

Rapporteurs

Jeremy Henley, Prof, Bristol UK
Guillaume Bossis, Dr, CR1 CNRS/HDR, Montpellier

Titre : Etude des mécanismes de régulation synaptique de la balance sumoylation/désumoylation

Résumé

La SUMOylation est une modification post-traductionnelle essentielle pour toutes les cellules eucaryotes. C'est un processus enzymatique qui permet la liaison covalente du polypeptide SUMO sur des résidus de lysine de protéines cibles. Les SUMO protéases (SENP) déconjuguent SUMO des protéines SUMOylées et sont donc critiques pour maintenir l'équilibre physiologique entre la forme modifiée et non modifiée d'un substrat. Les synapses se composent de deux compartiments : l'élément présynaptique ou terminaison axonale et le compartiment postsynaptique également appelé épine dendritique. Les synapses sont des structures très riches en protéines qui sont centrales pour la transmission et la plasticité synaptique. Il existe de nombreux éléments impliquant la SUMOylation au niveau des synapses où elle régule la fonction de multiples protéines. La dérégulation de la balance SUMOylation / déSUMOylation a notamment été mise en évidence dans plusieurs pathologies cérébrales présentant un dysfonctionnement de la fonction synaptique. Pour envisager le développement de nouvelles stratégies thérapeutiques de ces maladies, il est indispensable de mieux comprendre les mécanismes moléculaires régissant cet équilibre.

Mon laboratoire de thèse a préalablement montré que l'activation des récepteurs métabotropiques du glutamate (mGluR) augmente de façon transitoire le temps de résidence post-synaptique de l'enzyme de conjugaison de la SUMOylation Ubc9. Cette rétention transitoire est dépendante de la cascade d'activation PLC/PKC et qui conduit à l'augmentation des niveaux de sumoylation synaptique et à la régulation de la communication neuronale. Cependant, aucune donnée n'est aujourd'hui disponible dans la littérature concernant la régulation de la désumoylation synaptique. Au cours de ma thèse, j'ai combiné l'utilisation de l'imagerie en temps réel sur cellules vivantes avec des approches de biochimie et d'agents pharmacologiques spécifiques pour identifier les mécanismes de régulation du transport de la déSUMOylase SENP1. J'ai ainsi démontré que l'activation neuronale augmente les niveaux synaptiques de SENP1. Cette augmentation synaptique de SENP1 résulte de la modification de la vitesse de diffusion de l'enzyme entre les dendrites et les synapses d'une part, et d'autre part, de l'augmentation drastique du temps de rétention synaptique de l'enzyme. Je rapporte également que ce mécanisme de régulation dynamique de SENP1 implique l'activation directe des récepteurs mGlu du groupe I.

Pour résumé, mon travail révèle que l'équilibre SUMOylation / déSUMOylation repose sur une régulation spatio-temporelle distincte des deux enzymes Ubc9 et SENP1. De plus, je suggère la participation d'autres acteurs de la signalisation (comprenant la PKC) dans la régulation du transport synapto-dendritique de SENP1. Mon travail met ainsi en lumière de nouveaux mécanismes de régulation du processus de SUMOylation synaptique qui sont importants pour la communication cérébrale.

Mots clés : synapse, modification post-traductionnelle, sumoylation, SENP1

Title: Investigating the molecular pathways driving the sumoylation/desumoylation balance in rat hippocampal synapses

Abstract

Sumoylation is a vital posttranslational protein modification that takes place in all eukaryotic cells. Sumoylation occurs as an enzymatic process that conjugates SUMO peptides to target proteins. SUMO proteases (SENP) deconjugate SUMO from modified proteins and thus are critical for maintaining the balanced levels of SUMOylated and un-SUMOylated substrates required for normal physiology. Neuronal synapses consist of two compartments: presynaptic - the axon terminals and postsynaptic - dendritic spines. Synapses are protein-rich structures that are essential to synaptic transmission and plasticity. There is a strong evidence that sumoylation occurs in synapses and regulates the function of synaptic proteins. Indeed, distortion of the SUMO balance has been linked to several pathologies with dysfunctional synaptic function. Gaining a deeper understanding into the molecular mechanisms regulating the SUMO balance is a prerequisite to envisaging the development of novel therapeutic strategies.

My PhD host laboratory has previously shown that the activation of mGlu5 receptors transiently increases the postsynaptic residency time of the SUMO-conjugating enzyme Ubc9 in a PLC/PKC-dependent manner increasing synaptic sumoylation levels and regulating neuronal communication. However, to date there have been no reports on the regulation of desumoylation at synapses. During my PhD thesis, I used a combination of real-time live-cell confocal imaging, biochemistry and pharmacological approaches to identify SENP1 (SENtrin specific Protease 1) regulatory mechanisms at synapses. I provided evidence that synaptic activation increases SENP1 protein levels at synapses at a time-scale that is distinct from the Ubc9 enzyme. I showed that the increase in synaptic SENP1 upon synaptic activation is a result of two processes: Although (a) fewer SENP1 proteins enter into spines at low diffusion speed (b) a significant proportion of SENP1 becomes immobile and is retained in spines. I demonstrate that the regulatory mechanism of this SENP1 dynamics involves direct activation of Group I mGlu receptors.

Altogether, I propose that the SUMO balance is achieved via a distinct spatio-temporal regulation of Ubc9 and SENP1 enzymes at synapses. Moreover, I suggest a participation of additional signalling players (incl. PKC) in SENP1 regulation at synapses. These findings reveal novel mechanisms and add to the understanding of the SUMO balance in neuronal communication.

Keywords : synapse, post-translational modification, sumoylation, SENP1

mé rodině,

to my family,

á ma famille,

ACKNOWLEDGEMENTS

"If the only prayer you say in your entire life is 'Thank you,' it will be enough." – Meister Eckhart

"Barn's burnt down / Now I can see the moon." – Mizuta Masahide

First, I wish to thank the members of my dissertation committee: Prof Jeremy Henley, Dr Guillaume Bossis, Prof Jacques Noël and Dr Stéphane Martin for generously offering their expertise and time to review this document.

Mé největší díky patří mé rodině, která po celou dobu mých studií stála při mně a podporovala mě. Prošli jsme si časy v odloučení a stesku ale v lásce a vzpomínkách. Bez vás, maminko, tatínku, sestřicko, Františku, Nicolko, Martínku a Matine bych to nezvládla. Upřímně a z celého sdrce vám děkuji.

My next heartfelt thank you belongs to my darling Anouar. Your enthusiasm, honesty, humbleness and love made me a better person. You encouraged me and scientifically advised which helped me immensely. Thank you. Je voudrais également exprimer ma gratitude à la famille d'Anouar. Je remercie Aicha, Fredj, Tarek, Sami, Rakia, Hatem, et tous les petits qui m'ont toujours donné le sourire. Je vous remercie de votre soutien et de la délicieuse nourriture tunisienne.

It is a genuine pleasure to express my gratitude to my supervisor Dr Stéphane Martin. I sincerely appreciate your guidance, expertise, patience, support and help that you devoted to me throughout the years. Your dedication to research will always serve me as an example. Thank you.

This thesis is the result of a team effort and therefore I would like to thank all my colleagues from the "SM" team: Gwénola Poupon, Carole Gwizdek, Marta Prieto García, Alessandra Folci and Marie Pronot. Gwen, thank you for your help. More than that however, I feel thankful to have met such an honest and perceptive person like you. Thank you for being a friend. Carole, thank you for your advice and support during my PhD. I admire your pedagogical attitude and passion for science, both of which I believe you have passed on to me. Thank you for that.

Cocolinas (Marta and Ale), thank you for your participation in this project and your lovely friendship. A special thanks goes to Marta for an incredible batch of V3. Marie, you helped me greatly and I very much appreciate your effort. We all had great fun in and outside the lab which kept me going and I will never forget these times. Thank you guys.

A big thank you goes to my other dear friends and colleagues: Jana, Denisa, Liudmyla, Magda, Sandrine, Nedra, Amine and Aisling. Thank you for making me feel like I never left home.

I also thank to all the members of the “IPMC” and “Signalife” communities. A very big thank you to Frédèric Brau and Sophie Abelanet for their imaging advice and help. Here comes the time for the spinning-disc microscope to be used by someone else than me. Tell them to be nice with it.

Last, but not least, I would like to thank the PhD program Labex Signalife for funding my PhD project and Dr Beck for her administrative support.

SUMMARY

Sumoylation is a vital posttranslational protein modification that takes place in all eukaryotic cells. Sumoylation occurs as an enzymatic process that conjugates SUMO peptides to target proteins. SUMO proteases (SENP) deconjugate SUMO from modified proteins and thus are critical for maintaining the balanced levels of SUMOylated and un-SUMOylated substrates required for normal physiology. Neuronal synapses consist of two compartments: presynaptic - the axon terminals and postsynaptic - dendritic spines. Synapses are protein-rich structures that are essential to synaptic transmission and plasticity. There is a strong evidence that sumoylation occurs in synapses and regulates the function of synaptic proteins. Indeed, distortion of the *SUMO balance* has been linked to several pathologies with dysfunctional synaptic function. Gaining a deeper understanding into the molecular mechanisms regulating the *SUMO balance* is a prerequisite to envisaging the development of novel therapeutic strategies.

My PhD host laboratory has previously shown that the activation of mGlu5 receptors transiently increases the postsynaptic residency time of the SUMO-conjugating enzyme Ubc9 in a PLC/PKC-dependent manner increasing synaptic sumoylation levels and regulating neuronal communication. However, to date there have been no reports on the regulation of **desumoylation at synapses**. During my PhD thesis, I used a combination of real-time live-cell confocal imaging, biochemistry and pharmacological approaches to identify **SENP1** (SENtrin specific Protease 1) **regulatory mechanisms at synapses**. I provided evidence that **synaptic activation increases SENP1 protein levels at synapses at a time-scale that is distinct from the Ubc9 enzyme.** I showed that the increase in synaptic SENP1 upon synaptic activation is a **result of two processes: Although (a) fewer SENP1 proteins enter into spines at low diffusion speed (b) a significant proportion of SENP1 becomes immobile and is retained in spines**. I demonstrate that the regulatory mechanism of this SENP1 dynamics involves direct activation of **Group I mGlu receptors.**

Altogether, I propose that the *SUMO balance* is achieved via a distinct spatio-temporal regulation of Ubc9 and SENP1 enzymes at synapses. Moreover, I suggest a participation of additional signalling players (incl. PKC and CaMKII) in SENP1 regulation at synapses. These

findings reveal novel mechanisms and add to the understanding of the *SUMO balance* in neuronal communication.

LIST OF CONTENTS

LIST OF FIGURES

1. INTRODUCTION

2. RESULTS AND DISCCUSSION

3. PERSPECTIVES

LIST OF TABLES

1. INTRODUCTION

Introduction

1. Introduction

This introduction is aimed to provide an overview of the anatomical and cellular features of the hippocampal formation. I further discuss the structure of a typical excitatory synapse, which is followed by a description of the mechanisms of glutamatergic transmission. In the last part, I focus on posttranslational modifications that play important roles at the synapse. Sumoylation is discussed in detail as it is the topic of my thesis. I believe that providing this information facilitates understanding into the thesis subject which concerns the investigation into regulatory mechanisms of postsynaptic desumoylation. I have to admit that the process of acquiring this background knowledge including a vast literature review and the write-up process was a very useful exercise.

1.1 The hippocampus

It is not a coincidence that the hippocampus is the most studied part of the brain serving as a model system for neurobiological studies. Its intrinsic structure has draught the attention of anatomists since ancient Egypt (~300 B.C.). Alexandrian scholars observed on the horizontal midsection of the hippocampus a curved structure resembling horns of the ram deity Ammon ***(Fig. 1A)***, and therefore named it *cornu ammonis* in Latin. This terminology survived until now as the acronym (CA) for hippocampal subregions. The name 'hippocampus' was first used by the

Figure 1.

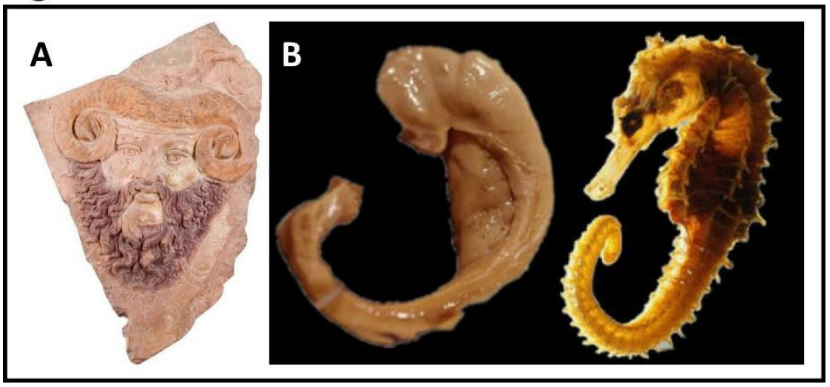

Figure 1. **Historical reminder of hippocampal terminology. A.** A terracotta cast of ram-horned Jupiter Ammon, 1st century A.D. (Museo di Scultura Antica Giovanni Barracco, Rome, http://en.museobarracco.it/). **B.** Comparison of the dissected human hippocampus (left) with sea horse *Hippocampus leria* (right). Adapted from The Hippocampus Book (Andersen et al., 2007).

Bolognese anatomist Guilio Cesare Aranzi (circa 1564) undeniably because of its similarity with the sea horse ***(Fig. 1B)***, genus *Hippocampus*, where *hippo* means in ancient Greek 'horse' and *kampos* 'sea monster'. However, it was not until the late 19th century that the Spanish physician Dr Santiago Ramón y Cajal **(Fig. 2A)** mostly with the use of the Golgi method ***(Fig. 3)*** depicted the cellular organisation of many tissues structures including the structure of nerve cells and neuromuscular junction. These findings were published in 1893 as *Manual de Histología Normal y Técnica Micrográfica*. Later, Ramón y Cajal set himself for a thorough study of the nervous system and published his observations along with a more detailed cellular organisation of the hippocampus (***Fig. 2B***) in *Histologie du système nerveux de l'homme & des vertébrés* in 1909. Simultaneously, Karoly Schaffer, a Hungarian neurologist, was interested in hippocampal axonal fibres and their length, and found that they have short as well as long branches connecting with other areas of the cortex. He discovered the so-called 'collateral fiber system' that connects the CA3 to the CA1 region of the hippocampus, known today as Schaffer collaterals. Another pioneering neuroanatomist Rafael Lorente de Nó (1934) bolstered the work of Ramón y Cajal by adding to the study of the many hippocampal cell types and their arborisations, and distinguished the hippocampal subregions CA1, CA2 and CA3.

Until 1930s the hippocampus was thought to be part of the olfactory system, perhaps due to its size in macrosmatic animals (e.g. rodents and insectivores) as it is considerably large in the

Figure 2.

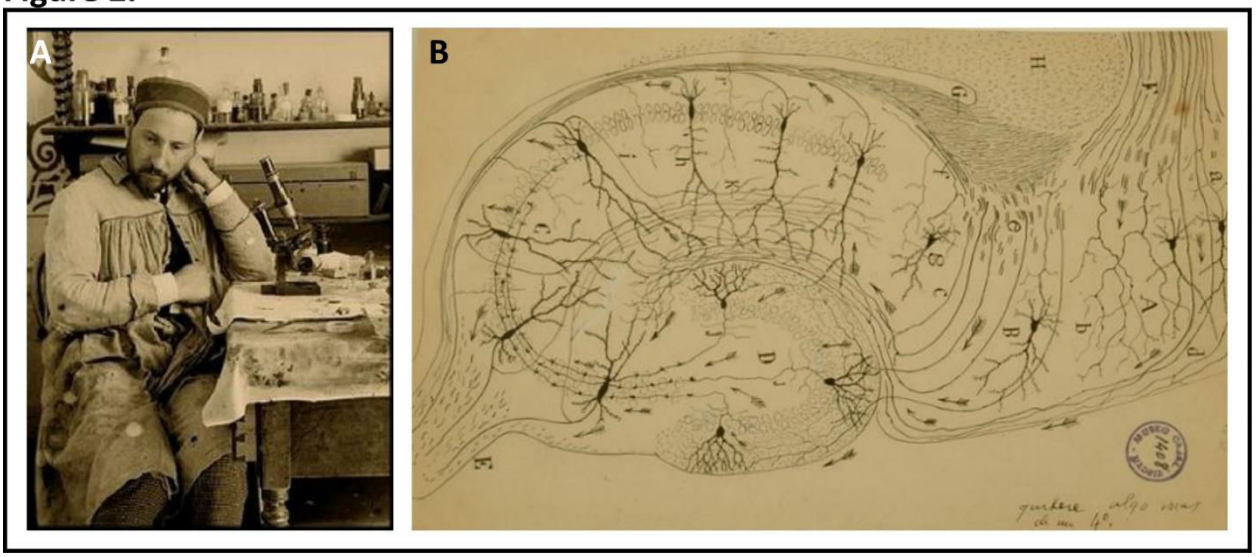

Figure 2. **Discovery of hippocampal structure**. **A.** Santiago Ramón y Cajal, the 'Father of modern Neuroscience'. **B.** Cellular organisation of the rat hippocampus by S. Ramón y Cajal. Both images were taken and modified from (Swanson et al., 2017).

context of the whole brain. This view was challenged throughout the years since the hippocampus was not found to be directly connected with the olfactory bulb (a review by (Brodal, 1947)). Another important influencer in the field of neuroanatomy was James Papez who proposed the existence of a circuit (known as Papez circuit, 1937) that interconnected cortical and subcortical structures including the hippocampus and supposedly mediated emotions. The most prominent functional importance of the hippocampus was uncovered about 60 years ago when patient H. M. suffered from amnesia due to surgical excision of the medial temporal lobe for epilepsy relief performed by Dr Scoville (1957). Since then, the hippocampus has been extensively studied for its involvement in memory. Early experiments on hippocampectomized primates and rodents, however, failed to bring a convincing proof of memory deficits. Nonetheless, some of the observations included defects in exploration, habituation to novelty and navigation, which prompted the idea of existence of more than one type of memory. An important milestone pro-hippocampus-mediated memory was made with the introduction of a more appropriate behavioural test – the object recognition task – by David Gaffan (1974) and its optimization for use in the monkey by Mortimer Mishkin and Jean Delacour (1975). Nowadays, the hippocampus is accepted to be part of the 'limbic system', a term that was first used by the French neurologist Pierre Paul Broca (1878), which mediates not only memory formation but also emotions, motivation, learning, spatial navigation and olfaction.

Figure 3.

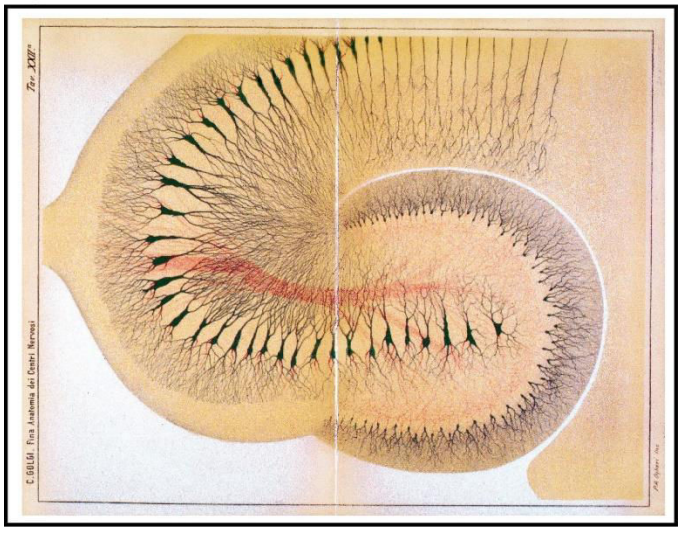

Figure 3: **Section of the rabbit hippocampus stained with the original Golgi method** (1886). Source: The Hippocampus Book (Andersen et al., 2007).

❖ Neuroanatomy of the hippocampal formation

The hippocampal formation (***Fig. 4 and 6***) is widely accepted to refer to several closely related regions: the **dentate gyrus**, **hippocampus proper** (CA1, CA2 and CA3), **subicular complex** and **entorhinal cortex**. Although the volume of the human hippocampus is about 100 times that of the rat and 10 times that of the monkey, the basic hippocampal architecture, particular cellular organisation and 'sea horse' shape is present throughout all mammals. The hippocampus is buried in the medial temporal lobe of the human brain, whereas in rat it is localised rather rosto-caudally. An intriguing feature of the hippocampal formation is that it is largely nonreciprocal, with unidirectional projections. This is different from what we see in neocortical areas where it is normal practice that region A projects into region B and region B projects back to region A, showing a large degree of reciprocity. Much of the neocortical input to the hippocampal formation is received through the entorhinal cortex. As depicted in ***Figure 4***, the entorhinal cortex

Figure 4.

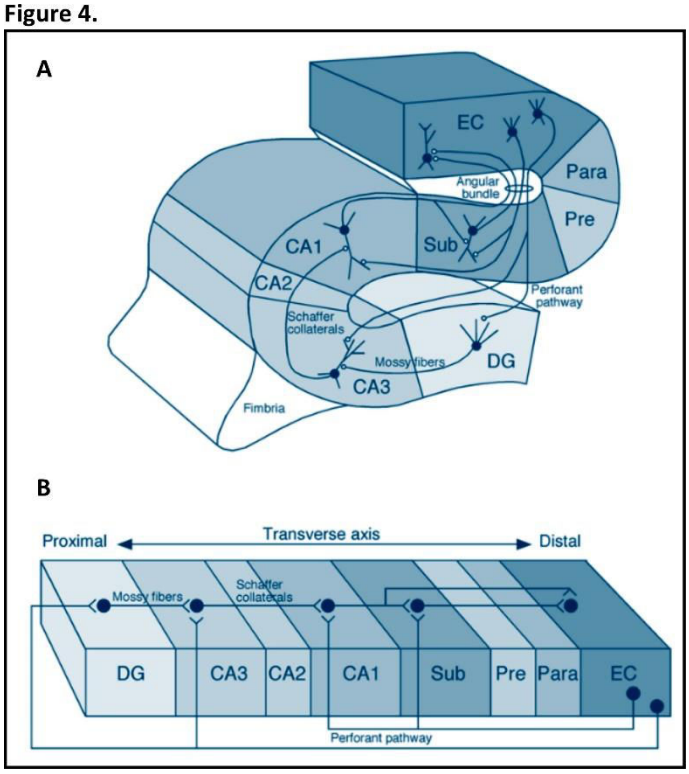

Figure 4. **The hippocampal formation. A**. Neurons in layer II of the entorhinal cortex (EC) project to the dentate gyrus and the CA3 region via the perforant pathway. Neurons in layer III of EC project to CA1 and the subiculum (Sub) via the perforant and alvear pathways. The granule cells of the dentate gyrus (DG) project to CA3 via mossy fibre projections. CA3 pyramidal neurons project to CA1 via Schaffer collaterals. CA1 pyramidal neurons project to Sub. Both CA1 and Sub neurons project back to the deep layers of EC. **B**. Projections along the transverse axis of the hippocampal formation.

sends axons to the dentate gyrus, however, the dentate gyrus does not project to the entorhinal cortex. Granule cell axons of the dentate gyrus called **mossy fibres** project towards the pyramidal cells of the CA3 region and again this pathway is unidirectional; so are the projections from CA3 to CA1 called **Schaffer collaterals**, and CA1 to the subiculum.

It should be emphasized that no brain region functions in isolation. The regions of the hippocampal formation are innervated by and send projections to other brain nuclei, which is vital for their function. There are three major fibre bundles providing input innervation to the hippocampal formation. The first is the **angular bundle** containing fibres that originate in the entorhinal cortex and innervate the dentate gyrus, hippocampus and subiculum. The second pathway is the **fimbria-fornix pathway** that interconnects the hippocampal formation with the basal forebrain, hypothalamus and brain stem. The third major fibre system is called **dorsal and ventral hippocampal commissures** and contain some 350,000 fibres. They connect one hippocampal formation of one hemisphere with the hippocampal formation of the contralateral hemisphere.

To follow on the architectonic organisation of the hippocampal formation, the specific regions will be separately and briefly described below. For the sake of simplicity, this will be done taking the rodent hippocampal formation as a model system.

A. Dentate gyrus

The dentate gyrus (DG) has three distinct layers, from the superficial side: **molecular layer**, **granule cell layer** and **polymorphic cell layer** (see scheme in ***Fig. 5***). The principal cells, that is to say those that project out of DG, are the **granule cells** whose cell bodies (10 µm x 18 µm) lay within the granule cell layer. There are about 1.2 x 10^6 granule cells in one dentate gyrus. The granule neuron has a very specific cone-shaped dendritic tree extending its branches in the molecular cell layer. Granule cells have spiny dendrites with estimates between 3600-5600 spines per cell depending on their particular localisation along the granule cell layer. Interestingly, the number of granule cells does not vary in adult animals, however, young animals that were exposed to enriched environments show bigger dentate gyri with more granule cells in adulthood. Except granule cells, the dentate gyrus contains local interneurons that unlike the granule cells do not project to other areas of the hippocampal formation. The pyramidal basket

cell is the most studied interneuron. Their cell bodies are localised at the edge of the granule cell layer. The name 'basket' comes from the appearance of the cone-like axonal plexus that surrounds and connects with cell bodies of granule cells. The basket neuron has usually one principal apical aspiny dendrite extending to the molecular layer and several basal dendrites in the polymorphic cell layer. Basket cells are positive for the μ-aminobutyric acid (GABA) and thus provide an inhibitory input. The molecular cell layer is mostly occupied by dendrites and axons, however, it also contains cell bodies of interneurons named MOPP (molecular layer performant path-associated) and chandelier cells that are axo-axonic cells innervating the axon initial segment of granule cells. In regard to the polymorphic cell layer, that is also referred to as the hilus, the most common cell type is the **mossy cell** with large triangular or multipolar cell bodies (25-35 μm). Mossy cells are further characterized by large, complex and dense spines that are called **thorny excrescences** located on proximal dendrites. These spines form glutamatergic synapses with large boutons of mossy fibre axons of granule cells (as depicted in ***Fig. 5***). Of note, the word 'mossy' is used in two distinct cell types: mossy fibres of granule cells and mossy cells, which can be confusing but it is apt considering the mossy appearance of both.

Noteworthy, the dentate gyrus receives major excitatory innervations from the entorhinal cortex (***Fig. 4***) through so called perforant pathway for the fact that the fibres leaving the angular bundle perforate the subiculum. A population of hypothalamic cells sends mostly glutamatergic projections to granule cells; and noradrenergic and dopaminergic projections are received from the brain stem. The subcortical regions send only few inputs towards the dentate gyrus and the most prominent is the one from septal nuclei using acetylcholine or GABA as a neurotransmitter. Importantly, the dentate gyrus is a source of **adult neural stem cells** that reside in the **subgranular zone** and give rise to new granule cells throughout the life. The dentate gyrus plays a substantial role in cognition and emotions. The cognitive functions relate to spatial memory. In particular, DG has been involved in so called pattern separation, the ability to distinguish between similar experiences which is crucial for episodic memory, its storage and retrieval. The emotional function of DG involves the regulation of mood and anxiety, and it has also been associated with behaviours with a strong component of stress and fear (reviewed in (Scharfman, 2016)).

B. Hippocampus proper

Alike the dentate gyrus, the hippocampus proper, also referred to as Ammon's horn, has a curved structure (***Fig. 6***). It is divided into three subregions: CA1, CA2 and CA3 (***Fig. 4 and 6***). These subregions have laminar architecture with five layers, superficially: *stratum alveole* (ALV), *stratum oriens* (OR), *stratum pyramidale* (PYR), *stratum radiatum* (RAD) and *stratum lacunosum moleculare* (LAC-MOL; ***Fig. 5***). The CA3 field contains an additional thin acellular layer the *stratum lucidum* occupied by mossy fibres. Stratum alveole presents a fibre-rich thin layer. Stratum oriens contains basal dendrites of pyramidal cells and several types of interneurons. Moreover, some of the fibres connecting CA3 to CA3 and CA3 to CA1 (Schaffer collaterals) are also located in stratum oriens. The somata of hippocampal principal cells, called pyramidal cells, lay in the stratum pyramidale. They are tightly packed in CA1 and more loosely in CA2 and CA3. Owing to the U shape of the hippocampus, the CA1 pyramidal cells are upside down compared to CA3. Stratum radiatum consists of connecting fibres of CA3 to CA3 neurons, and Schaffer collaterals. The lacunosum moleculare layer is formed mostly by fibres from the entorhinal cortex and thalamus. Numerous interneurons are also scattered in both strata radiatum and lacunosum moleculare.

Figure 5.

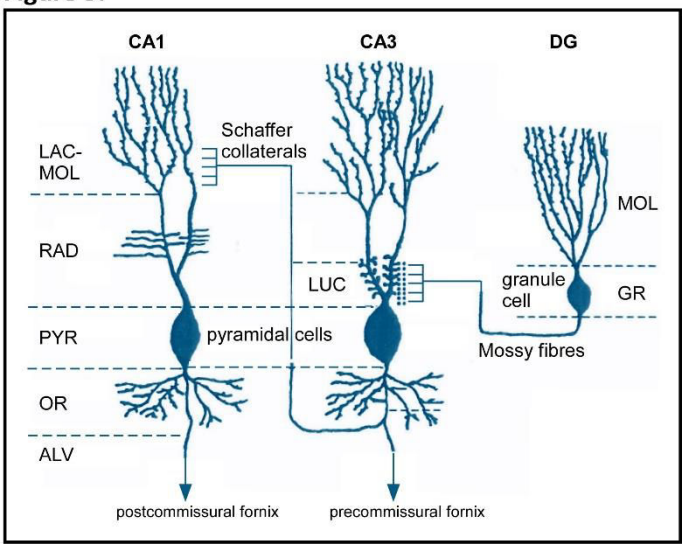

Figure 5. **The tri-neural circuit between principal cells of the hippocampal formation**. A scheme of axonal terminations of principal cells on target principal cells. Axons of the dentate gyrus (DG) granule cells, termed mossy fibres, innervate the giant excrescences of CA3 pyramidal cells. CA3 axons called Schaffer collaterals terminate on the CA1 dendrites. The names of individual layers are also indicated and further described within the text. The image was taken and adapted from (Hammond, 2001).

Figure 6.

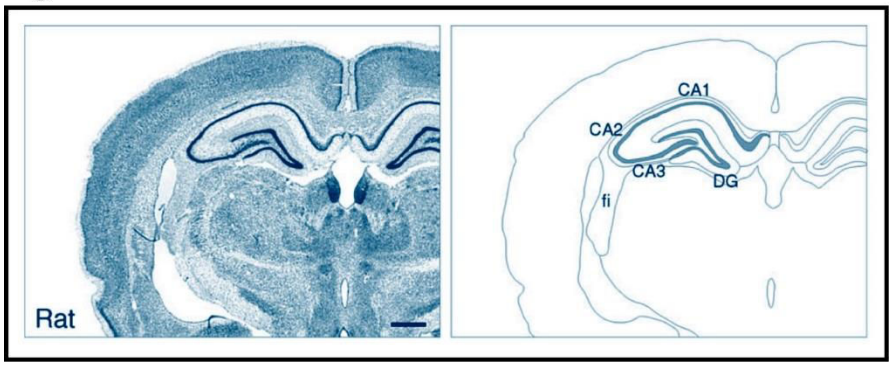

Figure 6. **Nissl-stained section (left) and line drawing (right) illustrating the general organization of the hippocampal formation in the rat**. Scale bar = 1 mm. Taken and modified from The Hippocampus Book (Andersen et al., 2007).

Pyramidal cells are the most numerous cell type found not only in the hippocampus but also in the cerebral cortex and amygdala. Although the pyramidal neurons present a certain degree of variability, their cellular architecture is stereotypical. Cell bodies of pyramidal cells tend to have a teardrop/rounded pyramid shape. They have a longer apical dendritic tree that extends from the pointy end of the soma and is terminated by a dendritic turf. The basal portion of the pyramidal cell forms a basal cluster of shorter dendrites. Apical dendrites of hippocampal pyramidal neurons pass through the stratum radiatum and ramify in stratum lacunosum moleculare, whereas basal dendrites arborize in stratum oriens. The pyramidal cells of the CA3 region that are closest to the DG do not extend their dendrites to stratum lacunosum moleculare and therefore are not influenced by projections from the entorhinal cortex, but synapse with mossy fibres of DG. Dendrites of pyramidal cells have numerous spines. The most prominent are the thorny excrescences of CA3 cells forming synapses with mossy fibres. Axons of pyramidal cells run through stratum alveus emitting numerous collaterals before leaving the Ammon's horn through the pre- and postcommissural fornixes (axon bundles; ***Fig 5***).

There is a vast literature concerning studies performed on the CA1 pyramidal neurons, especially focused on synaptic transmission and plasticity. This is mostly attributed to their morphology, cell viability in culture and well trackable connections with CA3. The dendrites of

CA1 neurons are covered with about 30,000 spines that receive excitatory synaptic inputs (Megias et al., 2001). Thus, density and morphology of dendritic spines has been used as a functional measure for excitatory efficacy that is closely correlated with cognitive function including memory formation. Indeed, changes in spine density and morphology have been reported in many neurological disorders. For instance, a massive loss of synapses in CA1 region is associated with cognitive decline in murine models of Alzheimer's disease (Perez-Cruz et al., 2011) (Merino-Serrais et al., 2011) (Lazcano et al., 2014). On the other hand, a neurodevelopmental disorder - the Fragile X syndrome is characterized by an increased number of immature dendritic spines in the CA1 region (reviewed in (He and Portera-Cailliau, 2013)). Under physiological conditions, the highest density of spines is found in strata radiatum and oriens, much lower in stratum lacunosum moleculare. Asymmetrical synapses, which are presumably excitatory, can be also formed on dendritic shafts usually in the apical dendritic tuft. It was estimated that about 1,700 inhibitory symmetrical synapses converge on a single CA1 pyramidal neuron targeting usually the soma, axon and spine-free proximal apical and proximal basal dendrites (Megias et al., 2001).

CA2 pyramidal neurons have been long overlooked probably due to the small size of the CA2 region when compared to CA1 or CA3. More recent studies have determined their particular synaptic properties and involvement in social and spatial memory and pathological conditions such as schizophrenia (reviewed in (Dudek et al., 2016) (Srinivas et al., 2017)). CA2 pyramidal neurons can be distinguished from the CA1 and CA3 pyramidal cells based on morphology, connectivity and molecular markers. According to Lorent de Nó (1934), CA2 pyramidal cell dendrites lack thorny excrescences that form synapses with mossy fibres from DG and are characteristic of the CA3 pyramidal neuron dendrites; although we now know that this is variable between species. More recent discoveries identified specific axonal projections from the thalamus that are indicative of the boundary between CA2 and CA3 fields. In addition, CA2 pyramidal neurons project mainly to stratum oriens of CA1, whereas CA3 pyramidal neurons project to stratum radiatum of CA1. Furthermore, there are more parvalbumin- and reelin-expressing interneurons in CA2 than in CA1 or CA3. Interestingly, the CA2 field is relatively

resistant to injury as well as to induction of plasticity processes such as long-term plasticity (LTP). Intriguing, however, is the finding that the CA2 pyramidal cells possess all proposed plasticity mediators characteristic of CA1 neurons. The research laboratory of Dr Serena M. Dudek has carried out extensive studies on the CA2 area concerning plasticity processes. In the past years, they showed that one possible cue for plasticity resistance could be through changes in calcium dynamics. Her team also proposed the RGS14 (Regulator of G-protein Signalling 14) scaffold protein to play a key role in suppression of LTP in CA2 pyramidal cells (Simons et al., 2009) (Lee et al., 2010) (Vellano et al., 2011). In addition, given the high resistance of the CA2 region to apoptosis, CA2 may prove a suitable model to study diseases with impairments in social and spatial memory processing.

The CA3 region receives three major excitatory inputs: from mossy fibres of DG, from EC and local from the CA3 neurons. This unique interconnectivity makes the CA3 network highly excitable. For this reason, the CA3 region has attracted increasing attention for its role in memory and susceptibility to seizures and degeneration. CA3 pyramidal neurons are morphologically very similar to CA1 neurons, however, the CA3 neurons are on average larger. The largest CA3 neurons are in the distal and smallest in the proximal portion of CA3 to DG. The dendritic ramification is characterised by a shorter basal dendritic tree within stratum oriens, a short apical dendritic trunk in stratum lucidum that arborizes into two or more long apical trunks. These long apical trunks further ramify into shorter dendritic branches in stratum radiatum and long dendritic trunks continue to stratum lacunosum moleculare. As mentioned above, CA3 neurons are studded with thousands of dendritic spines. The most apparent are the thorny excrescences that form about 40 clusters on each CA3 neuron. Generally, these branched dendritic spines synapse with a single mossy fibre bouton. A single CA3 neuron projects its axon to all CA3, CA2 and CA1 regions. These axons are myelinated with abundant boutons. The estimates show between 15,000 and 60,000 synapses that can be formed by a single CA3 axon. Some CA3 axon boutons also innervate interneurons which interestingly happens at a single release site. As in CA1 this single synapse is very powerful able to generate an action potential in the postsynaptic interneuron. In regard to the high excitability, the CA3 neurons show a typical bursting pattern

comprising of several action potentials that last 30 to 50 ms. Because the CA3 pyramidal neurons do not possess a large primary apical dendrite like the CA1 neurons, only a restricted number of studies have focused on the dendritic excitability and ion channels in CA3 (Andersen et al., 2007).

C. Subicular complex

The subicular complex (***Fig. 4***) including prosubiculum, subiculum, presubiculum, postsubiculum and parasubiculum forms a continuum of the CA1 as it begins where the Schaffer collaterals end (reviewed in (Andersen et al., 2007) (Ding, 2013) (O'Mara, 2005)). The pyramidal cells of the subicular complex are more disperse compared to the tightly packed layer of CA1 pyramidal cells. Despite the fact that the subicular complex constitutes the major output of the hippocampal formation it is a poorly investigated brain structure. Some of its roles were identified in the encoding and retrieval of memory, and in neurodegenerative disease and epilepsy. The subicular pyramidal neuron has a typical morphology with dendrites comprising spines. The subiculum receives input from CA1 as well as EC layer II and III. Importantly, the subicular output innervates local areas: EC layer V, presubiculum and parasubiculum and also more distant cortical structures such as the prefrontal cortex, olfactory nucleus, thalamus, amygdaloid complex and others. The particular subicular cortices can be identified based on the expression of specific genes and neurochemicals.

D. Entorhinal cortex

The name ‘’entorhinal’’ is based on its position as it is partially enclosed by the olfactory – rhinal sulcus. Early studies of the entorhinal cortex by Ramón y Cajal and Lorente de Nó defined the cytoarchitectonic organisation which is today accepted with some minor changes: EC is divided into two main subregions, the medial and lateral EC, both of which have a 6-layer laminar structure with four cellular and two acellular layers. Much interest devoted to EC has begun in early 1990s with the discovery that this brain area was prone to early neurodegeneration in Alzheimer’s disease (Van Hoesen et al., 1991). The entorhinal cortex plays an indispensable role

Figure 7.

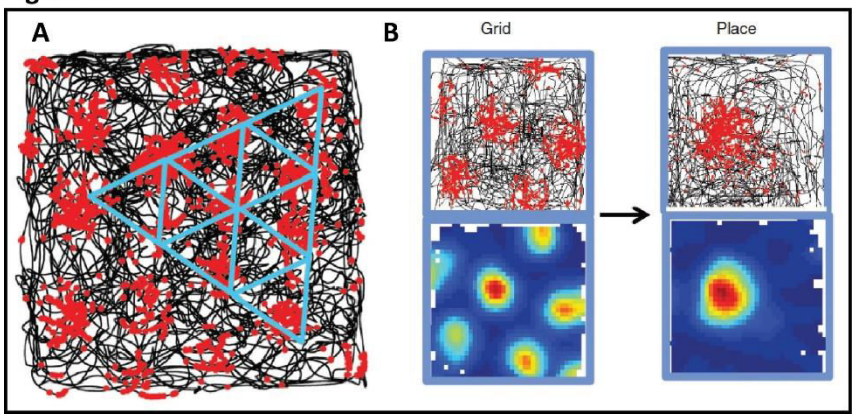

Figure 7. **Grid and place cells**. **A.** An EC grid cell firing pattern. The black trace shows the trajectory of a foraging rat in part of a 1.5-m-diameter-wide square field. Spike locations of the grid cell are in red. Each red dot corresponds to one spike. Blue equilateral triangles illustrate the regular hexagonal structure of the grid pattern. **B.** Grid cell (left) and place cell (right) firing and activity. The top part shows trajectories with spike locations. The bottom color-coded rate maps show high activity (red) and low activity (blue) firing. Grid cells are thought to provide much, but not all, of the entorhinal spatial input to place cells. Adapted from (Moser et al., 2015).

in the feedforward and feedback flow of information bridging the hippocampus and the neocortex. Recent studies provide evidence that the medial EC processes spatial information, whereas the lateral EC governs pathways encoding object information. A famous trio of scientists (John O'Keefe and Edward and May-Britt Moser) who were awarded the Nobel Prize in Physiology or Medicine in 2014 made a breakthrough discovery of a "GPS system" in the brain – the place and grid cells (***Fig. 7***). Place cells are CA1/CA3 hippocampal pyramidal neurons that fire specifically based on spatial localisation. Even more interesting is the finding that the firing of place cells does not depend on the local CA3/dentate gyrus innervation but rather the spatial information is received from the medial EC. The medial EC neurons are highly responsive to change in position. These neurons show a firing field pattern with regularly shaped triangular or hexagonal grids, thence called grid cells (reviewed in (Moser et al., 2015)). The realisation about where we are in space provides one of the most fundamental information for survival. The crucial function of place and grid cells function is evident in Alzheimer's disease where disorientation is a common early symptom.

1.2 Neuronal synapse

Most studies investigating synapses have been carried out using the hippocampal circuitry as a model system. Therefore, the previous chapter aimed at introducing the hippocampal formation so it would set the niche for further characterization of synapses, to which the current chapter is devoted.

The notion that a contact between two neurons is the place where information transmission occurs was first suggested by Ramon y Cajal in 1888. Later, an English neurophysiologist Charles Scott Sherrington (1897) introduced the term 'synapse' (from the Greek "to clasp") to give a name to these specialized zones of interneuronal communication. Currently, the synapse is no longer seen only as a static junction between neurons but a very dynamic organelle whose function is tightly regulated in time and space owing to the constituting molecular interactions (Choquet and Triller, 2013). Deciphering the structure and molecular organisation of synapses is an essential step toward understanding the molecular mechanisms that underlie synaptic transmission and plasticity - processes that are the foundation of physiological brain function. Noteworthy, there is a tendency to see cellular reactions as linear, but particularly in neurites, differential concentrations, position as well as the reactive state of soluble and bound synaptic proteins determine the regulatory cues in these highly dynamic and precise processes that mediate both presynaptic and postsynaptic portions of neurotransmission.

Primarily, neuronal synapses can be characterized based on the type of transmission – chemical and electrical. Electrical transmission is mediated via so called gap junctions, i.e. electrical synapses, through a direct cytoplasmic exchange of ions and small molecules between neighbouring neurons. Importantly, the two types of neurotransmission coexist and interact in both the developing and adult brain (Pereda, 2014) (Nagy et al., 2018). This introduction will describe and refer to the most abundant form of transmission at chemical synapses composed of axonal termini (boutons) and dendritic spines in the hippocampus.

❖ **Chemical synapses**

A characteristic of chemical synapses is the presence of a synaptic cleft – a gap between the axonal terminus of a presynaptic neuron and the dendritic specialisation of a postsynaptic neuron (reviewed in (Harris and Weinberg, 2012) (Hammond, 2001) (Pickel and Segal, 2014) (Nicholls et al., 2012)). The process of transmission is mediated by a change in electrical potential in the presynaptic cell that consequently leads to the release of neurotransmitter molecules. Chemical synapses are either excitatory or inhibitory depending on the neuromodulatory effect the neurotransmitter has on the receiving postsynaptic neuron. A large body of literature describes the prototypical chemical neuron-to-neuron synapses that are indeed the most abundant and extensively studied synapses in the brain. The synaptic complex is a basic unit of each functional chemical synapse. It comprises of three components: the presynapse, cleft and postsynapse. The synaptic complex shows a particular asymmetric organisation. The most prominent asymmetric trait is the presence of synaptic vesicles (40-60 nm) exclusively in the presynapse and a submembraneous electron-dense zone in the postsynapse. Additionally, the synaptic complex is surrounded by modulatory astroglial processes. Thus the synaptic complex together with astroglia can be seen as a mesh-like structure on an electron microscopy section (***Fig. 8***). Excitatory synapses are formed mainly on dendritic spines, unlike the inhibitory synapses that preferably connect to the cell soma and axonal initial segments with only small percentage found

Figure 8.

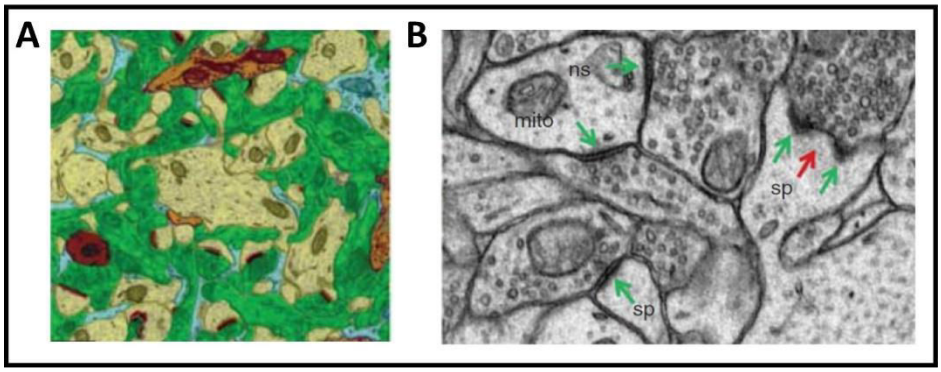

Figure 8. **Synaptic complex in the CA1 region of the hippocampus**. **A.** An electron microscopy section that was colour coded to show excitatory axon (green), spiny dendrites (yellow), an aspiny dendrite (dark red), sparse inhibitory axons (orange) and astroglial processes (light blue). **B.** Asymmetric synapses (green arrows), a non-spiny dendrite (ns) with a mitochondrion (mito), two dendritic spines (sp) of which one has a perforated PSD (red arrow). Adapted from (Harris and Weinberg, 2012).

along spiny and aspiny dendrites, hence the sparse distribution of inhibitory synapses that can be seen in the synaptic complex (***Fig. 8***).

This part of introduction will summarize the existing knowledge of the structure, types and composition of the synaptic complex.

A. The presynapse

The first piece of evidence pointing to the synapse as a dynamic organelle came with the finding that neurotransmission relies upon calcium-driven fusion of neurotransmitter-filled vesicles with presynaptic membrane. This notion was further reinforced by the discovery of endocytic pathway that dynamically recycles these vesicles (Heuser and Reese, 1973).

a) Presynaptic trafficking

During neuronal development, upon neuronal cell determination and morphogenesis, synapses are to be formed. The majority of synaptic material required for synaptic formation is synthesized in the cell body and transported over long distances to and from synaptic loci by microtubules-associated molecular motors. The molecular organization of axonal versus dendritic microtubules differs. According to *in vivo* studies, axonal microtubules (MTs) have their minus ends oriented exclusively toward the cell body, whereas dendritic microtubules show mixed orientation with more abundant distal plus-ends in vertebrates when compared to invertebrates (reviewed in (Chia et al., 2013); (Stone et al., 2008)). However, it is not only the polarity of MTs itself that is critical in determining whether molecular cargoes will be targeted toward the presynapse or postsynapse, the microtubule-associated proteins (MAPs) also play an important role. Upon genetic manipulations, presynaptic cargoes can be misplaced into dendrites, as shown in mutants for kinesin and other MT-binding proteins such as UNC-33 and UNC-44 in *Ceanorhabditis elegans* (Seeger and Rice, 2010) (Maniar et al., 2011).

Axonal trafficking of biomolecules can be classified based on the direction toward the cell body as retrograde, or toward the axonal terminus as anterograde. Anterograde trafficking is carried out by kinesins. These motor proteins are important for both the export of cargo molecules from the Golgi apparatus and their subsequent transport to destination sites. The exact mechanisms of cargo sorting and loading remain to be determined.

An average pyramidal neuron possesses thousands of synapses. What are the exact signalling cues that regulate how cargoes get distributed between synapses is yet to be elucidated. Most of the investigations into the molecular mechanisms of axonal trafficking have been performed in *C. elegans* and *Drosophila melanogaster*. The axonal anterograde transport includes kinesin-3 motor proteins KIF1A and KIF1Bβ that were shown to transport synaptic vesicle-associated proteins in the form of SV precursors to presynaptic sites (Sabo et al., 2006). Binding of motor molecules onto the MTs is followed by ATP hydrolysis that initiates the transport along MT tracks. The lack of KIF1A and KIF1Bβ reduced the number of SVs as well as SV proteins in the presynapse (Chia et al., 2013). The kinesin-1 motor complex transports presynaptic membrane proteins such as SNAP-25, Bassoon, Piccolo, RIM and syntaxin-1. Upon reaching the end of microtubules, molecular cargoes are unloaded for delivery to presynaptic sites presumably by additional local regulatory cues (Yagensky et al., 2016). For instance, one local regulatory mechanism involves the small GTPase Rab3. DENN/MADD, a Rab3 guanine nucleotide exchange factor, binds to the kinesin-3 complex and promotes anterograde transport of synaptic vesicles associated with Rab3 in the GTP-bound state (Niwa et al., 2008). Depleting DENN/MADD of its enzymatic activity or locking Rac3 in GTP-bound state impairs transport of these vesicles to distal presynaptic sites (Niwa et al., 2008). Phosphorylation presents another mechanism capable of controlling distal axonal cargo targeting. Phosphorylation of kinesins by the GSK3β kinase leads to cargo release (Morfini et al., 2004). GSK3β is selectively active in growth cones and thereby most likely participates in formation of synapses *de novo* (Morfini et al., 2004). A mechanism controlling cargo pausing and loading has also been documented along MTs *en route*. Loss-of-function mutations in *arl-8* that encodes the small G-protein ARL-8 lead to proximal accumulation of presynaptic specializations and loss of synapses in distal axons, which results in defects in neurotransmission in *C. elegans* (Wu et al., 2013). Thereafter, ARL-8 and JNK were reported to act in an antagonistic way to balance cargo self-assembly and facilitate cargo trafficking *en route* (Klassen et al., 2010) (Wu et al., 2013). An interesting phenomenon has been described in the process of synaptic vesicle recycling. The recycled material shuttles between local as well as remote boutons involving both kinesin and dynein motors. Remarkably, the retrogradely

transported vesicles are likely to be captured by distal as opposed to proximal presynaptic sites (Maeder et al., 2014).

Sustained and optimal presynaptic function requires the molecular motor dynein, which mediates retrograde transport of biomolecules from the presynapse to the nucleus. In response to synaptic activity, retrograde movement of messenger molecules functions as a feedback signal that triggers changes in gene expression. In turn, specific products of gene expression can regulate the strength of synaptic transmission (Panayotis et al., 2015). For instance, calcium ion waves implement fast response synapse to soma communication and are most efficient for synapses localised closer to the soma. Slower and long distance synapse to soma communication involves extracellular signalling molecules, neurotrophins, such as BDNF (brain derived neurotrophic factor). Principally, neurotrophins bind to their receptors (Trk [tyrosine kinase] or p75NTR) at the presynaptic membrane which triggers receptor autophosphorylation and activation of downstream signalling cascades via MAPK, PLCγ and PI3K (Pazyra-Murphy et al., 2009).

In addition to changes in gene expression, retrograde transport is crucial for degradation and turnover of unwanted or damaged proteins and organelles. During axonal development, protein degradation at the axonal tip decreases with an enhanced retrograde transport of the ubiquitin-proteasome system (UPS) (Hsu et al., 2015). In regard to mature presynapses, previous studies demonstrated that the UPS functions rather locally within synaptic boutons to acutely control levels of presynaptic proteins and thereafter the efficacy of neurotransmission (Speese et al., 2003). Autophagy, however, is a degradation mechanism that depends on the retrograde transport of presynaptic components. These components including synaptic vesicles and α-synuclein are cleared via autophagosomes. This degradation pathway is quite challenging since autophagosomes must be transported across long distances to lysosomes that usually reside in the cell soma. A recent study implicated JIP1, a kinesin-1 activator that binds dynein, and the autophagosomal protein LC3 in the clearance of presynaptic proteins. Preventing JIP1 binding to

LC3 results in defects in retrograde trafficking of autophagosomes as well as impairment of autophagosomes fusion with lysosomes (Fu et al., 2014b).

Noteworthy, although kinesin and dynein motors mediate unidirectional traffic, they are known to bind synaptic cargoes simultaneously. Axonal microtubule tracks are not continuous. They can break, or encounter various obstacles and therefore the option of switching between the two directions is very convenient for bypassing such difficulties. Importantly, these opposite-polarity motors were found to activate one another and this way efficiently carry synaptic cargoes in either direction.

MT motors also respond to presynaptic plasticity processes. Repetitive stimulation of neurons in culture enhances the formation of new presynaptic boutons, a process that is dependent upon trafficking of presynaptic components by kinesin-1. Similarly, mice that were placed in an enriched environment expressed increased levels of kinesin-3 motor KIF1A which is directly correlated with increased trafficking of presynaptic cargoes (Kondo et al., 2012).

b) Structure and composition of presynaptic termini

The excitatory axospinous synapses in the stratum radiatum of the hippocampal CA1 are prototypic and highly abundant synapses formed predominantly by unmyelinated axons. Most of these axons are the Schaffer collaterals originating in the CA3 region. The axonal termini often form swellings referred to as boutons that are filled with many neurotransmitter-containing

Figure 9.

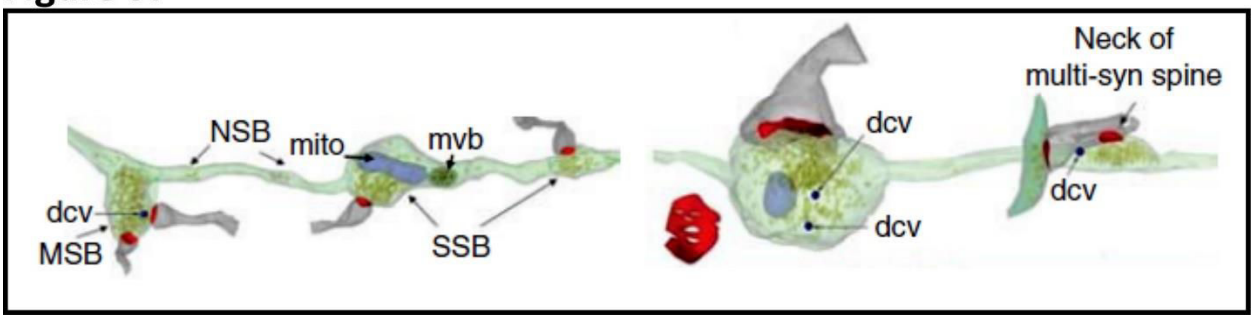

Figure 9. **Axonal boutons and dendritic spines**. (Left and right), 3D reconstructions of axons and axonal boutons (light green) of Schaffer collaterals. Synaptic vesicles are visible within each bouton. Dendritic spines (grey) with PSD (red) converge onto synaptic boutons. In the right panel, a red disc represents a reconstructed PSD from the depicted dendritic spine. Abbreviations: dcv, dense core vesicles; MSB, multi-synaptic bouton; SSB, single synaptic bouton; NSB, non-synaptic bouton; mito, mitochondrion; mvb, multivesicular body. Taken from (Harris and Weinberg, 2012).

vesicles and can be clearly seen by electron microscopy ***(Fig. 9)***. The majority (~75%) of axonal boutons establish a single contact synapse, about 21% form multi-synapse contacts and ~4% lack their postsynaptic counterpart (Sorra et al., 2006). These pre-existing but unconnected boutons are an advantage when it comes to rapid synaptogenesis as there is no need for generation of presynaptic termini *de novo* (Petrak et al., 2005) (Harris and Weinberg, 2012). Another type of axonal bouton that is worth mentioning is the robust bouton of granule neurons of the dentate gyrus that converge onto multiple thorny excrescences of CA3 pyramidal neurons ***(Fig. 10)***. In the cerebellum, large specialized axonal termini termed synaptic glomeruli can be found. These originate from cerebellar granule cells and synapse with dendritic spines of Purkinje neurons.

Figure 10.

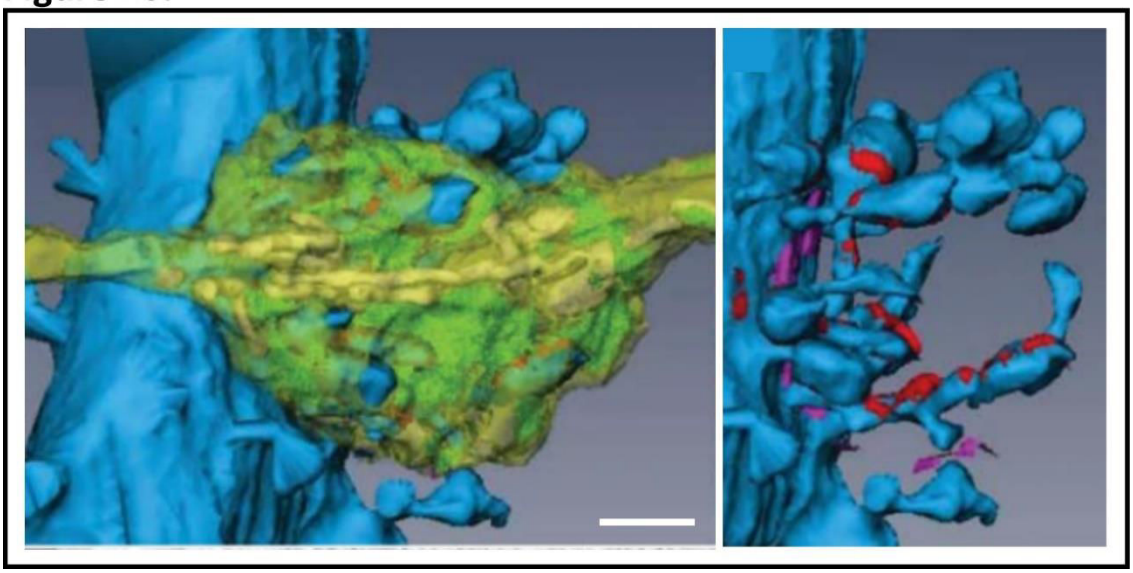

Figure 10**. 3D reconstruction of a mossy fibre bouton and CA3 thorny excrescences**. Left, a mossy fibre bouton (yellow-green) converging onto thorny excrescences (blue spines). Right, CA3 thorny excrescences with reconstructed synaptic (red) and non-synaptic connections (magenta). Scale bar 1 µm. Taken from (Harris and Weinberg, 2012).

The active zone

At chemical synapses, action potentials trigger calcium influx into the presynaptic terminal, which typically leads to the fusion of SVs with the presynaptic active zone membrane and neurotransmitter release. The active zone (AZ) is a biomolecule-rich electron-dense region that can be found in the proximity to the presynaptic membrane opposed to the postsynaptic density.

Typically, many synaptic vesicles occupy this region ready to dock and release neurotransmitter molecules. Intriguingly, AZ can be visualised as cytoplasmic dense projections that are organized into a presynaptic grid-like structure ***(Fig 11A)***. Why AZ adopts this particular shape is uncertain but it most likely has to do with SV mobilization and release as suggested by (Fernandez-Busnadiego et al., 2010). The excitatory SVs measure ~35 nm in diameter and are filled with glutamate molecules. Emerging evidence suggests that SVs are not a homogenous population of organelles and can be discriminated both structurally and molecularly. There exist at least three types of SV pools depending on SV availability for membrane mobilization and release: resting, recycling and readily releasable pools ***(Fig. 11B)***. The existence of different pools of SVs is obvious during a phenomenon called synaptic depression. Upon repetitive bursts of action potentials (APs) a reduction in postsynaptic response can be measured reflecting the fact that the RRP empties and another AP comes before this pools gets replenished. Oftentimes, a homeostatic lower steady level of transmission is established, in which the release is balanced by the slow refilling (Alabi and Tsien, 2012). In hippocampal synaptic boutons, only a few vesicles have the readily releasable pool status. After the readily releasable pool gets discharged (short 10-40 Hz stimulation), neurotransmitter release occurs from the secondary glutamate depot – the recycling pool. This total releasable pool of SVs (including both recycling and readily releasable pools) represents as little as ~100 vesicles. On the other hand, the resting pool is defined as a set of vesicles that are extremely reluctant to trafficking toward the AZ membrane and remain unreleased even after prolonged stimulation. Although the resting pool represent about 75% of total SV content in a presynaptic terminal, the physiological function of these vesicles remains unclear.

The release of SVs can be evoked in three distinct ways ***(Fig. 11B)***: a. synchronous vesicle release – electrical stimulation precedes synchronous currents that are triggered in the postsynaptic cell; b. asynchronous – a delayed vesicle fusion upon a stimulus; c. spontaneous – occurs in the absence of action potential, releases a very small portion of SVs and generates miniature postsynaptic currents (Crawford and Kavalali, 2015). The release of SV content is mediated by exocytosis, a well-orchestrated process that relies on spatial organisation and dynamics of fusion machinery components. Three-step SV release has been well documented:

Figure 11.

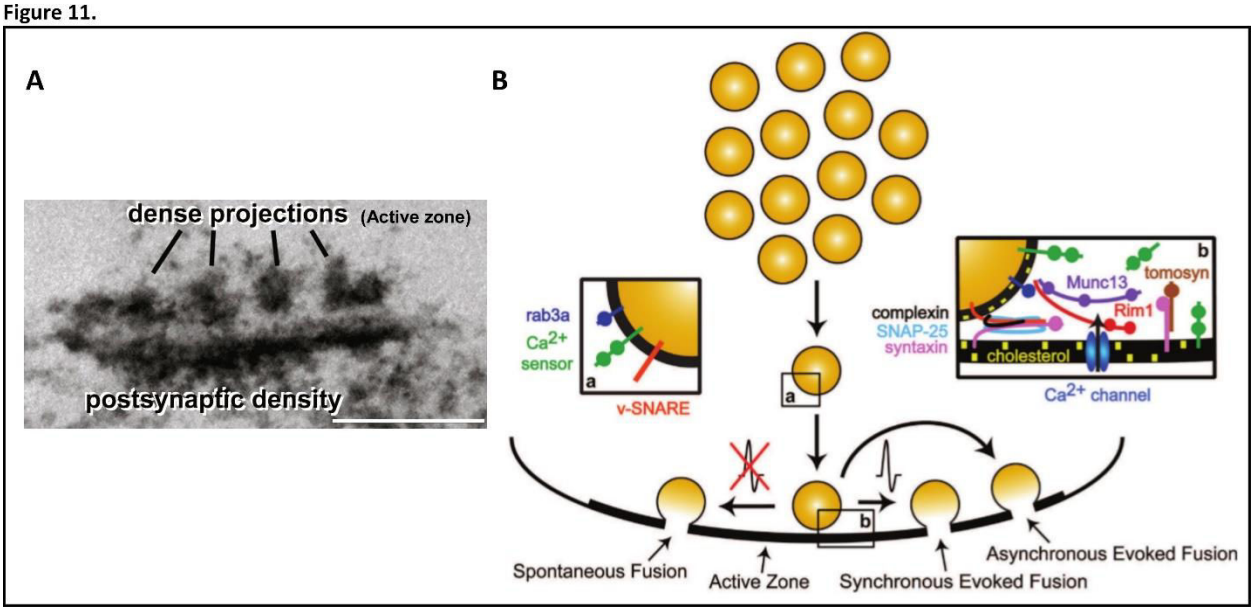

Figure 11. **Dense projections of the active zone and heterogeneity of the synaptic vesicle pool**. **A.** Electron micrograph of a phosphotungstic acid stained synapse with pre- and postsynaptic specializations, scale bar = 200 nm (taken from (Sudhof, 2012). **B.** A scheme of synaptic vesicles that are shuttled to the active zone for fusion and neurotransmitter release: synchronously, in response to an action potential; asynchronously after an action potential; or spontaneously, in the absence of action potentials. Vesicular proteins (a) confer heterogeneity to synaptic vesicle populations while cytosolic and plasma membrane molecules (b) coordinate with vesicular proteins to determine the fusion process. Taken from (Crawford and Kavalali, 2015).

SVs attachment to the plasma membrane (docking), fusion-preparatory phase (priming) and Ca^{2+} influx-dependent fusion (Milovanovic and Jahn, 2015). The SNARE (soluble N-ethylmaleimide-sensitive factor attachment protein receptor) family of proteins lies at the centre of the SV release process. v-SNARE (vesicular SNARE) proteins bind to target membrane SNARE (t-SNARE) proteins to form a complex that is essential for the fusion of vesicular and plasma membranes. Canonically, the component of v-SNARE VAMP2 (vesicle-associated membrane protein 2, also known as synaptobrevin-2) binds to the members of t-SNARE syntaxin 1 and SNAP-25 (synaptosomal-associated protein of 25 kDa) to bring the juxtaposed membranes together for fusion and neurotransmitter release. This process is catalysed by Ca^{2+} binding to the calcium sensor synaptotagmin 1 (Crawford and Kavalali, 2015) (Sudhof, 2013). The SV membrane contains a range of proteins important for exocytosis. Evidence suggests that some v-SNAREs, calcium sensors and other vesicular proteins are involved in SV trafficking to segregate vesicle pools prior to the release. Thus, expression of these membrane proteins on SVs could function as a molecular code predictive of their function within the presynapse (Wilhelm et al., 2014).

- v-SNARE proteins

The majority of neurotransmission is driven by the most abundant v-SNARE protein VAMP2. Depleting VAMP2 in cultured mouse hippocampal neurons leads to complete abolishment of evoked neurotransmission while spontaneous neurotransmission persists although at a decreased level (Deak et al., 2004). VAMP1 is also involved in synchronous SV release and was suggested to serve as a synchronizer of fusion events. Its expression in the CNS is more variable and higher in the periphery when compared to VAMP2. Importantly, VAMP1 knock-out mice show defects in both synchronously evoked and spontaneous SV release (Zimmermann et al., 2014). Albeit better known for its roles in endosomal trafficking and trans-Golgi network, VAMP4, another v-SNARE member, facilitates evoked release of SVs (Raingo et al., 2012). The v-SNARE vps10p tail interactor 1 (vti1) protein was discovered not long ago to reside in a specific subset of SVs as they are trafficked to the presynaptic membrane independently of VAMP2-containing vesicles. Depletion of vti1a causes minor deficits in spontaneous neurotransmission event (Ramirez et al., 2012). VAMP7 promotes neurite outgrowth and is enriched in SVs of hippocampal mossy fibre terminals. VAMP7-positive SVs fuse with presynaptic membrane in response to action potential-independent events (Bal et al., 2013).

- Calcium sensors associated with synaptic vesicles

Synaptotagmins are well described SV membrane proteins that following calcium binding catalyse membrane fusion. Synaptotagmin-1 (syt1) promotes synchronous evoked SV fusion. Syt1 is the most abundant synaptotagmin at the mammalian presynapse. Cultured mouse neurons depleted from syt1 do not express synchronous SV release, whereas asynchronous release is potentiated. Syt-2 has the same properties like syt-1, however it is expressed less abundantly. Syt-2 possesses the ability of Ca^{2+}-dependent phospholipid binding and both Ca^{2+}-dependent and independent binding to t-SNAREs (see thereafter).

In addition to v-SNAREs and calcium sensors, other SV-associated proteins have been involved in vesicle guidance to different SV pools and consequent release. The Rab3 small GTPase-deficient hippocampal neurons exhibit slightly increased evoked but normal

spontaneous release, while Rab3 depletion from neuromuscular junctions leads to decreased yet otherwise unaffected evoked release (Geppert et al., 1997) (Crawford and Kavalali, 2015). Synapsin 1 and synapsin 2 also play a role in evoked neurotransmission release, possibly regulating the likelihood of synchronous release (Crawford and Kavalali, 2015).

- t-SNARE proteins

Important for SV identity and membrane fusion are many proteins and protein complexes that reside within the target plasma membrane. These are the t-SNARE proteins and plasma membrane calcium sensors and calcium channels. The t-SNARE protein syntaxin 1 is abundantly expressed in the CNS, especially at the presynapse. Prior to binding to v-SNAREs, syntaxin 1 dimerizes with another t-SNARE protein, SNAP-25. This dimer binds to VAMP4, VAMP7 and syt-2. A knock-out of syntaxin 1 in *D. melanogaster* completely abolishes all forms of neurotransmission except for some rare asynchronous SV release. Preventing syntaxin 1 from binding to the SNARE complex destabilizes the SNARE complex formation and results in severely impaired evoked neurotransmission in both the *Drosophila* (Fergestad et al., 2001) and mammalian hippocampal neurons (Mishima et al., 2002). Undoubtedly, according to many studies on syntaxin 1 and its isoforms, these proteins are essentially involved in the guidance of SV for fusion, thus modulation and expression of different forms of neurotransmission (Crawford and Kavalali, 2015) (Mishima et al., 2014) (Zhou et al., 2013). SNAP-25 does not bear a transmembrane domain and anchors in the presynaptic membrane by palmitoylated cysteine residues and its interaction with syntaxin 1. Similarly, as for syntaxin 1, SNAP-25 is crucial for evoked neurotransmission but dispensable for spontaneous neurotransmission. SNAP-23 is structurally related to SNAP-25 but expresses lower affinity to syt1. In vitro, SNAP-23-dependent SV docking occurs at lower Ca^{2+} concentration when compared to SNAP25-dependent docking. Evidence suggests that SNAP-25 and SNAP-23 could function to a certain degree in a redundant fashion (Sorensen et al., 2003). In addition, SV release is promoted by calcium sensors and calcium channels that are embedded in the presynaptic membrane. According to electron microscopy imaging of hippocampal neurons, synaptotagmin 7 localises into the presynaptic membrane rather than synaptic vesicles. It exhibits high calcium affinity and slow kinetics, which

points to its involvement in coordinated delayed SV release events. Multimeric transmembrane voltage-gated calcium channels like N-type, P/Q-type, R-type and L-type are also known to directly interact with the fusion machinery. They participate in both excitatory and inhibitory spontaneous fusion events.

Despite this intense research, it is currently not clear how the readily releasable pool is assembled and maintained. In addition, to the above-described molecular players that participate in RRP assembly and SV exocytosis, the cytosolic proteins Munc-18 and Munc-13 also play a substantial role in SV priming/fusion. Latest research shows that primed vesicles are instable in the absence of Munc13-1 or Munc18-1 as they get de-primed and fall back into a non-releasable state. Thus, Munc13-1 and Munc18-1 stabilize primed synaptic vesicles by preventing de-priming (He et al., 2017).

- Actin cytoskeleton

In addition to the microtubule cytoskeleton that carries out long-range axonal trafficking, actin-dependent mechanisms often organize local protein complexes in subcellular domains such as the presynapse (Chia et al., 2013). Depolymerization of F-actin reduces the size and number of synapses in cultured immature, but not mature, hippocampal neurons (Zhang and Benson, 2001). Indeed, presynaptic F-actin levels rise in newly-made synapses (Zhang and Benson, 2002). The exact function of presynaptic actin is still unclear, however, it was suggested to act as a scaffold that provides mechanical stability, and recruits and stabilizes presynaptic assembly proteins (Sankaranarayanan et al., 2003). Similarly, AZ proteins have been shown to affect F-actin assembly. For instance, loss of Piccolo results in loss of Profilin 2, a mediator of F-actin polymerization (Waites et al., 2011). Importantly, actin-associated motors myosins of class II and VI are present at the presynapse (Kneussel and Wagner, 2013). Myosins II have been implicated in neurotransmitter release and synaptic vesicle motility during evoked activity (Peng et al., 2012); and myosins VI act in both pre- and postsynaptic BNDF signalling as they bind BDNF receptor TRKB. The lack of myosin VI leads to deficits in synaptic transmission in mice (Yano et al., 2006).

- Mitochondria

Synaptic transmission is an ATP- and Ca^{2+}-dependent process. Hence, mitochondria, the energy power plants and calcium buffering system, are another integral component of axons and presynaptic boutons. In hippocampal CA1 neurons only 41% of presynaptic termini contain mitochondria. On the contrary, many mitochondria can reside in large boutons (Harris and Weinberg, 2012). The assembly of the MT motor adaptor KIF5, Milton (Trak) and Ca^{2+}-binding mitochondria outer membrane receptor Miro drives mitochondrial anterograde transport toward axon terminals (Sheng, 2014). Of note, a recent study provided evidence that synapses are highly enriched in ATP in spite of containing little portion of mitochondrial membranes (Chavan et al., 2015). This finding suggests that other still undefined local mechanisms involved in ATP concentrating or production could be present at the presynapse.

- Synaptic vesicle recycling machinery

Sustained neuronal activity requires repeated exo- and endocytosis of SVs. To forestall the expansion of the presynaptic plasma membrane and a corresponding loss of lateral membrane tension, a recycling endocytosis occurs following SV fusion (reviewed in (Soykan et al., 2016) and (Rizzoli, 2014)). Two models of synaptic recycling were suggested based on early electron microscopy analysis (1970s) of frog neuromuscular junctions: "kiss and run" (or bulk) and clathrin-mediated endocytosis. As aptly stated by Shigeki Watanabe *''The kiss-and-run mechanism is like refilling the same bottle: The same vesicle that has just undergone fusion is retrieved and refilled. The clathrin-mediated mechanism is like moulding a new bottle from a used one: the old vesicle is resorbed into the plasma membrane and must be subsequently remoulded''* (Watanabe, 2015). Nevertheless, the mechanisms of SV recycling have been challenged in many aspects and need more investigation.

B. The postsynapse

Coming to the presynapse-juxtaposed synaptic part, the postsynapse, a special attention will be devoted to the composition and function of the glutamatergic postsynaptic compartment –

the **dendritic spine – in which the study of my PhD thesis is set in**. Here, I specifically discuss the morphology and molecular composition of spines with a brief mention of the dendrito- and spinogenesis processes. The postsynaptic membrane receptors that carry out glutamatergic neurotransmission will be discussed in **Chapter 1.3**.

Axonal presynaptic terminals converge onto dendritic specialisations of a postsynaptic neuron with built-in membrane receptors for neurotransmitter binding. Such molecular interactions evoke electrical and biochemical changes in the postsynaptic cell and further propagation of the transmitted signal. The nature of such a signal can be dual: excitatory or inhibitory depending on the identity of the neurotransmitter. In the mammalian brain, the most abundant form of excitatory neurotransmission is mediated by glutamate.

a) Morphology of dendritic spines

Dendritic spines present a great variability in size and shape ***(Fig. 12)***. Importantly, the morphology, distribution and density often reflect on functional properties of spines. At first, dendritic spines were considered an artefact caused by silver staining precipitation. However, their reoccurrence made Ramón y Cajal (1888) believe that these protuberances occur as natural structures (Garcia-Lopez et al., 2007). Spines are present at an average density of 1-10 spines per 10 µm of dendritic length, reaching up to thousands of spines on a single pyramidal neuron. They come in different lengths varying from 0.2 to 2 µm and volumes from 0.001 to 1 μm^3. Typical spines consist of three basic compartments: (1) a delta-shaped junction connecting the spine to the dendritic shaft, (2) a constricted neck, and (3) a bulbous head contacting the axonal bouton (Hotulainen and Hoogenraad, 2010). Generally, these typically-shaped large spines called *mushroom spines* represent ~10% of all spines in DG of an adult rat. On the other hand, *thin spines* without a bulbous head make up the majority of ~75%. *Stubby spines* lack an obvious spine neck and account for ~10%. Finally, *spines located on dendritic shafts* without a visible dendritic protrusion represent ~5% ***(Fig. 12)***. Notably, *filopodia* are considered the immature precedent stage of mature dendritic spines. The most complex set of spine shapes (thorny excrescences), present all the above-mentioned spine types and are found in the CA3 region where giant

Figure 12.

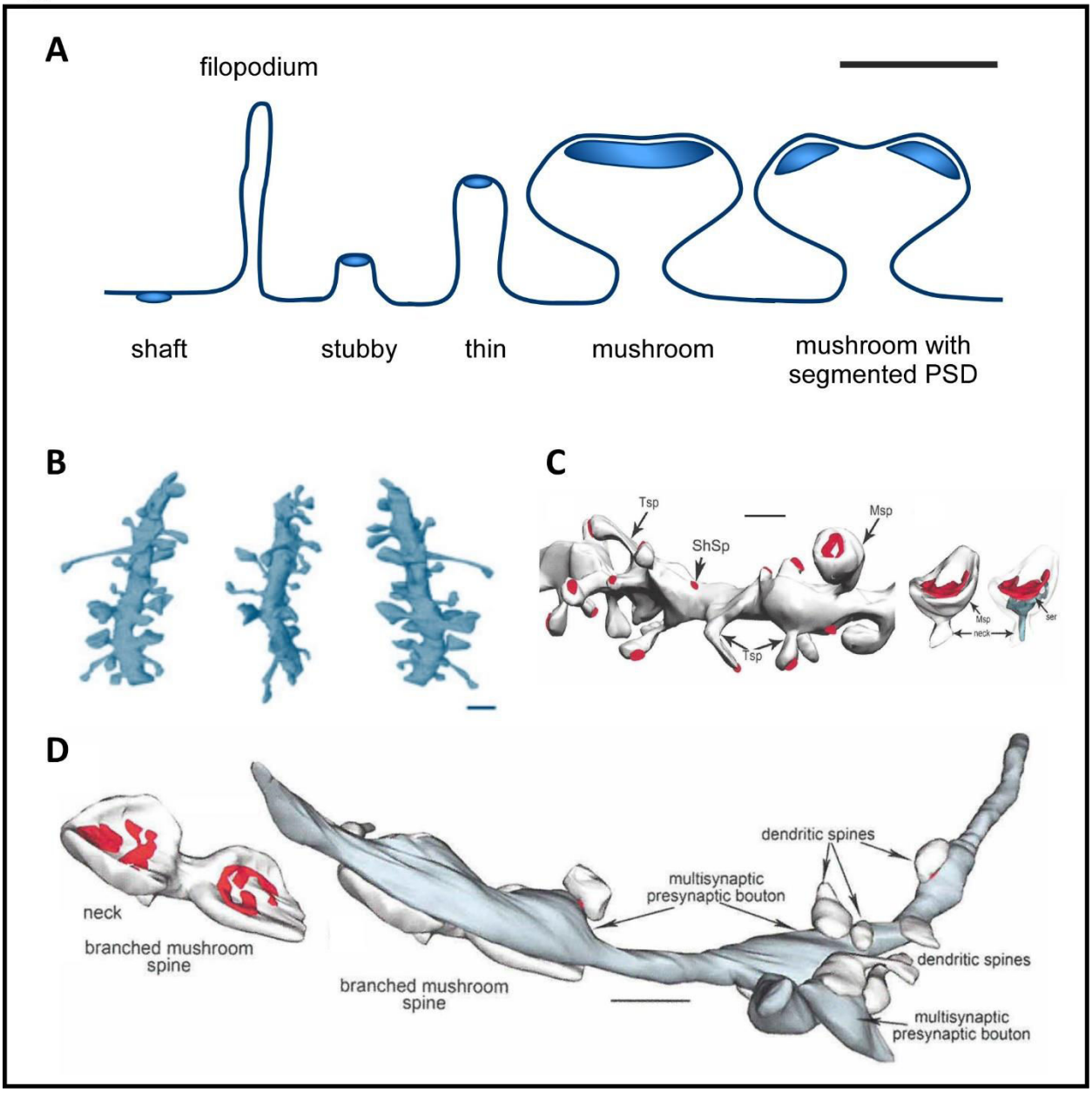

Figure 12. **Dendritic spine morphology**. **A.** A schematic of spine shape categories. Approximate scale bar = 1 µm. Adapted from (Pickel and Segal, 2014). **B.** Three views of a 3D reconstruction of a section of a CA1 dendrite from the stratum radiatum, illustrating the density of dendritic spines and their diverse shapes. Source: The Hippocampus Book (Andersen et al., 2007). **C.** 3D reconstruction of a dendrite segment from the rat dentate gyrus showing thin spines (Tsp), a shaft spine (ShSp) and mushroom spines (MSp). In red are postsynaptic densities. On the right, smooth ER (ser) is depicted with in an MSp. **D.** Left, a branched mushroom spine reconstruction with PSDs. Right, axonal segment (light blue) converging onto spines including the branched spine depicted on the left. Adapted from (Pickel and Segal, 2014). Scale bars = 1 µm.

boutons of mossy fibres from the dentate gyrus synapse with CA3 pyramidal neurons. The spine shape is not a fixed feature as it is subjected to an activity-dependent remodelling. For instance,

LTP enlarges the spine head (Park et al., 2006), which is correlated with an increase in synaptic AMPAR (Watson et al., 2017); whereas LTD reduces it (Zhou et al., 2004). Destabilisation of spines can eventually lead to their complete disappearance usually through the stubby stage (Alvarez and Sabatini, 2007). Importantly, dendritic spine dynamics lead to weakening or strengthening of synaptic connections and are thus widely believed to underpin learning and memory in the brain (Jedlicka et al., 2008) (Matsuzaki et al., 2004).

b) Dendritic and spinal cytoskeleton

Three major cytoskeletal components are present in neuronal arborisations (axons and dendrites): microfilaments (actin filaments, 7 nm), intermediate filaments (keratin family of proteins, 8-15 nm) and microtubules (α- and β-tubulin, 25 nm with 15 nm lumen). Microtubules constitute the major cytoskeletal component of dendrites, whereas dendritic spines contain mainly actin microfilaments ***(Fig. 13)***. However, over the past years, actin was shown to participate in dendritic growth and microtubules were reported to invade spines (Hoogenraad and Bradke, 2009). The particular dendritic arborisation is a function of development in response to specific cues that eventually results in formation of functional synapses. *In vivo* imaging showed that dendritic development is a multistage process that begins shortly after axon specification. First, dendrites undergo initial elongation without branching. Then, dendrites begin to form branches to fill in their dendritic fields and connect with axons. Finally, before establishing a mature interconnected neuronal network, a large proportion of synaptic connections undergo pruning (Kreutz and Sala, 2012). This elimination process is a normal stage of brain development in both vertebrates and invertebrates. In mammals, soon after birth, as much as 50% of neurons undergo apoptosis and extensive pruning. Another peak of synapse elimination can be seen slightly later in the maturing brain (adolescent stage) (Semple et al., 2013). All these dynamic processes precede the establishment of a fully mature brain where dendritic and axonal trees become stable and plasticity occurs rather rarely in basal conditions.

The actin cytoskeleton in dendritic arborisation and spines

Spines are actin-rich structures (see ***Fig. 13***). The actin cytoskeleton is indispensable for spine morphogenesis, hence synaptic signalling. β- and γ-actin are major isoforms highly prevalent in neurons. Actin is found as soluble monomeric G-actin and polar filaments of polymerized F-actin. The ratio G/F-actin is thought to be responsible for spine plasticity (Kreutz and Sala, 2012). Previous research has shown that synaptic stimulation rapidly changes the equilibrium between G-actin and F-actin. The expression of LTP shifts the G/F-actin ratio toward F-actin (increase in F-actin filaments) and enlarges spines, whereas LTD induction shifts the ratio toward G-actin (decrease in F-actin filaments) and causes spines to shrink (Okamoto et al., 2004). There are a few striking differences between actin filaments in dendritic spines versus in conventional filopodia of other cell types or even neuronal growth cones. First, in all other known filopodia, the actin cytoskeleton is composed of unidirectional actin, whereas spines are composed of actin filaments with two ends, one growing more rapidly (barbed end) than the other (pointed end), which results in the treadmilling of actin subunits from the barbed end to the pointed end. Second, actin forms a mix of both branched and unbranched filaments found throughout all compartments of the spine, while conventional filopodia are built of linear parallel actin bundles. Third, the associated molecular nucleators differ. In ordinary filopodia, actin filaments are assembled by linear actin nucleators such as formins. On the contrary, the principal nucleator of actin branching and remodelling within dendritic spines is the actin-related proteins 2 and 3 (Arp2/3) complex (Racz and Weinberg, 2008) (Wegner et al., 2008). Actin polymerization and remodelling is controlled by a large set of regulatory molecules that respond to synaptic activity and are downstream of synaptic receptors including the Arp2/3 complex and its activators. For instance, cortactin is an actin nucleation-promoting factor that recruits and localizes Arp2/3 into spines. Shank proteins were recently shown to bind cortactin and this interaction stabilized actin cytoskeleton in spines (MacGillavry et al., 2016). WAVE-1 (WASP-family verprolin homology protein-1), another crucial Arp2/3 activator, serves as a signal transducer through Rho GTPase Rac-1. Genetic disruption of Arp2/3 or its activators revealed important roles in the regulation of morphology and number of spines (Hotulainen and Hoogenraad, 2010). Actin polymerization is further helped by profilin proteins. Upon stimulation, profilins translocate to dendritic spines.

Figure 13.

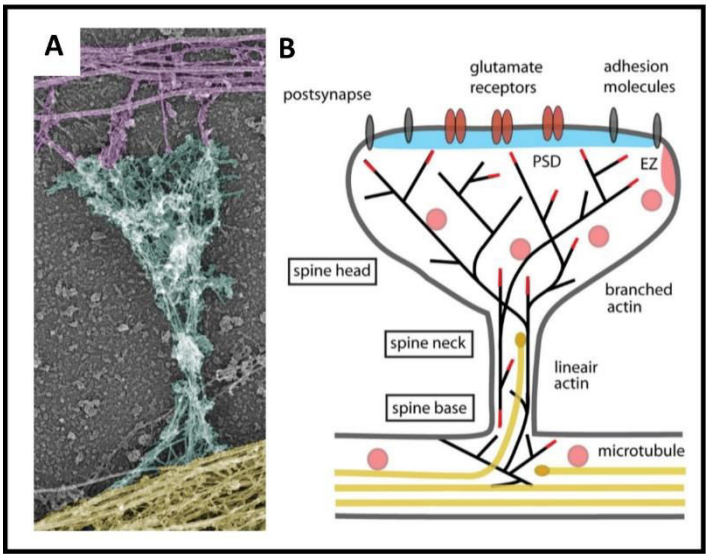

Figure 13: **Cytoskeletal organization of dendritic spines**. **A.** Actin and microtubule cytoskeleton organization in a mature dendritic spine from cultured hippocampal neurons visualized by electron microscopy (EM). Axonal cytoskeleton (purple), dendritic shaft (yellow), dendritic spine (cyan). The spine head typically contains a dense network of short crosslinked branched actin filaments, whereas the spine neck contains loosely arranged actin filaments, both branched and linear. Some branched filaments are at the base of spines and frequently reside directly on microtubules in the dendritic shaft. Image courtesy of Drs. Farida Korobova and Tatyana Svitkina (University of Pennsylvania, Philadelphia, PA). **B.** A schematic of a mushroom spine showing the postsynaptic density (in blue) with adhesion molecules and glutamate receptors. Actin filaments are represented in black lines (barbed ends in red), microtubules cytoskeleton in yellow. The endocytic zone (EZ) is located lateral to the PSD in extrasynaptic regions of the spine. Recycling endosomes (pink) localise in the shaft and spines. A small fraction of microtubules in mature dendrites are dynamic and transiently enter dendritic spines. The microtubule plus-ends are symbolized as yellow ovals. Images were taken from (Hotulainen and Hoogenraad, 2010).

Profilins change actin-associated ADP nucleotide to ATP and promote barbed-end polymerization (Pollard et al., 2000). Preventing profilin targeting destabilizes dendritic spines (Ackermann and Matus, 2003). Myosins are large (~520 kDa; two ~220 kDa heavy chains and two paris of light chains of variable size) actin-anchored mechanoenzymes that hydrolyze ATP to produce movement and force. Three classes of myosins are found within dendrites and dendritic spines (Kneussel and Wagner, 2013). Class II non-muscle myosins localise to the spine neck and proximal spine head and co-fractionate with PSD. Their function has been established in the regulation of spine morphology and dynamics in cultured hippocampal neurons (Kneussel and Wagner, 2013). Myosin IIb is required for spine maturation resulting in mushroom-shaped spines upon NMDAR activation (Hodges et al., 2011). Local blebbistatin (myosin II ATPase blocker) application causes depression of AMPAR-mediated excitatory currents in CA1 neurons. Indeed, the insights into the

myosin IIb-mediated LTP have been provided and published in the study of Rex and colleagues (Rex et al., 2010). Similarly, the myosin V class is found within the PSD and has been involved in LTP induction (Wang et al., 2008). Upon LTP, myosin Vb associates with GluA1-containing recycling endosomes and drives their delivery into spines which is followed by membrane fusion and AMPAR membrane incorporation resulting in spine surface growth (Wang et al., 2008). On the other hand, myosin Va is a transporter of endoplasmic reticulum (ER) into spines, a step required for LTD induction. Rodents with *myo5a* mutations lack the smooth endoplasmic reticulum (ER) that is normally present in spines of Purkinje neurons (Wagner et al., 2011). Moreover, these neurons fail to respond to LTD, which depends upon the mGluR1-induced calcium release from ER in spines, and disrupts the parallel fibre-Purkinje cell communication (Wagner et al., 2011) (Miyata et al., 2000). The third class of synaptic myosins are myosins VI. Myosin VI was reported to directly regulate AMPAR trafficking to the postsynapse (Nash et al., 2010). The loss of myosin VI in mice decreases spin number and length in the CA1 region (Osterweil et al., 2005). There are many actin-associated proteins that have been identified to play important role in structural spine plasticity and extensive research still continues (Hayashi et al., 2002a) (Kreutz and Sala, 2012).

The role of microtubules in dendritic arborisation and spines

Alike in axons, dendritic microtubules (MTs) are composed of α- and β-tubulin heterodimers that connect in a head-to-tail fashion forming tubule-like structures with a hollow lumen (Gu and Zheng, 2009) (Pickel and Segal, 2014). In dendrites of mammalian neurons, however, the MT orientation is of a mixed polarity with both distally and proximally oriented plus and minus ends (Yau et al., 2016). This is very important, because the molecular motors dynein and kinesin are capable of bidirectional transport of cargoes. Several MT-associated proteins have been identified to regulate MT dynamics and dendritic transport and hence dendritic development. These include MAPs (microtubule-associated proteins), MT plus-end tracking proteins (+TIP), MT polymerizing and severing proteins and tubulin regulating proteins (Poulain and Sobel, 2010). The well-studied MAP2 protein is a substrate for different kinases and its phosphorylation state has been shown to impact on dendritic arborisation (Diez-Guerra and Avila, 1993). As an example,

the *c-jun* N-terminal kinase 1 (JNK1) phosphorylation of MAP2 promotes dendritic elongation (Bjorkblom et al., 2005). On the other hand, loss of JNK1 leads to MAP2 dephosphorylation causing dendritic shortening with a high level of branching as shown in cerebellar granule neurons (Podkowa et al., 2010).

Whether MTs are present in dendritic spines has been a controversial topic, however, evidence suggests that transient occurrence of MTs in spines indeed takes place ***(Fig. 13)***. For instance, neuronal depolarization was shown to trigger MT polymerization and invasion into spines (Hu et al., 2008). This activity-dependent MT spine entry is most likely regulated by synaptic NMDA receptors (Merriam et al., 2011), whereas stimulation of both synaptic and extrasynaptic NMDARs suppresses dendritic MT dynamics and MT entry into spines (Kapitein et al., 2011). Furthermore, the MT invasion into spines was reported to be associated with both spine enlargement (Merriam et al., 2011) and increased PSD-95 content (Hu et al., 2011). Interestingly, it was suggested that MT spine entry could directly regulate the transport of molecular cargoes to and from spines (Schapitz et al., 2010). The most recent piece of data indicates that the MT entry occurs at the specific sites of the spine base in response to synapse-specific calcium transients and is further dependent on F-actin and MT-associated protein drebrin (Merriam et al., 2013). It should be, however, taken into consideration that in the abovementioned studies the presence of MT in spines was detected using solely the MT-associated protein, the +TIP protein EB3. Thus, it would be of interest to the broad neuroscientific community to confirm these findings using additional MT markers and trackers.

As mentioned previously, excitatory synapses are principally formed on dendritic spines, whereas inhibitory neurotransmission occurs generally on dendritic shafts, cell bodies and axon initial segments. Not only the localisation of axonal innervation can help predict the type of neurotransmission but more importantly the molecular composition of the postsynapse. Excitatory synapses are characterised by the presence of the postsynaptic density (PSD), an electron-dense region, formed by protein complexes that adhere to the postsynaptic membrane. On the other hand, inhibitory synapses do not possess a clear PSD because the molecular

composition of an inhibitory postsynapse is much more simplified and less enriched in proteins (Pickel and Segal, 2014) (Sheng and Kim, 2011).

c) Components of the PSD

The PSD is essentially a disc-like proteinaceous organelle localised to the tip of a dendritic spine and held together by a myriad of adhesion molecules, membrane receptors, scaffolds, cytoskeleton elements and a host of other signalling molecules. An average PSD has 360 nm in diameter and contains a total molecular mass of 1.1 +/- 0.4 gigadaltons which can be imagined as 10,000 proteins of 100 kDa (Chen et al., 2005). Notably, the PSD protein composition is modifiable by neuronal activity to allow for weakening or strengthening of synaptic connections. Owing to the PSD importance in synaptic transmission, the composition of the PSD has been extensively analysed since 1970s when the first experiments of synaptosomes gradient purification and detergent-based PSD isolation were performed (Davis and Bloom, 1973) (Sheng and Kim, 2011). Later, electron microscopy imaging revealed the prominent membrane thickening of the PSD (Siekevitz, 1985). Mass spectrometry and immunoprecipitation analyses have yielded a common set of ~300 PSD proteins (Collins et al., 2006) (Dosemeci et al., 2007). In an average size glutamatergic PSD, calcium-calmodulin dependent kinases CaMKIIα and CaMKIIβ are the most abundant proteins with ~4800 and ~800 copies, respectively. Additionally, about 400 copies of the PSD-95 family (~300 copies of PSD-95 only) and ~360 copies of SynGAP (synapse specific Ras/Rap GTPase activating protein) are present. Interestingly, only ~15-20 copies of NMDA and AMPA receptors, that mediate the majority of excitatory neurotransmission in the brain, are contained within the PSD (Sheng and Kim, 2011).

PSD-95 is the best studied PSD scaffold protein since its identification in early 1990s. Some of this attention can be attributed to the genetic polymorphisms that were found to cosegregate with mental disease (Feyder et al., 2010). The PSD-95 subfamily belongs to the membrane-associated guanylate kinase (MAGUK) family characterized by the presence of at least one PDZ domain that plays important roles in anchoring and stabilising membrane proteins. The PSD-95 group of proteins is formed by four distinct genes encoding PSD-95 (SAP90, synapse-associated

protein 90), PSD-93, SAP102 and SAP97. All members have three PDZ domains, one SH3 (SRC homology) domain and one GK (guanylate kinase) domain. PSD-95 localises close to the postsynaptic membrane ~12 nm, a distance that correlates with the finding that PSD-95 directly interacts with the C-terminal of GluN2 subunit of NMDAR, which stabilizes NMDAR at the membrane (Prybylowski et al., 2005). In addition, PSD-95 also binds to AMPARs. The PSD-95-mediated receptor recruitment to the membrane is crucial for functional coupling of these receptors with downstream signalling players in the PSD.

As recently shown, decreased levels of the PSD-95 group of proteins result in smaller PSDs and significant reduction of synaptic transmission by AMPARs and NMDARs in cultured rat hippocampal neurons (Chen et al., 2015). In regard to synaptic plasticity events, some discrepancies still need to be addressed to clarify whether PSD-95 actively participates in the expression of long term potentiation (LTP). Interesting, however, is the finding that synaptic potentiation induced by overexpression of PSD-95 is able to convert silent synapses into functional synapses (Ehrlich and Malinow, 2004). In contrast, consistent data suggest that PSD-95 is functionally involved in long term depression (LTD). This form of plasticity is impaired by RNAi knockdown or genetic disruption of PSD-95 in mice, while enhanced upon PSD-95 overexpression (Ehrlich et al., 2007) (Sheng and Kim, 2011). In general, the activity-dependent redistribution of synaptic PSD-95 is associated with increase or loss of AMPARs and changes in glutamate-receptor-induced signal transduction including CREB (cAMP-response element binding protein), and MAPK (mitogen-activated protein kinase), both of which are the mediators of synaptic plasticity.

Shank1-3, other members of the PSD protein assembly, are large proteins of ~200 kDa that are involved in dendritic spine growth and synaptic transmission. Mutations within genes coding for Shank proteins have been described in several forms of intellectual disability, which reflects the functional importance of these proteins (Bonaglia et al., 2001). Shanks do not only localize directly underneath the postsynaptic membrane but they extend up to 120 nm deep in the PSD. Shank proteins molecularly bridge two types of glutamatergic receptors: NMDAR and group I

Figure 14.

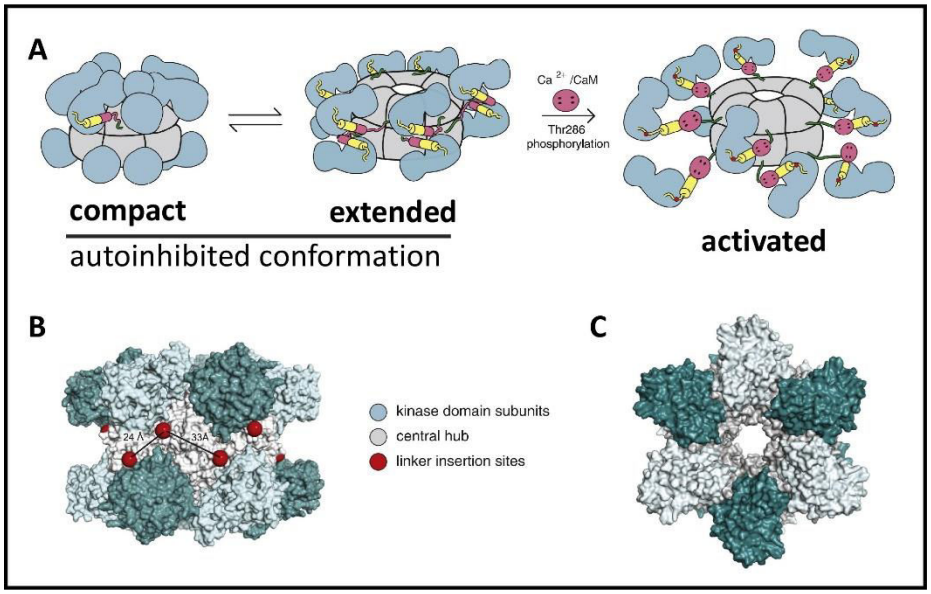

Figure 14. **Structure of CaMKII**. **A.** Schematic of a structural model of CaMKII dodecamer. According to the model, the CaMKII dodecamer exists in three conformations: (1) a closed inhibited/inactive conformation with the linker folded into the association domain, rendering it inaccessible for Ca^{2+}/CaM binding; (2) an extended inactive conformation with the linker extended outward; and (3) a fully extended active conformation with Ca^{2+}/CaM bound to the regulatory segment. Light blue segments represent the catalytic domains. **B and C**. Crystal structure model of the CaMKII dodecamer in its closed conformation. Side (B) and top (C) views. Taken from (Hell, 2014).

metabotropic GluRs. They further interact with GKAP (guanylate kinase associated protein), another highly abundant scaffold (Sheng and Kim, 2011). The Homer family (Homer 1-3) of scaffold/adaptor proteins are thought to act synergistically with Shank and regulate the localization and activity of target proteins such as the Group I mGluRs (Shiraishi-Yamaguchi and Furuichi, 2007). Beside scaffold proteins, additional signalling molecules are integral components of the PSD. These are: CaMKII (calcium/calmodulin-dependent protein kinase II), small GTPases (Ras, Rap, Rac, Rho, Ran and Arf), and their regulators GEFs (guanine exchange factors) and GAPs (GTPase-activating proteins).

CaMKII is a serine/threonine protein kinase and the most abundant synaptic protein that accounts for ~1-2% of total brain protein (reviewed in (Hell, 2014)). CaMKII is a holoenzyme formed by 12 catalytic kinase subunits (dodecamer) that prior to activation are in an autoinhibited conformation ***(Fig. 14)***. CaMKII is activated by binding of calcium ions, that influx through NMDARs, and calmodulin (CaM). This causes CaMKII relocation from the spine cytosol

to the PSD within less than 2 min (Otmakhov et al., 2004). Upon Ca^{2+}/CaM biding, CaMKII can be autophosphoryled at T286, which leads to a persistent kinase activity beyond the Ca^{2+}/CaM detachment (Coultrap et al., 2010). CaMKIIα and CaMKIIβ, encoded by CAMK2A and CAMK2B genes, respectively, are the two most prevalent isoforms in the brain. In basal state, there is twice as much CaMKII in dendritic spines than in the shaft. The diffusion exchange of CaMKII between spine and shaft lasts approximately 1-5 min (<1s for free GFP; (Loriol et al., 2014)) with respect to 15% of CaMKII that remains immobile in spines after 30 min in unstimulated conditions. Protein-protein interactions play a critical role in retention of CaMKII in spines. α-actinin supports CaMKII binding to F-actin filaments. Upon Ca^{2+}/CaM binding CaMKII interaction with α-actinin is disrupted which allows for CaMKII redistribution toward PSD (Robison et al., 2005) (Hell, 2014). CaMKII and F-actin interactions in spines are mutually important: F-actin anchors CaMKII and CaMKII stabilizes and bundles F-actin, which regulates spine size (Lin and Redmond, 2008). This kinase can be also anchored to the PSD by association with L-type Ca^{2+} channels that are required for CaMKII-dependent phosphorylation and activation of CREB (Wheeler et al., 2012). Moreover, a direct association of activated CaMKII with GluN2B subunit of NMDAR is essential for CaMKII recruitment to PSD (Halt et al., 2012). CaMKII binding to GluN2B is also a prerequisite for CaMKII-dependent phosphorylation of the GluA1 subunit of AMPAR that results in an increase of AMPAR conductivity during LTP (Kristensen et al., 2011). Although the exact mechanisms are yet to be discovered, one of the most intriguing outcome of CaMKII activation is an increased incorporation of AMPAR into the postsynaptic membrane followed by the expression of LTP (Bosch et al., 2014). It is for this reason that CaMKII is considered the central regulator of synaptic plasticity underlying learning and memory.

Importantly, upon synaptic activation CaMKII was also found to shape the synaptic content by controlling protein turnover through the recruitment proteasomes in dendritic spines (Bingol et al., 2010). Ca^{2+} influx via NMDARs augments CaMKII accumulation in stimulated spines just before proteasome accumulation. The ability of CaMKII to recruit proteasomes depends on its activation by Ca^{2+}/CaM, autophosphorylation on T286, and binding to GluN2B (Hamilton et al., 2012). The particular way of CaMKII activation and binding to its docking site on GluN2B and to proteasome, assures that proteasome accumulation mainly occurs in activated spines. These

findings indicate that CaMKII can play a structural role by functioning as an activity-dependent, autoregulated postsynaptic proteasome scaffold. Regulation of synaptic protein repertoire is an important mechanism not only for LTP but also for activity-induced formation (Hamilton et al., 2012) and stabilization (Hill and Zito, 2013) of new spines.

Small GTPases are a type of G-proteins that function as molecular switches driving the Mg^{2+}-dependent hydrolysis of active state GTP (guanosine triphosphate) into inactive GDP (guanosine diphosphate). It is for this reason that small GTPases are involved in many synaptic signal transduction pathways. At the postsynapse, these enzymes were reported to regulate synaptic structure and function, and consequently they have been associated with various brain diseases. Ras family of small GTPases regulates the CaMKII and NMDAR-dependent synaptic delivery of AMPAR during LTP. On the contrary, Rap mediates synaptic removal of AMPAR upon LTD (Zhu et al., 2002). Rho GTPases direct the actin dynamics in the formation and remodelling of spines (Ba et al., 2013). GAPs (GTPase-activating proteins) and GEFs (guanine nucleotide exchange factors) catalyse the activation of small GTPases and are as well crucially implicated in the regulation of synaptic structure and function (Duman et al., 2015). SynGAP is highly enriched at excitatory synapses. *De novo* mutations resulting in dysfunctional SynGAP are associated with autism spectrum disorders that are characterised by impaired excitatory synaptic function. This is most likely due to the imbalance excitation-inhibition as genetic deletion of SynGAP increases excitatory synaptic strength. Importantly, NMDAR and CaMKII act as upstream regulators of SynGAP (Wang et al., 2013).

1.3 The mechanisms of glutamatergic neurotransmission

Glutamate, one the non-essential amino acids, is the major excitatory neurotransmitter in vertebrates. I would like to pinpoint, however, that glutamate is also an important metabolic molecule in the brain. The blood-brain barrier (BBB) prevents dietary and stored lipids from reaching the brain. Unlike other organs, the brain's mass is limited by the cranial bones, and only a limited amount of glucose is stored in the form of glycogen and no adipose tissue is present in

the brain as a backup source of energy. This leaves the brain dependent on blood-circulating glucose directly from food or the energy supplier - the liver (providing glucose through glycogenolysis and gluconeogenesis). Over the past two decades, the role of glutamate as an energy-providing biomolecule in the brain has been scientifically supported. Karaca *et al.* provided evidence that glutamate is an essential energy-providing substrate of astrocytic glutamate dehydrogenase (GDH). Preventing glutamate oxidation by GDH increases the ADT/ATP ratio and promotes hepatic glucose production (Karaca et al., 2015). In general, the metabolic production of glutamate happens as follows: Glucose crosses the BBB and reaches neuronal cells either directly or via endothelial and astrocytic cells (through plasma membrane glucose transporters [GLUT]). Glucose then undergoes cytosolic glycolytic break down resulting in the production of pyruvate, which enters the tricarboxylic acid cycle (TCA). One of the TCA products is α-ketoglutarate, a GDH substrate generating glutamate (*de novo* production of glutamate). Glutamate can be further converted into glutamine by glutamine synthetase (astrocyte- and oligodendrocyte-specific enzyme) or γ-amino butyric acid (GABA) by glutamate decarboxylase (restricted to GABAergic neurons). Both astrocytes and neurons contain glutamine transporters and so glutamine can be taken up by neurons and converted by the mitochondrial glutaminase to glutamate.

Apart from being a bioenergetic substrate, glutamate functions as a major excitatory neurotransmitter that is highly present throughout the brain and spinal cord. The extremely high concentrations of glutamate in the brain tissue are tightly regulated to prevent excitotoxicity. The extracellular glutamate that is released by synaptic vesicles must be rapidly cleared up in the scale of a millisecond. Some of the synaptic cleft glutamate is endocytosed and recycled by neurons and the rest is taken up by astrocytes through the excitatory amino acid transporters (EAATs) primarily localised on synaptic astrocytic processes (Niciu et al., 2012).

❖ Glutamate receptors

The typical glutamatergic neurotransmission occurs between axonal terminals and dendritic spines (axo-dendritic/spinous transmission). Released glutamate activates a family of glutamatergic receptors consisting of ionotropic glutamate receptors (iGluRs) and metabotropic

glutamate receptors (mGluRs). iGluRs are membrane-embedded tetrameric complexes that upon glutamate binding function as cation channels for Na^+, K^+ and some also pass Ca^{2+}. On the contrary, mGluRs have seven transmembrane domains and signal through coupled G-proteins and second messenger systems.

A. Ionotropic glutamate receptors

iGluR are assembled in the endoplasmic reticulum as tetramers, often dimers of dimers (reviewed in (Karakas et al., 2015) (Pickel and Segal, 2014)). As shown in ***Figure 15***, each subunit has two ligand-binding domains (S1 and S2) that are necessary for glutamate binding, three transmembrane domains (M1, M3 and M4), and an ion pore-lining region (M2). Interestingly, RNA editing of glutamine to arginine makes the channel impermeable to Ca^{2+}. Three major classes of iGluR have been identified based on a specific molecule selectivity (reviewed in (Niciu et al., 2012) (Pickel and Segal, 2014)): N-methyl-D-aspartate receptors (NMDARs), α-animo-3-hydroxy-5-methyl-4-isoxazole propionic acid receptors (AMPARs) and kainate receptors (KARs). Three families of NMDARs have been identified: GluN1, GluN2 and GluN3. Four different genes encode the subunits of AMPAR: GluA1 – GluA4; and five subtypes of KARs are known to date: GluK1 – GluK5.

Figure 15.

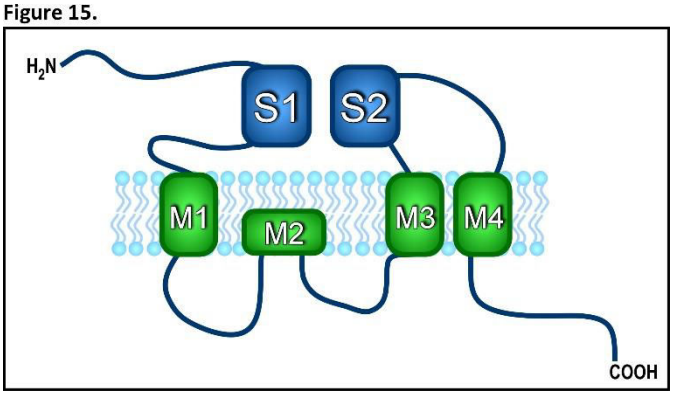

Figure 15. **Subunit composition of ionotropic glutamate receptor**. Each subunit of ionotropic glutamate receptors (NMDA, AMPA and kainate receptors) is composed of three transmembrane domains (M1, 3 and 4) and one re-entrant loop (M2). Moreover, glutamate binding is localised in a pocket that is formed by two extracellular domains (S1 and S2). S1 is present in the N-terminal loop and S2 is found between M3 and M4. The C-terminus varies in length depending on the subunit specificity. Adapted from (Sanz-Clemente et al., 2013).

a) NMDA receptors

NMDARs possess the highest affinity for glutamate (EC_{50}: 1 µM). NMDARs display a broad functional diversity. They differ in subunit composition, biophysical and pharmacological properties, their interacting partners as well as subcellular localisations (reviewed in (Vyklicky et al., 2014)). Moreover, the NDMAR subunit expression differs throughout the development and also in mature brain ***(Fig. 16B)***. Seven distinct subunits belonging to three NMDAR families have been identified: one GluN1 subunit, four GluN2 subunits (GluN2A-D) encoded by four distinct genes, and two separate genes coding for GluN3A and GluN3B subunits. All NMDARs contain an obligatory GluN1 homodimer coupled with a homodimer or heterodimer constituting of other GluN2/3 subunits ***(Fig. 16A)***. The ubiquitously-expressed GluN1 subunits are present throughout the brain from the embryonic day 14 (E14). GluN1 knock-out mice die shortly after birth of respiratory failure suggesting that the GluA1 subunits are indispensable for neurodevelopment (Tsien et al., 1996). In addition, the CA1-restricted GluN1 knock-out mice show defects in synaptic plasticity and spatial learning (Tonegawa et al., 1996). Although there is only one gene encoding the GluN1 subunit, the NMDAR composition gets more complex as the product of the GluN1 gene can be alternatively spliced into eight distinct isoforms (GluN1-1a-4a and GluN1-1b-4b).

NMDARs have some unique properties that distinguish them from other iGluRs. Firstly, they require a co-agonist activation. Several binding co-agonist sites have been identified to regulate the channel opening (two obligatory co-ligands: glutamate and glycine or D-serine; polyamines and cations such as Mg^{2+}, Zn^{2+} and H^{+}). Secondly, NMDAR channels are permeable for Ca^{2+} ions. And thirdly, they show slow deactivation kinetics owing to slow glutamate unbinding. Apart from glutamate, NMDARs bind other known ligands. These are the short-chain dicarboxylic amino acids (NMDA, aspartate, …). Interestingly, the open-NMDAR binds Mg^{2+} to prevent cation flux, while Zn^{2+}, although also divalent, does not have such an effect. GluN2 binds glutamate and several competitive antagonists such as D-AP5, while the GluN1 subunit binds glycine (Niciu et al., 2012) (Paoletti et al., 2013).

Figure 16.

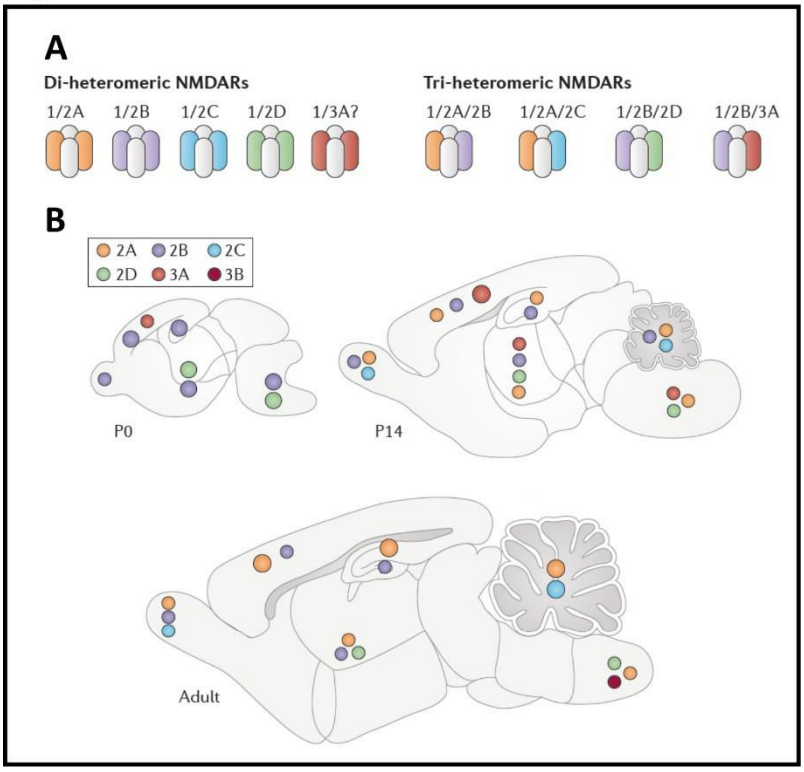

Figure 16. **NMDAR subunit diversity and expression pattern**. **A**. Various populations of NMDARs that are thought to exist in the CNS. **B**. The expression profile of different NMDAR subunits throughout the mouse brain development. Taken from (Paoletti et al., 2013).

The intracellular cytosolic domains of NMDARs are the least conserved regions, thus they provide subunit-specific functions involved in receptor trafficking, localisation and downstream signalling. They directly interact with PDZ domain-containing proteins of the PSD e.g. the MAGUK family. Such an interaction can stabilize NMDARs in the postsynapse, like in the case of GluN2B subunit (Prybylowski et al., 2005). Phosphorylation (for instance by cyclin-dependent kinase 5, protein kinase A and C and SRC tyrosine kinase) of the PDZ-binding motif in NMDAR subunits also accounts for the mobility and membrane stability of the receptor subunits (Paoletti et al., 2013). Importantly, CaMKII interacts more strongly with GluN2B and this interaction has major implications in the regulation of AMPAR synaptic content, expression of synaptic plasticity and synapse maturation (Wang et al., 2011) (Gambrill and Barria, 2011).

In cultured neurons, GluN2A synaptic delivery requires synaptic activity, whereas GluN2B does not (Barria and Malinow, 2002). GluN2B was additionally reported to undergo synaptic

clearance upon phosphorylation of the PDZ-binding domain by casein kinase 2 (CK2) (Sanz-Clemente et al., 2010). This finding indicates that alterations in synaptic activity control the synaptic NMDAR subunit content.

Although AMPARs are considered the prototypic receptor mediators of synaptic plasticity, NMDARs are also dynamically regulated in response to LTP and LTD events. Some important discoveries have been made in regard to NMDAR involvement in LTP and LTD (reviewed in (Luscher and Malenka, 2012)). NMDA-mediated LTP (LTP_{NMDA}) requires stronger induction and develops slower, which is in line with slower mobility of NMDARs. A rise of postsynaptic Ca^{2+} precedes LTP_{NMDA} and can happen without changes in AMPAR-mediated transmission. An increase in synaptic content of certain subunits of NMDAR (shown for GluN2D and GluN2A) has been detected. Under particular stimulation protocols LTD_{NMDA} occurs without the accompanying LTD_{AMPA}. LTD-mediated dynamin-dependent internalisation of NMDARs has been shown in CA1-CA3 and CA3-CA3 synapses. The precise mechanisms of NMDAR-mediated synaptic plasticity events remain to be addressed. In the context of AMPAR-mediated LTP/LTD, NMDAR provide an indispensable source of Ca^{2+}. Some hypothesize that the composition of NMDARs could dictate whether LTP_{AMPA} or LTD_{AMPA} is expressed. The GluN2A plays a crucial role in LTP_{AMPA} as mice lacking GluN2A show reduced LTP at CA3-CA1 synapses, and a complete loss of LTP in the *superior colliculus* (optic tectum) and cerebellar granule cells (Zhao and Constantine-Paton, 2007) (Andreescu et al., 2011). On the other hand, loss of GluN2B abolishes LTD in the CA1 region. This suggests that GluN2A could be specifically implicated in LTP_{AMPA} while GluN2B in LTD_{AMPA} induction.

Owing to the importance of NMDAR in synaptic function, defects due to hypo- and hyperfunction of NMDARs have been described in numerous neurological and psychiatric illnesses. After brain injury, glutamate levels rise, which has a cytotoxic effect leading to neuronal death (Lai et al., 2011). NMDARs act as major excitotoxicity mediators and thus much effort has been put into developing NMDAR antagonists that would exhibit neuroprotective function. Unfortunately, many of these broad-spectrum molecules showed intolerable side effects, and

therefore could not be used in clinics. For this reason, the focus of the pharmacological research shifted toward developing subunit selective therapeutics. Pharmacological disruption of the interaction between GluN2B subunits has been successful in ischemic brain injury in rodents (Aarts et al., 2002), non-human primates (Cook et al., 2012) and also humans (Hill et al., 2012). In contrast, potentiating NMDAR function could be beneficial in some neuropsychiatric conditions that display attenuated NMDAR function. Schizophrenic patients show reduced NMDAR-mediated neurotransmission in GABAergic interneurons that results in imbalanced excitation and inhibition and could explain psychosis and perturbed cognitive function in these patients (Moghaddam and Javitt, 2012) (Paoletti et al., 2013). Intriguingly, the use of NMDAR antagonists in healthy humans causes schizophrenia-like symptoms and worsen the symptoms in schizophrenics. Until now, however, enhancing NMDAR activity by elevating glycine or D-serine levels has gained mixed results (Moghaddam and Javitt, 2012).

b) AMPA receptors

AMPARs are tetrameric receptors composed of combinations of four subunits GluA1 - GluA4 ***(Fig. 17)*** with the turnover from 10h to 2 days (Henley and Wilkinson, 2016). Estimates show that rodent hippocampus and cortex contain synaptic AMPARs composed mainly of GluA1-GluA2 or GluA1-GluA3 heteromers (Lu et al., 2009). GluA4 is a less abundant subunit that is tightly developmentally regulated and sparsely expressed at excitatory synapses in the adult brain (Zhu

Figure 17.

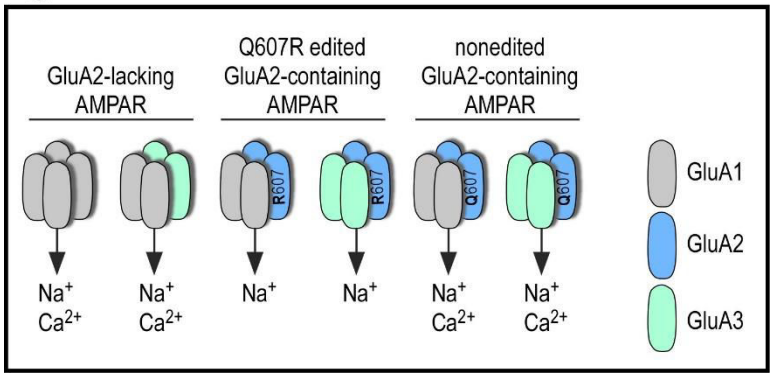

Figure 17. **Subunit composition and ion permeability of AMPAR**. RNA editing of the GluA2 subunit determines calcium permeability of AMPARs. AMPARs that lack the GluA2 subunit, or an unedited GluA2 subunit are calcium-permeable. AMPAR that contain an edited GluA2 subunit do not gate calcium. Not shown: GluA3 homomers, (calcium permeable), GluA2 homomers (calcium permeability depends on the RNA editing) and GluA4 (similar to GluA1). Adapted from (Henley and Wilkinson, 2013).

et al., 2000). AMPAR trafficking (including exo- and endocytosis) and surface diffusion have been well studied mechanisms owing to their implications in synaptic plasticity. It is widely believed that LTP is induced following these steps: 1. activity-dependent CaMKII phosphorylation of the C-terminal part of GluA1 (this subunit is indispensable for the initial stages of LTP), 2. GluA1 interaction with PDZ-containing PSD proteins, and 3. GluA1-GluA2 recruitment at the synapses. On the contrary, the GluA2 subunits-mediated endocytosis is responsible for the opposite plasticity phenomenon (LTD). However, as discussed in a review by Henley and Wilkinson (Henley and Wilkinson, 2016), this AMPAR dogma has been, in recent years, challenged by newly emerging scientific evidence. Intriguingly, some complete contradictory data emerged in a study using single-cell molecular replacement strategy in CA1 mouse neurons. According to (Granger et al., 2013) upon strong LTP induction no specific AMPAR subunits were required for the expression of LTP. Moreover, LTP could be still induced in the concomitant absence of AMPAR subunits that were replaced by KAR subunits (Granger et al., 2013). However, a reserve pool of AMPAR that is present at the synapse and presumably does not undergo the LTP-induced trafficking is mandatory, as neurons with markedly reduced AMPAR pools showed LTP impairment (Granger et al., 2013). One should, however, take into account that these experiments were performed under very intense saturating LTP protocols, which could potentially drive a non-physiological AMPAR subunit substitutions. Undeniably, even if considering the conditions of the experimental procedure, a hippocampal LTP mechanism independent of AMPA receptor subunit specificity is a significant discovery, and future research will need to disclose more details. One possible clue could derive from the PSD itself. AMPARs do not bind to PSD proteins directly but through the interaction of their auxiliary domains with the transmembrane AMPAR regulatory proteins (TARPs) (Coombs and Cull-Candy, 2009). CaMKII phosphorylation of stargazin, a TARP, increases its binding to PSD-95. Such a mechanism could possibly explain the subunit-nonspecific increase in AMPARs at the synapse driving LTP. However, there is a hitch as stargazin does not bind to KARs, and thus this model does not explain the AMPAR-KAR subunit substitution.

A new piece of evidence from the Humeau and Choquet labs shows that AMPAR membrane diffusion is mandatory for expression of LTP and hippocampal memory *in vivo* (Penn et al., 2017). They used biotin crosslinking strategy to immobilize surface AMPARs and prevent them from lateral diffusion. In normal conditions upon LTP induction, AMPARs diffuse almost freely from a surface pool toward into the postsynaptic membrane increasing their synaptic localisation hence synaptic potentiation. Preventing AMPAR surface diffusion resulted in attenuated LTP and led to defects in early phases of hippocampal-dependent fear learning in the mouse (Penn et al., 2017). This study clearly shows that manipulating AMPAR surface diffusion *in vivo* specifically affects learning but does not modify basal transmission which offers a new approach for further investigations into synaptic memory (Penn et al., 2017).

An extra level of complexity in the mechanisms of AMPAR-mediated neurotransmission is given by transcriptional editing. In the adult brain, the majority (~99%) of GluA2 are present in an alternatively edited form. This RNA editing results in a charge change (glutamine to arginine at position 607) and renders the GluA2-containing AMPARs impermeable to calcium ions. Both Ca^{2+}-permeable and -impermeable AMPA receptors harbour important functions in synaptic plasticity. LTP stimulation evokes an initial synaptic insertion of homotetrameric GluA1 AMPARs. In contrast, selective blocking of AMPARs that lack GluA2 (eliminating Ca^{2+}-impermeable AMPAR) prevents LTP expression but no effect was observed when this selective blocker was used after the establishment of LTP. This means that Ca^{2+}-impermeable AMPAR are needed for the initial LTP induction but are dispensable as they get possibly replaced by Ca^{2+}-permeable AMPAR during the maintenance of LTP (Plant et al., 2006) (Jaafari et al., 2012).

c) Kainate receptors

NMDARs and AMPARs mediate the majority of fast excitatory neurotransmission in the brain. KARs on the other hand, despite being closely homologous with AMPAR, play distinct and quite diverse roles that are correlated with their subcellular localisation and signalling pathways. Importantly, KARs are expressed at both presynaptic and postsynaptic elements (reviewed in (Lerma and Marques, 2013) (Carta et al., 2014). They occur as homo- or heterotetramers

assembled by combination of five distinct subunits (GluK1-5) resulting in receptors with different kinetics and affinities for kainate. Moreover, GluK1-3 have different C-terminal splice isoforms, and GluK1 and GluK2 are subjected to RNA editing, adding to the diversity of KARs. The GluK4 and GluK5 subunits seem not to undergo such processings. Unlike NMDARs and AMPARs, kainate receptors can in addition signal via G-proteins acting rather as metabotropic receptors. Due to these unique signalling properties they have been identified to play roles in a variety of neuronal functions. To begin, KARs are involved in synaptic transmission and modulation of neuronal network excitability. In addition, KARs have been also reported to participate in developmental maturation of the brain (Lerma and Marques, 2013). Transient kainate stimulation has been shown to change KARs surface expression. Recently, it was reported that kainate induces an increase in AMPARs at the synaptic membrane in an NMDAR-independent manner leading to changes in dendritic spine structure including enhanced growth and maturation (Petrovic et al., 2017). The pathway responsible for this spine plasticity was identified to involve postsynaptic GluK2-containg KARs and endosomal vesicle recycling (Petrovic et al., 2017).

B. Metabotropic glutamate receptors

The function of metabotropic glutamate receptors is not carried out through the cation flux as in the case of ionotropic glutamate receptors (although they do modulate the function of iGluRs). mGluRs, members of the G-protein coupled receptor family (GPCR), modify synaptic transmission and neuronal excitability via trimeric G-proteins and associated signal transduction pathways (reviewed in (Bhattacharyya, 2016) and (Kalinowska and Francesconi, 2016)). mGluRs belong to class C GPCR (including $GABA_B$ receptors, Ca^{2+} sensing receptors, pheromone receptors and taste receptors) that differs from class A by the presence of a large extracellular N-terminal domain with a ligand-binding site for glutamate. mGluRs are further subdivided into 3 functional groups according to their sequence homology, G-protein coupling and ligand selectivity: Group I (mGluR 1 and 5), Group II (mGluR 2 and 3) and Group III (mGluR 4, 6, 7 and 8) (Niswender and Conn, 2010). Group I mGluRs exert their effects in two ways: Glutamate binding leads to the activation of phospholipase C that cleaves phosphatidylinositol 4,5-bisphosphate (PIP_2). The products of this cleavage are (1) the inositol-3-phosphate (IP_3) that is involved in the release of

intracellular calcium stores and (2) diacylglycerol (DAG) that activates PKC ((Kalinowska and Francesconi, 2016), ***Fig. 18***). On the other hand, the Group II and III elicit their roles via inhibitory G-proteins (G_i) that decrease the levels of intracellular cAMP through the inhibition of the adenylyl cyclase/protein kinase A pathway.

a) Group I mGluRs

Group II and III mGluRs are involved in presynaptic inhibition via affecting both excitatory glutamatergic and inhibitory GABAergic neurotransmission. To this end, the focus of this part will be on the postsynaptic Group I mGluRs as these receptors play substantial roles in neuronal development and multiple forms of synaptic plasticity including learning and memory. In addition, Group I mGluRs have been extensively studied in the correlation with various neurological and neuropsychiatric disorders and are subject of drug discovery (see (Niswender and Conn, 2010) for a comprehensive review). Finally, Group I mGluRs have been implicated in a

Figure 18.

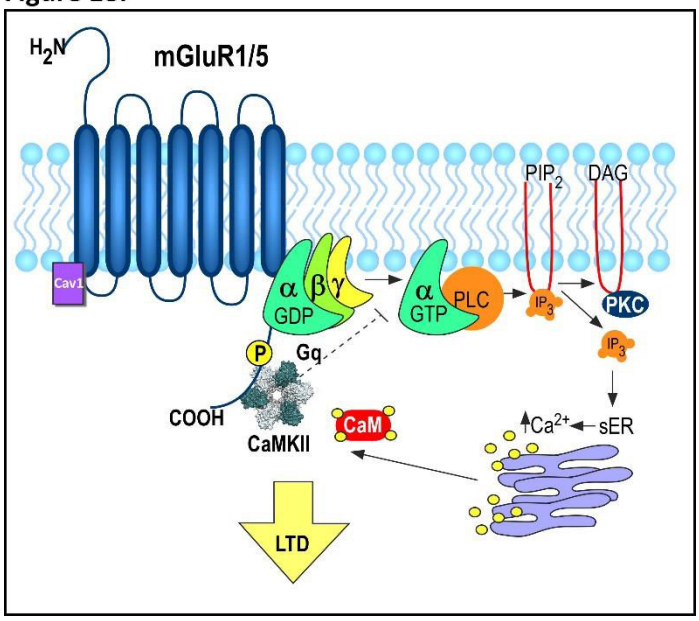

Figure 18. **Signal transduction of Group I mGluRs**. mGluR1/5 activate G_q proteins upon glutamate binding. This leads to PLC activation and hydrolysis of PIP2, which rises the intracellular levels of IP_3 and DAG. IP_3 stimulates calcium release from ER, and DAG activates PKC. A mechanism that is depicted in the scheme is the feedback loop of Group I mGluRs activation: The rise in intracellular calcium leads to CaM-dependent CaMKII activation that phosphorylates the receptor at its C-terminus resulting in receptor desensitisation and blockade of the PLC cascade (Jin et al., 2013a). This mechanism is potentially involved in LTD induction (Kalinowska and Francesconi, 2016). Calveolin-1 is an adaptor protein involved in the control of the mGluR1/5 internalisation rate.

previous study from our laboratory (Loriol et al., 2014) as well as in **my PhD project as being modulators of synaptic sumoylation** (**Annexed Article 3**).

mGluR1 is highly expressed in the hippocampus, cerebellum, olfactory bulb and the thalamus. mGluR5 is expressed in the hippocampus, cortex, striatum and olfactory bulb and at low levels in the cerebellum. Activation of mGluR1 or mGluR5 does not induce the same strength of responses, which is largely the result of a different amino acid coupling to the G-protein. Interestingly, the synaptic membrane composition also plays a role in the function of Group I mGluRs. These receptors contain a cholesterol binding motif. It has been reported that an increase in membrane cholesterol leads to an enhanced agonist-mediated activation of mGluR1, whereas a drop in membrane cholesterol content inhibits the mGluR1-dependent ERK activation (Kumari et al., 2013).

In the CNS, LTD can be triggered either via the activation of NMDA receptors or mGluRs. Group I mGluR stimulation with the selective agonist DHPG was shown to transiently induce activation of CaMKIIα in the hippocampus ***(Fig. 18)***. CaMKIIα binds to the membrane proximal segment of the C-terminal tail of mGluR1 (Jin et al., 2013a) and mGluR5 (Jin et al., 2013b). Autophosphorylated CaMKIIα binds mGluR1 with high affinity and phosphorylates the receptor at Thr871. As a result, CaMKII-dependent phosphorylation leads to a desensitization of mGlu1-dependent activation of the PLC pathways, thus providing a feedback mechanism relevant to regulation of mGluR1 activity (Jin et al., 2013a). In contrast, autophosphorylated CaMKIIα has a reduced affinity for mGluR5, whereby CaMKIIα interaction with the receptor is occluded by calmodulin competition for the same binding site (Jin et al., 2013b). At hippocampal Schaffer collateral-CA1 synapses, activation of Group I mGluRs with DHPG or by paired-pulse low frequency stimulation induces LTD (mGluR-LTD) by a mechanism that requires *de novo* protein synthesis (Huber et al., 2000). Application of CaMKII inhibitors impairs expression of mGluR-LTD, while concurrently inhibiting *de novo* protein synthesis elicited by Group I mGluRs (Mockett et al., 2011). This indicates that synaptic signalling by Group I mGluRs to CaMKII – possibly via their physical interaction – is critical for efficient expression of synaptic plasticity.

Another piece of evidence suggests that mGluR-mediated MAP kinase activation triggers the mGluR-LTD in pyramidal hippocampal neurons (Mao et al., 2005). Moreover, the scaffolding protein Homer 1, which interacts with group I mGluRs, has been shown to participate in this type of LTD (Mao et al., 2005). According to several reports, it seems that NMDAR-dependent LTD and mGluR-dependent LTD are mechanistically different but share a common mechanism involving the endocytosis of AMPARs (Luscher and Huber, 2010). Noteworthy, research suggests that the mGluR-LTD and NMDAR-LTD can coexist in the hippocampus (Huber et al., 2001). Understanding the molecular mechanisms underlying mGluR driven LTD and protein synthesis has gained much research interest since aberrant mGluR-LTD has been reported in the mouse model of Fragile X syndrome, the leading cause of intellectual disability and autism. **Importantly, our laboratory (including my participation) found that mGluR5 activation promotes sumoylation of FMRP, a protein whose mutations co-segregate with Fragile X syndrome, and that this process is crucial for proper spine density and maturation (Annexed Article 2, Khayachi *et al*., 2018).** This finding could have further implications when developing new therapeutics that target Group I mGluRs and are used for a treatment in variety of neurological disorders.

Upon G-protein unbinding, mGluRs like many GPCRs undergo desensitisation, a negative feedback to prevent chronic activation. Several strategies of desensitisation have been observed. For instance, phosphorylation and endocytosis have been identified as mechanisms involved in the desensitization of mGluRs. Phosphorylation (by CaMKII, PKC or G-protein coupled protein kinases [GRKs]) triggers binding of adaptor proteins like e.g. β-arrestin which interferes with receptor coupling to G-proteins and thus the receptor fails to generate the second messenger response despite the presence of a ligand (Krupnick and Benovic, 1998). In contrast, PKA phosphorylation seems to inhibit mGluR1 desensitisation. In regard to receptor endocytosis, group I mGluRs undergo rapid internalization following ligand exposure (Mundell et al., 2001) (Mundell et al., 2004) (Choi et al., 2011). The internalization of Group I mGluRs starts as early as 1 min after ligand exposure and maximum internalization was observed 30 min post-ligand application. Receptors recycle back to the plasma membrane in about 2.5 h – 3 h (Pandey et al., 2014) (Mahato et al., 2015). The endocytosis is often a part of the desensitisation process

involving β-arrestin binding, which facilitates the targeting of receptors for clathrin-mediated endocytosis (Ferguson et al., 1996).

Ubiquitination, another posttranslational modification, also targets group I mGluRs and regulates their internalisation. Recently, Gulia and colleagues reported that both mGluR1 and mGluR5 are subjected to ubiquitination by the E3 ubiquitin ligase Siah-1A (Gulia et al., 2017). The K1112 mutation to arginine inhibits mGluR internalisation. In addition, knocking down endogenous Siah-1A results in an increased mGluR-mediated endocytosis of AMPAR (Gulia et al., 2017). These result suggest a synergistic role between ubiquitination, mGluRs and AMPARs. More investigation into this subject could shed light on the involvement of posttranslational modifications of mGluRs in the expression of synaptic plasticity.

1.4 Posttranslational modifications implicated in synaptic function

Multiple posttranslational modifications (PTMs) occur at both presynaptic and postsynaptic elements to regulate the function of synaptic proteins, thereafter the synaptic function. PTMs are carried out by an enzyme or enzymatic machinery in a spatial-temporal manner in response to a range of stimuli, typically to synaptic and neuronal activity. In general, PTMs can alter target proteins activity, trafficking (localisation), stability and interactions (protein-protein interactions). Some important synaptic PTMs were already briefly discussed throughout the introduction. Therefore, in this chapter I aim to summarize the findings on the most relevant PTMs in synaptic function, dedicating most of the attention to **sumoylation - the subject of my PhD work**.

A. Phosphorylation

It has been over 50 years (1959) since protein phosphorylation was first discovered as a critical biological regulatory mechanism by Krebs and Fischer (Fischer et al., 1959), for which they jointly received the Nobel Prize in 1992. More than 20 years ago the first crystal structure of a

kinase, the receptor tyrosine kinase, was solved (McDonald et al., 1995). Protein kinases constitute one of the largest gene families and have been recurrently associated with many diseases (review by (Chico et al., 2009)). It is for this reason, that they have become a major drug target second only to G-protein coupled receptors. Thus, intensive research investigations into the process and consequences of phosphorylation are under way in all biological fields.

Protein phosphorylation is an essential and the most studied PTM. It is a reversible modification carried out by kinases that catalyse the addition of phosphate (PO_4, from ATP) to a polar group of various amino acids; and reversed by different enzymes called phosphatases. This PTM changes target proteins from hydrophobic apolar to hydrophilic polar leading to alterations in conformation thus functional and interacting properties, including changes in protein stability, localisation, activity and protein-protein interations. Protein phosphorylation events occur mainly on serine (86.4%), threonine (11.8%), and tyrosine residues (1.8%; (Ardito et al., 2017).

a) Presynaptic phosphorylation

In the past, synaptic phosphoproteins were identified by *in vitro* assays using extracted or purified proteins. Based on this classical approach, several synaptic phosphoproteins and their kinases were identified. In the presynapse, syntaxin1A, synaptobrevin (VAMP) and SNAP25 were shown to be phosphorylated by CaMKII; synaptobrevin and SNAP25 also by PKC, and synaptotagmin1 and syntaxin1A by casein kinase II (CK2; (Bennett et al., 1993) (Kataoka et al., 2000). Nowadays, phosphoproteomics, an advanced mass spectrometry approach, is widely used as it permits the identification of phosphorylation sites in a robust, global and quantitative manner. Oftentimes however, the functional relevance of these modifications is uncovered later with many to be yet elucidated. In regards to presynaptic proteins, phosphorylation has been perhaps not surprisingly implicated in the regulation of synaptic vesicle assembly/release. As an example, CaMKII phosphorylation of syntaxin 3B that is found specifically at retinal ribbon synapses has been shown to modulate the assembly of the SNARE complex and regulate the exocytosis of synaptic vesicles at these synapses (Liu et al., 2014). Another example comes from a recent study reporting that phosphorylation by different kinases on the same effector protein can have differential functional consequences. PKA phosphorylation of SNAP25 (at Thr138)

inhibits SNARE complex assembly, whereas PKC phosphorylation on a different phosphosite (Ser187) promotes SNARE complex formation. Interestingly however, activation of both kinases resulted in increased exocytosis (Gao et al., 2016). It should be emphasized, that this study was performed in PC12 cells, that present a mixture of neuroblastic and eosinophilic cells, and therefore the outcome of PKA and PKC SNAP25 phosphorylation in postmitotic neurons could differ. More recently, Katayama and colleagues provided evidence using a knock-in mouse model (where the phosphorylation site in SNAP-25 Ser187 is replaced by alanine) that the PKC phosphosite Ser187 in SNAP25 plays indeed a crucial role in synaptic vesicle dynamics. Moreover, the results suggested that Ser187 phosphorylation has a great influence on synaptic functions in the CNS, and may regulate higher brain functions and prevent excessive synaptic activity such as an epileptic seizure through inhibition of presynaptic plasticity (Katayama et al., 2017).

As pointed above, certain presynaptic proteins have multiple phosphorylation sites that can simultaneously undergo opposing changes in their phosphorylation states with different functional consequences. A prototypic example are synapsins. While phosphorylation by CaMKII on Ser9, Ser566 and Ser603 upon stimulation decreases actin binding and increases exocytosis of synaptic vesicles, the tyrosine-kinase Src phosphorylation of synapsin at Tyr301 has the opposite effect (Cesca et al., 2010). Moreover, MAPK and Cdk5 phosphorylation at serine residues (62, 67, 549 and 551) is downregulated upon synaptic stimulation resulting in a decreased binding of synapsin to actin filaments, possibly presenting a mechanism that regulates the ratio between resting and recycling synaptic vesicle pools (Verstegen et al., 2014).

Noteworthy, a recent phosphoproteomic study has investigated the alterations in phosphorylation of important presynaptic proteins in rat brain synaptosomes upon exocytosis stimulation. The active zone proteins such as dynamin 1, synapsin 1, Piccolo, Bassoon, Munc13, RIM and others, exhibited concurrent changes in phosphorylation and dephosphorylation at multiple positions, some of them previously unknown. This report further reinforced the complexity of the molecular switch that this PTM offers to target proteins. Functional studies will have to be carried out to further examine the involvement of these new presynaptic phosphorylation sites in synaptic function (Kohansal-Nodehi et al., 2016).

b) Postsynaptic phosphorylation

The involvement of postsynaptic phosphorylation and phosphoproteins in synaptic function, especially synaptic plasticity is nicely reviewed in (Lee, 2006). A more recent publication by Li *et al*. identifies LTP-regulated phosphoproteins at the PSD, many of which have been associated with brain disease (Li et al., 2016). In this part I will focus only on the most important historic findings and add some of the newest insights into the regulation of postsynaptic proteins by phosphorylation. By no means I will provide an exhaustive list of all phosphorylation-related regulatory mechanisms but rather a hint of the importance of this PTM at the postsynapse.

It is generally believed, that a rise in intracellular calcium through NMDARs is the key determinant of LTP and LTD induction. Furthermore, many kinases and phosphatases present different sensitivity to calcium increase as they target NMDARs either directly or indirectly via associated phosphoproteins within a common macromolecular complex. Postsynaptic CaMKII, PKC, PKA, cGMP-dependent protein kinase (PKG), casein kinase II (CKII) and MAPK, and phosphatases (protein phosphatase 1, 2A and 2B [PP1, 2A and 2B]) have been all implicated in synaptic plasticity (reviewed by (Blackwell and Jedrzejewska-Szmek, 2013)). CaMKII hypothesis (Lisman, 1994) states that moderate increase in calcium preferentially activates PP2B leading to dephosphorylation and deactivation of CaMKII and induction of LTD, whereas more robust calcium influx triggers CaMKII autophosphorylation. This hypothesis was later replenished by the AMPAR trafficking phenomenon. Many phosphorylation sites have been identified on the intracellular carboxy-tail of NMDAR to regulate the receptor function. Importantly, this regulation is dependent on the developmental stage of neurons. Protein tyrosine kinases (PTK) and protein tyrosine phosphatases (PTP) are necessary for maintaining NMDAR function.

Figure 19.

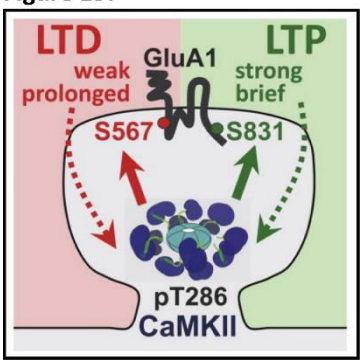

Figure 19. **CaMKII phosphorylation of GluA1 subunit of AMPAR can mediate differential plasticity responses**. Weak but prolonged NMDAR stimulation inducing LTD or strong but brief inducing LTP, both lead to CaMKII autophosphorylation at T286, which generates autonomous kinase activity. However, a stronger further stimulation of CaMKII by Ca^{2+}/CaM during LTP leads to phosphorylation of traditional CaMKII substrates (such as S831 on GluA1), whereas the autonomous CaMKII activity without such further stimulation after LTD stimuli favours phosphorylation of S567 on GluA1. The phosphorylation of CaMKII S831 or S567 promotes synaptic potentiation or depression, respectively. Taken from (Coultrap et al., 2014).

Application of PTK inhibitors or exogenous PTP (Wang et al., 1996) depresses NMDA receptor currents. Most of the Src family of PTK (i.e. Src, Fyn, Yes, and Lyn) localise in the PSD and associate with NMDARs (Salter and Kalia, 2004). Src serves as the major PTK regulating basal NMDAR function, and its activity is thought to be counteracted the striatal enriched tyrosine phosphatase (STEP) (Salter and Kalia, 2004). In addition, the GluN1, GluN2A, and GluN2B subunits of NMDAR can be regulated by phosphorylation on serine residues by PKA and PKC. For instance, the dispersal of NMDAR to extrasynaptic sites has been proposed to rely on PKC Ser890 phosphorylation of GluN1 (Tingley et al., 1997) (Fong et al., 2002). Another regulatory mechanism of phosphorylation involves NMDAR trafficking from endoplasmic reticulum (ER) that depends on PKC and PKA phosphorylation around the ER retention motif that is present in certain isoforms of GluN1 (Scott et al., 2003). As already mentioned, CaMKII is the most abundant protein at the postsynapse, and therefore it is not surprising that it plays major roles in synaptic function including plasticity events. It phosphorylates an array of receptors and other PSD proteins regulating their functions (Lee, 2006) (Gambrill and Barria, 2011) (Hell, 2014). This topic has been already partially covered in previous chapters regarding the PSD composition and individual glutamate receptors, therefore I will only briefly mention some of the key regulatory mechanisms of phosphorylation by CaMKII. Traditionally, hippocampal LTP of synaptic strength requires Ca^{2+} influx via postsynaptic NMDA receptors and calmodulin binding to CaMKII leading to CaMKII activation by autophosphorylation at T286; since preventing this site from phosphorylation (T286A) fails to express LTP (Giese et al., 1998) (Lucchesi et al., 2011). The constitutively active autophoshorylated state of CaMKII allows it to tightly associate with PSD members. Translocation of CaMKII to dendritic spines and its prolonged residency (synaptic trapping) has been widely observed upon LTP induction (Lee et al., 2009). It has been proposed that CaMKII provides anchoring sites for AMPAR following LTP (Jackson and Nicoll, 2011). This kinase also contains two autoinhibitory sites T305 and T306, which are the binding sites of Ca^{2+}/calmodulin, and prevent further activation upon an immediate calcium rise, which would otherwise result in excitotoxicity. Moreover, the autoinhibition decreases CaMKII affinity toward PSD (Coultrap and Bayer, 2012). Intriguingly, a 2014 study showed that CaMKII and its phospho-T286-induced "autonomous" activity is also required for the expression of LTD ((Coultrap et al., 2014), ***Fig. 19***).

LTP induces CaMKII phosphorylation of the AMPAR subunit GluA1 at S831, whereas LTD induces CaMKII-mediated phosphorylation at S567, a site whose phosphorylation is known to mediate a decrease in synaptic GluA1 localization. Thus, this work uncovered a mechanism of differential regulation of AMPAR/CaMKII-mediated synaptic plasticity: CaMKII phosphorylation of GluA1 S831 is favoured by LTP-type stimuli (strong but brief), whereas CaMKII phosphorylation of GluA1 S567 is favoured by LTD-type stimuli (weak but prolonged; (Coultrap et al., 2014)).

Recently, a novel regulatory postsynaptic mechanism involving CaMKII was demonstrated in Purkinje cells (Sugawara et al., 2017). The activity-dependent PKC-mediated phosphorylation of CaMKIIβ was found to be triggered by Group I mGluRs but not calcium influx. The Ser315 phosphorylation interferes with CaMKIIβ F-actin binding, therefore preventing F-acting bundling and increasing the immaturity of dendritic spines. In conclusion, the phosphorylation state of Ser315 is a driving force for equilibrated spinogenesis on distal dendrites of Purkinje cells (Sugawara et al., 2017).

PSD-95, the second most abundant PSD protein is also a target of phosphorylation. Kim *et al*. (2007) reported that PSD-95 phosphorylation by Jun N-terminal kinase 1 (JNK1) at Ser295 is regulated by synaptic activity leading to the accumulation of PSD-95 in spines, thereafter synaptic potentiation. Additionally, JNK1 phosphorylation of PSD-95 is Rac-1 dependent and Ser295 dephosphorylation is important for AMPAR internalisation-mediated LTD (Kim et al., 2007). Not long after this report, PSD-95 was reported to be involved in an activity-dependent spine growth. In response to local synaptic stimulation (glutamate uncaging), PSD-95 gets rapidly trafficked out of spines to allow for spine growth that is followed by a reestablishment of higher PSD-95 levels at the synapse (Steiner et al., 2008). This finding was further supported by the data from Wu *et al.* (2017), who proposed a model whereby increased dynamics of synaptic PSD-95 upon chemical LTP (cLTP) is a prerequisite for structural rearrangement of dendritic spines (Wu et al., 2017). In the first case, Ser73 on PSD-95 was identified to be targeted by CaMKII whose phosphorylation destabilised PSD-95 in the PSD and led to PSD-95 and SHANK1 trafficking out of spines to terminate spine growth (Steiner et al., 2008). In the second instance, Ser561 phosphorylation

carried out by the microtubule affinity-regulating kinase (MARK also known as Par1) was reported to regulate a conformational switch in PSD-95 between the SH3 and GK domains. Moreover, preventing phosphorylation stabilized PSD-95 interaction with its binding partners and decreased its synaptic dynamics resulting in unresponsiveness to LTP stimulation. On the other hand, a phosphomimetic mutant showed enhanced dynamic properties (Wu et al., 2017). Another level of PSD-95 regulation by phosphorylation was revealed by Nelson *et al*. (2013) providing evidence that Thr19 phosphorylation by GSK-3β (a widely expressed kinase with a broad range of biological implications [reviewed in (Peineau et al., 2008)] including cell polarity, axon guidance, neuronal plasticity, phosphorylation of tau [involved in formation of neurofibrillary tangles in Alzheimer's Disease], as well as it is a target of Li^+ treatment in bipolar disorder) destabilises PSD-95 in spines and is essential for AMPAR internalisation during the expression of LTD in CA1 hippocampal neurons (Nelson et al., 2013). Altogether, these findings bolster the fact that phosphorylation/dephosphorylation take place on diverse sites of target proteins having various and often opposing functional consequences to balance physiological processes.

B. Palmitoylation

Lipid modifications regulate diverse aspects of neuronal protein trafficking and function by increasing their hydrophobicity and facilitating their insertion into cellular membranes (reviewed in (Fukata and Fukata, 2010)). Palmitoylation, is the most common lipid modification that frequently occurs in neurons. Palmitoylation is defined as the addition of 16-carbon palmitic acid to specific cysteine residues via the formation of a thioester bond. Most palmitoylation is reversible due to the unstable thioester bond (S-palmitoylation), however a stable irreversible amide bond has been also reported (N-palmitoylation) e.g. in Sonic hedgehog (Pepinsky et al., 1998)). Recent advances in the detection of palmitoylated proteins enabled to identify 68 already known and more than 200 new palmitoylation substrates in rat brain synaptosomes and cultured cortical neurons. Moreover, palmitoylation (palmitoyl acyl transferases, PATs) and depalmitoylation (palmitoyl protein thioesterases, PPTs) enzymes have been identified. PATs share a common domain known as the DHHC cysteine-rich domain that consists of ~50 amino acids with a conserved Asp-His-His-Cys region. In mammals, 23 kinds of DHHC proteins are

predicted. Importantly, many neuronal and synaptic proteins have been found to be palmitoylated. For instance, PSD-95 postsynaptic targeting relies on palmitoylation (Topinka and Bredt, 1998). Incubation of neurons with a palmitoylation inhibitor 2-bromopalmitate significantly decreases PSD-95 palmitoylation; and many DHHC proteins are able to enhance PSD-95 palmitoylation. It was shown that palmitoylation has a rapid turnover effect on PSD-95, which was surprising considering that PSD-95 was thought to be quite stable at the PSD where it anchors transmembrane proteins (Kang et al., 2008). Functionally, PSD-95 palmitoylation-depalmitoylation cycles could play a role in synaptic plasticity. PSD-95 palmitoylation decreases when synaptic activity increases, whereas tetrodotoxin-induced activity blockade potentiates PSD-95 palmitoylation and its accumulation in spines in cultured neurons (Noritake et al., 2009). Moreover, an increase in synaptic AMPARs is dependent on DHHC-mediated palmitoylation of PSD-95. Correspondingly, the activity-evoked depalmitoylation of PSD-95 promotes AMPAR endocytosis (Noritake et al., 2009). The PSD-95 protein is just one example to illustrate the significance of this PTM in the trafficking and function of target proteins. Other proteins such as small GTPases, G-proteins, glutamate receptors, scaffolds and cell adhesion molecules were reported to be palmitoylated. In addition, the functional importance of single PATs and PPTs starts to emerge. Not long ago, the microRNA miR138 has been shown to target the depalmitoylation enzyme APT1 and in this way negatively regulate dendritic spine size. In this line, APT1 knock-down leads to reduction in spine volume (Siegel et al., 2009). Finally, considering the abundant presence of this PTM in neurons, defects in palmitoylation have been linked to psychiatric disease (Chen et al., 2004), neurodegenerative (Huang et al., 2004) and neurodevelopmental disorders (Raymond et al., 2007).

Recently, Woolfrey and colleagues reported that the kinase anchor protein AKAP79/150 is an LTD-related substrate of CaMKII (Woolfrey et al., 2017). CaMKII inhibition prevented LTD-induced AKAP79/150 removal from dendritic spines, while CaMKII-mediated phosphorylation impaired AKAP79/150 interaction with F-actin and facilitated spine removal. Moreover, AKAP79/150 spine removal additionally required AKAP79/150 de-palmitoylation regulated also by CaMKII. This depalmitoylation was required for AKAP79/150 trafficking as well as for structural LTD (Woolfrey

et al., 2017). Altogether, these data provide evidence of an active participation of palmitoylation and a possible interplay between phosphorylation and palmitoylation of AKAP79/150 in synaptic plasticity.

C. Ubiquitination

Eukaryotic cells have evolutionarily developed protein degradation strategies, the ubiquitin proteasome system (UPS) and lysosomes, to control protein levels, prevent non-specific protein degradation and thus maintain proper cell homeostasis. The UPS degrades most of the intracellular and soluble proteins and also some membrane proteins if extracted from the membranes into the cytosol. Lysosomes, on the other hand, are mainly responsible for the degradation of membrane and endocytosed proteins but can also digest cytosolic proteins via autophagy. The enzymatic process resulting in protein modification by ubiquitination is essential prior to protein degradation through the UPS. This pathway was first described in 1975 by the pioneering work of Aaron Ciechanover, Avram Hershko and Irwin Rose (Ciechanover et al., 1980) (Hershko et al., 1980), for which they jointly received the Nobel Prize in Chemistry in 2004. Although the most prominent role of the UPS system is protein degradation, over the years, ubiquitination has been also implicated in signal transduction, endocytosis and DNA repair. Given the unique morphology of neurons, this PTM is particularly interesting as local proteomes undergo tight regulation within different subcellular domains (i.e. dendritic spines) in response to neuronal stimulation. The importance of this PTM is also highlighted by the fact that malfunctions of the UPS result in accumulation of misfolded and damaged ubiquitin-positive proteins and lead to different pathologies such as neurodegenerative diseases (Parkinson's, Alzheimer's and Huntington's).

Ubiquitin is a highly conserved protein of 76 amino acids (8.5 kDa). In the process of ubiquitination, ubiquitin is covalently conjugated to proteins, typically on their lysine residues, that are to be degraded in the proteasome. In the mouse brain, there is about 40% of free (non-conjugated) and 60% conjugated ubiquitin. Out of the conjugated ubiquitin, ~90% exist as monoubiquitination and ~10% form poly-ubiquitin chains (Hallengren et al., 2013). Ubiquitination is carried out with the participation of four different enzymes: E1 (ubiquitin-

activating enzyme), E2 (ubiquitin-conjugating enzyme), E3 (ubiquitin-protein ligase) and E4 (chain elongation factors). In the presence of ATP, ubiquitin is covalently linked to E1, and then transferred onto E2. Ubiquitin conjugation is catalysed by E3 from E2 to a target protein. Both E3 and E4 can catalyse ubiquitin chain elongation. Ubiquitin has seven lysines all of which can be used for chain extension via the ubiquitin-ubiquitin isopeptide bond. The K48 polyubiquitin chains (most abundant) lead the substrate via diffusion, or the aid of chaperons and other shuttling factors to the proteasome (Hallengren et al., 2013). The most common cytoplasmic proteasome is the 26S proteasome composed of ~30 different proteins that are arranged in a barrel-like proteolytic core (20S, ~700 kDa) and a cap unit on one or either end of the core (19S, ~900 kDa). The 26S proteasome is involved in many essential neuronal processes, including the synaptic strength regulation by modulating the presynaptic (Willeumier et al., 2006) as well as postsynaptic (Ehlers, 2003) proteomes.

Over the past years, we have gained important insights into the molecular mechanisms that underlie the synaptic plasticity phenomena and will be briefly described below. A 2006 report by Bingol and Schuman demonstrates that under basal conditions proteasomes are equally distributed between dendritic shaft and spines, however this changes upon neuronal depolarisation (KCl application), which evokes a redistribution of proteasomes from dendritic shaft to spines within minutes. Moreover, application of the NMDAR blocker AP5 prevents this redistribution suggesting that activation of NMDAR specifically recruits proteasomes to spines. The proteasomes in spines were shown to be catalytically active and this effect was further accompanied by more than a 60% increase in ubiquitinated synaptic proteins (Bingol and Schuman, 2006). These data clearly showed an activity-dependent proteasome redistribution toward the synapse suggesting an active shaping of the local proteome in spines. In line with the idea that proteasomes sculpt the synaptic proteome, thus the spine structure and function, Hamilton *et al*. applied acute inhibition of the proteasome in combination with local glutamate uncaging, which led to a rapid reduction of spine outgrowth. Moreover, the upstream players necessary for the activity-dependent spine outgrowth were identified to be NMDAR and CaMKII (Hamilton et al., 2012). Ubiquitination is also critically important for the internalisation of Group

I mGluRs. Blocking the E1 enzyme inhibits the ligand-mediated endocytosis of Group I mGluRs. Moreover, the K63 polyubiquitin chains of the mGluR1 and the E3 ubiquitin ligase Siah1A were shown to be indispensable for the process of mGluR1 internalisation (Gulia et al., 2017). The above data prompt a possible involvement of synaptic proteolysis in the expression of synaptic plasticity. Indeed, over the past years, experimental evidence supported the involvement of the UPS in both short- and long-term plasticity events. At excitatory glutamatergic synapses, Arc, the activity-regulated cytoskeleton-associated protein, is thought to serve as a major regulator of synaptic plasticity mainly due to its facilitation of AMPAR endocytosis. Arc is ubiquitinated by and associates with E3 ubiquitin ligase Triad3A at endocytic sites in dendrites and spines (Mabb et al., 2014). Deficient Triad3A results in loss of surface AMPAR, whereas overexpression of Triad3A increases surface AMPAR. Altogether, controlling Arc levels by Triad3A was shown to regulate the expression of LTD in hippocampal neurons (Mabb et al., 2014). A couple of years ago, Sun *et al*. demonstrated that UBE3A, an ubiquitin E3 ligase involved in Angelman syndrome, regulates synaptic plasticity in learning and memory (Sun et al., 2015). UBE3A was shown to ubiquitinate the small-conductance potassium (SK2) channels resulting in their endocytosis and removal from synapses. UBE3A-deficient mice displayed impaired hippocampal long-term synaptic plasticity that was manifested by deficits in cognitive function (Sun et al., 2015). Proteasome-independent action of ubiquitination has also been implicated in synaptic plasticity. The cytoplasmic polyadenylation element-binding protein 3 (CPEB3) mediates long-lasting changes of synaptic efficacy and long-term memory and has been shown to be monoubiquitinated by Neuralized1, an E3 ubiquitin ligase, in mouse hippocampal cultures. CPEB3 activation by monoubiquitination leads to the growth of new dendritic spines and increased expression of the AMPA receptor subunits resulting in enhanced hippocampal-dependent memory and synaptic plasticity (Pavlopoulos et al., 2011).

In conclusion, local ubiquitination that often precedes UPS proteolysis is essential for the regulation of synaptic protein repertoire, and thus synaptic function and plasticity.

D. Sumoylation

In summary, until this point, the introduction paved the way throughout important biological knowledge that will largely facilitate the understanding of the investigation **into the regulation of synaptic sumoylation balance – the main aim of my PhD thesis project**. Naturally, in this last part of introduction, I will define the enzymatic SUMO pathway and give an overview of our current knowledge on the function and dysfunction of protein sumoylation at the mammalian synapse (also partially reviewed in (Schorova and Martin, 2016), **Annexed Article 1**).

Sumoylation is a ubiquitous and vital post-translational modification regulating many biological processes. More than 20 years ago, sumoylation was simultaneously discovered by several groups as a modification of nuclear proteins such as the Ran GTPase activating protein (RanGAP1; (Matunis et al., 1996) (Mahajan et al., 1997)). Although the majority of sumoylation localises in the nucleus, many important extranuclear roles have been reported since. The essential role of sumoylation is given by the fact that either knocking-down or deleting genes or components of sumoylation causes cell-cycle arrest in yeast (Johnson and Blobel, 1997) and is lethal in rodent models (Hayashi et al., 2002b) (Nacerddine et al., 2005) (Cheng et al., 2007). Disruption of sumoylation in developing brain has also fatal consequences (Fu et al., 2014a), indicating that this process is vital to both embryonic and postnatal development of the brain**. In spite of a large body of data implicating sumoylated substrates in synapse formation, synaptic communication and plasticity, it is yet to unveil the regulatory cues that control for an equilibrated sumoylation and desumoylation at a given time and space in the mammalian brain.**

Sumoylation is a highly evolutionarily conserved (from yeast to mammals) enzymatic pathway ***(Fig. 20)***, which covalently but reversibly conjugates the Small Ubiquitin-like Modifier (SUMO) protein (~100 amino acids, ~11 kDa) to lysine residues of target proteins (Matunis et al., 1996) (Mahajan et al., 1997). SUMO conjugation is catalysed by the sole SUMO-conjugating enzyme, Ubc9. Sumoylation pathways is analogous to ubiquitination, and SUMO polypeptides share ~18% homology with ubiquitin. Five SUMO paralogs have been identified in humans until now. SUMO1-

3 are ubiquitously expressed (Hay, 2005) (Geiss-Friedlander and Melchior, 2007), whereas SUMO4 expression is restricted to the spleen, the kidney and the lymphatic nodes (Bohren et al., 2004) (Guo et al., 2004) and SUMO5 is expressed in the lung and spleen (Liang et al., 2016). SUMO2 and SUMO3 are nearly identical except for three additional N-terminal residues within the SUMO3 sequence; therefore, they are generally referred to as SUMO2/3. On the contrary, SUMO1 shares only ~50% sequence identity with SUMO2/3. SUMO1 and SUMO2/3 modify an overlapping set of target proteins; but they differ in their properties and subcellular abundance with the amount of free available SUMO2/3 being much larger than that of SUMO1. The SUMO-targeted lysine often resides within a specific consensus site defined as ψ-K-x-D/E, where ψ corresponds to a large hydrophobic residue, K stands for lysine, x is any amino acid, and D/E are glutamate and aspartate acid residues, respectively (Rodriguez et al., 2001) (Sampson et al., 2001). Importantly however, many lysines that do not lay within the consensus sequence have been discovered to be targeted by sumoylation, and many of the lysine residues contained within the SUMO consensus sites have been reported as not sumoylated (reviewed in (Flotho and Melchior, 2013) and (Henley et al., 2014)). Noteworthy, in most cases the determination of the sumoylation status was achieved in basal unstimulated conditions. Therefore, caution should be taken to state with certainty that a given protein is not a SUMO substrate since only a small percentage of any protein is sumoylated at steady state (Hay, 2005) (Nayak and Muller, 2014).

The SUMO enzymatic pathway ***(Fig. 20)*** is highly dynamic and must be tightly controlled as it drastically influences the function of many proteins targeted by this PTM. Despite a covalent SUMO binding, sumoylation is reversible through the isopeptidase activity of desumoylation enzymes (see (Hickey et al., 2012) for a comprehensive review on SUMO proteases). In addition, prior to entering the sumoylation pathway, SUMO precursors must be matured (a hydrolytic cleavage to expose the carboxyl-terminal diglycine motif) by desumoylation enzymes. Several SUMO proteases effectively mediate desumoylation and some also SUMO maturation. In humans, six SENP proteases have been described (SENP1, 2, 3, 5, 6 and 7). These SENP enzymes differ in their subcellular localization and SUMO selectivity (Hickey et al., 2012). Recently, several additional SUMO proteases have been identified, DeSumoylating Isopeptidase 1 and 2 (DeSI1 and

Figure 20.

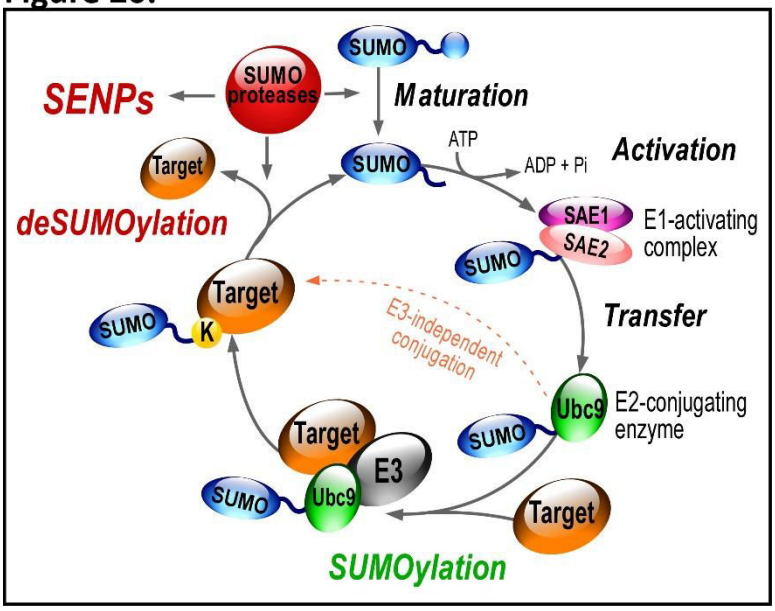

Figure 20. **The SUMO enzymatic pathway**. SUMO paralogs are synthesized as inactive precursors that are first matured by the hydrolase activity of specific desumoylases called SENPs. SUMO activation is an ATP-dependent step leading to formation of a thioester bond between the SUMO-activating subunit SAE2 of the E1 enzymatic heterodimer SAE1/SAE2 and the matured SUMO protein. SUMO is then transferred onto the active (C93) cysteine residue of Ubc9, E2-conjugating enzyme. Ubc9 is able to catalyse the sumoylation reaction of the target lysine residue on the substrate either directly or in combination with one of the existing SUMO E3 ligases. Importantly, sumoylation is readily reversible and sumoylated proteins can be efficiently desumoylated via the isopeptidase activity of a variety of SUMO proteases including SENPs, DeSI1/2 and/or USPL1.

DeSI2; (Shin et al., 2012)) and USPL1 (Ubiquitin-Specific Protease-Like 1; (Schulz et al., 2012)). Both SUMO conjugation and deconjugation control the dynamic equilibrium between the sumoylated and desumoylated state of many proteins. Since this PTM regulates many proteins involved in essential developmental processes (Gwizdek et al., 2013) and synaptic functions (Schorova and Martin, 2016) (Henley et al., 2014), dysregulation of the sumoylation/desumoylation balance may directly link the SUMO process to a number of pathophysiological conditions (see ***Table 1*** and review (Schorova and Martin, 2016) **Annexed Article 1**, for detailed description).

Synaptopathy	Implicated SUMO targets and machinery	Effects	References
Down syndrome	*SUMO3*	SUMO3 gene is localised on Hsa21. SUMO3 overdose leads to imbalanced/deregulated sumoylation.	(Gardiner, 2006)
Rett syndrome	*MeCP2*	Some MeCP2 mutations found in patients reported to decrease MeCP2 sumoylation. Lack of MeCP2 sumoylation leads to abnormal synaptic density.	(Cheng et al., 2014) (Tai et al., 2016)
Parkinson's disease	*α-Synuclein*	Sumoylated by SUMO1 and SUMO2/3. PD patients show increased α-Syn sumoylation. α-Syn sumoylation promotes α-Syn aggregation. Another pathogenic mechanism could include inter-neuronal spreading of α-Syn.	(Krumova et al., 2011), (Kim et al., 2011), (Kunadt et al., 2015) (Rott et al., 2017)
	DJ-1	A PD mutation disrupts DJ-1 sumoylation and decreases its solubility.	(Shinbo et al., 2006)
	Parkin	Increase in its E3 ligase activity by non-covalent SUMO1 modification. Parkin also associates with and targets the SUMO E3 ligase RanBP2 for degradation. Direct implication in PD is still lacking.	(Um and Chung, 2006)
Huntington's disease	*Huntingtin*	Sumoylation may act as a prevention mechanism of huntingtin accumulation.	(Steffan et al., 2004), (O'Rourke et al., 2013)
Alzheimer's disease	*SAE2, Ubc9, SENP3*	Single Nucleotide Polymorphisms of these genes co-segregate with AD.	(Corneveaux et al., 2010), (Grupe et al., 2007), (Ahn et al., 2009), (Weeraratna et al., 2007)
	Aβ	Unclear results about whether sumoylation of Aβ enhances or decreases its aggregation.	(Li et al., 2003), (Zhang and Sarge, 2008), (Dorval et al., 2007)
	Tau	Proportion between sumoylated and ubiquitinated Tau can regulate its degradation/accumulation. Hyper-phosphorylated toxic Tau is immunoreactive for SUMO1.	(Dorval and Fraser, 2006), (Luo et al., 2014)

Table 1. **Implication of sumoylation in synaptopathies.**

In the following sections, I discuss **sumoylation in the context of presynaptic and postsynaptic functions** (as reviewed in (Schorova and Martin, 2016), **Annexed Article 1**) and more importantly, I provide an **update of the newest discoveries and controversies in the field of synaptic sumoylation**.

a) Presynaptic sumoylation

The activity-dependent neurotransmitter release is a highly dynamic process that depends upon tight regulation provided mainly by PTMs, including sumoylation.

Feligioni *et al*. used a synaptosomal preparation protocol to trap exogenous matured SUMO1 polypeptides or the catalytically active domain of the desumoylation enzyme SENP1 in synaptosomes to respectively increase or decrease the presynaptic sumoylation levels and measure the impact of sumoylation on glutamate release. They reported that the increase in presynaptic sumoylation reduced Ca^{2+} influx and decreased glutamate release upon KCl depolarization. In contrast, decreasing presynaptic sumoylation by introducing SENP1 into synaptosomes led to an enhanced Ca^{2+} influx and glutamate release in KCl-stimulated conditions (Feligioni et al., 2009). This study was the first to provide evidence for a direct role of sumoylation at the presynapse via modulation of calcium influx and glutamate release, although the molecular pathway and presynaptic proteins targeted by this PTMs were not described at that time. Since then, several key axonal and presynaptic proteins have been reported to be sumoylated and a better view of the complexity of sumoylation as well as the regulatory role of sumoylation at the presynapse is now clearly emerging ***(Fig. 21)***.

• La protein

The human La protein was originally identified as an auto-antigen in an immune system disorder called Sjogren's syndrome. Levels of circulating anti-La antibodies are used for the diagnosis of this autoimmune syndrome. La is the smallest member (46kDa) but the most abundant of the La-related protein (LARP) family (reviewed in (Stavraka and Blagden, 2015)). Its RNA-interacting motif RRM allows the binding, protection and axonal transport of many mRNAs. Importantly, La has been reported to be a sumoylation substrate (van Niekerk et al., 2007). Sumoylated La binds to dynein allowing its retrograde axonal transport. Conversely, the native non-sumoylated La interacts with kinesin and undergoes anterograde axonal transport. This pioneering work uncovered sumoylation as a key regulatory mechanism in mRNAs trafficking

toward their local translation sites, an essential process for the maintenance of axonal protein pools that are required for synaptic transmission.

• Synapsin Ia

Synapsins are presynaptic proteins that are essential for the establishment, clustering and release of SVs (Cesca et al., 2010). Synapsin Ia (SynIa) is involved in maintaining the reverse pool of SV that is required upon long lasting neuronal stimulation. Tang and collaborators demonstrated that SynIa is sumoylated at the K687 residue and that this sumoylation potentiates

Figure 21.

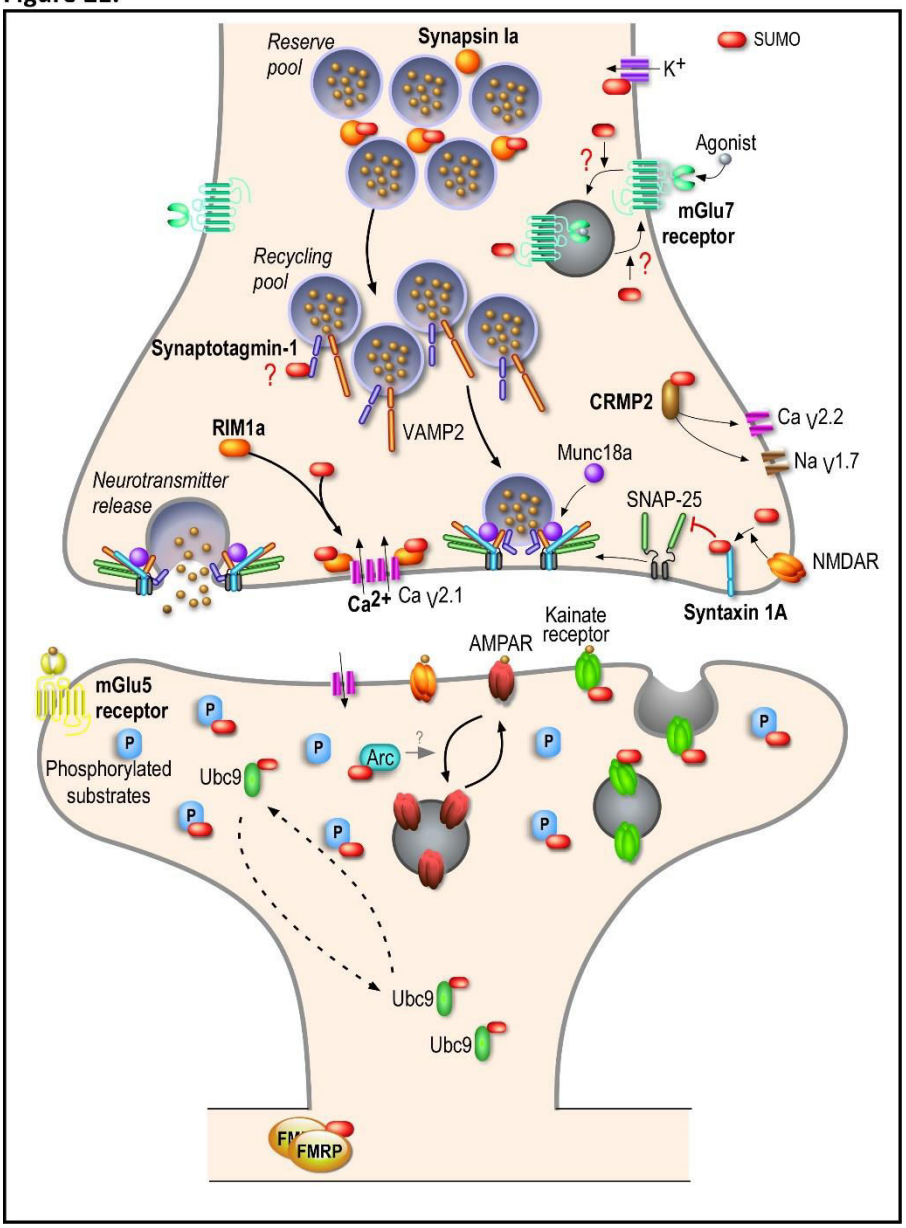

Figure 21 (Continued). **Sumoylation at the synapse**. The sumoylation enzymatic machinery localises at the synapse and several pre- and postsynaptic proteins have been identified to be sumoylated. (1) **Presynaptic sumoylation** emerges as a central protein modification acting at several stages of the neurotransmitter release mechanism. Sumoylation of **Synapsin Ia** (SynIa) potentiates its association with synaptic vesicles and thus participates in the clustering of these vesicles at the presynapse. **Synaptotagmin-1** is sumoylated *in vivo* but the precise function of this modification is still not known. **Syntaxin-1A** sumoylation is evoked upon NMDAR activation leading to a decreased binding to SNAP-25 and VAMP-2 and thus acting as a key presynaptic regulator of vesicle endocytosis. **RIM1α** sumoylation is required for presynaptic exocytosis since depolarization-evoked vesicle exocytosis with a non-sumoylatable RIM1α mutant is dramatically impaired. This effect is mainly due to a defect in presynaptic calcium entry following neuronal activation since RIM1α sumoylation enables the binding to $Ca_V2.1$ calcium channels and coordinates the presynaptic Ca^{2+} entry. **CRMP2** is a SUMO substrate and dynamically reduces Ca^{2+} entry through the presynaptic voltage-gated Ca^{2+} channel $Ca_V2.2$. CRMP2 sumoylation is also believed to regulate the membrane expression of the sodium channel $Na_V1.7$. **K_V potassium channels** play critical roles in neuronal excitability and sumoylation of a number of these channels ($K_V1.1$, $K_V2.1$, $K_V7.2$, $K_V7.3$) has been reported to act as a molecular regulator of their intrinsic activity. Question marks in red indicate that the physiological consequences of the target protein sumoylation are still not clearly defined. **mGluR7** is sumoylatable both *in vitro* but also *in vivo* in rat hippocampal and cortical neurons. mGluR7 agonist activation triggers the endocytosis of the WT mGluR7 but not the internalization of its non-sumoylatable mutant suggesting that sumoylation acts on the endocytic pathway. However, overexpressing the desumoylase SENP1 increases the pool of internalized mGluR7, which rather implies that mGluR7 sumoylation is important for recycling of these receptors back to the plasma membrane and not for the receptor endocytosis per se. (2) **Postsynaptic sumoylation** plays important roles in neuronal maturation and synaptic plasticity. First evidence of postsynaptic protein sumoylation was provided for **kainate receptors**. KAR sumoylation promotes receptor internalisation. **Arc** is also a sumoylation substrate. Arc levels decrease upon attenuated synaptic activity leading to an increase in AMPAR at the membrane. The exact mechanisms are yet to be discovered. The **Ubc9** enzyme is regulated by activation of mGluR5, which leads to Ubc9 transient trapping in spines due to an enhanced ability of Ubc9 to recognise synaptic PKC-phosphorylated substrates. Prolonged residency of Ubc9 at the postsynapse results in increased synaptic sumoylation levels and modulation of neuronal communication. **FMRP** protein is targeted by sumoylation. mGluR5-mediated FMRP sumoylation is essential for proper spine maturation and control of dendritic spine density. See text for more details and references.

its association with SVs participating in the clustering and anchoring of these vesicles at the presynapse (Tang et al., 2015); ***Fig. 21***). The lysine-687-to-arginine mutation resulted in a complete absence of SynIa sumoylation, a decrease in number of releasable SVs and impaired exocytosis (Tang et al., 2015). Interestingly, the A548T mutation in SynIa that co-segregates with autism also impairs SynIa sumoylation. Defects in SynIa sumoylation may therefore be involved in the pathophysiology of neurological disorders through a presynaptic SUMO-dependent deregulation of SynIa function at the presynapse. Altogether, sumoylation of SynIa appears to be critical for the activity-dependent neurotransmitter release and may therefore actively participate in synaptic transmission and synaptic plasticity.

• Syntaxin-1A

The exocytosis of SVs is mediated through the action of the SNARE protein complex that includes the 35-kDa-membrane protein Syntaxin-1A (Stx1A), SNAP-25, VAMP-2 and additional proteins such as Munc18, Synaptotagmins and RIM1α ***(Fig. 21)***. Stx1A has been reported to be important in neuronal survival (Kofuji et al., 2014), neurotransmitter release and recycling of SVs (Watanabe et al., 2013). The role of Stx1A in synaptic function is also supported by studies reporting a possible involvement of Stx1A in the pathophysiology of autism with Stx1A mRNA expression levels being significantly higher in autistic patients compared to controls (Nakamura et al., 2008). Interestingly, Stx1A has recently been reported a novel sumoylation target (Craig et al., 2015). Stx1A sumoylation is evoked upon NMDA receptor activation or KCl-depolarization in hippocampal neurons. This activity-dependent sumoylation occurs at three lysines (K252, 253 and 256) leading to a reduced Stx1A binding to SNAP-25 and VAMP-2, but not to Munc18a. Importantly, neuronal expression of the non-sumoylatable form of Stx1A, leads to a significant increase in presynaptic vesicle endocytosis (Craig et al., 2015), which suggests that Stx1A sumoylation is critically involved in maintaining the balance between SV endocytosis/exocytosis. How exactly the sumoylated form of Stx1A enhances SV endocytosis as well as how Stx1A desumoylation occurs in this context is yet to be investigated.

• Synaptotagmin-1

Membrane fusion at presynaptic sites involves not only the SNARE proteins but also several other presynaptic factors to orchestrate neurotransmission in a timely dependent way (reviewed in (Sudhof, 2013)). Among these are calcium sensor proteins called Synaptotagmins. To date, sixteen isoforms of synaptotagmins have been identified in mammals that either co-localise with SVs or are distributed at the plasma membrane. Owing to the calcium sensing properties, Syt1 importantly participates in neurotransmitter release ***(Fig. 21)***.

The Fraser lab used a proteomic approach on transgenic mice that exclusively over-expressed the human form of SUMO1 in neurons (Matsuzaki et al., 2015). They identified many SUMO1 targets that were neuron- and synapse-specific. Syt1 among them displayed up-regulated

sumoylation in these transgenic mice (Matsuzaki et al., 2015). Using field potential recording in acute hippocampal slices from SUMO1-transgenic brains, they reported a deficit in basal transmission suggesting a decrease in synaptic activity and/or a loss of functional synapses. They also showed that a form of short-term synaptic plasticity dependent on presynaptic mechanisms named paired pulse facilitation is impaired in SUMO1-transgenic brain slices, which suggests that SUMO1 over-expression leads to functional presynaptic mechanisms defects (Matsuzaki et al., 2015). Moreover, SUMO1-over-expressing hippocampal cells exhibit a dramatic loss of dendritic spines that results in the impairment of contextual fear memory (Matsuzaki et al., 2015). Despite these deleterious alterations in SUMO1-transgenic mice, the functional significance of Syt1 sumoylation remain unexplained. Clearly, the hyper-sumoylation of Syt1 in SUMO1-transgenic mice cannot be taken as the unique cause of all the physiological deficits reported in these animals. **Nevertheless, this work clearly highlighted the importance of a controlled equilibrium between sumoylation and desumoylation, since a small and uncompensated increase in neuronal sumoylation directly impacts synaptic architecture, cell communication and memory formation.**

• RIM1α (Rab3-interacting molecule 1α)

Among the members of the presynaptic active zone that have been extensively studied are the RIM protein family. RIMs are proteins that interact either directly or indirectly with several presynaptic proteins including Rab3a, synapsin-1, Syt1A, Munc13-1, and the voltage-gated Ca^{2+} channels (Calakos et al., 2004) and are thus important for synaptic transmission ***(Fig. 21)***. Although, RIM1α has been implicated in the docking/priming of synaptic vesicles and also in short and long-term synaptic plasticity (Castillo et al., 2002; Dulubova et al., 2005), the regulatory mechanisms underlying RIM1α presynaptic function have not been fully elucidated. The Henley lab reported that RIM1α is a SUMO substrate (Girach et al., 2013). They showed that RIM1α sumoylation occurs only on lysine 502 independently of neuronal activity. Using molecular replacement experiments, they substituted the endogenous RIM1α by the non-sumoylatable RIM1α-K502R mutant, in hippocampal neurons. While the presynaptic localisation of both the WT and non-sumoylatable RIM1α remained unchanged, there was a marked decrease in the

depolarization-evoked SV exocytosis in the K502R mutant indicating that RIM1α sumoylation is required for presynaptic exocytosis (Girach et al., 2013). RIM1α sumoylation was found to enable the clustering of Cav2.1 calcium channels via its binding to RIM1α-SUMO. Altogether, (Girach et al., 2013) uncovered an additional important presynaptic function for the SUMO process.

• CRMP2 (Collapsin response mediator protein 2)

CRMP2 is a microtubule-binding protein that was primarily identified for its roles in the regulation of axonal guidance, neuronal polarity and more recently presynaptic functions including axonal transport and neurotransmitter release (for a comprehensive review, see (Ip et al., 2014), ***Fig. 21***). CRMP2 dynamically interacts with the presynaptic N-type voltage-gated Ca^{2+} channel (CaV2.2) and disruption of this complex reduces pain in a rodent model of neuropathic pain. Thus, investigation into CRMP2 mechanisms of action is a prerequisite for the understanding of its role in pain (Brittain et al., 2011). CRMP2 has been reported to be sumoylated *in vitro* on lysine 374. Using calcium imaging on primary rat cultures of dorsal root ganglion (DRG) neurons, the non-sumoylated form of CRMP2 was shown to affect calcium influx in depolarized DRGs when compared to WT CRMP2 expression, suggesting that CRMP2 sumoylation acts as a negative modulator of presynaptic calcium influx (Ju et al., 2013).

Later, the same group confirmed that both the WT and the SUMO-deficient CRMP2 are robustly expressed in catecholaminergic cells (CAD) and that both forms are able to promote neurite outgrowth in rat DRG neurons (Dustrude et al., 2013). They have also reported that the sodium channel NaV1.7 is regulated by CRMP2 sumoylation. Preventing sumoylation by over-expressing SENP1 and SENP2 enzymes in WT CRMP2-expressing CAD cells decreased the NaV1.7 currents and accordingly, they showed a significant decrease in the levels of surface expressed NaV1.7 in CAD cells expressing the SUMO-deficient form of CRMP2. NaV1.7 currents were also decreased in sensory neurons expressing the non-sumoylatable CRMP2-K374A (Dustrude et al., 2013).

Overall these two reports highlight the putative function of CRMP2 sumoylation in the regulation of the two ion channels. However, the authors did not demonstrate that CRMP2 is sumoylated *in vivo* nor did they determined whether the SUMO modification directly modifies the activity or the surface expression of the two channels targeted by CRMP2. Further work will therefore be required to clarify the functional role of CRMP2 sumoylation at presynaptic sites.

• Kv channels (Voltage-gated potassium ion channels)

Kv channels form potassium-selective pores spanning the plasma membrane ***(Fig. 21)*** and are essential to generating action potentials and controlling neuronal excitability. In human, mutations in Kv channels subunits have been implicated in epilepsies and sudden unexplained death in epilepsy (SUDEP).

Potassium Kv1.1 channels are abundantly expressed in the brain and localize in large axons where they form tetramers with Kv1.2 subunits. These channels regulate the action potential propagation, neuronal firing and neurotransmitter release (Dodson and Forsythe, 2004). Mutations within the human gene encoding Kv1.1 have been associated with partial epilepsy and episodic ataxia in humans (Zuberi et al., 1999). Knock-in mice with Kv1.1 mutations also exhibit hippocampal hyperexcitability, severe epilepsy and premature death (Glasscock et al., 2007). Qi and colleagues engineered a post-natal deficient SENP2 mouse model that develops spontaneous seizures and sudden death (Qi et al., 2014). They reported that the SENP2 deficiency results in increased levels of sumoylation for several potassium channels known to impact neuronal excitability including the Kv1.1 that is modified by both SUMO1/2 and colocalizes with SENP2 in hippocampal neurons. However, the sumoylation of Kv1.1 did not significantly affect its channel properties and activity. Interestingly, the authors have also reported in this work that the Kv7.2 is hyper-sumoylated by SUMO2/3 in hippocampal neurons. Kv7 potassium channels play critical roles in neuronal excitability. Two Kv7 members, Kv7.2 and Kv7.3, are highly expressed in neurons and generate the M-current that is important for firing action potentials. Strikingly, the hyper-sumoylation of Kv7.2 resulted in a significant decrease in the depolarizing M-current in SENP2-deficient hippocampal CA3 neurons and consequently led to neuronal hyperexcitability, severe seizures and ultimately, to sudden death of mice by a maximum of 8 weeks of age (Qi et al.,

2014). Interestingly, these symptoms were prevented by administration of an approved anti-epileptic drug called retigabine. This drug acts as a specific Kv7.2 opener and counteracts neuronal hyperexcitability. However, how this drug impacts the sumoylation levels of Kv7.2/7.3 in hippocampal neurons has not been so far investigated.

Plant and colleagues reported a functional role of Kv2.1 sumoylation in hippocampal neurons (Plant et al., 2011). Kv2.1 potassium channels are important in neurons for activity-dependent excitability. They reported that sumoylation occurs at the lysine 470 residue and showed that two Kv2.1 subunits have to be modified within a functional Kv2.1 tetramer to produce the full SUMO response. Kv2.1 sumoylation led to a 35 mV shift in the half-maximal activation voltage of the functional channel, which resulted in its increased sensitivity to depolarization (Plant et al., 2011). Therefore, sumoylation of Kv2.1 channels provides a way to directly control neuronal excitability.

• Metabotropic glutamate receptors

The Group III mGluRs typically exert presynaptic inhibitory functions. In the past years, several Group III mGluRs have been shown to be sumoylated mainly *in vitro* but some also *in vivo*. To date, no compelling evidence exist regarding the functional roles of SUMO modification in Group III mGluRs, except for mGluR7 (Dutting et al., 2011; Tang et al., 2005; Wilkinson and Henley, 2011; Wilkinson et al., 2008).

mGluR7 is widely expressed at the presynapse modulating excitatory neurotransmission as well as synaptic plasticity by inhibiting neurotransmitter release (reviewed in (Niswender and Conn, 2010)). C-terminal truncated forms of mGluR7 were found to be sumoylated at the K889 residue *in vitro* (Wilkinson and Henley, 2011; Wilkinson et al., 2008). In a recent study, Choi and collaborators confirmed that mGluR7 is a SUMO substrate in vitro (Choi et al., 2016). They have also shown that these receptors are sumoylated *in vivo* both in rat hippocampi and primary cortical neurons with the K889 residue identified as the sole sumoylation site. While, mGluR7 can be sumoylated by both SUMO1 and SUMO2/3 in HEK293T cells, only SUMO1 conjugation was reported in hippocampal homogenates (Choi et al., 2016). Since the sumoylation process has

been directly involved in the endocytosis of glutamate receptors in hippocampal neurons (Martin et al., 2007b), the authors investigated whether sumoylation has an effect on mGluR7 internalization ***(Fig. 21)***. Constitutive agonist-independent endocytosis of the non-sumoylatable mGluR7-K889R mutant was increased compared to the WT control receptor. Addition of L-AP4, an mGluR7 agonist, to the cells expressing WT receptors triggered mGluR7 endocytosis. The increase in agonist-evoked mGluR7 endocytosis was not seen for the non-sumoylatable mutant. The authors attributed this lack of effect to the sumoylation process directly acting on the endocytic pathway. However, they cannot rule out that sumoylation rather impacts on the recycling properties of the pathway. It is indeed likely that sumoylation acts after the endocytosis of mGluR7 by preventing the recycling of the non-sumoylatable receptor. This is in line with their data showing that the overexpression of SENP1, which prevents sumoylation, leads to an increase in the internalized population of WT mGluR7 similar to the values measured for the endocytosed population of the non-sumoylatable mutant in absence of SENP1. This may be explained by a decrease in the SUMO-dependent recycling of internalized mGluR7 to the plasma membrane leading to an increased intracellular pool of receptors. Since this pathway was not assessed, it is difficult to conclude about the exact role of mGluR7 sumoylation in the internalization/recycling process. Since mGlu7Rs are primarily expressed at presynaptic sites (Niswender and Conn, 2010) and this work (Choi et al., 2016) examined the postsynaptic endocytic properties of an over-expressed tagged version mGluR7, it implies that further work will now be necessary to assess the functional impact of mGluR7 sumoylation at presynaptic sites and whether its SUMO modification influences neuronal excitability and/or synaptic transmission and plasticity.

b) Postsynaptic sumoylation

The first demonstration that sumoylation acts directly within the postsynapse has been provided in 2007 with the immunodetection of many unidentified sumoylated substrates in rat hippocampal PSD-95-positive synaptic fractions as well as with the immunolocalisation of the sole SUMO conjugating enzyme Ubc9 (Martin et al., 2007a). In addition, the first synaptic sumoylated substrate was characterized i.e., the kainate receptor (KAR) subunit GluK2, which has

opened new avenues for investigation of the sumoylation process in the brain (Martin et al., 2007a).

Although the precise mechanisms are still lacking, synaptic sumoylation has been shown to play an active role in the control of postsynaptic AMPAR surface expression during chemically evoked synaptic plasticity. Upon chemical LTP, Jaafari and colleagues observed an increase in both dendritic and synaptic SUMO1 immunoreactivity as well as a large increase in Ubc9 and SUMO1 mRNAs in soma and dendrites (Jaafari et al., 2013). Interestingly, the over-expression of a catalytically active domain of the desumoylase SENP1, but not its catalytically inactive mutant, prevented the increase in SUMO1 mRNA and in surface expressed AMPAR upon Chem-LTP (Jaafari et al., 2013).

A year later, the sumoylation process was reported as indispensable for the expression of LTP (Lee et al., 2014). By combining the use of WT or catalytically inactive forms of the cell permeable TAT-Ubc9 and LTP protocols in acute CA1 hippocampal slices, the authors showed that LTP is significantly reduced when sumoylation is prevented by the dominant negative Ubc9 mutant (Lee et al., 2014). This LTP inhibition was observed without any impact on basal transmission. The authors confirmed their initial results using the catalytic domain of the desumoylase SENP1 in the patch pipette as used previously in (Martin et al., 2007a). They showed that inclusion of the active SENP1, but not its catalytically inactive mutant, fully blocked the induction of LTP in CA1 pyramidal neurons confirming that the SUMO pathway is involved in the expression of long-term plasticity events (Lee et al., 2014). They subsequently demonstrated that infusion of the dominant negative form of TAT-Ubc9 *in vivo* impairs the hippocampal-dependent learning and memory (Lee et al., 2014).

• Regulatory mechanisms of sumoylation at the postsynapse

Despite numerous publications demonstrating the postsynaptic involvement of sumoylation, some of the mechanisms regulating this PTM were reported much later (Loriol et al., 2014). Using a combination of pharmacological tools with synaptic biochemistry and restricted

photobleaching/photoconversion of individual hippocampal spines, our group demonstrated that the synaptic diffusion of Ubc9 is regulated by synaptic activity on a rapid timescale. The synapto-dendritic diffusion of Ubc9 remains unchanged upon the activation of NMDA receptors but is altered by the activation of mGluR5 ***(Fig. 21)***. Increasing synaptic activity by the application of a $GABA_A$ receptor antagonist or direct activation of mGlu5R prolongs the synaptic residency of Ubc9 in a PKA-independent but PKC-dependent manner. The Ubc9 transient trapping in spines is a result of the enhanced ability of Ubc9 to recognise synaptic PKC-phosphorylated substrates, that consequently leads to an increase in synaptic sumoylation levels and modulation of neuronal communication (Loriol et al., 2014). Despite this first demonstration of an activity-dependent regulation of postsynaptic sumoylation, future work will be required to identify the nature of synaptic SUMO substrates, which will further help to better understand the functions of synaptic sumoylation.

As a matter of fact, our laboratory (with my participation) has been working on identifying the native **endogenous synaptic SUMO2-ylome** from young rat brains using a mass spectrometry approach. This ongoing work has yielded many already known as well as novel synaptic sumoylation substrates. Additional experiments are being performed to confirm the specificity of identified proteins before these data will be submitted for publication. To follow up on the story of synaptic regulation of Ubc9, I have investigated the **molecular mechanisms behind the synaptic diffusion of the desumoylation enzyme SENP1 (the subject of my PhD thesis)**. This work will greatly add to the general knowledge of synaptic sumoylation and provide insights into the mechanisms that control for the activity-dependent equilibrium between sumoylation and desumoylation at the mammalian synapse (Schorova *et al.*, in preparation; **Annexed Article 3**).

• FMRP (Fragile X Mental Retardation Protein)

FMRP is an mRNA binding protein, a component of the RNA granules that transport translationally repressed mRNAs to synaptic sites, where synaptic activity promotes their translation in an mGluR5-dependent manner. Loss of FMRP leads to the most common monogenic cause of autism and intellectual disability, the Fragile X syndrome (FXS; for a review see (Maurin et al., 2014)). At the cellular level, the absence of FMRP leads to a pathological hyper-

abundance of long thin (immature) dendritic filopodia in *Fmr1* $^{-/y}$ rodents (Mientjes et al., 2006). Presumably, these structural synaptic defects translate into previously reported impairments in synaptic transmission and plasticity as well as deficits in social and cognitive behaviours in the FXS animal models (Mientjes et al., 2006).

FMRP-containing RNA granules often localise at the base of dendritic spines (Bassell, 2011). Upon synaptic activation, mRNAs are released from the granules for local translation (Maurin et al., 2014). FMRP phosphorylation inhibits the translation of associated mRNAs, whereas dephosphorylation promotes it (Narayanan et al., 2007) (Niere et al., 2012). Moreover, mGluR5 activation induces FMRP dephosphorylation and subsequent ubiquitination targeting FMRP for the UPS degradation (Nalavadi et al., 2012). Our team now provides evidence that FMRP is a sumoylation target *in vivo* (Khayachi *et al.*, 2018; **Annexed Article 2**, ***Fig. 21***). In response to mGluR5 activation, we identify three lysines (K88, 130 and 614) as the major sumoylated residues in FMRP. Preventing sumoylation on these lysines (K to R mutations) leads to a complete loss of FRMP sumoylation. We report that reintroducing WT FMRP into *Fmr1* $^{-/y}$ neurons restores the mature phenotype of dendritic spines, whereas the non-sumoylatable FMRP mutant fails to do so. Interestingly, the expression of the non-sumoylatable FMRP in WT neurons reverses the WT phenotype toward the FXS-like phenotype. These results clearly demonstrate that FMRP sumoylation is essential for spine density and maturation. However, what are the molecular mechanisms behind sumoylation of FMRP in the regulation of spine maturation?

To address this, we performed extensive biochemical and live imaging analyses to evidence the essential role of sumoylation in FMRP-mediated neuronal function. We expressed the non-sumoylatable form of FMRP in *Fmr1*$^{-/y}$ neurons, which did not affect the mRNA binding within dendritic RNA granules nor their transport along dendrites. In addition, these granules still contained known RNA-binding proteins commonly present in RNA granules. Intriguingly however, the non-sumoylatable FMRP-containing RNA granules were significantly larger starting from 48h post-transfection. In normal conditions, FMRP forms homodimers within RNA granules, which was a characteristic that remained unaffected upon the expression of the non-

sumoylatable FMRP in *Fmr1* $^{-/y}$ neurons. We then used live imaging to test the dissociation ability of FMRP from RNA granules. We measured that the exit of WT FMRP from granules upon Dendra2-FMRP photoconversion was much faster when compared to the non-sumoylatable mutant. Upon mGluR5 activation, WT FMRP dissociation was further enhanced, whereas no effect was detected in the non-sumoylatable mutant. Taking into account the impaired dynamics of the non-sumoylatable FMRP within the RNA granules and that this mutant is still able to bind mRNA and form homodimers, we reasoned that sumoylation may play a role in disruption of these homodimers and therefore their release from RNA granules. To test this, we performed an *in vitro* sumoylation assay ***(Fig. 22A)***. After the immobilisation of WT GST-FMRP to the Glutathione-Sepharose beads, WT His-FMRP was added to form GST-FMRP – His-FMRP dimers. Then, the addition of a sumoylation reaction (E1, E2 and SUMO) will have supposedly disrupted these dimers ***(Fig. 22A)***. Indeed, His-FMRP was detected in the unbound fraction confirming our hypothesis that sumoylation promotes FMRP homodimers dissociation.

In short, we found that mGluR5-mediated FMRP sumoylation is essential for proper spine maturation and control of dendritic spine density through a mechanism possibly involving FMRP dissociation from dendritic mRNA granules ***(Fig. 22B)***. This is a significant discovery that may

Figure 22.

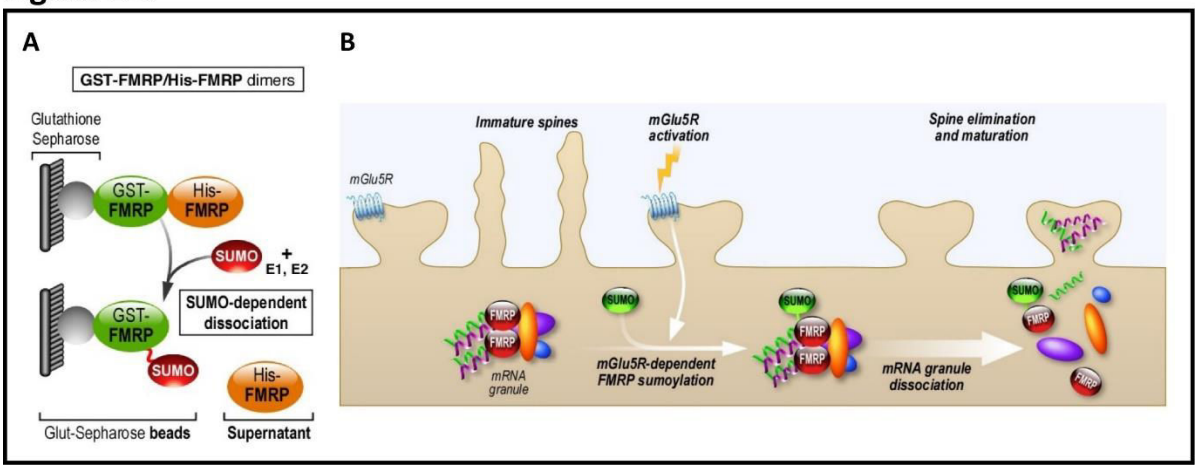

Figure 22: **In vitro FMRP sumoylation assay and FMRP mechanism of action in dendrites**. **A.** Schematic of the SUMO-dependent dissociation assay showing the release of His-FMRP from the immobilized sumoylated GST-FMRP into the supernatant. **B.** Model of the mGlu5R-dependent regulation of FMRP function by sumoylation. The activity-dependent sumoylation of FMRP is a key step to dissociate FMRP from dendritic mRNA granules and consequently to regulate spine elimination and maturation.

prove useful when developing new therapeutic strategies for FXS (Khayachi *et al*., 2018; **Annexed Article 2**).

• Kainate receptors

The GluK2 subunit directly interacts with the conjugating enzyme Ubc9 and is a sumoylation substrate in rat hippocampal neurons ((Martin et al., 2007a), ***Fig. 21***). GluK2 sumoylation by SUMO1 occurs in an activity-dependent manner on its C-terminal domain at the single lysine K886. Importantly, several additional reports have confirmed GluK2 sumoylation in neurons (Choi et al., 2016; Konopacki et al., 2011; Zhu et al., 2012). At the postsynapse, binding of glutamate or kainate to GluK2 leads to its sumoylation at the plasma membrane and represents a trigger for the activated receptors to be internalized. Interestingly, postsynaptic KAR responses at hippocampal Mossy fiber-CA3 synapses decrease when postsynaptic sumoylation is promoted by infusing SUMO1 postsynaptically and conversely, postsynaptic responses largely increase upon desumoylation by the infusion of SENP1 catalytic domain (Martin et al., 2007a). Consistent with earlier publication (Martin and Henley, 2004), PKC activation has been shown to be essential to GluK2 internalization (Chamberlain et al., 2012; Konopacki et al., 2011). PKC phosphorylation at serine 868 in GluK2 is a prerequisite for its sumoylation and its subsequent endocytosis that occurs during LTD of KAR-mediated synaptic transmission (Chamberlain et al., 2012; Konopacki et al., 2011). Thus, these data revealed that the activity-dependent interplay between phosphorylation and sumoylation of GluK2 is important for KAR-mediated synaptic communication and plasticity.

• Arc (Activity-regulated cytoskeleton-associated protein/activity-regulated gene 3.1)

Transcription of Arc gene is strongly induced by synaptic activity. Arc mRNAs are rapidly transported into dendrites where they undergo local translation at synaptic sites. Arc exhibits key roles in protein synthesis-dependent forms of synaptic plasticity and in consolidating different forms of memory (reviewed in (Bramham et al., 2010)).

The Henley group reported that Arc is a sumoylation substrate with the lysine 110 and 268 residues being the sites of sumoylation ((Craig and Henley, 2012), ***Fig. 21***). A new piece of data by Nair and co-workers showed that upon LTP consolidation the newly synthesized Arc undergoes rapid SUMO1-ylation *in vivo* in the dentate gyrus of live adult rats (Nair et al., 2017). SUMO1-ylated Arc is concentrated in synaptic and cytoskeletal fractions. In addition, the SUMO1-modified Arc was omitted from the PSD-95-, CaMKIIβ- and dynamin 2-containing protein complexes, where the unmodified Arc is usually detected upon basal conditions. On the other hand, in the cytoskeletal fraction, SUMO1-Arc was reported to form complexes with drebrin A, a regulator of F-actin stability in spines. These results evidence a model in which SUMO1-ylation targets Arc for regulation of actin cytoskeletal dynamics during *in vivo* LTP (Nair et al., 2017).

Altogether, the data from the above sections clearly establish that the sumoylation machinery is partly targeted to, localized and regulated at pre- and postsynaptic sites to modulate, in an activity-dependent manner, the levels of synaptic sumoylation and in turn, the synaptic function. Furthermore, a growing number of SUMO substrates have been recently identified in axons, dendrites and synapses and were shown to fulfil essential physiological functions on synaptic communication and plasticity (Chamberlain et al., 2012; Chao et al., 2008; Craig et al., 2015; Craig and Henley, 2012; Girach et al., 2013; Jaafari et al., 2013; Konopacki et al., 2011; Loriol et al., 2014; Loriol et al., 2013; Martin et al., 2007a; Shalizi et al., 2007; Shalizi et al., 2006; Tai et al., 2016; Tang et al., 2015) **providing additional evidence that the sumoylation process is an essential modulator of synaptic function.**

NOTE

The existence of synaptic sumoylation was directly challenged by the laboratory of Nils Brose

A certain discrepancy arose with a study using a double-tagged His-HA-SUMO1 knock-in (KI) mouse model in combination with mass spectrometry analysis. The authors failed to detect any synaptic SUMO substrates nor did they localise His-HA-SUMO1 at synapses (Tirard et al., 2012). The explanation for these rather physiologically improbable results could be the decreased levels

of SUMO1 conjugation by ~20-30% reported in the brains of KI animals compared to WT animals (Tirard et al., 2012). Moreover, the ~20-30% decrease in SUMO1-ylation in the brains of KI animals was accompanied by a corresponding increase in SUMO2/3-ylation indicating a compensatory effect. This suggests that the dual SUMO1 tag impairs the sumoylation process, and therefore the His-HA-SUMO1 KI model seems unsuitable for sumoylation studies. Indeed, in our laboratory, we have the experience (unpublished data) of a very poor HA-SUMO conjugation capacity, compared to other tags (e.g. His, myc, GFP, …), and for this reason we aim to eschew using the HA-SUMO constructs. It should be also emphasized, that synaptic sumoylation occurs at quite low levels, when compared to e.g. nuclear SUMO-conjugation, therefore in the His-HA-SUMO1 KI mice that have ~20-30% less of overall brain SUMO1-ylation, the synaptic sumoylation levels may simply become too low and below the detection sensitivity of the methods employed.

Despite the significant controversy of this study and especially the use of the His-HA-SUMO1 KI model (Tirard et al., 2012), the same laboratory went on to argue against the SUMO1-modification of many already identified and validated synaptic sumoylation substrates, once again using mainly the His-HA-SUMO1 KI model (Daniel et al., 2017), omitting the assessment of these substrates in WT rodents. The distressing conclusion of this report was the non-existing functional relevance of SUMO1-modification at the synapse. The scientific community of neuronal sumoylation (including our laboratory), was therefore instigated to react and published a commentary questioning this latter report in a step by step rationalising of this misleading piece of research data (Wilkinson et al., 2017). In brief, first, Tirard and co-workers do not provide a comparison of SUMO1-ylation between KI and WT mice or rat, nor they examine the very likely compensation by SUMO2/3-ylation of synaptic proteins. Second, no functional studies were performed to devaluate synaptic SUMO1-modification in synaptic and neuronal function. Third, they used an anti-GluK2 antibody for GluK2 detection that is unable to recognise the sumoylated form of GluK2 because its epitope is masked by the SUMO protein binding. Forth, they provide a very vague nuclear staining in both KI and WT neurons, suggesting that the synaptic staining is most likely below the threshold of detection (Wilkinson et al., 2017).

Nonetheless, a large body of studies from independent groups worldwide including ours demonstrate that SUMO1- and SUMO2/3-ylation take place in neurons and at synapses to regulate neuronal and synaptic function.

1.5 Subject of thesis study:

Investigating the molecular pathways driving the sumoylation/desumoylation balance in rat hippocampal synapses.

❖ SENtrin specific Proteases (SENPs)

The sumoylation state of a protein is a key determinant that regulates target proteins' function. The levels of protein sumoylation are delicately regulated by the SUMO-conjugation (E1/Ubc9/E3) and SUMO-deconjugation (SUMO proteases). These pathways work in synergy to respond to diverse molecular stimuli. SUMO-deconjugation is catalysed by three families of cysteine proteases: Ulp/SENP, DeSI and USPL. SENP proteases are the mammalian counterparts of the yeast Ulp1 and Ulp2 enzymes ***(Fig. 23B)***. There are six human SENPs (SENP1-3 and 5-7; ***Fig 23A***). SENP proteases differ in their subcellular localisation ***(Table 2)***, SUMO paralog specificity, the efficiency of endopeptidase and isopeptidase activity and the ability to cleave monomeric SUMO or poly-SUMO chains ***(Fig. 23C)***. All SENPs contain a conserved C-terminal catalytic domain

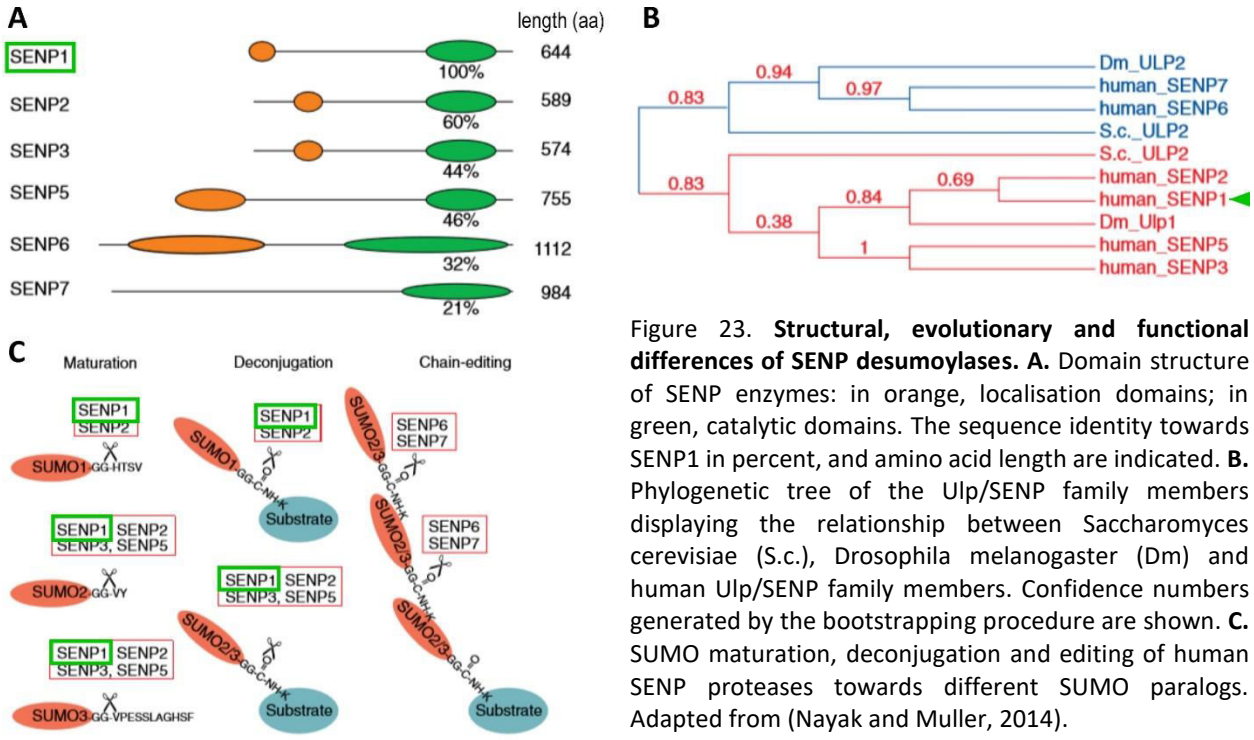

Figure 23. **Structural, evolutionary and functional differences of SENP desumoylases. A.** Domain structure of SENP enzymes: in orange, localisation domains; in green, catalytic domains. The sequence identity towards SENP1 in percent, and amino acid length are indicated. **B.** Phylogenetic tree of the Ulp/SENP family members displaying the relationship between Saccharomyces cerevisiae (S.c.), Drosophila melanogaster (Dm) and human Ulp/SENP family members. Confidence numbers generated by the bootstrapping procedure are shown. **C.** SUMO maturation, deconjugation and editing of human SENP proteases towards different SUMO paralogs. Adapted from (Nayak and Muller, 2014).

and an N-terminal domain that is likely involved in their subcellular localisation and protein-protein interactions ***(Fig. 23A)***.

SUMO protease	Subcellular localisation
SENP1	Mainly nucleus and subnuclear structures. Also cytoplasm and other cytosolic compartments such as the **SYNAPSE.**
SENP2	Mainly nucleus and subnuclear structures. Also cytoplasm and other cytosolic compartments.
SENP3	Nucleolus, and extranuclear compartments such as mitochondria
SENP5	Nucleolus, and extranuclear compartments such as mitochondria and the **SYNAPSE.**
SENP6	Nucleus and cytosol including the **SYNAPSE**
SENP7	Nucleoplasm

Table 2. **Subcellular localisation of SENP proteases**. Adapted from (Henley et al., 2014). See text for more references.

Sentrin-specific protease 1 (SENP1)

Importantly, three of the SUMO proteases: SENP1, SENP5 and SENP6, have been reported to be present at synapses (Loriol et al., 2012) (Loriol et al., 2013) (Akiyama et al., 2017), therefore they presumably play a role in synaptic function. In my PhD thesis, I focused on the study of the sentrin-specific protease 1. SENP1 is a SUMO-maturing and SUMO-deconjugating enzyme expressed ubiquitously in all eukaryotic cells. Knocking-out SENP1 (SENP1 $^{-/-}$) leads to severe anaemia due to erythropoiesis defects, and causes embryonic or early postnatal lethality (E15.5 – P1) in mice (Yu et al., 2010) (Cheng et al., 2007). Specifically in the brain, the exact function of SENP1 is yet to be determined. However, a 2014 study showed that the ablation of functional SENP2 in the neural progenitor cells by Nestin-Cre (SENP2$^{\Delta SUMO}$-Nes) causes paralysis (at P16) and death in mice by 3 weeks of age (Fu et al., 2014a). Although the mutant embryos developed normally, in early postnatal life, these mice started to display severe neurodegeneration. The underlying mechanism was identified to involve SENP2 regulation of SUMO1-modification of dynamin-related protein 1 (Drp1) that controls mitochondrial dynamics. Targeted disruption of SENP2 induced neurodegeneration through promotion of Drp1 sumoylation and mitochondrial

fragmentation leading to cell death (Fu et al., 2014a). Future research could address the brain-specific role of SENP1 applying a similar strategy. In regard to SENP1 disruption in non-neuronal cells, RNAi knockdown of SENP1 was shown to induce p53-dependent senescence in human fibroblasts (Yates et al., 2008). SENP1 was also reported to play a crucial role in chromosome segregation during mitosis, and nucleoporin homeostasis in HeLa cells (Cubenas-Potts et al.,

Figure 24.

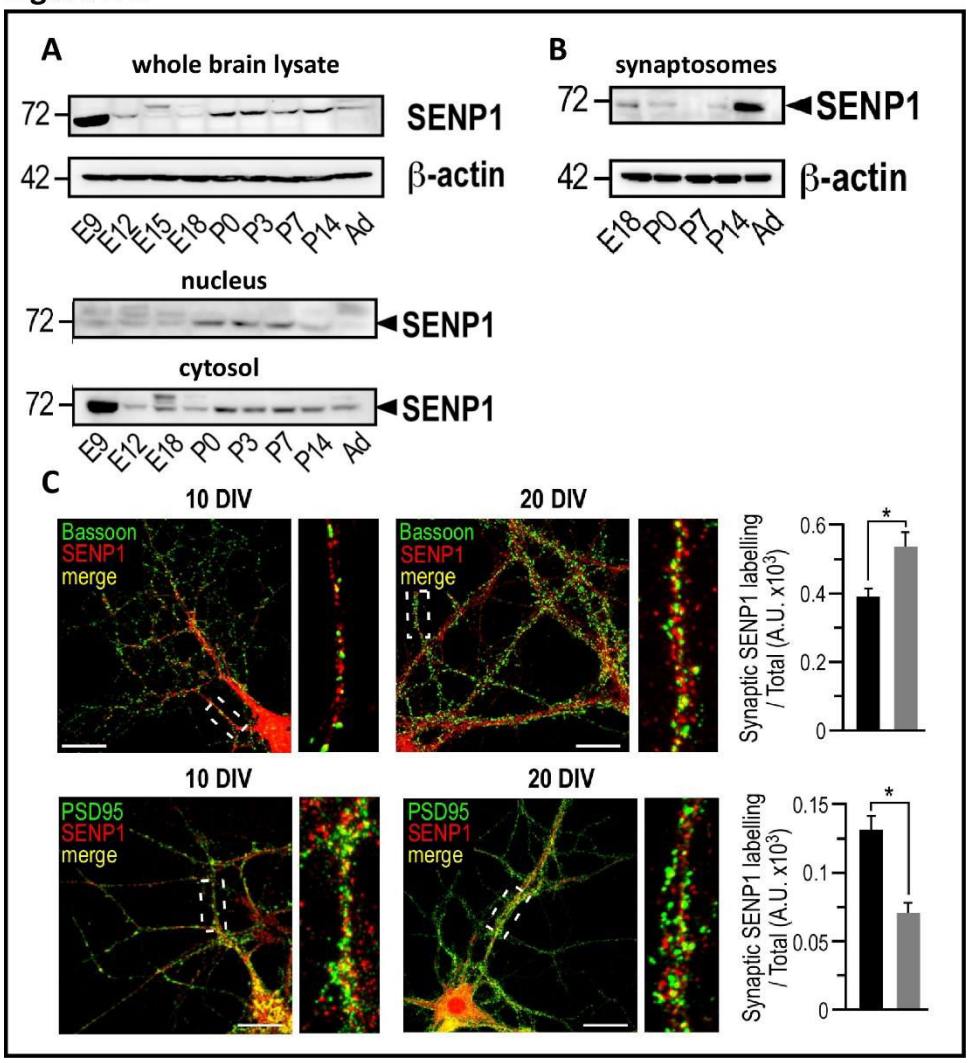

Figure 24. **Developmental regulation of SENP1 distribution in the rat brain. A.** Immunoblots of whole rat brain homogenates, nuclear and cytosolic fractions (obtained via subcellular fractionation of whole brains). **B.** Immunoblots of the synaptosomal preparation (obtained through subcellular fractionation of whole brains and sucrose gradient separation). All Immunoblots were prepared with samples at different ages as indicated: from the embryonic day 9 (E9) to adult stage (Ad). **C.** Confocal images of fixed rat hippocampal neurons (10 and 20 DiV) that were immunolabeled for a presynaptic (Bassoon) marker, postsynaptic (PSD-95) marker and SENP1. On the right are graphical quantifications of the colocalisation of SENP1 and a synaptic marker. Scale bars = 20 µm Taken and adapted from (Loriol et al., 2012).

2013) (Chow et al., 2014). According to these studies we can state that SENP1 is an essential and tightly spatiotemporally regulated protein with key cellular regulatory functions.

Our team has previously shown that endogenous SENP1 protein levels are dynamically regulated and change during brain development in the rat ((Loriol et al., 2012), ***Fig. 24***). The highest expression was found at the earliest time point examined (E9), followed by a marked decrease until birth (P0) when the levels slightly rise and are established low in the adult brain ((Loriol et al., 2012), ***Fig. 24A***). Upon neuronal cell fractionation, nuclear SENP1 levels were shown to be low during embryonic development with a slight increase early postnatally (P0-P7), and very low levels of SENP1 were detected in the nuclei of the adult brain ((Loriol et al., 2012),

Figure 25.

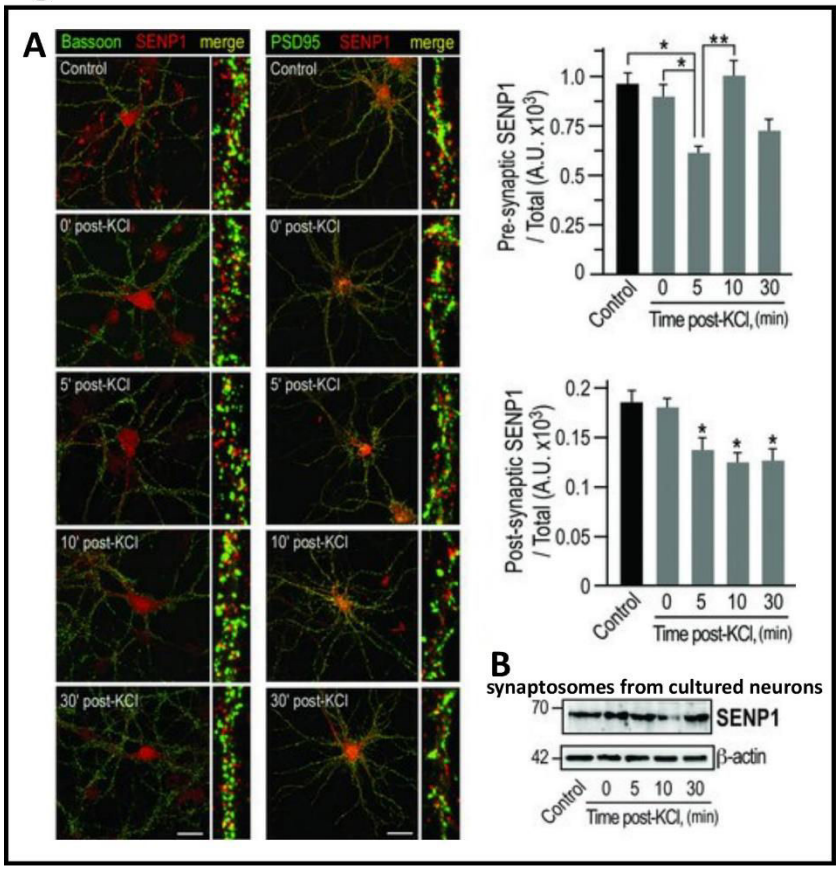

Figure 25. **Neuronal activity-dependent regulation of SENP1 redistribution at the synapse. A.** Confocal images of rat hippocampal neurons (20 DiV) that were stimulated with KCl (60 mM, 90s) and fixed at different time points post-KCl as indicated. Immunolabeling was performed for a presynaptic (Bassoon, left) marker, postsynaptic (right, PSD-95) marker and SENP1. On the right are graphical quantifications of the colocalisation of SENP1 and a synaptic marker. Scale bars = 20 µm **B.** Immunoblots of synaptosomal preparations (obtained through subcellular fractionation of neuronal homogenates and sucrose gradient separation). Prior to synaptosomal preparation, neurons were treated with KCl (60 mM, 90s) and homogenised at different time point post-KCl as indicated. Taken and adapted from (Loriol et al., 2013).

Fig. 24A). Cytosolic expression of SENP1 was high at E9, then decreased and stabilized at low levels early postnatally and in the adult brain ***(Fig. 24A)***. Interesting however, is the finding that SENP1 is found at very high levels in synaptosomes from adult rat brains compared to late embryonic and early postnatal brains ((Loriol et al., 2012), ***Fig. 24B***). In cultured hippocampal neurons, SENP1 colocalisation with the presynaptic marker Bassoon increases during neuronal maturation (10 DiV vs 20 DiV). On the other hand, SENP1 colocalisation with the postsynaptic marker PSD-95 decreases upon neuronal maturation (10 DiV vs 20 DiV; (Loriol et al., 2012), ***Fig. 24C***). These data clearly demonstrate a fine developmental regulation of SENP1 expression in the maturing rat brain. Our laboratory has also examined the activity-dependent redistribution of endogenous SENP1 at synapses in cultured rat hippocampal neurons ((Loriol et al., 2013), ***Fig. 25***). Upon KCl-evoked depolarisation of neurons (90s exposure to 60 mM KCl), SENP1 levels were measured according to the colocalisation with presynaptic (Bassoon) and postsynaptic (PSD-95) markers at 4 time points (0, 5, 10 and 30 min). SENP1 staining was strongly decreased 5 min after depolarisation at presynaptic sites. This SENP1 decrease was transient as SENP1 levels were restored after 10 min post-depolarisation ***(Fig. 25A)***. At the postsynapse, SENP1 colocalisation with PSD-95 decreased and remained decreased even 30 min post-depolarisation ***(Fig. 25A)***. Noteworthy, whole synaptosomal preparation (pre- and post-synaptic fraction) from 20 DiV hippocampal neurons showed that synaptic SENP1 levels do not change following KCl depolarisation ((Loriol et al., 2013), ***Fig. 25B***) These results suggest that SENP1 is regulated at synaptic sites in response to changes in neuronal activity. **The mechanisms of SENP1 regulation at synapses have been investigated in my PhD thesis and are presented in this manuscript** as well as in the **Annexed Article 3** (Schorova *et al.*, in preparation).

Working hypothesis

The posttranslational modification by sumoylation is a vital eukaryotic process. In the central nervous system, extra-nuclear sumoylation has emerged as a crucial mechanism regulating functions of many neuronal proteins, being involved in neuronal differentiation and survival, and the control of synaptic formation, plasticity and transmission. Moreover, disruption to the protein sumoylation/desumoylation balance in the brain has been implicated in severe neurological diseases ***(Table 1)***. Therefore, prior to being able to provide innovative therapeutic strategies, it is inevitable to understand the regulatory mechanisms leading to both protein sumoylation and desumoylation. Recent data from our laboratory have elucidated some of the regulatory cues of the sole SUMO-conjugating enzyme Ubc9 at postsynaptic sites ***(Fig. 26)***. Using live-imaging and biochemical approaches Loriol and co-workers showed that Ubc9 is transiently trapped in dendritic spines in response to mGluR5 activation. Moreover, Ubc9 trapping occurs via its recognition to PKC-phosphorylated proteins. Synaptic sumoylation levels increase upon mGluR5/PKC activation at synapses after 10 min of agonist treatment of isolated synaptosomes.

Figure 26.

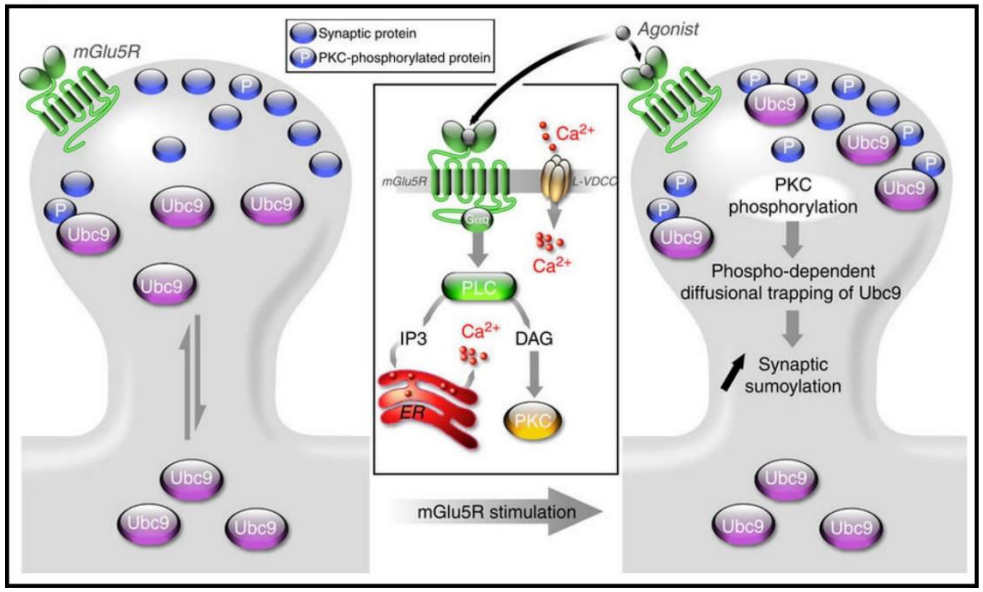

Figure 26. **Schematic model of Ubc9 regulation at postsynaptic sites.** Ubc9 enzyme diffuses between dendritic shaft and spine. Upon the mGluR5/PLC/PKC cascade activation, PKC phosphorylates synaptic proteins, which consequently leads to Ubc9 transient trapping in spines and increase in synaptic sumoylation levels (Loriol et al., 2014). Until now, the synaptic regulation of SUMO proteases has not been investigated.

Importantly, the half time of Ubc9 synapto-dendritic diffusion is ~0.5 s, and the mGluR5/PKC-driven trapping prolongs this time to ~1 s (Loriol et al., 2014). I intentionally refer to the findings on Ubc9, as I have used similar approaches to investigate the regulatory pathways of SENP1 synapto-dendritic diffusion, adding to the knowledge of how the balance between sumoylation and desumoylation at synapses is regulated.

To advance our understanding of the sumoylation/desumoylation balance at synapses, I aimed, in my PhD thesis, to identify the regulatory cues of the desumoylation enzyme SENP1 at rat hippocampal synapses. **My results show that SENP1 synaptic localisation increases upon sustained synaptic activity. This finding prompted me to investigate in detail the following objectives:**

1. ***What are the dynamic properties (synaptic entry vs exit) of SENP1 synapto-dendritic diffusion that could explain SENP1 synaptic targeting?***
2. ***Activation of which glutamatergic receptor/s leads to an increase in synaptic SENP1?***
3. ***Upon the identification of upstream receptor/s, what are the further signalling players in SENP1 diffusion?***
4. ***What are the effects on synaptic sumoylation levels when activating SENP1 upstream regulators that have been identified in previous objectives?***

By accomplishing these objectives, I will propose the first ever conception for regulation of synaptic sumoylation balance.

Experimental approaches

To unveil the regulatory mechanisms of SENP1 at synapses I used a range of experimental approaches such as **microscopy imaging** (including spinning disc confocal microscopy: fluorescence recovery after photobleaching [FRAP] and photoconversion; and classical confocal microscopy of immuno-labelled fixed cells), **biochemistry** (purification of PSD-enriched fractions from cultured neurons and Western blot), all of which were performed in combination with **pharmacological intervention** to target putative SENP1 upstream regulators. For all the abovementioned techniques I used mature primary rat cortical and hippocampal neurons in culture aged 18-21 DIV. Importantly, these cultures contain ~90% of glutamatergic pyramidal neurons, whereas GABAergic interneurons represent ~10%. Cultures were prepared from 17-day-old foetal wild-type Wistar rats as previously described (Loriol et al., 2013).

1. Live-cell imaging to dissect the dynamic properties of SENP1 spino-dendritic diffusion

a) Long duration time-lapse imaging

One of the first questions that I asked when investigating the upstream signalling of synaptic SENP1 was whether changes in synaptic activity by pharmacological means alter SENP1 spino-dendritic distribution. To probe the dynamic behaviour of SENP1, Sindbis virus for mRNA delivery to express GFP-SENP1 in neurons was implemented. I used time-lapse live-cell spinning disc confocal imaging together with a perfusion system for a direct media exchange. I used bicuculline, a $GABA_A$ receptor inhibitor, to potentiate glutamate release and thus to trigger synaptic activation. The fluorescence intensities were analysed in dendritic spines and shafts to detect changes in SENP1 spino-dendritic redistribution throughout the duration of each experiment recording.

b) Synaptic entry vs exit of SENP1

Time-lapse imaging itself, however, cannot reveal protein's kinetic properties (i.e. type of movement such as free diffusion, transient or more stable bindings to scaffolds or other cellular components; as well as measurement of mobility speed and mobile/immobile fractions). To understand the kinetic properties of SENP1 spino-dendritic diffusion I used two complementary advanced imaging techniques: Fluorescence Recovery After Photobleaching (FRAP; ***Fig. 27***) and photoconversion ***(Fig. 28)***. FRAP enables to determine the diffusion properties of SENP1 entry into dendritic spines (described in more detail in ***Fig. 27***). On the other hand, photoconversion provides information about synaptic exit of SENP1 ***(Fig. 28)***. A combination of these two imaging techniques, as used throughout my thesis project, is important to understand how different pharmacological interventions, and therefore neuronal/synaptic activation together with the

Figure 27.

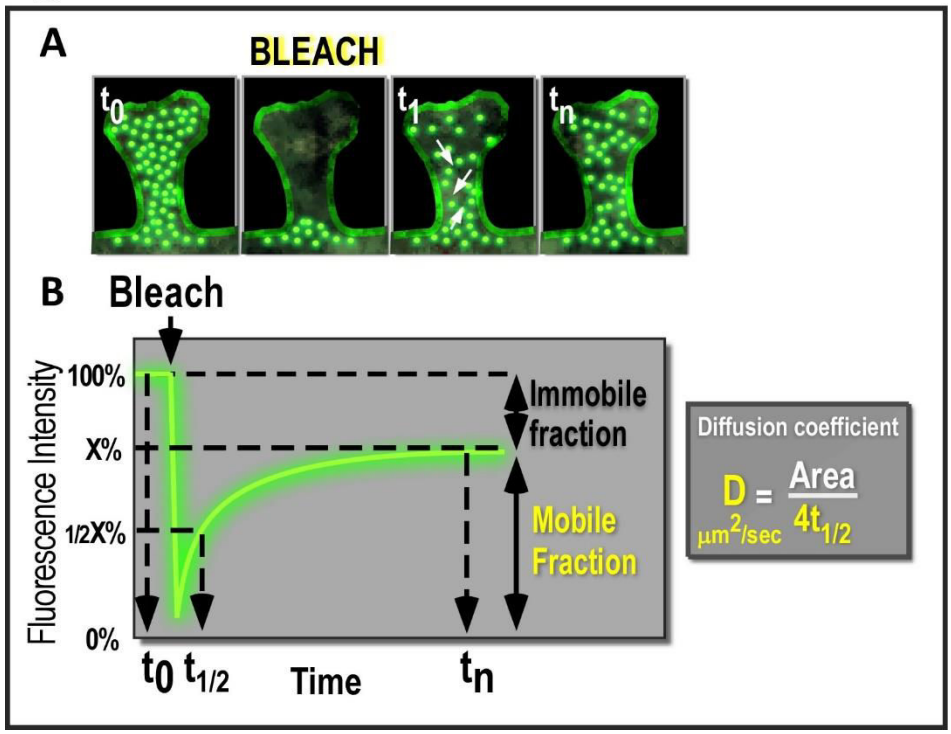

Figure 27. **The principle of Fluorescence Recovery After Photobleaching (FRAP)**. **A.** A high power laser beam targeted to a restricted area, here a dendritic spine, photobleaches exogenously expressed fluorescently labelled proteins (e.g. GFP-SENP1). As the non-bleached molecules from dendritic shaft diffuse toward a spine, a fluorescence recovery can be observed. **B.** A typical FRAP curve, from which several diffusion properties can be determined: *half time of recovery* ($t_{1/2}$) that represents recovery time of 50% of fluorescence of the mobile fraction; *mobile and immobile fractions* stand for the percentage of fluorescence that did and did not recovered, respectively. *Diffusion coefficient* represents the speed of recovery and can be calculated based on the size of the bleach area and the half time recovery.

action of putative regulators of SENP1, affect SENP1 spino-dendritic dynamics. In doing so, I aimed to identify novel upstream regulatory mechanisms of SENP1 at synapses.

Figure 28.

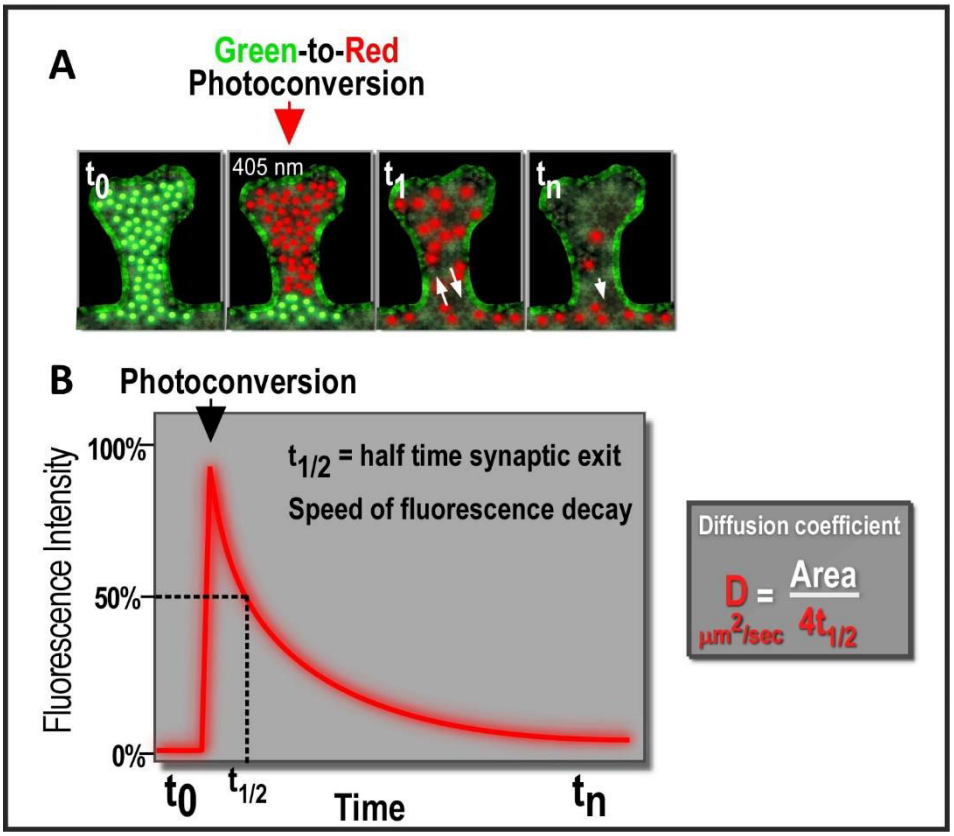

Figure 28. **The principle of photoconversion. A.** Restricted photoconversion in cells expressing a protein of interest conjugated to a photoswitchable fluorescent tag (here Dendra2-SENP1) allows to track the movement of photoconverted molecules from a restricted area, here a dendritic spine. Dendra2 photoconversion is triggered by 405nm laser beam leading to its conformational change and excitation at 561 nm (Chudakov et al., 2007). **B.** A typical photoconversion curve showing the decay of fluorescence as photoconverted molecules exit from a restricted area. Speed of fluorescence decay is given by diffusion coefficient and is calculated based on the size of photoconverted area and half time fluorescence decay/synaptic exit.

2. Investigation into endogenous synaptic SENP1

To examine whether the findings that concern exogenously expressed SENP1 apply to the endogenous SENP1, and therefore may be of a functional importance to the neuronal/synaptic function, I used corresponding pharmacological treatments as in live-cell imaging, but this time I performed immunocytochemistry to quantify SENP1 localisation in dendritic spines using the postsynaptic marker PSD-95. In addition, I performed subcellular fractionation from cultured rat

cortical neurons and measured SENP1 levels in PSD fractions to investigate the level of SENP1 at synapses upon synaptic activation. Here, I describe the isolation of PSD fraction that is referred to as the Triton Insoluble Fraction (TIF):

Triton X-insoluble Fraction (TIF) isolation

TIF fractions were prepared according to established protocols (Gardoni et al., 2009; Gardoni et al., 2003) (Phair and Misteli, 2001) using 18-20 DIV rat cortical neurons (5 x 100 mm dishes per condition with 2.5 x 10^6 cells). Prior to the isolation neurons were treated for 40 min with control solution (Earle's buffer + vehicle), or with Earle's buffer containing bicuculline (10 µM) or DHPG (50 µM). Neurons were then immediately cooled down on ice and homogenized in ice-cold sucrose buffer (1 mM HEPES pH 7.4; 0.32 M sucrose; 1 mM EDTA; 1 mM $MgCl_2$, 1 mM $NaHCO_3$; Mammalian protease inhibitors [Roche] containing 20 mM NEM [Sigma-Aldrich]). Nuclear proteins were removed from the synaptosomal preparation by centrifugation at 200g for 5 min (this step was repeated two times). Post-nuclear fractions were further centrifuged at 13,000g for 15 min to isolate crude synaptosomal fractions. Crude fractions were then resuspended in lysis buffer (75 mM KCl, 1% Triton X100 in presence of 20 mM NEM) and TIF fractions purified by centrifugation at 100,000g for 1h. Finally, TIF fractions were collected and resuspended in Urea-containing lysis buffer (50 mM Tris-HCl pH 6.8, 2% SDS, 10% glycerol and 8M Urea). Protein concentrations were determined (BioRad) and samples were heated at 95°C in Laemmli buffer for 10 min.

3. Pharmacological intervention to target SENP1 upstream regulators

The pharmacological targeting of key steps in intracellular signalling is a common approach for identifying regulatory mechanisms of studied pathways. I acquired this approach and used specific agonists and antagonist to target key neuronal receptors such as $GABA_A$, NMDAR and GluR1/5 to dissect upstream regulatory mechanisms of SENP1 at synapses. Moreover, I used specific pharmacological agents to block or destabilise additional regulatory molecules, e.g. microtubules, which could play a role in SENP1 regulation at synapses. Importantly, all these pharmacological agents were previously validated for use in neuronal cultures:

- *Bicuculline*: $GABA_A$ receptor competitive antagonist (Curtis et al., 1970). Its application leads to increase in glutamate release and thus potentiation of synaptic activation. Used at 10 µM concentration.
- *AP5*: NMDAR antagonist (Davis et al., 1992). Used at 50 µM.
- *DHPG*: mGluR1 and 5 selective agonist (Ito et al., 1992). Used at 50 µM.
- *MPEP*: selective non-competitive antagonist of mGluR5 (Gasparini et al., 1999). Used at 30 µM.
- *JNJ 16259685*: highly-potent non-competitive mGluR1 antagonist (Lavreysen et al., 2004). Used at 500 nM.
- *Tetrodotoxin* (TTX): inhibitor of sodium channel conductance (Gleitz et al., 1996). TTX was used to diminish high excitability in neuronal cultures. Used at 2 µM.
- *Nocodazole:* disrupts microtubule dynamics by binding to β−tubulin (Vasquez et al., 1997). Used at 33 µM.

Results and Discussion

2. Results and Discussion

The efficient delivery of cellular components to the location of their function is a fundamental mechanism of cellular biology. Macromolecular mobility can happen through diffusion due to the random walk of molecules (efficient for short [µm] distances) or long distance energy-requiring active transport (e.g. vesicle movement involving microtubules and molecular motors). Diffusion of molecules in well diluted environments follows simple and well-established physical principles. However, the inside of a cell presents a complex environment with many obstacles, such as macromolecular crowding, viscosity, physical barriers as well as specific and non-specific bindings, that the diffusing molecules must overcome to reach their destination (Perlson and Holzbaur, 2007). Protein mobility in neurons has attracted much attention owing to their particular shape (long distance trafficking and diffusion) and the phenomenon of synaptic transmission underlying brain function, that is on the molecular level governed by the trafficking of an immense number of molecules. According to the literature and own experience throughout my PhD, SENP1 is a cell-diffusing protein with both diffused (dispersed) and localised expression within a cell (Cubenas-Potts et al., 2013) (Chow et al., 2014). For instance, SENP1 localises to the nuclear pore complexes, and together with SENP2 to the kinetochores during mitosis in HeLa cells (Cubenas-Potts et al., 2013). What is also apparent is that SENP1 can shuttle between the nucleus and the cytoplasm through a nuclear export sequence (Kim et al., 2005). In neurons, SENP1 is also present at synapses (Loriol et al., 2012). The dynamic regulation of protein redistribution at synapses during neuronal maturation or KCl depolarisation has been observed not only for SENP1 and Ubc9 but also for other sumoylation machinery members (Loriol et al., 2012) (Loriol et al., 2013). Such findings strongly suggest functional implications of the sumoylation process at synapses, which has been widely evidenced by previous research (reviewed in (Schorova and Martin, 2016), **Annexed Article 1**). Ubc9 synaptic redistribution is regulated through the mGluR5/PLC/PKC signalling cascade (Loriol et al., 2014). Since the sumoylation process must duly work in a balance, i.e. both sumoylation and desumoylation take place in a time-coordinated manner, it is highly desirable to uncover the molecular mechanisms driving redistribution of a desumoylation enzyme such as SENP1 at synapses. I anticipate that

research into the understanding of the sumoylation/desumoylation balance will add to the fundamental knowledge of cellular physiology with far reaching implications in the pathogenesis of many diseases where this balance is dysregulated.

Indeed, disruption of the sumoylation-desumoylation balance has been recurrently associated with neurological diseases (reviewed in (Henley et al., 2014) and (Schorova and Martin, 2016), **Annexed Article 1**). In order to understand the mechanisms driving the "SUMO balance" in neurons and at mammalian synapses, we need to complement the findings on the Ubc9 synaptic regulation (Loriol et al., 2014) by investigation into the **desumoylation pathway**. Here, I present my PhD work that aimed to identify the **regulatory mechanisms of the SENP1 enzyme at the synapse**. Some of these findings can be also found in the **Annexed Article 3.**

I. Is SENP1 spino-dendritic diffusion regulated by synaptic activity?

a) Validation of experimental tools

- *Is GFP-SENP1 an active desumoylation enzyme?*

For the purpose of the investigation into the regulatory mechanisms of SENP1 trafficking at synapses I largely worked with exogenously expressed fluorescently tagged SENP1. To verify that GFP-SENP1 is functionally active in cells, I transfected COS7 cells with plasmids encoding for GFP, GFP-SENP1 and the inactive GFP-SENP1 mutant (C603S), respectively. As can be seen from ***Figure 29***, over-expression of GFP-SENP1 but not its inactive mutant C603S decreases the overall SUMO1- and SUMO2/3-modified protein levels ***(Fig. 29A and B)***.

Figure 29.

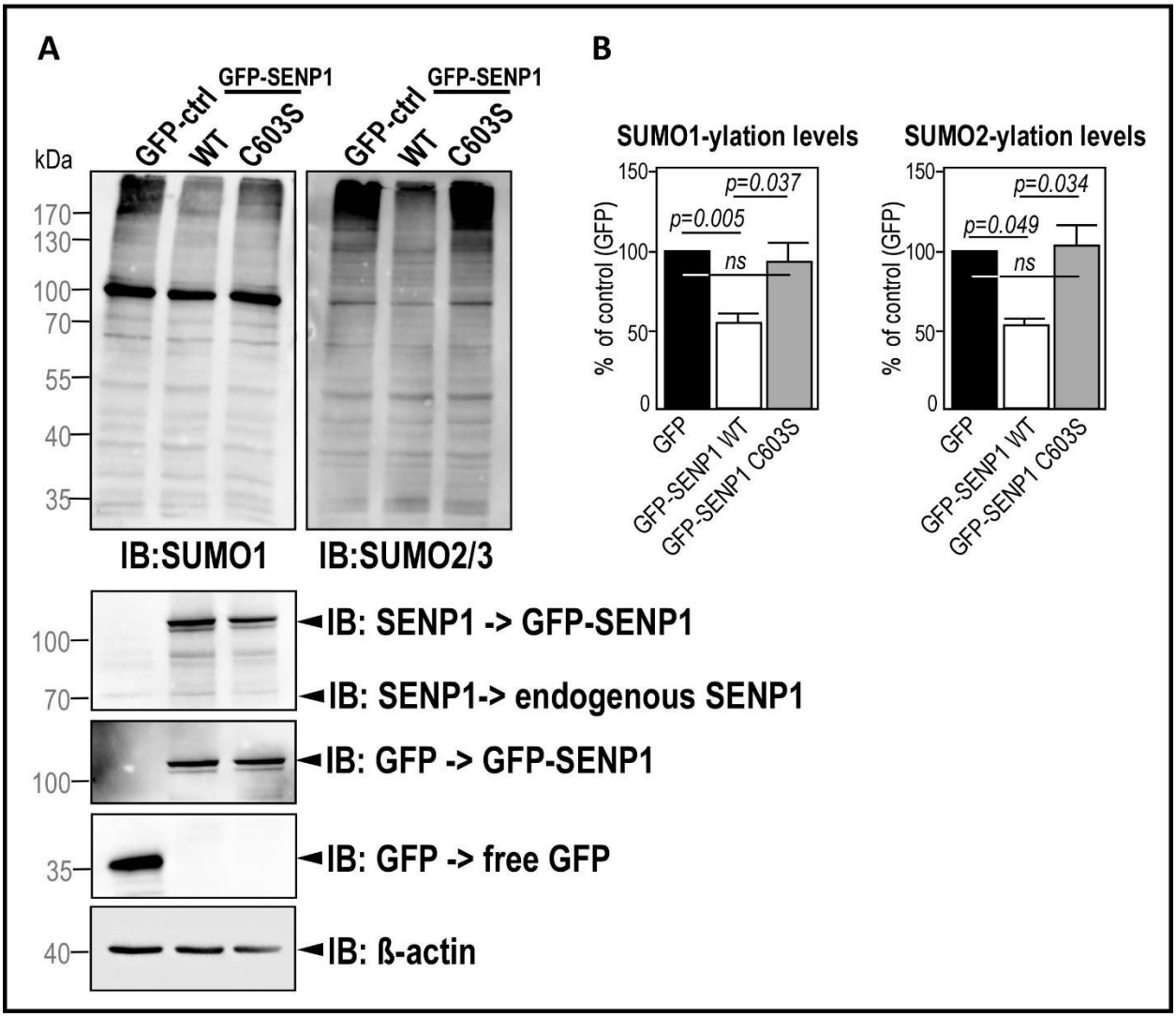

Figure 29. **Expression of WT GFP-SENP1 decreases SUMO1/2/3-modified protein levels in COS7 cells**. **A.** Representative Western Blots of SUMO1- and SUMO2/3-modified protein levels upon expression of GFP, WT GFP-SENP1 and the inactive GFP-SENP1 mutant (C603S). **B.** Quantitative representation of SUMO1- and SUMO2/3-modified protein levels normalised to GFP-ctrl +/- SEM (SUMO1: WT GFP-SENP1 [52.2 +/- 7.5 %] and GFP-SENP1 C603S [87.2 +/- 13.7 %]; SUMO2: WT GFP-SENP1 [50.7 +/- 6.7 %] and GFP-SENP1 C603S [103.6 +/- 22.7 %]) from 3 independent experiments. Statistics: One-way ANOVA with Tukey post hoc test. NS, not significant. P-values are indicated.

- *Is GFP-SENP1 distributed as the endogenous SENP1 in cultured rat hippocampal neurons?*

Here, I checked that both GFP-SENP1 and endogenous SENP1 are expressed at a steady state at synapses in rat hippocampal neurons that were principally used throughout this study. As shown in ***Figure 30 and 31***, both endogenous SENP1 and WT GFP-SENP1 localise to the nucleus as well as the cytoplasm including secondary dendrites and dendritic spines (colocalisation with

Figure 30.

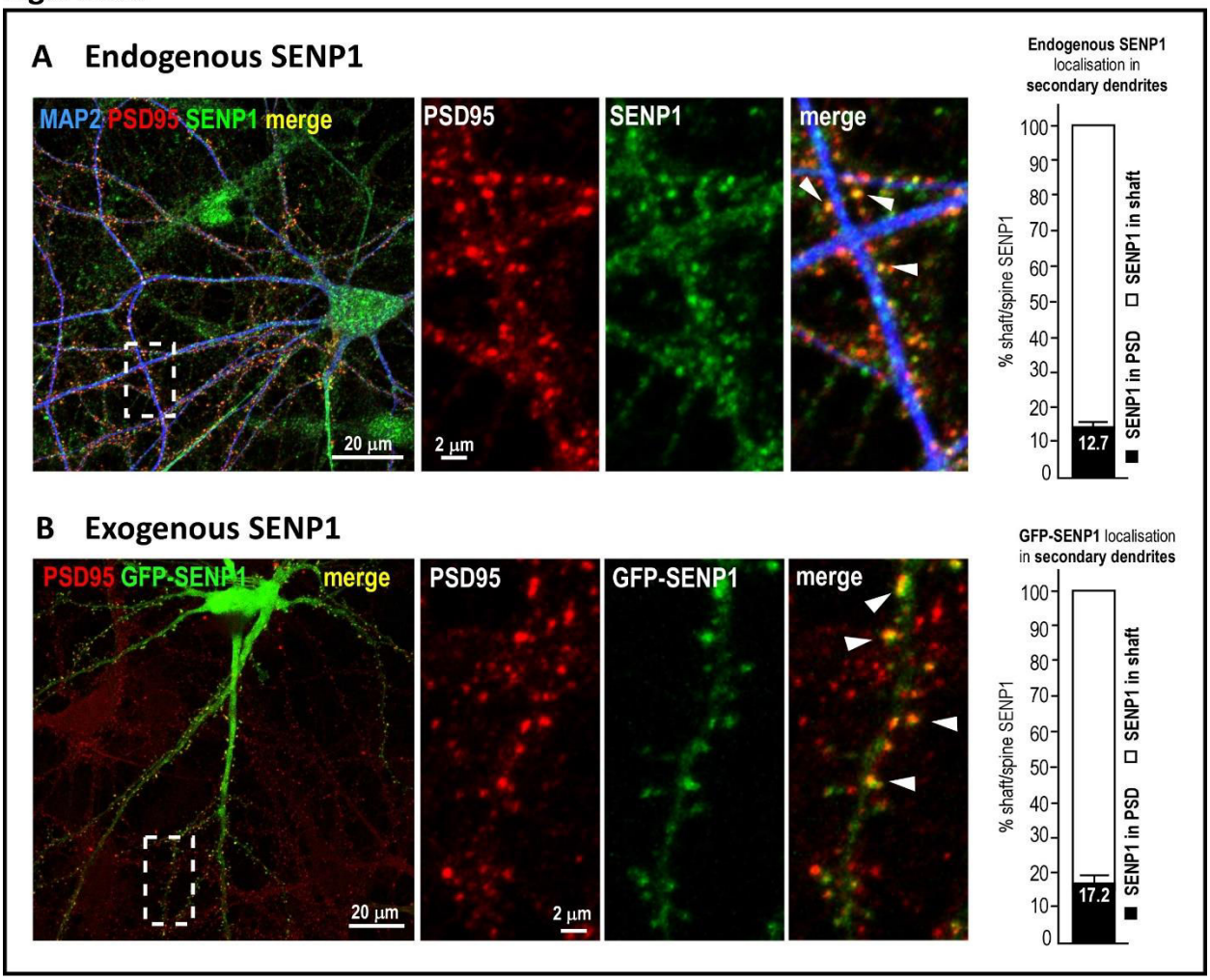

Figure 30. **Distribution of SENP1 in dendrites and spines**. **A.** Representative image of a 19 DIV rat hippocampal neuron immunolabelled for the neuronal marker MAP2 (blue), synaptic marker PSD-95 (red) and SENP1 (green). Graph on the right indicates the percentage of SENP1 staining in spines (12.7 +/- 0.4 %) and dendritic shafts (83.8 +/- 0.4 %) of secondary dendrites (n= 26 neurons). **B.** Representative image of a 19 DIV rat hippocampal neuron expressing WT GFP-SENP1 (green) and immunolabelled for PSD-95 (red). Graph on the right indicates the percentage of GFP-SENP1 localisation in spines (17.2 +/- 1.1 %) and dendritic shafts (82.8 +/- 1.1 %) of secondary dendrites (n= 2 neurons).

the postsynaptic marker PSD-95, ***Fig. 30A and B***). In regard to the endogenous SENP1, approximately 12.7 % of SENP1 that is found **within secondary dendrites** accounts for synaptic SENP1, i.e. in colocalisation with PSD-95 (***Fig. 30A***). Colocalisation of WT GFP-SENP1 with PSD-95 represents about 17.2 % indicating that WT GFP-SENP1 behaves similarly to the endogenous SENP1 (***Fig. 30B***). As it is well established that the majority of SENP1 expression is localised to the

nucleus, ***Figure 31*** further displays enlarged views of high nuclear localisation of both endogenous SENP1 (***Fig. 31A***) and GFP-SENP1 (***Fig. 31B***).

Figure 31.

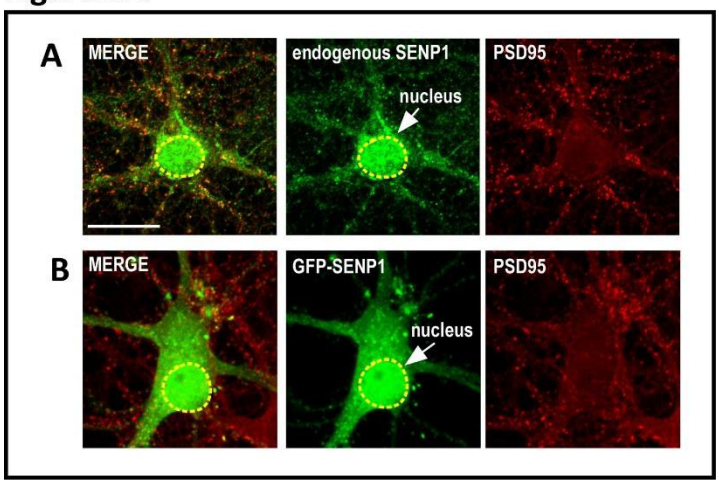

Figure 31. **Nuclear localisation of SENP1 in neurons**. **A.** Representative images of a 19 DIV rat hippocampal neuron immunolabelled for SENP1 (green) and the synaptic marker PSD-95 (red). **B.** Representative images of a 19 DIV rat hippocampal neuron expressing WT GFP-SENP1 (green) and immunolabelled for PSD-95 (red). Scale bar = 20 µm.

Since my thesis project is built around SENP1 live-imaging in cultured neurons, these initial experiments were important to demonstrate that exogenously expressed SENP1 localises at synapses and is functionally active.

b) Does an increase in synaptic activity alter the subcellular distribution of GFP-SENP1?

Synaptic activation leads to glutamate release which triggers a set of signalling cascades that eventually converge to changes in neuronal communication – the fundamental process of brain functioning ***(Fig. 32A)***. To test whether SENP1 spino-dendritic diffusion is altered upon an increase in synaptic activity I performed live-cell confocal imaging in the course of bicuculline (a $GABA_A$ receptor antagonist) administration to potentiate glutamate release and hence synaptic activity. Primary hippocampal neurons (18-21 DiV) virally transduced to express WT GFP-SENP1 were imaged following this work flow ***(Fig. 32B)***: First, neurons were kept at 37 °C in Earle's buffer (EB) solution (control solution) for 5 min prior to imaging for stabilisation; then, imaging was performed in control solution for 5-10 min before this medium was exchanged for control solution containing 10 µM bicuculline. Upon bicuculline addition, neurons were imaged for 30-40 min prior to the washout. As seen in ***Figure 32B and C***, a sustained increase in synaptic activity increases synaptic localisation of WT GFP-SENP1 in a time-dependent manner and plateaus at about 30 min of bicuculline treatment (increase by ~40 % of initial levels), with a corresponding decrease in dendritic shaft (by ~20 % of initial shaft levels). This WT GFP-SENP1 redistribution towards spines is reversible when a washout (control) solution is applied. Noteworthy, after recovering the basal level of activity, WT GFP-SENP1 remains in dendritic shaft at low levels even after 20 min post-washout. Since the experimental set up (lack of CO_2 microscope chamber) does not permit to image living neurons for longer periods of time (the overall health of cultured neurons decreases, which may introduce a significant bias into the analysis), I could argue that it takes longer than 30 minutes to reach the initial levels of WT GFP-SENP1 in dendritic shaft. However, considering that WT GFP-SENP1 fluorescence intensity in spines reaches the initial levels upon a washout, it is plausible to think that a concurrent degradation of WT GFP-SENP1 takes place in the shaft. To test this, it would be interesting to perform the very same experiment in the presence of inhibitors of proteasomal or lysosomal degradation. Additionally, a photobleaching artefact may account for some of the fluorescence intensity loss. We can see from the whole field fluorescence that about 5 % of fluorescence intensity is lost in the course of acquisition, including spines and shafts. This would mean that if the curves (***Fig. 32C***) were

corrected for bleaching, the WT GFP-SENP1 fluorescence may not be fully recovered in spines upon a washout and the shaft fluorescence would reach closer to the basal levels. I performed such a correction for photobleaching (***Fig. 32D***), upon which it is clear that a 30-minute washout is not sufficient to reach the initial levels of WT GFP-SENP1 in spines. This could be a result of an activation of signalling cascades that have a long-lasting effect on WT GFP-SENP1 spino-dendritic redistribution pointing to synaptic plasticity events. Indeed, changes in synaptic strenght require

Figure 32.

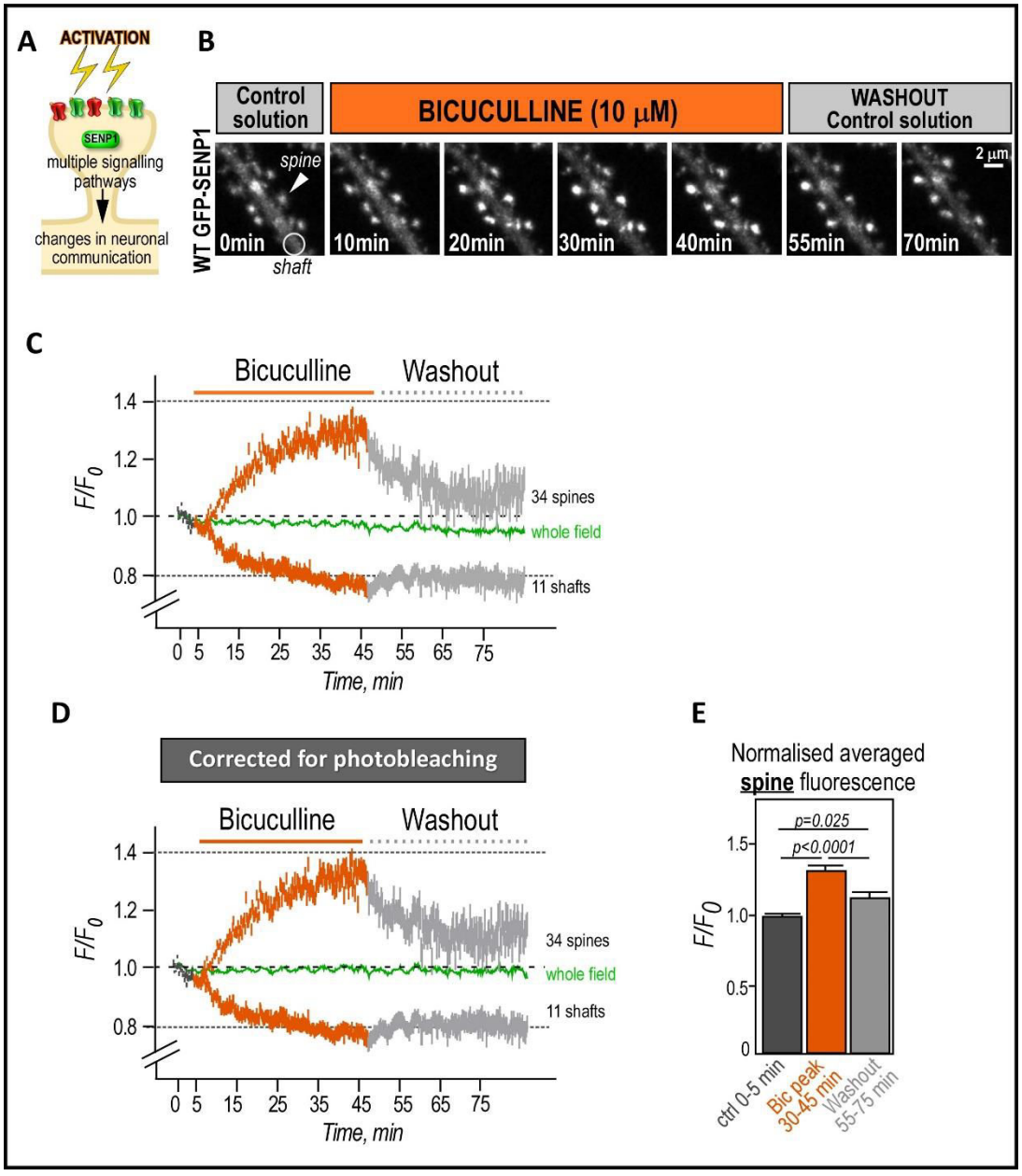

Figure 32 (Continued). **Activity-dependent redistribution of WT GFP-SENP1 into spines. A.** Scheme showing synaptic stimulation that leads to glutamate receptor activation and triggers a number downstream signalling pathways resulting in changes in neuronal communication. **B.** Workflow protocol of bicuculline (10 µM) treatment and representative confocal images (5-stack z-projection) of time-lapse recording of a GFP-SENP1 expressing rat hippocampal neuron (shown is a segment of a secondary dendrite with spines). **C.** Corresponding quantification of a representative experiment showing +/- SEM of normalised fluorescence intensity in spines (n=34), shafts (n=11) and whole dendritic tree field (green) in the course of incubation with control solution, bicuculline (10 µM) and during washout. **D.** Photobleaching correction was applied to measurements from C. **E.** Graphical representation of normalised mean fluorescence intensity from 34 spines pre-bicuculline (0-5 min, 1.003 +/- 0.0005, dark grey), high peak fluorescence intensity upon bicuculline treatment (30-45 min, mean = 1.304 +/- 0.027, orange), and low peak fluorescence intensity upon washout (55-70 min, mean = 1.14 +/- 0.04, light grey). Statistical test: Paired, parametric one-way ANOVA with Tukey post hoc test. P-values are indicated.

precise regulation of protein composition at the synapse. These include not only receptor proteins (e.g. AMPAR, (Henley and Wilkinson, 2013)) but also regulatory molecules such as kinases and scaffoding proteins. Neuronal activation triggers calcium flux and spikes throughout activated neurons. CaMKII has been shown to be recruited to activated synapses where calcium locally raises inducing spine plasticity (Lee et al., 2009). Moreover activated CaMKII serves as a docking hub for proteins and protein complexes such as proteasomes in dendritic spines.

Figure 33.

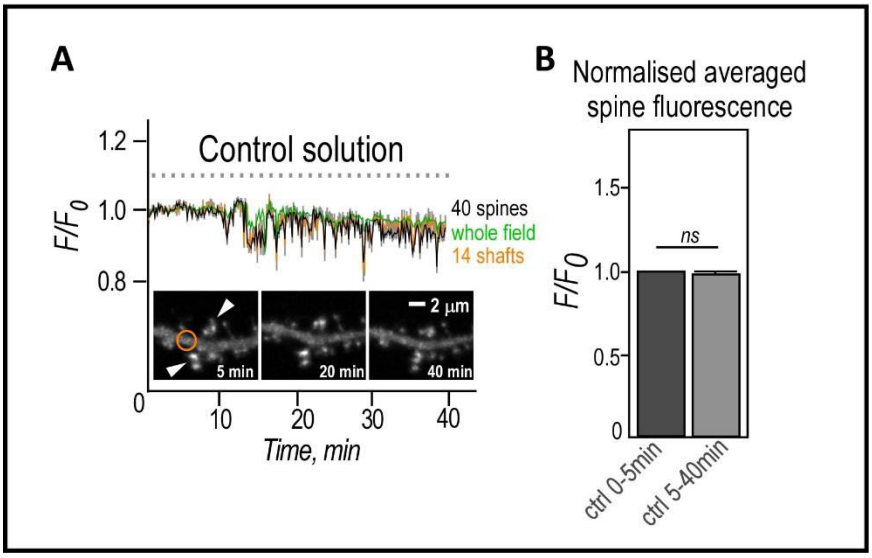

Figure 33. **Synapto-dendritic redistribution of WT GFP-SENP1 under basal/control neuronal activity**. **A.** Graphical representation and corresponding confocal images of time-lapse recording of a WT GFP-SENP1 expressing hippocampal neuron in control solution. Curves +/- SEM represent mean value of indicated numbed of spines (black), shafts (orange) and whole dendritic tree field (green). **B.** Bar graph shows spine mean fluorescence intensity +/- SEM during 0-5 min (dark grey) and 5-40 min (light grey). Number = 40 spines. Statistical test: Paired, non-parametric t-test. NS, not significant.

To verify that WT GFP-SENP1 does not undergo redistribution towards spines in the absence of synaptic stimulation, neurons were recorded for 40 min in control solution only (**Fig. 33**). As depicted in **Figure 33A** and **B**, WT GFP-SENP1 levels remain unchanged in dendritic spines and shafts throughout the course of recording. The evident oscillations were caused by a minor movement in the z-axis during acquisition. Notably, as in the previous experiment (***Fig. 32***), about a 5 % fluorescence decrease was measured in the course of acquisition in all regions measured (spines, shafts and field). As mentioned above, this rundown was most likely caused by photobleaching due to the acquisition protocol that constitutes of a 5-stack image being taken every 10 s with 300 ms exposure for the duration of 40 min and fits well with the previous experiment shown in ***Figure 32***.

It is important to uncover the biological reasons of SENP1 accumulation in spines. I assume that a sustained/chronic synaptic activation does not reflect physiological conditions and therefore, a significant increase in synaptic SENP1 could be a consequence of a pathological state. Moreover, such a robust accumulation of SENP1 in spines (by ~40%) would credibly impair the sumoylation/desumoylation balance further worsening synaptic defects. Thus, it would be very interesting to examine SENP1 levels at synapses in diseased conditions that are known for exacerbated synaptic/neuronal activity such as epilepsy. Importantly, the host laboratory has previously reported that Ubc9 transient trapping in spines increases synaptic SUMO1-ylation levels within 10 min of synaptic activation in intact synaptosomes *in vitro* (Loriol et al., 2014). Accordingly, SENP1 accumulation in spines starts to be apparent after this 10-minute time point. It will therefore be of interest first, to carry out time-lapse imaging of neurons expressing GFP-Ubc9 in the course of synaptic activation to examine the Ubc9 spino-dendritic redistribution; and second, to measure the sumoylation levels at synapses after prolonged synaptic activation at several time points (10 to 50 min of chronic stimulation). I have already performed one preliminary experiment with a 40-minute chronic synaptic activation suggesting that indeed sustained synaptic activation changes SUMO1/2/3-ylation levels in the synapse. This result is presented later in ***Figure 51***. Should all the above mentioned points be addressed, it may provide

additional evidence for the sumoylation/desumoylation balance being a vital physiological requirement.

SENP1 accumulation in dendritic spines is specifically triggered by synaptic activation. This implies a functional importance of desumoylation at synapses.

c) What are the dynamic properties of WT GFP-SENP1 spino-dendritic exchange upon synaptic activation?

- *Investigating SENP1 dynamics of synaptic entry.*

To gain understanding into dynamic properties of WT GFP-SENP1 synaptic entry in stimulated conditions, I performed FRAP experiments in control and bicuculline conditions ***(Fig. 34)***. Neurons were pre-treated or not with bicuculline for 10 min prior to FRAP spine photobleaching. I observed that the entry of WT GFP-SENP1 into spines was much slower (ctrl: ~0.0135 vs bic: ~0.0087 $\mu m^2/s$) and the mobile fraction much lower (ctrl: ~74.5 % vs bic: ~59.73 %) than in control condition, suggesting that rather a retention than a potentiated influx of WT GFP-SENP1 into spines might be the mechanism behind the increase of SENP1 synaptic localisation in bicuculline treated i.e. activated neurons.

Importantly however, considering that the effect of synaptic activation on WT GFP-SENP1 synaptic diffusion peaks at about 30 min post-treatment, I reasoned that this time-dependent effect would be further evidenced by FRAP experiments at different time points post-bicuculline treatment. Indeed, as seen from ***Figure 35***, the longer the bicuculline treatment the more robust was the effect on WT GFP-SENP1 synaptic entry diffusion ***(Fig. 35)***. This result suggests an important time-dependent effect of synaptic activity on WT GFP-SENP1 spino-dendritic diffusion (spine entry and/or retention).

Figure 34.

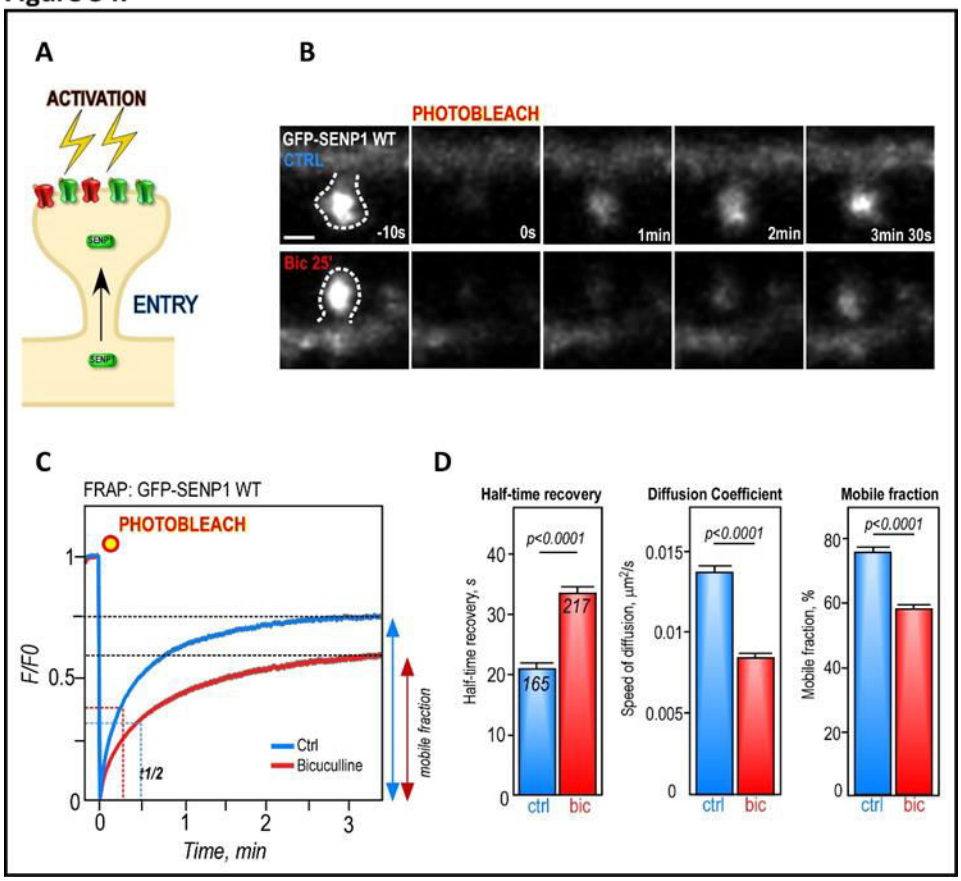

Figure 34. **SENP1 postsynaptic entry is regulated by synaptic activity**. **A.** Scheme showing the purpose of FRAP which is to determine the entry movement of GFP-SENP1 diffusing molecules upon synaptic activation into spines **B.** Representative FRAP recordings of WT GFP-SENP1-expressing spines of rat hippocampal neurons (19 DIV) in control and bicuculline (25 min sustained treatment) conditions. **C.** FRAP curves showing mean values (+/- SEM) of fluorescence intensity of bleached spines in control (blue) and bicuculline (sustained treatment of 10-50 min, red) conditions. **D.** FRAP measurements +/- SEM: half-time recovery ($t_{1/2}$, ctrl [20.79 +/- 1 s] and bic [33.94 +/- 1.3 s]); diffusion coefficient (ctrl [0.0135 +/- 0.0007 µm^2/s] and bic [0.0087+/-0.0005 µm^2/s]); and mobile fraction (ctrl [74.5 +/- 1.1 %] and bic [59.73 +/- 1.4 %]). Spine number ctrl= 165 and bic= 217 from at least 5 different cultures. Statistics: $t_{1/2}$ and diff. coef. were analysed by Mann-Whitney and Fm by parametric t-test. P-values are indicated.

Due to this time-dependent effect, I decided to separate the FRAP recordings of 10-25 min and 25-50 min of sustained bicuculline treatment. As shown in ***Figure 36***, such a separation gives rise to two distinct populations. In the first population (10-25 min of sustained bicuculline treatment), the effect of enhanced synaptic activity on SENP1 diffusion is already apparent, mostly in terms of half time recovery and speed of diffusion (***Fig. 36C***). However, the fraction of mobile SENP1 that enters the spine head is comparable at this time frame with non-treated condition (***Fig. 36C***). Sustained synaptic activation that lasts for more than 25 min (25-50 min)

dramatically decreases the fraction of SENP1 that diffuses into spines (***Fig. 36C***). These data reinforce the time-dependent regulation of SENP1 spino-dendritic diffusion and show that SENP1 spino-dendritic targeting gradually decreases in response to sustained synaptic activation.

Figure 35.

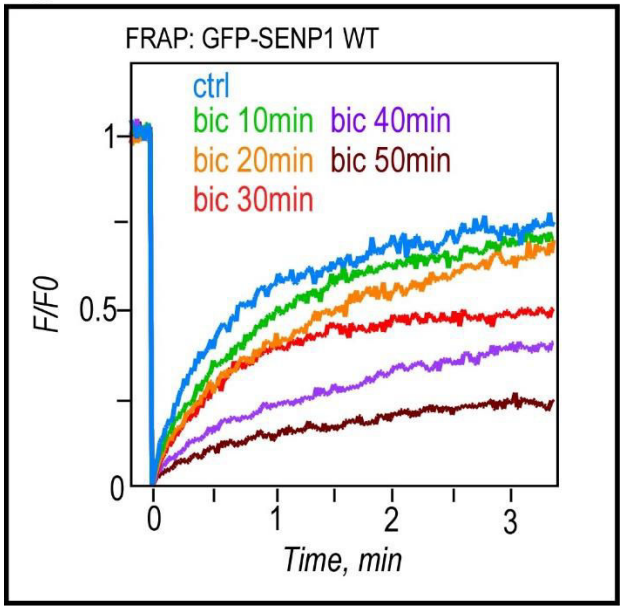

Figure 35. **SENP1 synaptic entry is regulated by synaptic activity in a time-dependent manner**. Each curve represents a mean value of 3 spines from 3 independent FRAP experiments in control (blue) and bicuculline (10 µM) conditions after indicated times of incubation.

SENP1 synaptic entry gradually decreases in response to sustained synaptic activation.

Figure 36.

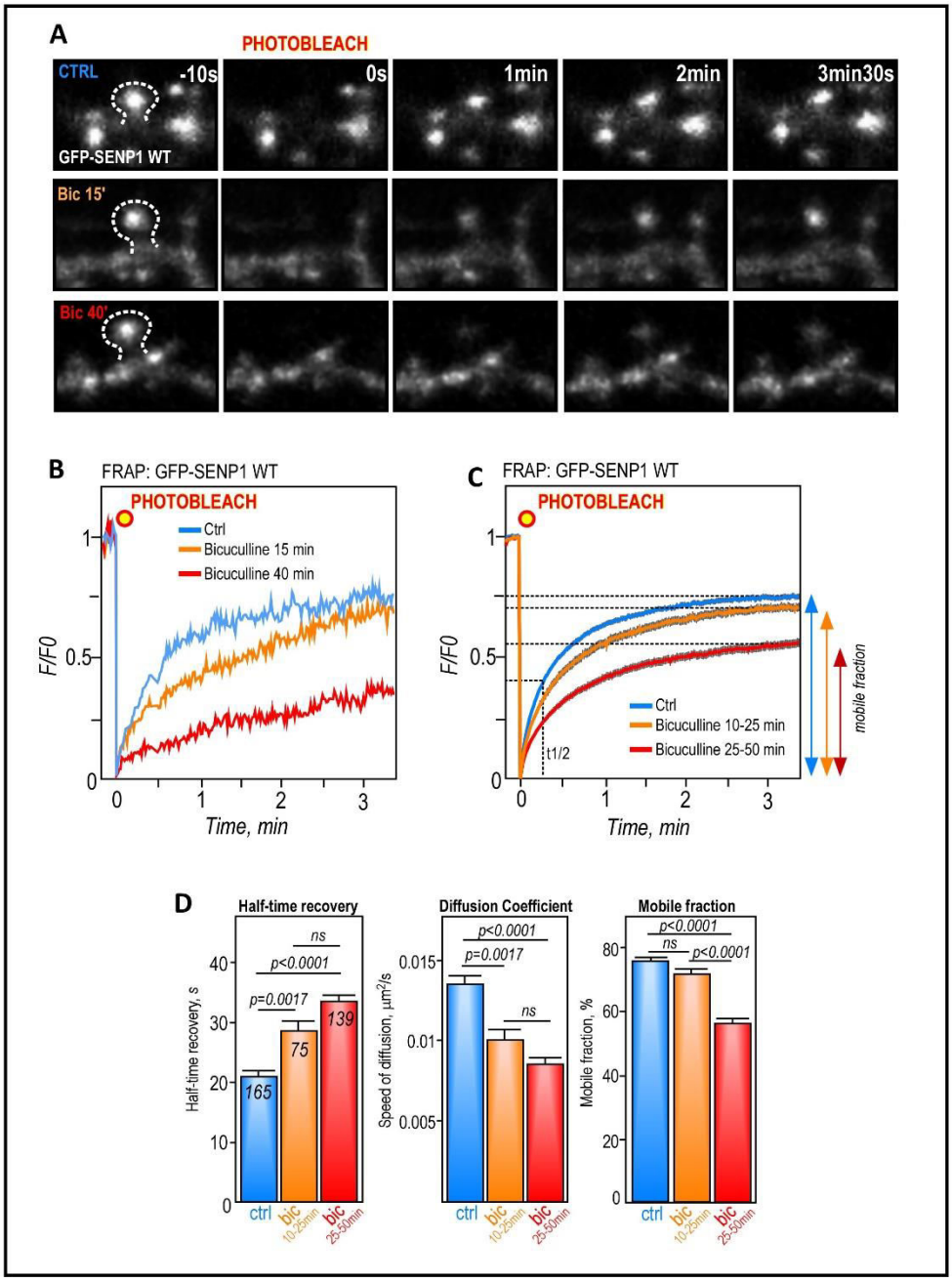

Figure 36. **SENP1 postsynaptic entry is regulated by synaptic activity in a time-dependent manner**. **A.** Representative FRAP recordings of WT GFP-SENP1-expressing spines of rat hippocampal neurons (19 DIV) in control and bicuculline (15 and 40 min of sustained treatment) conditions. **B.** FRAP curves corresponding to images in A. **C.** FRAP curves showing mean values (+/- SEM) of fluorescence intensity of bleached spines in control (blue) and bicuculline (sustained treatment of 10-25 min [orange] and 25-50 min [red]) conditions. **D.** FRAP measurements +/- SEM: half-time recovery ($t_{1/2}$, ctrl [20.79 +/- 1 s], bic 10-25min [28.25 +/- 2 s], and bic 25-50 min [33.58 +/- 1.6 s]); diffusion coefficient (ctrl [0.0135 +/- 0.0007 µm^2/s], bic 10-25 min [0.01 +/- 0.0008 µm^2/s], and bic 25-50 min [0.0087 +/- 0.0007 µm^2/s]); and mobile fraction (ctrl [74.5 +/- 1.1 %], bic 10-25 min [71.2 +/- 1.7 %], and bic 25-50 min [56.2 +/- 1.8 %]). Spine number ctrl= 165, bic 10-25 min= 75, and bic 25-50 min= 139 from at least 5 different cultures. Statistics: $t_{1/2}$ and diff. coef. were analysed by Kruskal-Wallis ANOVA and Fm by parametric ANOVA with Tukey post hoc test. P-values are indicated.

- *Investigating SENP1 synaptic exit*

To test whether the increase in SENP1 synaptic localisation is due to a decreased exit of SENP1 from spines I used photoconversion of Dendra2-SENP1 expressed in neurons. As above, neurons were pre-treated or not for 10 min with bicuculline prior to photoconversion. I observed that upon bicuculline treatment, the exit of Dendra2-SENP1 from spines was significantly slower when compared to basal condition (***Fig. 37***). This result indicates that increasing synaptic activity leads to SENP1 transient retention/trapping in spines. Once again, the robustness of Dendra2-SENP1 retention in spines was dependent upon the duration of bicuculline treatment demonstrating that SENP1 is regulated by sustained synaptic activity in a time-dependent manner (***Fig. 37***).

Figure 37.

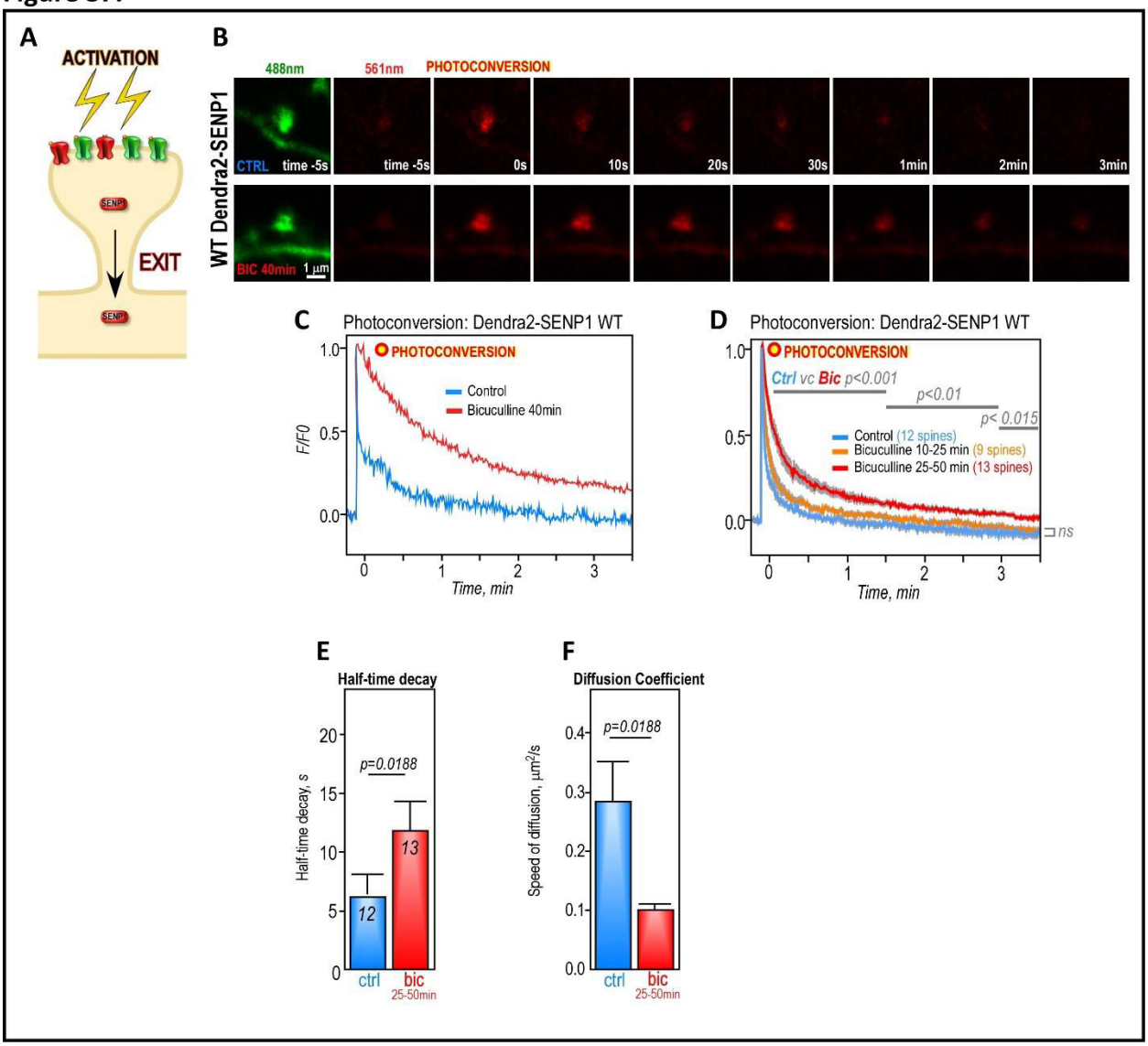

Figure 37 (Continued). **Synaptic exit of WT Dendra2-SENP1. A.** Scheme showing the purpose of the photoconversion experiment which is to determine the dynamics of the exit diffusion of WT Dendra2-SENP1 from spines upon synaptic activation. **B.** Representative confocal images of WT Dendra2-SENP1-expressing rat hippocampal neurons (19 DIV) during a photoconversion experiment in control and bicuculline (duration of treatment: 40 min) conditions. **C.** Typical fluorescence decay curves showing the diminishment of fluorescence as photoconverted WT Dendra2-SENP1 molecules exit from spines. The curves correspond to the images in B. **D.** Graph displaying fluorescence decay curves as mean values (+/- SEM) from 12 spines in control, 9 spines in bicuculline (duration of treatment 10-25 min) and 13 spines in bicuculline (duration of treatment 25-50 min) conditions. **E.** Graphical representation of half time fluorescence decay that corresponds to the ctrl (blue, 6.13 +/- 1.8 s) and bic (red, 25'-50', 11.9 +/- 2.6 s) curves in D. **F.** Graphs of fluorescence decay speed in ctrl (0.279 +/- 0.065 $\mu m^2/s$) and bic (0.105 +/- 0.020 $\mu m^2/s$) conditions. Number of cultures = 3. Statistics: multiple t-test in D and Mann-Whitney test in E and F. P-values are indicated.

I reason that the combination of a decreased entry to with an increased retention of SENP1 in spines is the mechanism responsible for SENP1 accumulation in spines upon sustained synaptic activation. This implies that molecular mechanisms that regulate the direction of SENP1 movement in and out of spines must work in synergy to maintain the sumoylation/desumoylation balance. The identification of these molecular cues regulating SENP1 spino-dendritic diffusion is described later in the results section.

The combination of a decreased entry to and a prolonged retention of SENP1 in spines is in favour of SENP1 synaptic accumulation as a result of a sustained synaptic activation.

- *Does synaptic localisation of endogenous SENP1 increase upon sustained synaptic activity?*

To answer this question, I performed immunolabelling of endogenous SENP1 in rat hippocampal neurons following a treatment with control or bicuculline-containing solutions. Taking into consideration that endogenous SENP1 is present at synapses at lower concentrations than in over-expression system, samples were analysed only for the peak time-point of bicuculline effect as seen in the live-cell imaging (30-40 min). I carried out a colocalisation analysis of SENP1 with the postsynaptic marker PSD-95 by assessing three measurements: *PSD-95 size of area* (PSD-95 Area), *SENP1 mean fluorescence intensity within PSD-95 area* (SENP1 in PSD-95) and *SENP1 total mean fluorescence intensity* (SENP1 Total). Using an ImageJ macro that was purposely tailored for this analysis in collaboration with Dr Brau (IPMC microscopy platform) I analysed secondary dendrites for the colocalisation of SENP1 with PSD-95. As shown in ***Figure 38***, firstly, the PSD-95 area, that was used as a mask for the colocalisation analysis with SENP1, remains unchanged between control and bicuculline conditions. Secondly, increasing synaptic activity does not affect the total SENP1 fluorescence intensity, which is expected given the time course of 40 minutes, in which very little protein synthesis (of ~70 kDa SENP1) takes place. Nevertheless, this was an important indicator of the non-toxicity of the bicuculline treatment or the vehicle over the 40-minute period of the experiment. Third, and a very exciting finding is that bicuculline-triggered synaptic activation results in an increased SENP1 intensity within the PSD-95 area demonstrating that SENP1 accumulates at the postsynapse upon bicuculline treatment.

This result is in agreement with the live-cell imaging experiments (***Fig. 32***) and indicates that the redistribution of endogenous SENP1 into dendritic spines is regulated upon synaptic activation.

Figure 38.

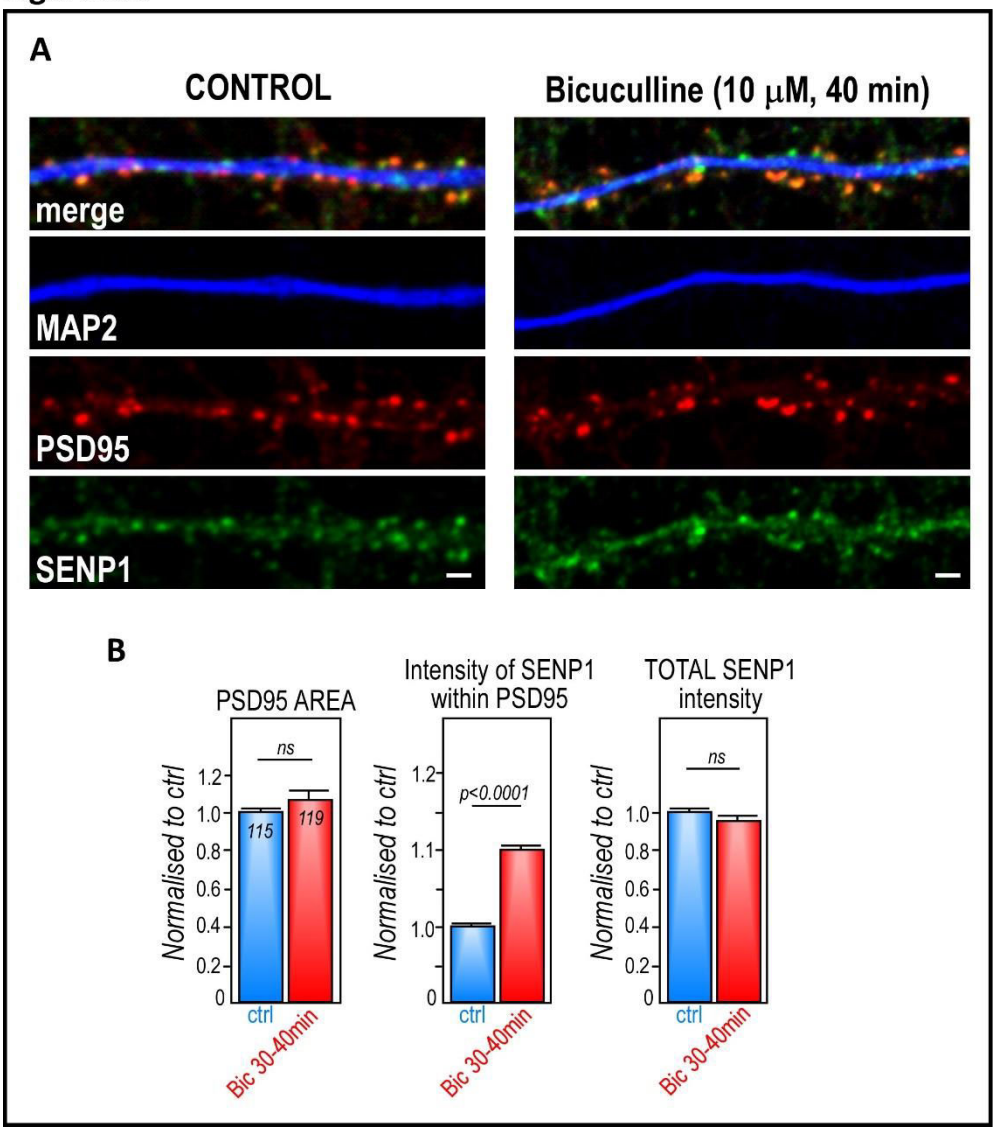

Figure 38. **Endogenous SENP1 localisation at synapses**. **A.** Immuno-labelling of fixed primary hippocampal neurons in control and bicuculline (40 min treatment) conditions. Scale bar = 2 μm. **B.** Quantitative representation of control-normalised size of PSD-95 area, fluorescence intensity of SENP1 within PSD-95 area, and total SENP1 staining from 4 different cultures and at least 6 neurons (DIV 18-21) analysed/culture. Number of segments of secondary dendrites is indicated. Statistics: two-tailed unpaired t-test. P-value is indicated. NS, not significant.

An alternative way to quantify protein levels at the synapse is by biochemical means. In order to provide additional evidence for synaptic levels of endogenous SENP1 in response to synaptic activation I aimed to purify synaptosomes from cultured cortical neurons (18-20 DIV). I carried out synaptosomal preparation using an already published protocol (Loriol et al., 2013), however, I did not succeed in synaptosomes enrichment upon sucrose gradient ultracentrifugation (***Fig.***

Figure 39.

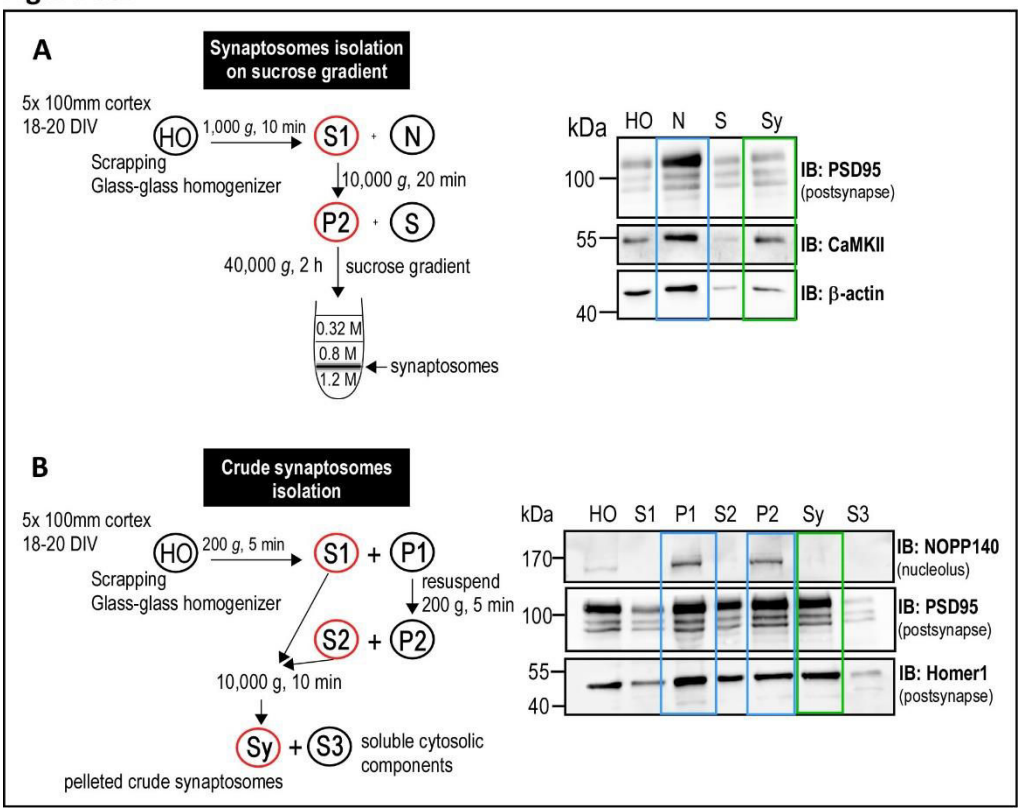

Figure 39. **Synaptosomal preparation from cultured cortical neurons**. Step-by-step scheme of synaptosomal isolation on sucrose gradient and a corresponding Western blot of different fractions from 5x 10 cm Petri dishes (2.5 mil cells/dish). Immuno-detection was performed for PSD-95 (postsynaptic marker), CaMKII (enriched in postsynapse) and β-actin (enriched in postsynapse). Lanes labels: total homogenate (HO), nuclear fraction (N), supernatant (S, soluble cytoplasmic components) and synaptosomes (Sy). Loaded 15 µg/lane. In blue and green rectangles are shown protein enrichments in nuclear but not synaptic fraction, respectively. **B** Step-by-step scheme of crude synaptosomal isolation and a corresponding Western blot of fractions from 5x 10 cm in diameter Petri dishes (2.5 mil cells/dish). In blue and green rectangles are shown protein enrichments in nuclear but not synaptic fraction, respectively.

39A). Although I introduced several modifications into the protocol, I was unable to visualise synaptosomal fraction in the sucrose gradient, which prevented me from collecting the correct synaptosomal fraction (***Fig. 39A***). I also performed purification of crude synaptosomes (without sucrose gradient) but found that most of the synaptic material was pelleted at earlier steps (P1 and P2) together with nuclei (***Fig. 39B***). I therefore acquired a different approach – isolation of so called Triton Insoluble Fraction (TIF) following previously published protocols ((Gardoni et al., 2003) and (Gardoni et al., 2009), also described in *Experimental approaches* in the section **1.5; Fig. 40A** and **Annexed Article 3**). Briefly, neurons were treated with control or bicuculline-containing solution for 40 min. After this time, neurons were homogenised and a nuclei-

Figure 40.

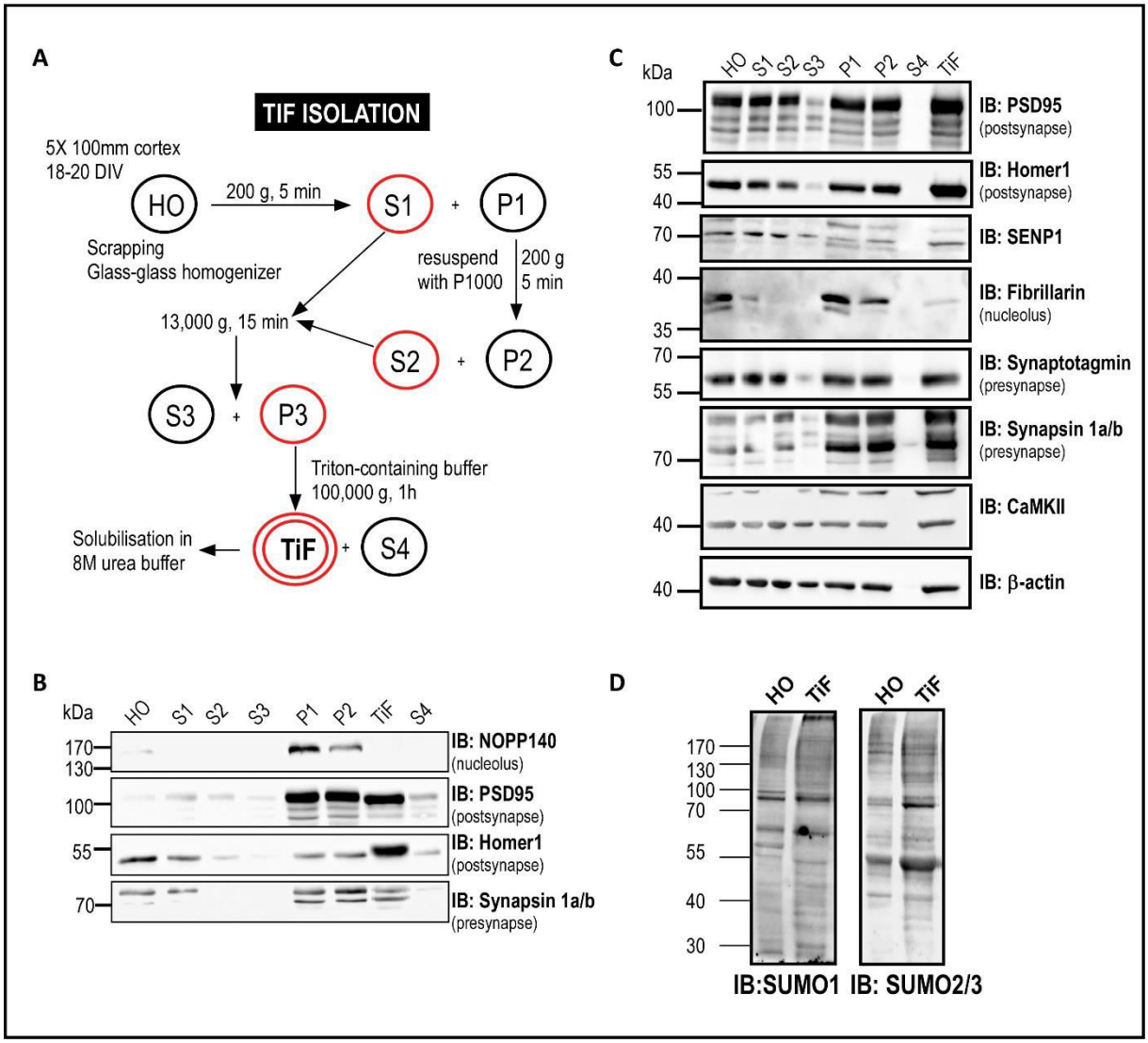

Figure 40. **TIF preparation from primary cortical neurons**. **A.** Step-by-step scheme of TIF isolation. **B.** Western blot analysis of TIF purity isolation displaying fractions from different steps indicated in A. Immuno-detection was performed for NOPP140 (nuclear marker), PSD-95 (postsynaptic marker), Homer1 (postsynaptic marker) and synapsin 1a/b (presynaptic marker). Lanes labels: total homogenate (HO), supernatant 1, 2 and 3 (S1,2 and 3), pellets 1 and 2 (P1 and 2), triton insoluble fraction (TIF) and supernatant 4 (S4). Loaded 10 µg of total protein/lane. **C.** Additional Western blot analysis of TIF purity isolation different from B displaying fractions from different steps indicated in A. Immuno-detection was performed for PSD-95 (postsynaptic marker), Homer1 (postsynaptic marker), SENP1, fibrillarin (nuclear marker), synaptotagmin (presynaptic marker), synapsin 1a/b (presynaptic marker), CaMKII (enriched in postsnapse) and β-actin. Lanes are labelled as in B. Loaded 15 µg of protein/lane. **D.** Western blot showing the presence of SUMO1/2/3-modified proteins in HO (loaded 15 µg) and TIF (loaded 40 µg) fractions.

containing fraction removed from cellular homogenate by a low-speed centrifugation to prevent contamination by nuclear SENP1 proteins. The supernatant containing cytosolic fraction including synapses was spun down at high speed to form a firm pellet. Pelleted cellular

components were lysed and solubilised with a buffer containing 1% TritonX100. The PSD macromolecular complex consists of many highly packed proteins (supposedly also SENP1) that are resistant to high percentage of TritonX100 solubilisation. Upon solubilisation, non-PSD complex proteins are solubilised into the solution whereas PSD complexes remain intact. Then, to pellet PSD complexes, a high speed ultracentrifugation was performed. In the last step of TIF isolation, PSD complexes were stringently denaturised in 8M urea buffer and Western Blot was performed to test the purity of each fraction for markers of cellular compartments (***Fig. 40B*** and ***C***), the presence of SUMO-modified proteins (***Fig. 40D***) as well as SENP1 protein levels that were quantified (***Fig. 41***). Of note, Homer1 and PSD95, the postsynaptic scaffolds, were used as loading controls (***Fig. 41***) since both are prominent components of PSD and therefore TIF fractions, and their distribution within spines is presumably correlated with the spine size. However, I am aware that more optimisation and seeking a better loading control for assessment of protein levels in TIF fraction is needed. Possibly, α- and β-tubulin may present more suitable loading controls for TIF fraction as they are found within PSD as previously described (Kelly and Cotman, 1978). I also considered using actin, but the levels were highly variable and I therefore decided to omit its use as a loading control. Ideally, a well optimised Bradford protein assay combined with appropriate loading control will yield results that accurately reflect the levels of SENP1 protein in PSD under studied conditions. In conclusion, although more experiments are being conducted at the

Figure 41.

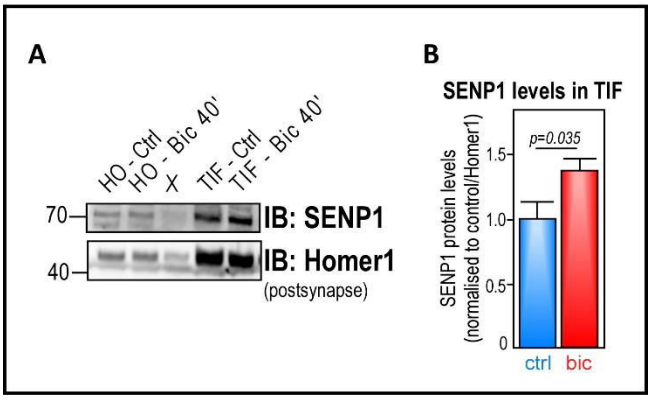

Figure 41. **SENP1 protein levels in TIF fraction**. **A.** Representative Western blot of cellular homogenate (HO) and TIF fractions in control and bicuculline (40 min) conditions. Immuno-detection was performed for SENP1 and Homer1. **B.** Quantifications of normalised SENP1 levels in TIF fractions in control and bicuculline conditions. The bars represent mean values +/- SEM from 3 independent experiments. SENP1 normalisation was performed with levels of Homer1. Statistics: Paired t-test.

moment, the present results suggest that sustained synaptic activation leads to an enrichment of endogenous SENP1 in PSD/TIF traction (***Fig. 41***).

Synaptic activation leads to an accumulation of endogenous SENP1 at synaptic sites.

II. Activation of which glutamatergic receptors is responsible for the regulation of SENP1 spino-dendritic diffusion?

Glutamate is the major excitatory neurotransmitter in the brain. Glutamate receptor binding triggers a plethora signal transduction cascades via the redistribution and binding of signalling molecules. Since the application of bicuculline, the $GABA_A$ receptor antagonist, to neurons is known to result in glutamate release, I expected a direct participation of glutamate receptor activation in the regulation of SENP1 synaptic redistribution.

a) Are NMDA receptors involved in SENP1 spino-dendritic redistribution?

NMDA receptors are voltage- and ligand-gated ion channels that largely contribute to synaptic plasticity and intracellular Ca^{2+} transients. Increased calcium ion concentration in postsynaptic neuron contributes to the rearrangement of scaffolding proteins, the increase of postsynaptic area and the decrease of resistance during synaptic transmission resulting in the formation of LTP (Pastalkova et al., 2006). In addition, Ca^{2+} is an important second messenger that activates several crucial protein kinases, such as PKA, CaMKII and MAPK that activate further downstream signalling pathways. Therefore, I aimed to examine whether NMDAR activation could specifically regulate SENP1 redistribution at synapses. In order to target NMDARs, I used the NMDAR antagonist, AP5 (Davis et al., 1992). I performed FRAP experiments on GFP-SENP1-expressing primary hippocampal neurons in the absence or presence of AP5. Interestingly, application of AP5 alone affects SENP1 spine entry dynamics that is comparable with

bicuculline-treated conditions (***Fig. 42***, $t_{1/2}$ mean +/- SEM: **AP5** [**30.1** +/- 1.2 s] vs **bic** [**33.6** +/- 1.6 s] and speed of diffusion (**AP5** [0.0085 +/- 0.0004 µm^2/s] vs **bic** [0.0087 +/- 0.0007 µm^2/s]), whereas mobile fraction in AP5 condition is similar to control (**Fm** mean +/- SEM: **AP5** [**72** +/- 1 %] vs **ctrl** [**75** +/- 1 %] vs **bic** [**56** +/- 1.8 %]). It is difficult to explain the slight effect of AP5 itself on SENP1 dynamics, however, multiple compensatory effects of an activity potentiation of different glutamatergic receptors could play a role. Nevertheless, the pre-incubation with AP5 does not reverse the bicuculline-induced effect on SENP1 diffusion (***Fig. 42***) and therefore, blocking NMDAR activity does not interfere with SENP1 synaptic redistribution upon increased synaptic activity. I can thus conclude that NMDARs are not involved in bicuculline-mediated SENP1 synaptic redistribution.

Synaptic activation regulates SENP1 redistribution at post-synaptic sites in an NMDAR-independent manner.

Figure 42.

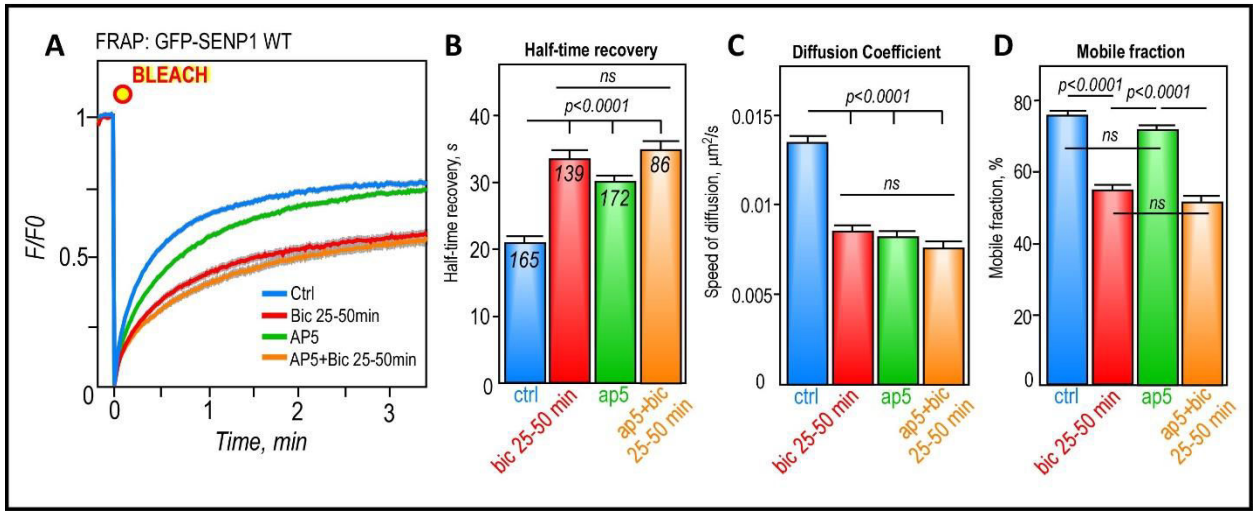

Figure 42. **The role of NMDAR in SENP1 regulation at synapses**. **A.** FRAP curves showing mean values (+/- SEM) of fluorescence intensity of bleached spines in control (blue), bicuculline (sustained treatment of 25-50 min, red), AP5 (green) and AP5+bicuculline (25-50 min, orange) conditions. **B.** FRAP measurements +/- SEM: Half-time recovery ($t_{1/2}$, ctrl [20.79 +/- 1 s], bic 25-50 min [33.58 +/- 1.6 s], AP5 [30.05 +/- 1.2 s] and AP5+bic [35.01 +/- 2.2 s]). **C.** Diffusion coefficient (ctrl [0.0135 +/- 0.0007 µm^2/s], bic 25-50 min [0.0087 +/- 0.0007 µm^2/s], AP5 [0.0085 +/- 0.0004 µm^2/s] and AP5+bic [0.0079 +/- 0.0006 µm^2/s]). **D.** Mobile fraction (ctrl [74.5 +/- 1.1 %], bic 25-50 min [56.2 +/- 1.8 %], AP5 [72 +/- 1 %] and AP5+bic [54 +/- 2%]). Spine number ctrl = 165, bic 25-50 min = 139, AP5 = 172, AP5+bic = 86 from at least 4 different cultures. Statistics: $t_{1/2}$ and diff. coef. were analysed by Kruskal-Wallis ANOVA and Fm by parametric ANOVA with Tukey post hoc test. P-values are indicated.

b) Are Group I mGlu receptors involved in SENP1 spino-dendritic redistribution?

Stimulation of Group I metabotropic glutamate receptors (mGluR1 and mGluR5) also leads to activation of a wide range of signalling pathways. mGluRs couple to Gα(q) proteins, activating phospholipase C leading to formation of DAG and IP3 that is followed by the activation of a plethora of kinases such as PKC. In addition, Group I mGluR activation modulates a myriad of ion channels, such as calcium and potassium channels. Group I mGluRs can also activate other downstream protein kinases, such as ERK1/2 and AKT, which are implicated in cellular growth, differentiation, and survival. mGluR1/5 are localised perisynaptically, right outside the postsynaptic membrane specializations, and are crosslinked through the interaction with Homer1 to a number of PSD proteins that regulate synaptic signalling and plasticity. Group I mGluRs has been also implicated in many types of brain disease such as Alzheimer's disease and Fragile X syndrome. Importantly, my host laboratory has previously reported that the sole sumoylation enzyme Ubc9 is regulated by the activation of mGluR5 followed by the activation of the PLC/PKC cascade that leads to Ubc9 transient trapping at synapses (Loriol et al., 2014). Moreover, we have also reported that the FMRP protein, of which gene mutations result in Fragile X syndrome, is sumoylated in a mGluR5 activation-dependent manner leading to changes in spine frequency and maturation (Khayachi et al. 2018, **Annexed Article 2**). Altogether, these results strongly evidence the involvement of Group I mGluR in synaptic function, control of the overall sumoylation balance as well as regulation of specific SUMO-target interactions.

To follow up on the SENP1 upstream regulatory mechanisms, I tested for the involvement of **Group I mGluRs**. I used the mGluR1/5 agonist DHPG to specifically activate these receptors and performed FRAP assays on WT GFP-SENP1-expressing primary hippocampal neurons (***Fig. 43***). Restricted photobleaching of spines was performed in the range of 10-50 minutes of the duration of DHPG treatment. DHPG treatment of 10 to 25 minutes significantly altered the entry diffusion of WT GFP-SENP1 to spines (***Fig. 43***), increasing the $\mathbf{t_{1/2}}$ (Ctrl **23.4** +/- 1.35 s vs DHPG [10'-25'] **29** +/- 1.3 s), decreasing **speed of diffusion** (Ctrl **0.013** +/- 0.001 $\mu m^2/s$ vs DHPG [10'-25'] **0.008** +/- 0.0004 $\mu m^2/s$) and reducing the **mobile fraction** (Ctrl **73.9** +/- 1.55 % vs DHPG [10'-25'] **66** +/- 1.3 %). DHPG effect on WT GFP-SENP1 spino-dendritic redistribution was further enhanced when a

longer exposure to DHPG 25 to 50 minutes was applied. The entry redistribution of WT GFP-SENP1 to spines was further reduced (***Fig. 43***) with $\mathbf{t_{1/2}}$ (DHPG [25'-50'] **34** +/- 1.12 s), **speed of**

Figure 43.

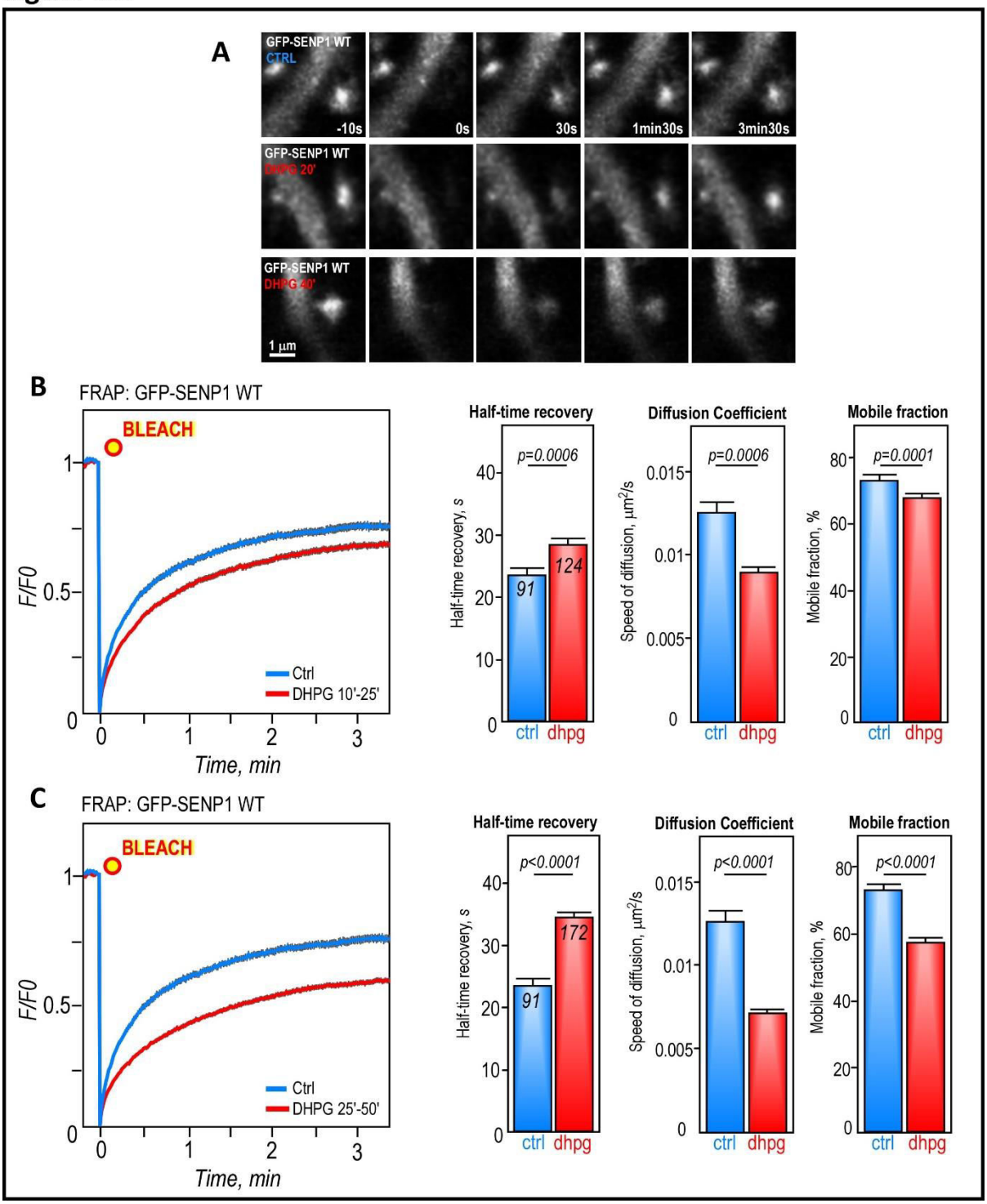

Figure 43 (Continued). **Activation of mGluR1/5 regulates SENP1 postsynaptic entry**. **A.** Representative FRAP recordings of WT GFP-SENP1-expressing spines of rat hippocampal neurons (19 DIV) in control and DHPG-treated (20 and 40 min of sustained treatment) conditions. **B.** FRAP curves showing mean values (+/- SEM) of fluorescence intensity of bleached spines in control (blue) and DHPG (red, sustained treatment of **10-25 min**) conditions. FRAP measurements +/- SEM: half-time recovery ($t_{1/2}$, ctrl [23.4 +/- 1.35 s] and DHPG 10'-25' [29 +/- 1.3 s]); diffusion coefficient (ctrl [0.013 +/- 0.001 $\mu m^2/s$] vs DHPG 10'-25' [0.008 +/- 0.0004 $\mu m^2/s$]); and mobile fraction (ctrl [74.0 +/- 1.55 %] vs DHPG 10'-25' [66 +/- 1.3 %]. **C.** FRAP curves showing mean values (+/- SEM) of fluorescence intensity of bleached spines in control (blue) and DHPG (red, sustained treatment of **25-50 min**) conditions. FRAP measurements +/- SEM: half-time recovery ($t_{1/2}$, ctrl [23.4 +/- 1.35 s] and DHPG 25'-50' [34 +/- 1.12 s]); diffusion coefficient (ctrl [0.013 +/- 0.001 $\mu m^2/s$] vs DHPG 25'-50' [0.0071 +/- 0.0003 $\mu m^2/s$]); and mobile fraction (ctrl [73.9 +/- 1.55 %] vs DHPG 25'-50' [58.4 +/- 1.35 %]. Spine number ctrl= 91, DHPG 10'-25'= 124, and DHPG 25'-50'= 172 from at least 4 different cultures. Statistics: $t_{1/2}$ and diff. coef. were analysed by non-parametric t-test and Fm by parametric t-test. P-values are indicated.

diffusion (DHPG [25'-50'] **0.0071** +/- 0.0003 $\mu m^2/s$) and **mobile fraction** (DHPG [25'-50'] **58.4** +/- 1.35 %). This result shows that sustained DHPG treatment has a similar effect on WT GFP-SENP1 synaptic diffusion as bicuculline. Moreover, a similar dependency on the sustained duration of mGluR1/5 receptors activation was also observed when compared between 10-25 and 25-50 minutes of DHPG exposure (***Fig. 43***).

Colocalisation analysis of endogenous SENP1 with PSD95 in the absence or presence of DHPG was performed to determine SENP1 protein levels at the postsynapse. As depicted in ***Figure 44***, a sustained DHPG treatment (40 min) leads to a significant ~14 % increase in SENP1 immunoreactivity within PSD95-positive sites (***Fig. 44B***). At the same time, there are no significant changes in the size of PSD95-positive area, nor in total SENP1 protein levels (***Fig. 44B***). Altogether, I showed that activation of Group I mGluRs increases protein levels of endogenous SENP1 in spines suggesting that these receptors regulate endogenous SENP1 accumulation of at the postsynapse.

Additionally, I performed TIF isolation to determine the protein levels of endogenous SENP1 in the PSD fraction upon DHPG treatment. Once again, protein levels were determined using PSD95 as a loading control (***Fig. 45***). Initially, I aimed to use β-tubulin as a loading control, however, β-tubulin levels in the TIF fraction were very high (***Fig. 45A***) and therefore the bands could not be used for quantification and protein level normalisation. This point will need to be addressed and concentration of loaded proteins optimised in future experiments. Data from TIF

isolations from four different neuronal cultures are presented in ***Figure 45*** showing control, DHPG and MPEP-DHPG stimulations. Activation of mGluR1/5 with DHPG led to a significant increase in SENP1 levels in PSD (ctrl: 1, DHPG: 1.8 +/- 0.23) which was partially reversed by the addition on MPEP (MPEP+DHPG: 1.6). This finding is in agreement with FRAP experiments that suggest a retention of GFP-SENP1 in spines upon DHPG treatment as well as the immuno-detection showing an increase in endogenous SENP1 at synapses after sustained DHPG stimulation (***Fig. 44***). Here, I clearly demonstrated that the activation of mGluR1/5 regulates the

Figure 44.

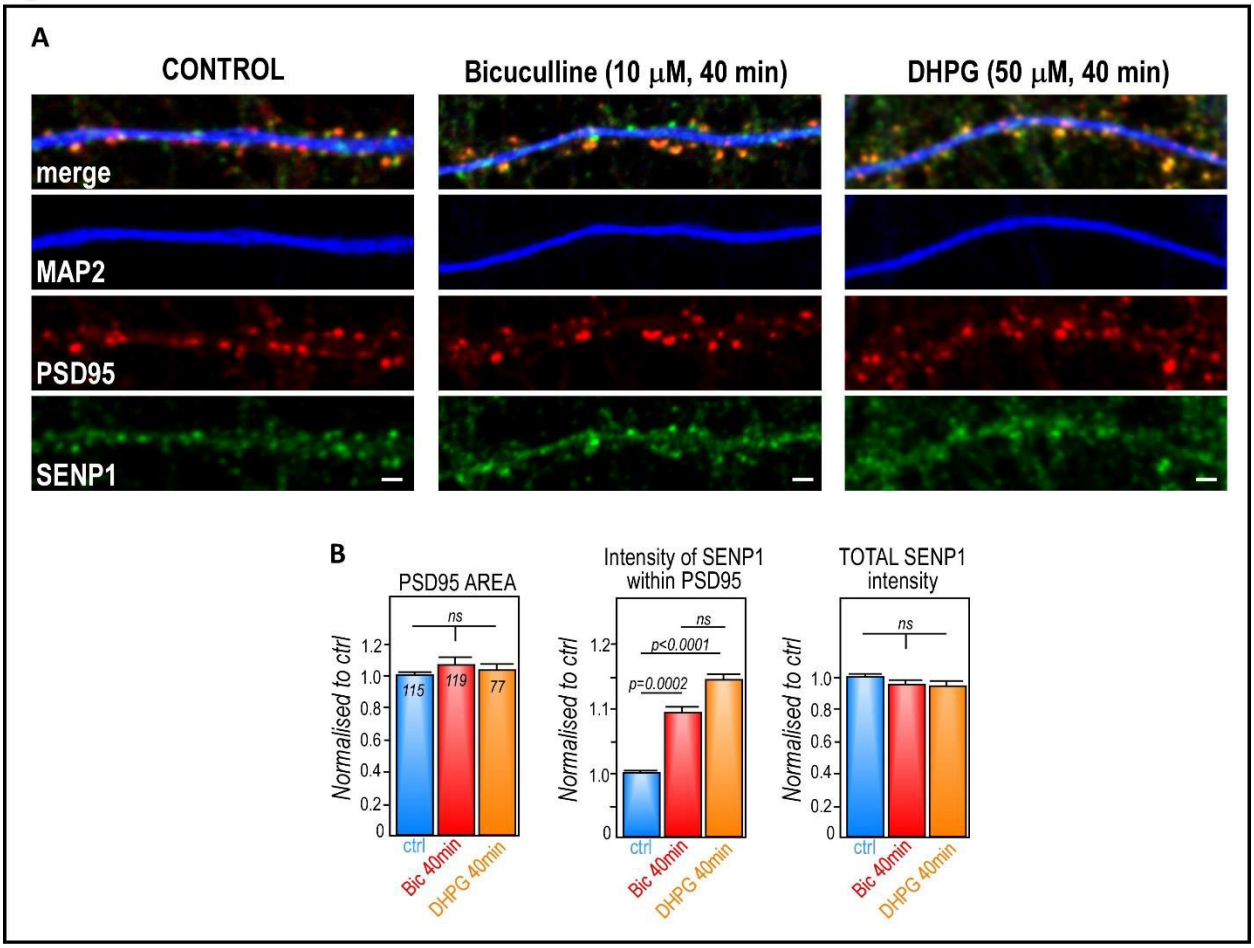

Figure 44. **Localisation of endogenous SENP1 at synapses**. **A.** Immuno-labelling of cold-methanol fixed primary hippocampal neurons in control, bicuculline (40 min treatment) and DHPG (40 min treatment) conditions. **B.** Quantitative representation in arbitrary units +/- SEM of control-normalised size of **PSD-95 area** (ctrl: 1 +/- 0.057, bic: 1.087 +/- 0.08, DHPG: 1.043 +/- 0.062); **fluorescence intensity of SENP1 within PSD-95 area** (ctrl: 1+/- 0.012, bic: 1.09 +/- 0.016, DHPG: 1.139 +/- 0.025); and **total SENP1** staining (ctrl: 1 +/- 0.02, bic: 0.96 +/- 0.027, DHPG: 0.95 +/- 0.032) from 3 different cultures and at least 6 neurons analysed per condition in each culture. Number of secondary dendrites is indicated. Statistics: One-way ANOVA, post hoc: Tukey. Significant p-values are indicated. Scale bar = 2 μm.

level of endogenous SENP1 in PSD. Although only one experiment examining the SENP1 protein levels upon MPEP+DHPG treatment was performed, it is likely that mGluR5 plays at least a partial role in the regulation of SENP1 synaptic distribution. Noteworthy, these results suggest a functional importance as disrupted mGluR1/5 signalling, that has been repeatedly implicated in a number of neurological conditions, could consequently trigger a dysregulation of the sumoylation/desumoylation balance leading to synaptic defects.

Figure 45.

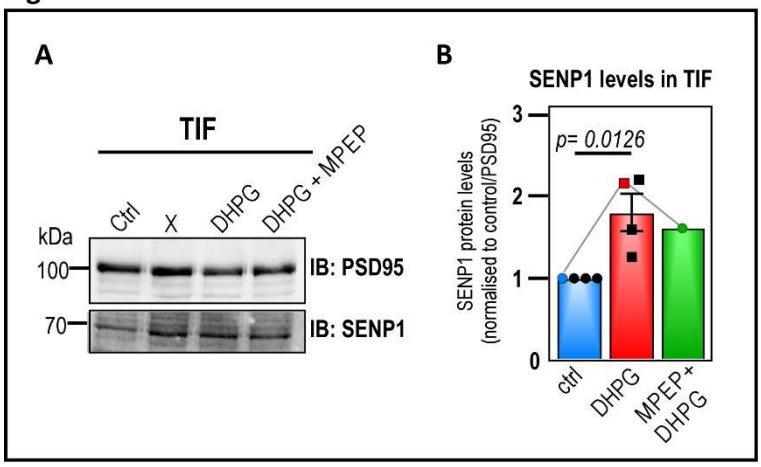

Figure 45. **Activation of Group I mGluRs increases endogenous SENP1 levels at PSD**. **A.** Representative Western Blot of TIF fractions from ctrl, DHPG- and DHPG+MPEP-treated cortical neurons (19 DIV). 15 µg of protein was loaded per lane. Immuno-detection was performed for PSD95 and SENP1. **B.** Quantitative representation of control-normalised SENP1 levels in TIF +/- SEM in DHPG (1.8 +/- 0.23) condition from 4 different neuronal cultures and DHPG+MPEP (1.6) from 1 culture. Grey lines and coloured point mark the quantification of SENP1 levels from A. PSD95 levels were used as a loading control. Statistics: Paired t-test. P-value is indicated.

The activation of mGluR1/5 regulates SENP1 synaptic redistribution leading to an accumulation of SENP1 at synapses.

In order to identify which one of the two Group I mGlu receptors activation is responsible for SENP1 regulation at synapses I applied an mGluR5 antagonist, the MPEP compound, and performed FRAP experiments in unstimulated and stimulated conditions. Neurons were pre-incubated for 10 min with MPEP before bicuculline addition for another at least 25 min and then FRAP was performed. As seen from ***Figure 46***, the effect of MPEP itself on SENP1 spino-dendritic diffusion was significant with an increase in half time recovery (t1/2: ctrl [20.84 +/- 1s] vs MPEP [26.5 +/- 1.1 s]) and concurrent decrease in diffusion speed (diff. coef.: ctrl [0.0135 +/- 0.0007 $\mu m^2/s$] vs MPEP [0.010 +/- 0.0004 $\mu m^2/s$]). Although significantly lower, the mobile fraction of SENP1 upon MPEP action is not as low as it is in bic and MPEP+bic conditions (Fm: ctrl [74.9 +/- 1 %] vs MPEP [70.1 +/- 1.1 %] vs bic [56.2 +/- 1.8 %] vs MPEP+bic [64.4 +/- 2.1 %]). This rather complex result confirms that mGluR5 may play at least a partial regulatory role on SENP1 at synapses as already proposed for the endogenous SENP1 (***Fig. 45***). To follow on these findings, I carried out similar FRAP assays but this time with the use of DHPG as a synaptic activity-promoting compound that acts on both mGluR1 and mGluR5. It can be appreciated from ***Figure***

Figure 46.

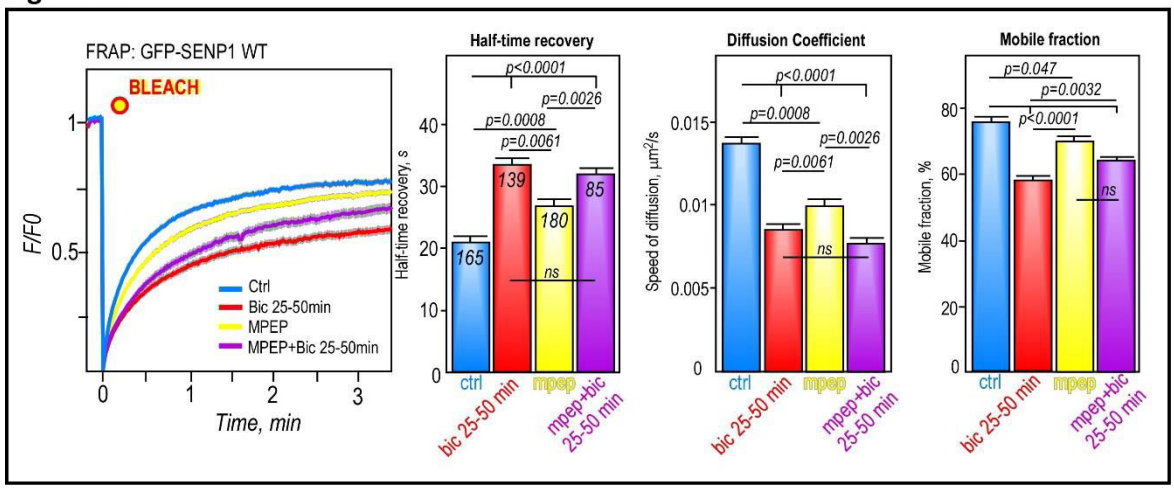

Figure 46. **mGluR5 participates in the regulation of SENP1 synaptic diffusion**. **A.** FRAP curves from FRAP experiments of WT GFP-SENP1-expressing spines of rat hippocampal neurons (18-20 DIV) showing mean values (+/- SEM) of fluorescence recovery in bleached spines in **control** (blue), **bicuculline** (red, sustained treatment of **25-50 min**), **MPEP** (yellow) and **MPEP+bic** (purple, sustained treatment of bic **25-50 min**) conditions. **B.** FRAP measurements +/- SEM: half-time recovery (**$t_{1/2}$**, ctrl [20.84 +/- 1 s], bic [33.6 +/- 1.6 s], MPEP [26.5 +/- 1.1 s] and MPEP+bic [33.75 +/- 1.8 s]); **diffusion coefficient** (ctrl [0.0135 +/- 0.0007 $\mu m^2/s$], bic [0.0088 +/- 0.0007 $\mu m^2/s$], MPEP [0.010 +/- 0.0004 $\mu m^2/s$] and MPEP+bic [0.0081 +/-0.0007 $\mu m^2/s$]); and **mobile fraction** (ctrl [74.0 +/- 1 %], bic [56.2 +/- 1.8 %], MPEP [70.1 +/- 1.1 %] and MPEP+bic [64.4 +/- 2.1 %]). Spine numbers are indicated and come from at least 3 different cultures. Statistics: $t_{1/2}$ and diff. coef. were analysed by Kruskal-Wallis and Fm by parametric ANOVA with the posthoc Tukey test. P-values are indicated.

47, despite of a low spine n-number in MPEP and MPEP+DHPG conditions, that specific activation of Group I mGluRs by DHPG and simultaneous blocking of mGluR5 reverses the effect of DHPG

Figure 47.

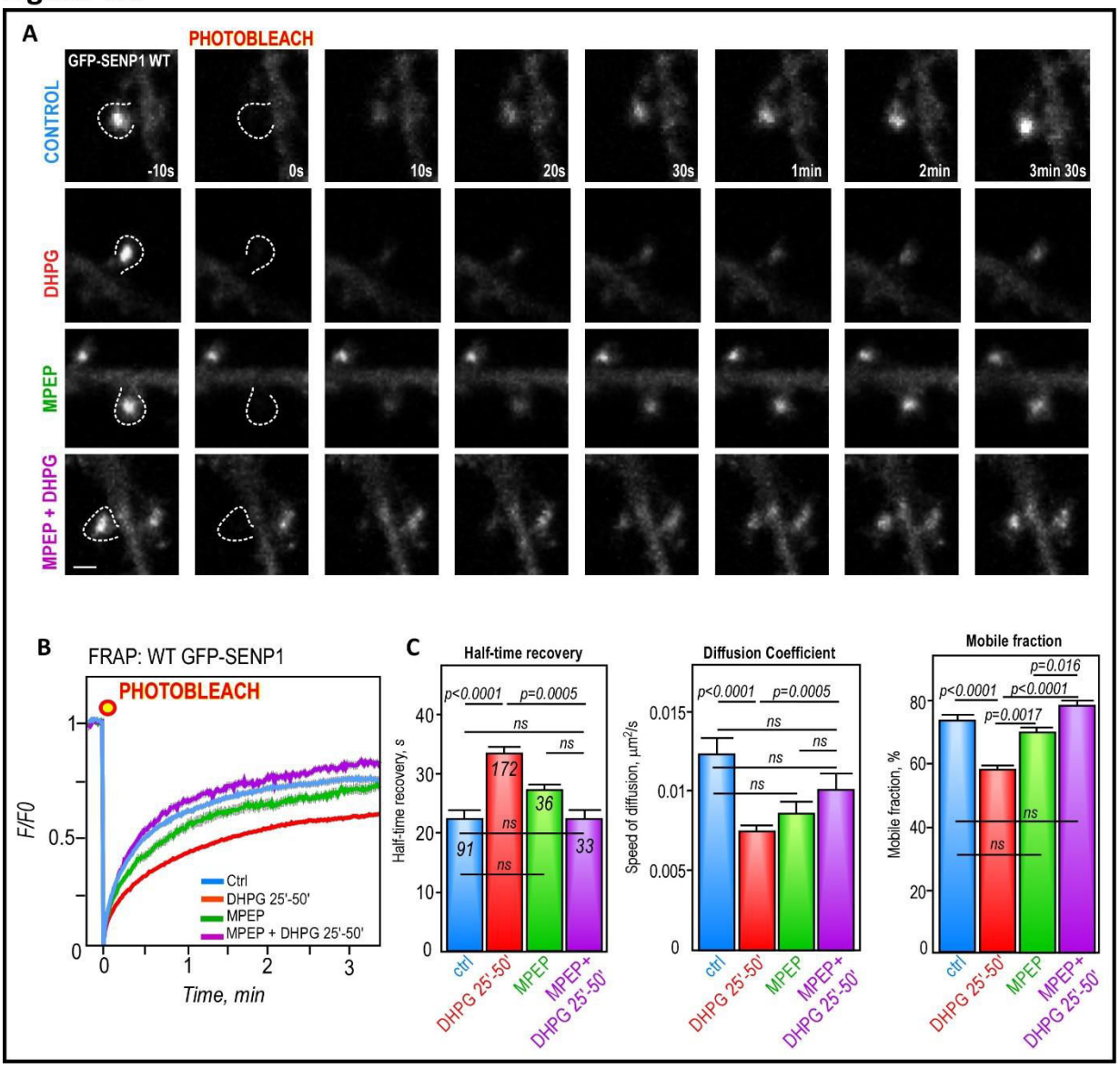

Figure 47. **SENP1 synaptic diffusion is mGluR5-dependent**. **A.** Representative FRAP recordings of WT GFP-SENP1-expressing spines of rat hippocampal neurons (19 DIV) in control, DHPG (sustained treatment of 25-50 min), MPEP and MPEP+DPHG (sustained DHPG treatment of 25-50 min) conditions. Scale bar = 1 µm. **B.** FRAP curves showing mean values (+/- SEM) of fluorescence recovery in bleached spines in **control** (blue), **DHPG** (red), **MPEP** (green) and **MPEP+DHPG** (purple) conditions. **C.** FRAP measurements +/- SEM: half-time recovery (**$t_{1/2}$**, ctrl [23.4 +/- 1.4 s], DHPG [34.0 +/- 1.1 s], MPEP [27.5 +/- 1.7 s] and MPEP+DHPG [23.3 +/- 2 s]); **diffusion coefficient** (ctrl [0.0126 +/- 0.0012 µm^2/s], DHPG [0.0071 +/- 0.0003 µm^2/s], MPEP [0.0082 +/- 0.0006 µm^2/s] and MPEP+DHPG [0.012 +/-0.001 µm^2/s]); and **mobile fraction** (ctrl [74.0 +/- 1.6 %], DHPG [58.4 +/- 1.2 %], MPEP [68.1 +/- 2.1 %] and MPEP+DHPG [79.0 +/- 1.5 %]). Spine numbers are indicated and come from at least 2 different cultures. Statistics: $t_{1/2}$ and diff. coef. were analysed by Kruskal-Wallis and Fm by parametric ANOVA with the posthoc Tukey test. P-values are indicated.

with the time and speed of fluorescence recovery as well as mobile fraction being comparable to control condition (***Fig. 47***). Significant changes can be seen again between control and MPEP-only conditions (***Fig. 47***). It should be also noted, that neuronal cultures present a high level of spontaneous activity and therefore blocking a receptor, of which activity mediates SENP1 synaptic regulation, may potentiate the activity of an alternative receptor/pathway. I therefore used tetrodotoxin (TTX) to verify whether reducing spontaneous neuronal activity could explain this discrepancy. To this end, neurons were pre-treated with 2 µM TTX for 10 min prior to the addition of MPEP (***Fig. 48***). Indeed, TTX addition prevented the changes in SENP1 diffusion when blocking mGluR5 by MPEP. Altogether, these findings confirm a direct participation of mGluR5 in SENP1 spino-dendritic diffusion.

Figure 48.

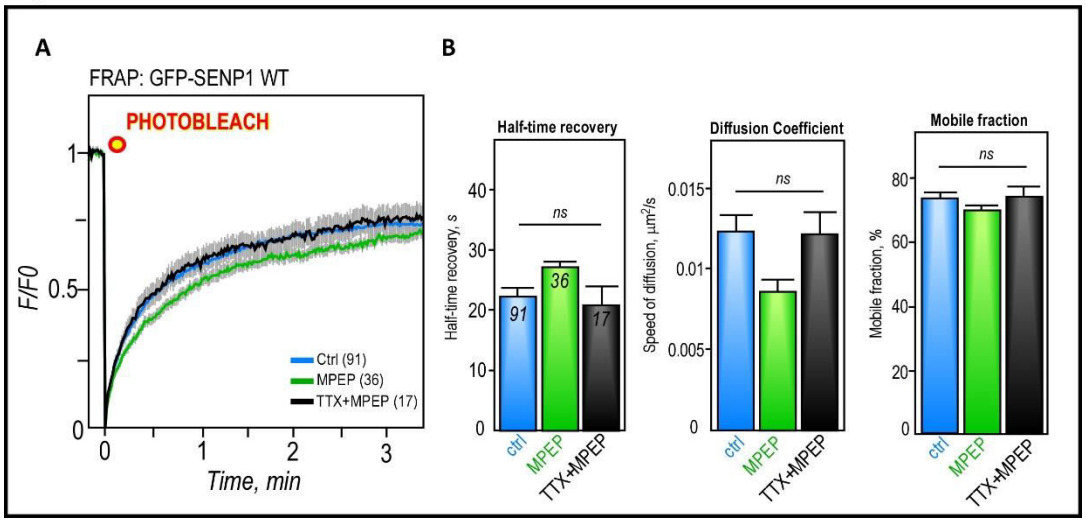

Figure 48. **Application of TTX reduces spontaneous neuronal activity**. FRAP curves showing mean values (+/- SEM) of fluorescence recovery in bleached spines in **control** (blue), **MPEP** (green) and **TTX+MPEP** (black) conditions. B. FRAP measurements +/- SEM: **half-time recovery** ($t_{1/2}$, ctrl [23.4 +/- 1.4 s], MPEP [27.5 +/- 1.7 s] and TTX+MPEP [21.9 +/- 3.4 s]); **diffusion coefficient** (ctrl [0.0126 +/- 0.0012 µm^2/s], MPEP [0.0082 +/- 0.0006 µm^2/s] and TTX+MPEP [0.0123 +/-0.0018 µm^2/s]); and **mobile fraction** (Fm, ctrl [74.0 +/- 1.6 %], MPEP [68.1 +/- 2.1 %] and TTX+MPEP [74.3 +/- 4.8 %]). Spine numbers are indicated. Experiments were performed with at least 2 different cultures. Statistics: $t_{1/2}$ and diff. coef with Kruskal-Wallis and Fm with parametric ANOVA with Tukey post hoc test. NS, not significant.

SENP1 synaptic redistribution is regulated in an mGluR5 activity-dependent manner.

III. Is SENP1 trafficking dependent upon microtubules?

SENP1 presence at the postsynapse is likely a result of dendritic protein trafficking/diffusion, although local translation may also occur. The spino-dendritic exchange of SENP1 is regulated on an intermediate timescale (~tens of seconds, ***Fig. 34***). In the previous sections, we could appreciate a particular SENP1 mobility which suggests that SENP1 most likely undergoes a transient binding diffusion before reaching its destination (due to its size and interactions). I highlighted the different types of protein mobility in ***Figure 49***, indicating that SENP1 diffuses with short transient binding to yet unknown structures. This points to a question as to what are the interacting structures/molecules that slow down SENP1 spino-dendritic diffusion? Considering that microtubule processes enter into dendritic spines rather rarely and stop usually at the spine base or neck, I reasoned that microtubules could act for delivery of SENP1 to the spine neck where SENP1 molecules would be released and would either diffuse to the spine head or would be handed off to the actin-bound motor protein myosin. It is well established that synaptic plasticity depends upon synaptic activation that triggers biophysical changes of the cytoskeleton. Group I mGluRs have been linked to microtubule function. In particular, mGluR5 has been shown to closely associate with microtubules (Paquet and Smith, 2003). Moreover, mGluR1/5 activation has been reported to reduce the formation of microtubules (Huang and Hampson, 2000). Since SENP1 synaptic redistribution is regulated by mGluR5, I wanted to examine whether preventing microtubule polymerisation/depolymerisation could affect the dynamics of SENP1 redistribution into spines.

Figure 49.

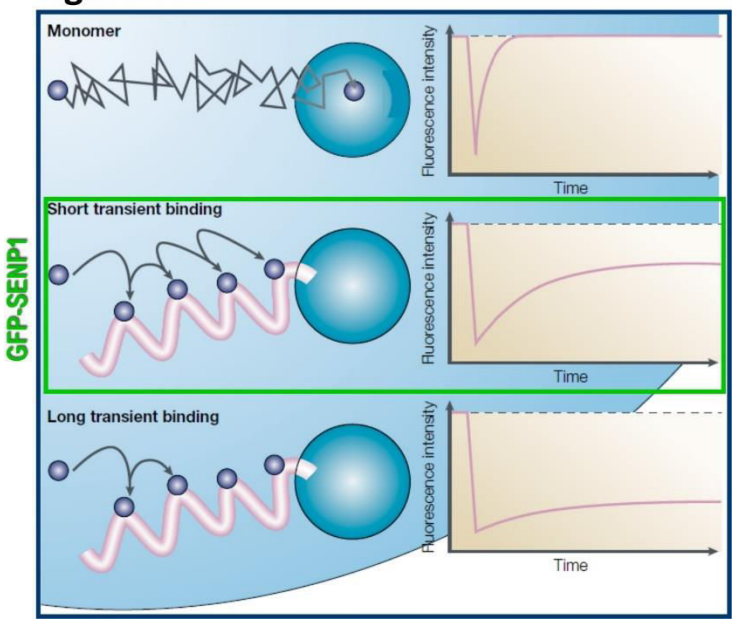

Figure 49**. FRAP measurements can determine the binding properties of studied proteins.** Protein mobility can be divided into three basic kinds: free diffusion, short transient binding and long transient binding. Usually a monomeric protein undergoes rapid diffusion, therefore a fast recovery in FRAP can be recorded (such as free GFP). On the other hand, proteins that transiently interact with relatively more immobile structures, e.g. the cytoskeleton, show intermediate kinetics. This type of kinetics can be seen for GFP-SENP1 (green rectangle). Proteins that bind to cellular components for longer periods of time recover with slow kinetics. Taken and modified from (Phair and Misteli, 2001).

To do this, I performed time-lapse imaging of WT GFP-SENP1-expressing rat hippocampal neurons in the course of a treatment with nocodazole (***Fig. 50***), a potent microtubule destabilising agent. Interestingly, nocodazole effect mimicked the bicuculline-induced increase in GFP-SENP1 localisation in spines, which was reversed upon a washout with control solution (***Fig. 50***). This finding importantly suggests that microtubule stability is requisite for SENP1 removal from spines. More experiments will now have to be carried out with the combination of DHPG and MPEP (mGluR5 antagonist) together with nocodazole to be certain of mGluR5 activation and microtubules being the driving mechanism of SENP1 spino-dendritic exchange/exit. Possibly, an investigation into the involvement of particular microtubule or actin-bound motor proteins could yield more detailed insights into SENP1 regulation at synapses. Moreover, regulatory proteins/structures that have been already reported to accumulate in spines upon stimulation could be also considered as potential participants in SENP1 regulation. Some of these are CaMKII (Otmakhov et al., 2004), proteasomes (Bingol et al., 2010), lysosomes (Goo et al., 2017), and PSD proteins (Kim et al., 2007).

Figure 50.

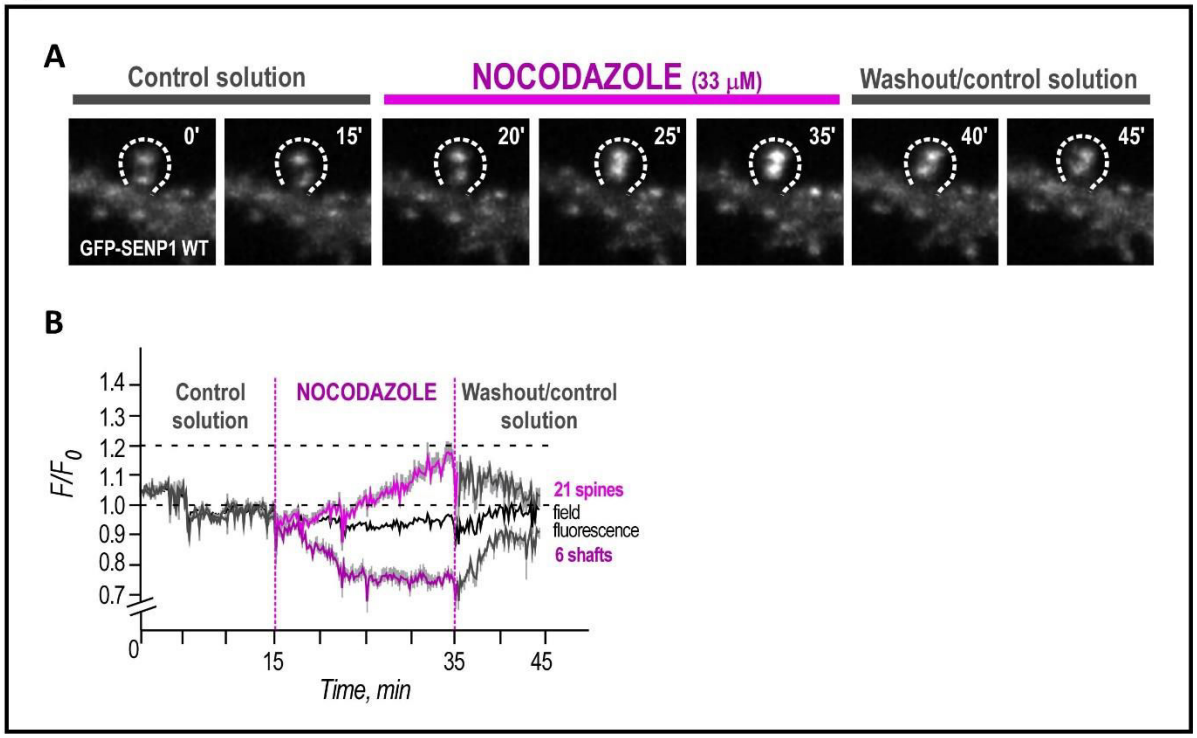

Figure 50**. Microtubule stability is involved in spino-dendritic exchange of WT GFP-SENP1. A**. Confocal images of a WT GFP-SENP1-expressing neuron during a time-lapse imaging in the course of the treatment with control (0-15 min), nocodazole (33 µM, 15-35 min) and washout (35-45 min) solutions. **B.** Corresponding quantification of a representative experiment showing +/- SEM of normalised fluorescence intensity in spines (n=21), shafts (n=6) and whole dendritic tree field in the course of the treatment with control solution, nocodazole (33 µM, in purple) and during washout.

SENP1 synaptic exit is likely mediated by microtubules.

IV. Does SENP1 accumulation in spines affect SUMO1/2/3-ylation levels in the PSD?

To examine the levels of sumoylation at synapses, I performed TIF isolation from cortical cultured neurons that were treated or not with bicuculline, DHPG and DHPG+MPEP (***Fig. 51***). It should be noted that TIF fraction may not be a representative fraction of a whole synapse (as it only represents the PSD environment, i.e. a specific set of proteins), and therefore the preliminary results presented in ***Figure 51*** need to be validated in synaptosomal preparation. Nevertheless, I wish to discuss these results since they represent an important functional read-out of SENP1 accumulation at synapses; but at the same time keeping in mind that this point must be correctly addressed by future experiments. Here I show that synaptic activation by both bicuculline and DHPG (40-minute sustained treatment) leads to an increase in SUMO1-ylated protein levels in TIF (bic: ~144% and DHPG: 166% of control, ***Fig. 51***). Interestingly, stimulation by DHPG with a simultaneous blocking of mGluR5 by MPEP reverses, although only partially, the increase in SUMO1-ylation seen upon DHPG treatment (~128% of control). In regard to SUMO2/3-ylation, only sustained bicuculline treatment increased the levels of overall SUMO2/3-ylation by ~28%, whereas the activation of mGluR1/5 by DHPG did not change the levels of SUMO2/3-ylation in TIF after 40 min of sustained treatment (***Fig. 51***). However, the application of mGluR5 antagonist MPEP together with DHPG led to a drop in SUMO2/3-ylation by ~16% in comparison with control (***Fig. 51***). Altogether, the present results indicate that SUMO1-ylation increases likely in response to the activation of Group I mGluRs. Although the S2/3-ylation levels remain unchanged in response to Group I mGluR activation, a certain level of regulation by these receptors can be noticed when blocking specifically mGluR5 by MPEP. For the time being no conclusive remarks can be drawn other than that the SUMO1/2/3-ylated levels of synaptic proteins in TIF undergo changes in response to sustained synaptic activation.

From previous experiments presented above, I demonstrated that SENP1 gradually accumulates in spines. This is, however, not reflected by decreased SUMO1/2/3-ylation levels at the 40-minute time point of sustained synaptic stimulation. Notably, this does not imply that desumoylation does not take place, but rather that sumoylation prevails. It could be also

hypothesized that the catalytic activity of accumulating SENP1 is inhibited by an unknown pathway (perhaps as a protective mechanism against excessive and unwanted desumoylation at the synapse). Only when synaptic activity returns to basal levels, SENP1 may be released from the inhibited state and desumoylate its substrates. To address these discrepancies, cultured neurons should be first, treated for several time points with control solution and upon sustained synaptic activation (e.g. 0, 10, 20, 30 and 40 min). And second, a protocol introducing a washout upon synaptic stimulation prior to the lysis and TIF isolation should be used. Then, SENP1 and SUMO1/2/3-ylation levels as well as Ubc9 levels can be determined and compared along the time course of different length of the treatment.

I would like to mention that our laboratory has already published findings reporting increased SUMO1/2/3-ylation levels in stimulated conditions in synapses (endpoint of a 10-minute sustained stimulation, (Loriol et al., 2014)). However, these experiments were performed *in vitro* on intact synaptosomes. Therefore, they cannot reflect on the counteractivity of both sumoylation and desumoylating enzymes that would diffuse from the shaft into the spine upon stimulation to balance sumoylation levels. These previous findings provide insights only into the immediate effects of the sumoylation machinery and the "SUMO pool" on synaptic proteins, all of which are already available in the synapse. What can be, however, appreciated is that indeed, under such experimental conditions, SUMO-conjugation predominates SUMO-deconjugation (Loriol et al., 2014). Here I present a different approach, in which neurons were treated prior the PSD (TIF) isolation reflecting the outcome of the dynamic shaft-spine exchange of both sumoylation and desumoylation enzymes that takes place within the 40-minute incubation under control or treated conditions (but examined only at the end point of 40 minutes). It will be important to carry out corresponding biochemical and imaging assays and examine the levels and kinetics of Ubc9 together with SENP1 and alternatively other desumoylation enzymes (e.g. SENP5 and SENP6) as well as the levels of SUMO1/2/3-conjugation at multiple time points. This will provide a more complete picture of the synaptic regulation of the sumoylation machinery as a whole.

Figure 51.

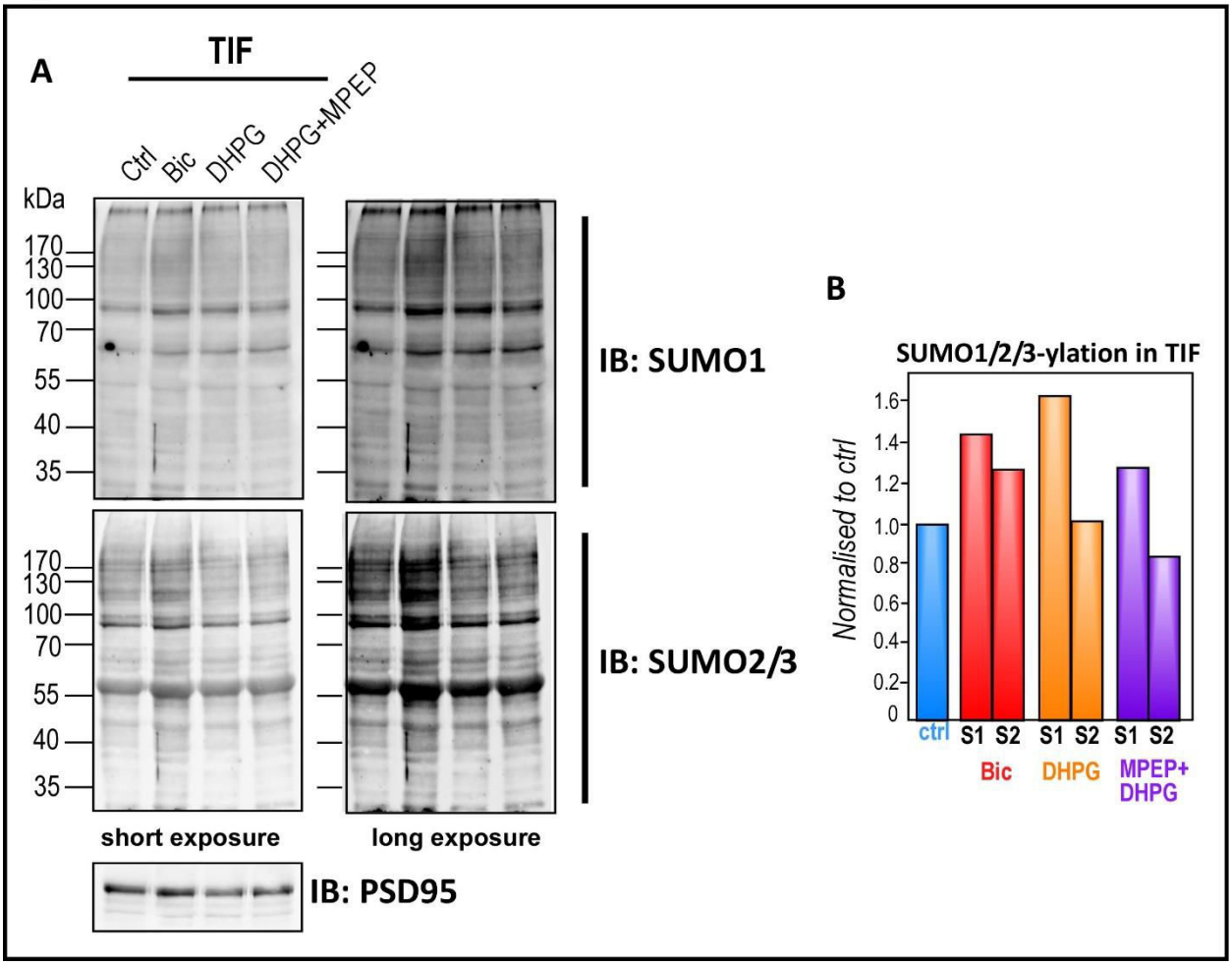

Figure 51. **Sustained synaptic activation alters SUMO1/2/3-ylation levels in TIF fraction. A**. Western Blots of TIF fractions isolated from 19DIV primary cortical neurons treated or not with bicuculline, DHGP and MPEP+DHPG for a sustained stimulation of 40 min. Loaded was 40 µg of protein per lane. Immuno-detection was performed for SUMO1, SUMO 2/3 and PSD95. PSD95 levels were used as a loading control. **B.** Corresponding quantification of Western Blots in A normalised to control: Bic (S1: 1.44; S2: 1.28), DHPG (S1: 1.66; S2: 1.04), MPEP+DHPG (S1: 1.28; S2: 0.84).

Synaptic activation changes SUMO1/2/3-ylation levels in the TIF fraction.

V. Is the catalytic activity of SENP1 important for its spino-dendritic redistribution?

To address this question, I performed time-lapse imaging and FRAP experiments using hippocampal neurons expressing GFP-SENP1 with a point mutation in its nucleotide sequence leading to the substitution of Cysteine for Serine at position 603 (C603S) which abolishes SENP1 catalytic activity (Bailey and O'Hare, 2004). Interestingly, as for the WT enzyme, GFP-SENP1 C603S showed an accumulation in dendritic spines in the course of bicuculline treatment (***Fig. 52A and B***). This accumulation was partially reversed upon a washout with control solution (***Fig. 52A and B***). Moreover, GFP-SENP1 C603S displayed a similar diffusion behaviour like WT GFP-SENP1 with a slower speed of fluorescence recovery and lower mobile fraction upon synaptic activation (***Fig. 53***). This result indicates that GFP-SENP1 is regulated upon synaptic activation at postsynaptic sites independently of its catalytic capabilities. This finding was unexpected as I

Figure 52.

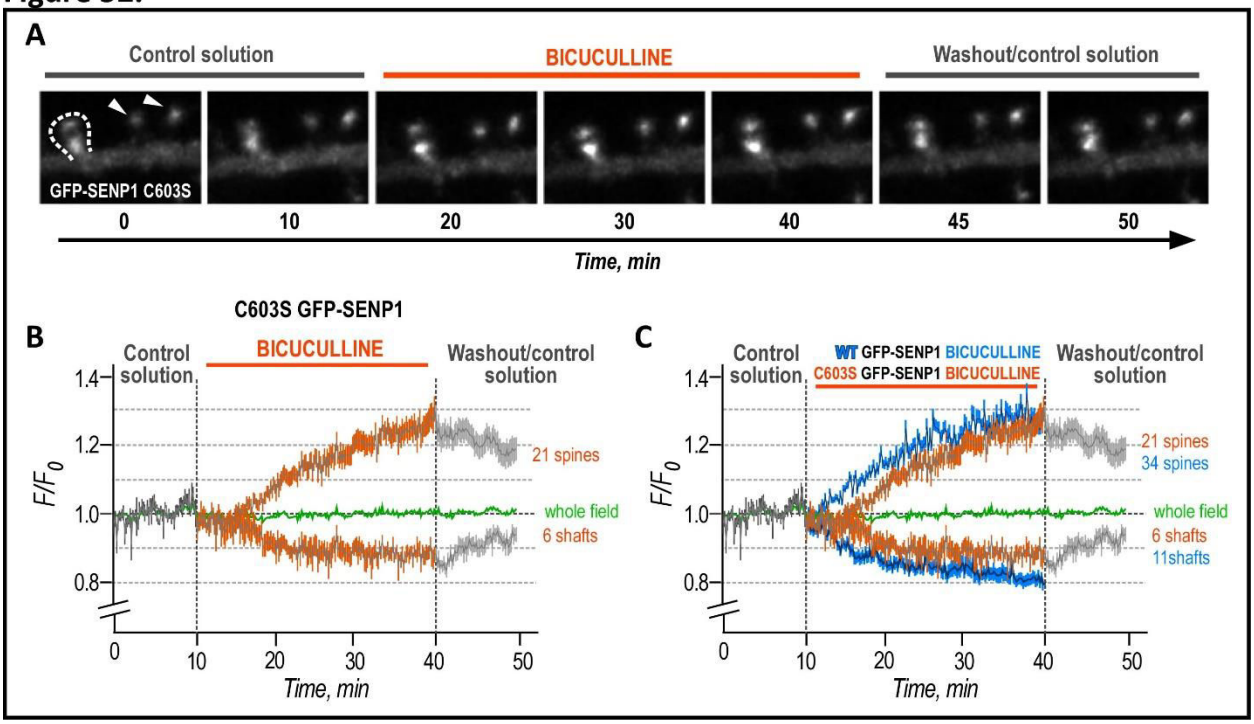

Figure 52**. Synaptic activation triggers accumulation of GFP-SENP1 C603S in spines. A**. Confocal images of a GFP-SENP1 C603S-expressing neuron during a time-lapse imaging in the course of treatment with control (0-10 min), bicuculline (10-40 min) and washout (40-50 min) solutions. **B.** Corresponding quantification of a representative experiment showing mean curve +/- SEM of normalised fluorescence intensity in spines (n=21), shafts (n=6) and whole dendritic tree field in the course of treatment with control solution, bicuculline (10 µM, in orange) and during washout. **C.** Graph as in B with additionally pasted curves +/- SEM (blue) from time-lapse recording of WT GFP-SENP1 during the course of 30-minute bicuculline treatment from Fig. 32.

hypothesized that WT SENP1 would be regulated toward an increase of its synaptic localisation for the specific purpose of catalysing desumoylation of synaptic substrates, which would be prevented by perturbing its catalytic activity, but this turned out not to be the case.

What can be, however, appreciated is different spino-dendritic kinetics between WT and C603S GFP-SENP1 from both time lapse (***Fig. 52***) and FRAP experiments (***Fig. 53C and D***). In ***Figure 52C*** I combined the quantifications of spine and shaft fluorescence intensities in neurons expressing WT and C603S GFP-SENP1 in the course of bicuculline treatment (30 min of sustained activation). It is apparent that GFP-SENP1 C603S accumulates in spines with slower dynamics but resulting in similar abundance of GFP-SENP1 C603S in spines at the peak of bicuculline effect as for WT GFP-SENP1. This suggest that GFP-SENP1 C603S may be physically stalled in the shaft. The rundown of GFP-SENP1 in the shaft does also manifest distinct dynamics between WT and C603S GFP-SENP1 (***Fig. 52C***). The FRAP experiments demonstrate that the half time recovery and speed of diffusion between WT and C603S GFP-SENP1 in basal condition (blue bars in ***Fig. 53D***) differ substantially. It is clear that WT GFP-SENP1 diffuse into spines faster than the mutant GFP-SENP1 in unstimulated conditions. This difference is nearly completely diminished upon bicuculline-induced and sustained activity (red and orange bars in ***Fig. 53D***). Mobile fractions, however, remain similar in unstimulated conditions between WT and C603S GFP-SENP1, with a comparable reduction upon stimulation with bicuculline (***Fig. 53D***). Altogether, these observations imply that GFP-SENP1 C603S may be stalled in shaft for a longer period of time in comparison to the WT form of GFP-SENP1. A mechanism involved in C603S GFP-SENP1 stalling could include more persistent interactions with molecular partners/cellular structures (as pointed out in section III) or substrate proteins due to the amino acid mutation. Upon synaptic activation, different forms of interactions may be potentiated and persist with sustained synaptic stimulation for both WT and mutant forms of GFP-SENP1. To gain more insight into the dynamic properties of GFP-SENP1 C603S, the exit from spines will have to be also examined using Dendra2-SENP1 C603S photoconversion as previously done for WT GFP-SENP1 in ***Figure 37***.

The mechanism of GFP-SENP1 synaptic targeting is independent of its catalytic site/activity.

Figure 53.

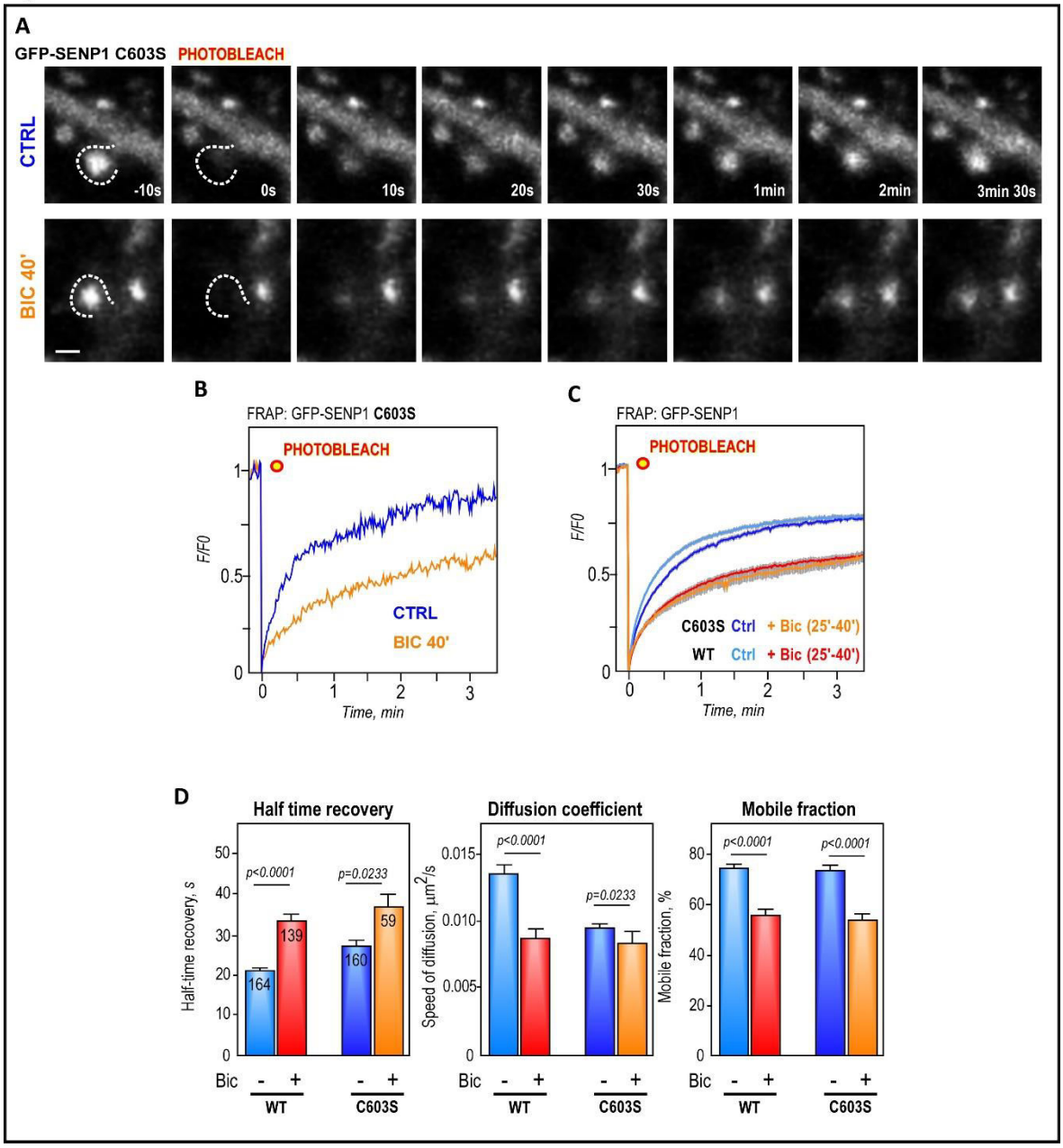

Figure 53. **Synaptic redistribution of GFP-SENP1 C603S is regulated by synaptic activity**. **A.** Representative FRAP recordings of GFP-SENP1 C603S-expressing spines of rat hippocampal neurons (19 DIV) in control and bicuculline (40 min of sustained treatment) conditions. Scale bar 1 µm. **B.** FRAP curves corresponding to images in A. **C.** FRAP curves showing mean values (+/- SEM) of fluorescence intensity of bleached spines for **WT** and **C603S GFP-SENP1** in control (light and dark blue) and bicuculline (red and orange, 25-50 min of sustained bic treatment) conditions. **D.** FRAP measurements +/- SEM: **half-time recovery** ($t_{1/2}$, **WT**: ctrl [20.79 +/- 1 s], bic 25-50 min [33.58 +/- 1.6 s]; **C603S**: ctrl [27.4 +/- 1.2 s], bic [36.8 +/- 3.6 s]); **diffusion coefficient** (**WT**: ctrl [0.0135 +/- 0.0007 µm^2/s], bic 25-50 min [0.0087 +/- 0.0007 µm^2/s]; **C603S:** ctrl [0.0092 +/- 0.0004 µm^2/s], bic [0.0084 +/- 0.001 µm^2/s]); and **mobile fraction** (**WT**: ctrl [74.5 +/- 1.1 %], and bic 25-50 min [56.2 +/- 1.8 %]; **C603S:** ctrl [73.9 +/- 1 %], bic [54.2 +/- 2.6 %]). Spine number WT: ctrl= 165 and bic 25-50 min= 139; C603S: ctrl= 160 and bic 25-50 min= 59, from at least 5 different cultures for WT and 2 different cultures for C603S GFP-SENP1. Statistics: $t_{1/2}$ and diff. coef. were analysed with Mann-Whitney t-test and Fm with parametric t-test. P-values are indicated.

Perspectives

3. Perspectives

The posttranslational modification by SUMO proteins has emerged as an important mechanism regulating synaptic proteins instantly associated with synaptic function. This is evidenced by defective 'SUMO balance' that has been closely associated with neurodevelopmental as well as neurodegenerative diseases. Moreover, sumoylation does not occur only in the brain as it is a ubiquitous PTM. A dysregulated sumoylation/desumoylation balance occurs in many other pathological conditions such as the aetiology of cancer. Current research in this field is intensively focused on gaining more insights into the consequences of sumoylation of proteins with proto-oncogenic and tumour-suppressor roles. Due to the magnitude of its effects on cell function and ubiquitous presence it is difficult at the moment to envisage what kind of pharmacological interventions could be developed in the future to target the sumoylation machinery to bring sumoylation and desumoylation back to balance. Prior to this challenging objective, many fundamental questions are yet to be addressed. One of them includes the regulatory mechanisms of the SUMO-conjugation and SUMO-deconjugation processes.

In my PhD thesis I aimed at dissecting the molecular mechanisms of SENP1 regulation at synapses to complement the findings on Ubc9 (Loriol et al., 2014) and get a better picture of how the sumoylation/desumoylation balance is established at synapses. I identified mGluR5 receptors as upstream regulators of SENP1 synaptic diffusion (as previously identified also for Ubc9). Moreover, I showed that microtubules may additionally play a role in SENP1 dynamic spino-dendritic processes. Strikingly, however, the complex results suggest that additional players may be involved. This prompted me to investigate SENP1 interacting proteins that may regulate SENP1 at synapses.

In order to identify SENP1 protein partners and/or substrates I performed Mass Spectrometry analysis of GFP-pulled down (-trapped) GFP-SENP1 expressed in cultured neurons (***Fig. 54***). By doing this, I wanted to identify important regulatory players that could be further studied by molecular and cellular means for their involvement in SENP1 regulation in neurons and perhaps other cell types. However, due to a low level of GFP-SENP1 expression, I did not perform

subcellular fractionation to enrich the sample in synaptic proteins. Despite this discrepancy, the MS analysis on whole cell lysate yielded some interesting results including highly abundant synaptic proteins. What stroke me was the presence of both CaMKII and PKC as highly enriched SENP1 interactors/substrates. Indeed, it has been previously suggested that SENP1 may be a phosphorylation target (based on high scores from phospho-sites prediction softwares and immuno blot analyses that revealed higher molecular band species (Bailey and O'Hare, 2004)). Moreover, sumoylation and phosphorylation are two PTMs that have been on several occasions found to work in a crosstalk introducing an additional level of complexity for the regulation of target proteins. For instance, SENP1-dependent desumoylation of PKC has been shown to regulate kainate-activation dependent endocytosis of glycine receptors (Sun et al., 2014). Since

Figure 54.

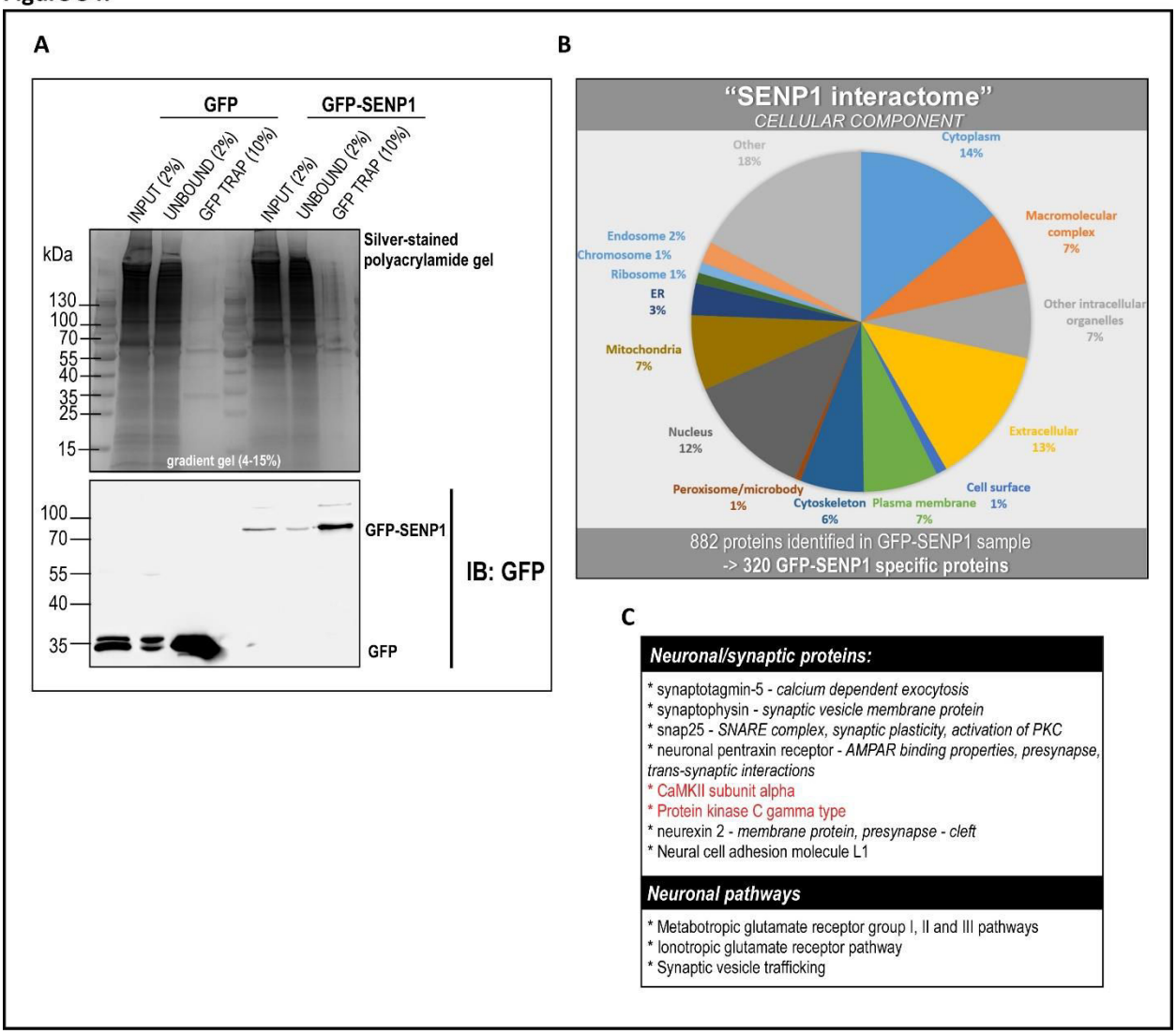

Figure 54 (Continued). **Mass spectrometry to identify SENP1 interactome**. **A.** GFP (control) and GFP-SENP1 proteins were virally expressed in cultured cortical neurons (17DIV). GFP-trap (*ChromoTek*) was performed to pull-down GFP and GFP-SENP1, respectively, with interacting partners. Samples (input 2%, unbound fraction 2 % and GFP-trapped fraction 10%) were loaded in a 4-15% gradient gel and silver-stained, or Western blot was performed (bottom membrane) to verify the presence of GFP and GFP-SENP1 in trapped fractions. **B.** Output data from MS analysis showing a categorization of SENP1-specific interactome based on cellular component. **C.** Some of the neuronal/synapse-specific proteins that have been already shown sumoylated and/or desumoylated by SENP1, as well as interesting regulatory molecules.

PKC has been already involved in the regulatory signalling cascade of SUMO-conjugation (Loriol et al., 2014), I hypothesized that in addition to PKC being a target of SENP1, this desumoylation enzyme could be in turn regulated by PKC. To this end, I performed some preliminary FRAP experiments implementing chelerythrine, a well-known inhibitor of PKC, and PMA, a PKC activator, to see whether SENP1 spino-dendritic exchange was affected by PKC blockage and/or activation (***Fig. 54***). I found that PKC activation speeded up SENP1 recovery in spines but led to a dramatic drop in the mobile fraction, suggesting that SENP1 may be actively trapped at synapses upon PKC activation. Moreover, I recorded a strong time-dependent effect of PKC activation on SENP1 spino-dendritic diffusion (***Fig. 54A***). On the other hand, blocking PKC without subsequent synaptic activation slowed down SENP1 recovery but had a little effect on mobile fraction. Together, these results, although very preliminary, indicate that PKC is a part of the signalling pathway regulating SENP1 spino-dendritic redistribution. More experiments will have to be carried out implementing PKC activators and inhibitors with simultaneous targeting of the Group I mGluRs especially focusing on mGluR5 to experimentally evidence the involvement of PKC in mGluR-dependent SENP1 regulation at synapses. Moreover, to further prove that SENP1 is a phosphorylation target, a phosphorylation-specific antibody that recognises a phosphorylated form of SENP1 could be implemented. To this end, we will compare levels of phosphorylated SENP1 in basal unstimulated and stimulated conditions. Synaptic activation leads to phosphorylation of many synaptic substrates (Woolfrey and Dell'Acqua, 2015), therefore at this point I hypothesised that PKC-dependent phosphorylation of SENP1 could at least partly drive the SENP1 action toward establishing the sumoylation/desumoylation balance at synapses. This fits well with the previous finding showing that Ubc9 gets transiently retained in spines upon the mGluR5/PLC/PKC cascade activation. Considering the time frame of Ubc9 diffusion and transient

trapping (~1-2 s) and SENP1 diffusion (~ 30 s), it is obvious that these processes must be sequentially regulated, perhaps by phosphorylation/dephosphorylation of the SUMO machinery members including SENP1.

CaMKII, another crucial synaptic kinase, that has been to date only predicted to be sumoylated in a yeast-two-hybrid screen in the *Drosophila* (Long and Griffith, 2000), was

Figure 55.

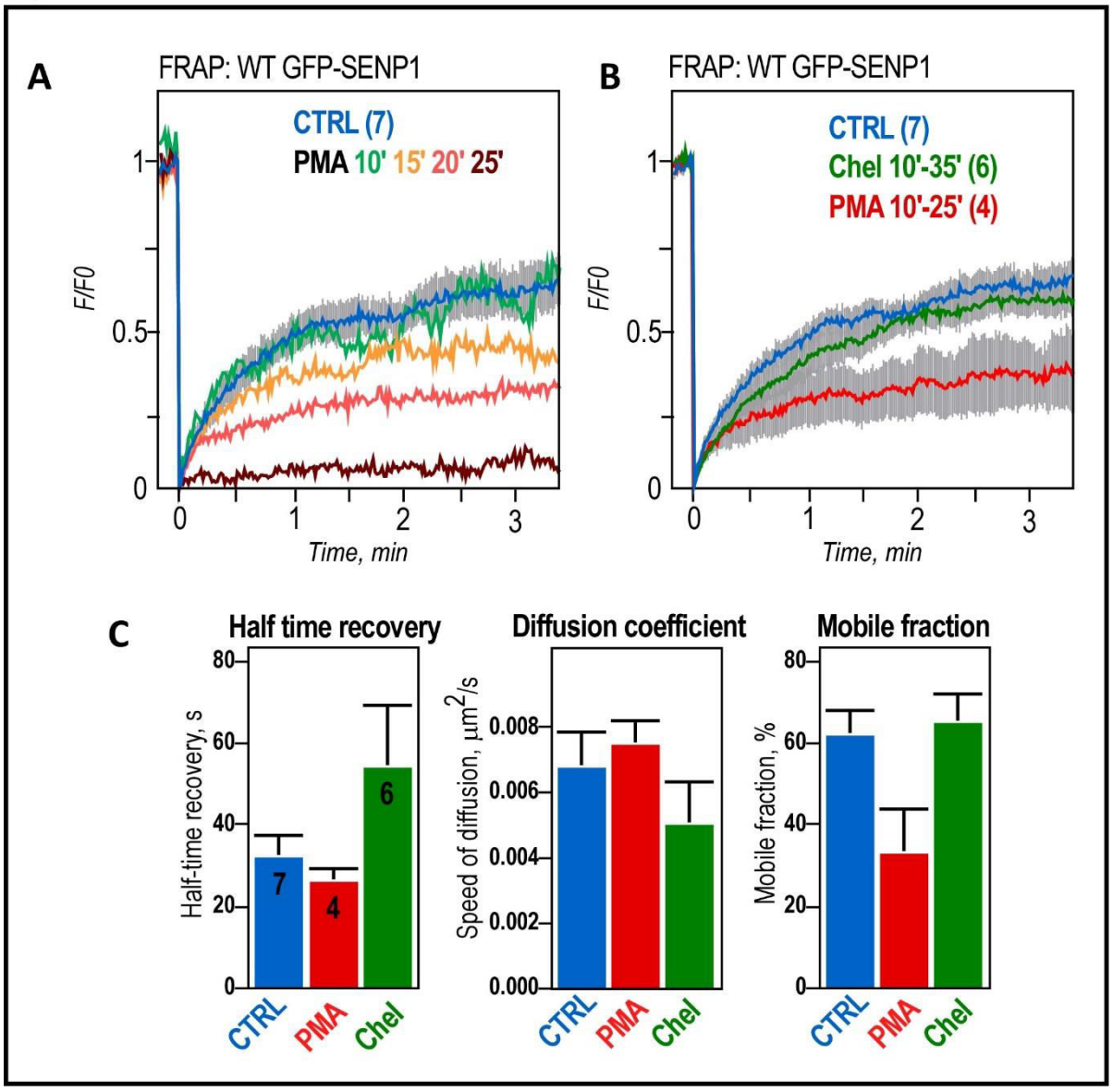

Figure 55. **PKC may play a role in the regulation of SENP1 spino-dendritic exchange. A.** Frap curves in control (blue, 7 spines) and PMA (upon sustained treatment of 10, 15, 20 and 25 min, each curve represents 1 spine). **B.** FRAP curves +/- SEM in control (7), chelerythrine (chel, 6) and PMA (spines 1-4 from A pulled together) conditions. **C.** FRAP measurements for control, PMA and chelerythrine corresponding to B.

detected in my MS analysis as a specific interactor of SENP1. I also performed FRAP experiments to examine whether blocking CaMKII by the inhibitor KN93, would affect the dynamic properties of SENP1 spino-dendritic diffusion. We can see from ***Figure 56A*** that pre-incubation with KN93 coupled with synaptic activation by bicuculline has a slight effect on the fluorescence recovery of SENP1 (compare the magenta and red curves). However, the addition of KN93 did not reverse the bicuculline effect of SENP1 dynamics as can be seen from t1/2, diffusion coefficient as well as mobile fraction. Although there might be a certain degree of regulation implying once again a more complex regulation of SENP1 at synaptic sites in comparison to Ubc9 (Loriol et al., 2014).

Figure 56.

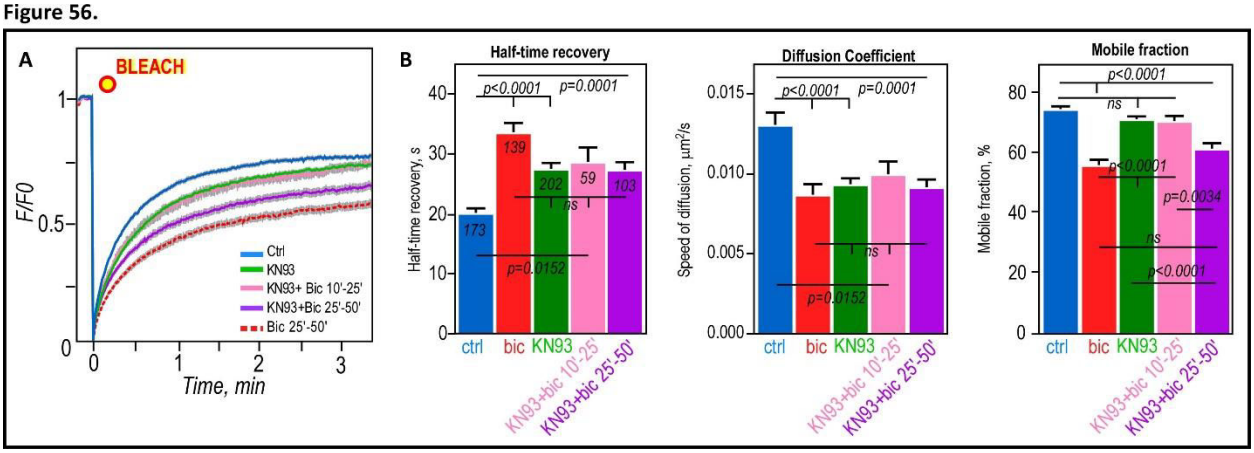

Figure 56. **CaMKII may play a role in the regulation SENP1 spino-dendritic diffusion**. **A.** FRAP curves +/- SEM from control (n spines= 173), bicuculline (139), KN93 (202), KN93+bic 10-25min (59) and KN93+bic 25-50 min (103). **B.** FRAP measurements +/- SEM corresponding to A.

mGluR5 activation can trigger the activation of both PKC and CaMKII (***Fig. 57***). Although the effect of CaMKII on SENP1 regulation seems only partial, since IP_3 binding to smooth ER leads to a release of calcium from the ER stores, it would be very interesting to investigate the effect of calcium availability in the cell on SENP1 diffusion. Specific pharmacological agents can be used e.g. to target ER calcium ATPase and prevent it from pumping calcium ions into ER therefore leading to an increase intracellular calcium levels (thapsigargin); or BAPTA, a calcium chelator. Caution will have to be taken to use appropriate and previously published concentration of these agents as their application may cause cellular stress and lead to apoptosis.

Figure 57.

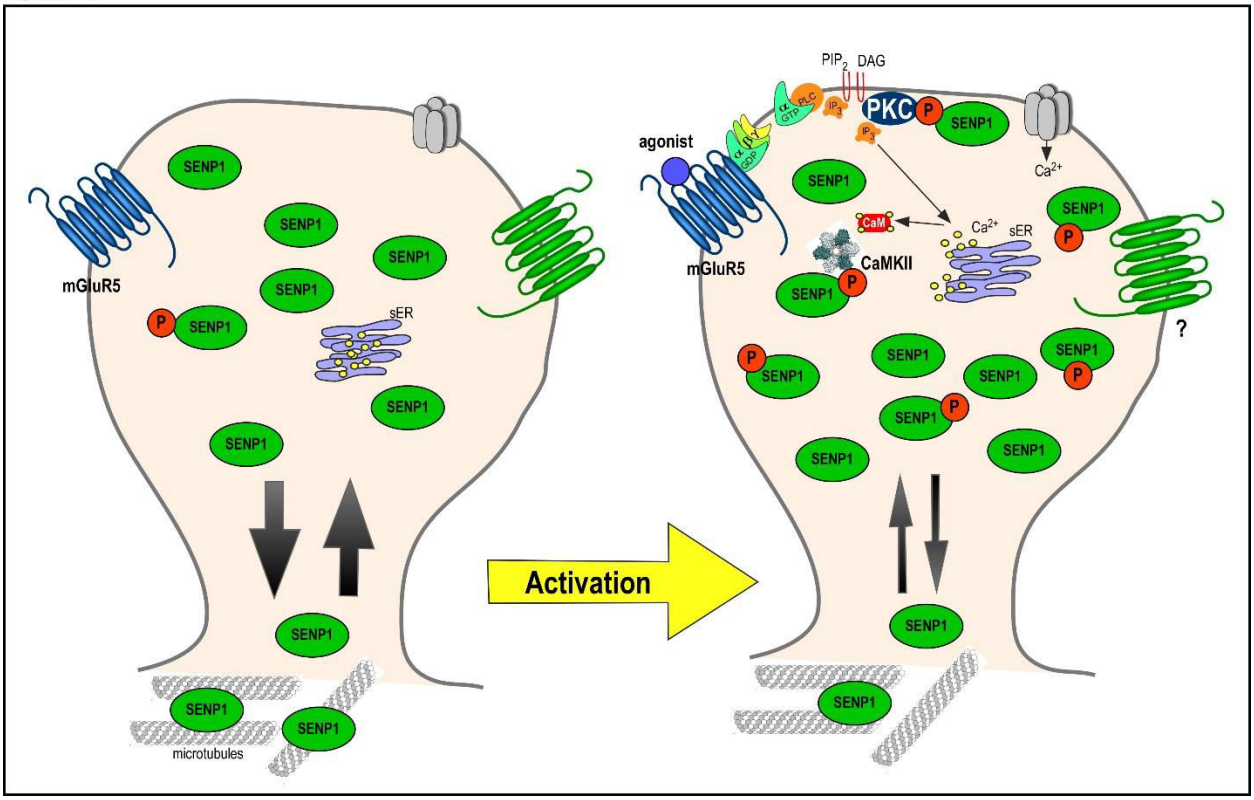

Figure 57. **Scheme of the newly identified and putative regulatory mechanisms of SENP1 spino-dendritic diffusion.** (1) In basal conditions SENP1 molecules diffuse at a relatively fast speed between the shaft and spines. The exit of SENP1 proteins may be partially dependent on microtubules. (2) Upon synaptic activation (primarily through mGluR5 receptors), PKC and CaMKII get activated and trigger phosphorylation of synaptic substrates including SENP1. This leads to SENP1 synaptic trapping and accumulation. (3) I hypothesize that Ubc9-sumoylated substrates at the synapse will be sequentially desumoylated by SENP1 with a significant time shift that is necessary for the protein targets to perform their synaptic functions. Upon stabilisation, these proteins are rapidly desumoylated by the accumulated SENP1, which might be SENP1 dephosphorylation-dependent process. Then SENP1 gets rapidly trafficked out of spines.

Conclusion

4. Conclusion

The posttranslational modification by sumoylation has been proven a vital regulatory mechanism at synapses. Indeed, unbalanced sumoylation is an emerging feature of neuropathological conditions including synaptopathies. A very important objective that must be addressed prior to envisaging the development of novel therapeutic strategies aimed at targeting this posttranslational process, is the identification of signalling cues that drive sumoylation and desumoylation of synaptic proteins. Our laboratory has previously published that Ubc9 undergoes a transient trapping in spines in response to the activation of the mGluR5/PLC/PKC cascade increasing synaptic sumoylation levels. This finding implies that desumoylation must dynamically take place to establish balanced sumoylation levels.

To this end, I used in my thesis project live-imaging, biochemical and cell biology approaches to identify the regulatory mechanisms of SENP1 diffusion at synapses. In summary, the results show that a sustained synaptic activation leads to accumulation of SENP1 at synapses. This accumulation is immediately reversible upon the establishment of basal levels of activity. I also provide evidence that SENP1 spino-dendritic diffusion is regulated by synaptic activity specifically through mGluR5 receptors. I suggest that additional regulatory molecules may play a role in SENP1 regulation at synapses. These include microtubules, PKC and CaMKII.

I hypothesize that the activation of mGluR5 triggers the activation of PKC and CaMKII leading to the phosphorylation of synaptic substrates including SENP1, which reduces SENP1 spino-dendritic diffusion. Phosphorylated substrates function as a molecular ‘glue’ for Ubc9 that gets transiently trapped in spines and rapidly sumoylates synaptic proteins. Once these proteins perform their function, SENP1 is activated (perhaps by dephosphorylation) and desumoylates synaptic substrates establishing the basal state of sumoylation. To confirm this hypothesis, additional experiments will have to be carried out.

Annex

ARTICLE 1

Sumoylation in synaptic function and dysfunction

(Published in Frontiers in Synaptic Neuroscience, April 2016)

Lenka Schorova and Stéphane Martin

Institut de Pharmacologie Moléculaire et Cellulaire, Centre National de la Recherche Scientifique (UMR7275), University of Nice—Sophia-Antipolis, Laboratory of Excellence "Network for Innovation on Signal Transduction, Pathways in Life Sciences", Valbonne, France.

This specialised review on synaptic sumoylation was jointly written by myself and my supervisor Dr Martin. We briefly discuss the SUMO pathway and give more detailed overview of our current knowledge of sumoylation at both the presynaptic and postsynaptic compartments. Moreover, we collected data that evidenced the involvement of the sumoylation process in synaptic plasticity. In the last part, we focus on describing research that have implicated aberrant sumoylation in diseases of the synapse (jointly called synaptopathies) such as Down syndrome, Parkinson's disease, Huntingon's disease and Alzheimer's disease.

I worked on this review at the beginning of my second year of PhD. Therefore, collecting literature and gaining general understanding into the overall problematics of synaptic sumoylation helped me greatly in pursuing my PhD project.

frontiers in Synaptic Neuroscience

REVIEW
published: 28 April 2016
doi: 10.3389/fnsyn.2016.00009

Sumoylation in Synaptic Function and Dysfunction

*Lenka Schorova and Stéphane Martin**

Institut de Pharmacologie Moléculaire et Cellulaire, Centre National de la Recherche Scientifique (UMR7275), University of Nice—Sophia-Antipolis, Laboratory of Excellence "Network for Innovation on Signal Transduction, Pathways in Life Sciences", Valbonne, France

Sumoylation has recently emerged as a key post-translational modification involved in many, if not all, biological processes. Small Ubiquitin-like Modifier (SUMO) polypeptides are covalently attached to specific lysine residues of target proteins through a dedicated enzymatic pathway. Disruption of the SUMO enzymatic pathway in the developing brain leads to lethality indicating that this process exerts a central role during embryonic and post-natal development. However, little is still known regarding how this highly dynamic protein modification is regulated in the mammalian brain despite an increasing number of data implicating sumoylated substrates in synapse formation, synaptic communication and plasticity. The aim of this review is therefore to briefly describe the enzymatic SUMO pathway and to give an overview of our current knowledge on the function and dysfunction of protein sumoylation at the mammalian synapse.

Keywords: synapse, post-translational modification, sumoylation, desumoylation, SUMO

OPEN ACCESS

Edited by:
Martín Cammarota, Federal University of Rio Grande do Norte, Brazil

Reviewed by:
Marco Feligioni, European Brain Research Institute (EBRI) 'Rita Levi-Montalcini', Italy
Gustavo Paratcha, National Scientific and Technical Research Council (CONICET), Argentina

***Correspondence:**
Stéphane Martin
martin@ipmc.cnrs.fr

Received: *07 March 2016*
Accepted: *08 April 2016*
Published: *28 April 2016*

Citation:
Schorova L and Martin S (2016) Sumoylation in Synaptic Function and Dysfunction. Front. Synaptic Neurosci. 8:9. doi: 10.3389/fnsyn.2016.00009

INTRODUCTION

As the mammalian brain develops, crucial sequential processes take place for a functional neuronal circuitry to be established. These processes are as follows: embryonic neurogenesis that gives rise to neuronal cells from the progenitors within the neural tube; migration of these newly born neurons to their destination area that is followed by maturation and formation of interneuronal connections. The spatiotemporal regulation of these processes, which results in the formation and the stabilization of synaptic connections, participates in the shaping of a physiologically active and functional brain circuitry. The formation of a mature functional synaptic contact starts with an axonal outgrowth until the growth cone reaches a target neuron. The axonal growth cone transforms into a presynaptic terminal that is characterized by the presence of neurotransmitter-filled synaptic vesicles and faces the postsynaptic area i.e., the dendritic spine, which is enriched in neurotransmitter receptors. The functional synapse is capable of integrating an electrical signal into biochemical changes, a process referred to as synaptic transmission. Importantly, the term "synaptic plasticity" regroups a wide range of molecular mechanisms that allow the modification of the strength and efficacy of synaptic transmission, and thereby underpin the ability of the brain to respond to environmental changes and/or experiences, and consequently underlie cognitive functions.

The molecular composition and organization of a mature synapse is incredibly complex. It has been estimated that "an average" synapse contains 300,000 proteins (Wilhelm et al., 2014). As these proteins mediate synaptic transmission and plasticity their interactions must be regulated both in time and space and this is mostly achieved by posttranslational modifications (PTMs).

Accordingly, it is widely accepted that most types of plasticity are expressed through changes in the number of postsynaptic glutamate receptors and these changes are regulated by PTMs (for a comprehensive review, see Yokoi et al., 2012). For instance, both CaMKII and PKC phosphorylation of the GluA1 subunit of AMPA receptors (AMPARs) increase single-channel conductance of AMPARs leading to expression of long-term potentiation (LTP) in the hippocampus. In addition, previous studies have reported that PKC-phosphorylation of the AMPAR subunit GluA2 regulates its protein-protein interactions in the cerebellum leading to the expression of an activity-dependent long-term decrease in synaptic strength known as long-term depression (LTD; Matsuda et al., 2000). It has also been shown that the synaptic function can be regulated via other PTMs. Ubiquitination is a reversible PTM that can direct target proteins for degradation through the ubiquitin proteasome system (UPS). Bingol and Schuman (2006) reported that proteasome constituents and ubiquitin moiety are present in dendrites and upon neuronal activation the dendritic UPS moves into spines to shape the synaptic protein composition and subsequently the synaptic function. Interestingly, sumoylation has recently emerged as an essential PTM in the central nervous system (CNS) that profoundly alters protein activity, stability and subcellular localization, controls protein-protein interactions, and is important for the brain development and the regulation of synaptic communication (for recent reviews see Gwizdek et al., 2013; Henley et al., 2014). Moreover, perturbations in neuronal sumoylation have been implicated in numerous pathological conditions (reviewed in Dorval and Fraser, 2007; Martin et al., 2007b; Martin, 2009; Krumova and Weishaupt, 2012; Lee et al., 2013; Henley et al., 2014).

THE ENZYMATIC MACHINERY OF SMALL UBIQUITIN LIKE MODIFIERS

Sumoylation is an evolutionarily conserved enzymatic pathway, analogous to the ubiquitination process, which covalently and reversibly conjugates a small protein of ∼100 amino acids, called Small Ubiquitin-like Modifier(SUMO, ∼11 kDa), to lysine residues of target proteins (Matunis et al., 1996; Mahajan et al., 1997).

Four SUMO paralogs have been identified in humans until now. SUMO1–3 are ubiquitously expressed (Hay, 2005; Geiss-Friedlander and Melchior, 2007) whereas SUMO4 expression seems restricted to the spleen, the kidney and the lymphatic nodes (Bohren et al., 2004; Guo et al., 2004). SUMO2 and SUMO3 are nearly identical except three additional N-terminal residues within the SUMO3 sequence; therefore they are generally referred to as SUMO2/3. On the contrary, SUMO1 shares only ∼50% sequence identity with SUMO2/3. SUMO1 and SUMO2/3 modify an overlapping set of target proteins; but they differ in their properties and subcellular abundance with the amount of free available SUMO2/3 being much larger that of SUMO1.

In most cases, the SUMO-targeted lysine resides within a specific consensus site defined as ψ-K-x-D/E, where ψ corresponds to a large hydrophobic residue, K stands for lysine, x is any amino acid, and D/E are glutamate and aspartate acidic residues respectively (Rodriguez et al., 2001; Sampson et al., 2001). Importantly, not all consensus sequences are sumoylated and not all SUMO-target proteins are modified within this particular motif. Several additional sumoylation sites were identified, which revealed that the sequences flanking the target lysine residue are critical to determine whether a site can be SUMO-modified or not (reviewed in Flotho and Melchior, 2013; Henley et al., 2014). It is also important to note that many of the lysine residues contained within SUMO consensus sites are reported as not sumoylated. However, in most cases the determination of such sumoylation status was achieved in basal unstimulated conditions. Therefore, caution should be taken to definitively state that a given protein is not a SUMO substrate since only a small proportion of a specific protein is sumoylated at steady state (Hay, 2005).

The sumoylation/desumoylation cycle (**Figure 1**) starts with the cleavage of inactive SUMO precursor proteins by the hydrolase activity of the SENtrin-specific Protease (SENP, Mukhopadhyay and Dasso, 2007; Hickey et al., 2012) enzymes so the C-terminal di-glycine motif on SUMO is uncovered for conjugation. Mature SUMOs are then activated by the SAE1 and SAE2 (SUMO-activating enzyme subunit 1 and 2; also named AoS1/Uba2 in rodents) heterodimer complex in an ATP-dependent manner. Afterwards, SUMO conjugation to target substrate proteins is carried out by the sole conjugating enzyme of the SUMO system, Ubc9 (**Figure 1**). This conjugation step can be achieved either directly or in combination with an E3 SUMO ligase (Bernier-Villamor et al., 2002). These E3 proteins assist the sumoylation step either by bringing the substrate and the SUMO-Ubc9 in close proximity or by enhancing the transfer rate of SUMO onto the substrate (reviewed in Gareau and Lima, 2010; Flotho and Melchior, 2013). In the brain, the mechanisms, by which these E3 SUMO ligases operate and how they participate in the SUMO process to enhance sumoylation in neurons, are still largely unknown. However recent evidence suggests that these E3 ligases may be extremely important to tightly regulate the synaptic function.

The sumoylation/desumylation cycle (**Figure 1**) is highly dynamic and must be tightly controlled as it drastically influences the function of many proteins targeted by this PTM. Despite a covalent SUMO binding, sumoylation is a reversible process due to the isopeptidase activity of specific enzymes (see Hickey et al., 2012, for a comprehensive review on SUMO proteases). The desumoylation enzymes allow the removal of the SUMO moieties from modified substrates leaving non-sumoylated proteins and matured SUMOs available to re-enter the SUMO pathway. Several SUMO proteases effectively mediate this desumoylation process. In humans, six SENP proteases have been described (SENP1, 2, 3, 5, 6 and 7). These desumoylation enzymes differ in their subcellular localization and SUMO selectivity (Hickey et al., 2012). Recently, several additional SUMO proteases have been identified, DeSumoylating Isopeptidase 1 and 2 (DeSI1 and DeSI2; Shin et al., 2012) and USPL1 (Ubiquitin-Specific Protease-Like 1; Schulz et al., 2012). These SUMO proteases together with the SUMO-conjugating pathway convey

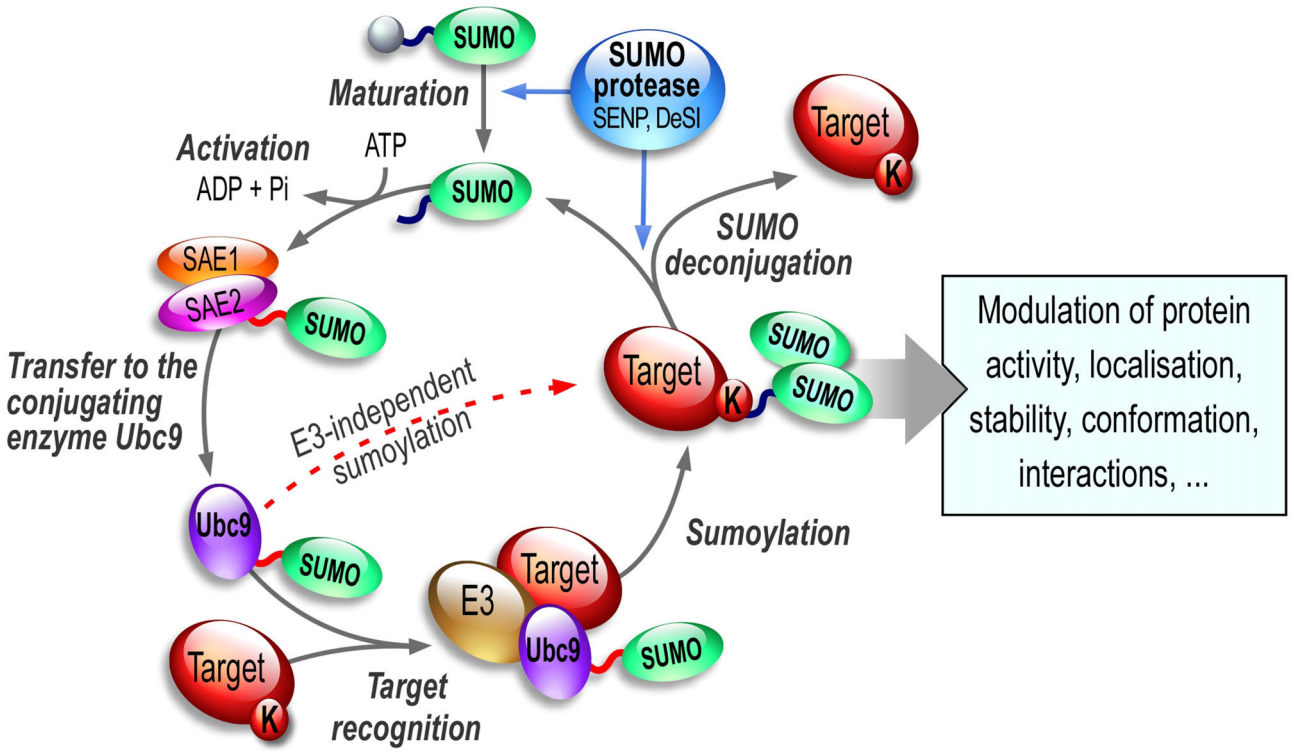

FIGURE 1 | The SUMO enzymatic pathway. SUMO paralogs are synthesized as inactive precursors that are first matured by the hydrolase activity of specific desumoylases called SENPs. SUMO activation is an ATP-dependent step leading to formation of a thioester bond between the SUMO-activating subunit SAE2 of the E1 enzymatic heterodimer SAE1/SAE2 and the activated SUMO. SUMO is then transferred onto the active (C93) cysteine residue of Ubc9, the sole E2-conjugating enzyme of the SUMO system. Ubc9 is able to catalyze the sumoylation reaction of the target lysine residue on the substrate either directly or in combination with one of the existing SUMO E3 ligases. Importantly, sumoylation is readily reversible and sumoylated proteins can be efficiently desumoylated via the isopeptidase activity of a variety of SUMO proteases including SENPs, DeSI1/2 and/or USPL1.

an essential role to allow the dynamic equilibrium between the sumoylated and desumoylated state of many proteins. Since sumoylation participates in the regulation of many proteins involved in essential developmental processes and synaptic functions, dysregulation of the sumoylation/desumoylation balance may directly link the SUMO process to a number of pathophysiological conditions (see thereafter, "Sumoylation in Synaptopathies" Section).

SUMOYLATION IN BRAIN DEVELOPMENT, NEURONAL MATURATION AND SYNAPSE FORMATION

Sumoylation in Brain Development

Sumoylation acts throughout the neuronal cell to dynamically modulate protein function and consequently SUMO enzymatic machinery members present a widespread subcellular distribution including the nucleus (Martin et al., 2007a; Loriol et al., 2012; Wang et al., 2012; Hasegawa et al., 2014), the mitochondrial surface (Guo et al., 2013), the dendritic shaft and both pre- and postsynaptic elements (Martin et al., 2007a; Feligioni et al., 2009; Loriol et al., 2012, 2013, 2014; Gwizdek et al., 2013; Luo et al., 2013; Hasegawa et al., 2014).

To date, three separate studies have examined the spatiotemporal distribution of the sumoylation machinery members in the developing rodent brain with consistent results (Watanabe et al., 2008; Loriol et al., 2012; Hasegawa et al., 2014). The expression levels of both Ubc9 and SUMO1 mRNA are developmentally regulated in the rat brain, with higher expression levels before birth (Watanabe et al., 2008). Only recently, we reported that the protein expression levels of sumoylated proteins, the SUMO-activation enzyme SAE1, the SUMO-conjugating Ubc9 and the two desumoylation enzymes SENP1 and SENP6 are developmentally regulated in the rat brain (Loriol et al., 2012). SUMO1/2/3-conjugated protein levels are at their maximum at embryonic day 12, followed by a slow decrease until birth. SUMO1-modified protein levels progressively decrease until the adult stage. However, a second increasing phase occurs for SUMO2/3-ylated substrates just after birth. Interestingly, while the overall sumoylation slowly decreases after birth reaching relatively low levels in the adult brain, there are progressively more SUMO substrates within synaptic compartments (Loriol et al., 2012). The relative accumulation in synaptic SUMO substrates in aged rat brain

is also consistent with an enrichment of the sumoylation enzymes AoS1 and Ubc9 in dendritic spines of fully mature rat neurons.

More recently, Hasegawa et al. (2014) combined immunohistochemical and immunoblot analyses on mouse brain at various developmental stages and also showed a developmental distribution of all SUMO moieties and the SUMO-conjugating enzyme Ubc9. During embryonic development, sumoylation occurred in the nucleoplasm of nestin-positive neural stem cells. Although the total amount of SUMO-modified proteins decreased during postnatal mouse brain development similar to the developing rat brain (Loriol et al., 2012), a persistent accumulation of SUMO2/3 was detected in neural progenitor populations in neurogenic regions throughout life (Hasegawa et al., 2014). In addition, a strong SUMO1-immunoreactivity was observed in large projection neurons in the brainstem suggesting that SUMO1- and SUMO2/3-modified proteins exert specific functions in the mouse brain.

The abundance and distribution of the sumoylation machinery play a critical role during embryonic and postnatal development. For instance, it was previously thought that SUMO2 and SUMO3 paralogs act in a totally redundant manner. Wang et al. (2014) recently revealed that SUMO2 is the predominantly expressed isoform in early embryonic stages of mouse development. Indeed, SUMO3-KO mice are viable while SUMO2 deficiency in mice leads to severe developmental delay and embryonic lethality, which strongly suggests that the spatiotemporal expression of these SUMO moieties, and not their functional differences (the two paralogs being almost identical), is a critical factor during the brain development.

Fu et al. (2014) investigated the role of SENP2 in the brain development by engineering a mouse model that expressed SUMO-protease activity-deficient SENP2 in neural progenitors. The authors showed that SENP2 is indispensable for the brain development. Indeed, SENP2 loss of function evoked an increase in neuronal sumoylation levels eventually leading to a robust post-natal neurodegeneration resulting in paralysis and death of the mice by three weeks of age (Fu et al., 2014). They also demonstrated that this neurodegeneration is the consequence of the hyper-sumoylation of Drp1 (Dynamin-related protein 1), which promoted its enhanced association with mitochondria and their subsequent fragmentation leading to neuronal apoptosis. Altogether, these data confirmed the importance of a controlled balance between the sumoylation and desumoylation state of a protein in the developing brain.

Sumoylation in Neuronal Maturation and Synapse Formation

We have reported, that the sumoylation enzymes AoS1, Ubc9 as well as the SUMO proteases SENP1 and SENP6 were differentially redistributed in pre- and postsynaptic areas during neuronal maturation (Loriol et al., 2012). We further showed that the redistribution of the sumoylation machinery in and out of synapses is also observed upon neuronal depolarization and that this enzymatic redistribution impacts the synaptic levels of sumoylation (Loriol et al., 2013). Altogether, these data suggested that the SUMO process and the involved SUMO targets are not only important for the brain development but also for the maturation of neuronal cells and consequently for synaptic function.

MeCP2 (Methyl CpG Binding Protein 2)

Hundreds of mutations within the MeCP2 gene, which is located on the X-chromosome, have been linked to neurodevelopmental disorders, most frequently to Rett syndrome in females but also to some forms of autism, and schizophrenia. The Rett syndrome is behaviorally characterized by a developmental stagnation in early childhood associated with severe cognitive impairment and autistic features, the loss of spoken language and hand use. The encoded MeCP2 protein is a DNA-binding protein expressed ubiquitously and acts as a transcriptional repressor that fulfils key roles during the synaptic development (Guerrini and Parrini, 2012). Sumoylation of MeCP2 regulates its interaction with the transcriptional repression complex HDAC1/2 and preventing sumoylation in MeCP2 at the K223 residue leads to abnormal gene expression and impaired synaptic density (Cheng et al., 2014).

More recently, Tai et al. (2016) reported that MeCP2 is modified on different lysine residues e.g., K353 and K412, but failed to detect the K223 sumoylation. They showed that phosphorylation is required for MeCP2 sumoylation and that the SUMO E3 ligase PIAS actively participates in MeCP2 modification. They also elegantly demonstrated that MeCP2 sumoylation in the hippocampus is induced by several factors including the activation of NMDA receptors (NMDARs), the Insulin-like growth factor (IGF-1) and the Corticotropin-Releasing Factor (CRF) revealing a previously unsuspected activity-dependent regulation of MeCP2 sumoylation. Importantly, preventing MeCP2 sumoylation using the non-sumoylatable K412R MeCP2 mutant leads to a decrease in its DNA binding ability whereas a MeCP2-SUMO1 fusion significantly increases its DNA binding capabilities (Tai et al., 2016). Altogether, these data reinforce the idea that MeCP2 sumoylation is essential to its function and acts as a central regulator of MeCP2 function in the brain.

MEF2 Proteins (Myocyte-Enhancer Factor 2)

The establishment of functional synaptic circuits relies on the concomitant activity-dependent formation and elimination of synapses. MEF2 members form a family of four evolutionarily conserved transcriptional factors (MEF2A, B, C and D) that were first identified in muscle differentiation. They are also expressed throughout the brain including areas involved in cognitive functions (cortex, hippocampus, amygdala, striatum; reviewed in Rashid et al., 2014). Mutations within MEF2 genes have been directly linked to various pathological conditions including epilepsies, autism, and some neurodegenerative disorders (Flavell and Greenberg, 2008; Li et al., 2008; Yin et al., 2012) suggesting that these brain diseases could be

triggered by abnormal MEF2-dependent gene transcription programs. Notably, MEF2 s are involved in several important neurodevelopmental processes including cell differentiation, dendritic morphogenesis, synapse formation, pruning and synaptic plasticity.

MEF2 activities are regulated through several PTMs including acetylation (Grégoire and Yang, 2005; Shalizi et al., 2007), phosphorylation (Flavell et al., 2006; Kang et al., 2006) and sumoylation (Grégoire and Yang, 2005; Zhao et al., 2005; Shalizi et al., 2006, 2007; Lu et al., 2013). A decade ago, Shalizi et al. (2006) investigated the SUMO-dependent repression of MEF2A in the developing cerebellar cortex. They demonstrated that there is an activity-dependent switch from a sumoylated MEF2A at the lysine 403 to its acetylated state leading to MEF2A activation and inhibition of dendritic claw differentiation and consequently to synapse disassembly (Shalizi et al., 2006). They used overexpression and knockdown strategies to show that PIASx is a MEF2 SUMO-E3 ligase linking this E3 protein to postsynaptic dendritic claw morphogenesis in the cerebellar cortex and confirming the essential role of protein sumoylation in the developing brain (Shalizi et al., 2007). MEF2A was also reported to be sumoylated both *in vitro* and *in vivo* at the lysine 395 residue and the E3 SUMO ligase PIAS1 enhances its sumoylation and subsequently decreases its transcriptional activity (Riquelme et al., 2006).

More recently, the Bonni's group reported that MEF2A sumoylation participates in presynaptic differentiation in the rat brain (Yamada et al., 2013). Indeed, while the *in vivo* knockdown of MEF2A in the rat cerebellar cortex increases the density of orphan presynaptic sites, the sumoylated transcriptional repressor form of MEF2A drives the suppression of these sites via the direct repression of the gene encoding the presynaptic protein Synaptotagmin 1 (Yamada et al., 2013).

Lu et al. (2013) have engineered SENP2 knockout embryos and used *in vivo* SUMO assays to demonstrate that SENP2, but not SENP1, is the MEF2A desumoylating enzyme. They also showed via co-expression of SENP2 and MEF2A with a luciferase reporter gene a SENP2-dependent increase in MEF2A transcriptional activity (Lu et al., 2013) further highlighting the importance of the SUMO process in the transcriptional regulation mediated by MEF2A.

MEF2C, another member of the MEF2 family, is also a sumoylation substrate (Kang et al., 2006). Sumoylation at K391 repressed MEF2C transcriptional activity without altering its DNA-binding properties. Interestingly, phosphorylation at S396 in MEF2C, five residues downstream of the sumoylation site, potentiated MEF2C sumoylation (Kang et al., 2006). The phospho-deficient S396A mutant of MEF2C showed a reduced sumoylation *in vivo* with the concurrent increase in its transcriptional activity further confirming that the regulation of MEF2 activities is controlled by the crosstalk between phosphorylation and sumoylation.

The last member of the MEF2 family to be reported a SUMO substrate is MEF2D. MEF2D sumoylation occurs at the lysine 439 residue (Grégoire and Yang, 2005). The authors showed that the K439 SUMO2/3-ylation of MEF2D strongly decreases its transcriptional activity. In agreement with this, they demonstrated that SENP3 activity is able to increase the transcriptional activity of MEF2D by lowering its sumoylation (Grégoire and Yang, 2005). The same group reported that the kinase Cdk5 promotes MEF2D phosphorylation at the serine 444 residue leading to an increased sumoylation of the protein and consequently to the inhibition of the transcriptional activity of MEF2D (Grégoire et al., 2006). Altogether, these data indicate that the transcriptional activity of MEF2 proteins is tightly regulated through the interplay between several PTMs, e.g., phosphorylation, acetylation and sumoylation, to tightly control the developmental expression of essential target genes involved in brain development and plasticity.

FOXP2 (Forkhead Box Protein P2)

FOXP2 belongs to the forkhead box (FOX) family of transcription factors. Disruption of the FOXP2 gene has been implicated in a rare and severe form of autosomal-dominant language and speech disorder (Lai et al., 2001). This disorder was first described in a British family (known as the KE family), in which half of their members struggle to develop coordinated orofacial movements. These patients also express incomprehensive written and spoken language, but they do not show any cognitive impairment. All the affected family members carry the missense arginine to histidine mutation at position 553 (R553H) in FOXP2, which abolishes its DNA binding and consequently fails to repress transcription of many target genes (Lai et al., 2001). FOXP2 is mainly expressed during neuronal differentiation in many brain areas including the cortex, basal ganglia, thalamus and hippocampus (Lai et al., 2003). Importantly, FOXP2 regulates expression of genes that are important for neuronal development and synaptogenesis. For instance, FOXP2 regulates the expression of DISC1 that is involved in neurogenesis, synapse regulation, neuronal outgrowth, migration, differentiation and proliferation (reviewed in Brandon and Sawa, 2011).

Only recently, three independent studies reported that FOXP2 is sumoylated *in vitro* and *in vivo* by all SUMO paralogs predominantly at the lysine 674 residue (Estruch et al., 2016; Meredith et al., 2016; Usui et al., 2016). They further showed that FOXP2 interacts with the E3 SUMO ligases PIAS1 and PIAS3 promoting FOXP2 sumoylation (Estruch et al., 2016; Usui et al., 2016) whereas SENP2 activity significantly decreases its sumoylation (Usui et al., 2016). The FOXP2-PIAS1/3 interaction leads to redistribution of FOXP2 to the nuclear speckles. Interestingly, abolition of the sumoylation site via the K674R mutation did not cause any changes in FOXP2 stability, transcriptional repression or dimerization with the WT sumoylatable form of FOXP2. The subcellular localization of FOXP2 K674R mutant was reported both *in vitro* and *in vivo* to be increased in the cytoplasm and decreased in the nucleus (Usui et al., 2016). Importantly, the human etiological FOXP2 R553H mutation led to a dramatic decrease in the ability of FOXP2 R553H to be sumoylated

(Meredith et al., 2016). They further showed that the pathogenic R553H mutation negatively influences the interaction between FOXP2 and the PIAS ligases (Estruch et al., 2016; Meredith et al., 2016).

The cerebellum harbors important motor coordination and speech functions and the expression of FOXP2 in the cerebellum is restricted to Purkinje cells (PC). Usui et al. (2016) have reported that FOXP2 sumoylation is increased during neuronal differentiation in the cerebellum suggesting a key role for sumoylation in cerebellar development. They further showed using mouse neural progenitor cells that overexpression of the WT form of FOXP2 results in long neurites expressing either the immature neuronal marker Tuj1 or the mature neuronal marker MAP2. Interestingly, the overexpression of the SUMO-deficient K674R FOXP2 mutant failed to promote elongation of Tuj1- and MAP2-positive neurites as effectively as the WT FOXP2 indicating that FOXP2 sumoylation is essential to neuronal maturation. *In utero* electroporation to knockdown FOXP2 expression in the cerebellum led to a dramatic reduction in dendritic outgrowth and arborization of PC (Usui et al., 2016). This reduction was rescued by re-expression of the WT sumoylatable form of FOXP2 but not its sumoylation-deficient K674R mutant. Strikingly, the impairments in cerebellum-based motor behaviors such as righting reflex or negative geotaxis observed in FOXP2 knockdown mice were rescued with the expression of the WT form of FOXP2, but not with its sumoylation-deficient K674R mutant confirming the essential role of FOXP2 sumoylation in the developing cerebellum (Usui et al., 2016).

A knock-in mouse model expressing the pathogenic R552H FOXP2 mutation (corresponding to the human FOXP2 R553H mutation) exhibited an immature development of the cerebellum with impaired neuronal migration and autism-related deficits such as decreased ultrasonic vocalizations (Fujita et al., 2008). These vocalization defects were rescued by introducing the WT form of FOXP2 but not its sumoylation-deficient mutant (Usui et al., 2016) further demonstrating that impaired FOXP2 sumoylation could participate in the etiology of FOXP2-related developmental verbal/vocal communication in mammals.

CASK (Calcium/Calmodulin-Dependent Serine Protein Kinase)

CASK is a member of the membrane-associated guanylate kinase (MAGUK) protein family. MAGUK proteins have scaffolding properties and interact with many proteins involved in spinogenesis. CASK expression is high in the mammalian brain and extremely critical as its genetic deletion in mice causes neonatal lethality. Mutations within the CASK gene on the X-chromosome have been identified in human patients presenting severe neurological defects, microcephaly and mental impairments, highlighting an essential role of the CASK protein during the brain development (Hsueh, 2009; Hackett et al., 2010).

At the molecular level, CASK binds to a myriad of proteins important for embryonic development, synapse formation and plasticity (Hsueh, 2006). For instance, CASK interacts with the adhesion molecules, e.g., neurexin and syndecans, with cytoplasmic adaptor proteins such as Mint1, SAP97 and CIP98, and with calcium channel proteins. CASK also participates in the regulation of synaptic transmission via its indirect interaction with vesicles that transport the NMDAR subunit NR2B to the plasma membrane (Huang and Hsueh, 2009; Setou et al., 2000).

CASK functions as a multidomain scaffolding protein and has been shown to be sumoylated on the lysine 679 residue (Chao et al., 2008). The sumoylation of CASK reduces the interaction between CASK and the protein 4.1. Mammalian 4.1 proteins are known to act as hubs for cytoskeleton-membrane protein organization and cellular signaling. Notably, protein 4.1 connects spectrin to the actin cytoskeleton and this interaction is crucial for spinogenesis (Huang and Hsueh, 2009). Therefore, in order to evaluate the role of CASK sumoylation in spinogenesis, the authors fused SUMO1 to CASK and overexpressed this chimearic construct in hippocampal neurons. They showed a dramatic impairment in spine number and size (Chao et al., 2008) indicating that CASK sumoylation is essential for spinogenesis. Interestingly, CASK is also expressed presynaptically and future research could therefore shed light on the role of CASK sumoylation in synaptic vesicles (SVs) trafficking and/or neurotransmitter release.

PRESYNAPTIC SUMOYLATION

The main function of the presynaptic terminal is to orchestrate the release of neurotransmitter from SVs upon neuronal depolarization (reviewed in Südhof and Rizo, 2011; Südhof, 2013). This essential activity-dependent process requires a tightly controlled spatiotemporal regulation of protein-protein interactions between a myriad of molecules to achieve the calcium-dependent fusion of SVs with the presynaptic membrane and the subsequent release of the neurotransmitter in the synaptic cleft. These dynamic events are mostly regulated via PTMs and sumoylation is clearly emerging as a key process at the presynapse.

Feligioni et al. (2009) used a modified synaptosomal preparation protocol to trap exogenous conjugatable SUMO1 polypeptides or the catalytically active domain of the desumoylation enzyme SENP1 in synaptosomes to respectively increase or decrease the presynaptic sumoylation levels and measure the impact of sumoylation on glutamate release. They reported that the increase in presynaptic sumoylation reduced Ca^{2+} influx and decreased glutamate release upon KCl depolarization. In contrast, decreasing presynaptic sumoylation by introducing SENP1 into synaptosomes led to an enhanced Ca^{2+} influx and glutamate release in KCl-stimulated conditions (Feligioni et al., 2009). This study was the first to provide evidence for a direct role of the SUMO process at the presynapse via modulation

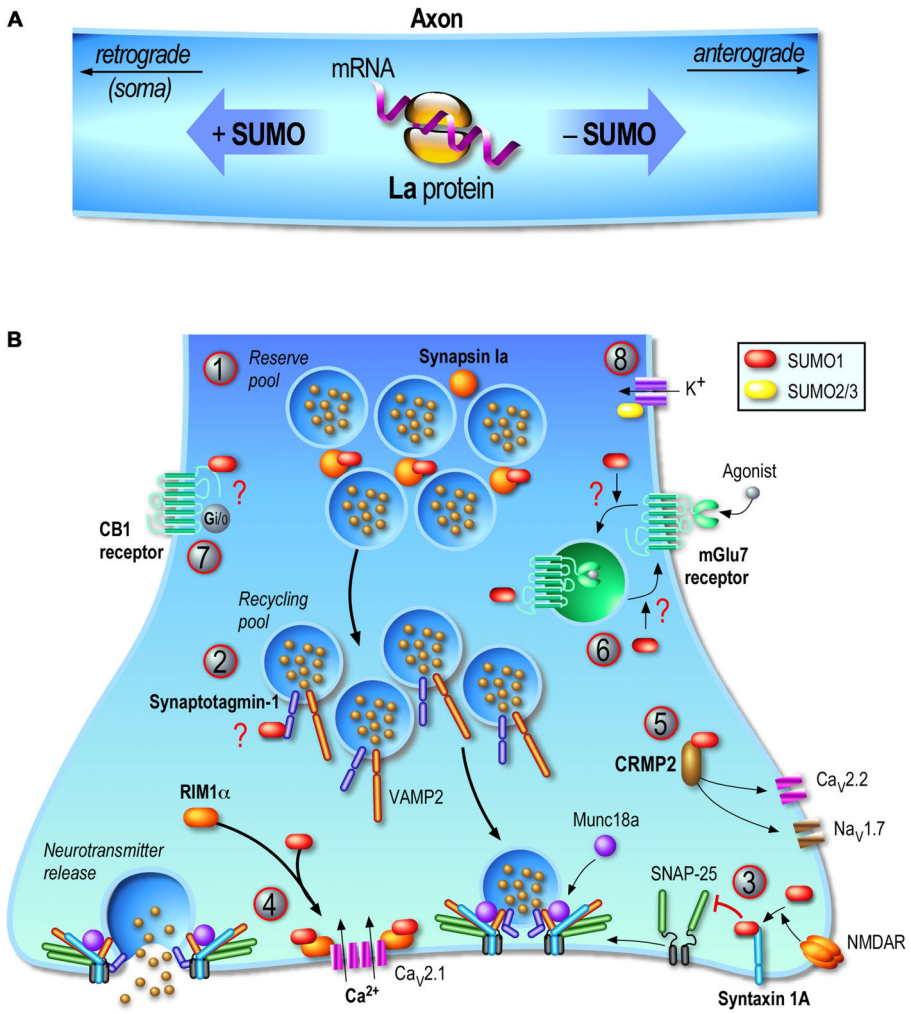

FIGURE 2 | Regulation of the presynaptic function by sumoylation. Consistent with the emerging presynaptic functions of sumoylation, its enzymatic machinery is localized at the presynapse and several presynaptic proteins are SUMO subtrates. **(A)** Transport of mRNAs along axons is a key mechanism to dynamically control the function of proteins in growth cones. The axonal mRNA-binding protein **La** is a SUMO substrate. La is transported toward the end of the axon by its association to kinesins while sumoylated La proteins are bound to dyneins and therefore undergo retrograde transport toward the soma. **(B)** Presynaptic sumoylation emerges as a central protein modification acting at several stages of the neurotransmitter release mechanism. **(1)** Sumoylation of **Synapsin Ia** (Synla) potentiates its association with synaptic vesicles and thus participates in the clustering of these vesicles at the presynapse. **(2) Synaptotagmin-1** is sumoylated *in vivo* but the precise function of this modification is still not known. **(3) Syntaxin-1A** sumoylation is evoked upon NMDA receptor (NMDAR) activation leading to a decreased binding to SNAP-25 and VAMP-2 and thus acting as a key presynaptic regulator of vesicle endocytosis. **(4) RIM1α** sumoylation is required for presynaptic exocytosis since depolarization-evoked vesicle exocytosis with a non-sumoylatable RIM1α mutant is dramatically impaired. This effect is mainly due to a defect in presynaptic calcium entry following neuronal activation since RIM1α sumoylation enables the binding to Cav2.1 calcium channels and coordinates the presynaptic Ca^{2+} entry. **(5) CRMP2** is a SUMO substrate and dynamically reduces Ca^{2+} entry through the presynaptic voltage-gated Ca^{2+} channel CaV2.2. CRMP2 sumoylation is also believed to regulate the membrane expression of the sodium channel NaV1.7. **(6) mGluR7** is sumoylatable both *in vitro* but also *in vivo* in rat hippocampal and cortical neurons. mGluR7 agonist activation triggers the endocytosis of the WT mGluR7 but not the internalization of its non-sumoylatable mutant suggesting that sumoylation acts on the endocytic pathway. However, overexpressing the desumoylase SENP1 increases the pool of internalized mGluR7, which rather implies that mGluR7 sumoylation is important for recycling of these receptors back to the plasma membrane and not for the receptor endocytosis *per se*. **(7)** Activation of **CB1 receptors** in rat cortical neurons increases the overall SUMO1 conjugation. CB1 receptors are potentially sumoylated in resting cells but not in CB1 receptor-activated conditions. However, the confirmation that these receptors are sumoylated at presynaptic sites and whether the SUMO modification impacts presynaptic endocannabinoid functions are still not determined. **(8) Kv potassium channels** play critical roles in neuronal excitability and sumoylation of a number of these channels (Kv1.1, Kv2.1, Kv7.2, Kv7.3) have been reported to act as molecular regulators of their intrinsic activity. Question marks in red indicate that the physiological consequences of the target protein sumoylation are still not clearly defined.

of calcium influx and glutamate release but the molecular pathway and presynaptic proteins targeted by this PTMs were not described at that time. Since then, several key axonal and presynaptic proteins have been reported to be the target of the SUMO system and a better view about the complexity of this process as well as the functional role of sumoylation at the presynapse is now emerging (**Figure 2**).

La Protein

The human La protein was originally identified as an auto-antigen in an immune system disorder called Sjogren's syndrome. Levels of circulating anti-La autoantibodies are used for the diagnosis of this autoimmune syndrome but also in cases of systemic lupus erythematosus and neonatal lupus syndrome. La is the smallest member (46kDa) but the most abundant of the La-related protein (LARP) family (reviewed in Stavraka and Blagden, 2015). Its particular LAM motif adopts a special conformation commonly seen in DNA transcription factors and its RNA-interacting motif RRM allows the binding, protection and axonal transport of many mRNAs. However, how the expression and function of La are regulated remains largely unexplored. To date, it has been shown that phosphorylation of La regulates its activity and possibly its ability to recognize mRNAs. Two kinases, CK2 and Akt, have been so far identified to phosporylate the La protein (Broekhuis et al., 2000; Brenet et al., 2009; Bayfield et al., 2010). Furthermore, (van Niekerk et al., 2007) reported that La is a SUMO substrate and that sumoylated La binds to dynein allowing its retrograde axonal transport. Conversely, the native non-sumoylated La interacts with kinesin and undergoes anterograde axonal transport (**Figure 2A**). This pioneer study showed that sumoylation is a key regulatory mechanism for transporting mRNAs towards their local translation sites, which represents a crucial process for the maintenance of the axonal and growth cone pool of proteins that are required for synaptic transmission.

Kv Channels (Voltage-Gated Potassium Ion Channels)

Kv channels form potassium-selective pores that span through the plasma membrane and are essential for the generation of action potentials and the control of neuronal excitability. Mutations in subunits forming some of these channels have been implicated in epilepsies and sudden unexplained death in epilepsy (SUDEP). Investigations into the regulatory roles of sumoylation on potassium channel activities have revealed exciting features. However, most of these works were not achieved in neurons since Kv channels also regulate the excitability of many non-neuronal cells (recently reviewed in Wu et al., 2016). Hereafter, we describe the functional effects of sumoylation of voltage-gated potassium channels in the CNS.

Potassium Kv1.1 channels are abundantly expressed in the brain and localize in large axons where they form tetramers with Kv1.2 subunits. These channels regulate action potential propagation, neuronal firing and neurotransmitter release (Dodson and Forsythe, 2004). Mutations within the human gene encoding Kv1.1 have been associated with partial epilepsy and episodic ataxia in humans (Zuberi et al., 1999). Knock-in mice with Kv1.1 mutations also exhibit hippocampal hyperexcitability, severe epilepsy and premature death (Glasscock et al., 2007). Qi et al. (2014) engineered a post-natal deficient SENP2 mouse model that develops spontaneous seizures and sudden death. They also reported that the SENP2 deficiency results in increased levels of sumoylation for several potassium channels known to impact neuronal excitability including the Kv1.1 that is modified by both SUMO1/2 and colocalizes with SENP2 in hippocampal neurons. However, the sumoylation of Kv1.1 did not significantly affect its channel properties and activity. Interestingly, the authors have also reported in this work that the Kv7.2 is hyper-sumoylated by SUMO2/3 in hippocampal neurons. Kv7 potassium channels play critical roles in neuronal excitability. Two Kv7 members, Kv7.2 and Kv7.3, are highly expressed in neurons and generate the M-current that is important for firing action potentials. Strikingly, the hyper-sumoylation of Kv7.2 resulted in a significant decrease in the depolarizing M-current in SENP2-deficient hippocampal CA3 neurons and consequently led to neuronal hyperexcitability, severe seizures and ultimately, to sudden death of mice by a maximum of 8 weeks of age (Qi et al., 2014). These symptoms were prevented by administration of an approved anti-epileptic drug retigabine. This effective drug acts as a specific Kv7.2 opener and counteracts neuronal hyperexcitability. However, how this drug impacts the sumoylation levels of Kv7.2/7.3 in hippocampal neurons has not been investigated.

Voltage-gated Kv2.1 channels have also been shown to be the target of the SUMO system. While sumoylation of these channels was initially demonstrated in native pancreatic cells where it regulates beta-cell excitability (Dai et al., 2009), Plant et al. (2011) reported a functional role of Kv2.1 sumoylation in hippocampal neurons. Kv2.1 potassium channels are important in neurons for determining the activity-dependent excitability. They reported that sumoylation occurs at the lysine 470 residue and showed that two Kv2.1 subunits have to be modified within a functional Kv2.1 tetramer to produce full SUMO response. Kv2.1 sumoylation led to a 35 mV shift in the half-maximal activation voltage of the functional channel, which resulted in its increased sensitivity to depolarization (Plant et al., 2011). Therefore, sumoylation of Kv2.1 channels provides a way to directly control neuronal excitability.

Synapsin Ia

Synapsins are synaptic proteins essential for the establishment, clustering and release of presynaptic vesicles (Cesca et al., 2010). Synapsin Ia (SynIa) is involved in maintaining the reverse pool of synaptic vesicles that is required when neuronal stimulation lasts for longer period of time. Tang et al. (2015) demonstrated that SynIa is sumoylated at the K687 residue and this sumoylation potentiates its association with synaptic vesicles participating in the clustering and anchoring of these vesicles into the presynaptic element (**Figure 2B**). The lysine-687 to arginine mutation resulted in complete absence of SynIa sumoylation, decrease in the number of releasable synaptic vesicles and impaired exocytosis (Tang et al., 2015). Notably, the A548T mutation in SynIa that co-segregates with autism also impairs SynIa sumoylation. Defects in SynIa sumoylation may therefore be involved in the pathophysiology of neurological disorders through a SUMO-dependent deregulation of SynIa function at the presynapse. Altogether, sumoylation of SynIa appears to be

critical for the activity-dependent release of neurotransmitter and may therefore actively participate in synaptic transmission and potentially in long-term synaptic plasticity events.

Syntaxin-1A

The activity-dependent exocytosis of neurotransmitters at presynaptic sites and the subsequent recycling of synaptic vesicles are essential processes underlying synaptic communication. The exocytotic event is mediated through the action of the SNARE (Soluble N-ethylmaleimide sensitive factor Attachment protein REceptor) protein complex that includes the 35 kDa-membrane protein Syntaxin-1A (Stx1A), SNAP-25 and VAMP-2, and additional proteins such as Munc18, Synaptotagmins and RIM1α (**Figure 2B**). Stx1A has been reported to be important in neuronal survival (Kofuji et al., 2014), neurotransmitter release and recycling of SV (Watanabe et al., 2013). The role of Stx1A in neurotransmitter release is also supported by studies reporting a possible involvement of Stx1A in the pathophysiology of autism with Stx1A mRNA expression levels being significantly higher in autistic patients compared to controls (Nakamura et al., 2008). Furthermore, the STX1A gene, which is located at the chromosome 7q11.23, has been found duplicated in patients with speech delay and autism spectrum behaviors (Berg et al., 2007; Depienne et al., 2007). All these findings therefore converge to the idea that Stx1A is critically important for synapse formation, presynaptic function and neuronal transmission in the developing brain.

Interestingly, Stx1A has been recently reported as a novel presynaptic sumoylation target (Craig et al., 2015). Stx1A sumoylation is evoked upon NMDAR activation or following KCl-depolarization in hippocampal neurons. This activity-dependent sumoylation occurs at three lysine sites (K252, 253, 256) and reduces Stx1A binding to SNAP-25 and VAMP-2, but not to Munc18a. Importantly, neuronal expression of a non-sumoylatable form of Stx1A via the mutation of the three SUMO sites into arginine residues, leads to a significant increase in presynaptic vesicle endocytosis (Craig et al., 2015). This suggests that Stx1A sumoylation is critically involved in the maintenance of the balance between SV endocytosis/exocytosis and subsequently in neurotransmitter release. However, how exactly the sumoylated form of Stx1A enhances SV endocytosis as well as how Stx1A desumoylation occurs in this context has not yet been investigated.

Synaptotagmin-1

Membrane fusion is a key mechanism occurring for many processes including protein/lipid transport, hormone and neurotransmitter release. Membrane fusion at presynaptic site involves not only the SNARE proteins but also several other presynaptic factors to orchestrate neurotransmission in a timely dependent way (reviewed in Südhof and Rizo, 2011; Südhof, 2013). Among these are calcium sensor proteins called synaptotagmins. To date, 16 isoforms of synaptotagmins have been identified in mammals that either colocalize with synaptic/secretory vesicles or are distributed at the plasma membrane. Although not directly related to presynaptic exocytotic function, Dai et al. (2011) reported that SENP1 overexpression enhances insulin exocytosis in pancreatic β-cells via the association of SUMO1 to Synaptotagmin VII. More interesting is the presynaptic function of Synaptotagmin-1 (Syt1) sumoylation. Syt1 is well known to exert important roles at the presynapse to sense the calcium influx that arises through the activated voltage-gated calcium channels and thus Syt1 participates in neurotransmitter release (**Figure 2B**).

To assess the role of sumoylation in neuronal function, the Fraser lab used a proteomic approach on transgenic mice that exclusively over-expressed the human form of SUMO1 in neurons (Matsuzaki et al., 2015). The effect of this over-expression was a simultaneous increase in the level of non-conjugated SUMO1 proteins and in the proportion of high molecular weight SUMO1-modified targets in transgenic brains compared to WT brains. The levels of protein expression of the SUMO enzymes as well as the free fraction of SUMO2/3 proteins in transgenic brain remained similar to those measured in WT animals. Using mass spectrometry, the authors confirmed that many of these SUMO1 targets were neuron and synapse-specific. Importantly, the authors described the sumoylation of Syt1 and showed that Syt1 sumoylation was upregulated in these transgenic mice (Matsuzaki et al., 2015). Using field potential recording in acute hippocampal slices from SUMO1-transgenic brains, they reported a deficit in basal transmission suggesting a decrease in synaptic activity and/or a loss of functional synapses. They also showed that a form of short-term synaptic plasticity dependent on presynaptic mechanisms, named paired pulse facilitation, is impaired in SUMO1-transgenic brain slices, which suggests that SUMO1 over-expression leads to defects in functional presynaptic mechanisms (Matsuzaki et al., 2015). They further showed that SUMO1-over-expressing hippocampal cells exhibit a dramatic loss of dendritic spines that leads to impairment in contextual fear memory (Matsuzaki et al., 2015). While the over-expression of SUMO1 in neurons leads to multiple alterations, the functional and physiological functions of Syt1 sumoylation are yet to be described. Clearly, the hyper-sumoylation observed for Syt1 in SUMO1-transgenic mice cannot be taken as the unique cause to explain all the physiological deficits reported in these animals. However, this work confirmed the importance of a controlled equilibrium between sumoylation and desumoylation since a small and uncompensated increase in neuronal sumoylation directly impacts synaptic architecture, cell communication and memory formation.

RIM1α (Rab3-Interacting Molecule 1α)

Among the proteins of the presynaptic active zone that have been extensively studied are the RIM protein family. RIMs interact either directly or indirectly with several presynaptic proteins including Rab3a, synapsin-1, Syt1A, Munc13–1, and the voltage-gated Ca^{2+} channels (Calakos et al., 2004). These scaffolding proteins are crucial to the active zone function and consequently to synaptic transmission (**Figure 2B**). Specifically, RIM1α has been implicated in the docking/priming of synaptic vesicles but also in short and long-term synaptic plasticity (Castillo

et al., 2002; Dulubova et al., 2005). It is now generally believed that RIM1α plays key roles in diverse presynaptic functions, however, the regulatory mechanisms at the presynaptic site have not been fully elucidated. A recent study from the Henley lab reported that RIM1α is a SUMO substrate (Girach et al., 2013). They showed that RIM1α sumoylation occurs only on the lysine 502 residue independently of the neuronal activity. Using molecular replacement experiments, they have substituted the endogenous RIM1α in hippocampal neurons by the non-sumoylatable RIM1α-K502R mutant. While the presynaptic localization of both the WT and non-sumoylatable exogenous RIM1α remained unchanged, there was a marked decrease in the depolarization-evoked SV exocytosis with the K502R mutant indicating that RIM1α sumoylation is required for presynaptic exocytosis (Girach et al., 2013). They further demonstrated that the outcome measurements of the mutant were due to a defect in calcium entry following depolarization since RIM1α sumoylation enables the clustering of Cav2.1 calcium channels. Altogether, (Girach et al., 2013) uncovered an additional important presynaptic function for the SUMO process. As there are other isoforms of RIM proteins that are involved in modulation of presynaptic functions, it would be of interest to investigate whether and how sumoylation can impact on these proteins.

CRMP2 (Collapsin Response Mediator Protein 2)

CRMP2 is a microtubule-binding protein that was originally identified for its roles in regulation of axonal guidance in neuronal polarity and more recently, in presynaptic functions including axonal transport and neurotransmitter release (for a recent review on CRMP2 see Ip et al., 2014). CRMP2 dynamically interacts with the presynaptic N-type voltage-gated Ca^{2+} channel (CaV2.2) and disruption of this complex reduces pain in a rodent model of neuropathic pain. Thus, investigation into CRMP2 mechanisms of action is of interest to understand its role in pain and identify potential therapeutic targets (Brittain et al., 2011). CRMP2 has been reported to be sumoylated *in vitro* on the lysine 374 residue and preventing CRMP2 sumoylation did not impair its ability to promote neurite outgrowth (Ju et al., 2013). Using calcium imaging on primary rat cultures of dorsal root ganglion (DRG) neurons, the authors showed that the non-sumoylated form of CRMP2 differentially affects the calcium influx in depolarized DRGs when compared to WT CRMP2 expression suggesting that CRMP2 sumoylation acts as a negative modulator of presynaptic calcium influx.

The same group later confirmed that both the WT and the SUMO-deficient CRMP2 are robustly expressed in catecholaminergic cells (CAD) and are able to promote neurite outgrowth in rat DRG neurons (Dustrude et al., 2013). They have also reported that the sodium channel NaV1.7 is regulated by CRMP2 sumoylation. Preventing sumoylation by over-expressing SENP1 and SENP2 enzymes in WT CRMP2-expressing CAD cells decreased the NaV1.7 currents. Accordingly, there was a significant decrease in the levels of surface-expressed NaV1.7 in CAD cells expressing the SUMO-deficient form of CRMP2. NaV1.7 currents were also decreased in sensory neurons expressing the non-sumoylatable CRMP2 K374A mutant (Dustrude et al., 2013).

Overall these two reports highlight the putative function of CRMP2 sumoylation in the regulation of calcium and sodium channels; however, the authors did not demonstrate CRMP2 sumoylation *in vivo*. It is also to be determined whether CRMP2 sumoylation directly modifies the activity or the surface expression of the two channels. Further work will therefore be required to clarify the functional role of CRMP2 sumoylation at presynaptic sites.

Metabotropic Glutamate Receptors

Metabotropic glutamate receptors (mGluRs) form a family of G-protein coupled receptors that are centrally involved in excitatory neurotransmission and synaptic plasticity. mGluRs are divided into three groups based on their sequence homology, G-protein coupling and ligand specificity (reviewed in Niswender and Conn, 2010). The group III consists of mGluR4, 6, 7 and 8, and is of particular interest since these receptors typically exert presynaptic inhibitory functions. In the past years, several group III mGluRs have been shown to be sumoylated mainly *in vitro* but also *in vivo*, however until recently, there was no compelling evidence regarding the functional roles for such modifications (Tang et al., 2005; Wilkinson et al., 2008; Dütting et al., 2011; Wilkinson and Henley, 2011).

The functional role of sumoylation in mGluRs has been so far addressed solely for the mGluR7. These receptors are widely expressed presynaptically and modulate excitatory neurotransmission as well as synaptic plasticity by inhibiting neurotransmitter release (reviewed in Niswender and Conn, 2010). C-terminal truncated forms of mGluR7 were found to be sumoylated at the K889 residue *in vitro* (Wilkinson et al., 2008; Wilkinson and Henley, 2011). In a recent study, Choi et al. (2016) confirmed that mGluR7 is a SUMO substrate *in vitro*. They have also shown that these receptors are sumoylated *in vivo* in both the rat hippocampus and primary cortical neurons with the mGluR7-K889 residue identified as the sole sumoylation site. While mGluR7 can be sumoylated by both SUMO1 and SUMO2/3 in HEK293T cells, only SUMO1 conjugation was reported in hippocampal homogenates (Choi et al., 2016). Since the sumoylation process has been directly involved in the endocytosis of glutamate receptors in hippocampal neurons (Martin et al., 2007a), the authors investigated whether sumoylation has an effect on mGluR7 internalization (**Figure 2B**). Constitutive agonist-independent endocytosis of the non-sumoylatable mGluR7 K889R mutant was increased compared to the WT control receptor. Addition of L-AP4 mGluR7 agonist to the cells expressing WT receptors triggers the endocytosis of mGluR7. This increase in agonist-evoked mGluR7 endocytosis was not seen for the non-sumoylatable mGluR7. The authors attributed this lack of effect to the sumoylation process directly acting on the endocytic pathway. However, they cannot rule out that sumoylation rather impact on the recycling properties of the pathway. It is indeed likely that sumoylation acts after the

endocytosis of mGluR7 by preventing the recycling of the non-sumoylatable receptor. This is in line with their data showing that overexpression of SENP1, which prevents sumoylation, leads to an increase in the internalized population of WT mGluR7 similar to the values measured for the endocytosed population of the non-sumoylatable mutant in the absence of SENP1. This could be explained by a decrease in the SUMO-dependent recycling of internalized mGluR7 to the plasma membrane that leads to an increased intracellular pool of receptors. Since this pathway was not assessed, it is difficult to conclude about the exact role of mGluR7 sumoylation in the internalization/recycling process. Furthermore, mGluR7s are primarily expressed at presynaptic sites (Niswender and Conn, 2010). Since the current work (Choi et al., 2016) examined the postsynaptic endocytic properties of an over-expressed tagged version mGluR7, it implies that further work will now be necessary to assess the functional impact of mGluR7 sumoylation at presynaptic sites and whether this SUMO modification influences neuronal excitability and/or synaptic transmission and plasticity.

Cannabinoid Receptor 1

The endocannabinoid system fulfils complex neuromodulatory functions in brain development and synaptic plasticity (reviewed in Lu and Mackie, 2016). It is composed of endogenous cannabinoid substrates (endocannabinoids), receptors and enzymes that synthesize and degrade endocannabinoids. Strikingly, impairments of the endocannabinoid system have been implicated in several psychiatric disorders. The most abundant endocannabinoid receptors, CB1 and CB2, belong to the family of G-protein coupled receptors, which primarily couple to G proteins of the Gi and Go classes. Their activation leads to inhibition of adenylyl cyclases and modulation of presynaptic voltage-dependent calcium channels as well as certain potassium channels (Lu and Mackie, 2016). CB1 and CB2 receptors are involved in a number of physiological functions, such as gene transcription, cell motility and synaptic communication. CB1 receptors are highly expressed in the cortex, basal ganglia, hippocampus, and the cerebellum. CB1 receptors are primarily present at presynaptic terminals (**Figure 2B**) while CB2 receptors, which are expressed at a much lower level in the CNS, are mainly expressed in microglia and vascular elements. Activation of CB1 receptors in rat cortical neurons leads to an increase in the overall SUMO1 conjugation as well as an increase in the levels of free SUMO1 (Gowran et al., 2009). The authors further showed that CB1 receptors were potentially sumoylated in basal but not in CB1 receptor-activated conditions (Gowran et al., 2009). However, there have been no reports so far regarding which CB1 receptor residues are sumoylated and whether the SUMO modification regulates presynaptic endocannabinoid functions.

In recent years, a lot of work has been achieved regarding the identification of presynaptic SUMO target proteins and the function of sumoylation at the presynapse, placing the SUMO pathway as a key regulator of protein-protein interactions within this highly crowded environment. Despite these efforts it is still unknown how is this timely dependent sumoylation/desumoylation process orchestrated and future work will be required to decipher how the targeting, the trafficking and the activity of the sumoylation and desumoylation enzymes are regulated in an activity-dependent manner at presynaptic sites.

POSTSYNAPTIC SUMOYLATION

Spines are small protrusions on dendritic membranes receiving inputs from axonal termini. Dendritic spines represent the postsynaptic elements that consist in a head connected to the dendritic shaft by a narrow neck and contain multiple synaptic actors, which interact in a coordinated manner to allow synaptic communication. The first demonstration that sumoylation acts directly within the synapse has been provided in 2007 with the immunodetection of many unidentified sumoylated substrates in rat hippocampal PSD95-positive synaptic fractions as well as with the immunolocalization of the sole SUMO conjugating enzyme Ubc9 at postsynaptic sites (Martin et al., 2007a). This work has also identified and characterized the first synaptic sumoylated substrate i.e., the kainate receptor (KAR) subunit GluK2, and therefore has opened new avenues for investigation of the sumoylation process in the brain (Martin et al., 2007a).

Kainate Receptors

Kainate receptors are ionotropic glutamate receptors that are functionally active as tetramers composed of the subunits GluK1–5 (formerly named GluR5–7, KA1 and KA2). KARs play important roles for synaptic transmission as well as neuronal excitability (Contractor et al., 2011). They are expressed at many synapses both pre- and postsynaptically but also extrasynaptically, where they regulate neuronal excitability. At the presynapse, they participate in the release of neurotransmitters, whereas postsynaptically they contribute to synaptic transmission. The GluK2 subunit directly interacts with the conjugating enzyme Ubc9 and is a sumoylation substrate in rat hippocampal neurons (Martin et al., 2007a). GluK2 sumoylation by SUMO1 occurs in an activity-dependent manner on its C-terminal domain at the single lysine 886 residue. Since this report, several additional studies have confirmed the SUMO state of GluK2 in neurons (Konopacki et al., 2011; Zhu et al., 2012; Choi et al., 2016). Agonist activation causes the endocytosis of GluK2 receptors via a PKC-dependent pathway (Martin and Henley, 2004). Interestingly, the binding of glutamate or kainate to GluK2 leads to its sumoylation at the plasma membrane and represents a trigger for the activated receptors to be internalized. Interestingly, postsynaptic KAR responses at hippocampal mossy fiber-CA3 synapses decrease when postsynaptic sumoylation is promoted by infusing SUMO1 postsynaptically and conversely, postsynaptic responses largely increase in desumoylation conditions using infusion of the catalytic domain of SENP1 (Martin et al., 2007a). Consistent with earlier publication (Martin and Henley, 2004), PKC activation has been shown

to be essential to GluK2 internalization (Konopacki et al., 2011; Chamberlain et al., 2012). PKC phosphorylation at the serine 868 in GluK2 is a prerequisite for its sumoylation and subsequent endocytosis (Konopacki et al., 2011; Chamberlain et al., 2012).

Arc (Activity-Regulated Cytoskeleton-Associated Protein/Activity-Regulated Gene 3.1)

The immediate early gene Arc is capable of coupling changes in neuronal activity to synaptic plasticity events in a tightly regulated way (reviewed in Bramham et al., 2010). Arc is a unique gene required for consolidation of synaptic plasticity and LTP. Transcription of Arc gene is strongly induced by synaptic activity. Arc mRNAs are rapidly transported into dendrites where they undergo local translation at synaptic sites. Therefore it is not surprising that Arc exhibits key roles in protein synthesis-dependent forms of synaptic plasticity and in consolidating different forms of memory (Bramham et al., 2010). Interestingly, Arc levels are also controlled by ubiquitination and proteasomal degradation as it was shown that defective Arc ubiquitination increases Arc levels leading to the concurrent decrease in synaptic AMPAR receptors (Greer et al., 2010).

AMPAR are heterotetrameric (GluA1-A4) glutamate-gated ion channels that underpin the vast majority of fast excitatory glutamate neurotransmission in the CNS. Interestingly, a chronic abolishment of neuronal activity promotes AMPARs membrane expression and in contrast an increase in neuronal activity leads to decreased surface AMPARs. However, the mechanisms, by which the number and composition of AMPARs change, are still not fully understood. To date, it is believed that Arc participates in the internalization of AMPAR from the plasma membrane through its interaction with the endocytic endophilin-3 and dynamin-2 proteins (Chowdhury et al., 2006).

The Henley group reported that Arc is a sumoylation substrate with the lysine 110 and 268 residues being the sites of sumoylation (Craig et al., 2012). They also showed that the suppression of network activity with the sodium channel blocker tetrodotoxin (TTX) induces SENP1 degradation leading to the concurrent increase in SUMO1- and SUMO2/3-modified protein levels in rat cortical neurons in primary culture (Craig et al., 2012). The level of Arc proteins was dramatically reduced in TTX conditions independently of its sumoylatable ability indicating that sumoylation does not exert any stabilizing effect on Arc. The prolonged exposure to TTX also directly increases the membrane expression of GluA1 subunits of AMPARs, a process named synaptic scaling (Turrigiano, 2008). This effect in surface-expressed AMPAR in TTX condition was prevented when the catalytic domain of SENP1 was expressed, revealing the involvement of the SUMO process in this homeostatic scaling effect (Craig et al., 2012). However, how the SUMO process participates in the regulation of AMPAR levels at the plasma membrane, how Arc sumoylation levels are modulated by the TTX treatment and how Arc sumoylation impacts on AMPAR trafficking still remain open questions.

Regulation of the Sumoylation Pathway at the Postsynapse

Despite numerous publications demonstrating the postsynaptic involvement of sumoylation, it is only recently that some of the mechanisms regulating this post-translational system at the post synapse were reported (Loriol et al., 2014; **Figure 3**). Indeed, using a combination of pharmacological tools with synaptic biochemistry and restricted photobleaching/photoconversion of individual hippocampal spines, our group demonstrated that the synaptic diffusion of Ubc9, the sole conjugating enzyme of the sumoylation pathway, is regulated by synaptic activity on a rapid timescale. The synapto-dendritic diffusion of Ubc9 remained unchanged upon the activation of NMDARs but was altered through the activation of group I metabotropic mGluR5 receptors (see Niswender and Conn, 2010 for a comprehensive review on mGluRs signaling pathways). Increasing synaptic activity with a $GABA_A$ receptor antagonist or directly activating mGlu5R increases the synaptic residency time of Ubc9 in a PKA-independent but PKC-dependent manner. This transient synaptic diffusional trapping of Ubc9 enhanced its recognition to synaptic PKC-phosphorylated substrates and consequently leads to the increase in synaptic sumoylation (Loriol et al., 2014; **Figure 3**). However, despite this first demonstration that the sumoylation pathway is activity-dependently regulated at postsynaptic sites, future work will now be required to identify the nature of these synaptic mGlu5R-activated SUMO substrates to further decipher the synaptic functions of sumoylation.

Altogether, the data from the above sections clearly establish that the sumoylation machinery is partly targeted to, localized and regulated at pre- and postsynaptic sites to modulate in an activity-dependent manner the levels of synaptic sumoylation and in turn, the synaptic function. Furthermore, a growing number of SUMO substrates were recently identified in axons, dendrites and synapses and shown to fulfil essential physiological functions on synaptic communication and plasticity (Shalizi et al., 2006, 2007; Martin et al., 2007a; Chao et al., 2008; Konopacki et al., 2011; Chamberlain et al., 2012; Craig et al., 2012, 2015; Girach et al., 2013; Jaafari et al., 2013; Loriol et al., 2013, 2014; Tang et al., 2015; Tai et al., 2016) revealing the sumoylation process as an essential modulator of the synaptic function. Strikingly however, a study combining the use of a double-tagged His-HA-SUMO1 knock-in mouse model and mass spectrometry analysis failed to detect any synaptic SUMO substrates nor any colocalization between His-HA-SUMO1 at synapses (Tirard et al., 2012). The explanation for these rather stark differences is still unclear but the authors demonstrated that the levels of SUMO conjugation decreased in the knock-in model compared to WT animal suggesting that the dual SUMO tag partly impairs the sumoylation process. The direct outcome of this observation is that the synaptic sumoylation levels may become too low and below the detection sensitivity of their analysis method. Despite these data, an increasing number of exciting studies from independent groups worldwide including ours is now available demonstrating that sumoylation takes place in neurons and at synapses to regulate synaptic communication.

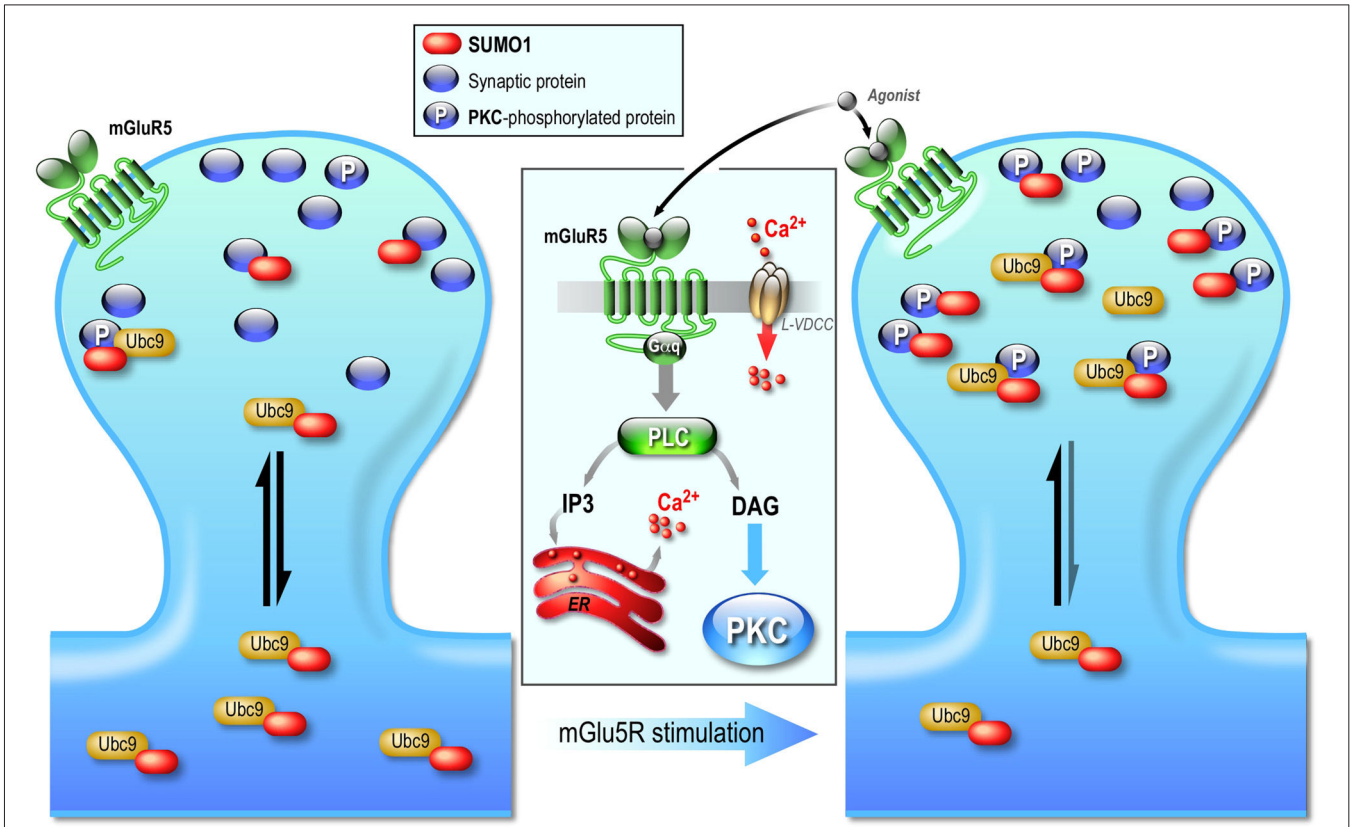

FIGURE 3 | Postsynaptic regulation of the SUMO pathway. The diffusion of Ubc9, the sole conjugating enzyme of the SUMO system is regulated by synaptic activity. Neuronal activation increases the residency time of the SUMO-conjugationg enzyme Ubc9 at the post-synapse. This synaptic regulation is independent of NMDAR activation but involves an mGlu5R-dependent signaling pathway that leads to PKC activation. The effect of this activity-dependent PKC phosphorylation is the increased anchoring of Ubc9 to synaptic phosphorylated protein substrates, which ultimately enhances sumoylation at synapses. Activation of mGlu5R therefore promotes a transient diffusional trapping of Ubc9 in activated spines via a PKC-dependent pathway, which in turn contributes in the regulation of neuronal excitability.

SUMOYLATION IN SYNAPTIC PLASTICITY

Synaptic plasticity is characterized by the ability of a synapse to change in strength over long periods of time and this process is now widely accepted as the cellular model of learning and memory. Sumoylation, as described above, is centrally involved in the fine-tuning of neuronal excitability and the regulation of several pre- and postsynaptic proteins important for synaptic transmission. In recent years, several pieces of evidence have accumulated implicating the sumoylation process in plasticity events.

Phosphorylation of the cAMP-responsive element binding protein (CREB) at the serine 133 residue via different signaling cascades, e.g., Ras/ERK, Akt kinase, calcium/calmoduin-dependent kinases II and IV, protein kinase A, regulates memory formation and neuronal survival during development and leads to transcription of genes required for activity-dependent brain plasticity, which makes CREB a prototypic transcriptional factor of cognitive function of the brain (Cohen and Greenberg, 2008; Bell et al., 2013). In an in-depth study published recently, Chen et al. (2014) investigated the role of CREB sumoylation and its interplay with phosphorylation in the rat hippocampal CA1 region. They showed that CREB sumoylation is enhanced in the presence of PIAS1, and NMDA injection in the CA1 region increases CREB sumoylation. Moreover, the spatial training in rats increases CREB phosphorylation after 1 day of training. After 2 and 5 days the phospho-CREB levels remained unchanged compared to untrained control animals, whereas CREB sumoylation increased significantly suggesting a molecular regulatory switch between phosphorylation and sumoylation during this learning process. In addition, CREB sumoylation enhanced the transcription of growth factor Brain-Derived Neurotrophic Factor (BDNF). Transduction of CREB-SUMO1 fusion vector to the rat CA1 region increased spatial learning and memory, whereas PIAS1 knock-down decreased CREB sumoylation and impaired spatial learning and memory (Chen et al., 2014). Importantly, the authors provided evidence that preventing CREB phosphorylation completely abolishes CREB sumoylation, however preventing CREB sumoylation on two most prominent sumoylation sites increases CREB phosphorylation in the CA1 region. Clearly, there is a regulatory interplay between these two modifications and it will be of interest to examine whether deregulation of the CREB phosphorylation/sumoylation crosstalk is relevant in cognitive disorders.

LTP (Long-Term Potentiation)

LTP is characterized by a long-lasting increase in synaptic strength that involves in most cases an activity-dependent increase in the functionality and the number of postsynaptic AMPAR (Kneussel and Hausrat, 2016).

Jaafari et al. (2013) applied a chemically-induced LTP assay (Chem-LTP) on cultured rat hippocampal neurons to investigate the role of sumoylation in AMPARs surface expression. This pharmacological approach was previously reported to significantly increase the surface level of AMPARs (Lu et al., 2001). Chem-LTP led to an increase in dendritic and synaptic SUMO1 immunoreactivity as well as a large increase in Ubc9 and SUMO1 mRNAs in soma and dendrites. Interestingly, the over-expression of a catalytically active domain of the desumoylase SENP1, but not its catalytically inactive mutant, prevented the increase in SUMO1 mRNA and in surface expressed AMPAR upon Chem-LTP (Jaafari et al., 2013). These results are in favor of an active role of the sumoylation process in the control of AMPAR surface expression during LTP. However, the precise mechanism by which the SUMO process acts on AMPAR surface expression is still not clear.

The prion-like Cytoplasmic Polyadenylation Element-Binding protein 3 (CPEB3) regulates the translation of several mRNAs involved in synaptic plasticity (Pavlopoulos et al., 2011; Fioriti et al., 2015). Previous studies reported that CPEB exists as a soluble inactive or insoluble aggregate-prone active protein (Si et al., 2010), both of which localize at the synapse (Drisaldi et al., 2015). When aggregated, active CPEB3 can initiate the translation of specific target mRNAs such as those coding for the AMPAR subunits GluA1 and GluA2 (Pavlopoulos et al., 2011; Fioriti et al., 2015). Interestingly, sumoylation of CPEB3 by SUMO2 was shown to regulate its oligomerization capacity and neuronal activity-dependent translation of target mRNAs (Drisaldi et al., 2015). In basal state CPEB3 is sumoylated and acts as a translation repressor. *In vitro* and *in vivo* stimulation of hippocampal neurons triggered CPEB3 desumoylation leading to its aggregation and mRNA translation. The authors found that the uncleavable SUMO2-CPEB3 construct is soluble compared to the non-sumoylated CPEB3 and showed a decreased ability to aggregate leading to inhibition of mRNA translation. Stimulation of hippocampal neurons with glycine led to an increase in the number of filopodia (immature spines), which was not observed when neurons expressed SUMO2-CPEB3 (Drisaldi et al., 2015). Importantly, CPEB3 was reported to induce SUMO2 mRNA translation upon glycine stimulation. These data suggest that the SUMO process operates as a regulatory loop influencing the translation activity of CPEB3, which in turn modulates the levels of SUMO2 mRNA.

The sumoylation process is required for the expression of LTP (Lee et al., 2014). Indeed, by combining the use of WT or catalytically inactive forms of the cell permeable TAT-Ubc9 and LTP protocols in acute CA1 hippocampal slices, the authors showed that LTP is significantly reduced when sumoylation is prevented by the dominant negative Ubc9 mutant (Lee et al., 2014). This LTP inhibition was observed without any impact on basal transmission. Lee et al. (2014) confirmed their initial results using the catalytic domain of the desumoylase SENP1 in the patch pipette as used previously (Martin et al., 2007a). They showed that inclusion of the active SENP1, but not its catalytically inactive mutant, fully blocked the induction of LTP in CA1 pyramidal neurons confirming that the SUMO pathway is involved in the expression of long-term plasticity events (Lee et al., 2014). They subsequently demonstrated that infusion of the dominant negative form of TAT-Ubc9 *in vivo* impairs the hippocampal-dependent learning and memory (Lee et al., 2014).

More recently, several MeCP2 gene mutations in patients with Rett syndrome patients were shown to decrease MeCP2 sumoylation (Tai et al., 2016). The authors also demonstrated that the re-expression of the WT form of MeCP2 in CA1 hippocampal neurons rescued the deficits of social interaction and the CA1-LTP impairment observed in MeCP2 conditional knockout mice. Interestingly, re-expression of the non-sumoylatable K412R form of MeCP2 in these conditional knockout mice was not able to rescue the LTP in CA1 hippocampal neurons with measured values similar to those obtained in MeCP2 KO animals (Tai et al., 2016). Altogether, these data reveal a crucial role of MeCP2 sumoylation in social interaction and synaptic plasticity, and suggest that erratic MeCP2 sumoylation may directly participate in the etiology of Rett syndrome.

LTD (Long-Term Depression)

LTD is a ubiquitous form of activity-dependent long-lasting reduction of synaptic strength characterized by a decrease in the surface expression of neurotransmitter receptors that often results from the remodeling of their intracellular protein-interacting partners via PTMs.

As depicted above, the agonist-dependent sumoylation of the GluK2 subunit at the lysine 886 leads to the internalization of the sumoylated KAR complexes (Martin et al., 2007a). This process requires a PKC-phosphorylation of the GluK2 C-terminus at the serine 868 residue prior to its sumoylation (Konopacki et al., 2011). Interestingly, it was also reported that both the PKC-phosphorylation of the serine 868 and the subsequent sumoylation are required for the internalization of KARs that occurs during LTD of KAR-mediated synaptic transmission at rat hippocampal mossy fiber synapses (Chamberlain et al., 2012). Thus, this work revealed that the interplay between phosphorylation and sumoylation of GluK2 is important for activity-dependent KAR synaptic plasticity.

SUMOYLATION IN SYNAPTOPATHIES

The human synaptic proteome is composed of hundreds of different proteins in many copies and mutations in the encoding genes lead to more than hundred brain disorders (reviewed in van Spronsen and Hoogenraad, 2010; Grant, 2012). Spine architecture, synaptic proteome and neuronal functions are strongly correlated features, which is never more apparent than in pathological conditions. Notably, synaptopathies that are characterized by alterations in spine morphology,

TABLE 1 | Sumoylation in synaptopathies.

Synaptopathy	Implicated SUMO targets and machinery	Effects	Reference
Down syndrome, Trisomy 21	*SUMO3*	SUMO3 gene is localized on Hsa21. SUMO3 overdose leads to imbalanced/deregulated sumoylation.	Gardiner (2006)
Parkinson's disease	*α-Synuclein*	Sumoylated by SUMO1 and SUMO2/3. Involved in protein aggregation. Another pathogenic mechanism could include inter-neuronal spreading of α-Syn.	Kim et al. (2011), Krumova et al. (2011), and Kunadt et al. (2015)
	DJ-1	PD mutation disrupts DJ-1 sumoylation and decreases its solubility.	Shinbo et al. (2006)
	Parkin	Increase in its E3 Ubiquitin ligase activity by non-covalent SUMO1 modification. Parkin also associates with and targets the SUMO E3 ligase RanBP2 for degradation. Direct implication with PD is still lacking.	Um and Chung (2006)
Huntington's disease	*Huntingtin*	Sumoylation may act as a prevention mechanism for huntingtin accumulation.	Steffan et al. (2004) and O'Rourke et al. (2013)
Alzheimer's disease	*SAE2, Ubc9, SENP3*	Single Nucleotide Polymorphisms in these genes co-segregate with AD.	Grupe et al. (2007), Weeraratna et al. (2007), Ahn et al. (2009), and Corneveaux et al. (2010)
	Aβ	Unclear results about whether sumoylation of Aβ enhances or decreases its aggregation.	Li et al. (2003), Dorval et al. (2007), and Zhang and Sarge (2008)
	Tau	Proportion between sumoylated and ubiquitinylated Tau can regulate its degradation/accumulation. Hyper-phosphorylated Tau is immunoreactive for SUMO1.	Dorval and Fraser (2006) and Luo et al. (2014)

synapse number and synaptic function are increasingly seen as central feature in major psychiatric, brain developmental and neurodegenerative diseases. These diseases constitute a major social and economic burden in our societies and it is therefore essential to gain a better insight into the underlying molecular and cellular mechanisms prior to developing effective diagnostic, preventative and eventually therapeutic strategies.

Since the sumoylation pathway is emerging as a critical regulator of neuronal and synaptic function under normal conditions, it is not surprising to see more and more publications reporting defective sumoylation events in wide range of brain disorders. In this section, we review the current knowledge regarding the multiple sumoylation anomalies reported in synaptopathies (**Table 1**).

Down Syndrome (DS)

The DS or trisomy 21, is caused by an extra copy of all or parts of the long arm of the human chromosome 21 (Hsa21) and is the most common chromosomal abnormality with about 1:1000 births worldwide (Loane et al., 2013). Clinical features are multiple with mild to severe intellectual disabilities, learning defects in short- and long-term memory formation, typical craniofacial appearance, hypotonia and premature aging (Perluigi and Butterfield, 2012). On the neuroanatomical side, DS patients show reduction in brain size and weight, as well as a decrease in neuronal density associated with synaptic abnormalities (Kaufmann and Moser, 2000).

DS is believed to result from a gene dosage imbalance leading to the increased expression of normal chromosome 21 genes. Accordingly, the overexpression of specific genes located in the long arm of Hsa21, such as DS Critical Region 1 (DSCR1), the Amyloid-beta Precursor Protein (APP) and the dual-specificity tyrosine (Y)-phosphorylation regulated kinase 1A (DYRK1A) genes have been reported in DS patients (Antonarakis et al., 2004; Shukkur et al., 2006). However, several studies have also shown that individual loci were not responsible on their own for specific anatomical and functional features of DS (Roper and Reeves, 2006; Shukkur et al., 2006).

Interestingly, the SUMO3 gene is located on the long arm of the Hsa21 and it was reported that there is an increase in SUMO3-modified proteins in the human hippocampus of post-mortem DS patient (Gardiner, 2006). This increase in SUMO3-sumoylation impacts a large number of target proteins that may include important molecular pathways involved in the synaptic function and disruption of their sumoylation/desumoylation balance may explain at least in part, some of the synaptic defect observed in the patients. Therefore it would be of great interest to identify and functionally characterize the increased SUMO3 target proteins in DS to evaluate whether this imbalanced sumoylation may account for some of the reported DS features.

Parkinson's Disease (PD)

PD is a neurodegenerative condition caused by impairments of striatal dopaminergic neurotransmission, and ultimately leads to gradual loss of dopaminergic neurons in the substantia

nigra. Loss of these neuronal projections toward the striatum is directly correlated with the symptoms of the disease as the striatal structure is responsible for the control of voluntary movements. Accordingly, PD patients show significant decline in motor and non-motor functions, which are symptomatically expressed as resting tremor, muscle rigidness, impaired balance as well as speech and writing difficulties. Only 5% of the PD patients are diagnosed with genetic form of PD and the etiology of PD is yet to be fully elucidated. A cellular hallmark of the disease is the formation of intraneuronal inclusions known as Lewy bodies (LBs) that are often positive for SUMO1, ubiquitin and α-synuclein (for a recent review, see Vijayakumaran et al., 2015), therefore linking the SUMO pathway to the disease.

Sumoylation of α-Synuclein (αSYN)

The major component of LBs is αSYN, a small protein of 14 kDa encoded by the SNCA gene on chromosome 4. About 18 mutations in this gene have been directly linked to familial forms of PD and generally associate with the early-onset form of the disease, which typically appears before the age of 50.

The physiological functions of αSYN are still not clearly established but the protein is mainly localized at presynaptic sites where it is believed to regulate neurotransmitter release via its direct association to SNARE-proteins (reviewed in Calo et al., 2016). Structurally, αSYN contains an N-terminal membrane-binding domain, a hydrophobic core centrally involved in protein-protein aggregation, and an acidic C-terminal tail. Under physiological conditions, αSYN is able to fold into soluble tetra- and octameric protein structures. In LBs, αSYN misfolding leads to cytotoxic aggregates containing insoluble αSYN of high molecular weight species. It should be noted that recent experimental data showed that the intermediate oligomeric species of αSYN are toxic and most likely precede the formation of LBs in PD (Karpinar et al., 2009; Winner et al., 2011; Peelaerts et al., 2015).

αSYN was shown to be modified by SUMO1 and SUMO2 in cultured cells and in mammalian brain, and SUMO1 was also found in the brain of PD patients at the periphery of LBs co-localizing with αSYN, which raises the possibility that the SUMO pathway plays a role in protein aggregation (Dorval and Fraser, 2006; Kim et al., 2011; Krumova et al., 2011). Krumova et al. (2011) engineered a transgenic His-tagged SUMO2 mouse model and reported that sumoylation of αSYN occurs at the lysine 96 and 102 residues. They further showed that αSYN sumoylation reduces its propensity to aggregate in dopaminergic neurons of a rat model of PD. However, another study published almost simultaneously that sumoylation of αSYN promotes αSYN aggregates formation (Oh et al., 2011). Intriguingly, aggregates and inclusions formed as a result of impaired proteasome activity contain the sumoylated form of αSYN (Kim et al., 2011). Since the sumoylation of αSYN does not affect its ubiquitination, a proteasomal dysfunction may result in the accumulation of sumoylated αSYN and subsequently in αSYN toxic aggregation (Kim et al., 2011). Of note, a study that was performed in yeast confirmed the protective role of sumoylation against αSYN aggregation (Shahpasandzadeh et al., 2014). Moreover, this study showed that phosphorylation of αSYN can be additionally important for αSYN clearance through proteosomal degradation and suggested that sumoylation could modulate the interaction of αSYN with different kinases influencing its degradation (Shahpasandzadeh et al., 2014). Whether there is an active interplay between these two modifications of αSYN and whether they play a cell protective function against PD in the mammalian brain remains to be tested.

Interestingly, the extracellular spreading of αSYN has been reported in PD and Kunadt et al. (2015) have recently examined the possibility that sumoylation could serve as a regulatory mechanism for the sorting and the extracellular vesicular release of αSYN in neurons. They showed that sumoylation of proteins can mediate their extracellular sorting via the Endosomal Sorting Complex Required for Transport (ESCRT) into the extracellular vesicle pathway. Most importantly, they demonstrated that SUMO is recruited to ESCRT formation sites by the interaction with phosphoinositols and that sumoylation acts as a sorting signal for the extracellular vesicular release of αSYN (Kunadt et al., 2015). These data provide strong evidence for a role of the SUMO modification as a regulator of αSYN sorting to the extracellular space, possibly contributing to the interneuronal toxic spreading of αSYN reported in the disease and consequently to the etiology of PD.

Sumoylation of DJ-1

DJ-1 mutations have been linked to 1–2% of early-onset PD cases. DJ-1 is a molecular chaperone with cytoprotective functions under oxidative stress; in addition DJ-1 also acts as a transcriptional regulator. The DJ-1 protein is expressed in all brain regions, localizing to neurons and glial cells. DJ-1 is found within the cytoplasm, the nucleus, and in association with the mitochondria and the endoplasmic reticulum (reviewed in Eckermann, 2013). Interestingly, DJ-1 is present in presynaptic terminals, colocalizing with synaptophysin and associating with synaptic vesicles and also at the postsynapse, in dendritic spines (Usami et al., 2011) where it is involved in synaptic neurotransmission and induction of LTD (Wang et al., 2008).

Sumoylation of DJ-1 occurs on the lysine 130 residue and has been shown to increase upon UV irradiation. Moreover, this modification is necessary for DJ-1 to be in a fully activated form (Shinbo et al., 2006). The PD-associated DJ-1 mutation L166P leads to impaired DJ-1 sumoylation and decreases its solubility (Shinbo et al., 2006). Interestingly, the DJ-1 K130R mutation does not impact on the protein structure but rather leads to multi-/polysumoylation of the DJ-1 at alternative SUMO sites (Tao and Tong, 2003). Thus the elucidation of the exact synaptic function of DJ-1 sumoylation and how a defect in its sumoylation balance could impact synaptic function remains to be determined.

Overall, these findings highlight the key roles played by the sumoylation pathway in PD and we believe that the aim at clarifying the involvement of the SUMO process in the etiology of PD will become an active area of future research.

Sumoylation of Parkin

Although the loss-of-function mutations within the PARK2 gene, coding for the protein parkin, are the most common autosomal recessive juvenile causes of PD, the responsible molecular mechanisms remain unclear. Parkin is a RING-domain-containing E3 Ubiquitin ligase that is widely expressed throughout the CNS and can associate with PDZ scaffolding proteins at the postsynaptic membrane. Notably, parkin localizes to the majority of LBs in both familial and sporadic cases of PD. Recent findings suggest that parkin interacts with the KAR subunit GluK2 and regulates its neuronal function (Maraschi et al., 2014). Loss of parkin function, *in vitro* and *in vivo*, leads to GluK2 accumulation at the plasma membrane resulting in potentiated KAR current and consequently in the increase in KAR-dependent excitotoxicity presenting similar phenotype observed in autosomal recessive juvenile PD cases (Maraschi et al., 2014). Taking into account that GluK2 sumoylation regulates KAR endocytosis, neuronal excitability (Martin et al., 2007a) and synaptic plasticity (Chamberlain et al., 2012), it would be of high interest to see whether sumoylation could provide a rescue mechanism to down-regulate the increased surface expression and excitotoxicity seen in mouse brains that express the Parkin mutant causing autosomal recessive juvenile parkinsonism.

Importantly, parkin has also been shown to interact non-covalently with SUMO1 (Um and Chung, 2006). This interaction increased the E3 Ubiquitin ligase activity of parkin. Furthermore, it has been reported in this work that parkin specifically targets the SUMO E3 ligase RanBP2 for degradation (Um and Chung, 2006). Even though sumoylation of parkin or parkin substrates has not been directly involved in the pathogenesis of PD, it is reasonable to think, based on previous data, that sumoylation may directly impact on parkin's function and so on the pathophysiology of PD.

Huntington's Disease (HD)

Unlike PD, HD has a monogenic fully penetrant cause with autosomal dominant inheritance. It belongs to the group of polyQ disorders that arise as a consequence of an expansion of the CAG trinucleotide repeat (encoding for glutamine) in specific genes. In HD, the deleterious CAG expansion leads to a polyQ expansion ($\geq$ 40 instead of 23 glutamine residues in the normal Htt) within the amino-terminal domain of the Huntingtin (Htt) protein with the general agreement that longer polyQ expansions predict earlier onsets of the disease. Clinical hallmarks of HD are progressive motor decline leading to severe motor dysfunction, psychiatric disturbances and cognitive impairment. HD results from the toxic gain-of-function of expanded polyQ in Htt and its accumulation in affected neurons leads to neuronal cell death primarily in the striatum. Recent prevalence studies show that one individual in 7300 is affected in the western world (reviewed in Ross and Tabrizi, 2011).

Sumoylation of Huntingtin

Huntingtin is a large protein of 3144 amino acids (348 kDa) that folds into a superhelical structure with a hydrophobic core and serves as a scaffold protein. Htt is widely expressed in neurons and localizes both to the nucleus and the cytoplasm, shuttling between these two compartments. The cellular functions of Htt are still not well defined. Some studies suggested its roles in vesicular transport, regulation of gene transcription and RNA trafficking. Htt knockdown is lethal before the embryonic day 7.5 highlighting its critical role in embryonic development (Zeitlin et al., 1995). Htt indirectly interacts with NMDARs through PSD95 whereas presynaptic Htt is localized to synaptic vesicles, recycling endosomes and clathrin-coated vesicles (DiFiglia et al., 1995; Velier et al., 1998). Htt has been shown to influence the production and the transport of the growth factor BDNF in mice, and in cultured neurons Htt stimulates BDNF vesicle trafficking (Gauthier et al., 2004).

Importantly, several types of PTMs have been described for Htt including sumoylation and ubiquitination. A pathogenic fragment of Htt can be modified by both SUMO-1 and ubiquitin at the same lysine residue (Steffan et al., 2004). This group further showed that sumoylation stabilizes the pathogenic Htt fragment and reduces its ability to form aggregates in neuronal cell lines probably leading to a decrease in intracellular concentration of the toxic peptide (Steffan et al., 2004). Interestingly, genetic reduction of SUMO proteins in a *Drosophila* model of HD results in neuroprotection (Steffan et al., 2004). Moreover, potentiated sumoylation of mutant Htt that was caused by the action of the mutant Htt-specific SUMO E3 ligase Rhes, a striatal GTP-binding protein, displayed increased cytotoxicity (Subramaniam et al., 2009). Since sumoylation and ubiquitination of Htt occur on the same lysine residue and act in an antagonistic manner, it implies that the availability of the target lysine is critical for the degradation of Htt by the proteasome (Steffan et al., 2004). Because mutations that prevent these post-translational modifications on Htt reduce the pathology in *Drosophila*, it is likely that the balance between sumoylation and ubiquitination controls both the stability and the accurate targeting of Htt in neurons and that this tightly regulated balance is disrupted in HD.

More recently, O'Rourke et al. (2013) reported that Htt is sumoylated by both SUMO1 and SUMO2 primarily on the proximal lysine 6 and 9 residues and that PIAS1 is a SUMO E3 ligase for Htt. They further showed that genetic reduction of dPIAS in a mutant Htt *Drosophila* model of HD, which expresses mutant Htt, is protective confirming the previously reported positive role of sumoylation in HD (Steffan et al., 2004). The effect of Htt sumoylation by SUMO2 is the increase in the insoluble form of Htt in HeLa cells similar to the accumulation measured under proteasome inhibition. Importantly, this group also reported that the accumulation could be modulated by overexpression or acute knockdown of PIAS1 (O'Rourke et al., 2013). This supports the central role of the SUMO process in HD and also that a deregulated balance between sumoylation and desumoylation of Htt could participate in the etiology or in the aggravation of the disease. Accordingly, the authors reported an accumulation of SUMO2-modified proteins in insoluble fractions of HD post-mortem striata (O'Rourke et al., 2013).

Alzheimer's Disease (AD)

AD is the most common neurodegenerative condition causing severe memory deficits. AD accounts for more than 80% of dementia cases worldwide with no cure yet available (reviewed in Lee et al., 2013). Although the exact causes of AD are still much discussed, the pathology is characterized by the presence of intra- and extracellular protein aggregates mainly composed of Tau and β-amyloid (Aβ) proteins, which are toxic to the brain since they induce the loss of synapses, synaptic impairments and consequently, neuronal cell death (reviewed in Spires-Jones and Hyman, 2014).

Genetic studies have linked Single nucleotide polymorphisms (SNPs) in genes encoding the SUMO-activating enzyme SAE2 (Grupe et al., 2007; Corneveaux et al., 2010), the SUMO-conjugating enzyme Ubc9 (Ahn et al., 2009) and the desumoylase SENP3 (Weeraratna et al., 2007) to sporadic late onset AD. Immunohistological studies also revealed stronger SUMO immunoreactivities in hippocampal neurons of post-mortem AD brains compared to control patients (Li et al., 2003).

Sumoylation of Amyloid Precursor Protein (APP)

Interestingly, the APP from which Aβ is generated, and Tau have been both proposed to be substrates of the sumoylation machinery (reviewed in Spires-Jones and Hyman, 2014). Aβ is a small peptide of 4 kDa implicated in synaptic physiology and plasticity. The enzymatic machinery generating Aβ, which is composed of β- and γ-secretases, is partly localized in synaptic compartments. Aβ can directly bind to several synaptic receptors including NMDA and EphB2 receptors (De Felice et al., 2007; Simón et al., 2009). In cultured neurons the clustering of Aβ at excitatory synapses blocks the diffusion of mGlu5 receptors leading to increased calcium levels and hyperexcitability (Renner et al., 2010).

To date, the investigation into the effects of the sumoylation process in AD has generated mixed results. In 2003, the over-expression of SUMO3 was reported to dramatically reduce the Aβ production, whereas the expression of a SUMO3 form bearing the K11R mutation and therefore unable to form poly-SUMO chains displayed the opposite effect (Li et al., 2003). An additional work in 2008 showed that sumoylation of APP at the lysine 587 and 595 residues decreases the levels of Aβ aggregates in HeLa cells probably by altering the availability of the β-secretase cleavage (Zhang and Sarge, 2008). Conversely, two separate studies showed that sumoylation increases Aβ production independently of SUMO conjugation (Dorval et al., 2007) or via a mechanism involving the interaction of SUMO1 with BACE1, which is known to initiate the generation of Aβ (Yun et al., 2013). However, it should be noted that none of these studies examined the effects of Aβ sumoylation in neuronal cells. The authors rather used over-expression systems that might not reflect the exact mechanisms involved in the pathophysiology of AD. Considering the molecular complexity of AD and the off-target effects of SUMO over-expression, given the wide range of cellular pathway targeted by this modification, it will be of great interest to further address these discrepancies.

A more recent study examined the expression profile of the members of the SUMO machinery in the Tg2576 mouse model of AD that over-expresses APP (Nistico et al., 2014). They reported a significant increase in SUMO1-modified proteins and Ubc9 in the transgenic mice at 3 and 6 months of age compared to the WT littermates. SENP1 protein levels were also increased at the age of 3 months. On the contrary, the expression levels of SUMO2/3-modified proteins were markedly decreased at the age of 17 months and unchanged at the other examined stages (Nistico et al., 2014). This study thus supported the general belief of the field that the sumoylation/desumoylation balance is crucial and when deregulated it may participate in disease pathophysiology.

Sumoylation of Tau Protein

Tau is a microtubule-binding and stabilizing protein initially discovered to localize in axons (reviewed in Spires-Jones and Hyman, 2014). Recent data also suggest its roles in the regulation of protein composition at the postsynaptic density (Ittner et al., 2010). Moreover, tau was observed both in dendritic spines of normal as well as AD post-mortem brains (Tai et al., 2012). In AD, Tau is hyper-phosphorylated, detached from microtubules and aggregates into tangles within the somatodendritic region. It should be noted that not all neurons that have died display neurofibrillary tangles, suggesting that other pathological events must occur during the AD progression (Spires-Jones et al., 2014). Tau can be sumoylated in different cell types, mainly at the lysine 340 residue within a microtubule binding site (Dorval and Fraser, 2006). Tau sumoylation was affected upon proteasome inhibition suggesting that the lysine 340 residue is also a target for ubiquitination and that the balance between these two PTMs regulates Tau degradation (Dorval and Fraser, 2006). Intriguingly, the hyper-phosphorylated Tau aggregates stain positively for SUMO1 in an APP transgenic mouse model of AD, but not in post-mortem brain sections of AD patients (Pountney et al., 2003; Takahashi et al., 2008). In contrast, a recent study revealed that SUMO1 immunoreactivity colocalized with hyper-phosphorylated Tau in the cortex and hippocampal CA1 region of post-mortem AD brains, whereas no signal was measured for aged-matched control brains (Luo et al., 2014).

Sumoylation was also reported to promote Tau phosphorylation, and conversely, the hyper-phosphorylation of Tau induced Tau sumoylation (Luo et al., 2014). Luo et al. (2014) further showed that Tau sumoylation at the lysine 340 residue inhibited its ubiquitination and consequently its degradation. In addition, the exposure of cultured neurons to Aβ increased Tau-phosphorylation and sumoylation in a dose-dependent manner, which indicates that Aβ can act as an upstream regulator for tau phosphorylation and sumoylation (Luo et al., 2014). Altogether, these findings contribute to a better understanding of the role of sumoylation in AD and provide evidence for a putative mechanism explaining how the pathological accumulation of hyper-phosphorylated Tau occurs in AD brains.

CONCLUDING REMARKS

It is nowadays very clear that the sumoylation process acts as a major signaling pathway essential for the regulation of synaptic function. The available set of identified sumoylated substrates is rapidly expanding at the presynaptic site but is still quite limited in the postsynaptic area. We are, however, confident that the recent technical advances in the proteomic field will allow the identification of novel SUMO target proteins and that such neuronal and synaptic SUMOylomes will help to better assess the central role fulfilled by sumoylation in synaptic transmission and plasticity.

As highlighted in this review, the sumoylation process contributes to a wide range of regulatory actions in the developing brain, and also that disruption of the equilibrium between the sumoylated and non-sumoylated state of proteins is directly linked to several neurodevelopmental and neurodegenerative diseases. Therefore, the better comprehension of the mechanisms that regulate the spatiotemporal distribution, targeting and activity of the sumoylation machinery in neurons will certainly provide valuable information regarding how the sumoylation/desumoylation balance is orchestrated in the brain and at synapses.

We can now expect that the functional characterization of novel SUMO regulatory pathways as well as the discovery of additional sumoylated substrates at all stages of the brain development will facilitate a deeper understanding of the SUMO process in brain function and help evaluate its potential implication in pathological conditions.

AUTHOR CONTRIBUTIONS

LS and SM wrote the manuscript. All authors listed, have made substantial, direct and intellectual contribution to the work, and approved it for publication.

ACKNOWLEDGMENTS

We thank the members of the SM lab for fruitful discussions and Franck Aguila for excellent artwork. SM gratefully acknowledges the Jérôme Lejeune foundation and the "Agence Nationale de la Recherche" (ANR-15-CE16-0015-01) for financial support. We also thank the French Government for the "Investments for the Future" LabEx "SIGNALIFE" (ANR-11-LABX-0028-01). LS is a PhD fellow from the LabEx "SIGNALIFE".

REFERENCES

Ahn, K., Song, J. H., Kim, D. K., Park, M. H., Jo, S. A., and Koh, Y. H. (2009). Ubc9 gene polymorphisms and late-onset Alzheimer's disease in the Korean population: a genetic association study. *Neurosci. Lett.* 465, 272–275. doi: 10.1016/j.neulet.2009.09.017

Antonarakis, S. E., Lyle, R., Dermitzakis, E. T., Reymond, A., and Deutsch, S. (2004). Chromosome 21 and down syndrome: from genomics to pathophysiology. *Nat. Rev. Genet.* 5, 725–738. doi: 10.1038/nrg1448

Bayfield, M. A., Yang, R., and Maraia, R. J. (2010). Conserved and divergent features of the structure and function of La and La-related proteins (LARPs). *Biochim. Biophys. Acta* 1799, 365–378. doi: 10.1016/j.bbagrm.2010.01.011

Bell, K. F., Bent, R. J., Meese-Tamuri, S., Ali, A., Forder, J. P., and Aarts, M. M. (2013). Calmodulin kinase IV-dependent CREB activation is required for neuroprotection via NMDA receptor-PSD95 disruption. *J. Neurochem.* 126, 274–287. doi: 10.1111/jnc.12176

Berg, J. S., Brunetti-Pierri, N., Peters, S. U., Kang, S. H., Fong, C. T., Salamone, J., et al. (2007). Speech delay and autism spectrum behaviors are frequently associated with duplication of the 7q11.23 Williams-Beuren syndrome region. *Genet. Med.* 9, 427–441. doi: 10.1097/gim.0b013e3180986192

Bernier-Villamor, V., Sampson, D. A., Matunis, M. J., and Lima, C. D. (2002). Structural basis for E2-mediated SUMO conjugation revealed by a complex between ubiquitin-conjugating enzyme Ubc9 and RanGAP1. *Cell* 108, 345–356. doi: 10.1016/s0092-8674(02)00630-x

Bingol, B., and Schuman, E. M. (2006). Activity-dependent dynamics and sequestration of proteasomes in dendritic spines. *Nature* 441, 1144–1148. doi: 10.1038/nature04769

Bohren, K. M., Nadkarni, V., Song, J. H., Gabbay, K. H., and Owerbach, D. (2004). A M55V polymorphism in a novel SUMO gene (SUMO-4) differentially activates heat shock transcription factors and is associated with susceptibility to type I diabetes mellitus. *J. Biol. Chem.* 279, 27233–27238. doi: 10.1074/jbc.m402273200

Bramham, C. R., Alme, M. N., Bittins, M., Kuipers, S. D., Nair, R. R., Pai, B., et al. (2010). The Arc of synaptic memory. *Exp. Brain Res.* 200, 125–140. doi: 10.1007/s00221-009-1959-2

Brandon, N. J., and Sawa, A. (2011). Linking neurodevelopmental and synaptic theories of mental illness through DISC1. *Nat. Rev. Neurosci.* 12, 707–722. doi: 10.1038/nrn3120

Brenet, F., Socci, N. D., Sonenberg, N., and Holland, E. C. (2009). Akt phosphorylation of La regulates specific mRNA translation in glial progenitors. *Oncogene* 28, 128–139. doi: 10.1038/onc.2008.376

Brittain, J. M., Duarte, D. B., Wilson, S. M., Zhu, W., Ballard, C., Johnson, P. L., et al. (2011). Suppression of inflammatory and neuropathic pain by uncoupling CRMP-2 from the presynaptic Ca^{2+} channel complex. *Nat. Med.* 17, 822–829. doi: 10.1038/nm.2345

Broekhuis, C. H., Neubauer, G., van der Heijden, A., Mann, M., Proud, C. G., van Venrooij, W. J., et al. (2000). Detailed analysis of the phosphorylation of the human La (SS-B) autoantigen. (De)phosphorylation does not affect its subcellular distribution. *Biochemistry* 39, 3023–3033. doi: 10.1021/bi992308c

Calakos, N., Schoch, S., Südhof, T. C., and Malenka, R. C. (2004). Multiple roles for the active zone protein RIM1α in late stages of neurotransmitter release. *Neuron* 42, 889–896. doi: 10.1016/j.neuron.2004.05.014

Calo, L., Wegrzynowicz, M., Santivañez-Perez, J., and Grazia Spillantini, M. (2016). Synaptic failure and α-synuclein. *Mov. Disord.* 31, 169–177. doi: 10.1002/mds.26479

Castillo, P. E., Schoch, S., Schmitz, F., Südhof, T. C., and Malenka, R. C. (2002). RIM1α is required for presynaptic long-term potentiation. *Nature* 415, 327–330. doi: 10.1038/415327a

Cesca, F., Baldelli, P., Valtorta, F., and Benfenati, F. (2010). The synapsins: key actors of synapse function and plasticity. *Prog. Neurobiol.* 91, 313–348. doi: 10.1016/j.pneurobio.2010.04.006

Chamberlain, S. E., González-González, I. M., Wilkinson, K. A., Konopacki, F. A., Kantamneni, S., Henley, J. M., et al. (2012). SUMOylation and phosphorylation of GluK2 regulate kainate receptor trafficking and synaptic plasticity. *Nat. Neurosci.* 15, 845–852. doi: 10.1038/nn.3089

Chao, H. W., Hong, C. J., Huang, T. N., Lin, Y. L., and Hsueh, Y. P. (2008). SUMOylation of the MAGUK protein CASK regulates dendritic spinogenesis. *J. Cell Biol.* 182, 141–155. doi: 10.1083/jcb.200712094

Chen, Y. C., Hsu, W. L., Ma, Y. L., Tai, D. J., and Lee, E. H. (2014). CREB SUMOylation by the E3 ligase PIAS1 enhances spatial memory. *J. Neurosci.* 34, 9574–9589. doi: 10.1523/JNEUROSCI.4302-13.2014

Cheng, J., Huang, M., Zhu, Y., Xin, Y. J., Zhao, Y. K., Huang, J., et al. (2014). SUMOylation of MeCP2 is essential for transcriptional repression and hippocampal synapse development. *J. Neurochem.* 128, 798–806. doi: 10.1111/jnc.12523

Choi, J. H., Park, J. Y., Park, S. P., Lee, H., Han, S., Park, K. H., et al. (2016). Regulation of mGluR7 trafficking by SUMOylation in neurons. *Neuropharmacology* 102, 229–235. doi: 10.1016/j.neuropharm.2015.11.021

Chowdhury, S., Shepherd, J. D., Okuno, H., Lyford, G., Petralia, R. S., Plath, N., et al. (2006). Arc/Arg3.1 interacts with the endocytic machinery to regulate AMPA receptor trafficking. *Neuron* 52, 445–459. doi: 10.1016/j.neuron.2006.08.033

Cohen, S., and Greenberg, M. E. (2008). Communication between the synapse and the nucleus in neuronal development, plasticity and disease. *Annu. Rev. Cell Dev. Biol.* 24, 183–209. doi: 10.1146/annurev.cellbio.24.110707.175235

Contractor, A., Mulle, C., and Swanson, G. T. (2011). Kainate receptors coming of age: milestones of two decades of research. *Trends Neurosci.* 34, 154–163. doi: 10.1016/j.tins.2010.12.002

Corneveaux, J. J., Myers, A. J., Allen, A. N., Pruzin, J. J., Ramirez, M., Engel, A., et al. (2010). Association of CR1, CLU and PICALM with Alzheimer's disease in a cohort of clinically characterized and neuropathologically verified individuals. *Hum. Mol. Genet.* 19, 3295–3301. doi: 10.1093/hmg/ddq221

Craig, T. J., Anderson, D., Evans, A. J., Girach, F., and Henley, J. M. (2015). SUMOylation of Syntaxin1A regulates presynaptic endocytosis. *Sci. Rep.* 5:17669. doi: 10.1038/srep17669

Craig, T. J., Jaafari, N., Petrovic, M. M., Rubin, P. P., Mellor, J. R., Henley, J. M., et al. (2012). Homeostatic synaptic scaling is regulated by protein SUMOylation. *J. Biol. Chem.* 287, 22781–22788. doi: 10.1074/jbc.m112.356337

Dai, X. Q., Kolic, J., Marchi, P., Sipione, S., and Macdonald, P. E. (2009). SUMOylation regulates Kv2.1 and modulates pancreatic β-cell excitability. *J. Cell Sci.* 122, 775–779. doi: 10.1242/jcs.036632

Dai, X. Q., Plummer, G., Casimir, M., Kang, Y., Hajmrle, C., Gaisano, H. Y., et al. (2011). SUMOylation regulates insulin exocytosis downstream of secretory granule docking in rodents and humans. *Diabetes* 60, 838–847. doi: 10.2337/db10-0440

De Felice, F. G., Velasco, P. T., Lambert, M. P., Viola, K., Fernandez, S. J., Ferreira, S. T., et al. (2007). Aβ oligomers induce neuronal oxidative stress through an N-methyl-D-aspartate receptor-dependent mechanism that is blocked by the Alzheimer drug memantine. *J. Biol. Chem.* 282, 11590–11601. doi: 10.1074/jbc.m607483200

Depienne, C., Heron, D., Betancur, C., Benyahia, B., Trouillard, O., Bouteiller, D., et al. (2007). Autism, language delay and mental retardation in a patient with 7q11 duplication. *J. Med. Genet.* 44, 452–458. doi: 10.1136/jmg.2006.047092

DiFiglia, M., Sapp, E., Chase, K., Schwarz, C., Meloni, A., Young, C., et al. (1995). Huntingtin is a cytoplasmic protein associated with vesicles in human and rat brain neurons. *Neuron* 14, 1075–1081. doi: 10.1016/0896-6273(95)90346-1

Dodson, P. D., and Forsythe, I. D. (2004). Presynaptic K^+ channels: electrifying regulators of synaptic terminal excitability. *Trends Neurosci.* 27, 210–217. doi: 10.1016/j.tins.2004.02.012

Dorval, V., and Fraser, P. E. (2006). Small ubiquitin-like modifier (SUMO) modification of natively unfolded proteins tau and α-synuclein. *J. Biol. Chem.* 281, 9919–9924. doi: 10.1074/jbc.m510127200

Dorval, V., and Fraser, P. E. (2007). SUMO on the road to neurodegeneration. *Biochim. Biophys. Acta* 1773, 694–706. doi: 10.1016/j.bbamcr.2007.03.017

Dorval, V., Mazzella, M. J., Mathews, P. M., Hay, R. T., and Fraser, P. E. (2007). Modulation of Aβ generation by small ubiquitin-like modifiers does not require conjugation to target proteins. *Biochem. J.* 404, 309–316. doi: 10.1042/bj20061451

Drisaldi, B., Colnaghi, L., Fioriti, L., Rao, N., Myers, C., Snyder, A. M., et al. (2015). SUMOylation is an inhibitory constraint that regulates the prion-like aggregation and activity of CPEB3. *Cell Rep.* 11, 1694–1702. doi: 10.1016/j.celrep.2015.04.061

Dulubova, I., Lou, X., Lu, J., Huryeva, I., Alam, A., Schneggenburger, R., et al. (2005). A Munc13/RIM/Rab3 tripartite complex: from priming to plasticity? *EMBO J.* 24, 2839–2850. doi: 10.1038/sj.emboj.7600753

Dustrude, E. T., Wilson, S. M., Ju, W., Xiao, Y., and Khanna, R. (2013). CRMP2 protein SUMOylation modulates NaV1.7 channel trafficking. *J. Biol. Chem.* 288, 24316–24331. doi: 10.1074/jbc.M113.474924

Dütting, E., Schröder-Kress, N., Sticht, H., and Enz, R. (2011). SUMO E3 ligases are expressed in the retina and regulate SUMOylation of the metabotropic glutamate receptor 8b. *Biochem. J.* 435, 365–371. doi: 10.1042/BJ20101854

Eckermann, K. (2013). SUMO and Parkinson's disease. *Neuromolecular Med.* 15, 737–759. doi: 10.1007/s12017-013-8259-5

Estruch, S. B., Graham, S. A., Deriziotis, P., and Fisher, S. E. (2016). The language-related transcription factor FOXP2 is post-translationally modified with small ubiquitin-like modifiers. *Sci. Rep.* 6:20911. doi: 10.1038/srep20911

Feligioni, M., Nishimune, A., and Henley, J. M. (2009). Protein SUMOylation modulates calcium influx and glutamate release from presynaptic terminals. *Eur. J. Neurosci.* 29, 1348–1356. doi: 10.1111/j.1460-9568.2009.06692.x

Fioriti, L., Myers, C., Huang, Y. Y., Li, X., Stephan, J. S., Trifilieff, P., et al. (2015). The persistence of hippocampal-based memory requires protein synthesis mediated by the prion-like protein CPEB3. *Neuron* 86, 1433–1448. doi: 10.1016/j.neuron.2015.05.021

Flavell, S. W., and Greenberg, M. E. (2008). Signaling mechanisms linking neuronal activity to gene expression and plasticity of the nervous system. *Annu. Rev. Neurosci.* 31, 563–590. doi: 10.1146/annurev.neuro.31.060407.125631

Flavell, S. W., Cowan, C. W., Kim, T. K., Greer, P. L., Lin, Y., Paradis, S., et al. (2006). Activity-dependent regulation of MEF2 transcription factors suppresses excitatory synapse number. *Science* 311, 1008–1012. doi: 10.1126/science.1122511

Flotho, A., and Melchior, F. (2013). Sumoylation: a regulatory protein modification in health and disease. *Annu. Rev. Biochem.* 82, 357–385. doi: 10.1146/annurev-biochem-061909-093311

Fu, J., Yu, H. M., Chiu, S. Y., Mirando, A. J., Maruyama, E. O., Cheng, J. G., et al. (2014). Disruption of SUMO-specific protease 2 induces mitochondria mediated neurodegeneration. *PLoS Genet.* 10:e1004579. doi: 10.1371/journal.pgen.1004579

Fujita, E., Tanabe, Y., Shiota, A., Ueda, M., Suwa, K., Momoi, M. Y., et al. (2008). Ultrasonic vocalization impairment of Foxp2 (R552H) knockin mice related to speech-language disorder and abnormality of Purkinje cells. *Proc. Natl. Acad. Sci. U S A* 105, 3117–3122. doi: 10.1073/pnas.0712298105

Gardiner, K. (2006). Transcriptional dysregulation in down syndrome: predictions for altered protein complex stoichiometries and post-translational modifications and consequences for learning/behavior genes ELK, CREB and the estrogen and glucocorticoid receptors. *Behav. Genet.* 36, 439–453. doi: 10.1007/s10519-006-9051-1

Gareau, J. R., and Lima, C. D. (2010). The SUMO pathway: emerging mechanisms that shape specificity, conjugation and recognition. *Nat. Rev. Mol. Cell Biol.* 11, 861–871. doi: 10.1038/nrm3011

Gauthier, L. R., Charrin, B. C., Borrell-Pagès, M., Dompierre, J. P., Rangone, H., Cordelières, F. P., et al. (2004). Huntingtin controls neurotrophic support and survival of neurons by enhancing BDNF vesicular transport along microtubules. *Cell* 118, 127–138. doi: 10.1016/j.cell.2004.06.018

Geiss-Friedlander, R., and Melchior, F. (2007). Concepts in sumoylation: a decade on. *Nat. Rev. Mol. Cell Biol.* 8, 947–956. doi: 10.1038/nrm2293

Girach, F., Craig, T. J., Rocca, D. L., and Henley, J. M. (2013). RIM1α SUMOylation is required for fast synaptic vesicle exocytosis. *Cell Rep.* 5, 1294–1301. doi: 10.1016/j.celrep.2013.10.039

Glasscock, E., Qian, J., Yoo, J. W., and Noebels, J. L. (2007). Masking epilepsy by combining two epilepsy genes. *Nat. Neurosci.* 10, 1554–1558. doi: 10.1038/nn1999

Gowran, A., Murphy, C. E., and Campbell, V. A. (2009). Delta(9)-tetrahydrocannabinol regulates the p53 post-translational modifiers Murine double minute 2 and the small ubiquitin modifier protein in the rat brain. *FEBS Lett.* 583, 3412–3418. doi: 10.1016/j.febslet.2009.09.056

Grant, S. G. (2012). Synaptopathies: diseases of the synaptome. *Curr. Opin. Neurobiol.* 22, 522–529. doi: 10.1016/j.conb.2012.02.002

Greer, P. L., Hanayama, R., Bloodgood, B. L., Mardinly, A. R., Lipton, D. M., Flavell, S. W., et al. (2010). The angelman syndrome protein Ube3A regulates

synapse development by ubiquitinating arc. *Cell* 140, 704–716. doi: 10.1016/j.cell.2010.01.026

Grégoire, S., and Yang, X. J. (2005). Association with class IIa histone deacetylases upregulates the sumoylation of MEF2 transcription factors. *Mol. Cell. Biol.* 25, 2273–2287. doi: 10.1128/mcb.25.6.2273-2287.2005

Grégoire, S., Tremblay, A. M., Xiao, L., Yang, Q., Ma, K., Nie, J., et al. (2006). Control of MEF2 transcriptional activity by coordinated phosphorylation and sumoylation. *J. Biol. Chem.* 281, 4423–4433. doi: 10.1074/jbc.m509471200

Grupe, A., Abraham, R., Li, Y., Rowland, C., Hollingworth, P., Morgan, A., et al. (2007). Evidence for novel susceptibility genes for late-onset alzheimer's disease from a genome-wide association study of putative functional variants. *Hum. Mol. Genet.* 16, 865–873. doi: 10.1093/hmg/ddm031

Guerrini, R., and Parrini, E. (2012). Epilepsy in rett syndrome and CDKL5- and FOXG1-gene-related encephalopathies. *Epilepsia* 53, 2067–2078. doi: 10.1111/j.1528-1167.2012.03656.x

Guo, C., Hildick, K. L., Luo, J., Dearden, L., Wilkinson, K. A., and Henley, J. M. (2013). SENP3-mediated deSUMOylation of dynamin-related protein 1 promotes cell death following ischaemia. *EMBO J.* 32, 1514–1528. doi: 10.1038/emboj.2013.65

Guo, D., Li, M., Zhang, Y., Yang, P., Eckenrode, S., Hopkins, D., et al. (2004). A functional variant of SUMO4, a new I κ B α modifier, is associated with type 1 diabetes. *Nat. Genet.* 36, 837–841. doi: 10.1038/ng1391

Gwizdek, C., Cassé, F., and Martin, S. (2013). Protein sumoylation in brain development, neuronal morphology and spinogenesis. *Neuromolecular Med.* 15, 677–691. doi: 10.1007/s12017-013-8252-z

Hackett, A., Tarpey, P. S., Licata, A., Cox, J., Whibley, A., Boyle, J., et al. (2010). CASK mutations are frequent in males and cause X-linked nystagmus and variable XLMR phenotypes. *Eur. J. Hum. Genet.* 18, 544–552. doi: 10.1038/ejhg.2009.220

Hasegawa, Y., Yoshida, D., Nakamura, Y., and Sakakibara, S. (2014). Spatiotemporal distribution of SUMOylation components during mouse brain development. *J. Comp. Neuro.l* 522, 3020–3036. doi: 10.1002/cne.23563

Hay, R. T. (2005). SUMO: a history of modification. *Mol. Cell* 18, 1–12. doi: 10.1016/j.molcel.2005.03.012

Henley, J. M., Craig, T. J., and Wilkinson, K. A. (2014). Neuronal SUMOylation: mechanisms, physiology and roles in neuronal dysfunction. *Physiol. Rev.* 94, 1249–1285. doi: 10.1152/physrev.00008.2014

Hickey, C. M., Wilson, N. R., and Hochstrasser, M. (2012). Function and regulation of SUMO proteases. *Nat. Rev. Mol. Cell Biol.* 13, 755–766. doi: 10.1038/nrm3478

Hsueh, Y. P. (2006). The role of the MAGUK protein CASK in neural development and synaptic function. *Curr. Med. Chem.* 13, 1915–1927. doi: 10.2174/092986706777585040

Hsueh, Y. P. (2009). Calcium/calmodulin-dependent serine protein kinase and mental retardation. *Ann. Neurol.* 66, 438–443. doi: 10.1002/ana.21755

Huang, T. N., and Hsueh, Y. P. (2009). CASK point mutation regulates protein-protein interactions and NR2b promoter activity. *Biochem. Biophys. Res. Commun.* 382, 219–222. doi: 10.1016/j.bbrc.2009.03.015

Ip, J. P., Fu, A. K., and Ip, N. Y. (2014). CRMP2: functional roles in neural development and therapeutic potential in neurological diseases. *Neuroscientist* 20, 589–598. doi: 10.1177/1073858413514278

Ittner, L. M., Ke, Y. D., Delerue, F., Bi, M., Gladbach, A., van Eersel, J., et al. (2010). Dendritic function of tau mediates amyloid-β toxicity in Alzheimer's disease mouse models. *Cell* 142, 387–397. doi: 10.1016/j.cell.2010.06.036

Jaafari, N., Konopacki, F. A., Owen, T. F., Kantamneni, S., Rubin, P., Craig, T. J., et al. (2013). SUMOylation is required for glycine-induced increases in AMPA receptor surface expression (ChemLTP) in hippocampal neurons. *PLoS One* 8:e52345. doi: 10.1371/journal.pone.0052345

Ju, W., Li, Q., Wilson, S. M., Brittain, J. M., Meroueh, L., and Khanna, R. (2013). SUMOylation alters CRMP2 regulation of calcium influx in sensory neurons. *Channels (Austin)* 7, 153–159. doi: 10.4161/chan.24224

Kang, J., Gocke, C. B., and Yu, H. (2006). Phosphorylation-facilitated sumoylation of MEF2C negatively regulates its transcriptional activity. *BMC Biochem.* 7:5. doi: 10.1186/1471-2091-7-5

Karpinar, D. P., Balija, M. B., Kügler, S., Opazo, F., Rezaei-Ghaleh, N., Wender, N., et al. (2009). Pre-fibrillar α-synuclein variants with impaired β-structure increase neurotoxicity in Parkinson's disease models. *EMBO J.* 28, 3256–3268. doi: 10.1038/emboj.2009.257

Kaufmann, W. E., and Moser, H. W. (2000). Dendritic anomalies in disorders associated with mental retardation. *Cereb. Cortex* 10, 981–991. doi: 10.1093/cercor/10.10.981

Kim, Y. M., Jang, W. H., Quezado, M. M., Oh, Y., Chung, K. C., Junn, E., et al. (2011). Proteasome inhibition induces α-synuclein SUMOylation and aggregate formation. *J. Neurol. Sci.* 307, 157–161. doi: 10.1016/j.jns.2011.04.015

Kneussel, M., and Hausrat, T. J. (2016). Postsynaptic neurotransmitter receptor reserve pools for synaptic potentiation. *Trends Neurosci.* 39, 170–182. doi: 10.1016/j.tins.2016.01.002

Kofuji, T., Fujiwara, T., Sanada, M., Mishima, T., and Akagawa, K. (2014). HPC-1/syntaxin 1A and syntaxin 1B play distinct roles in neuronal survival. *J. Neurochem.* 130, 514–525. doi: 10.1111/jnc.12722

Konopacki, F. A., Jaafari, N., Rocca, D. L., Wilkinson, K. A., Chamberlain, S., Rubin, P., et al. (2011). Agonist-induced PKC phosphorylation regulates GluK2 SUMOylation and kainate receptor endocytosis. *Proc. Natl. Acad. Sci. U S A* 108, 19772–19777. doi: 10.1073/pnas.1111575108

Krumova, P., Meulmeester, E., Garrido, M., Tirard, M., Hsiao, H. H., Bossis, G., et al. (2011). Sumoylation inhibits α-synuclein aggregation and toxicity. *J. Cell Biol.* 194, 49–60. doi: 10.1083/jcb.201010117

Krumova, P., and Weishaupt, J. H. (2012). Sumoylation in neurodegenerative diseases. *Cell. Mol. Life Sci.* 70, 2123–2138. doi: 10.1007/s00018-012-1158-3

Kunadt, M., Eckermann, K., Stuendl, A., Gong, J., Russo, B., Strauss, K., et al. (2015). Extracellular vesicle sorting of α-Synuclein is regulated by sumoylation. *Acta Neuropathol.* 129, 695–713. doi: 10.1007/s00401-015-1408-1

Lai, C. S., Fisher, S. E., Hurst, J. A., Vargha-Khadem, F., and Monaco, A. P. (2001). A forkhead-domain gene is mutated in a severe speech and language disorder. *Nature* 413, 519–523. doi: 10.1038/35097076

Lai, C. S., Gerrelli, D., Monaco, A. P., Fisher, S. E., and Copp, A. J. (2003). FOXP2 expression during brain development coincides with adult sites of pathology in a severe speech and language disorder. *Brain* 126, 2455–2462. doi: 10.1093/brain/awg247

Lee, L., Dale, E., Staniszewski, A., Zhang, H., Saeed, F., Sakurai, M., et al. (2014). Regulation of synaptic plasticity and cognition by SUMO in normal physiology and Alzheimer's disease. *Sci. Rep.* 4:7190. doi: 10.1038/srep07190

Lee, L., Sakurai, M., Matsuzaki, S., Arancio, O., and Fraser, P. (2013). SUMO and Alzheimer's disease. *Neuromolecular Med.* 15, 720–736. doi: 10.1007/s12017-013-8257-7

Li, H., Radford, J. C., Ragusa, M. J., Shea, K. L., McKercher, S. R., Zaremba, J. D., et al. (2008). Transcription factor MEF2C influences neural stem/progenitor cell differentiation and maturation *in vivo*. *Proc. Natl. Acad. Sci. U S A* 105, 9397–9402. doi: 10.1073/pnas.0802876105

Li, Y., Wang, H., Wang, S., Quon, D., Liu, Y. W., and Cordell, B. (2003). Positive and negative regulation of APP amyloidogenesis by sumoylation. *Proc. Natl. Acad. Sci. U S A* 100, 259–264. doi: 10.1073/pnas.0235361100

Loane, M., Morris, J. K., Addor, M. C., Arriola, L., Budd, J., Doray, B., et al. (2013). Twenty-year trends in the prevalence of down syndrome and other trisomies in Europe: impact of maternal age and prenatal screening. *Eur. J. Hum. Genet.* 21, 27–33. doi: 10.1038/ejhg.2012.94

Loriol, C., Cassé, F., Khayachi, A., Poupon, G., Chafai, M., Deval, E., et al. (2014). mGlu5 receptors regulate synaptic sumoylation via a transient PKC-dependent diffusional trapping of Ubc9 into spines. *Nat. Commun.* 5:5113. doi: 10.1038/ncomms6113

Loriol, C., Khayachi, A., Poupon, G., Gwizdek, C., and Martin, S. (2013). Activity-dependent regulation of the sumoylation machinery in rat hippocampal neurons. *Biol. Cell* 105, 30–45. doi: 10.1111/boc.201200016

Loriol, C., Parisot, J., Poupon, G., Gwizdek, C., and Martin, S. (2012). Developmental regulation and spatiotemporal redistribution of the sumoylation machinery in the rat central nervous system. *PLoS One* 7:e33757. doi: 10.1371/journal.pone.0033757

Lu, H., Liu, B., You, S., Chen, L., Dongmei, Q., Gu, M., et al. (2013). SENP2 regulates MEF2A de-SUMOylation in an activity dependent manner. *Mol. Biol. Rep.* 40, 2485–2490. doi: 10.1007/s11033-012-2329-x

Lu, H. C., and Mackie, K. (2016). An introduction to the endogenous cannabinoid system. *Biol. Psychiatry* 79, 516–525. doi: 10.1016/j.biopsych.2015.07.028

Lu, W., Man, H., Ju, W., Trimble, W. S., MacDonald, J. F., and Wang, Y. T. (2001). Activation of synaptic NMDA receptors induces membrane insertion of new AMPA receptors and LTP in cultured hippocampal neurons. *Neuron* 29, 243–254. doi: 10.1016/s0896-6273(01)00194-5

Luo, J., Ashikaga, E., Rubin, P. P., Heimann, M. J., Hildick, K. L., Bishop, P., et al. (2013). Receptor trafficking and the regulation of synaptic plasticity by SUMO. *Neuromolecular Med.* 15, 692–706. doi: 10.1007/s12017-013-8253-y

Luo, H. B., Xia, Y. Y., Shu, X. J., Liu, Z. C., Feng, Y., Liu, X. H., et al. (2014). SUMOylation at K340 inhibits tau degradation through deregulating its phosphorylation and ubiquitination. *Proc. Natl. Acad. Sci. U S A* 111, 16586–16591. doi: 10.1073/pnas.1417548111

Mahajan, R., Delphin, C., Guan, T., Gerace, L., and Melchior, F. (1997). A small ubiquitin-related polypeptide involved in targeting RanGAP1 to nuclear pore complex protein RanBP2. *Cell* 88, 97–107. doi: 10.1016/s0092-8674(00)81862-0

Maraschi, A., Ciammola, A., Folci, A., Sassone, F., Ronzitti, G., Cappelletti, G., et al. (2014). Parkin regulates kainate receptors by interacting with the GluK2 subunit. *Nat. Commun.* 5:5182. doi: 10.1038/ncomms6182

Martin, S. (2009). Extranuclear functions of protein sumoylation in the central nervous system. *Med. Sci. (Paris)* 25, 693–698. doi: 10.1051/medsci/20092589693

Martin, S., and Henley, J. M. (2004). Activity-dependent endocytic sorting of kainate receptors to recycling or degradation pathways. *EMBO J.* 23, 4749–4759. doi: 10.1038/sj.emboj.7600483

Martin, S., Nishimune, A., Mellor, J. R., and Henley, J. M. (2007a). SUMOylation regulates kainate-receptor-mediated synaptic transmission. *Nature* 447, 321–325. doi: 10.1038/nature05736

Martin, S., Wilkinson, K. A., Nishimune, A., and Henley, J. M. (2007b). Emerging extranuclear roles of protein SUMOylation in neuronal function and dysfunction. *Nat. Rev. Neurosci.* 8, 948–959. doi: 10.1038/nrn2276

Matsuda, S., Launey, T., Mikawa, S., and Hirai, H. (2000). Disruption of AMPA receptor GluR2 clusters following long-term depression induction in cerebellar Purkinje neurons. *EMBO J.* 19, 2765–2774. doi: 10.1093/emboj/19.12.2765

Matsuzaki, S., Lee, L., Knock, E., Srikumar, T., Sakurai, M., Hazrati, L. N., et al. (2015). SUMO1 affects synaptic function, spine density and memory. *Sci. Rep.* 5:10730. doi: 10.1038/srep10730

Matunis, M. J., Coutavas, E., and Blobel, G. (1996). A novel ubiquitin-like modification modulates the partitioning of the Ran-GTPase-activating protein RanGAP1 between the cytosol and the nuclear pore complex. *J. Cell Biol.* 135, 1457–1470. doi: 10.1083/jcb.135.6.1457

Meredith, L. J., Wang, C. M., Nascimento, L., Liu, R., Wang, L., and Yang, W. H. (2016). The key regulator for language and speech development, FOXP2, is a novel substrate for SUMOylation. *J. Cell. Biochem.* 117, 426–438. doi: 10.1002/jcb.25288

Mukhopadhyay, D., and Dasso, M. (2007). Modification in reverse: the SUMO proteases. *Trends Biochem. Sci.* 32, 286–295. doi: 10.1016/j.tibs.2007.05.002

Nakamura, K., Anitha, A., Yamada, K., Tsujii, M., Iwayama, Y., Hattori, E., et al. (2008). Genetic and expression analyses reveal elevated expression of syntaxin 1A (STX1A) in high functioning autism. *Int. J. Neuropsychopharmacol.* 11, 1073–1084. doi: 10.1017/S1461145708009036

Nistico, R., Ferraina, C., Marconi, V., Blandini, F., Negri, L., Egebjerg, J., et al. (2014). Age-related changes of protein SUMOylation balance in the AβPP Tg2576 mouse model of Alzheimer's disease. *Front. Pharmacol.* 5:63. doi: 10.3389/fphar.2014.00063

Niswender, C. M., and Conn, P. J. (2010). Metabotropic glutamate receptors: physiology, pharmacology and disease. *Annu. Rev. Pharmacol. Toxicol.* 50, 295–322. doi: 10.1146/annurev.pharmtox.011008.145533

Oh, Y., Kim, Y. M., Mouradian, M. M., and Chung, K. C. (2011). Human Polycomb protein 2 promotes α-synuclein aggregate formation through covalent SUMOylation. *Brain Res.* 1381, 78–89. doi: 10.1016/j.brainres.2011.01.039

O'Rourke, J. G., Gareau, J. R., Ochaba, J., Song, W., Raskó, T., Reverter, D., et al. (2013). SUMO-2 and PIAS1 modulate insoluble mutant huntingtin protein accumulation. *Cell Rep.* 4, 362–375. doi: 10.1016/j.celrep.2013.06.034

Pavlopoulos, E., Trifilieff, P., Chevaleyre, V., Fioriti, L., Zairis, S., Pagano, A., et al. (2011). Neuralized1 activates CPEB3: a function for nonproteolytic ubiquitin in synaptic plasticity and memory storage. *Cell* 147, 1369–1383. doi: 10.1016/j.cell.2011.09.056

Peelaerts, W., Bousset, L., Van der Perren, A., Moskalyuk, A., Pulizzi, R., Giugliano, M., et al. (2015). α-Synuclein strains cause distinct synucleinopathies after local and systemic administration. *Nature* 522, 340–344. doi: 10.1038/nature14547

Perluigi, M., and Butterfield, D. A. (2012). Oxidative stress and down syndrome: a route toward Alzheimer-like dementia. *Curr. Gerontol. Geriatr. Res.* 2012:724904. doi: 10.1155/2012/724904

Plant, L. D., Dowdell, E. J., Dementieva, I. S., Marks, J. D., and Goldstein, S. A. (2011). SUMO modification of cell surface Kv2.1 potassium channels regulates the activity of rat hippocampal neurons. *J. Gen. Physiol.* 137, 441–454. doi: 10.1085/jgp.201110604

Pountney, D. L., Huang, Y., Burns, R. J., Haan, E., Thompson, P. D., Blumbergs, P. C., et al. (2003). SUMO-1 marks the nuclear inclusions in familial neuronal intranuclear inclusion disease. *Exp. Neurol.* 184, 436–446. doi: 10.1016/j.expneurol.2003.07.004

Qi, Y., Wang, J., Bomben, V. C., Li, D. P., Chen, S. R., Sun, H., et al. (2014). Hyper-SUMOylation of the Kv7 potassium channel diminishes the M-current leading to seizures and sudden death. *Neuron* 83, 1159–1171. doi: 10.1016/j.neuron.2014.07.042

Rashid, A. J., Cole, C. J., and Josselyn, S. A. (2014). Emerging roles for MEF2 transcription factors in memory. *Genes Brain Behav.* 13, 118–125. doi: 10.1111/gbb.12058

Renner, M., Lacor, P. N., Velasco, P. T., Xu, J., Contractor, A., Klein, W. L., et al. (2010). Deleterious effects of amyloid β oligomers acting as an extracellular scaffold for mGluR5. *Neuron* 66, 739–754. doi: 10.1016/j.neuron.2010.04.029

Riquelme, C., Barthel, K. K., and Liu, X. (2006). SUMO-1 modification of MEF2A regulates its transcriptional activity. *J. Cell. Mol. Med.* 10, 132–144. doi: 10.1111/j.1582-4934.2006.tb00295.x

Rodriguez, M. S., Dargemont, C., and Hay, R. T. (2001). SUMO-1 conjugation *in vivo* requires both a consensus modification motif and nuclear targeting. *J. Biol. Chem.* 276, 12654–12659. doi: 10.1074/jbc.m009476200

Roper, R. J., and Reeves, R. H. (2006). Understanding the basis for down syndrome phenotypes. *PLoS Genet.* 2:e50. doi: 10.1371/journal.pgen.0020050

Ross, C. A., and Tabrizi, S. J. (2011). Huntington's disease: from molecular pathogenesis to clinical treatment. *Lancet Neurol.* 10, 83–98. doi: 10.1016/s1474-4422(10)70245-3

Sampson, D. A., Wang, M., and Matunis, M. J. (2001). The small ubiquitin-like modifier-1 (SUMO-1) consensus sequence mediates Ubc9 binding and is essential for SUMO-1 modification. *J. Biol. Chem.* 276, 21664–21669. doi: 10.1074/jbc.m100006200

Schulz, S., Chachami, G., Kozaczkiewicz, L., Winter, U., Stankovic-Valentin, N., Haas, P., et al. (2012). Ubiquitin-specific protease-like 1 (USPL1) is a SUMO isopeptidase with essential, non-catalytic functions. *EMBO Rep.* 13, 930–938. doi: 10.1038/embor.2012.125

Setou, M., Nakagawa, T., Seog, D. H., and Hirokawa, N. (2000). Kinesin superfamily motor protein KIF17 and mLin-10 in NMDA receptor-containing vesicle transport. *Science* 288, 1796–1802. doi: 10.1126/science.288.5472.1796

Shahpasandzadeh, H., Popova, B., Kleinknecht, A., Fraser, P. E., Outeiro, T. F., and Braus, G. H. (2014). Interplay between sumoylation and phosphorylation for protection against α-synuclein inclusions. *J. Biol. Chem.* 289, 31224–31240. doi: 10.1074/jbc.M114.559237

Shalizi, A., Bilimoria, P. M., Stegmüller, J., Gaudillière, B., Yang, Y., Shuai, K., et al. (2007). PIASx is a MEF2 SUMO E3 ligase that promotes postsynaptic dendritic morphogenesis. *J. Neurosci.* 27, 10037–10046. doi: 10.1523/jneurosci.0361-07.2007

Shalizi, A., Gaudillière, B., Yuan, Z., Stegmuller, J., Shirogane, T., Ge, Q., et al. (2006). A calcium-regulated MEF2 sumoylation switch controls postsynaptic differentiation. *Science* 311, 1012–1017. doi: 10.1126/science.1122513

Shin, E. J., Shin, H. M., Nam, E., Kim, W. S., Kim, J. H., Oh, B. H., et al. (2012). DeSUMOylating isopeptidase: a second class of SUMO protease. *EMBO Rep.* 13, 339–346. doi: 10.1038/embor.2012.3

Shinbo, Y., Niki, T., Taira, T., Ooe, H., Takahashi-Niki, K., Maita, C., et al. (2006). Proper SUMO-1 conjugation is essential to DJ-1 to exert its full activities. *Cell Death Differ.* 13, 96–108. doi: 10.1038/sj.cdd.4401704

Shukkur, E. A., Shimohata, A., Akagi, T., Yu, W., Yamaguchi, M., Murayama, M., et al. (2006). Mitochondrial dysfunction and tau hyperphosphorylation in Ts1Cje, a mouse model for down syndrome. *Hum. Mol. Genet.* 15, 2752–2762. doi: 10.1093/hmg/ddl211

Si, K., Choi, Y. B., White-Grindley, E., Majumdar, A., and Kandel, E. R. (2010). Aplysia CPEB can form prion-like multimers in sensory neurons that contribute to long-term facilitation. *Cell* 140, 421–435. doi: 10.1016/j.cell.2010.01.008

Simón, A. M., Schiapparelli, L., Salazar-Colocho, P., Cuadrado-Tejedor, M., Escribano, L., Lopez De Maturana, R., et al. (2009). Overexpression of wild-type human APP in mice causes cognitive deficits and pathological features unrelated to Aβ levels. *Neurobiol. Dis.* 33, 369–378. doi: 10.1016/j.nbd.2008.11.005

Spires-Jones, T. L., Friedman, T., Pitstick, R., Polydoro, M., Roe, A., Carlson, G. A., et al. (2014). Methylene blue does not reverse existing neurofibrillary tangle pathology in the rTg4510 mouse model of tauopathy. *Neurosci. Lett.* 562, 63–68. doi: 10.1016/j.neulet.2014.01.013

Spires-Jones, T. L., and Hyman, B. T. (2014). The intersection of amyloid β and tau at synapses in Alzheimer's disease. *Neuron* 82, 756–771. doi: 10.1016/j.neuron.2014.05.004

Stavraka, C., and Blagden, S. (2015). The La-related proteins, a family with connections to cancer. *Biomolecules* 5, 2701–2722. doi: 10.3390/biom5042701

Steffan, J. S., Agrawal, N., Pallos, J., Rockabrand, E., Trotman, L. C., Slepko, N., et al. (2004). SUMO modification of Huntingtin and Huntington's disease pathology. *Science* 304, 100–104. doi: 10.1126/science.1092194

Subramaniam, S., Sixt, K. M., Barrow, R., and Snyder, S. H. (2009). Rhes, a striatal specific protein, mediates mutant-huntingtin cytotoxicity. *Science* 324, 1327–1330. doi: 10.1126/science.1172871

Südhof, T. C. (2013). Neurotransmitter release: the last millisecond in the life of a synaptic vesicle. *Neuron* 80, 675–690. doi: 10.1016/j.neuron.2013.10.022

Südhof, T. C., and Rizo, J. (2011). Synaptic vesicle exocytosis. *Cold Spring Harb. Perspect. Biol.* 3:a005637. doi: 10.1101/cshperspect.a005637

Tai, D. J., Liu, Y. C., Hsu, W. L., Ma, Y. L., Cheng, S. J., Liu, S. Y., et al. (2016). MeCP2 SUMOylation rescues Mecp2-mutant-induced behavioural deficits in a mouse model of rett syndrome. *Nat. Commun.* 7:10552. doi: 10.1038/ncomms10552

Tai, H. C., Serrano-Pozo, A., Hashimoto, T., Frosch, M. P., Spires-Jones, T. L., and Hyman, B. T. (2012). The synaptic accumulation of hyperphosphorylated tau oligomers in Alzheimer's disease is associated with dysfunction of the ubiquitin-proteasome system. *Am. J. Pathol.* 181, 1426–1435. doi: 10.1016/j.ajpath.2012.06.033

Takahashi, K., Ishida, M., Komano, H., and Takahashi, H. (2008). SUMO-1 immunoreactivity co-localizes with phospho-Tau in APP transgenic mice but not in mutant Tau transgenic mice. *Neurosci. Lett.* 441, 90–93. doi: 10.1016/j.neulet.2008.06.012

Tang, L. T., Craig, T. J., and Henley, J. M. (2015). SUMOylation of synapsin Ia maintains synaptic vesicle availability and is reduced in an autism mutation. *Nat. Commun.* 6:7728. doi: 10.1038/ncomms8728

Tang, Z., El Far, O., Betz, H., and Scheschonka, A. (2005). Pias1 interaction and sumoylation of metabotropic glutamate receptor 8. *J. Biol. Chem.* 280, 38153–38159. doi: 10.1074/jbc.m508168200

Tao, X., and Tong, L. (2003). Crystal structure of human DJ-1, a protein associated with early onset Parkinson's disease. *J. Biol. Chem.* 278, 31372–31379. doi: 10.1074/jbc.m304221200

Tirard, M., Hsiao, H. H., Nikolov, M., Urlaub, H., Melchior, F., and Brose, N. (2012). *In vivo* localization and identification of SUMOylated proteins in the brain of His6-HA-SUMO1 knock-in mice. *Proc. Natl. Acad. Sci. U S A* 109, 21122–21127. doi: 10.1073/pnas.1215366110

Turrigiano, G. G. (2008). The self-tuning neuron: synaptic scaling of excitatory synapses. *Cell* 135, 422–435. doi: 10.1016/j.cell.2008.10.008

Um, J. W., and Chung, K. C. (2006). Functional modulation of parkin through physical interaction with SUMO-1. *J. Neurosci. Res.* 84, 1543–1554. doi: 10.1002/jnr.21041

Usami, Y., Hatano, T., Imai, S., Kubo, S., Sato, S., Saiki, S., et al. (2011). DJ-1 associates with synaptic membranes. *Neurobiol. Dis.* 43, 651–662. doi: 10.1016/j.nbd.2011.05.014

Usui, N., Co, M., Harper, M., Rieger, M. A., Dougherty, J. D., and Konopka, G. (2016). Sumoylation of FOXP2 regulates motor function and vocal communication through Purkinje cell development. *Biol. Psychiatry* doi: 10.1016/j.biopsych.2016.02.008 [Epub ahead of print].

van Niekerk, E. A., Willis, D. E., Chang, J. H., Reumann, K., Heise, T., and Twiss, J. L. (2007). Sumoylation in axons triggers retrograde transport of the RNA-binding protein La. *Proc. Natl. Acad. Sci. U S A* 104, 12913–12918. doi: 10.1073/pnas.0611562104

van Spronsen, M., and Hoogenraad, C. C. (2010). Synapse pathology in psychiatric and neurologic disease. *Curr. Neurol. Neurosci. Rep.* 10, 207–214. doi: 10.1007/s11910-010-0104-8

Velier, J., Kim, M., Schwarz, C., Kim, T. W., Sapp, E., Chase, K., et al. (1998). Wild-type and mutant huntingtins function in vesicle trafficking in the secretory and endocytic pathways. *Exp. Neurol.* 152, 34–40. doi: 10.1006/exnr.1998.6832

Vijayakumaran, S., Wong, M. B., Antony, H., and Pountney, D. L. (2015). Direct and/or indirect roles for SUMO in modulating α-synuclein toxicity. *Biomolecules* 5, 1697–1716. doi: 10.3390/biom5031697

Wang, Y., Chandran, J. S., Cai, H., and Mattson, M. P. (2008). DJ-1 is essential for long-term depression at hippocampal CA1 synapses. *Neuromolecular Med.* 10, 40–45. doi: 10.1007/s12017-008-8023-4

Wang, L., Ma, Q., Yang, W., Mackensen, G. B., and Paschen, W. (2012). Moderate hypothermia induces marked increase in levels and nuclear accumulation of SUMO2/3-conjugated proteins in neurons. *J. Neurochem.* 123, 349–359. doi: 10.1111/j.1471-4159.2012.07916.x

Wang, L., Wansleeben, C., Zhao, S., Miao, P., Paschen, W., and Yang, W. (2014). SUMO2 is essential while SUMO3 is dispensable for mouse embryonic development. *EMBO Rep.* 15, 878–885. doi: 10.15252/embr.201438534

Watanabe, Y., Katayama, N., Takeuchi, K., Togano, T., Itoh, R., Sato, M., et al. (2013). Point mutation in syntaxin-1A causes abnormal vesicle recycling, behaviors and short term plasticity. *J. Biol. Chem.* 288, 34906–34919. doi: 10.1074/jbc.M113.504050

Watanabe, M., Takahashi, K., Tomizawa, K., Mizusawa, H., and Takahashi, H. (2008). Developmental regulation of Ubc9 in the rat nervous system. *Acta Biochim. Pol.* 55, 681–686.

Weeraratna, A. T., Kalehua, A., Deleon, I., Bertak, D., Maher, G., Wade, M. S., et al. (2007). Alterations in immunological and neurological gene expression patterns in Alzheimer's disease tissues. *Exp. Cell Res.* 313, 450–461. doi: 10.1016/j.yexcr.2006.10.028

Wilhelm, B. G., Mandad, S., Truckenbrodt, S., Kröhnert, K., Schafer, C., Rammner, B., et al. (2014). Composition of isolated synaptic boutons reveals the amounts of vesicle trafficking proteins. *Science* 344, 1023–1028. doi: 10.1126/science.1252884

Wilkinson, K. A., and Henley, J. M. (2011). Analysis of metabotropic glutamate receptor 7 as a potential substrate for SUMOylation. *Neurosci. Lett.* 491, 181–186. doi: 10.1016/j.neulet.2011.01.032

Wilkinson, K. A., Nishimune, A., and Henley, J. M. (2008). Analysis of SUMO-1 modification of neuronal proteins containing consensus SUMOylation motifs. *Neurosci. Lett.* 436, 239–244. doi: 10.1016/j.neulet.2008.03.029

Winner, B., Jappelli, R., Maji, S. K., Desplats, P. A., Boyer, L., Aigner, S., et al. (2011). *In vivo* demonstration that α-synuclein oligomers are toxic. *Proc. Natl. Acad. Sci. U S A* 108, 4194–4199. doi: 10.1073/pnas.1100976108

Wu, H., Chen, X., Cheng, J., and Qi, Y. (2016). SUMOylation and potassium channels: links to epilepsy and sudden death. *Adv. Protein Chem. Struct. Biol.* 103, 295–321. doi: 10.1016/bs.apcsb.2015.11.009

Yamada, T., Yang, Y., Huang, J., Coppola, G., Geschwind, D. H., and Bonni, A. (2013). Sumoylated MEF2A coordinately eliminates orphan presynaptic sites and promotes maturation of presynaptic boutons. *J. Neurosci.* 33, 4726–4740. doi: 10.1523/JNEUROSCI.4191-12.2013

Yin, Y., She, H., Li, W., Yang, Q., Guo, S., and Mao, Z. (2012). Modulation of neuronal survival factor MEF2 by kinases in Parkinson's disease. *Front. Physiol.* 3:171. doi: 10.3389/fphys.2012.00171

Yokoi, N., Fukata, M., and Fukata, Y. (2012). Synaptic plasticity regulated by protein-protein interactions and posttranslational modifications. *Int. Rev. Cell Mol. Biol.* 297, 1–43. doi: 10.1016/b978-0-12-394308-8.00001-7

Yun, S. M., Cho, S. J., Song, J. C., Song, S. Y., Jo, S. A., Jo, C., et al. (2013). SUMO1 modulates Aβ generation via BACE1 accumulation. *Neurobiol. Aging* 34, 650–662. doi: 10.1016/j.neurobiolaging.2012.08.005

Zeitlin, S., Liu, J. P., Chapman, D. L., Papaioannou, V. E., and Efstratiadis, A. (1995). Increased apoptosis and early embryonic lethality in mice nullizygous for the Huntington's disease gene homologue. *Nat. Genet.* 11, 155–163. doi: 10.1038/ng1095-155

Zhang, Y. Q., and Sarge, K. D. (2008). Sumoylation of amyloid precursor protein negatively regulates Aβ aggregate levels. *Biochem. Biophys. Res. Commun.* 374, 673–678. doi: 10.1016/j.bbrc.2008.07.109

Zhao, X., Sternsdorf, T., Bolger, T. A., Evans, R. M., and Yao, T. P. (2005). Regulation of MEF2 by histone deacetylase 4- and SIRT1 deacetylase-mediated lysine modifications. *Mol. Cell. Biol.* 25, 8456–8464. doi: 10.1128/mcb.25.19.8456-8464.2005

Zhu, Q. J., Xu, Y., Du, C. P., and Hou, X. Y. (2012). SUMOylation of the kainate receptor subunit GluK2 contributes to the activation of the MLK3-JNK3 pathway following kainate stimulation. *FEBS Lett.* 586, 1259–1264. doi: 10.1016/j.febslet.2012.03.048

Zuberi, S. M., Eunson, L. H., Spauschus, A., De Silva, R., Tolmie, J., Wood, N. W., et al. (1999). A novel mutation in the human voltage-gated potassium channel gene (Kv1.1) associates with episodic ataxia type 1 and sometimes with partial epilepsy. *Brain* 122, 817–825. doi: 10.1093/brain/122.5.817

Conflict of Interest Statement: The authors declare that the research was conducted in the absence of any commercial or financial relationships that could be construed as a potential conflict of interest.

ARTICLE 2

Sumoylation regulates FMRP-mediated dendritic spine elimination and maturation

(Accepted for publication by Nature Communications in January 2018)

Anouar Khayachi[1,#], Carole Gwizdek[1,#], Gwénola Poupon[1], Damien Alcor[2], Magda Chafai[1], Frédéric Cassé[1], Thomas Maurin[1], Marta Prieto[1], Alessandra Folci[1], Fabienne De Graeve[3], Sara Castagnola[1], Romain Gautier[1], **Lenka Schorova**[1], Céline Loriol[1], Marie Pronot[1], Florence Besse[3], Frédéric Brau[1], Emmanuel Deval[1], Barbara Bardoni[4] and Stéphane Martin[4]

[1] Université Côte d'Azur, CNRS, IPMC, 06560, France.
[2] Université Côte d'Azur, INSERM, C3M, 06200, France.
[3] Université Côte d'Azur, CNRS, INSERM, iBV, 06108, France.
[4] Université Côte d'Azur, INSERM, CNRS, IPMC, 06560 France.
[#] Equal contribution

Fragile X syndrome (FXS) is the most frequent cause of inherited intellectual disability and the best-understood single monogenic cause of autism. The functional absence of the Fragile X Mental Retardation Protein (FMRP), a component of mRNA granules that is centrally involved in RNA transport along neurites and local synaptic translation, leads to FXS. The precise regulatory mechanisms driving FMRP functions are still poorly understood and a matter of extensive debates. We report that FMRP is a sumoylation substrate *in vivo*. Using a combination of molecular biology, biochemical and advanced imaging-based approaches, we show that neuronal sumoylation of FMRP is rapidly triggered by the activation of mGlu5 receptors. We also demonstrate that FMRP sumoylation is essential to post-synaptic maturation as well as the regulation of spine frequency. We suggest that the underlying mechanism likely involves the SUMO-dependent regulation of FMRP-FMRP interactions within mRNA granules along dendrites. Importantly, the findings presented in this report provide a better understanding of the molecular pathways regulating FMRP function and we anticipate that it may lead to formulation of novel hypotheses for the design of future therapeutic approaches of FXS.

I directly participated in this study by performing some preliminary imaging experiments of FMRP mRNA granules in dendrites. I further helped with preparation of primary mouse hippocampal and mixed cultures. And finally I participated in the manuscript writing process.

Sumoylation regulates FMRP-mediated dendritic spine elimination and maturation

Anouar Khayachi[1,#], Carole Gwizdek[1,#], Gwénola Poupon[1], Damien Alcor[2], Magda Chafai[1], Frédéric Cassé[1], Thomas Maurin[1], Marta Prieto[1], Alessandra Folci[1], Fabienne De Graeve[3], Sara Castagnola[1], Romain Gautier[1], Lenka Schorova[1], Céline Loriol[1], Marie Pronot[1], Florence Besse[3], Frédéric Brau[1], Emmanuel Deval[1], Barbara Bardoni[4] and Stéphane Martin[4*]

[1] Université Côte d'Azur, CNRS, IPMC, 06560, France.

[2] Université Côte d'Azur, INSERM, C3M, 06200, France.

[3] Université Côte d'Azur, CNRS, INSERM, iBV, 06108, France.

[4] Université Côte d'Azur, INSERM, CNRS, IPMC, 06560 France.

*Correspondence: Stéphane Martin (martin@ipmc.cnrs.fr)

Institut de Pharmacologie Moléculaire et Cellulaire, Centre National de la Recherche Scientifique, UMR7275, 660 route des lucioles, 06560 Valbonne, France

Phone: (33) 49395-3461; Fax: (33) 49395-7708

# Equal contribution

Abstract

Fragile X syndrome (FXS) is the most frequent inherited cause of intellectual disability and the best-studied monogenic cause of autism. FXS results from the functional absence of the Fragile X Mental Retardation Protein (FMRP) leading to abnormal pruning and consequently to synaptic communication defects. Here we show that FMRP is a substrate of the Small Ubiquitin-like MOdifier (SUMO) pathway in the brain and identify its active SUMO sites. We unravel the functional consequences of FMRP sumoylation in neurons by combining molecular replacement strategy, biochemical reconstitution assays with advanced live-cell imaging. We first demonstrate that FMRP sumoylation is promoted by activation of metabotropic glutamate receptors. We then show that this increase in sumoylation controls the homomerization of FMRP within dendritic mRNA-granules which, in turn, regulates spine elimination and maturation. Altogether, our findings reveal the sumoylation of FMRP as a critical activity-dependent regulatory mechanism of FMRP-mediated neuronal function.

Introduction

In neurons, mRNA targeting to synapses and local synthesis of synaptic proteins are tightly regulated. Indeed, dysregulation of such processes leads to structural synaptic abnormalities and consequently to neurological disorders[1] classified as synaptopathies[2]. Among them, the Fragile X Syndrome (FXS) is the most frequent form of inherited intellectual disablility (ID) and a leading monogenic cause of autism with the prevalence of 1:4000 males and 1:7000 females. FXS results from mutations within the *FMR1* gene causing the loss of function of the RNA-binding protein FMRP. Localization studies revealed that FMRP is highly expressed in the Central Nervous System (CNS). FMRP binds a large subset of mRNAs in the mammalian brain and is a key component of RNA granules. These granules transport mRNA along axons and dendrites and are targeted to the base of active synapses to regulate local translation in an activity-dependent manner[3, 4, 5]. Therefore, the transport and the subsequent regulation of local translation are critical processes to brain development as they play essential roles in stabilizing and maturing synapses[3, 4]. According the role of FMRP in regulating translation at synapses, the loss of FMRP function in FXS leads to a patholological hyper-abundance of long thin immature dendritic protrusions called filopodia[6, 7]. These structural defects result from an abnormal post-synaptic maturation and/or a failure in the synapse elimination process[8]. An increased number of immature spines associated with severe changes in synaptic transmission and plasticity as well as in social and cognitive behaviours have also been reported in *Fmr1* knock-out (*Fmr1*$^{-/y}$) mouse models for FXS[4, 9, 10].

The majority of FMRP-containing mRNA granules localizes at the base of dendritic spines[3, 4]. Neuronal activation leads to the release of mRNAs from dendritic granules and their local translation at synapses (for a review, see[5]). Importantly, this activity-dependent process requires a tight spatiotemporal regulation involving many protein-protein interactions. Such a

regulation is mainly governed by post-translational modifications (PTMs). Previous reports have shown that FMRP function is regulated by phosphorylation, which inhibits translation of its associated mRNAs, whereas dephosphorylation of FMRP promotes their translation[11, 12]. Activation of metabotropic Glutamate Receptor 5 (mGlu5R) induces dephosphorylation of FMRP and its subsequent ubiquitination which ultimately leads to FMRP degradation via the ubiquitin-proteasome pathway[13, 14]. Thus, a deeper comprehension of the activity-dependent molecular mechanisms controlling FMRP is absolutely criticial to understanding the functional regulation of FMRP-mediated mRNA transport and local protein synthesis in physiological and pathological conditions, including FXS.

Sumoylation is a post-translational modification involved in many cellular signalling pathways. It consists in the covalent enzymatic conjugation of the Small Ubiquitin-like MOdifier (SUMO) protein to specific lysine residues of substrate proteins[15, 16]. The sumoylation process requires a dedicated enzymatic pathway[17, 18, 19]. SUMO paralogs (~100 amino acids; ~11 kDa) are conjugated to its substrates via the action of the E2-conjugating enzyme Ubc9. Sumoylation is a reversible process due to the activity of specific desumoylation enzymes called Sentrin-proteases (SENPs[20]). At the molecular level, sumoylation can modulate the dynamics of multi-protein complexes by preventing protein-protein interactions and/or by providing new binding sites for novel interactors[21, 22].

Sumoylation regulates a wide range of neurodevelopmental processes[18, 19, 23]. For instance, our group has demonstrated the spatiotemporal regulation of the SUMO system in the developing rat brain[24] and that sumoylation is regulated by neuronal activity[25] and the activation of mGlu5R[25, 26]. Sumoylation also influences various aspects of the neuronal function including neurotransmitter release[27, 28], spinogenesis[29, 30] and synaptic communication[31, 32, 33].

Here, we report that FMRP is a novel sumoylation substrate in neurons. We demonstrate that FMRP sumoylation is absolutely essential to maintaining the shape of mRNA granules in dendrites and to controlling both the spine density and maturation. We identify the active SUMO sites on FMRP and show that activation of mGlu5R rapidly induces FMRP sumoylation triggering the dissociation of FMRP from dendritic RNA granules to allow for local translation. Altogether, our findings shed light on sumoylation as an essential activity-dependent mechanism that tunes spine elimination and maturation in the mammalian brain.

Results

FMRP is sumoylated *in vivo*

Given the critical importance of FMRP in brain development and maturation, it is of particular interest to understand the molecular mechanisms regulating FMRP function. Thus, we investigated whether FMRP is subjected to sumoylation. To this end, we performed immunoblot analyses and control assays using several commercial as well as in-house anti-FMRP and anti-SUMO1 antibodies on rodent brain homogenates (**Fig. 1**; **Supplementary Fig. 1**). We first analyzed rat brain homogenates in absence or presence of NEM *(N-Ethyl Maleimide)* which protects proteins from desumoylation during the lysis process[31] (**Fig. 1a; Supplementary Fig. 1f**). FMRP is detected as isoforms ranging from 70 to 90 kDa. Interestingly, we found a higher molecular weight band at ~120 kDa that was detected only in the presence of NEM (**Fig. 1a**, Total lane). The densitometric analysis of the ratio between the sumoylated form of FMRP and the total level of FMRP in NEM-treated input lanes revealed that there is about 4% of sumoylated FMRP in all the conditions tested (**Supplementary Fig. 1c**). We confirmed the upper band to be the sumoylated form of FMRP by immunoprecipitation experiments with specific anti-FMRP antibodies and anti-SUMO1 immunoblot (**Fig. 1b**) or

with the converse experiment using anti-SUMO1 immunoprecipitation and anti-FMRP immunoblot (**Fig. 1c**). We also validated the sumoylation of FMRP in wild-type (WT) mouse brain homogenates (**Fig. 1d**). Accordingly, we were also able to co-immunoprecipitate the sole SUMO-conjugating enzyme Ubc9 from mouse brain homogenates using anti-FMRP antibodies (**Fig. 1e**). We further validated the sumoylation of FMRP *in vivo* using several combinations of FMRP/SUMO1 antibodies (**Supplementary Fig. 1d,e; g-j**) or in cultured neurons (**Supplementary Fig. 1k-n**). Immunolabeling experiments (**Fig. 1f**) showed that FMRP partially colocalizes with Ubc9 and SUMO1 in dendrites of mouse hippocampal neurons, providing further evidence of the interplay between FMRP and the SUMO pathway.

Sumoylation consists in the covalent binding of the SUMO moiety to a lysine residue of the consensus sequence on the substrate protein (Ψ**K**xD/E, where Ψ is a large hydrophobic residue, **K** is the target lysine, x can be any residue, and D/E are aspartate or glutamate[34]). To identify lysine residues in FMRP potentially targeted by the sumoylation system, we used SUMO-prediction softwares to analyze the primary sequence of FMRP and then alignment tools to assess whether these potential sites are evolutionary conserved across species (**Fig. 1g**). We identified three conserved residues, two proximal (K88, K130) and one distal (K614) lysines as putative targets of the SUMO system. To validate whether these lysine residues could be sumoylated, we performed site-directed mutagenesis combined with bacterial sumoylation assays[31, 35] (**Fig. 1h-i**). We demonstrated that FMRP sumoylation occurs at these residues (K88, K130, K614) and showed that their mutation into arginine residues (K-to-R mutation) abolishes the sumoylation of FMRP (**Fig. 1h,i**). We confirmed these data using sumoylation assays in mammalian COS7 cells in which the expression of the FMRP-K88,130,614R mutant prevents the sumoylation of FMRP (**Fig. 1j**). Consistent with the sumoylation of FMRP in the brain and according to our FMRP-SUMO1 models which were

computed using crystal structures available for the N-terminal part of FMRP, both lysine residues (K88 and K130) are clearly exposed and accessible to sumoylation with a Solvent Accessible Surface Area (ASA) of ~70% and ~45% respectively **(Fig. 1k,l)**. We therefore conclude that FMRP is a SUMO substrate *in vivo* and that its sumoylation can occur at its N-terminal K88 and K130 and C-terminal K614 residues.

FMRP sumoylation participates in dendritic spine regulation

FMRP is essential to proper spine stabilization and maturation[3, 4]. In FXS patients, the lack of functional FMRP leads to an immature neuronal morphology with a characteristic excess of abnormally long and thin filopodia[36]. Similar morphological defects are also present in *Fmr1*$^{-/y}$ mouse brains[37]. Thus, we hypothesized that FMRP sumoylation could be critical in maintaining the density and the maturation of dendritic spines. To address this point, we used attenuated Sindbis particles[38, 39, 40] to express either free GFP, the WT GFP-FMRP, the N-terminal K88,130R, C-terminal K614R or non-sumoylatable K88,130,614R GFP-FMRP mutants in cultured *Fmr1*$^{-/y}$ neurons at 17 days *in vitro* (17 DIV). We then analyzed and compared the morphology of dendritic spines 24h post-transduction (**Fig. 2a,b**). In GFP-expressing *Fmr1*$^{-/y}$ neurons, ~60% of protrusions showed an immature phenotype (*See the Methods section for the spine characterization;* **Fig. 2a,b**). Conversely, the expression of either FMRP WT or the K614R GFP-FMRP mutant, which behaves as the WT, promoted spine maturation (**Fig. 2a,b**). In stark contrast, expressing either the N-terminal K88,130R or the non-sumoylatable K88,130,614R GFP-FMRP mutant failed to promote spine maturation (**Fig. 2a,b**).

The excess of dendritic protrusions in neurons is a hallmark of FXS[6, 7]. Interestingly, the density of the protrusions was considerably decreased upon the expression of the WT or K614R mutant form of GFP-FMRP (**Fig. 2c**; GFP control, 7.22 ± 0.16 protrusions/10μm; GFP-FMRP

WT, 5.34 ± 0.13 protrusions/10μm; GFP-FMRP-K614R, 5.39 ± 0.13 protrusions/10μm) whereas expressing either the N-terminal K130R, the K88,130R GFP-FMRP mutants or the non-sumoylatable GFP-FMRP-K88,130,614R did not affect the spine density with measured values almost identical to control neurons expressing free GFP (**Fig. 2c**). Furthermore, re-expressing WT GFP-FMRP in *Fmr1*$^{-/y}$ neurons not only affected the spine number but also drastically reduced the mean length of immature spines from ~3.7 μm to less than 2.6 μm (**Fig. 2d**).

To individually assess the role of the N-terminal lysine residue, we quantified the morphological changes occuring in *Fmr1*$^{-/y}$ neurons expressing GFP-FMRP with a single mutated lysine residue (K88R or K130R; **Supplementary Fig. 2**). While the expression of both mutants promoted spine maturation similarly to GFP-FMRP WT **(Supplementary Fig. 2b,d)**, the K130R mutant failed to reduce the density of the protrusions (**Supplementary Fig. 2c**; GFP control, 7.22 ± 0.16 protrusions/10μm; WT, 5.34 ± 0.13 protrusions/10μm; K130R, 6.48 ± 0.15 protrusions/10μm) indicating that the integrity of the K130 residue is essential to maintain spine density. Altogether, the data above indicate that the integrity of both N-terminal lysine residues is critical for the regulation of spine density and maturation since the expression of the K-to-R mutant forms failed to restore the density and the maturity of dendritic spines in *Fmr1*$^{-/y}$ neurons. Our initial findings therefore support the role of the N-terminal sumoylation of FMRP in the regulation of spine elimination and maturation events.

To start assessing the functional effect of FMRP sumoylation, we compared synaptic transmission by measuring spontaneous miniature Excitatory PostSynaptic Currents (mEPSCs) in *Fmr1*$^{-/y}$ neurons expressing either GFP-FMRP **WT** or its non-sumoylatable **K88,130,614R** mutant (**Supplementary Fig. 3**). The comparison of cumulative distributions indicated that the

amplitude of mEPSCs (from 20 to 40 pA) was significantly increased in neurons expressing the mutant form of GFP-FMRP (**Supplementary Fig. 3a,b**). Moreover, intervals between mEPSC events (between 300 ms and 1 s) were slightly but significantly increased upon expression of GFP-FMRP-**K88,130,614R** when compared to GFP-FMRP **WT** indicating that the mEPSC frequency is decreased in mutant-expressing cells (**Supplementary Fig. 3a,c**). Data comparing mEPSC properties in WT and *Fmr1*$^{-/y}$ brain slices have been described in the literature with either a decrease, an increase or no changes in their amplitudes or frequencies, depending on the brain area recorded, the age of the animals and/or the associated genetic background [41, 42, 43]. To our knowledge, there are no available data on mEPSCs recorded from FMRP **WT**-expressing *Fmr1*$^{-/y}$ cultured hippocampal neurons and the results from **Supplementary fig. 3** indicate that restoring the expression of FMRP in *Fmr1*$^{-/y}$ neurons leads to changes in basal synaptic transmission, occurring most probably via both pre- and post-synaptic modifications. Additional experiments are now needed to precisely define the associated mechanisms and to address the electrophysiological consequences of FMRP sumoylation in synaptic plasticity *in vivo*.

Preventing FMRP sumoylation alters the size of mRNA granules

Since FMRP is an RNA-binding protein, we also examined whether the mutation of the sumoylation sites interferes with the RNA-binding capacity of FMRP by performing Cross-Linking and ImmunoPrecipitation (CLIP) assays (**Fig. 2e,f**). FMRP-CLIPed mRNAs from *Fmr1*$^{-/y}$ neurons expressing either the WT or K88,130,614R forms of GFP-FMRP were analyzed by qPCR to compare the abundance of some known FMRP target mRNAs (**Fig. 2e**). Our data showed that either forms of GFP-FMRP are able to bind target RNAs to similar extent (**Fig. 2f**).

Since preventing FMRP sumoylation with the K-to-R mutations does not affect the ability of FMRP to interact with its target RNAs, we hypothesized that FMRP sumoylation is involved in the transport of mRNAs along dendrites. To this purpose, we first examined the FMRP-containing granules along dendrites. We transfected *Fmr1*$^{-/y}$ neurons to express either the WT or K88,130R form of GFP-FMRP and performed smFISH experiments using Stellaris probes complementary to three known FMRP mRNA targets: GFP (for GFP-FMRP), PSD-95[44] and CaMKII mRNAs (**Fig. 3a-c**). Interestingly, the fluorescence of all three probe sets was detectable in GFP-positive granules from secondary dendrites containing either the WT or mutant K88,130R form of GFP-FMRP (**Fig. 3a-c**). Together with the CLIP experiments (**Fig. 2e,f**), this reveals that both WT and K88,130R GFP-FMRP-containing granules can travel along dendrites, carrying their mRNA cargoes.

We further characterized these mRNA granules using colocalisation assays to investigate whether known components of such granules[45, 46] are also present in WT and K88,130R-GFP-FMRP positive granules. As clearly depicted in **Fig. 3d-g**, both the WT and K88,130R GFP-FMRP granules colocalise with the ribosomal protein S6 (**Fig. 3d**) and the RNA binding proteins FXR1 (**Fig. 3e**), Staufen 1 (**Fig. 3f**) and Staufen 2 (**Fig. 3g**), indicating that these granules contain not only some of the target mRNAs of FMRP (**Fig. 3a-c**) but also several described components of such dendritic mRNA granules[45, 46].

We then measured the surface of dendritic GFP-FMRP-positive mRNA granules at different time points post-transfection (**Fig. 3h,i**). Interestingly, the expression of the K88,130R GFP-FMRP for 48 hours significantly increased the size of FMRP-containing granules compared to the WT GFP-FMRP-positive granules (**Fig. 3i**; WT 48h, 0.236 ± 0.017 μm^2; K88,130R 48h, 0.305 ± 0.020 μm^2). The difference in granule size between the WT and the K88,130R form of

GFP-FMRP was further enhanced after 72h of transfection (**Fig. 3i**; WT 72h, 0.265 ± 0.020 μm^2; K88,130R 72h, 0.440 ± 0.030 μm^2). All these data reveal that the expression of GFP-FMRP K88,130R results in larger FMRP-containing dendritic mRNA granules suggesting that FMRP sumoylation could participate in the regulation of FMRP interactions within these granules.

FMRP has been reported to form homodimers via its N-terminal 1-134 domain[47], where the sumoylatable K88 and K130 residues are localized. Thus, to assess whether the difference in granule size measured in figure **3i** results from abnormal interaction properties of FMRP homodimers directly inside dendritic granules, we performed Fluorescence Lifetime Imaging Microscopy (FLIM) experiments on neurons co-expressing WT or K88,130R GFP-FMRP with their respective WT or K88,130R mCherry-tagged constructs (**Fig. 4**; **Supplementary Fig. 4**). We observed a clear colocalisation of the mCherry/GFP-FMRP constructs in dendritic granules confirming the incorporation of the proteins into granules (**Fig. 4a,b**). The energy transfer known as Fluorescence Resonance Energy Transfer (FRET) from donor GFP towards the acceptor mCherry is quantified by the reduction of the donor fluorescence lifetime (**Fig. 4c**). We measured a significant reduction of the donor GFP-FMRP fluorescence lifetime in presence of mCherry-FMRP indicating that FMRP/FMRP interaction occurs in dendritic granules. Interestingly, we also found that this homomeric interaction is not affected by the K88,130R mutations (**Fig. 4c**).

Sumoylation triggers FMRP dissociation from mRNA granules

Our results so far indicate that preventing FMRP sumoylation directly impacts on the morphology of mRNA granules in dendrites (**Fig. 3h,i**) without altering the intrinsic FMRP/FMRP interacting properties within the granules (**Fig. 4**). Therefore, we investigated

whether the absence of FMRP sumoylation affects the dissociation of FMRP from dendritic granules. To assess the diffusion properties of FMRP in dendritic granules, we performed live-time restricted photoconversion experiments[48] in *Fmr1*$^{-/y}$ neurons expressing the photoswitchable WT or K88,130R Dendra2-FMRP constructs (**Fig. 5a,b**). Dendra2 is a green-to-red photoactivatable fluorescent protein that allows the real-time tracking of a photoconverted protein[49, 50]. We measured and compared the half-times of the decrease in red photoconverted fluorescence, which corresponds to the real time diffusion of WT and K88,130R Dendra2-FMRP out of dendritic granules (**Fig. 5b-d**). In basal conditions, the mean half-time of Dendra2-FMRP **WT** fluorescence dissociation from dendritic granules was significantly shorter than the value measured for the Dendra2-FMRP K88,130R mutant (**Fig. 5d**; Half time WT = 101.8 ± 4.5s *vs* Half time K88,130R = 165.3 ± 12.1s) indicating that the dissociation of WT FMRP from the granules is much faster than for the K88,130R mutant. These data strongly support the involvement of FMRP sumoylation in controlling the dissociation of the protein from dendritic mRNA granules.

Activation of mGlu5R regulates FMRP-mediated mRNA transport[51, 52] and also modulates its phosphorylation and ubiquitination[13, 14]. Interestingly, we previously showed that activation of these receptors also evokes sumoylation in cultured neurons[26]. This prompted us to assess whether the application of the mGluR agonist DHPG triggers FMRP sumoylation in neurons (**Fig. 5e**). We first confirmed that the activation of mGlu5R with DHPG is effective in our neuronal cultures and evokes an intracellular Calcium increase (**Supplementary Fig. 5**). Then, FMRP-immunoprecipitates were probed with specific anti-SUMO1 antibodies and revealed that sumoylation of FMRP is low in basal unstimulated conditions but rapidly increases after 1 and 5 min of DHPG treatment (DHPG 1 min, 1.28 ±0.12 fold/control; DHPG 5 min, 1.73 ± 0.2

fold/control; **Fig. 5e**) indicating that FMRP sumoylation is rapidly triggered by the mGlu5R activation.

These results led us to hypothesize that the activity-dependent sumoylation of FMRP controls FMRP dissociation from dendritic mRNA granules. To address this point, we pharmacologically stimulated mGlu5R in *Fmr1*$^{-/y}$ neurons expressing either Dendra2-FMRP WT or K88,130R and measured the dissociation properties of FMRP from dendritic granules using the photoconversion assay (**Fig. 5f,g**). Interestingly, mGlu5R stimulation enhanced the exit rate of the red photoconverted Dendra2-FMRP WT fluorescence from granules by ~40% (**Fig. 5f**). By contrast, mGlu5R activation had no effect on the dissociation of Dendra2-FMRP-K88,130R positive granules (**Fig. 5g**). These findings strongly support that the mGlu5R-dependent sumoylation of FMRP regulates the dissociation of FMRP from dendritic mRNA granules.

Sumoylation regulates homomeric FMRP-FMRP interaction

Our data demonstrate that FMRP sumoylation controls FMRP release from dendritic granules. To further assess the role of sumoylation in the regulation of FMRP-FMRP interaction, we combined pull-down assays with *in vitro* SUMO reactions and analyzed the impact of sumoylation on the dissociation of FMRP homomers (**Fig. 6**).

We purified GST- and His-tagged FMRP (1-160aa) fusion proteins and found that GST-FMRP(1-160) specifically interacts with His-FMRP(1-160aa) and forms N-terminal FMRP homodimers *in vitro* (**Fig. 6a**). We then performed an *in vitro* sumoylation assay[31] on purified FMRP(1-160aa) dimers to assess whether sumoylation promotes their dissociation (**Fig. 6b-d**). First, we verified that the immobilization of GST-FMRP(1-160aa) on the glutathione matrix

did not prevent the *in vitro* sumoylation of the protein (**Fig. 6c**). Incubation of immobilized GST-FMRP(1-160aa) with the sumoylation reaction mix gave rise to higher molecular weight bands corresponding to the sumoylated forms of GST-FMRP(1-160aa). These bands were absent in control conditions (**Fig. 6c**).

Next, we performed *in vitro* sumoylation assays on immobilized GST-FMRP – His-FMRP dimers (**Fig. 6d**). The pool of His-FMRP(1-160aa) released by sumoylation was separated from the remaining immobilized dimers by centrifugation of the glutathion beads. Proteins either in the supernatant or bound to the beads were both analyzed by immunoblotting with anti-FMRP antibodies. As seen in **Fig. 6d**, the release of His-FMRP(1-160aa) from the immobilized dimers was only promoted upon sumoylation with the concurrent decrease of the remaining His-FMRP(1-160aa) in the pelleted FMRP fraction. This particular set of data demonstrates that sumoylation promotes the dissociation of FMRP-FMRP dimers.

SUMO-deficient FMRP-expressing WT neurons show FXS phenotype

Collectively, our data clearly demonstrate that sumoylation of the N-terminal part of FMRP is essential to allow for the dissociation of the protein from dendritic mRNA granules and to promote spine elimination and maturation. To confirm the key involvement of FMRP sumoylation in neuronal maturation events, we hypothesized that the expression of the non-sumoylatable FMRP mutant could reverse the spine density and maturation of WT neurons. Thus, we expressed either the WT or the K88,130R mutant form of GFP-FMRP into WT mouse neurons (**Fig. 7**). WT neurons expressing GFP-FMRP-K88,130R resembled the GFP-expressing *Fmr1*$^{-/y}$ neurons (**Fig. 2**) with more than 67% of protrusions characterized by an immature phenotype (**Fig. 7a,b**). Similarly, the length of dendritic spines in WT neurons

expressing GFP-FMRP-K88,130R was also significantly increased (**Fig. 7c**; K88,130R, 3.77 ± 0.08 μm) comparable to the values measured in *Fmr1*$^{-/y}$ neurons (**Fig. 2d**).

Importantly, the density of dendritic spines was dramatically increased upon the expression of the K88,130R mutant (**Fig. 7a,d**; GFP control, 5.03 ± 0.17 protrusions/10μm; K88,130R, 6.33 ± 0.24 protrusions/10μm), comparable to the values obtained in *Fmr1*$^{-/y}$ neurons (**Fig. 2c**). Interestingly, the expression of the single **K130R** mutant in WT mouse neurons also leads to a significant increase in the density of the protrusions (**Fig. 7a,d**; GFP control, 5.03 ± 0.17 protrusions/10μm; **K130R**, 6.29 ± 0.41 protrusions/10μm) without altering the maturity of dendritic spines (**Fig. 7b,c**). As expected, expressing the WT form of GFP-FMRP in WT neurons did not affect any of the spine characteristics confirming the essential role of FMRP sumoylation in spine elimination and maturation processes.

Discussion

Here, we report for the first time that FMRP is a sumoylation target *in vivo*. We identify three sumoylatable residues, two of which lay within the N-terminal domain of FMRP and are the active SUMO sites. We further find that the activation of metabotropic mGlu5R promotes the sumoylation of FMRP and rapidly leads to the dissociation of FMRP from dendritic mRNA granules allowing for the regulation of spine elimination and maturation (**Fig. 7**). Thus, our work uncovers a novel activity-dependent role of sumoylation in the regulation of FMRP neuronal function.

We provide the first evidence that FMRP sumoylation is required for spine elimination and proper maturation. The initial step of spine formation is the emergence of immature long thin protrusions, which are later on eliminated or matured with enlargement of spine head[8]. A tight

balance between these processes is thus required for the development of a functional neuronal network. This is in line with our data showing a decrease in the density of protrusions when expressing FMRP in *Fmr1*$^{-/y}$ neurons, and an increased density in WT neurons expressing the SUMO-deficient form of FMRP. Such compensatory and deleterious effects support the idea that immature spines are overproduced and/or less efficiently eliminated when FMRP sumoylation is perturbed.

In correlation with our findings, the role of sumoylation at the post-synaptic compartment has already been described for several proteins[19]. For instance, sumoylation of the scaffolding calcium/calmodulin-dependent serine protein kinase (CASK) reduces CASK interaction with protein 4.1, a protein that connects spectrin to the actin cytoskeleton in dendritic spines. Mimicking CASK sumoylation dramatically impairs spine formation[53]. According to the importance of sumoylation in the post-synaptic formation and maturation, our findings demonstrate a role of sumoylation in spine elimination and maturation by tuning FMRP dimerization within dendritic mRNA granules. Altogether, these data shed light on the role of sumoylation as a critical molecular regulator in neuronal development and maturation.

Interestingly, we demonstrate that the sumoylation of FMRP is triggered upon mGlu5R activation. mGlu5R has been previously reported to differentially regulate FMRP function depending on its subcellular localization. For instance, a direct involvement of FMRP was shown in targeting and transport of several mRNAs from the soma along dendrites upon mGlu5R activation[52]. Furthermore, the repression of mRNA translation exerted by FMRP in dendrites is counteracted by the activation of mGlu5R[51]. Here, we unravel a novel activity-dependent regulation of the FMRP function. We show that mGlu5R-induced sumoylation of

FMRP drives its own dissociation from dendritic mRNA granules to regulate both spine elimination and maturation.

It has been previously described that FMRP is a target of mGluR-dependent post-translational modifications[11, 13, 14, 54, 55]. Activation of mGluRs in neurons induces a rapid dephosphorylation of FMRP C-terminal region as a result of an enhanced protein phosphatase 2A (PP2A) activity[11]. Conversely, mGluR activation that lasts longer than 5 minutes results in an mTOR-mediated PP2A suppression followed by rapid rephosphorylation of FMRP C-terminus by the ribosomal protein S6 kinase (S6K1)[11, 55]. Accordingly to the role of phosphorylation in controlling FMRP function, the lack of S6K1-dependent FMRP phosphorylation mimics FMRP loss-of-function and leads to an increased expression of the FMRP target mRNA SAPAP3[55]. In addition, Nalavadi and colleagues described a rapid ubiquitination of the C-terminal part of FMRP upon stimulation with the mGlu5R agonist DHPG in rat cultured neurons[14]. FMRP ubiquitination promotes a proteasome-mediated FMRP degradation, which in turn controls FMRP levels at the synapse. Interestingly, these authors showed that FMRP ubiquitination requires a prior FMRP-dephosphorylation carried by PP2A. Taken together, these pieces of evidence suggest a crosstalk between various post-translational modifications in the regulation of FMRP function. Here, we demonstrate that mGlu5R activation triggers a rapid sumoylation of FMRP. This event promotes the release of FMRP from transport mRNA granules. Thus, the present study adds another level of complexity to the post-translational regulation of FMRP and advances our understanding of the activity-dependent control of FMRP function in neurons. It will therefore be of future interest to examine whether the interplay between these post-translational modifications could take place to orchestrate the mGlu5R-dependent regulation of FMRP.

The present study shows that the activation of mGlu5R directly promotes FMRP sumoylation, regulating its neuronal function in spine elimination and maturation. Our work therefore raises the intriguing possibility that the impairment of FMRP sumoylation could contribute to FXS physiopathology. Recent publications have reported missense point mutations within the *FMR1* gene in patients affected by FXS. Importantly, these mutations lead to amino-acid changes close to the SUMO active sites of FMRP (F126S[56], R138Q[57]). Similarly to our data on the K88,130R FMRP mutant, the FXS R138Q mutation does not modify the expression of FMRP nor its RNA-binding properties, indicating that the pathogenicity is caused independently of the FMRP expression level and the ability of FMRP to bind mRNAs[58]. To date, no data have been reported regarding the functional impairment due to the F126S mutation. Our data report that the reintroduction of the FMRP WT but not the K88,130R mutant in *Fmr1*$^{-/y}$ neurons promotes spine maturation and elimination demonstrating that FMRP sumoylation is critical for these processes. Therefore, an interesting possible explanation could be that the F126S and R138Q FXS mutations, which are very close to the active K130-SUMO site, would directly impact on the mGlu5R-dependent regulation of FMRP sumoylation and consequently, on post-synaptic FMRP-driven regulatory events. Future work will have to be performed aiming at understanding the effect of these FXS mutations on FMRP sumoylation. These next exciting steps will allow assessing whether FMRP sumoylation defects participate in the pathophysiology of FXS patients, raising the possibility to identify new targets and potentially develop novel therapeutic approaches.

Methods

Constructs

GFP-FMRP was obtained by subcloning the isoform 1 of the human FMR1 sequence into the EcoR1/Pst1 site of the mammalian expression vector pEGFP-C2 (Clontech). GFP-/Dendra2-/GST-/His-FMRP mutant constructs were all made by site-directed mutagenesis using the Quick-change mutagenesis solution (Agilent). pSinRep5 constructs used to produce Sindbis particles were generated using the Gateway recombination technology (Invitrogen). All constructs were then entirely sequenced.

Building model for FMRP-SUMO1

Three X-ray structures of human FMRP are available in Protein Data Bank (PDB, http://www.rcsb.org; PDB ID: 4OVA residues 1-209 at 3.0Å resolution[59], 4QVZ residues 1-213 at 3.2Å resolution and 4QW2 residues 1-213 with the mutation R138Q at 3.0Å resolution[60]. The Solvent Accessible Surface Area (ASA) values for each residue have been calculated using Naccess tool[61] on all monomers of each PDB files (4 for 4OVA, 2 for 4QVZ and 2 for 4QW2). We calculated the average values for K88 and K130 for each structure. The classical parameters used are 1.4 for the radius of the "solvent" sphere and 25% for the threshold that determines if a residue is considered as buried or exposed. We utilized the X-ray structures of human FMRP PDB ID: 4OVA residues 1-209 at 3.0Å resolution[59] and of human SUMO1 PDB ID: 4WJQ at 1.35Å resolution[62]. To build models of FMRP modified with the SUMO1 protein, we first verified the shape compatibility and then used the Pymol software to manipulate the structures, make and visualize the FMRP-SUMO1 models.

Mouse lines and rat strain

All animals (3 to 10 month-old pregnant female Wistar rats from Janvier, St Berthevin, France; 3 to 10 month-old female C57BL/6 WT and *Fmr1* knockout *(Fmr1*$^{-/y}$*)* mice[10]) were handled in our facility in accordance with the European Council Guidelines for the Care and Use of Laboratory animals and approved by the Animal Care and Ethics Committee *(Comité Institutionnel d'Ethique Pour l'Animal de Laboratoire N°28, Nice, France; Project reference NCE/2012-63)*. All animals had free access to water and food. The light cycle was controlled as 12h light and dark cycle and the temperature was maintained at 23 ± 1°C. Protocols to prepare primary neuronal cultures from mouse embryos at E15.5 or at E18 for rats were also approved by the Animal Care and Ethics Committee *(Comité Institutionnel d'Ethique Pour l'Animal de Laboratoire N°28, Nice, France; Project reference NCE/2012-63).* All mice were maintained on a C57BL/6 genetic background whereas Wistar rats were exclusively from a commercial source (Janvier, St Berthevin, France). The *Fmr1* knockout (*Fmr1*$^{-/y}$) mouse line[10] was maintained on a C57BL/6 background.

Mouse and rat brain lysate preparation

Brain lysates were prepared as previously described[26] from post-natal P1-3 mouse or P5-7 rat brains. Briefly, freshly dissected brains were transfered in 5 volumes (w/v) of ice-cold sucrose buffer (10 mM Tris-HCl pH 7.4, 0.32 M sucrose) supplemented with a protease inhibitor cocktail (Sigma, 1/100), Pefabloc 0.5 mM (Roche), MG132 100 μM (Enzo), ALLN 100 μM (Sigma) and 20 mM freshly prepared NEM (Sigma) and homogenized at 4°C using a Teflon-glass potter and a motor-driven pestle at 500 rpm. Nuclear fraction and cell debris were pelleted by centrifugation at 1,000g for 10 min. The post-nuclear S1 fraction (supernatant) was collected and protein concentration measured using the BCA protein assay (Biorad).

Primary neuronal cultures

Hippocampal and cortical neurons were prepared from embryonic (E18) pregnant Wistar rats as previously described[26] or from WT or *Fmr1*$^{-/y}$ E15.5 pregnant C57BL/6 mice. Briefly, neurons were plated in Neurobasal medium (Invitrogen, France) supplemented with 2% B27 (Invitrogen), 0.5 mM glutamine and penicillin/streptomycin (Ozyme) on 60-mm dishes or 24-mm glass coverslips (VWR) pre-coated with poly-L-Lysine (0.5 mg mL^{-1}; Sigma). Neurons (800,000 cells per 60-mm dish or 110,000 cells per coverslip) were then fed once a week with Neurobasal medium supplemented with 2% B27 and penicillin/streptomycin for a maximum of 3 weeks.

Cell transfection

COS7 cells and primary neurons (14-16 DIV) were transfected using Lipofectamine 2000 (Invitrogen) according to the manufacturer's instructions and used 48-72h post-transfection.

Sindbis virus production and neuronal transduction

Attenuated Sindbis viral particles (SINrep(nsP2S726)) were prepared and used as previously described[38, 39, 40]. Briefly, cRNAs were generated from the pSinRep5 plasmid containing the sequence coding for WT or mutated GFP-FMRP constructs and from the defective helper (pDH-BB) plasmid using the Mmessage Mmachine SP6 solution (Ambion). cRNAs were then mixed and electroporated into BHK21 cells. Pseudovirions present in the culture medium were harvested 48h after electroporation and concentrated using ultracentrifugation on SW41Ti. Aliquots of resuspended Sindbis particles were then stored at -80°C until use. Neurons were transduced at a multiplicity of infection (MOI) of 0.1 to 2 and returned to the incubator at 37°C under 5% CO_2 for 24 to 30h depending on their subsequent utilisation.

Bacterial sumoylation assay in E. coli

Bacterial sumoylation assays were performed as previously described[31, 35]. Briefly, competent E. coli BL21(DE3) cells (Invitrogen, France) expressing pE1-E2SUMO1 were transformed with 1 μg of pET-expression plasmid (Novagen) to express the WT or non-sumoylatable forms of His-tagged FMRP were selected on LB-Agar plates containing chloramphenicol (50 μg mL^{-1}) and ampicillin (50 μg mL^{-1}). A 10 ml preculture was then used to inoculate 50 ml of LB containing chloramphenicol and ampicillin. After incubation under shaking at 37°C until OD600 reaches 0.7, cells were cooled down to 20°C and isopropyl-β-D-thiogalactopyranoside (IPTG) was added at a concentration of 1 mM. After 4 h at 20°C, bacteria were pelleted by centrifugation at 4°C at 7,000g and kept at -80°C until use. Pellets were resuspended in 1 ml lysis buffer (25 mM Tris pH 8, 300 mM KCl, 1 mM EDTA, 20% glycerol, 5% ethanol, 0.5% NP40, 0.5M Urea, 1 mM DTT) supplemented with proteases inhibitors (Leupeptine 1 μg mL^{-1}, Pepstatine 1 μg mL^{-1}, Aprotinine 1 μg mL^{-1}, Pefabloc 0.5 mM and freshly prepared NEM 20 mM) and incubated under rotation for 30 min at 4°C in the presence of 5 mg mL^{-1} Lysozyme. Bacterial cytoplasmic membranes were then solubilised by addition of 1 mg mL^{-1} sodium deoxycholate and released DNA digested by incubation with 50 μg mL^{-1} of DNAse I and 10 mM $MgCl_2$ for 30 min at 4°C. Cellular debris were pelleted by centrifugation at 20,000 g for 15 min at 4°C and supernatants were incubated with 40 μl of nickel agarose beads (Qiagen) for 2h at 4°C under gentle rotation. After three washes (25 mM Tris pH8, 50 mM KCl, 1 mM EDTA, 20% glycerol, 0.1% Triton X100, 0.5 M Urea, 1 mM DTT), purified proteins were eluted in 200 μl of βME-reducing sample buffer for 5 min at 95°C.

COS7 sumoylation assay

Mycoplasm-free COS7 cells (ATCC reference CRL-1651, Molsheim, France) at 60% of confluence in 6 wells plates were cotransfected using 1 μg of the eukaryotic expression vector pTL1-FMRP plasmid[63] or its derived non-sumoylatable mutants with 0.5 μg of mCherry or

mCherry-SUMO1 plasmids[26] and 0.5 μg of plasmid coding for Flag-Ubc9 using Lipofectamine 2000 (Invitrogen) according to the manufacturer's instructions. After 48h of expression, cells were washed once in PBS containing 20 mM NEM and reduced for 5 min at 95°C in βME-containing sample buffer.

CLIP analysis

To isolate neuronal mRNAs associated with WT and SUMO-deficient GFP-FMRP mutant, UV-crosslinking and FMRP immunoprecipitations were performed on 20 DIV *Fmr1*$^{-/y}$ neurons transduced (MOI of 3) at day 19 to express free GFP, the WT or the non-sumoylatable K88,130,614R form of GFP-FMRP. RNAs and proteins were cross-linked through 3 rounds of UV irradiation (400 mJ each; 254 nm). Cells were then scraped in ice cold PBS, collected by centrifugation and lysed in NP40 buffer as described in ref[64]. For each assay, 5 μg of affinity-purified rabbit anti-FMRP antibody (Ab#056) was used to immunoprecipitate 1 mg of neuronal extracts and 2% of the lysate was used for assessment of relative RNA expression in the input material. IPs were then carried out at 4°C for 4h and 2% of the homogenate and 10% of the immunoprecipitates were saved to check for the IP quality using anti-FMRP immunoblots. After 3 washes in lysis buffer (50 mM HEPES pH7.4, 150 mM NaCl, 0.5% NP40, 10 mM EDTA, 1 mM NaF, 0.5 mM DTT, protease and phosphatase inhibitors (Pierce), proteins were digested with proteinase K (1 μg mL^{-1}) for 30 min at 56°C. IP and input RNAs were purified through two successive rounds of phenol / chloroform extraction, then reverse transcribed using a mix of Oligo dT and random primers and Superscript II enzyme (Invitrogen) according to the manufacturer's protocol. RT reactions were diluted two times and 1 μl of diluted material was used for qPCR analysis. Relative enrichment of the amplified RNA in the IP versus the input in each condition was calculated with the $2^{-\text{deltaCt}}$ (Ct_{IP}-Ct_{input}).

Oligonucleotides (5' to 3') used in RNA work were as follows:

*Fmr1*_F:GAACAAAAGACAGCATCGCT; *Fmr1*_R:CCAATTTGTCGCAACTGCTC;

*Camk2a*_F:TATCCGCATCACTCAGTAC; *Camk2a*_R:GAAGTGGACGATCTGCCATTT;

*Sapap3*_F:ACCATGTAACCCCGGCTG; *Sapap3*_R:CCTTGATGTCAGGATCCCC;

*Fxr1*_F: GTGCAGGGTCCCGAGGT; *Fxr1*_R:GGTGGTGGTAATCGGACTTC;

*Kif3c*_F: GGTCCCATCCCAGATACAGA; *Kif3c*_R: CCAGAAAGCTGTCAAACCTC;

*Tubb3*_F: CGAGACCTACTGCATCGACA; *Tubb3*_R: CATTGAGCTGACCAGGGAAT;

*PP2a*_F:GTCAAGAGCCTCTGCGAGAA; *PP2a*_R:GCCCATGTACATCTCCACAC;

*β-actin*_F: ACGGCCAGGTCATCACTATTG; *β-actin*_R: CACAGGATTCCATACCCAAGA

*PSD95*_F:GGCGGAGAGGAACTTGTCC; *PSD95*_R:AGAATTGGCCTTGAGGGAGGA;

*Map1b*_F:TCCGATCGTGGGACACAAACCTG; *Map1b*_R:AGCACCAGCAGTTTATGGCGGG

Immunoprecipitation

Proteins from rodent brain lysates or cultured neurons were solubilized for 1h at 4°C under gentle rotation in lysis buffer (10 mM Tris-HCl pH7.5, 10 mM EDTA, 150 mM NaCl, 1% Triton X100, 0.1% SDS) supplemented with a protease inhibitor cocktail (Sigma, 1/100), Pefabloc 0.5 mM (Roche), MG132 100 μM (Enzo), ALLN 100 μM (Sigma) and 20 mM freshly prepared NEM (Sigma). Then, NaCl concentration was raised to 400 mM and lysates were sonicated for 10 sec, further incubated for 30 min at 4°C and clarified *(for primary neuronal extracts)* or not *(for brain homogenates)* at 20,000g at 4°C for 15 min. Supernatants were diluted 2.5 fold with lysis buffer devoid of NaCl and pre-cleared for 1h with a 50/50 mix of untreated and preblocked protein G-sepharose beads (Sigma) with a blocking buffer (PBS containing 5 mg mL^{-1} BSA, 5 mg mL^{-1} Dextran (40 kDa), 1 mg mL^{-1} Gelatin, Yeast t-RNA 0.1 mg mL^{-1} and Glycogen 0.1 mg mL^{-1}) for 1h at 4°C. Proteins (800 μg) from precleared lysates were incubated with either 8 μg of mouse monoclonal anti-SUMO1 antibody (Ab#D11, Santa

Cruz), 4 µg of custom rabbit anti-FMRP (Ab#056, **Supplementary Fig. 1**) or 12 µg commercially available rabbit anti-FMRP (#Ab17722, Abcam; **Supplementary Fig. 1**) antibodies (or their corresponding IgGs as IP control) for 1h at 4°C and then overnight at 4°C with 30 µl of pre-blocked protein G-sepharose beads (Sigma). Precipitates were washed 3 times with 1 ml lysis buffer and proteins were eluted by boiling the beads 5 min in βME-reducing sample buffer before SDS-PAGE.

Immunoblotting

Protein extracts were resolved by SDS-PAGE, transferred onto nitrocellulose membrane (Hybond-C Extra, Amersham or BioTraceNT, PALL), immunoblotted with the indicated concentration of primary antibodies and revealed using the appropriate HRP conjugated secondary antibodies (GE healthcare) or True Blot (Rockland, Tebu-Bio). Proteins were then identified using Immobilon Western (Millipore) or Western Lightning Ultra (Perkin Helmer) chemiluminescent solutions and images acquired on a Fusion FX7 system (Vilber Lourmat). Full-size blots for cropped gels can be found in **Supplementary figures 6,7**.

Immunocytochemistry

Neurons (18-21 DIV) were fixed in phosphate-buffered saline (PBS) containing 3.7% formaldehyde and 5% sucrose for 1h at room temperature (RT). Neurons were then permeabilized for 20 min in PBS containing 0.1% Triton X-100 and 10% Horse serum at RT and immunostained with either a rabbit monoclonal anti-S6 (1/200; Cell Signaling), a goat anti-Staufen1 (1/100; Santa-Cruz), a goat anti-Staufen2 (1/100; Santa-Cruz), a rabbit anti-FXR1 (1/100[65]), a mouse monoclonal anti-Ubc9 (1/50; BD Bioscience, France), a mouse anti-SUMO1 (1/50; Ab#D11, Santa-Cruz; 1/50 Ab#2F5-1, DSHB) or rabbit anti-FMRP (1/200; Custom Ab#056 or 1/50; Ab#4317S, Cell Signaling) antibodies in PBS containing 0.05% Triton X-100

and 5%HS. Cells were washed 3 times in PBS and incubated with the appropriate secondary antibodies (1/400) conjugated to Alexa488 or Alexa594, and mounted with Mowiol (Sigma) until confocal examination.

Ratiometric calcium imaging

Mouse cortical/hippocampal neurons (19-23 DIV) were loaded in neurobasal containing 20 μM Fura-2AM (Invitrogen) for 30 min. After 2 washes in physiological 1.6 mM Calcium-containing buffer (139 mM NaCl, 1.25 mM glucose, 15 mM Na_2HPO_4, 1.8 mM MgSO4, 1.6 mM $CaCl_2$, 3 mM KCl, 10 mM HEPES), Fura-2AM-loaded neurons were imaged at 37°C on an inverted AxioObserver microscope (Carl Zeiss) equipped with a 300W Xenon lamp (Suttler instruments) and a Fluar 40x (NA 1.4) oil immersion objective. Fura-2AM was sequentially excited at 340 and 380 nm and the emission monitored at 510 nm. Images were acquired with a cascade 512 EMCCD camera every 2s and digitized using Metafluor software (Roper scientific). The intracellular calcium concentration was estimated by measuring the F340/380nm ratio of fluorescence. Neurons were treated for 40s with 100 μM DHPG in 1.6 mM Calcium-containing buffer.

GFP-FMRP-associated granules analysis

Fmr1$^{-/y}$ neurons were cotransfected to express mCherry with the WT or the non-sumoylatable mutant form of GFP-FMRP either for 48h or 72h. Cells were then rinse twice in PBS and fixed in PBS containing 3.7% formaldehyde and 5% sucrose for 1h at RT and mounted with Mowiol until use.

smFISH assays. smFISH assays were performed as described previously in ref[44]. Briefly, *Fmr1*$^{-/y}$ neurons grown on glass-coverslips were transfected as above at 12 DIV to express the

WT or the K88,130R mutant form of GFP-FMRP for 48-60h. Cells were then fixed in PBS containing 4% formaldehyde for 10 min at RT. smFISH assays were performed as described previously in[44] with the following modified prehybridization buffer: Formamide 10%, NaCl 68.5 mM, KCl 1.35 mM, KH_2PO_4 1 mM, Na_2HPO_4 5 mM, SSC 2X (Euromedex), Dextran sulfate 10% (Sigma), Ribonucleoside Vanadyl complexes 10 mM (Sigma), BSA 2 mg mL^{-1}, Salmon sperm DNA 0.67 mg mL^{-1} (Sigma), yeast tRNA 0.67 mg mL^{-1} (Sigma). Neurons were incubated overnight at 37°C in the presence of GFP Quasar 570-labelled, PSD-95 or CamKII Quasar 670-labelled Stellaris probes (12.5 picomoles in 100 µl of prehybridization buffer), washed 2 times with pre-warmed 10% Formamide in 2X SSC for 20 min at 37°C, three times 1 min with 2X SSC and twice for 5 min with 2X SSC under mild agitation prior to coverslip mounting in Vectashield (Clinisciences).

GFP Stellaris probes (used to detect GFP-FMRP mRNA) labeled with Quasar 570 dye were (5' to 3') as follows: tcctcgcccttgctcaccat, atgggcaccaccccggtgaa, gtcgccgtccagctcgacca, cgctgaacttgtggccgttt, tcgccctcgccctcgccgga, ggtcagcttgccgtaggtgg, cggtggtgcagatgaacttc, ggccagggcacgggcagctt, taggtcagggtggtcacgag, tagcggctgaagcactgcac, gtgctgcttcatgtggtcgg, gcatggcggacttgaagaag, cgctcctggacgtagccttc, gtcgtccttgaagaagatgg, tcggcgcgggtcttgtagtt, ggtgtcgccctcgaacttca, ttcagctcgatgcggttcac, gtcctccttgaagtcgatgc, agcttgtgccccaggatgtt, gtggctgttgtagttgtact, ttgtcggccatgatatagac, caccttgatgccgttcttct, atgttgtggcggatcttgaa, gagctgcacgctgccgtcct, tgttctgctggtagtggtcg, agcacggggccgtcgccgat, caggtagtggttgtcgggca, ttgctcagggcggactgggt, atcgcgcttctcgttggggt, cgaactccagcaggaccatg, agagtgatcccggcggcggt, cttgtacagctcgtccatgc

PSD-95 Stellaris probes, labeled with Quasar 670 dye were (5' to 3') as follows: ctctatgatcttctcagctg, taggccctttgataagcttg, tgcgatgctgaagccaagtc, ctattatctccagggatgtg, ccttcgatgatcttggttac, aggatcttgtctccgatctg, tcatgcatgacatcctctag, atatgtgttcttcagggctg, ccacctttaggtacacaacg, catagctgtcactcaggtag, tatgaggttgtgatgtctgg, tagctgctatgactgatctc, tcaacaccattgaccgacag, tgttcatgactggcattgcg, tactgagcgatgatcgtgac, cgaatcggctatactcttct, ataagctgttcccgaagatc, tgatatagaagccccgcttg, ttgtcgtagtcaaacagggc, tcaagaaaccgcagtccttg, gctggcgtcaattacatgaa, catcggtctcactgtcagag, tttgctgggaatgaagccaa, tctcatagctcagaaccgag, aaggatgatgatggggcgag, agaagatcatcgttggcacg, aaacttgtcggggaactcgg, tcgtatgagggacacaggat, tatctcatattcccgcttag, cgggaggagacaaagtggta, tgaatgtccttctccatttt, cagcctcaatgaacttgtgc, tagaggtggctgttgtactg, gcattggctgagacatcaag, ggatgaagatggcgataggg, cgcttattgatctctagcac, agatctcttcaaagctgtcg, cttcgatgacacgtttcact

CaMKII Stellaris probes, labeled with Quasar 670 dye were (5' to 3') as follows:

tactcttctgtgaatcgggt, taatcttggcagcatactcc, cttcaacaagcggcagatgc, tcatggagtcggacgatatt, accagtaaccagatcgaaga, gccacaatgtcttcaaacag, ggcatcagcttcactgtaat, tccaagatctgctggataca, catctggtgacagtgtagca, ttcacagcagcgcccttgag, tatccaggtgtccctgcgaa, cttcctcagcacttctgggg, aggtccacgggcttcccgta, agatatacaggatgacgcca, ctggtcttcatcccagaacg, ctttgatctgctggtacagg, gatgggaaatcataggcacc, ggtgacggtgtcccattctg, tgatcagatccttggcttct, gggttgatggtcagcatctt, tcagcggccgtgatgcgttt, agatccatgggtgcttgaga, tctcctgtctgtgcatgcag, ctccggagaagttcctggtg, gtgctctcagaagattcctt, tcttcgtcctcaatggtggt, ttcctgtttgcgcactttgg, gctgctctgtcactttgata, ccattgcttatggcttcgat, cttcgtgtaggactcaaagt, ctgtcattccagggtcgcac, cccagggcctctggttcaaa, gaatcgatgaaagtccaggc, gggaccacaggttttcaaaa, tgactcgtcacccatcaggt, atgcggatataggcgatgca, gcctgcatccaggtactgag, cagacgcgggtctcctctga, atctgtggaagtggacgatc, cgagtacataggtggcaatg, aaatacacggaagtttggct, agatgtccgttaacgcaaaa, acagcattccatacaagagc, tatagctcacatgtaggcga, ctgagccttatgaagaagcc, ggattgtagatcctgcatgg, catggagcttgtcagatgag, tttgagcagtggtcattcaa

Analysis of spine morphology

Fmr1$^{-/y}$ or WT neurons were transduced at 18 DIV with Sindbis virus (MOI of 1) expressing free GFP, the WT or mutated forms of GFP-FMRP for either 24h (*Fmr1*$^{-/y}$ neurons) or 30h (WT neurons) before use. Cells were then fixed using PBS containing 3.7% formaldehyde and 5% sucrose for 1h at RT and mounted in Mowiol before confocal examination.

Confocal imaging

For fixed cells, confocal images (1024x1024) were acquired with a 63x oil immersion lens (numerical aperture NA 1.4) on an inverted TCS-SP5 confocal microscope (Leica Microsystems, Nanterre, France). Z-series of 6-8 images of randomly selected secondary dendrites were compressed into two dimensions using the maximum projection of the LASAF acquisition software (Leica). Manders' colocalisation parameters were computed using the JaCoP plug-in from the ImageJ software[66] when required.

For GFP-FMRP-containing granule measurements, two Z-series were acquired. The first was acquired at low laser intensity to clearly identify large granules without any pixel saturation and the second series was recorded at a higher laser intensity to detect smaller granules. These two Z-series were then averaged and compressed into two dimensions by a maximal projection.

Measurements of the surface of GFP-FMRP-containing granules along dendrites were determined automatically using an home-made ImageJ macro program. Briefly, granules and dendrites were segmented in each image, and the length of the denditric tree was measured after a step of skeletonization. The data were then imported in GraphPad Prism software for statistical analysis.

For dendritic spine imaging, Z-series of 6-8 images of secondary dendrites from GFP-expressing neurons were compressed into two dimensions by a maximal projection using the LASAF software. About 3000 to 4500 spines were analyzed per condition (2-4 dendrites per neuron and from 20-30 neurons per condition from 4 independent experiments which were done blind for 2 of them). At the time of acquisition, laser power was adjusted so that all spines were below the saturation threshold. To analyze dendritic protrusions, projection images were imported into NeuronStudio software[67], which allows for the automated detection of immature and mature dendritic spines. The length of individual spines was automatically measured and data were imported in GraphPad Prism software for statistical analysis. Mature spines were characterized by a head diameter ranging from 0.3 to 1 µm and a spine length between 0.4 and 3 µm. Immature spines corresponded to protrusions with a head diameter below 0.3 µm and a spine length ranging from 0.5 to 6 µm.

Fluorescence Lifetime Imaging (FLIM) experiments

Fmr1$^{-/y}$ neurons co-expressing mCherry with the WT or the non-sumoylatable mutant form of GFP-FMRP for 72h were fixed in PBS containing 3.7% formaldehyde and 5% sucrose for 1h at RT and mounted using Mowiol. FLIM was then performed on a Nikon A1R confocal laser-scanning microscope equipped with Time Correlated Single-Photon Counting (TCSPC) electronics (PicoHarp 300; PicoQuant). Excitation was obtained using a pulsed laser LDH-D-

C-485 (PicoQuant) at a repetition rate of 40 MHz allowing the acquisition of the full intensity decay. Fluorescence emission was collected by a hybrid photomultiplier detector (PicoQuant) through a 60X λS, NA 1.4, oil objective (Nikon Instruments) and band pass filter (520/35). The following parameters were kept constant for all acquisition: pixel size (70 nm, 512x512), pixel dwell time (4.8 µs) and acquisition time (5 min/image). So as to limit pile-up and to accumulate enough photons within the 5 min acquisition time, laser excitation power was adjusted to obtain a count rate between 0.4 and 2 MHz[68]. In these conditions, there was no measurable photobleaching. Each field of view was also acquired in conventional confocal mode. EGFP and mCherry channels were respectively acquired using the 488-nm excitation with the 525/50-nm band-pass detection and the 561-nm excitation with the 595/50-nm band-pass detection.

Fluorescence lifetime was measured by fitting the intensity decays with a monoexponential decay model reconvolved with experimental IRF (Instrument Response Function) using the software SymPhoTime (PicoQuant). Intensity decays were fitted pixel by pixel to provide FLIM images and calculated lifetimes represented using a pseudo-colour scale ranging from 1.7 to 2.2 ns. To improve robustness of the fit, IRF parameters were fixed as the IRF is expected to be invariant over the acquisition field. The robustness of the fit was assessed by the calculated standard weighted least square (X^2) and the residual[69]. Values of the reduced X^2 should be close to 1 and residue should be randomly distributed around zero. The average lifetime of the FLIM image (Tau, ns) was determined from the barycentre of the frequency histogram associated with the FLIM image. To calculate the fluorescence lifetime of individual granules, the intensity decay resulting from all the photons of the granule was fitted using a monoexponential model reconvolved with IRF.

To get enough photons at each pixel for an accurate intensity decay fit, only granules with more than 10,000 photons *(integrated number of photons over the decay)* were analysed, with a minimum pixel threshold of 500 counts for background rejection. To reach 10,000 photons per granules and to reject granules, which were largely out of focus, only granules larger than 0.35 μm^2 were analyzed *(segmentation using ImageJ)*. To avoid pulse pile up and to collect photons fast enough to meet the above criteria, count rate was kept between 0.4 and 4 MHz. Clusters with higher count rate were excluded from the analysis. In those conditions, the fluorescent lifetime was invariant.

Dendra2-FMRP-containing granule photoconversion experiments

Experiments were performed as previously described[26, 48]. Briefly, live *Fmr1*$^{-/y}$ neurons expressing the WT or mutated Dendra2-FMRP from were kept in Earle's buffer (25 mM HEPES-Tris pH 7.4, 140 mM NaCl, 5 mM KCl, 1.8 mM $CaCl_2$, 0.8 mM $MgCl_2$, 0.9 g L^{-1} glucose) on the heated stage (set at 37°C) of a Nikon Ti inverted microscope and imaged using an Ultraview spinning disk confocal system (Perkin Elmer, France). Cells were then stimulated or not with 50 μM DHPG in Earle's buffer. After a 10-min incubation time in either control or DHPG solution, Dendra2-FMRP-granules were photoconverted through a 100X/1.4 oil immersion objective for 30 ms using 405-nm laser light (50 mW, 15%). The red photoconverted Dendra2-FMRP was excited using a 561-nm laser light (50 mW, 17%) and 2D-time series (2 Hz) were collected for 10 min. The decrease in red fluorescence from the Dendra2-FMRP photoconverted granules was measured over time using Volocity 6.3 software and data expressed as the percentage of the initial red photoconverted fluorescence (F/F_0). Curves were fitted using a mono-exponential decay equation and data analysed using GraphPad Prism.

GST- and His-FMRP production and purification

GST- or His-FMRP (1-160) proteins were produced in E. coli BL21(DE3) cells (Invitrogen, France). A single colony was picked and used to inoculate 25 ml of LB broth supplemented with 50 μg mL^{-1} ampicillin. This was used to inoculate 500 mL of LB and was shaken at 37°C until OD_{600} reached 0.8. Cells were then transferred at 20°C and protein synthesis induced by addition of 1 mM IPTG (Sigma, France). After 4h at 20°C, cells were pelleted by centrifugation at 7000g for 5 minutes and then gently resuspended in ice-cold PBS and frozen at -80°C until use. Pellets were then resuspended in 5 mL lysis buffer (25 mM Tris-HCl pH8, 300 mM KCl, 1 mM EDTA, 20% glycerol, 5% ETOH, 0.5% NP40, 0.5 M Urea) supplemented with 1% protease inhibitor cocktail (Sigma Aldrich, France). Cells were disrupted by incubation with 1% lysozyme (Sigma, France) for 30 min at 4°C followed by another 30 min in the presence of 0.1% Deoxycholic acid, 10 mM MgCl2 and 200 ng μL^{-1} DNase. Lysates were then clarified by centrifugation at 10,000g for 15 min. GST- or His-tagged proteins were purified using either Glutathione gel (GE Healthcare) for GST- and GST-FMRP or Nickel resin (Qiagen) for His-fusion proteins. Proteins were then concentrated on Amicon 3-kDa cutoff filters (Millipore) by centrifugation and resuspended in PBS. Concentrations of purified proteins were determined using the BCA protein assay (Biorad) and protein quality assessed by SDS-PAGE and Coomassie Blue protein staining (Clinisciences).

GST-FMRP/His-FMRP dimerization

GST- (control) or GST-FMRP (1-160) fusion proteins (1μg) were incubated with an excess of 2 μg His-FMRP (1-160) for 2h at 4°C in dimerization buffer (50 mM Tris-HCl pH8, 150 mM NaCl, 2.5 mM MgCl2, 0.5% NP40, 0.5 mM DTT, 1% Protease inhibitor cocktail) to allow for GST-FMRP/His-FMRP dimerization. Then, 50 μl of glutathione beads (GE Healthcare) were added to the dimerization mix and incubated at 4°C for 2h. After five washes in dimerization

buffer at 4°C, immobilized GST-FMRP (1-160) – His-FMRP (1-160) dimers were processed for *in vitro* sumoylation assays.

***In vitro* SUMO assays**

Immobilized GST-FMRP/His-FMRP dimers were incubated with 0.15 μg of E1-activating complex (Enzo Life science), 0.1 μg of E2 Ubc9 (Enzo Life science), 3 μg of SUMO1-GG in 20 μl of *in vitro* SUMO reaction mix (20 mM HEPES pH 7.3, 110 mM KOAc, 2 mM $Mg(OAc)_2$, 0.5 mM EGTA, 1 mM DTT 0.05% Tween 20, 0.2 mg mL^{-1} Ovalbumin) including the ATP regenerating system (20 mM ATP, 10 mM Creatine phosphate, 3.5 U mL^{-1} of Creatine kinase and 0.6 U mL^{-1} of inorganic pyrophosphatase (Sigma Aldrich) for 2h at 30°C. After centrifugation for 5 min at 3,000g at 4°C, the supernatant containing the released His-FMRP(1-160) and the pellet containing the remaining immobilized GST-FMRP/His-FMRP dimers were denatured at 95°C for 10 min in 5x Laemmli buffer containing 7.5% β-mercaptoethanol and analyzed by immunoblotting with FMRP #2F5-1 antibodies.

Electrophysiological recordings

Patch clamp experiments were carried out at RT (22-25°C) on mixed cultured cortical/hippocampal neurons obtained from *FMRP*$^{-/y}$ mice (four different cultures). *FMRP*$^{-/y}$ neurons (18 DIV) were transduced for 24-26h with attenuated Sindbis virus to express GFP-FMRP **WT** or the non-sumoylatable GFP-FMRP-**K88,130,614R**. Patch pipettes displayed a resistance of 4 to 7 MΩ and filled with a solution containing (in mM): 2 Na_2-ATP, 130 $CsMeSO_4$, 5 CsCl, 2.5 $MgCl_2$, 1 Na-GTP, 5 EGTA and 10 HEPES (pH adjusted to 7.2 with CsOH). The extracellular bathing solution contained (in mM): 145 NaCl, 5 KCl, 2 $CaCl_2$, 2 $MgCl_2$, 10 HEPES, 10 Glucose, 0.02 Bicuculline and 0.00025 TTX (pH adjusted to 7.4 with NaOH). We used the whole-cell configuration to record miniature Excitatory PostSynaptic

Currents (mEPSCs) from GFP-positive neurons that were voltage-clamped at -70 mV *i.e.*, the estimated reversal potential for chloride. mEPSCs were recorded for 10 min, starting 1-2 min after the whole-cell mode was achieved and series resistances were monitored every 50 sec by injecting a 5 mV hyperpolarizing current for 10 ms. Data were sampled at 20 kHz, low-pass filtered at 5kHz (Axopatch 200B Molecular Devices), digitalized (Digidata 1440, Molecular Devices) and recorded using Clampex software (pClamp 10, Molecular Devices). Analysis of series resistances and mEPSCs were performed offline using Clampfit software (pClamp 10, Molecular Devices). mEPSCs were analyzed over periods of 200 sec for which series resistances were stable, *i.e.*, did not vary for more than 25%.

Data and statistical analysis

Statistical analyses were calculated using GraphPad Prism (GraphPad software, Inc). All data are expressed as mean ± SEM. Unpaired t-test (**Fig. 3i**) or non-parametric Mann-Whitney test (**Figs. 4c** and **5d,f,g**) were used to compare medians of two data sets. For spine morphogenesis experiments, values represent means ± SEM. Statistical significance for multiple comparison data sets was computed using a one-way analysis of variance (ANOVA) with a Bonferroni post-test (**Figs. 2b-d, 5e, 7b-d** and **Supplementary Fig. 2b-d**). Normality for all groups was verified using the Shapiro-Wilk test. According to the Levene variance test, variances were homogenous for the percentage of immature and mature spines (**Figs. 2b-d, 7b-d** and **Supplementary Fig. 2b-d**). For FLIM, data distributions were represented as box and whiskers plots displaying upper and lower quartiles, and maximum and minimum values in addition to median. For electrophysiological data, distributions were analyzed by a Kolmogorov-Smirnov test (**Supplementary Fig. 3b,c**). *$p<0.05$ was considered significant.

Data availability

All relevant data are available from the corresponding author upon reasonable request.

References

1. Penzes P, Cahill ME, Jones KA, VanLeeuwen JE, Woolfrey KM. Dendritic spine pathology in neuropsychiatric disorders. *Nat Neurosci* **14**, 285-293 (2011).

2. Grant SG. Synaptopathies: diseases of the synaptome. *Curr Opin Neurobiol* **22**, 522-529 (2012).

3. Bassell GJ. Fragile balance: RNA editing tunes the synapse. *Nat Neurosci* **14**, 1492-1494 (2011).

4. Darnell JC, Klann E. The translation of translational control by FMRP: therapeutic targets for FXS. *Nat Neurosci* **16**, 1530-1536 (2013).

5. Maurin T, Zongaro S, Bardoni B. Fragile X Syndrome: from molecular pathology to therapy. *Neurosci Biobehav Rev* **46 Pt 2**, 242-255 (2014).

6. Grossman AW, Elisseou NM, McKinney BC, Greenough WT. Hippocampal pyramidal cells in adult Fmr1 knockout mice exhibit an immature-appearing profile of dendritic spines. *Brain Res* **1084**, 158-164 (2006).

7. Patel AB, Loerwald KW, Huber KM, Gibson JR. Postsynaptic FMRP promotes the pruning of cell-to-cell connections among pyramidal neurons in the L5A neocortical network. *J Neurosci* **34**, 3413-3418 (2014).

8. Yan Z, Kim E, Datta D, Lewis DA, Soderling SH. Synaptic Actin Dysregulation, a Convergent Mechanism of Mental Disorders? *J Neurosci* **36**, 11411-11417 (2016).

9. Bakker CE. Fmr1 knockout mice: a model to study fragile X mental retardation. The Dutch-Belgian Fragile X Consortium. *Cell* **78**, 23-33 (1994).

10. Mientjes EJ*, et al.* The generation of a conditional Fmr1 knock out mouse model to study Fmrp function in vivo. *Neurobiol Dis* **21**, 549-555 (2006).

11. Narayanan U*, et al.* FMRP phosphorylation reveals an immediate-early signaling pathway triggered by group I mGluR and mediated by PP2A. *J Neurosci* **27**, 14349-14357 (2007).

12. Niere F, Wilkerson JR, Huber KM. Evidence for a fragile X mental retardation protein-mediated translational switch in metabotropic glutamate receptor-triggered Arc translation and long-term depression. *J Neurosci* **32**, 5924-5936 (2012).

13. Hou L, Antion MD, Hu D, Spencer CM, Paylor R, Klann E. Dynamic translational and proteasomal regulation of fragile X mental retardation protein controls mGluR-dependent long-term depression. *Neuron* **51**, 441-454 (2006).

14. Nalavadi VC, Muddashetty RS, Gross C, Bassell GJ. Dephosphorylation-induced ubiquitination and degradation of FMRP in dendrites: a role in immediate early mGluR-stimulated translation. *J Neurosci* **32**, 2582-2587 (2012).

15. Matunis MJ, Coutavas E, Blobel G. A novel ubiquitin-like modification modulates the partitioning of the Ran-GTPase-activating protein RanGAP1 between the cytosol and the nuclear pore complex. *J Cell Biol* **135**, 1457-1470 (1996).

16. Mahajan R, Delphin C, Guan T, Gerace L, Melchior F. A small ubiquitin-related polypeptide involved in targeting RanGAP1 to nuclear pore complex protein RanBP2. *Cell* **88**, 97-107 (1997).

17. Flotho A, Melchior F. Sumoylation: a regulatory protein modification in health and disease. *Annu Rev Biochem* **82**, 357-385 (2013).

18. Henley JM, Craig TJ, Wilkinson KA. Neuronal SUMOylation: mechanisms, physiology, and roles in neuronal dysfunction. *Physiol Rev* **94**, 1249-1285 (2014).

19. Schorova L, Martin S. Sumoylation in Synaptic Function and Dysfunction. *Front Synaptic Neurosci* **8**, 9 (2016).

20. Hickey CM, Wilson NR, Hochstrasser M. Function and regulation of SUMO proteases. *Nat Rev Mol Cell Biol* **13**, 755-766 (2012).

21. Kerscher O. SUMO junction-what's your function? New insights through SUMO-interacting motifs. *EMBO Rep* **8**, 550-555 (2007).

22. Meulmeester E, Melchior F. Cell biology: SUMO. *Nature* **452**, 709-711 (2008).

23. Gwizdek C, Casse F, Martin S. Protein sumoylation in brain development, neuronal morphology and spinogenesis. *Neuromolecular Med* **15**, 677-691 (2013).

24. Loriol C, Parisot J, Poupon G, Gwizdek C, Martin S. Developmental regulation and spatiotemporal redistribution of the sumoylation machinery in the rat central nervous system. *PLoS ONE* **7**, e33757 (2012).

25. Loriol C, Khayachi A, Poupon G, Gwizdek C, Martin S. Activity-dependent regulation of the sumoylation machinery in rat hippocampal neurons. *Biol Cell* **105**, 30-45 (2013).

26. Loriol C*, et al.* mGlu5 receptors regulate synaptic sumoylation via a transient PKC-dependent diffusional trapping of Ubc9 into spines. *Nat Commun* **5**, 5113 (2014).

27. Girach F, Craig TJ, Rocca DL, Henley JM. RIM1alpha SUMOylation is required for fast synaptic vesicle exocytosis. *Cell Rep* **5**, 1294-1301 (2013).

28. Craig TJ, Anderson D, Evans AJ, Girach F, Henley JM. SUMOylation of Syntaxin1A regulates presynaptic endocytosis. *Sci Rep* **5**, 17669 (2015).

29. Shalizi A*, et al.* A calcium-regulated MEF2 sumoylation switch controls postsynaptic differentiation. *Science* **311**, 1012-1017 (2006).

30. Shalizi A*, et al.* PIASx is a MEF2 SUMO E3 ligase that promotes postsynaptic dendritic morphogenesis. *J Neurosci* **27**, 10037-10046 (2007).

31. Martin S, Nishimune A, Mellor JR, Henley JM. SUMOylation regulates kainate-receptor-mediated synaptic transmission. *Nature* **447**, 321-325 (2007).

32. Chamberlain SE*, et al.* SUMOylation and phosphorylation of GluK2 regulate kainate receptor trafficking and synaptic plasticity. *Nat Neurosci* **15**, 845-852 (2012).

33. Craig TJ, Jaafari N, Petrovic MM, Rubin PP, Mellor JR, Henley JM. Homeostatic synaptic scaling is regulated by protein SUMOylation. *J Biol Chem* **287**, 22781-22788 (2012).

34. Sampson DA, Wang M, Matunis MJ. The small ubiquitin-like modifier-1 (SUMO-1) consensus sequence mediates Ubc9 binding and is essential for SUMO-1 modification. *J Biol Chem* **276**, 21664-21669 (2001).

35. Uchimura Y, Nakao M, Saitoh H. Generation of SUMO-1 modified proteins in E. coli: towards understanding the biochemistry/structural biology of the SUMO-1 pathway. *FEBS Lett* **564**, 85-90 (2004).

36. Comery TA*, et al.* Abnormal dendritic spines in fragile X knockout mice: maturation and pruning deficits. *Proc Natl Acad Sci U S A* **94**, 5401-5404 (1997).

37. Zeier Z, Kumar A, Bodhinathan K, Feller JA, Foster TC, Bloom DC. Fragile X mental retardation protein replacement restores hippocampal synaptic function in a mouse model of fragile X syndrome. *Gene Ther* **16**, 1122-1129 (2009).

38. Martin S, Bouschet T, Jenkins EL, Nishimune A, Henley JM. Bidirectional regulation of kainate receptor surface expression in hippocampal neurons. *J Biol Chem* **283**, 36435-36440 (2008).

39. Xiong H*, et al.* mTOR is essential for corticosteroid effects on hippocampal AMPA receptor function and fear memory. *Learn Mem* **22**, 577-583 (2015).

40. Xiong H*, et al.* Interactions between N-Ethylmaleimide-sensitive factor and GluA2 contribute to effects of glucocorticoid hormones on AMPA receptor function in the rodent hippocampus. *Hippocampus* **26**, 848-856 (2016).

41. Suvrathan A, Hoeffer CA, Wong H, Klann E, Chattarji S. Characterization and reversal of synaptic defects in the amygdala in a mouse model of fragile X syndrome. *Proc Natl Acad Sci U S A* **107**, 11591-11596 (2010).

42. Scharkowski F, Frotscher M, Lutz D, Korte M, Michaelsen-Preusse K. Altered Connectivity and Synapse Maturation of the Hippocampal Mossy Fiber Pathway in a Mouse Model of the Fragile X Syndrome. *Cereb Cortex*, (2017).

43. Gocel J, Larson J. Synaptic NMDA receptor-mediated currents in anterior piriform cortex are reduced in the adult fragile X mouse. *Neuroscience* **221**, 170-181 (2012).

44. Ifrim MF, Williams KR, Bassell GJ. Single-Molecule Imaging of PSD-95 mRNA Translation in Dendrites and Its Dysregulation in a Mouse Model of Fragile X Syndrome. *J Neurosci* **35**, 7116-7130 (2015).

45. Kanai Y, Dohmae N, Hirokawa N. Kinesin transports RNA: isolation and characterization of an RNA-transporting granule. *Neuron* **43**, 513-525 (2004).

46. Elvira G*, et al.* Characterization of an RNA granule from developing brain. *Mol Cell Proteomics* **5**, 635-651 (2006).

47. Adinolfi S*, et al.* The N-terminus of the fragile X mental retardation protein contains a novel domain involved in dimerization and RNA binding. *Biochemistry* **42**, 10437-10444 (2003).

48. Casse F, Martin S. Tracking the activity-dependent diffusion of synaptic proteins using restricted photoconversion of Dendra2. *Front Cell Neurosci* **9**, 367 (2015).

49. Gurskaya NG*, et al.* Engineering of a monomeric green-to-red photoactivatable fluorescent protein induced by blue light. *Nat Biotechnol* **24**, 461-465 (2006).

50. Chudakov DM, Lukyanov S, Lukyanov KA. Tracking intracellular protein movements using photoswitchable fluorescent proteins PS-CFP2 and Dendra2. *Nat Protoc* **2**, 2024-2032 (2007).

51. Antar LN, Afroz R, Dictenberg JB, Carroll RC, Bassell GJ. Metabotropic glutamate receptor activation regulates fragile x mental retardation protein and FMR1 mRNA localization differentially in dendrites and at synapses. *J Neurosci* **24**, 2648-2655 (2004).

52. Dictenberg JB, Swanger SA, Antar LN, Singer RH, Bassell GJ. A direct role for FMRP in activity-dependent dendritic mRNA transport links filopodial-spine morphogenesis to fragile X syndrome. *Dev Cell* **14**, 926-939 (2008).

53. Chao HW, Hong CJ, Huang TN, Lin YL, Hsueh YP. SUMOylation of the MAGUK protein CASK regulates dendritic spinogenesis. *J Cell Biol* **182**, 141-155 (2008).

54. Ceman S, O'Donnell WT, Reed M, Patton S, Pohl J, Warren ST. Phosphorylation influences the translation state of FMRP-associated polyribosomes. *Hum Mol Genet* **12**, 3295-3305 (2003).

55. Narayanan U*, et al.* S6K1 phosphorylates and regulates fragile X mental retardation protein (FMRP) with the neuronal protein synthesis-dependent mammalian target of rapamycin (mTOR) signaling cascade. *J Biol Chem* **283**, 18478-18482 (2008).

56. Quartier A*, et al.* Intragenic FMR1 disease-causing variants: a significant mutational mechanism leading to Fragile-X syndrome. *Eur J Hum Genet* **25**, 423-431 (2017).

57. Myrick LK, Nakamoto-Kinoshita M, Lindor NM, Kirmani S, Cheng X, Warren ST. Fragile X syndrome due to a missense mutation. *Eur J Hum Genet* **22**, 1185-1189 (2014).

58. Myrick LK*, et al.* Independent role for presynaptic FMRP revealed by an FMR1 missense mutation associated with intellectual disability and seizures. *Proc Natl Acad Sci U S A* **112**, 949-956 (2015).

59. Hu Y*, et al.* The amino-terminal structure of human fragile X mental retardation protein obtained using precipitant-immobilized imprinted polymers. *Nat Commun* **6**, 6634 (2015).

60. Myrick LK, Hashimoto H, Cheng X, Warren ST. Human FMRP contains an integral tandem Agenet (Tudor) and KH motif in the amino terminal domain. *Hum Mol Genet* **24**, 1733-1740 (2015).

61. Richmond TJ. Solvent accessible surface area and excluded volume in proteins. Analytical equations for overlapping spheres and implications for the hydrophobic effect. *J Mol Biol* **178**, 63-89 (1984).

62. Cappadocia L*, et al.* Structural and functional characterization of the phosphorylation-dependent interaction between PML and SUMO1. *Structure* **23**, 126-138 (2015).

63. Sittler A, Devys D, Weber C, Mandel JL. Alternative splicing of exon 14 determines nuclear or cytoplasmic localisation of fmr1 protein isoforms. *Hum Mol Genet* **5**, 95-102 (1996).

64. Hafner M*, et al.* Transcriptome-wide identification of RNA-binding protein and microRNA target sites by PAR-CLIP. *Cell* **141**, 129-141 (2010).

65. Khandjian EW*, et al.* Novel isoforms of the fragile X related protein FXR1P are expressed during myogenesis. *Hum Mol Genet* **7**, 2121-2128 (1998).

66. Bolte S, Cordelieres FP. A guided tour into subcellular colocalization analysis in light microscopy. *J Microsc* **224**, 213-232 (2006).

67. Rodriguez A, Ehlenberger DB, Dickstein DL, Hof PR, Wearne SL. Automated three-dimensional detection and shape classification of dendritic spines from fluorescence microscopy images. *PLoS One* **3**, e1997 (2008).

68. Becker W, Bergmann A, Hink MA, Konig K, Benndorf K, Biskup C. Fluorescence lifetime imaging by time-correlated single-photon counting. *Microsc Res Tech* **63**, 58-66 (2004).

69. Lakowicz JR. Principles of frequency-domain fluorescence spectroscopy and applications to cell membranes. *Subcell Biochem* **13**, 89-126 (1988).

Acknowledgements

We thank J. Henley, F. Melchior, G. Bossis, Y. Uchimura and H. Saitoh for sharing DNA plasmids and H. Leonhardt for the generous gift of mCherry antibodies. We gratefully acknowledge Rob Willemsen (Rotterdam, Nl) for the gift of *Fmr1*$^{-/y}$ mice. We also thank L. Davidovic and Samantha Zongaro for helpful discussion in the initial step of the work and F. Aguila for excellent artwork. We gratefully acknowledge the 'Fondation pour la Recherche Médicale' (Equipe labellisée #DEQ20111223747 to SM; #DEQ20140329490 to BB; #DEQ20110421309 to ED), the 'Agence Nationale de la Recherche' (ANR-15-CE16-0015-01 to SM, ANR-12-BSV4-0020, ANR-12-SVSE8-0022 and ANR-15-CE16-0015-02 to BB, ANR-13-BVS4-0009 to ED), the FRAXA foundation to TM, the French Muscular Dystrophy Association AFM-Téléthon to ED, the 'Jérôme Lejeune' (SM and BB) and 'Bettencourt-Schueller' (SM) foundations for financial support. We also thank the French Government for the "Investments for the Future" LabEx 'SIGNALIFE' (ANR-11-LABX-0028-01), LabEx 'ICST' (ANR-11-LABX-0015-01), the CNRS LIA "Neogenex" and the CG06 (AAP santé), GIS IBiSA (AO 2014) and Région PACA for the Microscopy and Imaging Côte d'Azur (MICA) platform funding. MPri, LS and SC are fellows from the international PhD "Signalife" LabEx program.

Author contributions

AK performed the majority of fixed granule work and all the neuronal architecture imaging experiments and some biochemistry. CG performed most of the molecular cloning, bacterial sumoylation assays, some of the bioinformatic analyses and some of the endogenous SUMO-protein work. AK, CL, FC, LS, AF, MPri, MPro and GP prepared neuronal cultures and biochemical tools. MC and ED performed and analyzed electrophysiology experiments. GP prepared viral particles and achieved the FMRP dimerization / sumoylation experiments. TM

and AK performed and analyzed CLIP experiments. SC and TM performed calcium imaging. FD and FBe performed and analyzed smFISH experiments. RG performed FMRP structural analysis with help from CG. FC and SM performed live-cell imaging experiments. FBr provided computational tools to analyze live imaging data. DA performed and analyzed FLIM experiments. BB provided some FMRP coding cDNAs and antibodies as well as input for the mRNA work. AK, CG and SM contributed to hypothesis development, experimental design and data interpretation. SM provided the overall supervision, the funding and wrote the article. All authors discussed the data and commented on the manuscript.

Competing financial interests: The authors declare no competing financial interests.

Figure legends

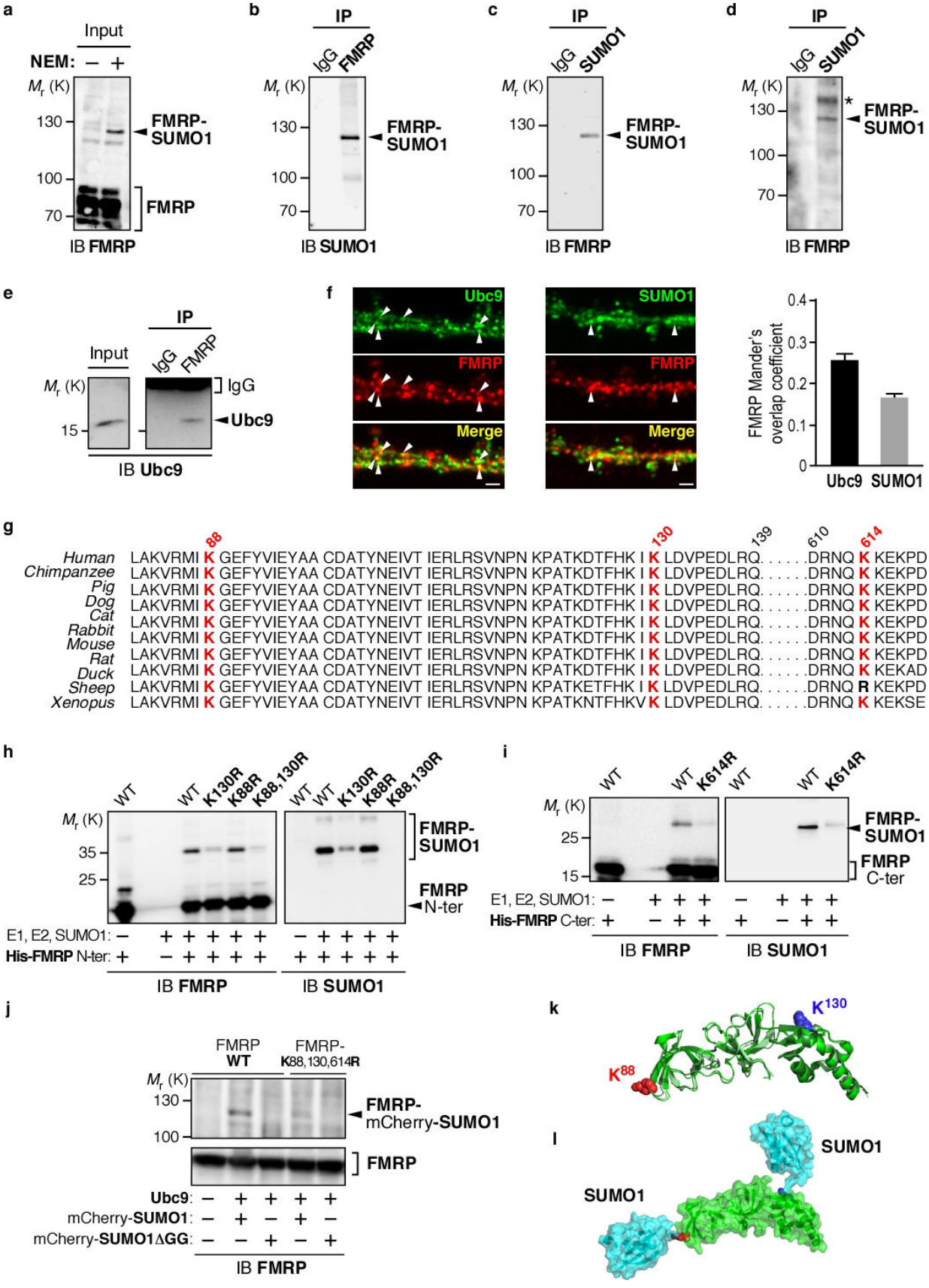

Figure 1

Figure 1. **FMRP is sumoylated *in vivo* in the rat and mouse brain and the SUMO system targets the conserved residues K88, 130 and 614 of FMRP**. **(a)** Representative immunoblot anti-FMRP (Ab#056) of P7 post-nuclear rat brain extracts prepared or not in the presence of the cysteine protease inhibitor NEM to prevent desumoylation. **(b)** Immunoblot anti-SUMO1 of NEM-treated P7 post-nuclear rat brain extracts subjected to immunoprecipitation with FMRP (Ab#056) antibody or control IgG. **(c)** Converse immunoblot with anti-FMRP (Ab#056) antibody of NEM-treated P7 post-nuclear rat brain extracts subjected to immunoprecipitation with SUMO1 antibody or control IgG. **(d)** Immunoblot anti-SUMO1 of NEM-treated P1 post-nuclear mouse brain extracts subjected to immunoprecipitation with FMRP (Ab#056) antibody or control IgG. *Non-specific band. **(e)** Immunoblot of post-nuclear mouse brain extracts (input) subjected to immunoprecipitation with FMRP antibody or control IgG and probed with anti-Ubc9 antibody. **(f)** Colocalisation assays performed on cultured mouse neurons (20 DIV) with antibodies directed against Ubc9, FMRP (Ab#4317), SUMO1. Bar, 2 μm. Degree of colocalisation (Manders' coefficient) between FMRP and Ubc9 or SUMO1. N = 3 independent primary cultures with 60 dendrites analyzed for each condition. **(g)** Sequence alignments showing the evolutionary conservation of the potential SUMO-targeted lysine residues (stars) within the consensus sumoylation sites of FMRP. **(h,i)** Bacterial sumoylation assay. Representative immunoblots of purified fractions of N- and C-terminal WT or mutated parts of His-FMRP in a recombinant bacterial system and probed with anti-FMRP (**h**, Ab#1C3) or (**i**, #17722) and anti-SUMO1 antibodies as indicated. **(j)** COS7 sumoylation assay. Immunoblots with anti-FMRP (Ab#056) antibody of full-length WT or lysine-mutated FMRP expressed in COS7 cells with mcherry-SUMO1 WT or mutated (ΔGG) to prevent its conjugation. **(k)** X-ray structures fitted of three human N-terminal FMRP (PDB: 4OVA in green, 4QVZ in light green, 4QW2 in dark green) shown in cartoon representation. K88 and K130 are shown in sphere representation in red and blue respectively. **(l)** Model of FMRP (PDB: 4OVA) and SUMO1 (PDB: 4WJQ) structural links in cartoon and surface representation (with transparency) respectively in green and light blue. Lysine residues 88 and 130 of FMRP are shown in sphere representation in red and blue respectively.

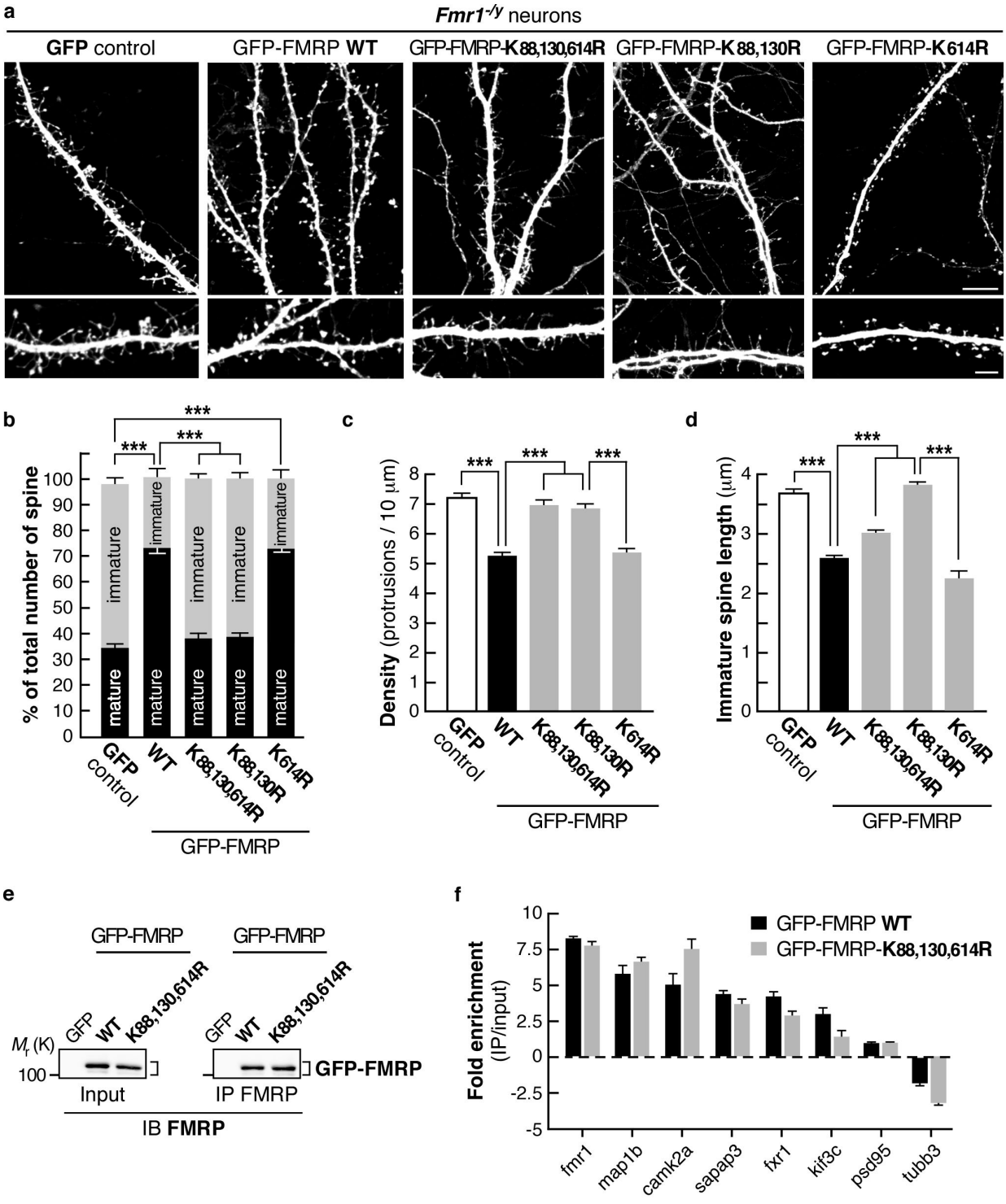

Figure 2

Figure 2. **The N-terminal sumoylation of FMRP is involved in the regulation of the spine density and maturation**. **(a)** Representative confocal images of dendrites from transduced *Fmr1*$^{-/y}$ neurons expressing free GFP, the WT or the non-sumoylatable K88,130,614R, K88,130R or K614R forms of GFP-FMRP for 24h. Bar, 10 µm. Enlargements of dendrites are

also shown. Bar, 5 μm. Histograms show the relative proportion of mature and immature dendritic spines **(b)** and the density of the protrusions **(c)** in GFP, in WT and mutated GFP-FMRP-expressing cells as shown in **(a)**. **(d)** Histograms of immature spine length measured from *Fmr1*$^{-/y}$ neurons expressing the indicated constructs. Data shown in **b-d** are the mean ± s.e.m and statistical significance determined by a one-way analysis of variance (ANOVA) with a Bonferonni post-test. N = ~4500 protrusions per condition from 4 independent experiments. ***p<0.001. **(e,f)** CLIP analysis from transduced *Fmr1*$^{-/y}$ cortical neurons expressing the WT or the K88,130,614R form of GFP-FMRP revealed that they bind the same RNA repertoire. **(e)** Representative immunoblots anti-FMRP of the indicated neuronal extracts subjected or not (Input) to immunoprecipitation (IP) with FMRP antibodies. GFP-expressing *Fmr1*$^{-/y}$ neurons were used as a negative control. **(f)** Enrichment (CLIPed/Input) of a set of FMRP-target RNA fragments in the indicated conditions. Several known RNA targets of FMRP (*fmr1, map1b, camk2a, sapap3, fxr1, kif3c and psd95*) as well as a non-targeted RNA (*tubb3*) were detected by quantitative PCR. Fold enrichment were calculated as described in the method section and did not show any statistical differences.

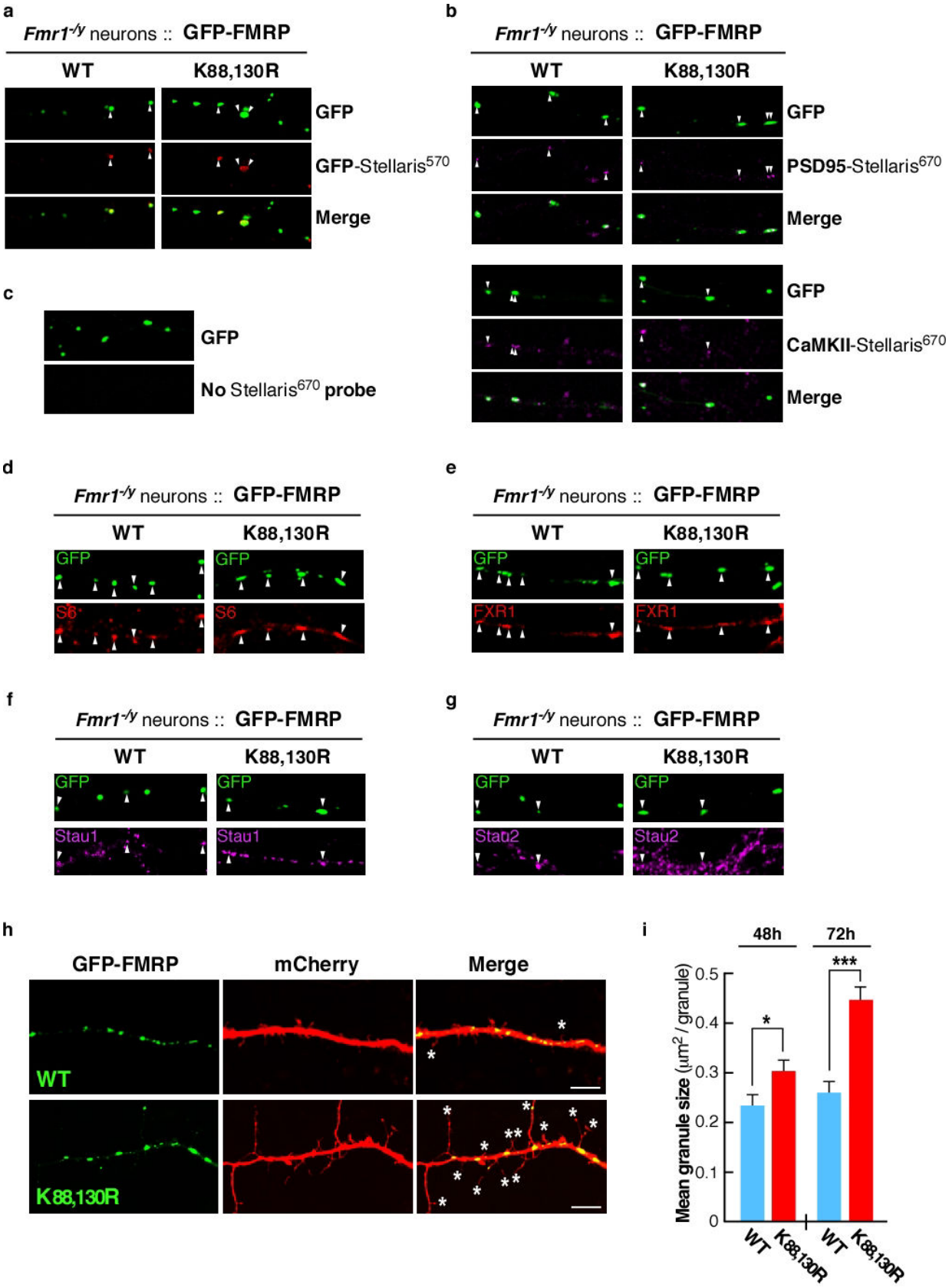
a
Fmr1-/y neurons :: GFP-FMRP
WT
K88,130R
GFP
GFP-Stellaris570
Merge
b
Fmr1-/y neurons :: GFP-FMRP
WT
K88,130R
GFP
PSD95-Stellaris670
Merge
GFP
CaMKII-Stellaris670
Merge
c
GFP
No Stellaris670 probe
d
Fmr1-/y neurons :: GFP-FMRP
WT
K88,130R
GFP
S6
e
Fmr1-/y neurons :: GFP-FMRP
WT
K88,130R
GFP
FXR1
f
Fmr1-/y neurons :: GFP-FMRP
WT
K88,130R
GFP
Stau1
g
Fmr1-/y neurons :: GFP-FMRP
WT
K88,130R
GFP
Stau2
h
GFP-FMRP
mCherry
Merge
WT
K88,130R
i
48h
72h
Mean granule size (µm2 / granule)
0.5
0.4
0.3
0.2
0.1
0
WT
K88,130R
WT
K88,130R

Figure 3

Figure 3. **Preventing FMRP sumoylation drastically impacts on the size of dendritic FMRP-containing mRNA granules**. **(a-c)** Representative images of WT and K88,130R GFP-FMRP expressing *Fmr1*$^{-/y}$ dendrites were hybridized with GFP **(a)**, PSD-95 **(b)** or CaMKII mRNA **(b)** using Stellaris probes. Arrowheads show the colocalisation between the indicated Stellaris signals and the GFP-FMRP granules. **(c)** GFP-FMRP-transfected neurons with no Stellaris probes were used as FISH controls. **(d-g)** Colocalisation assays performed on WT and K88,130R GFP-FMRP expressing *Fmr1*$^{-/y}$ neurons with antibodies directed against the S6 ribosomal protein **(d)**, FXR1 **(e)** and the RNA-binding proteins Staufen 1 **(f)** and Staufen 2 **(g)**. Arrowheads indicate the colocalisation with the GFP-FMRP positive mRNA granules. **(h)** Representative confocal images of dendrites from co-transfected *Fmr1*$^{-/y}$ neurons co-expressing free mCherry with either the WT or the K88,130R form of GFP-FMRP for 72h. Bar, 5 μm. **(i)** Histograms show the mean size of dendritic GFP-FMRP granules after 48h and 72h of expression. N = 190-460 granules per condition from 3-4 separate experiments. Data shown in **i** are the mean ± s.e.m. and statistical significance was determined using Unpaired t-test. *$p<0.05$; ***$p<0.0001$.

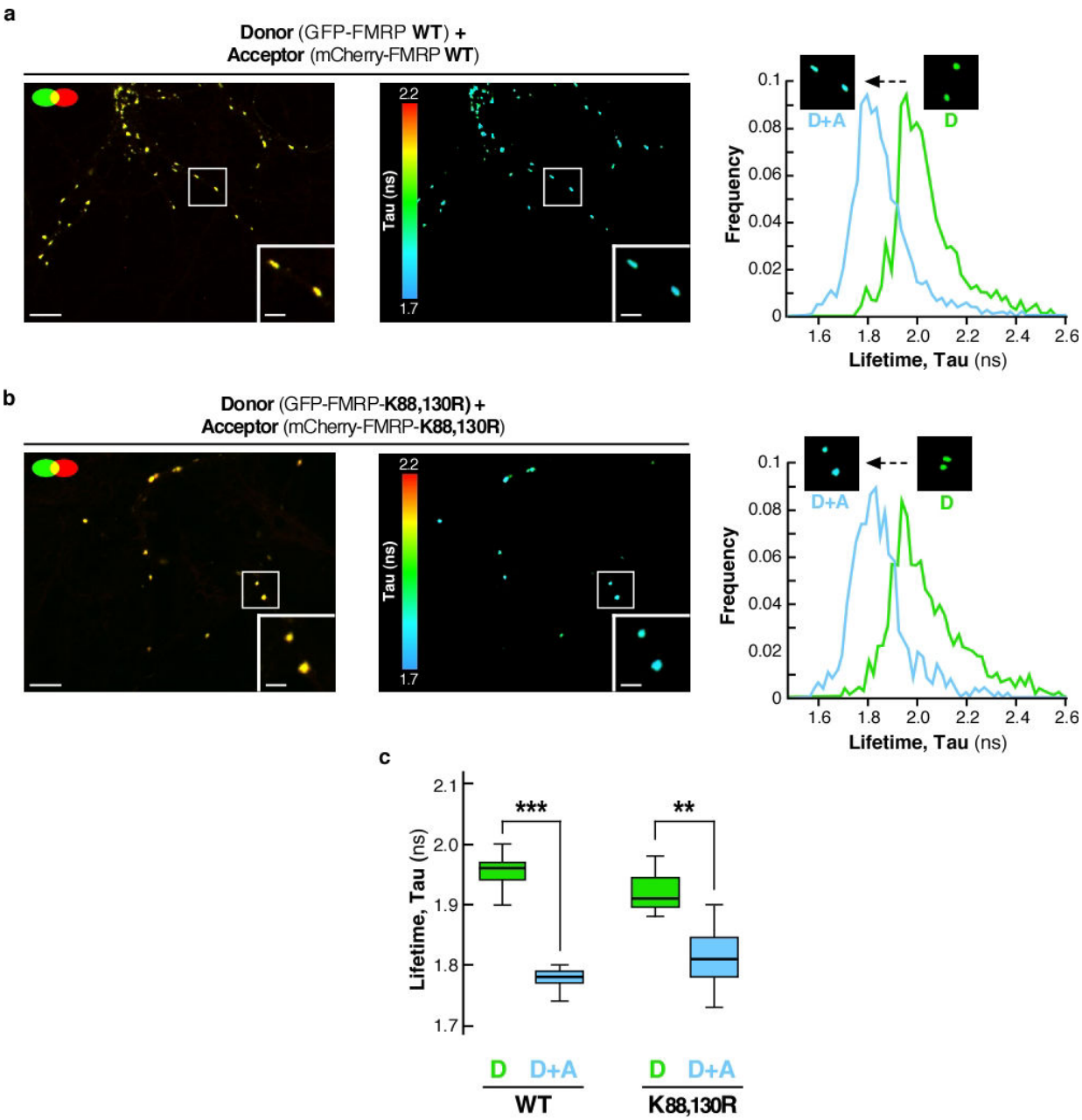

Figure 4

Figure 4. **Preventing the N-terminal sumoylation of FMRP by the K88,130R mutation does not alter the homomeric FMRP-FMRP interaction within dendritic mRNA granules.** **(a,c)** Analysis of GFP-FMRP/mCherry-FMRP interaction within dendritic mRNA granules by Fluorescence Life Time Imaging (FLIM). Representative confocal images showing the colocalisation of the WT **(a)** or the K88,130R **(b)** forms of GFP-FMRP and mCherry-FMRP (left images) in dendritic granules. FLIM images of the same field are shown on the right images **(a,b)** where fluorescence lifetime is represented using a pseudo-color scale ranging from 1.7 to 2.2 ns. Insets show representative clusters for each condition The third row represents the distribution histograms of GFP-FMRP fluorescence lifetime of the Donor (D)

alone in green and the Donor + Acceptor (D+A) in blue. FLIM images corresponding to the Donor alone condition are displayed in **Supplementary Fig. 3b**. **(c)** Box and whiskers plots show the variation of the lifetime determined from FLIM curves. This representation displays upper and lower quartiles, maximum and minimum values in addition to median. N = 114-189 granules per condition from 3 separate experiments. Statistical significance in **(c)** was determined by a non-parametric Mann-Whitney test. **p<0.01; ***p<0.0001.

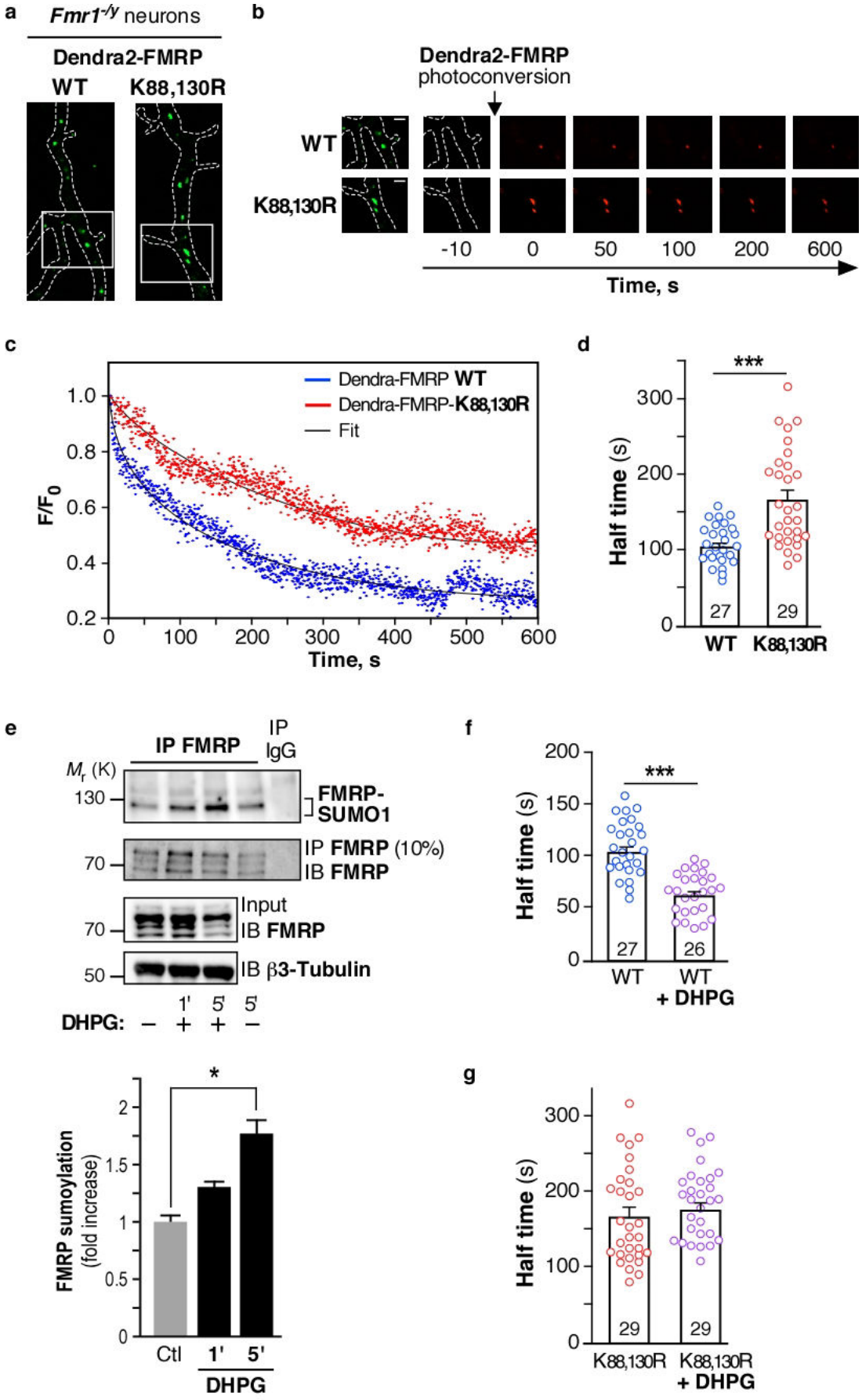
a
Fmr1-/y neurons
Dendra2-FMRP
WT
K88,130R
b
Dendra2-FMRP
photoconversion
WT
K88,130R
-10
0
50
100
200
600
Time, s
c
Dendra-FMRP WT
Dendra-FMRP-K88,130R
Fit
F/F0
Time, s
d
***
Half time (s)
27
29
WT
K88,130R
e
IP FMRP
IP
IgG
Mr (K)
130
FMRP-
SUMO1
70
IP FMRP (10%)
IB FMRP
Input
70
IB FMRP
50
IB β3-Tubulin
DHPG:
1'
5'
5'
f
***
Half time (s)
27
26
WT
WT
+ DHPG
*
FMRP sumoylation
(fold increase)
Ctl
1'
5'
DHPG
g
Half time (s)
29
29
K88,130R
K88,130R
+ DHPG

Figure 5

Figure 5. **Activation of mGlu5 receptors promotes FMRP sumoylation and leads to the release of FMRP from dendritic mRNA granules**. **(a)** Images of transfected *Fmr1*$^{-/y}$ dendrites expressing the WT or the non-sumoylatable K88,130R forms of GFP-FMRP before Dendra2-FMRP photoconversion are shown. **(b)** Time lapse series of confocal images of photoconverted Dendra2-FMRP red fluorescence in dendritic granules in basal unstimulated conditions. Enlargement of dendritic granules from the boxed area in (**a**) is also shown on the left. The decrease in red photoconverted Dendra2-FMRP fluorescence was then monitored over time. Scale bar, 1 μm. **(c)** Representative sample recording traces of normalized fluorescence from photoconverted WT or mutated Dendra2-FMRP in individual granules in basal unstimulated conditions. The thin traces (black) represent the corresponding fits. **(d)** Histograms with scatter plots of computed half time of photoconverted WT and K88,130R Dendra2-FMRP fluorescence diffusion in granules in basal conditions. The number of photoconverted granules is indicated on the bars. **(e)** Immunoprecipitation of FMRP (Ab#046) and immunoblotting for SUMO1. Control for the immunoprecipitated FMRP fractions is also depicted. Input lanes for FMRP and β3-tubulin are also shown. Quantification for DHPG-induced endogenous FMRP sumoylation in neurons over time is also indicated. The data are from three separate experiments and show the mean ± s.e.m. *p=0.0213. **(f)** Histograms with scatter plots of half time of photoconverted Dendra2-FMRP WT fluorescence diffusion in granules from *Fmr1*$^{-/y}$ neurons stimulated with DHPG. The number of photoconverted granules is indicated on the bars and the histogram/scatter plot in absence of stimulation is taken from **(d)**. **(g)** Histograms with scatter plots of half time of photoconverted Dendra2-FMRP-K88,130R fluorescence diffusion in granules in basal and DHPG-stimulated conditions. The histogram/scatter plot in absence of stimulation is taken from **(d)**. The number of photoconverted granules is indicated on the bars. Data shown in **d-f** and **g** are the mean ± s.e.m. Statistical significance in **d,f** and **g** was determined using a non-parametric Mann-Whitney test. Statistical significance in **(e)** was determined by an ANOVA with a Bonferroni post-test. *p<0.05; ***p<0.0001.

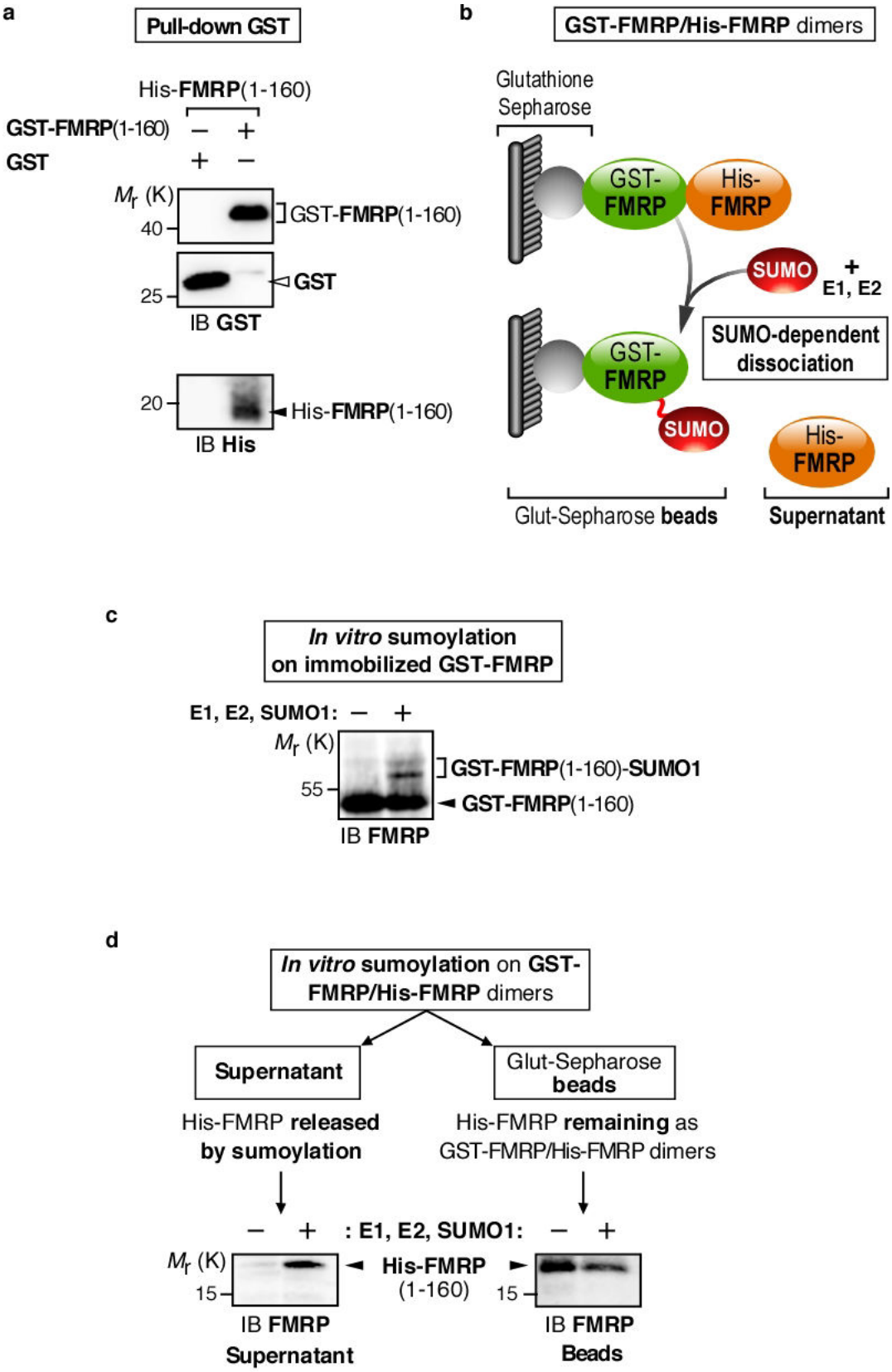
a
Pull-down GST
His-FMRP(1-160)
GST-FMRP(1-160) – +
GST + –
Mr (K)
40
GST-FMRP(1-160)
25
GST
IB GST
20
His-FMRP(1-160)
IB His
b
GST-FMRP/His-FMRP dimers
Glutathione Sepharose
GST-FMRP
His-FMRP
SUMO
+ E1, E2
SUMO-dependent dissociation
GST-FMRP
SUMO
His-FMRP
Glut-Sepharose beads
Supernatant
c
In vitro sumoylation on immobilized GST-FMRP
E1, E2, SUMO1: – +
Mr (K)
55
GST-FMRP(1-160)-SUMO1
GST-FMRP(1-160)
IB FMRP
d
In vitro sumoylation on GST-FMRP/His-FMRP dimers
Supernatant
Glut-Sepharose beads
His-FMRP released by sumoylation
His-FMRP remaining as GST-FMRP/His-FMRP dimers
– + : E1, E2, SUMO1: – +
Mr (K)
15
His-FMRP (1-160)
15
IB FMRP Supernatant
IB FMRP Beads

Figure 6

Figure 6. The N-terminal sumoylation of FMRP dissociates FMRP homomers. **(a)** GST pull-down of purified His-FMRP(1-160aa) with the N-terminal (1-160 amino acids) domain of FMRP fused to the GST protein. Free GST is used as a negative control. **(b)** Schematic diagram of the SUMO-dependent dissociation assay showing the release into the supernatant of His-FMRP from the immobilized sumoylated GST-FMRP fraction. **(c)** *In vitro* sumoylation assay on immobilized GST-FMRP(1-160aa). **(d)** *In vitro* sumoylation assay on GST-FMRP/His-FMRP dimers. Representative immunoblots anti-FMRP (Ab#2F5-1) following the SUMO-dependent dissociation of His-FMRP.

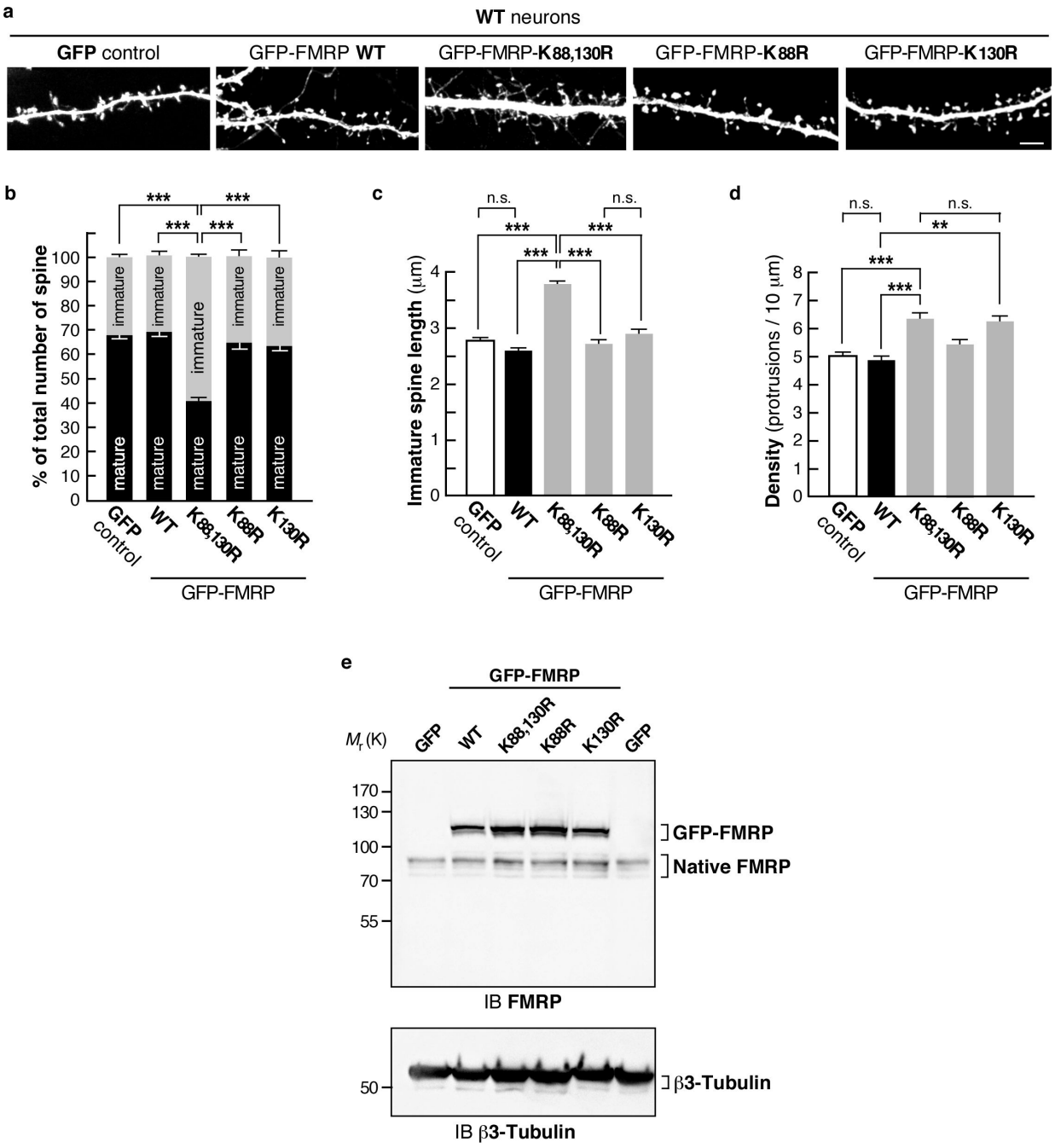

Figure 7

Figure 7. Spine density and maturation processes are intrinsically linked to the ability of FMRP to be sumoylated. (a) Representative confocal images of dendrites from transduced WT neurons expressing free GFP, the WT, K88R, K130R or K88,130R mutant forms of GFP-FMRP for 30h. Bar, 5 μm. Histograms show the relative proportion of mature and immature spines **(b)** and the density of the protrusions **(d)** in the indicated conditions shown in **(a)**. **(c)** Histograms of immature spine length measured from WT neurons expressing the indicated constructs. **(e)** Relative protein expression levels of the WT and mutant forms of GFP-FMRP in WT transduced neurons as in **(a)** showing a ~3-fold increase in the levels of exogenous GFP-

FMRP expression. Data shown in **b-d** are the mean ± s.e.m. Statistical significance in **b-d** was determined by a one-way analysis of variance (ANOVA) with a Bonferroni post-test. N = ~3000 spines per condition from 4 independent experiments. ***p<0.001; n.s, not significant.

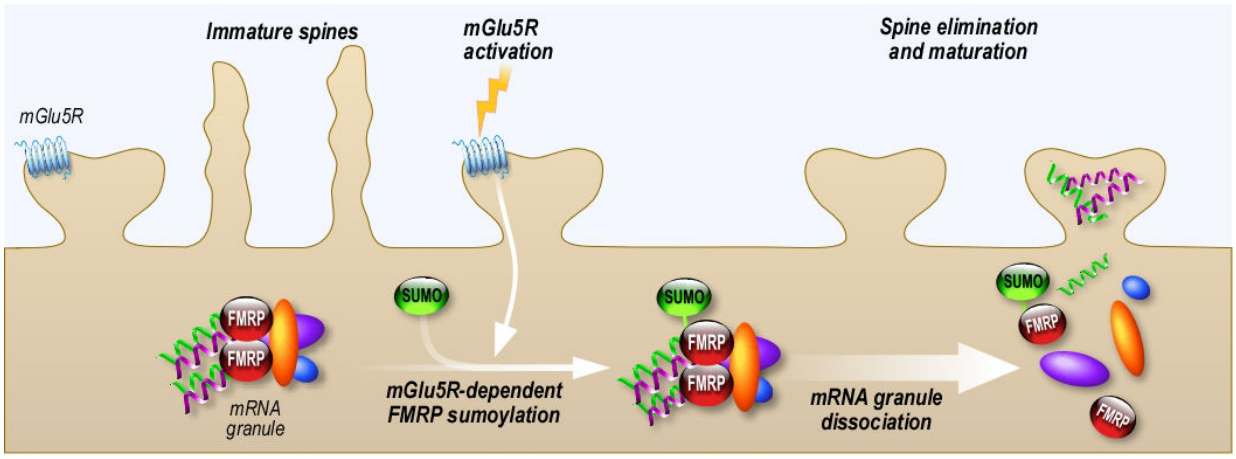

Figure 8

Figure 8. Schematic model for the mGlu5R-dependent regulation of FMRP function via the sumoylation process. The activity-dependent sumoylation of FMRP is a key step to dissociate FMRP from dendritic mRNA granules and consequently to regulate spine elimination and maturation.

Supplementary information

Sumoylation regulates FMRP-mediated dendritic spine elimination and maturation

Khayachi et al.

Supplementary information

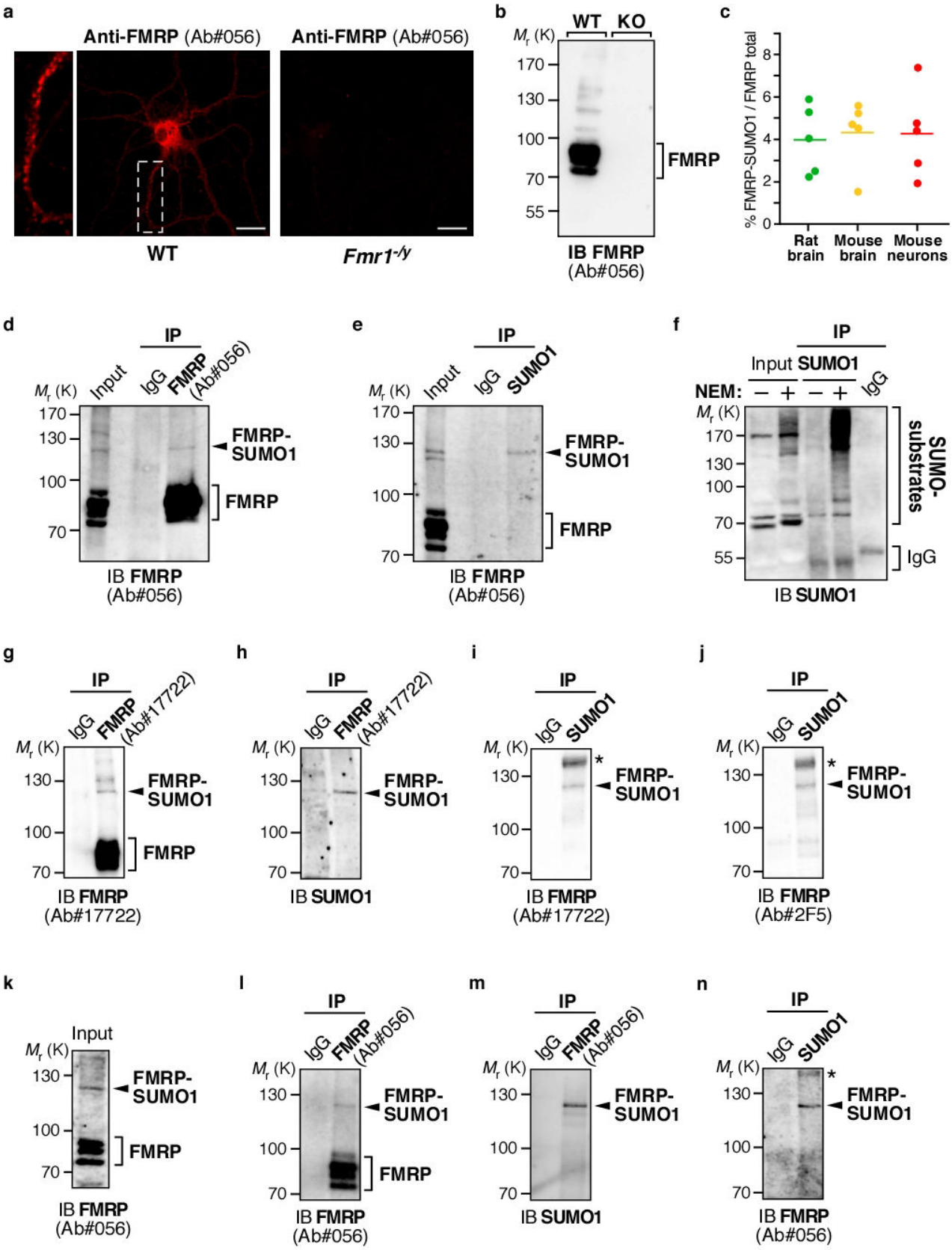

Supplementary Figure 1

Supplementary Figure 1. Characterization of the custom anti-FMRP (Ab#056) antibody and additional evidence for the *in vivo* and *in vitro* sumoylation of FMRP. (a) Immunostaining of

the endogenously expressed FMRP with the custom anti-FMRP antibody (Ab#056; 1 μg/mL) in WT mouse hippocampal neurons (18 DIV). Control immunostaining experiment with the custom anti-FMRP antibody (Ab#056; 1 μg/mL) on 18 DIV *Fmr1*$^{-/y}$ hippocampal neurons. Bar, 20 μm. **(b)** Representative immunoblot with the anti-FMRP (Ab#056) antibody of P7 post-nuclear WT and *Fmr1*$^{-/y}$ mouse brain extracts. **(c)** Scatter plots of the ratio between the intensity of FMRP-SUMO1 and the total amount of FMRP from input lanes (n=5 for each conditions) measured on FMRP immunoblots obtained from rat brain, mouse brain and mouse neuronal homogenates. Statistical analysis using an ANOVA with a Bonferonni post-test revealed no significant differences between the 3 conditions. **(d,e)** Immunoblots with the anti-FMRP (Ab#056) of NEM-treated P7 rat brain extracts subjected to immunoprecipitation with FMRP (Ab#056) **(d)** or anti-SUMO1 **(e)** antibodies. Input and control IgG lanes are also shown on the blots. **(f)** Control experiments demonstrating the protective role of NEM on protein sumoylation. Control and NEM-treated P7 rat brain homogenates were subjected to immunoprecipitation with anti-SUMO1 antibodies. Input and control IgG lanes are also shown on the blots. **(g,h)** Immunoblots with the anti-FMRP (Ab#17722; **g**) or anti-SUMO1 **(h)** antibodies of NEM-treated P7 rat brain extracts subjected to immunoprecipitation with FMRP (Ab#17722) antibody or control IgG. **(i,j)** Immunoblots with the anti-FMRP (**i**, Ab#17722; **j**, Ab#2F5-1) antibodies of NEM-treated P7 rat brain extracts subjected to immunoprecipitation with SUMO1 antibody or control IgG. *****Non-specific band. **(k)** Input blot with the anti-FMRP (Ab#056) antibody on homogenates from 18 DIV NEM-treated rat cortical neurons used in **l** and **m**. **(l,m)** Immunoblots with the anti-FMRP (Ab#056; **l**) or anti-SUMO1 **(m)** antibodies on neuronal extracts shown in **(k)** subjected to immunoprecipitation with FMRP (Ab#056) antibody or control IgG. **(n)** Immunoblot with anti-FMRP (Ab#056) antibody on homogenates from 18 DIV NEM-treated cortical neurons and subjected to immunoprecipitation with SUMO1 specific antibody or control IgG. *****Non-specific band.

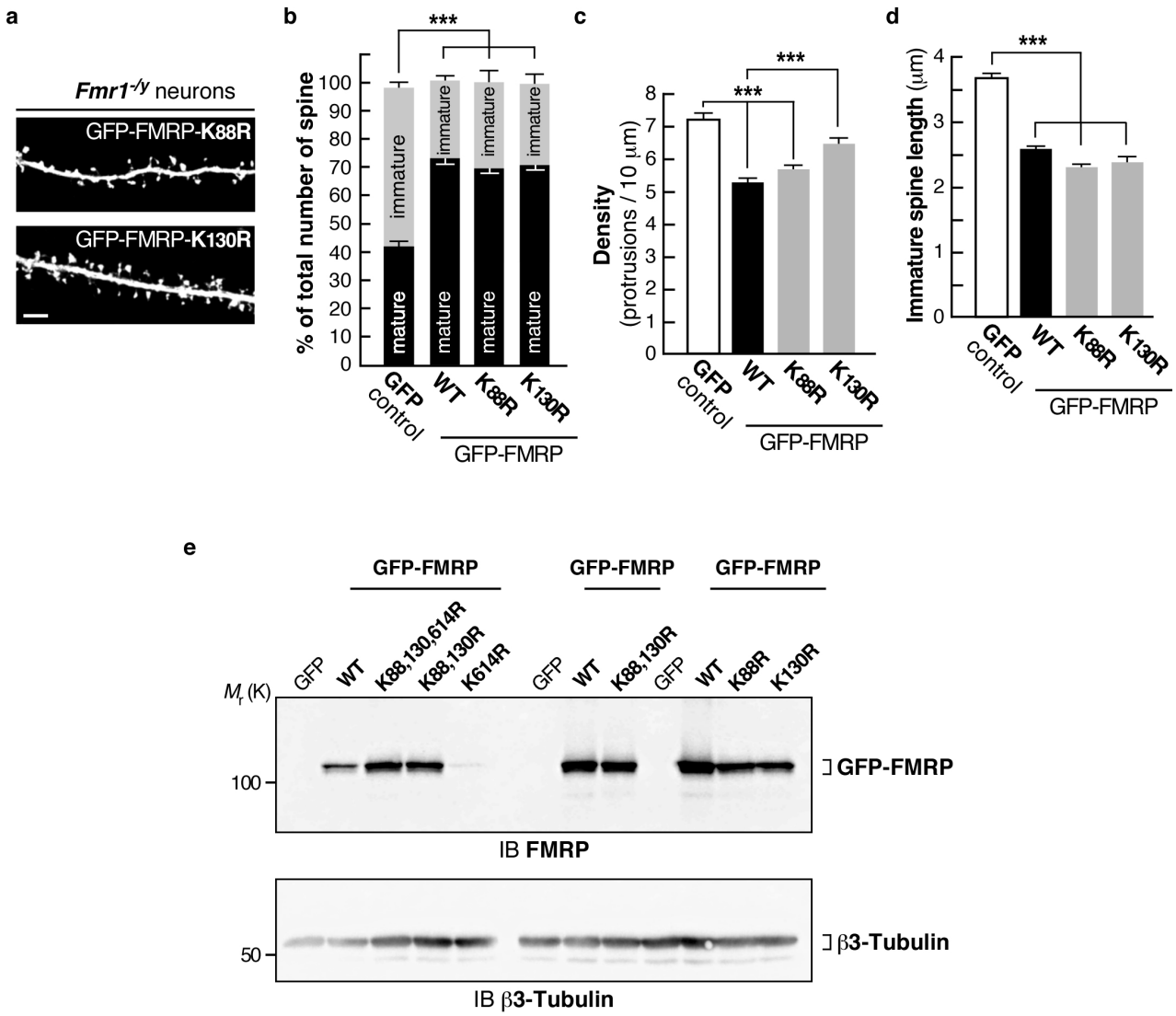

Supplementary Figure 2

Supplementary Figure 2. (a) Representative confocal images of dendrites from transduced *Fmr1*$^{-/y}$ neurons expressing the K88R or K130R mutant forms of GFP-FMRP for 24h. Bar, 5 µm. Histograms show the relative proportion of mature and immature spines **(b)** and the density of the protrusions **(c)** in the indicated conditions. **(d)** Histograms of immature spine length measured from *Fmr1*$^{-/y}$ neurons expressing the indicated constructs. Data shown in **b-d** are the mean ± s.e.m. Statistical significance in **b-d** was determined by a one-way analysis of variance (ANOVA) with a Bonferroni post-test. N = ~4500 spines per condition from 4 independent experiments. ***p<0.001. **(e)** Relative protein expression levels of the WT and mutant forms of GFP-FMRP in *Fmr1*$^{-/y}$ transduced neurons. Input lanes for β3-tubulin are also shown.

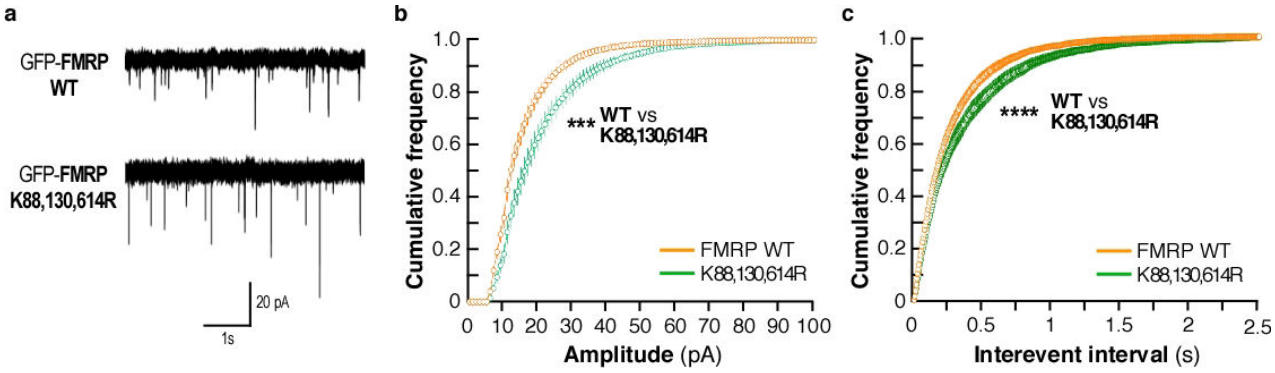

Supplementary Figure 3

Supplementary Figure 3. Sumoylation is involved in the regulation of FMRP function. **(a)** Representative sample traces from **WT** and **K88,130,614R** GFP-FMRP-positive *Fmr1*$^{-/y}$ neurons. Cumulative frequency for amplitudes **(b)** and interevent intervals **(c)** of mEPSCs recorded from GFP-FMRP **WT** and **K88,130,614R** expressing neurons (20 and 19 cells respectively from 4 different cultures). Statistical significance was determined by analysis of the amplitude and interevent interval distributions using a Kolmogorov-Smirnov test. ***p<0.001; ****p<0.0001.

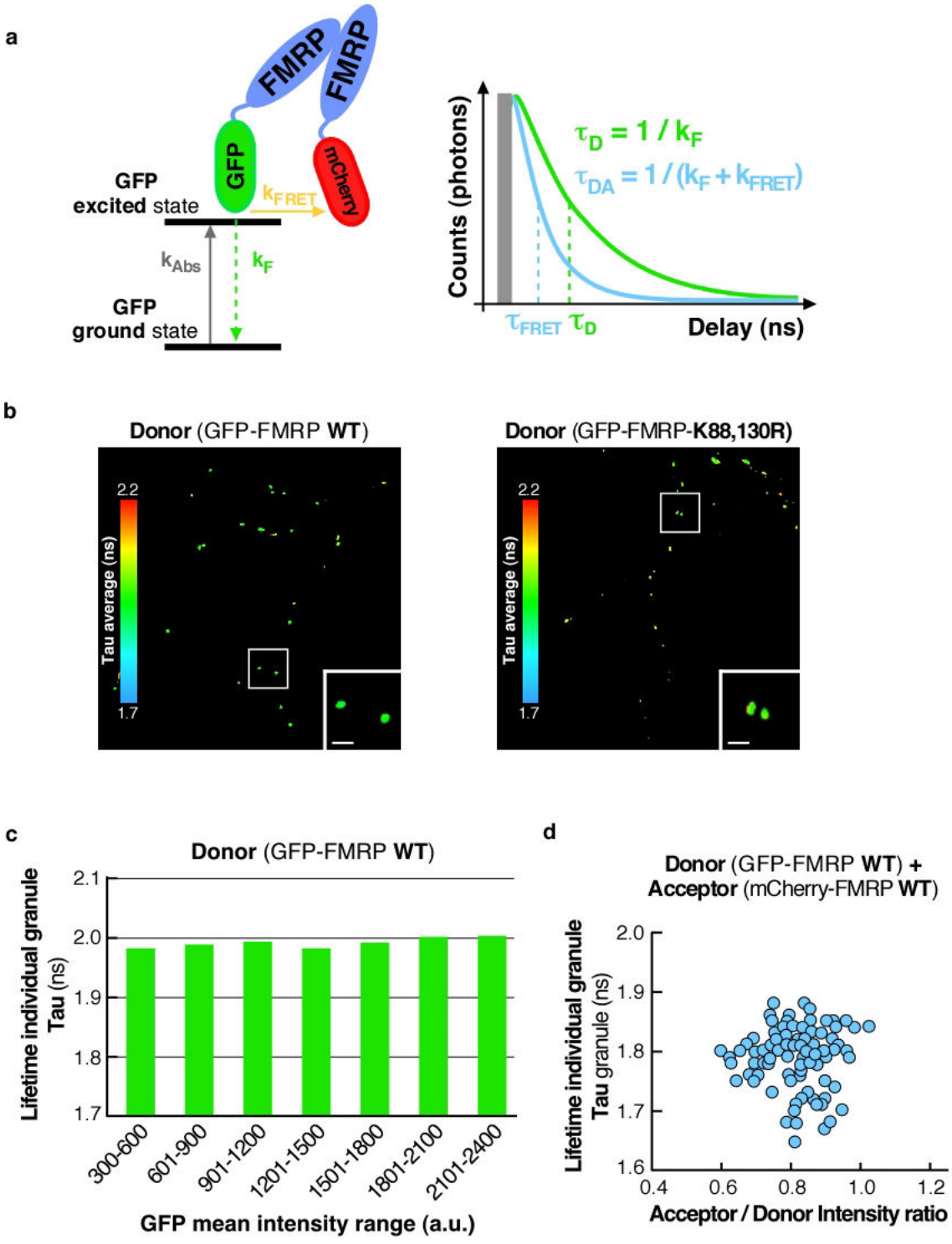

Supplementary Figure 4

Supplementary Figure 4. Control data for the FLIM experiments. (a) Original schematic representation of FLIM. When photophysical criteria are met (spectral overlap, distance…) Donor GFP in the excited state can transfer its energy to the acceptor mCherry. The possibility to relax by FRET provides an additional pathway to the radiative relaxation (emission of a photon).

Therefore the time spent by GFP in the excited state (fluorescence lifetime) is shortened in presence of FRET *i.e.* when the two proteins interact. Fluorescence lifetime can be expressed as a function of the kinetic constants of the relaxation processes (k_F and k_{FRET} for fluorescence and FRET respectively). As a result, the intensity decay in the presence of Acceptor (blue curve) is faster than in the case of Donor alone (green curve). **(b)** FLIM images of GFP-FMRP (Donor, D) alone in the WT and K88,130R forms. Fluorescence lifetime is represented using a pseudo-color scale ranging from 1.7 to 2.2 ns. Insets show representative clusters for each condition. **(c)** Average lifetime of individual granules is invariant with regards to the granule GFP intensity. The histogram represents the average lifetime of GFP-FMRP WT individual granules (n=172) over 3 independent experiments. Fluorescence lifetime was calculated for granules with sufficient photon counts (at least 500 Cnts/pixel and 10^4 Cnts/granule) and which were acquired with a count rate inferior to 4 MHz as detailed in the Methods. **(d)** Average lifetime of individual granules is randomly distributed over A/D intensity ratio. Represented granules correspond to neurons expressing WT forms of GFP-FMRP and mCherry-FMRP (n=171 granules over 2 independent experiments).

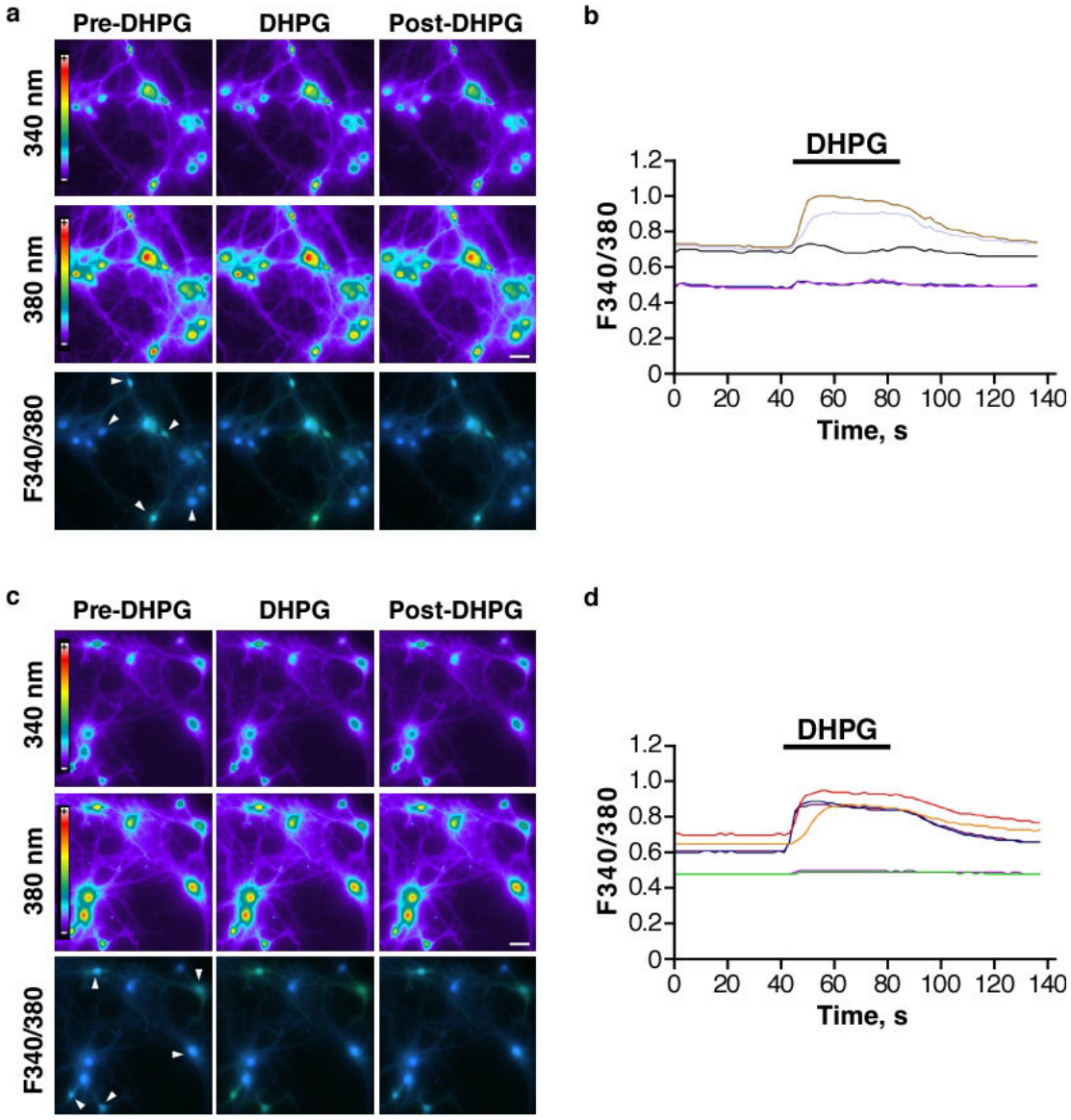

Supplementary figure 5

Supplementary Figure 5. Control intracellular calcium responses evoked by an mGlu5R activation in mouse WT and *Fmr1*$^{-/y}$ neurons. (a,c) Representative pseudocolored images of Fura-2 fluorescence ratio (340/380 nm) showing WT **(a)** and *Fmr1*$^{-/y}$ neurons **(c)** before (pre-DHPG), during (DHPG) and after (post-DHPG) an mGlu5R agonist stimulation. Bar, 20 μm. **(b,d)** Representative traces of Fura-2 fluorescence 340/380 nm ratio (F340/380) overtime showing an increase in intracellular Ca^{2+} concentration both in WT **(b)** and *Fmr1*$^{-/y}$ **(d)** neurons exposed to DHPG. Arrowheads in **(a)** and **(c)** point to neurons in which the F340/380 ratio is shown in **(b)** and **(d)** respectively.

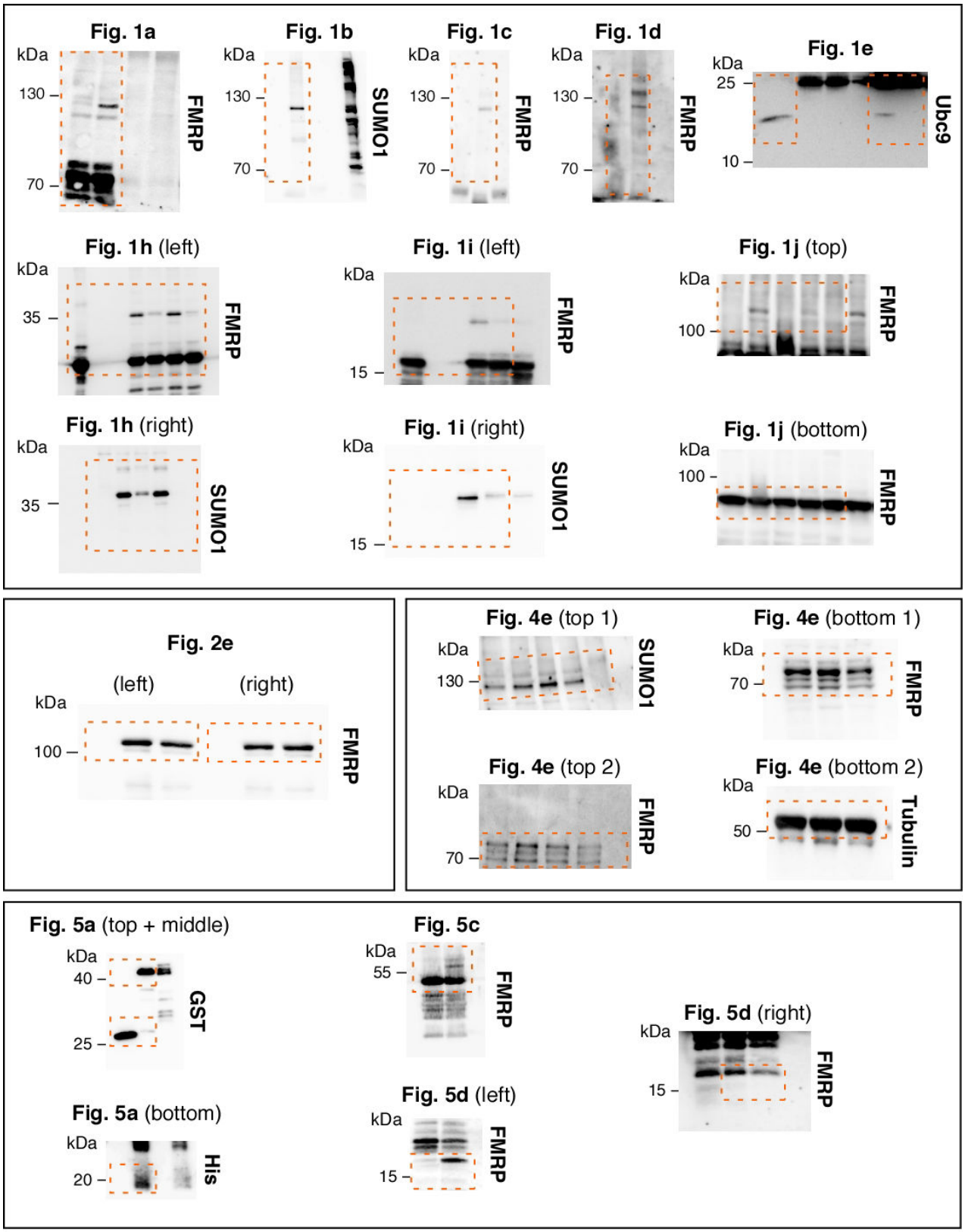

Supplementary figure 6

Supplementary Figure 6. Original uncropped blots. Orange boxed regions represent the portion used in **figures 1 to 5**.

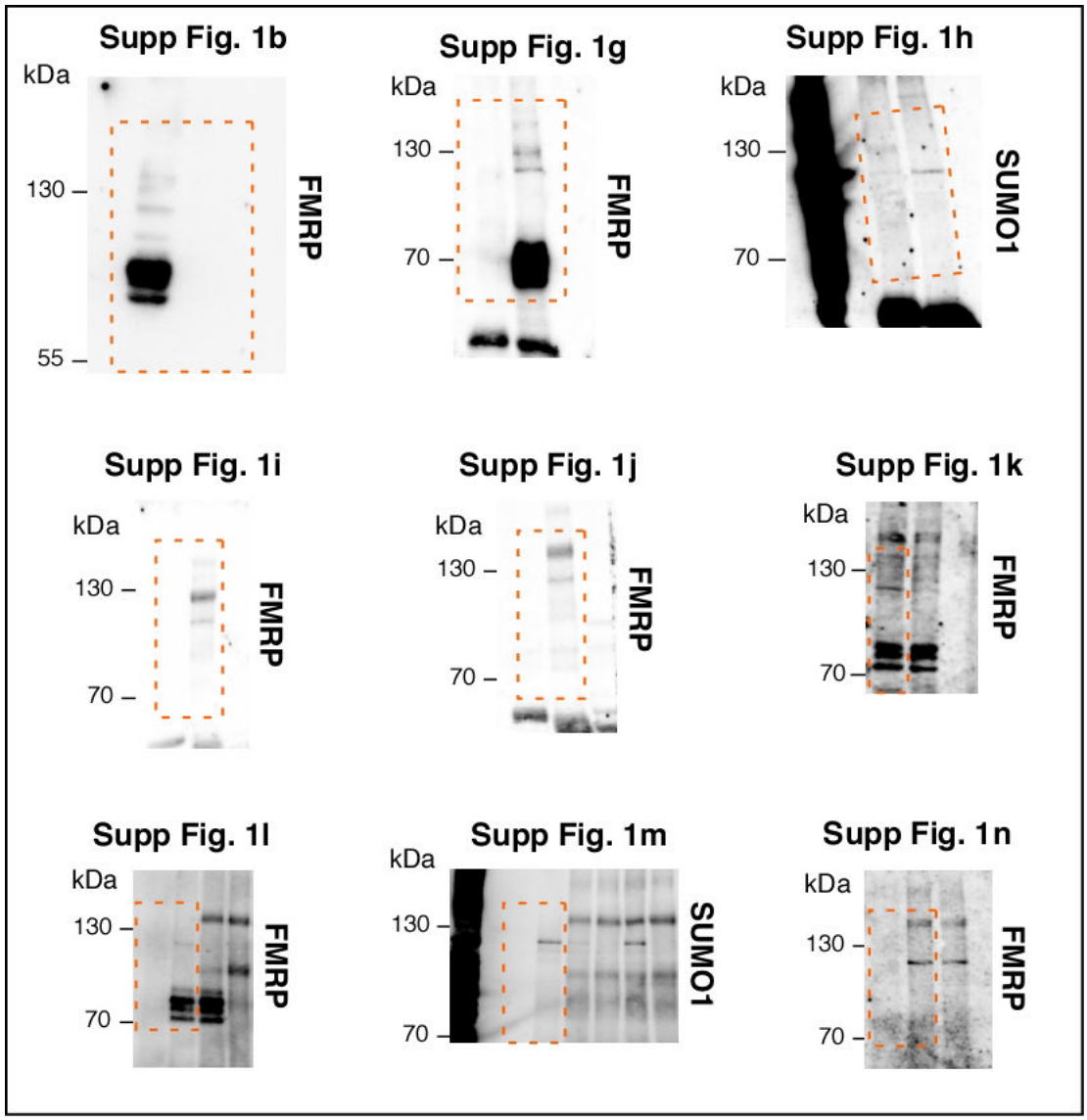

Supplementary figure 7

Supplementary Figure 7. Original uncropped blots. Orange boxed regions represent the portion used in the **Supplementary figure 1**.

ARTICLE 3

The mGlu5R activation regulates synaptic targeting and the level of the desumoylation enzyme SENP1 at synapses

(In preparation)

Lenka Schorova[1], Marie Pronot[1], Gwénola Poupon[1], Marta Prieto[1], Alessandra Folci[1], Anouar Khayachi[1], Frédéric Brau[1], Frédéric Cassé[1], Carole Gwizdek[1] and Stéphane Martin[*,1,2]

[1] Université Côte d'Azur, CNRS, IPMC, France.
[2] Université Côte d'Azur, INSERM, CNRS, IPMC, France.

This research article presents a study that aimed at uncovering the first regulatory pathway of SENP1 at hippocampal synapses. Using a combination of live-cell imaging, biochemistry and cell biology approaches we show that SENP1 spino-dendritic diffusion is regulated by synaptic activity. The underlying mechanism involves a direct activation of mGluR5 receptors, which triggers a dramatic decrease in the exit rate of SENP1 from dendritic spines, consequently leading to an accumulation of SENP1 at postsynaptic sites. We therefore provide the first ever evidence of a regulatory mechanism for the SENP1 enzyme at synapses with possible implications in further research into synaptic functions in health and disease.

This study is the main objective of my PhD thesis project. I have performed most of the experiments and data analyses. Although some supporting experiments will need to be carried out before submission, I anticipate that we will be able to send this report to a high impact factor journal by the end of April 2018.

The mGlu5R activation regulates the synaptic targeting and the level of the desumoylation enzyme SENP1 at synapses

Lenka Schorova[1], Marie Pronot[1], Gwénola Poupon[1], Marta Prieto[1], Alessandra Folci[1], Anouar Khayachi[1], Frédéric Brau[1], Frédéric Cassé[1], Carole Gwizdek[1] and Stéphane Martin[*,1,2]

[1] Université Côte d'Azur, CNRS, IPMC, France.

[2] Université Côte d'Azur, INSERM, CNRS, IPMC, France.

*Correspondence to: Stéphane Martin (martin@ipmc.cnrs.fr)

Institut de Pharmacologie Moléculaire et Cellulaire, Centre National de la Recherche Scientifique, UMR7275, 660 route des lucioles, 06560 Valbonne, France

Phone: (33) 49395-3461; Fax: (33) 49395-7708

Abstract

The sumoylation process is essential to the modulation of protein function, neurotransmission and plasticity and disruption of the sumoylation / desumoylation balance has been associated with several neurological conditions. However, the mechanisms regulating the equilibrium of the SUMO pathway are far from being understood. Here we show that the synapto-dendritic diffusion of the desumoylation enzyme SENP1 is regulated by synaptic activity. Synaptic activation triggers the targeting of SENP1 into dendritic spines independently of its enzymatic activity but via a pathway involving the activation of metabotropic mGlu5 glutamate receptors (mGlu5R). We used restricted photobleaching / photoconversion of individual hippocampal spines to measure the diffusion properties of SENP1 and show that the synaptic exit of SENP1 is decreased upon the activation of mGlu5R. The consequence of this is the enrichment of SENP1 levels at post-synaptic sites upon sustained mGlu5R activation. Altogether, our findings reveal the first activity-dependent regulation of SENP1 diffusion in neurons, which may have important implications for the regulation of the balance between sumoylation and desumoylation at the mammalian synapse.

Introduction

Synapses are highly specialized structures where neuronal transmission takes place. The efficacy of synaptic transmission depends on the correct arrangement of complex protein networks on both sides of the synapse. These dynamic processes are mainly regulated by post-translational modifications (PTMs) such as phosphorylation and ubiquitination[1]. Sumoylation is a PTM that consists in the covalent but reversible enzymatic conjugation of the Small Ubiquitin-like MOdifier (SUMO; ~100 amino acids; ~11 kDa) protein to specific lysine residues of substrate proteins[2,3]. Three functional SUMO proteins, SUMO1 and SUMO2/3, are expressed in the mammalian brain, SUMO2/3 being essentially almost identical. The enzymatic machinery of sumoylation is composed of the E1 heteromeric enzyme SAE1/SAE2, the sole E2 SUMO-conjugating enzyme Ubc9 and an E3 protein that may enhance the sumoylation of specific targets. At the molecular level, sumoylation can induce conformational changes and modulate the dynamics of multi-protein complexes by preventing protein-protein interactions and/or by providing a new platform for the interaction of a novel set of proteins[4,5].

Sumoylation is now clearly seen as a potent post-translational mechanism critical for the regulation of neuronal communication and plasticity[6,7,8]. It influences several aspects of the neuronal function including neurotransmitter release[9,10], spinogenesis[11,12] and synaptic communication[13,14,15]. Our group has also reported the spatiotemporal regulation of the SUMO system in the developing rat brain[16] and that sumoylation *per se* is regulated by neuronal activity[17] and the activation of mGlu5R[17,18].

Importantly, the basal levels of sumoylated proteins in a cell and in specific subcellular compartments must be tightly regulated. This occurs via the coordinated action of the conjugating enzyme Ubc9 and specific desumoylating enzymes called SENPs[19,20]. SENPs form

a family of six paralogs that are responsible for the maturation of SUMO precursors and for the removal of SUMO moieties from their substrate proteins. These enzymes differ in their subcellular localization and their specificity towards SUMO1 or SUMO2/3-modified proteins[19,20].

The sumoylation/desumoylation balance is a highly dynamic process, which allows the cells to specifically and quickly respond to either internal or external signalling cues. Generally, only a small amount of a specific substrate is sumoylated at any given time and space[20,21]. Therefore, the homeostasis of cell sumoylation first relies on the tight balance between the activities of the SUMO-conjugating and deconjugating enzymes but also on their subcellular and temporal localization. However, understanding the mechanisms regulating these enzymes for targeting and/or removal from specific cell compartments in a coordinated manner is absolutely essential to understand how the equilibrium between sumoylation and desumoylation is locally maintained.

Alterations of the sumoylation/desumoylation balance have been clearly linked to several pathological conditions, including cancer[22], neurodevelopmental[6] or neurodegenerative disorders[7,8]. However, despite the increasing number of newly identified SUMO substrates in the mammalian brain[8], the dynamic regulation of the sumoylation/desumoylation balance in neurons and at synapses is still poorly understood.

Here, we characterize the activity-dependent synaptic diffusion of the desumoylating enzyme SENP1 using live-imaging approaches on rat hippocampal neurons. We show that SENP1 is highly mobile in neurons and that its synapto-dendritic mobility is regulated by the activation of metabotropic glutamate 5 receptors (mGlu5R). The sustained activation of mGlu5R leads to

an increased synaptic localization of SENP1 occurring in a desumoylase-independent activity manner. The pharmacological activation of the mGlu5R pathway dramatically decreases the exit rate of SENP1 from dendritic spines resulting in a time-dependent increase in SENP1 at the synapse. Altogether, our data clearly indicate that the reversible synaptic enrichment of SENP1 into spines in mGlu5R-activated neurons is essential to counteract the Ubc9-driven increase in synaptic sumoylation[18] that preceded the synaptic entry of SENP1. We therefore uncovered an activity-dependent pathway for the neuron to control its level of desumoylation enzymes at the mammalian synapse.

Results

The neuronal diffusion of SENP1 is regulated by synaptic activity

The synapto-dendritic diffusion of the sole SUMO conjugating enzyme Ubc9 is regulated by synaptic activity[18]. Since the sumoylation/desumoylation process at synapses has to be balanced, we examine whether neuronal activity also regulates the synaptic diffusion of the desumoylation enzyme SENP1. Thus, we first expressed a GFP-tagged version of the SENP1 enzyme in rat hippocampal neurons **(Fig. 1; Supplementary figure 1)**. As expected, we observed the majority of SENP1 within the nucleus[19,20] indicating that the GFP tag does not impair the nucleocytoplasmic transport of the enzyme **(Supplementary figure 1a,b)**. A diffuse GFP fluorescence was also clearly detected along the dendritic shaft and as a punctuate GFP-SENP1 staining partly matching PSD95-synaptic sites **(Fig. 1a)**. Quantification of the distribution of GFP-SENP1 in basal conditions showed that ~17% of GFP-SENP1 fluorescence is associated with PSD95-positive spines of secondary dendrites **(Fig. 1b)**. A similar distribution was measured for the endogenous SENP1 enzyme with ~13% of the SENP1 immunoreactivity measured in PSD95-positive clusters **(Fig. 1c,d)**.

We then assessed GFP-SENP1 activity by expressing the WT GFP-tagged enzyme or its inactive C603S mutant in COS7 cells (**Fig. 1e-h**). As expected, expression of the WT form of GFP-SENP1 significantly decreased both SUMO1- and SUMO2-modified protein levels. By contrast, expression of the GFP-SENP1-C603S inactive mutant did not affect the overall level of sumoylated proteins (**Fig. 1g,h**). Altogether, these findings indicated that GFP-SENP1 is functional with a subcellular localization similar to the distribution reported for the endogenous desumoylation enzyme[16,17].

To investigate the dynamic redistribution of GFP-SENP1 in activated neurons, we combined time-lapse microscopy with the use of pharmacological drugs to potentiate synaptic activity. To this end, we stimulated GFP-SENP1-expressing hippocampal neurons with the $GABA_A$ receptor inhibitor bicuculline[18] and recorded the redistribution of GFP-SENP1 in real time (**Fig. 2a-c**). Synaptic activation with bicuculline led to a time-dependent increase in GFP-SENP1 localization peaking 25 min after the beginning of the treatment (**Fig. 2a-c; Supplementary video 1**). A concurrent decrease in GFP-SENP1 fluorescence was also measured in the dendritic shaft over the time course of the experiment (**Fig. 2a-c**). Interestingly, GFP-SENP1 fluorescence from the activated spines returned to initial levels when the bicuculline was exchanged for a control solution indicating that this activity-dependent increase in GFP-SENP1 synaptic localization is a fully reversible process (**Fig. 2a-c**). As an additional control, we also verified that the overall distribution of GFP-SENP1 remained unchanged in basal unstimulated conditions over the time course of these experiments (**Fig. 2d,e**).

To assess whether the enhanced bicuculline-induced synaptic SENP1 localization was due to an increased entry in and/or a decreased exit of GFP-SENP1 out of spines, we first assessed the diffusion properties of GFP-SENP1 using spine restricted Fluorescence Recovery After

Photobleaching (FRAP) experiments[18] (**Fig. 3**). To quantitatively measure the synapto-dendritic diffusion of GFP-SENP1, FRAP curves were individually fitted to get values for the mobile fraction and the rate of GFP-SENP1 fluorescence recovery (Half time of recovery; see the Method section for details). The mobile fraction refers to the percentage of GFP-SENP1 that moved from the shaft to the bleached spine area over the time course of the experiment. In unstimulated control conditions, we measured a ~75% recovery of the initial fluorescence indicating that the majority of bleached GFP-SENP1 molecules were dynamically exchanged with fluorescent GFP-SENP1 from the shaft (**Fig. 3d**). In resting neurons, the synaptic rate of GFP-SENP1 fluorescence recovery was ~21 seconds with a resulting diffusion coefficient of 0.0135 $\mu m^2\ s^{-1}$ (**Fig. 3e,f**). Interestingly, increasing synaptic activity by blocking inhibitory $GABA_A$ receptors with bicuculline for 10 to 25 minutes did not affect the ratio of mobile GFP-SENP1 molecules (**Fig. 3a-d**) but significantly increased the half time of GFP-SENP1 fluorescence recovery to 28 seconds (**Fig. 3e**) with the corresponding decrease in GFP-SENP1 diffusion coefficient to 0.010 $\mu m^2\ s^{-1}$ in spines (**Fig. 3f**). Since the mobile fraction of GFP-SENP1 remains unchanged in stimulated conditions concurrently to a delayed synapto-dendritic exchange of the enzyme indicate that there is an increase in the synaptic residency time of GFP-SENP1 in the activated neurons.

Taking into account that there is a time-dependent increase in the synaptic level of GFP-SENP1 in bicuculline-activated neurons, we measured the properties of SENP1 diffusion in sustained, i.e. >25 minutes, bicuculline-treated cells (**Fig. 3e**). Interestingly, the mobile fraction of GFP-SENP1 in spines was significantly decreased to less than 57% of the initial fluorescence indicating that the synapto-dendritic exchange of GFP-SENP1 molecules was dramatically reduced in these experimental conditions (**Fig. 3d**). The synaptic half time recovery of GFP-SENP1 fluorescence and the resulting diffusion coefficient were not significantly different

from values measured upon shorter bicuculline treatment (**Fig. 3e,f**). Altogether, these data suggest that the reduced mobile fraction of GFP-SENP1 is mainly due to a decreased exit of SENP1 from the spine rather than a slower entry rate.

To assess whether the desumoylation enzymatic activity could play a role in the regulation of SENP1 synapto-dendritic mobility, we measured the synaptic diffusion properties of the catalytically inactive SENP1-C603S mutant. We first verified that the C603S point mutation impairs its desumoylation activity **(Fig. 1e,f)**. We then performed FRAP experiments and analyzed the diffusion properties of the inactive GFP-SENP1-C603S in control and bicuculline-stimulated neurons (**Supplementary figure 2**). The mobile fraction in basal conditions was not significantly different from the active enzyme (**Fig. 3e,f**) with ~74% recovery of the initial fluorescence. In resting neurons, the half time of fluorescence recovery for GFP-SENP1-C603S was increased to 27s ($t_{1/2}$ = 21s for the WT) with a concurrent diffusion coefficient of 0.0092 $\mu m^2\ s^{-1}$ (**Supplementary figure 2d**) revealing a slower diffusion of the mutant enzyme into spines. Synaptic activation with bicuculline led to an increase in the half time of GFP-SENP1-C603S fluorescence recovery similar to the effect on the WT enzyme. The mobile fraction was reduced to ~54% (**Supplementary figure 2d**) as in bicuculline-treated WT GFP-SENP1-expressing neurons indicating that the mutation impairs the diffusion properties of SENP1 in basal but not stimulated conditions.

Activity-dependent trapping of SENP1 into spines

To confirm that the increase in synaptic SENP1 levels upon sustained (25-50 min) synaptic activation is due to the retention of the desumoylation enzyme in spines, we designed live-cell imaging experiments to visualize and measure the exit rate of SENP1 in control and activated conditions (**Fig. 4**). To achieve this, we first exchanged the GFP from GFP-SENP1 with the

green to red photoconvertible Dendra2[23,24] protein tag (Dendra2-SENP1). Then, using restricted Dendra2 photoconversion time-lapse microscopy[18,25], we recorded the decrease in the red photoconverted Dendra2-SENP1 fluorescence from dendritic spines in control and bicuculline-treated conditions (**Fig. 4a,b**). A 40-min bicuculline stimulation led to a significant decrease in both the exit rate of the red photoconverted fluorescence from the spines (Control half time decay, 6.10 ± 1.8s; Bicuculline, 11.90 ± 2.6s, Means ± s.e.m.; **Fig. 4c**) and the diffusion coefficient (Control, 0.289 ± 0.065 μm^2 s^{-1} ; Bicuculline, 0.115 ± 0.020 μm^2 s^{-1}, Means ± s.e.m.; **Fig. 4d**). These data strengthened the FRAP measurements (**Fig. 3**) further demonstrating that synaptic activation regulates the synapto-dendritic diffusion of SENP1 by reducing the exit of SENP1 from spines.

The synaptic retention of SENP1 is regulated by the activation of mGlu5 receptors

Activation of mGlu5 receptors leads to the transient synaptic trapping of the SUMO-conjugating enzyme Ubc9[18]. To investigate whether the activation of mGlu5R also regulates the synaptic diffusion of SENP1 we performed FRAP assays in the presence of the group 1 mGluR agonist DHPG (**Fig. 5**). GFP-SENP1-expressing neurons were stimulated with DHPG (50 μM) and GFP-SENP1-labeled spines were photobleached at various time points during the treatment. The mobile fraction of GFP-SENP1 was dropping from 74% to about 58% in DHPG-stimulated spines (**Fig. 5a-c**) similar to the values measured for bicuculline-treated WT GFP-SENP1 neurons (**Fig. 3**).

In DHPG-treated conditions, the half time of GFP-SENP1 fluorescence recovery was dramatically increased to values close to those measured in bicuculline-stimulated cells (**Fig. 5d**; Control, 23.4s ± 1.4; DHPG, 34.0 ± 1.1s, Means ± s.e.m.) indicating that the activation of mGlu1/5 receptors is essential to regulate the diffusion and trapping of SENP1 into spine.

Interestingly, the decreased synaptic diffusion of GFP-SENP1 in DHPG condition was fully prevented when neurons were pre-incubated with the specific mGlu5R antagonist MPEP (**Fig. 5**) revealing the specific involvement of mGlu5 receptors in the process. Altogether, these data indicate that mGlu5R activation is central to the time-dependent regulation of SENP1 at synapses.

The synaptic level of endogenous SENP1 is regulated upon activation of mGlu5 receptors

To further confirm the central role of mGlu5R activation in the regulation of SENP1 at synapses, we performed immunolabeling experiments in rat hippocampal neurons to measure the extent of colocalisation between the endogenous SENP1 and the postsynaptic marker PSD95 in basal and DHPG (50 μM)-treated conditions (**Fig. 6**). Consistent with the live imaging data (**Figs. 2-5**), the extent of SENP1 immunoreactivity in PSD95-positive clusters is significantly increased in DHPG-activated neurons (**Fig. 6a,b**). We also verified that there were no significant alterations of PSD95 and total SENP1 immunoreactivities upon the pharmacological treatments used (**Fig. 6c,d**). These findings further support the involvement of mGlu5 receptors in the dynamic targeting of the desumoylation enzymes into dendritic spines.

Finally, we evaluated the enrichment in endogenous SENP1 in post-synaptic fractions upon basal and activated conditions (**Fig. 7**). To this end we purified Triton X-insoluble post-synaptic density fractions (TiF[26,27]; **Fig. 7a**) from control, bicuculline and DHPG-treated rat cortical cultured neurons. TiF fractions were specifically enriched in synaptic PSD95 and Homer1 proteins and importantly, devoid of the nuclear protein NOPP140 revealing the absence of possible nuclear contamination (**Fig. 7b**). Interestingly, both the bicuculline and the DHPG treatments (**Fig. 7c,d**) led to an increase in the endogenous level of SENP1 in the TiF fraction further confirming the activity-dependent targeting of the enzyme in dendritic spines.

Discussion

Here, we uncovered for the first time, a regulatory pathway controlling the SENP1 targeting into dendritic spines providing additional insights into the regulation of the sumoylation balance at synapses. We demonstrated that SENP1 diffusion in neurons is regulated by the mGlu5 receptors in an activity-dependent manner. In particular, the activation of mGlu5Rs, which leads to a dramatic decrease in the exit rate of SENP1 from dendritic spines and consequently, to an accumulation of SENP1 at post-synaptic sites.

We previously demonstrated that the activation of mGlu5Rs in hippocampal neurons regulates the synaptic diffusion of Ubc9, the sole conjugating enzyme of the sumoylation pathway, by increasing its residency time at the synapse[18]. This work described for the first time a synaptic regulation of the SUMO machinery and highlighted the fast regulation of this process since this transient enzymatic modulation occurs within a sub-second to second time range. Here the regulation of SENP1 diffusion in and out of spines is rather slow when compared to the Ubc9 regulatory process. Indeed, values for the synapto-dendritic exchange of the desumoylation enzyme is within a 20-second range indicating that the mGlu5R activation sequentially leads to synaptic sumoylation and then, to the targeting of SENP1 into spines to balance the protein sumoylation levels. Interestingly, while we show here a clear synaptic enrichment of SENP1 into mGlu5R-activated spines, the sustained mGlu5R activation does not increase the synaptic levels of Ubc9[18]. This may uncover a differential regulation of both enzymes at the molecular level, despite the same initial, i.e. mGlu5R, activating pathway.

The synaptic targeting of other cytosolic enzymes important for synaptic regulatory functions such as the Ca^{2+}/calmodulin-dependent protein kinase II (CaMKII) is also regulated by

variations of synaptic activity[28,29]. However, the synaptic targeting of CaMKII is rather linked to the activation of an NMDA receptor-mediated calcium pathway[28]. In addition to its known synaptic accumulation, Lemieux and colleagues reported the dynamic recruitment of CaMKII to dendritic subdomains adjacent to the activated spines involving the interaction of the enzyme with microtubules, a prerequisite for CaMKII autophosphorylation[29]. The proteasome subunit Rpt1 is also targeted to spines in NMDAR-activated neurons and actively participate in the activity-dependent shaping of the synaptic protein content[30]. However, whether the activity-dependent targeting of CaMKII and/or Rpt1 to dendritic spines is also regulated by the activation of the mGlu5R pathway remains unexplored.

SENP5 was recently reported to be localized at least in part, at synaptic sites where it colocalizes with mitochondrial markers[31]. Despite this interesting descriptive aspect, the functional role of the desumoylase at synapses as well as its regulation in dendritic spines is still not available in the literature. On the same side, SENP2 has been closely associated to mitochondrial regulatory functions and for instance, it regulates Drp1 sumoylation and consequently mitochondrial fission[32]. Therefore, it would be interest to assess the activity-dependent diffusion properties of both SENP2 and SENP5 in hippocampal neurons. Despite the apparent lack of research on these proteins, the synaptic activity of these desumoylation enzymes may have important implications in neurological disorders involving mitochondrial alterations.

The current work also raises intriguing questions as to whether a deregulated mGlu5R-signaling impairs the sumoylation/desumoylation equilibrium. Since mGlu5Rs are involved in synaptic functions as well as in the aetiology of several neurological disorders, including schizophrenia, Fragile X syndrome or chronic pain[33], it is likely that anomalies of the mGlu5R-

signaling pathway in such diseased conditions could alter the synaptic targeting of SENP1 and consequently the synaptic levels of protein sumoylation.

Finally, future work will also have to assess whether the synaptic enrichment of SENP1 enzymes upon sustained synaptic activation, as in epilepsy or stroke, exerts a protective or a deleterious action.

Methods

Constructs

GFP-tagged full length WT human SENP1 in pEGFP-C2 is a generous gift from Dr Wang Min[34]. GFP-SENP1-C603S mutant construct was made by site-directed mutagenesis using Quick-change mutagenesis (Agilent). The constructs were entirely sequenced.

Rat strain

Wistar rats were exclusively from a commercial source (Janvier, St Berthevin, France). All animals were handled and treated in accordance with the European Council Guidelines for the Care and Use of Laboratory animals in our facility. Animals had free access to water and food. Lightning was controlled as a 12h light and dark cycle and the temperature maintained at 23 ± 1°C. Protocol to prepare primary neuronal cultures from rat embryos at E17 was approved by our local Animal Care and Ethics Committee *(Comité Institutionnel d'Ethique Pour l'Animal de Laboratoire N°28, Nice, France; Project reference NCE/2012-63).*

Cell culture

Hippocampal neurons were prepared from E17 pregnant rats as previously described[18,25]. Briefly, neurons were plated in Neurobasal medium (Invitrogen, France) supplemented with

2% B27 (Invitrogen), 0.5 mM glutamine and penicillin/streptomycin (Ozyme) on 100-mm dishes or 24-mm glass coverslips (VWR) pre-coated with poly-L-Lysine (0.5 mg mL^{-1}; Sigma). Neurons (3.10^6 cells per 100-mm dish or 110,000 cells per coverslip) were then fed once a week with Neurobasal medium supplemented with 2% B27 and penicillin/streptomycin for a maximum of 3 weeks.

Cell transfection

Mycoplasm-free COS7 cells (ATCC reference CRL-1651, Molsheim, France) were transfected with the indicated constructs using Lipofectamine 2000 (Invitrogen) according to the manufacturer's instructions and used 48-72h post-transfection.

Sindbis virus production and neuronal transduction

Attenuated Sindbis viral particles (SINrep(nsP2S726)) were prepared and used as previously described[35,36,37]. Briefly, cRNAs were generated from the pSinRep5 plasmid containing the sequence coding for the indicated GFP-SENP1 constructs and from the defective helper (pDH-BB) plasmid using the Mmessage Mmachine SP6 solution (Ambion). cRNAs were then electroporated into BHK21 cells. Pseudovirions present in the culture medium were harvested 72h after electroporation and concentrated using ultracentrifugation on SW41Ti. Aliquots of resuspended Sindbis particles were then stored at -80°C. Neurons were transduced at a multiplicity of infection (MOI) of 0.1 to 1 and returned to the incubator at 37°C under 5% CO_2 for 18 to 24h until use.

Immunocytochemistry

Hippocampal neurons (19 DIV) treated or not for 40 min with 50 μM DHPG or 10 μM Bicuculline at 37°C were fixed with Methanol for 20 min at -20°C and washed three times 5

minutes in PBS. Cells were then permeabilized for 1h in PBS containing 0.2% Triton X100, 0.2% of BSA and 5% Horse Serum (HS) at RT. Neurons were immunostained with a rabbit anti-SENP1 (1/200; Sigma-Aldrich), a mouse anti-PSD95 (1/500; Neuromab) and a guinea pig anti-MAP2 (1/1000; Synaptic System) overnight at 4°C in PBS containing 0.2% Triton X100, 0.2% of BSA. Cells were washed three times in PBS and incubated with the appropriate secondary antibodies conjugated to Alexa488, Alexa594 or Alexa 647 as indicated and mounted with Mowiol (Sigma). Confocal images (1024×1024 pixels) were acquired with a 63X oil-immersion lens (Numerical Aperture NA 1.4) on a confocal LSM780 microscope (Zeiss, Germany). Z-series of 5 images of randomly selected dendrites were compressed into two dimensions using the maximum projection algorithm of the Zeiss software. Quantification was performed using the ImageJ software and the synaptic enzymatic staining was measured with the use of an in-house ImageJ macro[18]. Briefly, confocal image of the synaptic marker was used to produce a mask after an automated intensity threshold. Masks were then applied to the corresponding images and the fluorescence intensity within the synaptic area was measured.

Live cell imaging

Protocols were performed as previously described[18,25,37]. Briefly, live GFP-SENP1 expressing neurons were kept on a heated stage (set at 37°C) on a Nikon Ti inverted microscope. GFP fluorescence was excited through a 60X oil-immersion lens (Numerical Aperture, 1.4) using a 488nm laser light (50 mW, 3%) and time series (15 Hz) were collected for 210 sec as a single image slice using a Perkin Elmer Ultra-View spinning disk solution.

Neurons were treated or not with 10 µM bicuculline or 50 µM DHPG in Earle's buffer (25 mM HEPES-Tris pH 7.4, 140 mM NaCl, 5 mM KCl, 1.8 mM $CaCl_2$, 0.8 mM $MgCl_2$, 0.9 g L^{-1} glucose) for 10-40 min in Earle's buffer. A 10 min preincubation at 37°C was achieved when

specific inhibitors were used. Pharmacological drugs (30 μM MPEP, 10 μM bicuculline or 50 μM DHPG) were all diluted in Earle's buffer.

FRAP measurements

Fluorescence intensity variations in spines were analyzed using the FRAP module of the Volocity 6.3 software. Fluorescence recovery curve in FRAP allows the direct determination of two parameters. First the difference between the basal level of fluorescence and the recovered plateau level after photobleaching reflects the immobile fraction of protein and conversely the mobile diffusible fraction. Immobile fractions reflect the direct or indirect binding of the protein of interest to cytoskeleton constituents. Second, the half time of recovery specifies the mobility of the diffusible fraction of the protein of interest. Fluorescence data were collected from regions of interest drawn around the fluorescence of GFP-SENP1. FRAP data were expressed as a percentage of initial fluorescence (average fluorescence value from the ten second imaging period immediately before photobleaching) over time and fitted with a single-phase exponential function ($f(t) = y + A^{e-kt}$) using the Volocity 6.3 software from Perkin Elmer. Mobile fraction (in %), half time of recovery (in seconds) and diffusion coefficient (in $\mu m^2\ s^{-1}$; D = photobleached spine area / $4t_{1/2}$) values were extracted for each experiment using the FRAP module of the Volocity 6.3 software. Curves were fitted using a one phase exponential association or mono-exponential decay equation as indicated and data statistically analyzed with Prism 7 (GraphPad software, Inc).

Dendra2-SENP1 photoconversion measurements[25]

The GFP tag from the GFP-SENP1 construct was exchanged for the photoswitchable Dendra2 protein[23,24] (Evrogen JSC, Russia). Individual Dendra2-SENP1-expressing spines were photoconverted for 30 msec using a 405 nm laser light (50 mW, 18%). The red photoconverted

Dendra2-SENP1 was excited using a 561 nm laser light (50 mW, 20%) and time series (10 Hz) were collected for 210 sec as a single image slice using a Perkin Elmer Ultra-View spinning disk solution. The decrease in red fluorescence from Dendra2-SENP1 photoconverted spines was measured over time using the Volocity 6.3 software and data expressed as a percentage of the initial red photoconverted fluorescence (F/F_0).

Triton X-insoluble Fraction (TiF) isolation

TiF fractions were prepared according to established protocols[26,27] using 18-20 DIV control and treated-rat cortical neurons (5 x 100 mm dishes per condition with 2.5 x 10^6 cells) for 40 min in control, bicuculline (10 μM) or DHPG (50 μM) in Earle's Buffer. Neurons were immediately cooled down on ice and homogenized in ice-cold sucrose buffer (1 mM HEPES pH 7.4, 0.32 M Sucrose, 1 mM EDTA, 1 mM $MgCl_2$, 1 mM $NaHCO_3$, Mammalian protease inhibitors (Roche) and 20 mM NEM (Sigma-Aldrich) to protect proteins from desumoylation). Nuclear proteins were removed from the synaptosomal preparation by centrifugation at 500g for 5 min. Post-nuclear fractions were further centrifuged at 13,000g for 15 min to isolate crude synaptosomal fractions. The crude fractions were then resuspended in lysis Buffer (75 mM KCl, 1% Triton X100, 20 mM NEM). Tif fractions were finally purified by centrifugation at 100,000g for 1h. TiF fractions were collected and resuspended in Urea-containing lysis buffer (50 mM Tris-HCl pH 6.8, 2% SDS, 10% glycerol and 8M Urea). Protein concentrations were determined (BioRad) and samples were boiled in Laemmli buffer for 10 min.

Immunoblotting

Transfected COS7 cells as indicated were homogenized in lysis buffer (10 mM Tris-HCl pH7.5, 10 mM EDTA, 150 mM NaCl, 1% Triton X100, 0.1% SDS) in presence of a mammalian protease inhibitor tablet (Roche), proteasome inhibitor MG132 (20 μM) and 20

mM NEM. Protein extracts were resolved by SDS-PAGE, transferred onto nitrocellulose membrane and immunoblotted with the following primary antibodies: mouse anti-SUMO1 (clone 21C7, DSHB), 1.7 $\mu g.mL^{-1}$; Mouse anti-SUMO2/3 (clone 8A2, DSHB), 1.9 $\mu g.mL^{-1}$; Rabbit anti-SENP1 1/250 (Sigma Prestige); Mouse anti-GFP 1/1000 (Roche, Germany); Mouse anti-PSD95 1/10000 (NeuroMab); Mouse anti-Homer1 1/1000 (Synaptic System); Mouse anti-Synapsin 1a/b 1/1000 (Santa-Cruz); Mouse anti-NOPP140 1/700 (Santa-Cruz); Standard loading controls were included using a mouse anti-β-actin antibody 1/1000 (Sigma) or a rabbit anti-Tubulin 1/10000 (Synaptic System) as indicated.

Statistical analysis

Statistical analyses were calculated using GraphPad Prism 7 (GraphPad software, Inc). Data were expressed as mean ± s.e.m. One-way ANOVA were performed with the indicated post-test for multiple comparison data sets. All data were tested for normal distribution. *$p<0.05$ was considered significant.

References

1. Mabb AM, Ehlers MD. Ubiquitination in postsynaptic function and plasticity. *Annu Rev Cell Dev Biol* 26, 179-210 (2010).

2. Matunis MJ, Coutavas E, Blobel G. A novel ubiquitin-like modification modulates the partitioning of the Ran-GTPase-activating protein RanGAP1 between the cytosol and the nuclear pore complex. *J Cell Biol* 135, 1457-1470 (1996).

3. Mahajan R, Delphin C, Guan T, Gerace L, Melchior F. A small ubiquitin-related polypeptide involved in targeting RanGAP1 to nuclear pore complex protein RanBP2. *Cell* 88, 97-107 (1997).

4. Kerscher O. SUMO junction-what's your function? New insights through SUMO-interacting motifs. *EMBO Rep* 8, 550-555 (2007).

5. Meulmeester E, Melchior F. Cell biology: SUMO. *Nature* 452, 709-711 (2008).

6. Gwizdek C, Casse F, Martin S. Protein sumoylation in brain development, neuronal morphology and spinogenesis. *Neuromolecular Med* 15, 677-691 (2013).

7. Henley JM, Craig TJ, Wilkinson KA. Neuronal SUMOylation: mechanisms, physiology, and roles in neuronal dysfunction. *Physiol Rev* 94, 1249-1285 (2014).

8. Schorova L, Martin S. Sumoylation in Synaptic Function and Dysfunction. *Front Synaptic Neurosci* 8, 9 (2016).

9. Girach F, Craig TJ, Rocca DL, Henley JM. RIM1alpha SUMOylation is required for fast synaptic vesicle exocytosis. *Cell Rep* 5, 1294-1301 (2013).

10. Craig TJ, Anderson D, Evans AJ, Girach F, Henley JM. SUMOylation of Syntaxin1A regulates presynaptic endocytosis. *Sci Rep* 5, 17669 (2015).

11. Shalizi A*, et al.* A calcium-regulated MEF2 sumoylation switch controls postsynaptic differentiation. *Science* 311, 1012-1017 (2006).

12. Shalizi A*, et al.* PIASx is a MEF2 SUMO E3 ligase that promotes postsynaptic dendritic morphogenesis. *J Neurosci* 27, 10037-10046 (2007).

13. Martin S, Nishimune A, Mellor JR, Henley JM. SUMOylation regulates kainate-receptor-mediated synaptic transmission. *Nature* 447, 321-325 (2007).

14. Chamberlain SE*, et al.* SUMOylation and phosphorylation of GluK2 regulate kainate receptor trafficking and synaptic plasticity. *Nat Neurosci* 15, 845-852 (2012).

15. Craig TJ, Jaafari N, Petrovic MM, Rubin PP, Mellor JR, Henley JM. Homeostatic synaptic scaling is regulated by protein SUMOylation. *J Biol Chem* 287, 22781-22788 (2012).

16. Loriol C, Parisot J, Poupon G, Gwizdek C, Martin S. Developmental regulation and spatiotemporal redistribution of the sumoylation machinery in the rat central nervous system. *PLoS ONE* 7, e33757 (2012).

17. Loriol C, Khayachi A, Poupon G, Gwizdek C, Martin S. Activity-dependent regulation of the sumoylation machinery in rat hippocampal neurons. *Biol Cell* 105, 30-45 (2013).

18. Loriol C*, et al.* mGlu5 receptors regulate synaptic sumoylation via a transient PKC-dependent diffusional trapping of Ubc9 into spines. *Nat Commun* 5, 5113 (2014).

19. Hickey CM, Wilson NR, Hochstrasser M. Function and regulation of SUMO proteases. *Nat Rev Mol Cell Biol* 13, 755-766 (2012).

20. Nayak A, Muller S. SUMO-specific proteases/isopeptidases: SENPs and beyond. *Genome Biol* 15, 422 (2014).

21. Hay RT. SUMO: a history of modification. *Mol Cell* 18, 1-12 (2005).

22. Seeler JS, Dejean A. SUMO and the robustness of cancer. *Nat Rev Cancer* 17, 184-197 (2017).

23. Gurskaya NG*, et al.* Engineering of a monomeric green-to-red photoactivatable fluorescent protein induced by blue light. *Nat Biotechnol* 24, 461-465 (2006).

24. Chudakov DM, Lukyanov S, Lukyanov KA. Using photoactivatable fluorescent protein Dendra2 to track protein movement. *Biotechniques* 42, 553, 555, 557 passim (2007).

25. Casse F, Martin S. Tracking the activity-dependent diffusion of synaptic proteins using restricted photoconversion of Dendra2. *Front Cell Neurosci* 9, 367 (2015).

26. Gardoni F*, et al.* Decreased NR2B subunit synaptic levels cause impaired long-term potentiation but not long-term depression. *J Neurosci* 29, 669-677 (2009).

27. Gardoni F*, et al.* The NMDA receptor complex is altered in an animal model of human cerebral heterotopia. *J Neuropathol Exp Neurol* 62, 662-675 (2003).

28. Thalhammer A, Rudhard Y, Tigaret CM, Volynski KE, Rusakov DA, Schoepfer R. CaMKII translocation requires local NMDA receptor-mediated Ca2+ signaling. *Embo J* 25, 5873-5883 (2006).

29. Lemieux M, Labrecque S, Tardif C, Labrie-Dion E, Lebel E, De Koninck P. Translocation of CaMKII to dendritic microtubules supports the plasticity of local synapses. *J Cell Biol* 198, 1055-1073 (2012).

30. Bingol B, Schuman EM. Activity-dependent dynamics and sequestration of proteasomes in dendritic spines. *Nature* 441, 1144-1148 (2006).

31. Akiyama H, Nakadate K, Sakakibara SI. Synaptic localization of the SUMOylation-regulating protease SENP5 in the adult mouse brain. *J Comp Neurol*, (2017).

32. Fu J*, et al.* Disruption of SUMO-specific protease 2 induces mitochondria mediated neurodegeneration. *PLoS Genet* 10, e1004579 (2014).

33. Wang H, Zhuo M. Group I metabotropic glutamate receptor-mediated gene transcription and implications for synaptic plasticity and diseases. *Front Pharmacol* 3, 189 (2012).

34. Li X*, et al.* SENP1 mediates TNF-induced desumoylation and cytoplasmic translocation of HIPK1 to enhance ASK1-dependent apoptosis. *Cell Death Differ* 15, 739-750 (2008).

35. Xiong H*, et al.* mTOR is essential for corticosteroid effects on hippocampal AMPA receptor function and fear memory. *Learn Mem* 22, 577-583 (2015).

36. Xiong H*, et al.* Interactions between N-Ethylmaleimide-sensitive factor and GluA2 contribute to effects of glucocorticoid hormones on AMPA receptor function in the rodent hippocampus. *Hippocampus* 26, 848-856 (2016).

37. Khayachi A*, et al.* Sumoylation regulates FMRP-mediated dendritic spine elimination and maturation. *Nat Commun* in press, (2018).

Acknowledgements

We thank Wang Min for sharing the GFP-SENP1 construct and Jeremy Henley for sharing pSinRep5 plasmids. We gratefully acknowledge the 'Agence Nationale de la Recherche' (ANR-15-CE16-0015-01) and the Bettencourt-Schueller foundation for financial support. We also thank the French Government for the 'Investments for the Future' LabEx 'SIGNALIFE' (ANR-11-LABX-0028-01) and Région PACA for the Microscopy and Imaging Côte d'Azur (MICA) platform funding. LS and MPri are fellows from the international PhD 'SIGNALIFE' LabEx program.

Author contributions

LS, MP performed all the live imaging experiments. LS, MP and AK performed biochemical experiments. GP and MPri prepared viral particles. AF, MP and LS performed the immunocytochemistry. LS, MP, AF and GP prepared neuronal cultures. FC performed some initial FRAP experiments. FBr provided computational tools to analyze imaging data. LS, CG and SM contributed to hypothesis development, experimental design and data interpretation. SM provided the overall supervision, the funding and wrote the manuscript. All authors discussed the data and commented on the manuscript.

Competing financial interests: The authors declare no competing financial interests.

Figure legends

Figure 1. GFP-SENP1 is catalytically active and distributed in dendrites and spines. (a) Representative image of a 19 DIV rat hippocampal neuron expressing WT GFP-SENP1 (green) and immunolabelled for PSD-95 (red). Scale bars: Left, 20 μm; Right, 2 μm. **(b)** Graphical representation indicates the percentage of GFP-SENP1 localisation in PSD-95 positive compartment (17.2 ± 1.1%) of secondary dendrites. **(c)** Representative images of a 19 DIV rat hippocampal neuron immunolabelled for the neuronal marker MAP2 (blue), synaptic marker PSD-95 (red) and SENP1 (green). Scale bars: Left, 20 μm; Right, 2 μm. **(d)** Graphical representation indicates the percentage of endogenous SENP1 staining in PSD-95 positive spines (12.7 ± 0.4%) of secondary dendrites (n = 26 neurons). **(e)** Representative immunoblots of SUMO1- and SUMO2/3-modified protein levels upon expression of GFP, WT GFP-SENP1 and the inactive GFP-SENP1 mutant (C603S) in COS7 cells. **(f)** Representative immunoblots for SENP1, GFP and β-actin in the indicated transfected conditions. **(g)** Quantitative representation of SUMO1-ylation levels normalized to control GFP ± SEM (SUMO1: WT GFP-SENP1 [52.2 ± 7.5%] and GFP-SENP1 C603S [87.2 ± 13.7%]). **(h)** Quantitative representation of SUMO2/3-ylation levels normalized to control GFP ± SEM (SUMO2: WT GFP-SENP1 [50.7 ± 6.7%] and GFP-SENP1 C603S [103.6 ± 22.7%]) from 3 independent experiments. Statistics: One-way ANOVA with Tukey post-hoc test. P-values are indicated.

Figure 2. Activity-dependent redistribution of GFP-SENP1 into spines. (a) Representative confocal images of a time-lapse recording of a GFP-SENP1 expressing rat hippocampal secondary dendrite in control and bicuculline (10 μM)-treated conditions as indicated on the top bars. **(b)** Quantification of time lapse experiments showing the variation of normalized fluorescence intensity ± SEM in spines (n = 34), shafts (n = 11) and whole dendritic area (green). **(c)** Graphical representation of mean fluorescence intensity ± SEM in spines in control

(dark grey), bicuculline plateau (orange, 1.29 ± 0.03) and washout (light grey, 1.07 ± 0.04). Statistical test: Paired, non-parametric one-way ANOVA with Tukey post-hoc test. P-values are indicated. **(d)** Graphical representation and corresponding confocal images of time-lapse recording of a GFP-SENP1-expressing hippocampal neuron in control solution. Curves represent mean values ± SEM of indicated numbed of spines (black), shafts (orange) and whole dendritic tree field (green). **(e)** Bar graph shows spine mean fluorescence intensity ± SEM during 0-5 min (dark grey) and 5-40 min (light grey) incubation with control solution. N = 40 spines. Statistical test: Paired, non-parametric t-test. ns, not significant.

Figure 3. SENP1 postsynaptic entry is regulated by synaptic activity in a time-dependent manner. **(a)** Representative FRAP recordings of GFP-SENP1-expressing spines in control and bicuculline (15 and 40 min of sustained treatment) conditions. Scale bar: 1 μm. **(b)** FRAP curves corresponding to images in **(a)**. **(c)** FRAP curves showing mean values ± SEM of fluorescence intensity of bleached spines in control (blue) and bicuculline (sustained treatment of 10-25 min [orange] and 25-50 min [red]) conditions. **(d)** Bars represent mobile fraction (ctrl [74.5 ± 1.1%], bic 10-25 min [71.2 ± 1.7%], and bic 25-50 min [56.2 ± 1.8%]; **(e)** half-time recovery (ctrl [20.79 ± 1 s], bic 10-25min [28.25 ± 2 s], and bic 25-50 min [33.58 ± 1.6 s]); **(f)** diffusion coefficient (ctrl [0.0135 ± 0.0007 $\mu m^2/s$], bic 10-25 min [0.01 ± 0.0008 $\mu m^2/s$], and bic 25-50 min [0.0087 ± 0.0007 $\mu m^2/s$]); and spine numbers (ctrl= 165, bic 10-25 min= 75, and bic 25-50 min = 139) from at least 5 different cultures. Statistics: $T_{1/2}$ and diff. coef. were analyzed by Kruskal-Wallis ANOVA and Fm by parametric ANOVA with Tukey post hoc test. P-values are indicated.

Figure 4. The synaptic exit of SENP1 is regulated by synaptic activity. (a) Representative confocal images of Dendra2-SENP1-expressing rat hippocampal neurons (19 DIV) during a

photoconversion experiment in control and bicuculline conditions. Scale bar: 1 µm. **(b)** Fluorescence decay curves showing the decrease in red fluorescence as photoconverted Dendra2-SENP1 molecules exit from spines. The curves correspond to the images in **(a)**. **(c)** Graph displaying fluorescence decay curves as mean values ± SEM from 12 spines in control and 13 spines in bicuculline (duration of treatment 25-50 min) conditions. Statistics: multiple t-test. **(d)** Graphical representations that corresponds to fluorescence decay curves in **(c)** showing **(d)** half time decay (ctrl: [6.1 ± 1.8 s] and bic: [11.9 ± 2.6 s]). **(e)** Diffusion coefficient of fluorescence decay (ctrl: [0.289 ± 0.065 $\mu m^2/s$] and bic: [0.115 ± 0.020 $\mu m^2/s$]). Statistics: Mann-Whitney. P-values are indicated. Number of cultures = 3.

Figure 5. SENP1 synaptic diffusion is mGluR5-dependent. **(a)** Representative FRAP recordings of WT GFP-SENP1-expressing spines in control, DHPG (sustained 25-50 min), MPEP and MPEP+DPHG (sustained 25-50 min) conditions. Scale bar = 1 µm. **(b)** FRAP curves showing mean values ± SEM of fluorescence recovery in bleached spines in control (blue), DHPG (red), MPEP (green) and MPEP+DHPG (magenta) conditions. **(c)** Mobile fraction (ctrl [74.0 ± 1.6%], DHPG [58.4 ± 1.2%], MPEP [68.1 ± 2.1%] and MPEP+DHPG [79.0 ± 1.5%]); **(d)** Half-time recovery ± SEM (ctrl [23.4 ± 1.4 s], DHPG [34.0 ± 1.1 s], MPEP [27.5 ± 1.7 s] and MPEP+DHPG [23.3 ± 2 s]); and **(e)** diffusion coefficient (ctrl [0.0126 ± 0.0012 $\mu m^2/s$], DHPG [0.0071 ± 0.0003 $\mu m^2/s$], MPEP [0.0082 ± 0.0006 $\mu m^2/s$] and MPEP+DHPG [0.012 ± 0.001 $\mu m^2/s$]). Spine numbers are indicated on the bars. Statistics: $T_{1/2}$ and diff. coef. were analysed by Kruskal-Wallis and Fm by parametric ANOVA with Tukey post hoc test. P-values are indicated.

Figure 6. Activity-dependent targeting of endogenous SENP1 to synapses. **(a)** Immuno-labelling of fixed primary hippocampal neurons for PSD95 (red) and SENP1 (green) in control

and DHPG (40 min) conditions. **(b)** Quantitative representation ± SEM of control-normalized fluorescence intensity of SENP1 within PSD-95 area (ctrl: 1 ± 0.026, DHPG: 1.374 ± 0.032); (c) size of PSD-95 area (ctrl: 1 ± 0.045, DHPG: 0.933 ± 0.052); and **(d)** total SENP1 staining (ctrl: 1 ± 0.064, DHPG: 1.053 ± 0.058) from 3 independent cultures and at least 6 neurons / condition / culture. Number of secondary dendrites is indicated on the bars. Statistics: One-way ANOVA with Tukey post hoc test. Significant p-values are indicated. Scale bar = 2 µm.

Figure 7. mGlu5R activation induces the increase of SENP1 in PSD fractions. **(a)** Step-by-step scheme of TIF (TritonX100-Insoluble Fraction) isolation. **(b)** Immunoblot analysis of TIF purity isolation displaying fractions from different steps indicated in **(a)**. Immunoblots were performed using NOPP140 (nuclear), PSD-95 (postsynaptic), Homer1 (postsynaptic) and synapsin 1a/b (presynaptic) markers. Lanes labels: total homogenate (HO), supernatant 1, 2 and 3 (S1, 2 and 3), pellets 1 and 2 (P1 and 2), triton insoluble fraction (TIF) and supernatant 4 (S4). Each lane was loaded with 10 µg of total protein. **(c)** Representative immunoblot of TIF fractions from ctrl and DHPG-treated cortical neurons (19 DIV). 15 µg of protein was loaded per lane. Immunodetection was performed for PSD95, SENP1 and β-tubulin. **(d)** Quantitative representation of control-normalized SENP1 levels in TIF ± SEM in control and DHPG (1.8 ± 0.23) conditions from 4 independent cultures. Statistics: Unpaired t-test. P-value is indicated.

Supplementary information

Supplementary figure 1. Nuclear localisation of SENP1 in neurons. **(a)** Representative confocal image of a 19 DIV rat hippocampal neuron immunolabelled for SENP1 (green) and the synaptic marker PSD-95 (red). **(b)** Representative confocal image of a 19 DIV rat hippocampal neuron expressing WT GFP-SENP1 (green) and immunolabelled for PSD-95 (red). Dashed circle indicates the nuclear borders. Scale bar = 20 µm.

Supplementary figure 2. The synaptic redistribution of SENP1 into spines does not rely on its catalytic activity. **(a)** FRAP curves showing mean values ± SEM of fluorescence intensity of bleached spines for WT and C603S GFP-SENP1 in control (light and dark blue) and bicuculline (red and orange, 25-50 min of sustained bic treatment) conditions. It should be noted that FRAP curves and histograms for WT GFP-SENP1 are taken from **Fig. 3c-f**, for comparison. **(b)** FRAP measurement ± SEM: mobile fraction (WT: ctrl [74.5 ± 1.1%], and bic 25-50 min [56.2 ± 1.8%]; C603S: ctrl [73.9 ± 1%], bic [54.2 ± 2.6%]); **(c)** half-time recovery (t1/2, WT: ctrl [20.79 ± 1 s], bic 25-50 min [33.58 +/- 1.6 s]; C603S: ctrl [27.4 ± 1.2 s], bic [36.8 ± 3.6 s]); and **(d)** diffusion coefficient (WT: ctrl [0.0135 ± 0.0007 $\mu m^2/s$], bic 25-50 min [0.0087 ± 0.0007 $\mu m^2/s$]; C603S: ctrl [0.0092 ± 0.0004 $\mu m^2/s$], bic [0.0084 ± 0.001 $\mu m^2/s$]). Spine number WT: ctrl= 164 and bic 25-50 min = 139; C603S: ctrl = 160 and bic 25-50 min = 59, from at least 5 different cultures for WT and 2 independent cultures for C603S GFP-SENP1. Statistics: T1/2 and diff. coef. were analyzed with Mann-Whitney t-test and Fm with parametric t-test. P-values are indicated.

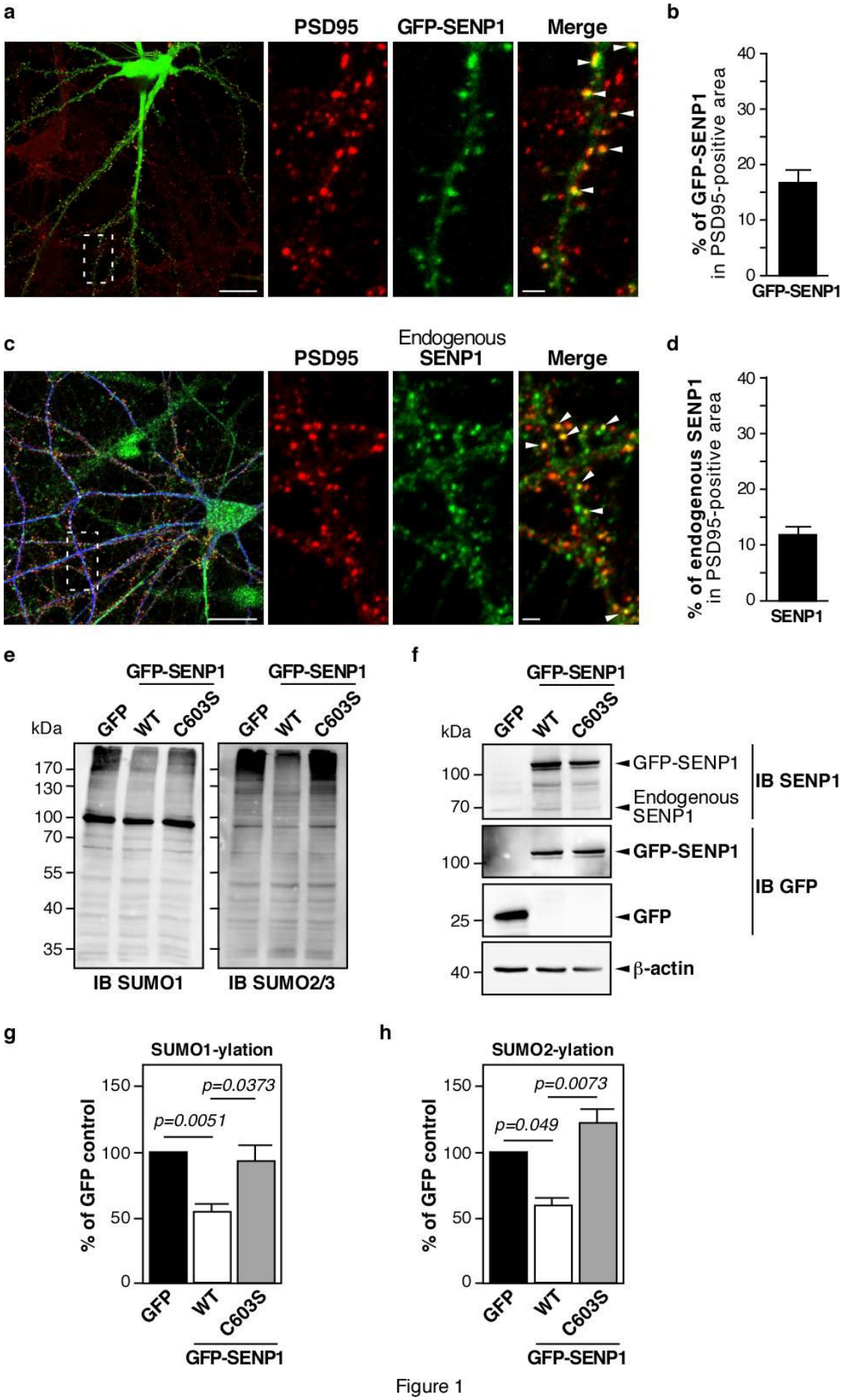
a
PSD95
GFP-SENP1
Merge
b
% of GFP-SENP1 in PSD95-positive area
40
30
20
10
0
GFP-SENP1
c
Endogenous SENP1
PSD95
Merge
d
% of endogenous SENP1 in PSD95-positive area
40
30
20
10
0
SENP1
e
GFP-SENP1
GFP-SENP1
kDa
GFP
WT
C603S
GFP
WT
C603S
170
130
100
70
55
40
35
IB SUMO1
IB SUMO2/3
f
GFP-SENP1
kDa
GFP
WT
C603S
100
70
GFP-SENP1
Endogenous SENP1
IB SENP1
100
GFP-SENP1
IB GFP
25
GFP
40
β-actin
g
SUMO1-ylation
% of GFP control
150
100
50
0
p=0.0373
p=0.0051
GFP
WT
C603S
GFP-SENP1
h
SUMO2-ylation
% of GFP control
150
100
50
0
p=0.0073
p=0.049
GFP
WT
C603S
GFP-SENP1

Figure 1

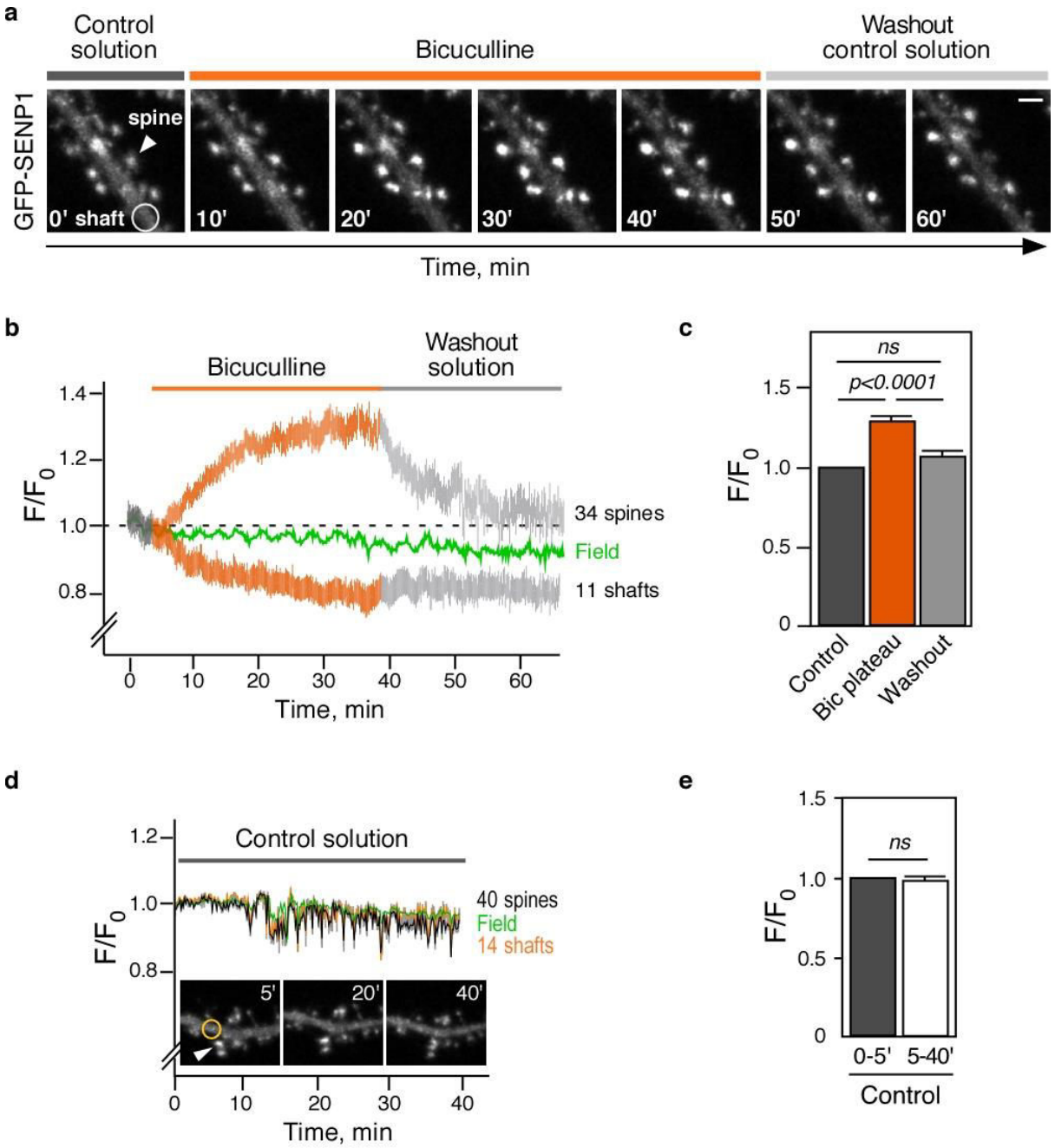
a
Control solution
Bicuculline
Washout control solution
GFP-SENP1
spine
0' shaft
10'
20'
30'
40'
50'
60'
Time, min
b
Bicuculline
Washout solution
F/F0
34 spines
Field
11 shafts
Time, min
c
ns
p<0.0001
F/F0
Control
Bic plateau
Washout
d
Control solution
F/F0
40 spines
Field
14 shafts
5'
20'
40'
Time, min
e
ns
F/F0
0-5'
5-40'
Control

Figure 2

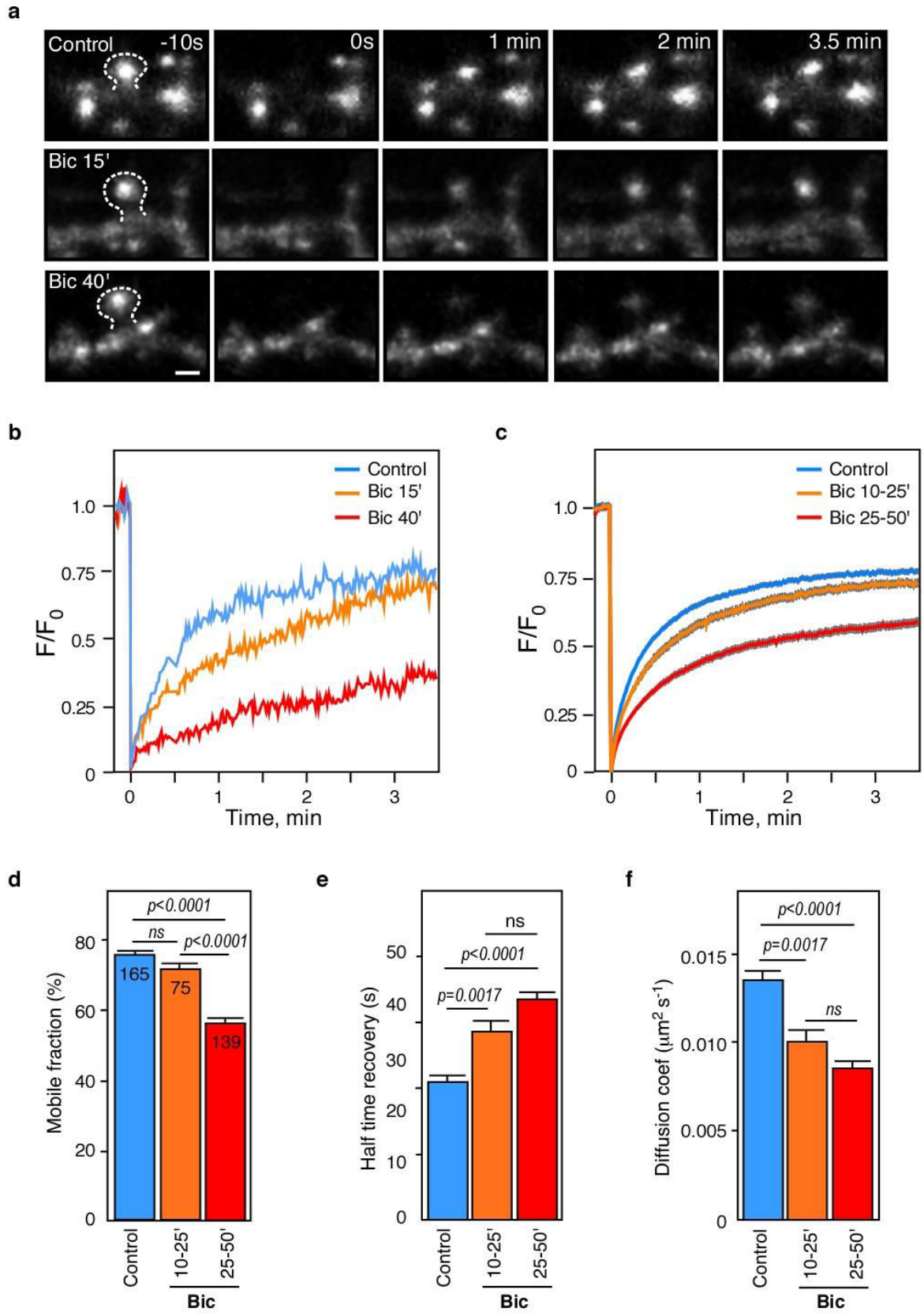
a
Control
-10s
0s
1 min
2 min
3.5 min
Bic 15'
Bic 40'
b
Control
Bic 15'
Bic 40'
F/F0
Time, min
c
Control
Bic 10-25'
Bic 25-50'
F/F0
Time, min
d
p<0.0001
ns
p<0.0001
165
75
139
Mobile fraction (%)
Control
10-25'
25-50'
Bic
e
ns
p<0.0001
p=0.0017
Half time recovery (s)
Control
10-25'
25-50'
Bic
f
p<0.0001
p=0.0017
ns
Diffusion coef (μm2 s-1)
Control
10-25'
25-50'
Bic

Figure 3

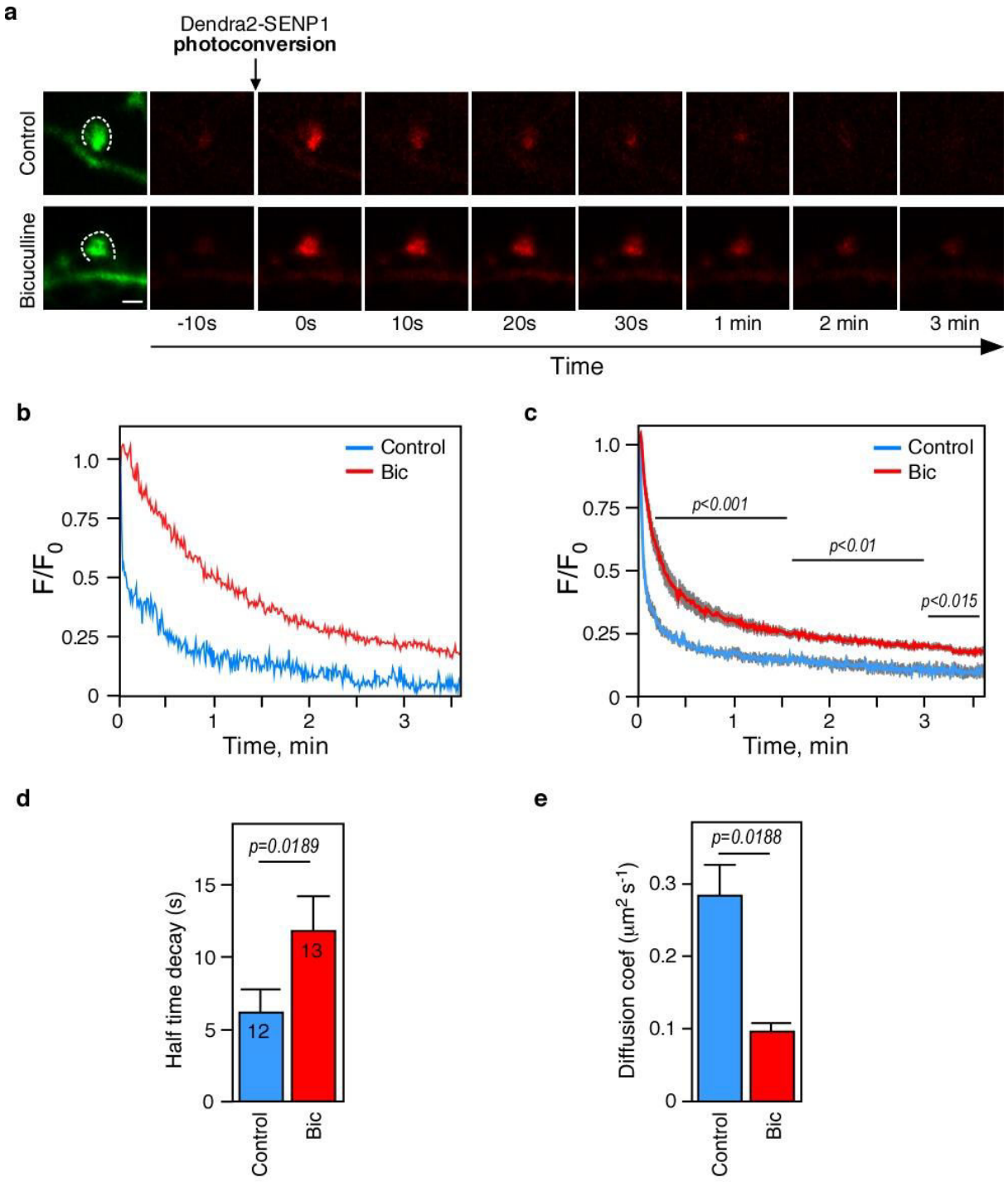
a
Dendra2-SENP1
photoconversion
Control
Bicuculline
-10s
0s
10s
20s
30s
1 min
2 min
3 min
Time
b
Control
Bic
F/F0
Time, min
c
Control
Bic
p<0.001
p<0.01
p<0.015
F/F0
Time, min
d
p=0.0189
Half time decay (s)
12
13
Control
Bic
e
p=0.0188
Diffusion coef (μm2 s-1)
Control
Bic

Figure 4

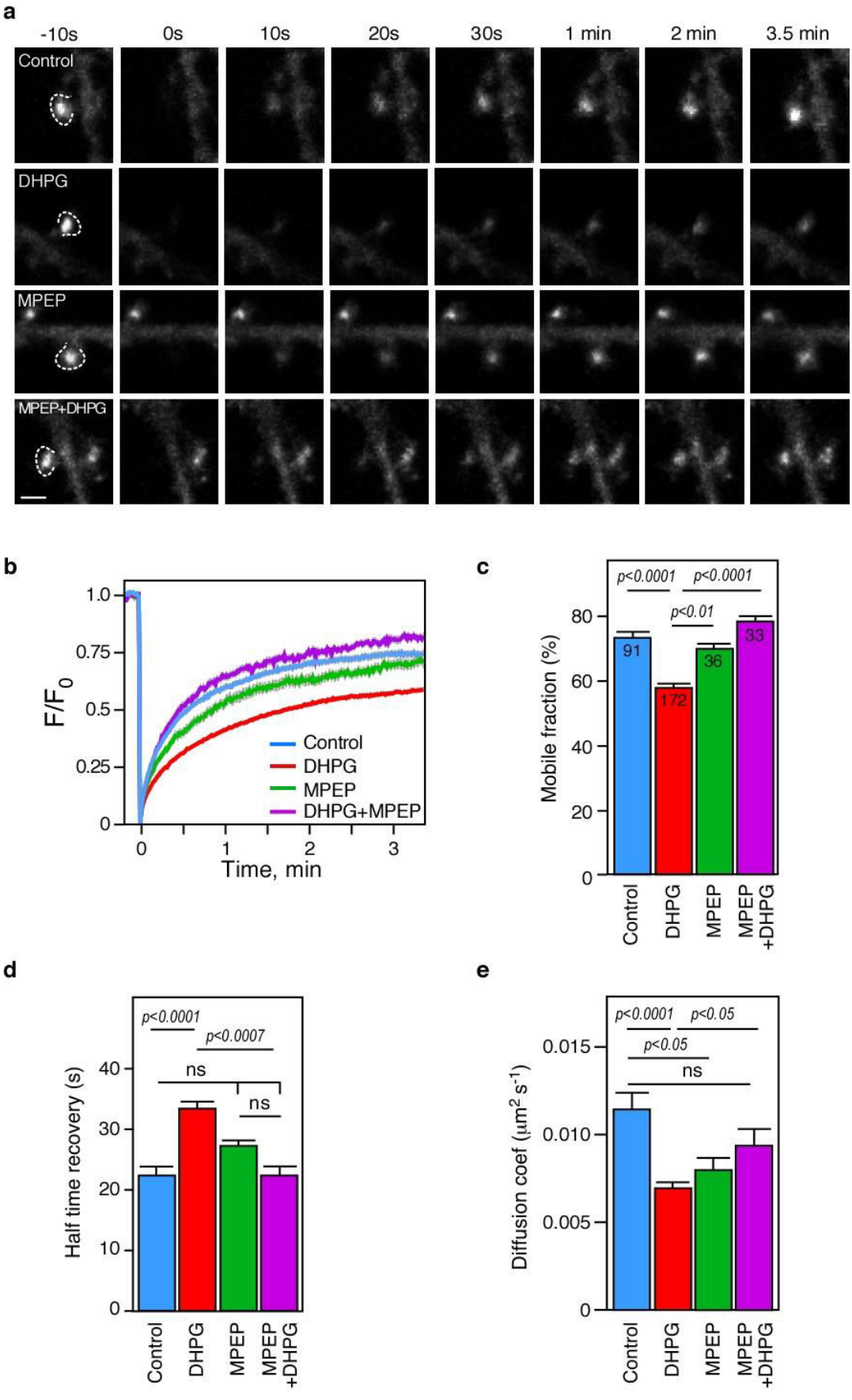
a
-10s
0s
10s
20s
30s
1 min
2 min
3.5 min
Control
DHPG
MPEP
MPEP+DHPG
b
F/F0
Time, min
Control
DHPG
MPEP
DHPG+MPEP
c
Mobile fraction (%)
p<0.0001
p<0.0001
p<0.01
91
172
36
33
Control
DHPG
MPEP
MPEP +DHPG
d
Half time recovery (s)
p<0.0001
p<0.0007
ns
ns
e
Diffusion coef (μm2 s-1)
p<0.0001
p<0.05
p<0.05
ns

Figure 5

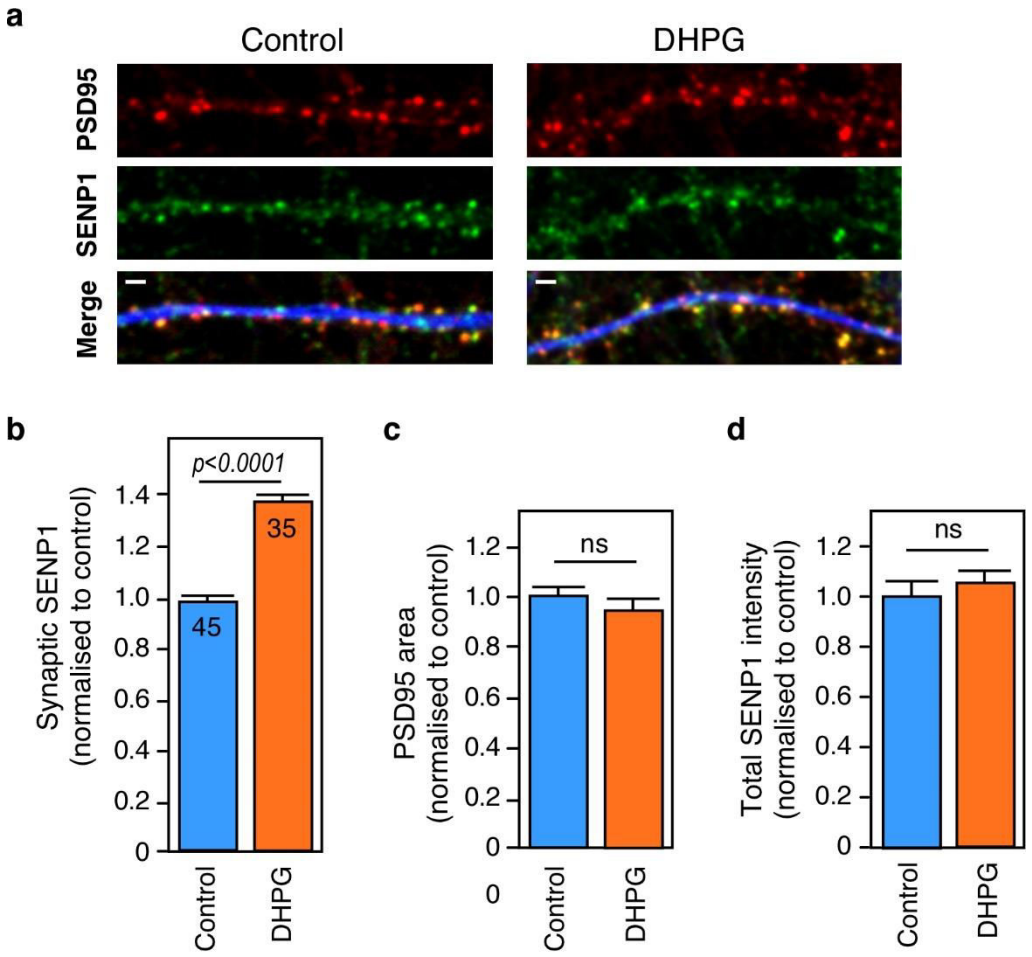
a
Control
DHPG
PSD95
SENP1
Merge
b
Synaptic SENP1
(normalised to control)
p<0.0001
45
35
Control
DHPG
c
PSD95 area
(normalised to control)
ns
Control
DHPG
d
Total SENP1 intensity
(normalised to control)
ns
Control
DHPG

Figure 6

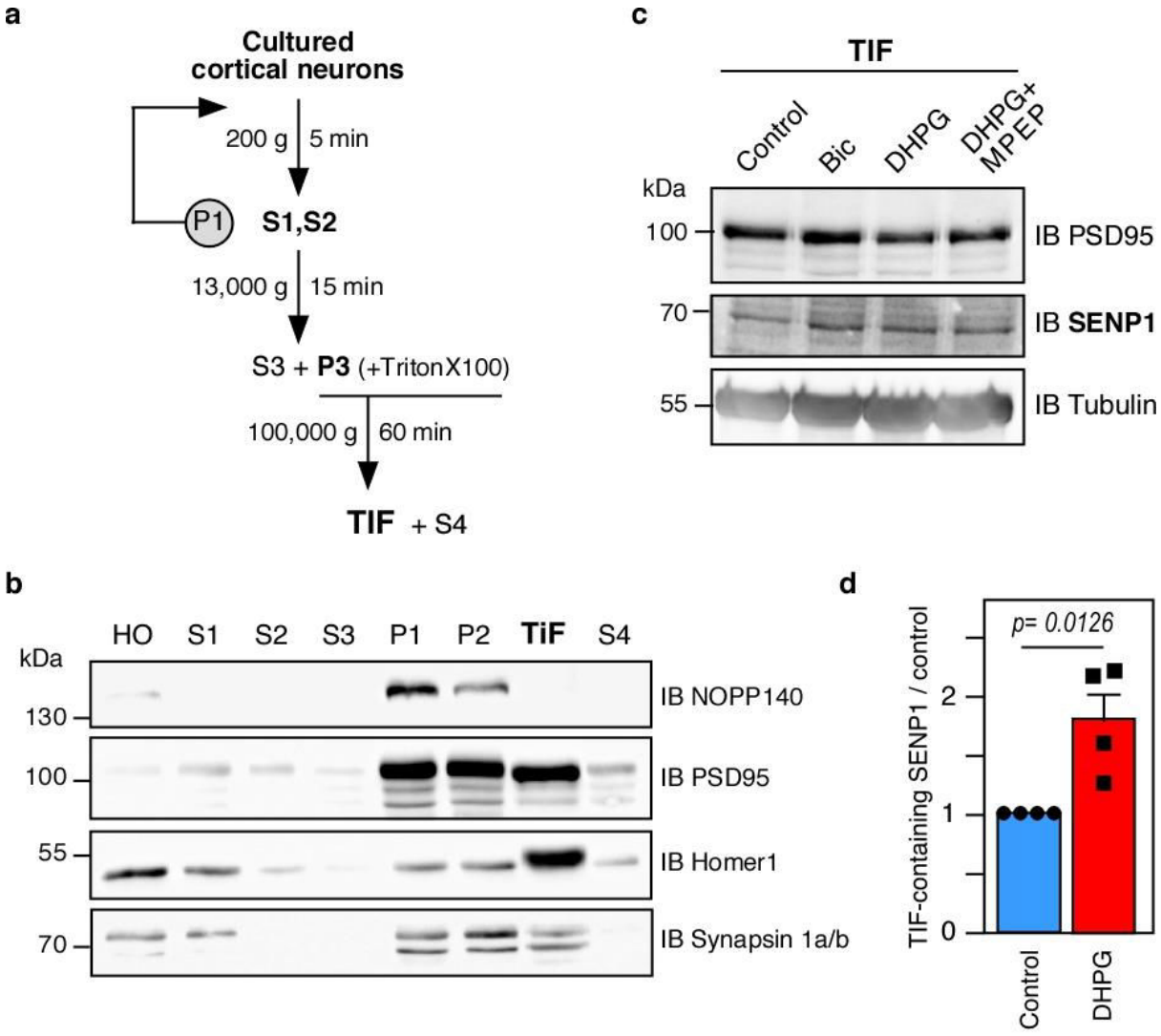
a
Cultured cortical neurons
200 g 5 min
P1
S1,S2
13,000 g 15 min
S3 + P3 (+TritonX100)
100,000 g 60 min
TIF + S4
c
TIF
Control
Bic
DHPG
DHPG+ MPEP
kDa
100
70
55
IB PSD95
IB SENP1
IB Tubulin
b
HO S1 S2 S3 P1 P2 TiF S4
kDa
130
100
55
70
IB NOPP140
IB PSD95
IB Homer1
IB Synapsin 1a/b
d
p= 0.0126
TIF-containing SENP1 / control
0
1
2
Control
DHPG

Figure 7

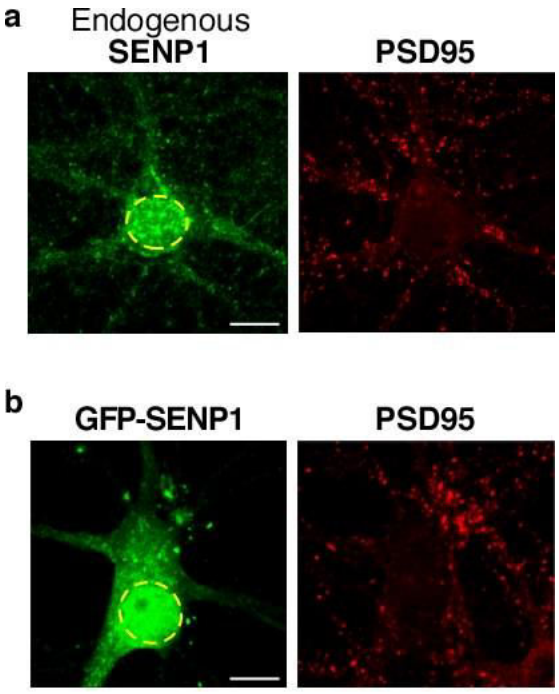

Supplementary figure 1

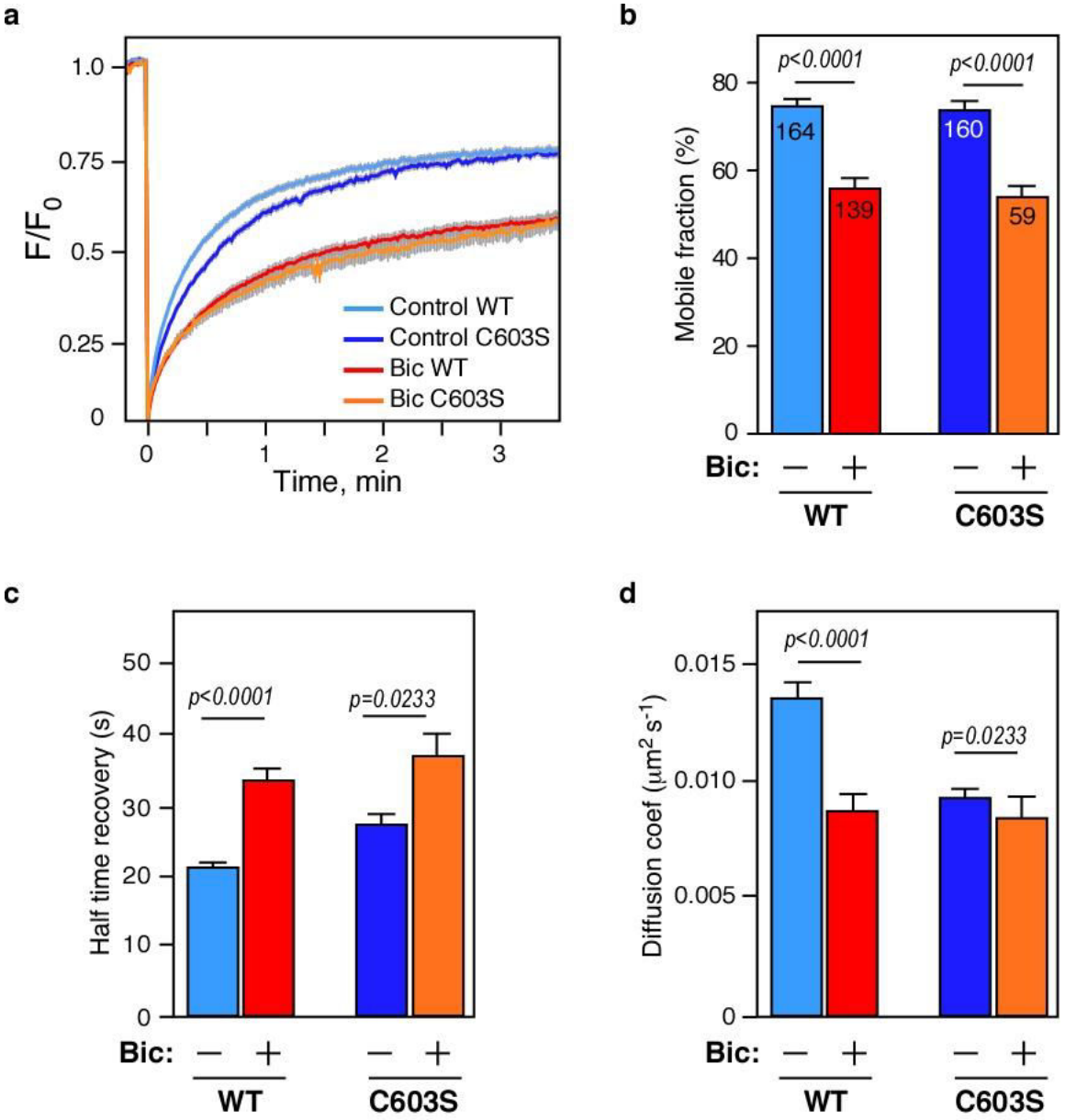

Supplementary figure 2

References

5. References

Aarts, M., Liu, Y., Liu, L., Besshoh, S., Arundine, M., Gurd, J.W., Wang, Y.T., Salter, M.W., and Tymianski, M. (2002). Treatment of ischemic brain damage by perturbing NMDA receptor- PSD-95 protein interactions. Science *298*, 846-850.

Ackermann, M., and Matus, A. (2003). Activity-induced targeting of profilin and stabilization of dendritic spine morphology. Nat Neurosci *6*, 1194-1200.

Ahn, K., Song, J.H., Kim, D.K., Park, M.H., Jo, S.A., and Koh, Y.H. (2009). Ubc9 gene polymorphisms and late-onset Alzheimer's disease in the Korean population: a genetic association study. Neurosci Lett *465*, 272-275.

Akiyama, H., Nakadate, K., and Sakakibara, S.I. (2017). Synaptic localization of the SUMOylation-regulating protease SENP5 in the adult mouse brain. J Comp Neurol.

Alabi, A.A., and Tsien, R.W. (2012). Synaptic vesicle pools and dynamics. Cold Spring Harb Perspect Biol *4*, a013680.

Alvarez, V.A., and Sabatini, B.L. (2007). Anatomical and physiological plasticity of dendritic spines. Annu Rev Neurosci *30*, 79-97.

Andersen, P., Morris, R., Amaral, D., Bliss, T., and O'Keefe, J. (2007). The Hippocampus Book (Oxford University Press).

Andreescu, C.E., Prestori, F., Brandalise, F., D'Errico, A., De Jeu, M.T., Rossi, P., Botta, L., Kohr, G., Perin, P., D'Angelo, E.*, et al.* (2011). NR2A subunit of the N-methyl D-aspartate receptors are required for potentiation at the mossy fiber to granule cell synapse and vestibulo-cerebellar motor learning. Neuroscience *176*, 274-283.

Ardito, F., Giuliani, M., Perrone, D., Troiano, G., and Lo Muzio, L. (2017). The crucial role of protein phosphorylation in cell signaling and its use as targeted therapy (Review). Int J Mol Med *40*, 271-280.

Ba, W., van der Raadt, J., and Nadif Kasri, N. (2013). Rho GTPase signaling at the synapse: implications for intellectual disability. Exp Cell Res *319*, 2368-2374.

Bailey, D., and O'Hare, P. (2004). Characterization of the localization and proteolytic activity of the SUMO-specific protease, SENP1. J Biol Chem *279*, 692-703.

Bal, M., Leitz, J., Reese, A.L., Ramirez, D.M., Durakoglugil, M., Herz, J., Monteggia, L.M., and Kavalali, E.T. (2013). Reelin mobilizes a VAMP7-dependent synaptic vesicle pool and selectively augments spontaneous neurotransmission. Neuron *80*, 934-946.

Barria, A., and Malinow, R. (2002). Subunit-specific NMDA receptor trafficking to synapses. Neuron *35*, 345-353.

Bassell, G.J. (2011). Fragile balance: RNA editing tunes the synapse. Nat Neurosci *14*, 1492-1494.

Bennett, M.K., Miller, K.G., and Scheller, R.H. (1993). Casein kinase II phosphorylates the synaptic vesicle protein p65. J Neurosci *13*, 1701-1707.

Bhattacharyya, S. (2016). Inside story of Group I Metabotropic Glutamate Receptors (mGluRs). Int J Biochem Cell Biol *77*, 205-212.

Bingol, B., and Schuman, E.M. (2006). Activity-dependent dynamics and sequestration of proteasomes in dendritic spines. Nature *441*, 1144-1148.

Bingol, B., Wang, C.F., Arnott, D., Cheng, D., Peng, J., and Sheng, M. (2010). Autophosphorylated CaMKIIalpha acts as a scaffold to recruit proteasomes to dendritic spines. Cell *140*, 567-578.

Bjorkblom, B., Ostman, N., Hongisto, V., Komarovski, V., Filen, J.J., Nyman, T.A., Kallunki, T., Courtney, M.J., and Coffey, E.T. (2005). Constitutively active cytoplasmic c-Jun N-terminal kinase 1 is a dominant regulator of dendritic architecture: role of microtubule-associated protein 2 as an effector. J Neurosci *25*, 6350-6361.

Blackwell, K.T., and Jedrzejewska-Szmek, J. (2013). Molecular mechanisms underlying neuronal synaptic plasticity: systems biology meets computational neuroscience in the wilds of synaptic plasticity. Wiley Interdiscip Rev Syst Biol Med *5*, 717-731.

Bohren, K.M., Nadkarni, V., Song, J.H., Gabbay, K.H., and Owerbach, D. (2004). A M55V polymorphism in a novel SUMO gene (SUMO-4) differentially activates heat shock transcription factors and is associated with susceptibility to type I diabetes mellitus. J Biol Chem *279*, 27233-27238.

Bonaglia, M.C., Giorda, R., Borgatti, R., Felisari, G., Gagliardi, C., Selicorni, A., and Zuffardi, O. (2001). Disruption of the ProSAP2 gene in a t(12;22)(q24.1;q13.3) is associated with the 22q13.3 deletion syndrome. Am J Hum Genet *69*, 261-268.

Bosch, M., Castro, J., Saneyoshi, T., Matsuno, H., Sur, M., and Hayashi, Y. (2014). Structural and molecular remodeling of dendritic spine substructures during long-term potentiation. Neuron *82*, 444-459.

Bramham, C.R., Alme, M.N., Bittins, M., Kuipers, S.D., Nair, R.R., Pai, B., Panja, D., Schubert, M., Soule, J., Tiron, A*., et al.* (2010). The Arc of synaptic memory. Exp Brain Res *200*, 125-140.

Brittain, J.M., Chen, L., Wilson, S.M., Brustovetsky, T., Gao, X., Ashpole, N.M., Molosh, A.I., You, H., Hudmon, A., Shekhar, A*., et al.* (2011). Neuroprotection against traumatic brain injury by a peptide derived from the collapsin response mediator protein 2 (CRMP2). J Biol Chem *286*, 37778-37792.

Brodal, A. (1947). The hippocampus and the sense of smell; a review. Brain *70*, 179-222.

Calakos, N., Schoch, S., Sudhof, T.C., and Malenka, R.C. (2004). Multiple roles for the active zone protein RIM1alpha in late stages of neurotransmitter release. Neuron *42*, 889-896.

Carta, M., Fievre, S., Gorlewicz, A., and Mulle, C. (2014). Kainate receptors in the hippocampus. Eur J Neurosci *39*, 1835-1844.

Castillo, P.E., Schoch, S., Schmitz, F., Sudhof, T.C., and Malenka, R.C. (2002). RIM1alpha is required for presynaptic long-term potentiation. Nature *415*, 327-330.

Cesca, F., Baldelli, P., Valtorta, F., and Benfenati, F. (2010). The synapsins: key actors of synapse function and plasticity. Prog Neurobiol *91*, 313-348.

Chamberlain, S.E., Gonzalez-Gonzalez, I.M., Wilkinson, K.A., Konopacki, F.A., Kantamneni, S., Henley, J.M., and Mellor, J.R. (2012). SUMOylation and phosphorylation of GluK2 regulate kainate receptor trafficking and synaptic plasticity. Nat Neurosci *15*, 845-852.

Chao, H.W., Hong, C.J., Huang, T.N., Lin, Y.L., and Hsueh, Y.P. (2008). SUMOylation of the MAGUK protein CASK regulates dendritic spinogenesis. J Cell Biol *182*, 141-155.

Chavan, V., Willis, J., Walker, S.K., Clark, H.R., Liu, X., Fox, M.A., Srivastava, S., and Mukherjee, K. (2015). Central presynaptic terminals are enriched in ATP but the majority lack mitochondria. PLoS One *10*, e0125185.

Chen, W.Y., Shi, Y.Y., Zheng, Y.L., Zhao, X.Z., Zhang, G.J., Chen, S.Q., Yang, P.D., and He, L. (2004). Case-control study and transmission disequilibrium test provide consistent evidence for association between schizophrenia and genetic variation in the 22q11 gene ZDHHC8. Hum Mol Genet *13*, 2991-2995.

Chen, X., Levy, J.M., Hou, A., Winters, C., Azzam, R., Sousa, A.A., Leapman, R.D., Nicoll, R.A., and Reese, T.S. (2015). PSD-95 family MAGUKs are essential for anchoring AMPA and NMDA receptor complexes at the postsynaptic density. Proc Natl Acad Sci U S A *112*, E6983-6992.

Chen, X., Vinade, L., Leapman, R.D., Petersen, J.D., Nakagawa, T., Phillips, T.M., Sheng, M., and Reese, T.S. (2005). Mass of the postsynaptic density and enumeration of three key molecules. Proc Natl Acad Sci U S A *102*, 11551-11556.

Cheng, J., Huang, M., Zhu, Y., Xin, Y.J., Zhao, Y.K., Huang, J., Yu, J.X., Zhou, W.H., and Qiu, Z. (2014). SUMOylation of MeCP2 is essential for transcriptional repression and hippocampal synapse development. J Neurochem *128*, 798-806.

Cheng, J., Kang, X., Zhang, S., and Yeh, E.T. (2007). SUMO-specific protease 1 is essential for stabilization of HIF1alpha during hypoxia. Cell *131*, 584-595.

Chia, P.H., Li, P., and Shen, K. (2013). Cell biology in neuroscience: cellular and molecular mechanisms underlying presynapse formation. J Cell Biol *203*, 11-22.

Chico, L.K., Van Eldik, L.J., and Watterson, D.M. (2009). Targeting protein kinases in central nervous system disorders. Nat Rev Drug Discov *8*, 892-909.

Choi, J.H., Park, J.Y., Park, S.P., Lee, H., Han, S., Park, K.H., and Suh, Y.H. (2016). Regulation of mGluR7 trafficking by SUMOylation in neurons. Neuropharmacology *102*, 229-235.

Choi, K.Y., Chung, S., and Roche, K.W. (2011). Differential binding of calmodulin to group I metabotropic glutamate receptors regulates receptor trafficking and signaling. J Neurosci *31*, 5921-5930.

Choquet, D., and Triller, A. (2013). The dynamic synapse. Neuron *80*, 691-703.

Chow, K.H., Elgort, S., Dasso, M., Powers, M.A., and Ullman, K.S. (2014). The SUMO proteases SENP1 and SENP2 play a critical role in nucleoporin homeostasis and nuclear pore complex function. Mol Biol Cell *25*, 160-168.

Chudakov, D.M., Lukyanov, S., and Lukyanov, K.A. (2007). Tracking intracellular protein movements using photoswitchable fluorescent proteins PS-CFP2 and Dendra2. Nat Protoc *2*, 2024-2032.

Ciechanover, A., Heller, H., Elias, S., Haas, A.L., and Hershko, A. (1980). ATP-dependent conjugation of reticulocyte proteins with the polypeptide required for protein degradation. Proc Natl Acad Sci U S A *77*, 1365-1368.

Collins, M.O., Husi, H., Yu, L., Brandon, J.M., Anderson, C.N., Blackstock, W.P., Choudhary, J.S., and Grant, S.G. (2006). Molecular characterization and comparison of the components and multiprotein complexes in the postsynaptic proteome. J Neurochem *97 Suppl 1*, 16-23.

Cook, D.J., Teves, L., and Tymianski, M. (2012). Treatment of stroke with a PSD-95 inhibitor in the gyrencephalic primate brain. Nature *483*, 213-217.

Coombs, I.D., and Cull-Candy, S.G. (2009). Transmembrane AMPA receptor regulatory proteins and AMPA receptor function in the cerebellum. Neuroscience *162*, 656-665.

Corneveaux, J.J., Myers, A.J., Allen, A.N., Pruzin, J.J., Ramirez, M., Engel, A., Nalls, M.A., Chen, K., Lee, W., Chewning, K.*, et al.* (2010). Association of CR1, CLU and PICALM with Alzheimer's disease in a cohort of clinically characterized and neuropathologically verified individuals. Hum Mol Genet *19*, 3295-3301.

Coultrap, S.J., and Bayer, K.U. (2012). CaMKII regulation in information processing and storage. Trends Neurosci *35*, 607-618.

Coultrap, S.J., Buard, I., Kulbe, J.R., Dell'Acqua, M.L., and Bayer, K.U. (2010). CaMKII autonomy is substrate-dependent and further stimulated by Ca2+/calmodulin. J Biol Chem *285*, 17930-17937.

Coultrap, S.J., Freund, R.K., O'Leary, H., Sanderson, J.L., Roche, K.W., Dell'Acqua, M.L., and Bayer, K.U. (2014). Autonomous CaMKII mediates both LTP and LTD using a mechanism for differential substrate site selection. Cell Rep *6*, 431-437.

Craig, T.J., Anderson, D., Evans, A.J., Girach, F., and Henley, J.M. (2015). SUMOylation of Syntaxin1A regulates presynaptic endocytosis. Sci Rep *5*, 17669.

Craig, T.J., and Henley, J.M. (2012). SUMOylation, Arc and the regulation homeostatic synaptic scaling: Implications in health and disease. Commun Integr Biol *5*, 634-636.

Crawford, D.C., and Kavalali, E.T. (2015). Molecular underpinnings of synaptic vesicle pool heterogeneity. Traffic *16*, 338-364.

Cubenas-Potts, C., Goeres, J.D., and Matunis, M.J. (2013). SENP1 and SENP2 affect spatial and temporal control of sumoylation in mitosis. Mol Biol Cell *24*, 3483-3495.

Curtis, D.R., Duggan, A.W., Felix, D., and Johnston, G.A. (1970). GABA, bicuculline and central inhibition. Nature *226*, 1222-1224.

Daniel, J.A., Cooper, B.H., Palvimo, J.J., Zhang, F.P., Brose, N., and Tirard, M. (2017). Analysis of SUMO1-conjugation at synapses. Elife *6*.

Davis, G.A., and Bloom, F.E. (1973). Isolation of synaptic junctional complexes from rat brain. Brain Res *62*, 135-153.

Davis, S., Butcher, S.P., and Morris, R.G. (1992). The NMDA receptor antagonist D-2-amino-5-phosphonopentanoate (D-AP5) impairs spatial learning and LTP in vivo at intracerebral concentrations comparable to those that block LTP in vitro. J Neurosci *12*, 21-34.

Deak, F., Schoch, S., Liu, X., Sudhof, T.C., and Kavalali, E.T. (2004). Synaptobrevin is essential for fast synaptic-vesicle endocytosis. Nat Cell Biol *6*, 1102-1108.

Diez-Guerra, F.J., and Avila, J. (1993). MAP2 phosphorylation parallels dendrite arborization in hippocampal neurones in culture. Neuroreport *4*, 419-422.

Ding, S.L. (2013). Comparative anatomy of the prosubiculum, subiculum, presubiculum, postsubiculum, and parasubiculum in human, monkey, and rodent. J Comp Neurol *521*, 4145-4162.

Dodson, P.D., and Forsythe, I.D. (2004). Presynaptic K+ channels: electrifying regulators of synaptic terminal excitability. Trends Neurosci *27*, 210-217.

Dorval, V., and Fraser, P.E. (2006). Small ubiquitin-like modifier (SUMO) modification of natively unfolded proteins tau and alpha-synuclein. J Biol Chem *281*, 9919-9924.

Dorval, V., Mazzella, M.J., Mathews, P.M., Hay, R.T., and Fraser, P.E. (2007). Modulation of Abeta generation by small ubiquitin-like modifiers does not require conjugation to target proteins. Biochem J *404*, 309-316.

Dosemeci, A., Makusky, A.J., Jankowska-Stephens, E., Yang, X., Slotta, D.J., and Markey, S.P. (2007). Composition of the synaptic PSD-95 complex. Mol Cell Proteomics *6*, 1749-1760.

Dudek, S.M., Alexander, G.M., and Farris, S. (2016). Rediscovering area CA2: unique properties and functions. Nat Rev Neurosci *17*, 89-102.

Dulubova, I., Lou, X., Lu, J., Huryeva, I., Alam, A., Schneggenburger, R., Sudhof, T.C., and Rizo, J. (2005). A Munc13/RIM/Rab3 tripartite complex: from priming to plasticity? EMBO J *24*, 2839-2850.

Duman, J.G., Mulherkar, S., Tu, Y.K., J, X.C., and Tolias, K.F. (2015). Mechanisms for spatiotemporal regulation of Rho-GTPase signaling at synapses. Neurosci Lett *601*, 4-10.

Dustrude, E.T., Wilson, S.M., Ju, W., Xiao, Y., and Khanna, R. (2013). CRMP2 protein SUMOylation modulates NaV1.7 channel trafficking. J Biol Chem *288*, 24316-24331.

Dutting, E., Schroder-Kress, N., Sticht, H., and Enz, R. (2011). SUMO E3 ligases are expressed in the retina and regulate SUMOylation of the metabotropic glutamate receptor 8b. Biochem J *435*, 365-371.

Ehlers, M.D. (2003). Activity level controls postsynaptic composition and signaling via the ubiquitin-proteasome system. Nat Neurosci *6*, 231-242.

Ehrlich, I., Klein, M., Rumpel, S., and Malinow, R. (2007). PSD-95 is required for activity-driven synapse stabilization. Proc Natl Acad Sci U S A *104*, 4176-4181.

Ehrlich, I., and Malinow, R. (2004). Postsynaptic density 95 controls AMPA receptor incorporation during long-term potentiation and experience-driven synaptic plasticity. J Neurosci *24*, 916-927.

Feligioni, M., Nishimune, A., and Henley, J.M. (2009). Protein SUMOylation modulates calcium influx and glutamate release from presynaptic terminals. Eur J Neurosci *29*, 1348-1356.

Fergestad, T., Wu, M.N., Schulze, K.L., Lloyd, T.E., Bellen, H.J., and Broadie, K. (2001). Targeted mutations in the syntaxin H3 domain specifically disrupt SNARE complex function in synaptic transmission. J Neurosci *21*, 9142-9150.

Ferguson, S.S., Downey, W.E., 3rd, Colapietro, A.M., Barak, L.S., Menard, L., and Caron, M.G. (1996). Role of beta-arrestin in mediating agonist-promoted G protein-coupled receptor internalization. Science *271*, 363-366.

Fernandez-Busnadiego, R., Zuber, B., Maurer, U.E., Cyrklaff, M., Baumeister, W., and Lucic, V. (2010). Quantitative analysis of the native presynaptic cytomatrix by cryoelectron tomography. J Cell Biol *188*, 145-156.

Feyder, M., Karlsson, R.M., Mathur, P., Lyman, M., Bock, R., Momenan, R., Munasinghe, J., Scattoni, M.L., Ihne, J., Camp, M.*, et al.* (2010). Association of mouse Dlg4 (PSD-95) gene deletion and human DLG4 gene variation with phenotypes relevant to autism spectrum disorders and Williams' syndrome. Am J Psychiatry *167*, 1508-1517.

Fischer, E.H., Graves, D.J., Crittenden, E.R., and Krebs, E.G. (1959). Structure of the site phosphorylated in the phosphorylase b to a reaction. J Biol Chem *234*, 1698-1704.

Flotho, A., and Melchior, F. (2013). Sumoylation: a regulatory protein modification in health and disease. Annu Rev Biochem *82*, 357-385.

Fong, D.K., Rao, A., Crump, F.T., and Craig, A.M. (2002). Rapid synaptic remodeling by protein kinase C: reciprocal translocation of NMDA receptors and calcium/calmodulin-dependent kinase II. J Neurosci *22*, 2153-2164.

Fu, J., Yu, H.M., Chiu, S.Y., Mirando, A.J., Maruyama, E.O., Cheng, J.G., and Hsu, W. (2014a). Disruption of SUMO-specific protease 2 induces mitochondria mediated neurodegeneration. PLoS Genet *10*, e1004579.

Fu, M.M., Nirschl, J.J., and Holzbaur, E.L.F. (2014b). LC3 binding to the scaffolding protein JIP1 regulates processive dynein-driven transport of autophagosomes. Dev Cell *29*, 577-590.

Fukata, Y., and Fukata, M. (2010). Protein palmitoylation in neuronal development and synaptic plasticity. Nat Rev Neurosci *11*, 161-175.

Gambrill, A.C., and Barria, A. (2011). NMDA receptor subunit composition controls synaptogenesis and synapse stabilization. Proc Natl Acad Sci U S A *108*, 5855-5860.

Gao, J., Hirata, M., Mizokami, A., Zhao, J., Takahashi, I., Takeuchi, H., and Hirata, M. (2016). Differential role of SNAP-25 phosphorylation by protein kinases A and C in the regulation of SNARE complex formation and exocytosis in PC12 cells. Cell Signal *28*, 425-437.

Garcia-Lopez, P., Garcia-Marin, V., and Freire, M. (2007). The discovery of dendritic spines by Cajal in 1888 and its relevance in the present neuroscience. Prog Neurobiol *83*, 110-130.

Gardiner, K. (2006). Transcriptional dysregulation in Down syndrome: predictions for altered protein complex stoichiometries and post-translational modifications, and consequences for learning/behavior genes ELK, CREB, and the estrogen and glucocorticoid receptors. Behav Genet *36*, 439-453.

Gardoni, F., Mauceri, D., Malinverno, M., Polli, F., Costa, C., Tozzi, A., Siliquini, S., Picconi, B., Cattabeni, F., Calabresi, P.*, et al.* (2009). Decreased NR2B subunit synaptic levels cause impaired long-term potentiation but not long-term depression. J Neurosci *29*, 669-677.

Gardoni, F., Pagliardini, S., Setola, V., Bassanini, S., Cattabeni, F., Battaglia, G., and Di Luca, M. (2003). The NMDA receptor complex is altered in an animal model of human cerebral heterotopia. J Neuropathol Exp Neurol *62*, 662-675.

Gasparini, F., Lingenhohl, K., Stoehr, N., Flor, P.J., Heinrich, M., Vranesic, I., Biollaz, M., Allgeier, H., Heckendorn, R., Urwyler, S.*, et al.* (1999). 2-Methyl-6-(phenylethynyl)-pyridine (MPEP), a potent, selective and systemically active mGlu5 receptor antagonist. Neuropharmacology *38*, 1493-1503.

Geiss-Friedlander, R., and Melchior, F. (2007). Concepts in sumoylation: a decade on. Nat Rev Mol Cell Biol *8*, 947-956.

Geppert, M., Goda, Y., Stevens, C.F., and Sudhof, T.C. (1997). The small GTP-binding protein Rab3A regulates a late step in synaptic vesicle fusion. Nature *387*, 810-814.

Giese, K.P., Fedorov, N.B., Filipkowski, R.K., and Silva, A.J. (1998). Autophosphorylation at Thr286 of the alpha calcium-calmodulin kinase II in LTP and learning. Science *279*, 870-873.

Girach, F., Craig, T.J., Rocca, D.L., and Henley, J.M. (2013). RIM1alpha SUMOylation is required for fast synaptic vesicle exocytosis. Cell Rep *5*, 1294-1301.

Glasscock, E., Qian, J., Yoo, J.W., and Noebels, J.L. (2007). Masking epilepsy by combining two epilepsy genes. Nat Neurosci *10*, 1554-1558.

Gleitz, J., Tosch, C., Beile, A., and Peters, T. (1996). The protective action of tetrodotoxin and (+/-)-kavain on anaerobic glycolysis, ATP content and intracellular Na+ and Ca2+ of anoxic brain vesicles. Neuropharmacology *35*, 1743-1752.

Goo, M.S., Sancho, L., Slepak, N., Boassa, D., Deerinck, T.J., Ellisman, M.H., Bloodgood, B.L., and Patrick, G.N. (2017). Activity-dependent trafficking of lysosomes in dendrites and dendritic spines. J Cell Biol *216*, 2499-2513.

Granger, A.J., Shi, Y., Lu, W., Cerpas, M., and Nicoll, R.A. (2013). LTP requires a reserve pool of glutamate receptors independent of subunit type. Nature *493*, 495-500.

Grupe, A., Abraham, R., Li, Y., Rowland, C., Hollingworth, P., Morgan, A., Jehu, L., Segurado, R., Stone, D., Schadt, E.*, et al.* (2007). Evidence for novel susceptibility genes for late-onset Alzheimer's disease from a genome-wide association study of putative functional variants. Hum Mol Genet *16*, 865-873.

Gu, J., and Zheng, J.Q. (2009). Microtubules in Dendritic Spine Development and Plasticity. Open Neurosci J *3*, 128-133.

Gulia, R., Sharma, R., and Bhattacharyya, S. (2017). A Critical Role for Ubiquitination in the Endocytosis of Glutamate Receptors. J Biol Chem *292*, 1426-1437.

Guo, D., Li, M., Zhang, Y., Yang, P., Eckenrode, S., Hopkins, D., Zheng, W., Purohit, S., Podolsky, R.H., Muir, A.*, et al.* (2004). A functional variant of SUMO4, a new I kappa B alpha modifier, is associated with type 1 diabetes. Nat Genet *36*, 837-841.

Gwizdek, C., Casse, F., and Martin, S. (2013). Protein sumoylation in brain development, neuronal morphology and spinogenesis. Neuromolecular Med *15*, 677-691.

Hallengren, J., Chen, P.C., and Wilson, S.M. (2013). Neuronal ubiquitin homeostasis. Cell Biochem Biophys *67*, 67-73.

Halt, A.R., Dallapiazza, R.F., Zhou, Y., Stein, I.S., Qian, H., Juntti, S., Wojcik, S., Brose, N., Silva, A.J., and Hell, J.W. (2012). CaMKII binding to GluN2B is critical during memory consolidation. EMBO J *31*, 1203-1216.

Hamilton, A.M., Oh, W.C., Vega-Ramirez, H., Stein, I.S., Hell, J.W., Patrick, G.N., and Zito, K. (2012). Activity-dependent growth of new dendritic spines is regulated by the proteasome. Neuron *74*, 1023-1030.

Hammond, C. (2001). Cellular and Molecular Neurobiology, 2nd edn (Elsevier).

Harris, K.M., and Weinberg, R.J. (2012). Ultrastructure of synapses in the mammalian brain. Cold Spring Harb Perspect Biol *4*.

Hay, R.T. (2005). SUMO: a history of modification. Mol Cell *18*, 1-12.

Hayashi, K., Ohshima, T., and Mikoshiba, K. (2002a). Pak1 is involved in dendrite initiation as a downstream effector of Rac1 in cortical neurons. Mol Cell Neurosci *20*, 579-594.

Hayashi, T., Seki, M., Maeda, D., Wang, W., Kawabe, Y., Seki, T., Saitoh, H., Fukagawa, T., Yagi, H., and Enomoto, T. (2002b). Ubc9 is essential for viability of higher eukaryotic cells. Exp Cell Res *280*, 212-221.

He, C.X., and Portera-Cailliau, C. (2013). The trouble with spines in fragile X syndrome: density, maturity and plasticity. Neuroscience *251*, 120-128.

He, E., Wierda, K., van Westen, R., Broeke, J.H., Toonen, R.F., Cornelisse, L.N., and Verhage, M. (2017). Munc13-1 and Munc18-1 together prevent NSF-dependent de-priming of synaptic vesicles. Nat Commun *8*, 15915.

Hell, J.W. (2014). CaMKII: claiming center stage in postsynaptic function and organization. Neuron *81*, 249-265.

Henley, J.M., Craig, T.J., and Wilkinson, K.A. (2014). Neuronal SUMOylation: mechanisms, physiology, and roles in neuronal dysfunction. Physiol Rev *94*, 1249-1285.

Henley, J.M., and Wilkinson, K.A. (2013). AMPA receptor trafficking and the mechanisms underlying synaptic plasticity and cognitive aging. Dialogues Clin Neurosci *15*, 11-27.

Henley, J.M., and Wilkinson, K.A. (2016). Synaptic AMPA receptor composition in development, plasticity and disease. Nat Rev Neurosci *17*, 337-350.

Hershko, A., Ciechanover, A., Heller, H., Haas, A.L., and Rose, I.A. (1980). Proposed role of ATP in protein breakdown: conjugation of protein with multiple chains of the polypeptide of ATP-dependent proteolysis. Proc Natl Acad Sci U S A *77*, 1783-1786.

Heuser, J.E., and Reese, T.S. (1973). Evidence for recycling of synaptic vesicle membrane during transmitter release at the frog neuromuscular junction. J Cell Biol *57*, 315-344.

Hickey, C.M., Wilson, N.R., and Hochstrasser, M. (2012). Function and regulation of SUMO proteases. Nat Rev Mol Cell Biol *13*, 755-766.

Hill, M.D., Martin, R.H., Mikulis, D., Wong, J.H., Silver, F.L., Terbrugge, K.G., Milot, G., Clark, W.M., Macdonald, R.L., Kelly, M.E*., et al.* (2012). Safety and efficacy of NA-1 in patients with iatrogenic stroke after endovascular aneurysm repair (ENACT): a phase 2, randomised, double-blind, placebo-controlled trial. Lancet Neurol *11*, 942-950.

Hill, T.C., and Zito, K. (2013). LTP-induced long-term stabilization of individual nascent dendritic spines. J Neurosci *33*, 678-686.

Hodges, J.L., Newell-Litwa, K., Asmussen, H., Vicente-Manzanares, M., and Horwitz, A.R. (2011). Myosin IIb activity and phosphorylation status determines dendritic spine and post-synaptic density morphology. PLoS One *6*, e24149.

Hoogenraad, C.C., and Bradke, F. (2009). Control of neuronal polarity and plasticity--a renaissance for microtubules? Trends Cell Biol *19*, 669-676.

Hotulainen, P., and Hoogenraad, C.C. (2010). Actin in dendritic spines: connecting dynamics to function. J Cell Biol *189*, 619-629.

Hsu, M.T., Guo, C.L., Liou, A.Y., Chang, T.Y., Ng, M.C., Florea, B.I., Overkleeft, H.S., Wu, Y.L., Liao, J.C., and Cheng, P.L. (2015). Stage-Dependent Axon Transport of Proteasomes Contributes to Axon Development. Dev Cell *35*, 418-431.

Hu, X., Ballo, L., Pietila, L., Viesselmann, C., Ballweg, J., Lumbard, D., Stevenson, M., Merriam, E., and Dent, E.W. (2011). BDNF-induced increase of PSD-95 in dendritic spines requires dynamic microtubule invasions. J Neurosci *31*, 15597-15603.

Hu, X., Viesselmann, C., Nam, S., Merriam, E., and Dent, E.W. (2008). Activity-dependent dynamic microtubule invasion of dendritic spines. J Neurosci *28*, 13094-13105.

Huang, K., Yanai, A., Kang, R., Arstikaitis, P., Singaraja, R.R., Metzler, M., Mullard, A., Haigh, B., Gauthier-Campbell, C., Gutekunst, C.A*., et al.* (2004). Huntingtin-interacting protein HIP14 is a palmitoyl transferase involved in palmitoylation and trafficking of multiple neuronal proteins. Neuron *44*, 977-986.

Huang, X.P., and Hampson, D.R. (2000). Inhibition of microtubule formation by metabotropic glutamate receptors. J Neurochem *74*, 104-113.

Huber, K.M., Kayser, M.S., and Bear, M.F. (2000). Role for rapid dendritic protein synthesis in hippocampal mGluR-dependent long-term depression. Science *288*, 1254-1257.

Huber, K.M., Roder, J.C., and Bear, M.F. (2001). Chemical induction of mGluR5- and protein synthesis--dependent long-term depression in hippocampal area CA1. J Neurophysiol *86*, 321-325.

Ip, J.P., Fu, A.K., and Ip, N.Y. (2014). CRMP2: functional roles in neural development and therapeutic potential in neurological diseases. Neuroscientist *20*, 589-598.

Ito, I., Kohda, A., Tanabe, S., Hirose, E., Hayashi, M., Mitsunaga, S., and Sugiyama, H. (1992). 3,5-Dihydroxyphenyl-glycine: a potent agonist of metabotropic glutamate receptors. Neuroreport *3*, 1013-1016.

Jaafari, N., Henley, J.M., and Hanley, J.G. (2012). PICK1 mediates transient synaptic expression of GluA2-lacking AMPA receptors during glycine-induced AMPA receptor trafficking. J Neurosci *32*, 11618-11630.

Jaafari, N., Konopacki, F.A., Owen, T.F., Kantamneni, S., Rubin, P., Craig, T.J., Wilkinson, K.A., and Henley, J.M. (2013). SUMOylation is required for glycine-induced increases in AMPA receptor surface expression (ChemLTP) in hippocampal neurons. PLoS One *8*, e52345.

Jackson, A.C., and Nicoll, R.A. (2011). The expanding social network of ionotropic glutamate receptors: TARPs and other transmembrane auxiliary subunits. Neuron *70*, 178-199.

Jedlicka, P., Vlachos, A., Schwarzacher, S.W., and Deller, T. (2008). A role for the spine apparatus in LTP and spatial learning. Behav Brain Res *192*, 12-19.

Jin, D.Z., Guo, M.L., Xue, B., Fibuch, E.E., Choe, E.S., Mao, L.M., and Wang, J.Q. (2013a). Phosphorylation and feedback regulation of metabotropic glutamate receptor 1 by calcium/calmodulin-dependent protein kinase II. J Neurosci *33*, 3402-3412.

Jin, D.Z., Guo, M.L., Xue, B., Mao, L.M., and Wang, J.Q. (2013b). Differential regulation of CaMKIIalpha interactions with mGluR5 and NMDA receptors by Ca(2+) in neurons. J Neurochem *127*, 620-631.

Johnson, E.S., and Blobel, G. (1997). Ubc9p is the conjugating enzyme for the ubiquitin-like protein Smt3p. J Biol Chem *272*, 26799-26802.

Ju, W., Li, Q., Wilson, S.M., Brittain, J.M., Meroueh, L., and Khanna, R. (2013). SUMOylation alters CRMP2 regulation of calcium influx in sensory neurons. Channels (Austin) *7*, 153-159.

Kalinowska, M., and Francesconi, A. (2016). Group I Metabotropic Glutamate Receptor Interacting Proteins: Fine-Tuning Receptor Functions in Health and Disease. Curr Neuropharmacol *14*, 494-503.

Kang, R., Wan, J., Arstikaitis, P., Takahashi, H., Huang, K., Bailey, A.O., Thompson, J.X., Roth, A.F., Drisdel, R.C., Mastro, R.*, et al.* (2008). Neural palmitoyl-proteomics reveals dynamic synaptic palmitoylation. Nature *456*, 904-909.

Kapitein, L.C., Yau, K.W., Gouveia, S.M., van der Zwan, W.A., Wulf, P.S., Keijzer, N., Demmers, J., Jaworski, J., Akhmanova, A., and Hoogenraad, C.C. (2011). NMDA receptor activation suppresses microtubule growth and spine entry. J Neurosci *31*, 8194-8209.

Karaca, M., Frigerio, F., Migrenne, S., Martin-Levilain, J., Skytt, D.M., Pajecka, K., Martin-del-Rio, R., Gruetter, R., Tamarit-Rodriguez, J., Waagepetersen, H.S.*, et al.* (2015). GDH-Dependent Glutamate Oxidation in the Brain Dictates Peripheral Energy Substrate Distribution. Cell Rep *13*, 365-375.

Karakas, E., Regan, M.C., and Furukawa, H. (2015). Emerging structural insights into the function of ionotropic glutamate receptors. Trends Biochem Sci *40*, 328-337.

Kataoka, M., Kuwahara, R., Iwasaki, S., Shoji-Kasai, Y., and Takahashi, M. (2000). Nerve growth factor-induced phosphorylation of SNAP-25 in PC12 cells: a possible involvement in the regulation of SNAP-25 localization. J Neurochem *74*, 2058-2066.

Katayama, N., Yamamori, S., Fukaya, M., Kobayashi, S., Watanabe, M., Takahashi, M., and Manabe, T. (2017). SNAP-25 phosphorylation at Ser187 regulates synaptic facilitation and short-term plasticity in an age-dependent manner. Sci Rep *7*, 7996.

Kelly, P.T., and Cotman, C.W. (1978). Synaptic proteins. Characterization of tubulin and actin and identification of a distinct postsynaptic density polypeptide. J Cell Biol *79*, 173-183.

Kim, M.J., Futai, K., Jo, J., Hayashi, Y., Cho, K., and Sheng, M. (2007). Synaptic accumulation of PSD-95 and synaptic function regulated by phosphorylation of serine-295 of PSD-95. Neuron *56*, 488-502.

Kim, Y.H., Sung, K.S., Lee, S.J., Kim, Y.O., Choi, C.Y., and Kim, Y. (2005). Desumoylation of homeodomain-interacting protein kinase 2 (HIPK2) through the cytoplasmic-nuclear shuttling of the SUMO-specific protease SENP1. FEBS Lett *579*, 6272-6278.

Kim, Y.M., Jang, W.H., Quezado, M.M., Oh, Y., Chung, K.C., Junn, E., and Mouradian, M.M. (2011). Proteasome inhibition induces alpha-synuclein SUMOylation and aggregate formation. J Neurol Sci *307*, 157-161.

Klassen, M.P., Wu, Y.E., Maeder, C.I., Nakae, I., Cueva, J.G., Lehrman, E.K., Tada, M., Gengyo-Ando, K., Wang, G.J., Goodman, M.*, et al.* (2010). An Arf-like small G protein, ARL-8, promotes the axonal transport of presynaptic cargoes by suppressing vesicle aggregation. Neuron *66*, 710-723.

Kneussel, M., and Wagner, W. (2013). Myosin motors at neuronal synapses: drivers of membrane transport and actin dynamics. Nat Rev Neurosci *14*, 233-247.

Kofuji, T., Fujiwara, T., Sanada, M., Mishima, T., and Akagawa, K. (2014). HPC-1/syntaxin 1A and syntaxin 1B play distinct roles in neuronal survival. J Neurochem *130*, 514-525.

Kohansal-Nodehi, M., Chua, J.J., Urlaub, H., Jahn, R., and Czernik, D. (2016). Analysis of protein phosphorylation in nerve terminal reveals extensive changes in active zone proteins upon exocytosis. Elife *5*.

Kondo, M., Takei, Y., and Hirokawa, N. (2012). Motor protein KIF1A is essential for hippocampal synaptogenesis and learning enhancement in an enriched environment. Neuron *73*, 743-757.

Konopacki, F.A., Jaafari, N., Rocca, D.L., Wilkinson, K.A., Chamberlain, S., Rubin, P., Kantamneni, S., Mellor, J.R., and Henley, J.M. (2011). Agonist-induced PKC phosphorylation regulates GluK2 SUMOylation and kainate receptor endocytosis. Proc Natl Acad Sci U S A *108*, 19772-19777.

Kreutz, M.R., and Sala, C.D. (2012). Synaptic plasticity : dynamics, development and disease (Wien: Springer).

Kristensen, A.S., Jenkins, M.A., Banke, T.G., Schousboe, A., Makino, Y., Johnson, R.C., Huganir, R., and Traynelis, S.F. (2011). Mechanism of Ca2+/calmodulin-dependent kinase II regulation of AMPA receptor gating. Nat Neurosci *14*, 727-735.

Krumova, P., Meulmeester, E., Garrido, M., Tirard, M., Hsiao, H.H., Bossis, G., Urlaub, H., Zweckstetter, M., Kugler, S., Melchior, F.*, et al.* (2011). Sumoylation inhibits alpha-synuclein aggregation and toxicity. J Cell Biol *194*, 49-60.

Krupnick, J.G., and Benovic, J.L. (1998). The role of receptor kinases and arrestins in G protein-coupled receptor regulation. Annu Rev Pharmacol Toxicol *38*, 289-319.

Kumari, R., Castillo, C., and Francesconi, A. (2013). Agonist-dependent signaling by group I metabotropic glutamate receptors is regulated by association with lipid domains. J Biol Chem *288*, 32004-32019.

Kunadt, M., Eckermann, K., Stuendl, A., Gong, J., Russo, B., Strauss, K., Rai, S., Kugler, S., Falomir Lockhart, L., Schwalbe, M.*, et al.* (2015). Extracellular vesicle sorting of alpha-Synuclein is regulated by sumoylation. Acta Neuropathol *129*, 695-713.

Lai, T.W., Shyu, W.C., and Wang, Y.T. (2011). Stroke intervention pathways: NMDA receptors and beyond. Trends Mol Med *17*, 266-275.

Lavreysen, H., Wouters, R., Bischoff, F., Nobrega Pereira, S., Langlois, X., Blokland, S., Somers, M., Dillen, L., and Lesage, A.S. (2004). JNJ16259685, a highly potent, selective and systemically active mGlu1 receptor antagonist. Neuropharmacology *47*, 961-972.

Lazcano, Z., Solis, O., Bringas, M.E., Limon, D., Diaz, A., Espinosa, B., Garcia-Pelaez, I., Flores, G., and Guevara, J. (2014). Unilateral injection of Abeta25-35 in the hippocampus reduces the number of dendritic spines in hyperglycemic rats. Synapse.

Lee, H.K. (2006). Synaptic plasticity and phosphorylation. Pharmacol Ther *112*, 810-832.

Lee, L., Dale, E., Staniszewski, A., Zhang, H., Saeed, F., Sakurai, M., Fa, M., Orozco, I., Michelassi, F., Akpan, N.*, et al.* (2014). Regulation of synaptic plasticity and cognition by SUMO in normal physiology and Alzheimer's disease. Sci Rep *4*, 7190.

Lee, S.E., Simons, S.B., Heldt, S.A., Zhao, M., Schroeder, J.P., Vellano, C.P., Cowan, D.P., Ramineni, S., Yates, C.K., Feng, Y.*, et al.* (2010). RGS14 is a natural suppressor of both synaptic plasticity in CA2 neurons and hippocampal-based learning and memory. Proc Natl Acad Sci U S A *107*, 16994-16998.

Lee, S.J., Escobedo-Lozoya, Y., Szatmari, E.M., and Yasuda, R. (2009). Activation of CaMKII in single dendritic spines during long-term potentiation. Nature *458*, 299-304.

Lerma, J., and Marques, J.M. (2013). Kainate receptors in health and disease. Neuron *80*, 292-311.
Li, J., Wilkinson, B., Clementel, V.A., Hou, J., O'Dell, T.J., and Coba, M.P. (2016). Long-term potentiation modulates synaptic phosphorylation networks and reshapes the structure of the postsynaptic interactome. Sci Signal *9*, rs8.

Li, Y., Wang, H., Wang, S., Quon, D., Liu, Y.W., and Cordell, B. (2003). Positive and negative regulation of APP amyloidogenesis by sumoylation. Proc Natl Acad Sci U S A *100*, 259-264.

Liang, Y.C., Lee, C.C., Yao, Y.L., Lai, C.C., Schmitz, M.L., and Yang, W.M. (2016). SUMO5, a Novel Poly-SUMO Isoform, Regulates PML Nuclear Bodies. Sci Rep *6*, 26509.

Lin, Y.C., and Redmond, L. (2008). CaMKIIbeta binding to stable F-actin in vivo regulates F-actin filament stability. Proc Natl Acad Sci U S A *105*, 15791-15796.

Lisman, J. (1994). The CaM kinase II hypothesis for the storage of synaptic memory. Trends Neurosci *17*, 406-412.

Liu, X., Heidelberger, R., and Janz, R. (2014). Phosphorylation of syntaxin 3B by CaMKII regulates the formation of t-SNARE complexes. Mol Cell Neurosci *60*, 53-62.

Long, X., and Griffith, L.C. (2000). Identification and characterization of a SUMO-1 conjugation system that modifies neuronal calcium/calmodulin-dependent protein kinase II in Drosophila melanogaster. J Biol Chem *275*, 40765-40776.

Loriol, C., Casse, F., Khayachi, A., Poupon, G., Chafai, M., Deval, E., Gwizdek, C., and Martin, S. (2014). mGlu5 receptors regulate synaptic sumoylation via a transient PKC-dependent diffusional trapping of Ubc9 into spines. Nat Commun *5*, 5113.

Loriol, C., Khayachi, A., Poupon, G., Gwizdek, C., and Martin, S. (2013). Activity-dependent regulation of the sumoylation machinery in rat hippocampal neurons. Biol Cell *105*, 30-45.

Loriol, C., Parisot, J., Poupon, G., Gwizdek, C., and Martin, S. (2012). Developmental regulation and spatiotemporal redistribution of the sumoylation machinery in the rat central nervous system. PLoS One *7*, e33757.

Lu, W., Shi, Y., Jackson, A.C., Bjorgan, K., During, M.J., Sprengel, R., Seeburg, P.H., and Nicoll, R.A. (2009). Subunit composition of synaptic AMPA receptors revealed by a single-cell genetic approach. Neuron *62*, 254-268.

Lucchesi, W., Mizuno, K., and Giese, K.P. (2011). Novel insights into CaMKII function and regulation during memory formation. Brain Res Bull *85*, 2-8.

Luo, H.B., Xia, Y.Y., Shu, X.J., Liu, Z.C., Feng, Y., Liu, X.H., Yu, G., Yin, G., Xiong, Y.S., Zeng, K.*, et al.* (2014). SUMOylation at K340 inhibits tau degradation through deregulating its phosphorylation and ubiquitination. Proc Natl Acad Sci U S A *111*, 16586-16591.

Luscher, C., and Huber, K.M. (2010). Group 1 mGluR-dependent synaptic long-term depression: mechanisms and implications for circuitry and disease. Neuron *65*, 445-459.

Luscher, C., and Malenka, R.C. (2012). NMDA receptor-dependent long-term potentiation and long-term depression (LTP/LTD). Cold Spring Harb Perspect Biol *4*.

Mabb, A.M., Je, H.S., Wall, M.J., Robinson, C.G., Larsen, R.S., Qiang, Y., Correa, S.A., and Ehlers, M.D. (2014). Triad3A regulates synaptic strength by ubiquitination of Arc. Neuron *82*, 1299-1316.

MacGillavry, H.D., Kerr, J.M., Kassner, J., Frost, N.A., and Blanpied, T.A. (2016). Shank-cortactin interactions control actin dynamics to maintain flexibility of neuronal spines and synapses. Eur J Neurosci *43*, 179-193.

Maeder, C.I., San-Miguel, A., Wu, E.Y., Lu, H., and Shen, K. (2014). In vivo neuron-wide analysis of synaptic vesicle precursor trafficking. Traffic *15*, 273-291.

Mahajan, R., Delphin, C., Guan, T., Gerace, L., and Melchior, F. (1997). A small ubiquitin-related polypeptide involved in targeting RanGAP1 to nuclear pore complex protein RanBP2. Cell *88*, 97-107.

Mahato, P.K., Pandey, S., and Bhattacharyya, S. (2015). Differential effects of protein phosphatases in the recycling of metabotropic glutamate receptor 5. Neuroscience *306*, 138-150.

Maniar, T.A., Kaplan, M., Wang, G.J., Shen, K., Wei, L., Shaw, J.E., Koushika, S.P., and Bargmann, C.I. (2011). UNC-33 (CRMP) and ankyrin organize microtubules and localize kinesin to polarize axon-dendrite sorting. Nat Neurosci *15*, 48-56.

Mao, L., Yang, L., Tang, Q., Samdani, S., Zhang, G., and Wang, J.Q. (2005). The scaffold protein Homer1b/c links metabotropic glutamate receptor 5 to extracellular signal-regulated protein kinase cascades in neurons. J Neurosci *25*, 2741-2752.

Martin, S., and Henley, J.M. (2004). Activity-dependent endocytic sorting of kainate receptors to recycling or degradation pathways. EMBO J *23*, 4749-4759.

Martin, S., Nishimune, A., Mellor, J.R., and Henley, J.M. (2007a). SUMOylation regulates kainate-receptor-mediated synaptic transmission. Nature *447*, 321-325.

Martin, S., Wilkinson, K.A., Nishimune, A., and Henley, J.M. (2007b). Emerging extranuclear roles of protein SUMOylation in neuronal function and dysfunction. Nat Rev Neurosci *8*, 948-959.

Matsuzaki, M., Honkura, N., Ellis-Davies, G.C., and Kasai, H. (2004). Structural basis of long-term potentiation in single dendritic spines. Nature *429*, 761-766.

Matsuzaki, S., Lee, L., Knock, E., Srikumar, T., Sakurai, M., Hazrati, L.N., Katayama, T., Staniszewski, A., Raught, B., Arancio, O.*, et al.* (2015). SUMO1 Affects Synaptic Function, Spine Density and Memory. Sci Rep *5*, 10730.

Matunis, M.J., Coutavas, E., and Blobel, G. (1996). A novel ubiquitin-like modification modulates the partitioning of the Ran-GTPase-activating protein RanGAP1 between the cytosol and the nuclear pore complex. J Cell Biol *135*, 1457-1470.

Maurin, T., Zongaro, S., and Bardoni, B. (2014). Fragile X Syndrome: from molecular pathology to therapy. Neurosci Biobehav Rev *46 Pt 2*, 242-255.

McDonald, N.Q., Murray-Rust, J., and Blundell, T.L. (1995). The first structure of a receptor tyrosine kinase domain: a further step in understanding the molecular basis of insulin action. Structure *3*, 1-6.

Megias, M., Emri, Z., Freund, T.F., and Gulyas, A.I. (2001). Total number and distribution of inhibitory and excitatory synapses on hippocampal CA1 pyramidal cells. Neuroscience *102*, 527-540.

Merino-Serrais, P., Knafo, S., Alonso-Nanclares, L., Fernaud-Espinosa, I., and DeFelipe, J. (2011). Layer-specific alterations to CA1 dendritic spines in a mouse model of Alzheimer's disease. Hippocampus *21*, 1037-1044.

Merriam, E.B., Lumbard, D.C., Viesselmann, C., Ballweg, J., Stevenson, M., Pietila, L., Hu, X., and Dent, E.W. (2011). Dynamic microtubules promote synaptic NMDA receptor-dependent spine enlargement. PLoS One *6*, e27688.

Merriam, E.B., Millette, M., Lumbard, D.C., Saengsawang, W., Fothergill, T., Hu, X., Ferhat, L., and Dent, E.W. (2013). Synaptic regulation of microtubule dynamics in dendritic spines by calcium, F-actin, and drebrin. J Neurosci *33*, 16471-16482.

Mientjes, E.J., Nieuwenhuizen, I., Kirkpatrick, L., Zu, T., Hoogeveen-Westerveld, M., Severijnen, L., Rife, M., Willemsen, R., Nelson, D.L., and Oostra, B.A. (2006). The generation of a conditional Fmr1 knock out mouse model to study Fmrp function in vivo. Neurobiol Dis *21*, 549-555.

Milovanovic, D., and Jahn, R. (2015). Organization and dynamics of SNARE proteins in the presynaptic membrane. Front Physiol *6*, 89.

Mishima, T., Fujiwara, T., and Akagawa, K. (2002). Reduction of neurotransmitter release by the exogenous H3 domain peptide of HPC-1/syntaxin 1A in cultured rat hippocampal neurons. Neurosci Lett *329*, 273-276.

Mishima, T., Fujiwara, T., Sanada, M., Kofuji, T., Kanai-Azuma, M., and Akagawa, K. (2014). Syntaxin 1B, but not syntaxin 1A, is necessary for the regulation of synaptic vesicle exocytosis and of the readily releasable pool at central synapses. PLoS One *9*, e90004.

Miyata, M., Finch, E.A., Khiroug, L., Hashimoto, K., Hayasaka, S., Oda, S.I., Inouye, M., Takagishi, Y., Augustine, G.J., and Kano, M. (2000). Local calcium release in dendritic spines required for long-term synaptic depression. Neuron *28*, 233-244.

Mockett, B.G., Guevremont, D., Wutte, M., Hulme, S.R., Williams, J.M., and Abraham, W.C. (2011). Calcium/calmodulin-dependent protein kinase II mediates group I metabotropic glutamate receptor-dependent protein synthesis and long-term depression in rat hippocampus. J Neurosci *31*, 7380-7391.

Moghaddam, B., and Javitt, D. (2012). From revolution to evolution: the glutamate hypothesis of schizophrenia and its implication for treatment. Neuropsychopharmacology *37*, 4-15.

Morfini, G., Szebenyi, G., Brown, H., Pant, H.C., Pigino, G., DeBoer, S., Beffert, U., and Brady, S.T. (2004). A novel CDK5-dependent pathway for regulating GSK3 activity and kinesin-driven motility in neurons. EMBO J *23*, 2235-2245.

Moser, M.B., Rowland, D.C., and Moser, E.I. (2015). Place cells, grid cells, and memory. Cold Spring Harb Perspect Biol *7*, a021808.

Mundell, S.J., Matharu, A.L., Pula, G., Roberts, P.J., and Kelly, E. (2001). Agonist-induced internalization of the metabotropic glutamate receptor 1a is arrestin- and dynamin-dependent. J Neurochem *78*, 546-551.

Mundell, S.J., Pula, G., McIlhinney, R.A., Roberts, P.J., and Kelly, E. (2004). Desensitization and internalization of metabotropic glutamate receptor 1a following activation of heterologous Gq/11-coupled receptors. Biochemistry *43*, 7541-7551.

Nacerddine, K., Lehembre, F., Bhaumik, M., Artus, J., Cohen-Tannoudji, M., Babinet, C., Pandolfi, P.P., and Dejean, A. (2005). The SUMO pathway is essential for nuclear integrity and chromosome segregation in mice. Dev Cell *9*, 769-779.

Nagy, J.I., Pereda, A.E., and Rash, J.E. (2018). Electrical synapses in mammalian CNS: Past eras, present focus and future directions. Biochim Biophys Acta *1860*, 102-123.

Nair, R.R., Patil, S., Tiron, A., Kanhema, T., Panja, D., Schiro, L., Parobczak, K., Wilczynski, G., and Bramham, C.R. (2017). Dynamic Arc SUMOylation and Selective Interaction with F-Actin-Binding Protein Drebrin A in LTP Consolidation In Vivo. Front Synaptic Neurosci *9*, 8.

Nakamura, K., Anitha, A., Yamada, K., Tsujii, M., Iwayama, Y., Hattori, E., Toyota, T., Suda, S., Takei, N., Iwata, Y.*, et al.* (2008). Genetic and expression analyses reveal elevated expression of syntaxin 1A (STX1A) in high functioning autism. Int J Neuropsychopharmacol *11*, 1073-1084.

Nalavadi, V.C., Muddashetty, R.S., Gross, C., and Bassell, G.J. (2012). Dephosphorylation-induced ubiquitination and degradation of FMRP in dendrites: a role in immediate early mGluR-stimulated translation. J Neurosci *32*, 2582-2587.

Narayanan, U., Nalavadi, V., Nakamoto, M., Pallas, D.C., Ceman, S., Bassell, G.J., and Warren, S.T. (2007). FMRP phosphorylation reveals an immediate-early signaling pathway triggered by group I mGluR and mediated by PP2A. J Neurosci *27*, 14349-14357.

Nash, J.E., Appleby, V.J., Correa, S.A., Wu, H., Fitzjohn, S.M., Garner, C.C., Collingridge, G.L., and Molnar, E. (2010). Disruption of the interaction between myosin VI and SAP97 is associated with a reduction in the number of AMPARs at hippocampal synapses. J Neurochem *112*, 677-690.

Nayak, A., and Muller, S. (2014). SUMO-specific proteases/isopeptidases: SENPs and beyond. Genome Biol *15*, 422.

Nelson, C.D., Kim, M.J., Hsin, H., Chen, Y., and Sheng, M. (2013). Phosphorylation of threonine-19 of PSD-95 by GSK-3beta is required for PSD-95 mobilization and long-term depression. J Neurosci *33*, 12122-12135.

Nicholls, J.G., Martin, A.R., Fuchs, P.A., Brown, D.A., Diamond, M.E., and Weisblat, D.A. (2012). From Neuron to Brain, 5th edn (Sinauer Associates Inc.,U.S.).

Niciu, M.J., Kelmendi, B., and Sanacora, G. (2012). Overview of glutamatergic neurotransmission in the nervous system. Pharmacol Biochem Behav *100*, 656-664.

Niere, F., Wilkerson, J.R., and Huber, K.M. (2012). Evidence for a fragile X mental retardation protein-mediated translational switch in metabotropic glutamate receptor-triggered Arc translation and long-term depression. J Neurosci *32*, 5924-5936.

Niswender, C.M., and Conn, P.J. (2010). Metabotropic glutamate receptors: physiology, pharmacology, and disease. Annu Rev Pharmacol Toxicol *50*, 295-322.

Niwa, S., Tanaka, Y., and Hirokawa, N. (2008). KIF1Bbeta- and KIF1A-mediated axonal transport of presynaptic regulator Rab3 occurs in a GTP-dependent manner through DENN/MADD. Nat Cell Biol *10*, 1269-1279.

Noritake, J., Fukata, Y., Iwanaga, T., Hosomi, N., Tsutsumi, R., Matsuda, N., Tani, H., Iwanari, H., Mochizuki, Y., Kodama, T*., et al.* (2009). Mobile DHHC palmitoylating enzyme mediates activity-sensitive synaptic targeting of PSD-95. J Cell Biol *186*, 147-160.

O'Mara, S. (2005). The subiculum: what it does, what it might do, and what neuroanatomy has yet to tell us. J Anat *207*, 271-282.

O'Rourke, J.G., Gareau, J.R., Ochaba, J., Song, W., Rasko, T., Reverter, D., Lee, J., Monteys, A.M., Pallos, J., Mee, L*., et al.* (2013). SUMO-2 and PIAS1 modulate insoluble mutant huntingtin protein accumulation. Cell Rep *4*, 362-375.

Okamoto, K., Nagai, T., Miyawaki, A., and Hayashi, Y. (2004). Rapid and persistent modulation of actin dynamics regulates postsynaptic reorganization underlying bidirectional plasticity. Nat Neurosci *7*, 1104-1112.

Osterweil, E., Wells, D.G., and Mooseker, M.S. (2005). A role for myosin VI in postsynaptic structure and glutamate receptor endocytosis. J Cell Biol *168*, 329-338.

Otmakhov, N., Tao-Cheng, J.H., Carpenter, S., Asrican, B., Dosemeci, A., Reese, T.S., and Lisman, J. (2004). Persistent accumulation of calcium/calmodulin-dependent protein kinase II in dendritic spines after induction of NMDA receptor-dependent chemical long-term potentiation. J Neurosci *24*, 9324-9331.

Panayotis, N., Karpova, A., Kreutz, M.R., and Fainzilber, M. (2015). Macromolecular transport in synapse to nucleus communication. Trends Neurosci *38*, 108-116.

Pandey, S., Mahato, P.K., and Bhattacharyya, S. (2014). Metabotropic glutamate receptor 1 recycles to the cell surface in protein phosphatase 2A-dependent manner in non-neuronal and neuronal cell lines. J Neurochem *131*, 602-614.

Paoletti, P., Bellone, C., and Zhou, Q. (2013). NMDA receptor subunit diversity: impact on receptor properties, synaptic plasticity and disease. Nat Rev Neurosci *14*, 383-400.

Paquet, M., and Smith, Y. (2003). Group I metabotropic glutamate receptors in the monkey striatum: subsynaptic association with glutamatergic and dopaminergic afferents. J Neurosci *23*, 7659-7669.

Park, M., Salgado, J.M., Ostroff, L., Helton, T.D., Robinson, C.G., Harris, K.M., and Ehlers, M.D. (2006). Plasticity-induced growth of dendritic spines by exocytic trafficking from recycling endosomes. Neuron *52*, 817-830.

Pastalkova, E., Serrano, P., Pinkhasova, D., Wallace, E., Fenton, A.A., and Sacktor, T.C. (2006). Storage of spatial information by the maintenance mechanism of LTP. Science *313*, 1141-1144.

Pavlopoulos, E., Trifilieff, P., Chevaleyre, V., Fioriti, L., Zairis, S., Pagano, A., Malleret, G., and Kandel, E.R. (2011). Neuralized1 activates CPEB3: a function for nonproteolytic ubiquitin in synaptic plasticity and memory storage. Cell *147*, 1369-1383.

Pazyra-Murphy, M.F., Hans, A., Courchesne, S.L., Karch, C., Cosker, K.E., Heerssen, H.M., Watson, F.L., Kim, T., Greenberg, M.E., and Segal, R.A. (2009). A retrograde neuronal survival response: target-derived neurotrophins regulate MEF2D and bcl-w. J Neurosci *29*, 6700-6709.

Peineau, S., Bradley, C., Taghibiglou, C., Doherty, A., Bortolotto, Z.A., Wang, Y.T., and Collingridge, G.L. (2008). The role of GSK-3 in synaptic plasticity. Br J Pharmacol *153 Suppl 1*, S428-437.

Peng, A., Rotman, Z., Deng, P.Y., and Klyachko, V.A. (2012). Differential motion dynamics of synaptic vesicles undergoing spontaneous and activity-evoked endocytosis. Neuron *73*, 1108-1115.

Penn, A.C., Zhang, C.L., Georges, F., Royer, L., Breillat, C., Hosy, E., Petersen, J.D., Humeau, Y., and Choquet, D. (2017). Hippocampal LTP and contextual learning require surface diffusion of AMPA receptors. Nature *549*, 384-388.

Pepinsky, R.B., Zeng, C., Wen, D., Rayhorn, P., Baker, D.P., Williams, K.P., Bixler, S.A., Ambrose, C.M., Garber, E.A., Miatkowski, K*., et al.* (1998). Identification of a palmitic acid-modified form of human Sonic hedgehog. J Biol Chem *273*, 14037-14045.

Pereda, A.E. (2014). Electrical synapses and their functional interactions with chemical synapses. Nat Rev Neurosci *15*, 250-263.

Perez-Cruz, C., Nolte, M.W., van Gaalen, M.M., Rustay, N.R., Termont, A., Tanghe, A., Kirchhoff, F., and Ebert, U. (2011). Reduced spine density in specific regions of CA1 pyramidal neurons in two transgenic mouse models of Alzheimer's disease. J Neurosci *31*, 3926-3934.

Perlson, E., and Holzbaur, E.L.F. (2007). Protein Trafficking in Neurons In Molecular Mobility in Cells Examined with Optical Methods (Elsevier).

Petrak, L.J., Harris, K.M., and Kirov, S.A. (2005). Synaptogenesis on mature hippocampal dendrites occurs via filopodia and immature spines during blocked synaptic transmission. J Comp Neurol *484*, 183-190.

Petrovic, M.M., Viana da Silva, S., Clement, J.P., Vyklicky, L., Mulle, C., Gonzalez-Gonzalez, I.M., and Henley, J.M. (2017). Metabotropic action of postsynaptic kainate receptors triggers hippocampal long-term potentiation. Nat Neurosci *20*, 529-539.

Phair, R.D., and Misteli, T. (2001). Kinetic modelling approaches to in vivo imaging. Nat Rev Mol Cell Biol *2*, 898-907.

Pickel, V., and Segal, M. (2014). The synapse : structure and function.

Plant, K., Pelkey, K.A., Bortolotto, Z.A., Morita, D., Terashima, A., McBain, C.J., Collingridge, G.L., and Isaac, J.T. (2006). Transient incorporation of native GluR2-lacking AMPA receptors during hippocampal long-term potentiation. Nat Neurosci *9*, 602-604.

Plant, L.D., Dowdell, E.J., Dementieva, I.S., Marks, J.D., and Goldstein, S.A. (2011). SUMO modification of cell surface Kv2.1 potassium channels regulates the activity of rat hippocampal neurons. J Gen Physiol *137*, 441-454.

Podkowa, M., Zhao, X., Chow, C.W., Coffey, E.T., Davis, R.J., and Attisano, L. (2010). Microtubule stabilization by bone morphogenetic protein receptor-mediated scaffolding of c-Jun N-terminal kinase promotes dendrite formation. Mol Cell Biol *30*, 2241-2250.

Pollard, T.D., Blanchoin, L., and Mullins, R.D. (2000). Molecular mechanisms controlling actin filament dynamics in nonmuscle cells. Annu Rev Biophys Biomol Struct *29*, 545-576.

Poulain, F.E., and Sobel, A. (2010). The microtubule network and neuronal morphogenesis: Dynamic and coordinated orchestration through multiple players. Mol Cell Neurosci *43*, 15-32.

Prybylowski, K., Chang, K., Sans, N., Kan, L., Vicini, S., and Wenthold, R.J. (2005). The synaptic localization of NR2B-containing NMDA receptors is controlled by interactions with PDZ proteins and AP-2. Neuron *47*, 845-857.

Qi, Y., Wang, J., Bomben, V.C., Li, D.P., Chen, S.R., Sun, H., Xi, Y., Reed, J.G., Cheng, J., Pan, H.L.*, et al.* (2014). Hyper-SUMOylation of the Kv7 potassium channel diminishes the M-current leading to seizures and sudden death. Neuron *83*, 1159-1171.

Racz, B., and Weinberg, R.J. (2008). Organization of the Arp2/3 complex in hippocampal spines. J Neurosci *28*, 5654-5659.

Raingo, J., Khvotchev, M., Liu, P., Darios, F., Li, Y.C., Ramirez, D.M., Adachi, M., Lemieux, P., Toth, K., Davletov, B.*, et al.* (2012). VAMP4 directs synaptic vesicles to a pool that selectively maintains asynchronous neurotransmission. Nat Neurosci *15*, 738-745.

Ramirez, D.M., Khvotchev, M., Trauterman, B., and Kavalali, E.T. (2012). Vti1a identifies a vesicle pool that preferentially recycles at rest and maintains spontaneous neurotransmission. Neuron *73*, 121-134.

Raymond, F.L., Tarpey, P.S., Edkins, S., Tofts, C., O'Meara, S., Teague, J., Butler, A., Stevens, C., Barthorpe, S., Buck, G.*, et al.* (2007). Mutations in ZDHHC9, which encodes a palmitoyltransferase of NRAS and HRAS, cause X-linked mental retardation associated with a Marfanoid habitus. Am J Hum Genet *80*, 982-987.

Rex, C.S., Gavin, C.F., Rubio, M.D., Kramar, E.A., Chen, L.Y., Jia, Y., Huganir, R.L., Muzyczka, N., Gall, C.M., Miller, C.A.*, et al.* (2010). Myosin IIb regulates actin dynamics during synaptic plasticity and memory formation. Neuron *67*, 603-617.

Rizzoli, S.O. (2014). Synaptic vesicle recycling: steps and principles. EMBO J *33*, 788-822.

Robison, A.J., Bartlett, R.K., Bass, M.A., and Colbran, R.J. (2005). Differential modulation of Ca2+/calmodulin-dependent protein kinase II activity by regulated interactions with N-methyl-D-aspartate receptor NR2B subunits and alpha-actinin. J Biol Chem *280*, 39316-39323.

Rodriguez, M.S., Dargemont, C., and Hay, R.T. (2001). SUMO-1 conjugation in vivo requires both a consensus modification motif and nuclear targeting. J Biol Chem *276*, 12654-12659.

Rott, R., Szargel, R., Shani, V., Hamza, H., Savyon, M., Abd Elghani, F., Bandopadhyay, R., and Engelender, S. (2017). SUMOylation and ubiquitination reciprocally regulate alpha-synuclein degradation and pathological aggregation. Proc Natl Acad Sci U S A *114*, 13176-13181.

Sabo, S.L., Gomes, R.A., and McAllister, A.K. (2006). Formation of presynaptic terminals at predefined sites along axons. J Neurosci *26*, 10813-10825.

Salter, M.W., and Kalia, L.V. (2004). Src kinases: a hub for NMDA receptor regulation. Nat Rev Neurosci *5*, 317-328.

Sampson, D.A., Wang, M., and Matunis, M.J. (2001). The small ubiquitin-like modifier-1 (SUMO-1) consensus sequence mediates Ubc9 binding and is essential for SUMO-1 modification. J Biol Chem *276*, 21664-21669.

Sankaranarayanan, S., Atluri, P.P., and Ryan, T.A. (2003). Actin has a molecular scaffolding, not propulsive, role in presynaptic function. Nat Neurosci *6*, 127-135.

Sanz-Clemente, A., Matta, J.A., Isaac, J.T., and Roche, K.W. (2010). Casein kinase 2 regulates the NR2 subunit composition of synaptic NMDA receptors. Neuron *67*, 984-996.

Sanz-Clemente, A., Nicoll, R.A., and Roche, K.W. (2013). Diversity in NMDA receptor composition: many regulators, many consequences. Neuroscientist *19*, 62-75.

Schapitz, I.U., Behrend, B., Pechmann, Y., Lappe-Siefke, C., Kneussel, S.J., Wallace, K.E., Stempel, A.V., Buck, F., Grant, S.G., Schweizer, M.*, et al.* (2010). Neuroligin 1 is dynamically exchanged at postsynaptic sites. J Neurosci *30*, 12733-12744.

Scharfman, H.E. (2016). The enigmatic mossy cell of the dentate gyrus. Nat Rev Neurosci *17*, 562-575.

Schorova, L., and Martin, S. (2016). Sumoylation in Synaptic Function and Dysfunction. Front Synaptic Neurosci *8*, 9.

Schulz, S., Chachami, G., Kozaczkiewicz, L., Winter, U., Stankovic-Valentin, N., Haas, P., Hofmann, K., Urlaub, H., Ovaa, H., Wittbrodt, J.*, et al.* (2012). Ubiquitin-specific protease-like 1 (USPL1) is a SUMO isopeptidase with essential, non-catalytic functions. EMBO Rep *13*, 930-938.

Scott, D.B., Blanpied, T.A., and Ehlers, M.D. (2003). Coordinated PKA and PKC phosphorylation suppresses RXR-mediated ER retention and regulates the surface delivery of NMDA receptors. Neuropharmacology *45*, 755-767.

Seeger, M.A., and Rice, S.E. (2010). Microtubule-associated protein-like binding of the kinesin-1 tail to microtubules. J Biol Chem *285*, 8155-8162.

Semple, B.D., Blomgren, K., Gimlin, K., Ferriero, D.M., and Noble-Haeusslein, L.J. (2013). Brain development in rodents and humans: Identifying benchmarks of maturation and vulnerability to injury across species. Prog Neurobiol *106-107*, 1-16.

Shalizi, A., Bilimoria, P.M., Stegmuller, J., Gaudilliere, B., Yang, Y., Shuai, K., and Bonni, A. (2007). PIASx is a MEF2 SUMO E3 ligase that promotes postsynaptic dendritic morphogenesis. J Neurosci *27*, 10037-10046.

Shalizi, A., Gaudilliere, B., Yuan, Z., Stegmuller, J., Shirogane, T., Ge, Q., Tan, Y., Schulman, B., Harper, J.W., and Bonni, A. (2006). A calcium-regulated MEF2 sumoylation switch controls postsynaptic differentiation. Science *311*, 1012-1017.

Sheng, M., and Kim, E. (2011). The postsynaptic organization of synapses. Cold Spring Harb Perspect Biol *3*.

Sheng, Z.H. (2014). Mitochondrial trafficking and anchoring in neurons: New insight and implications. J Cell Biol *204*, 1087-1098.

Shin, E.J., Shin, H.M., Nam, E., Kim, W.S., Kim, J.H., Oh, B.H., and Yun, Y. (2012). DeSUMOylating isopeptidase: a second class of SUMO protease. EMBO Rep *13*, 339-346.

Shinbo, Y., Niki, T., Taira, T., Ooe, H., Takahashi-Niki, K., Maita, C., Seino, C., Iguchi-Ariga, S.M., and Ariga, H. (2006). Proper SUMO-1 conjugation is essential to DJ-1 to exert its full activities. Cell Death Differ *13*, 96-108.

Shiraishi-Yamaguchi, Y., and Furuichi, T. (2007). The Homer family proteins. Genome Biol *8*, 206.
Siegel, G., Obernosterer, G., Fiore, R., Oehmen, M., Bicker, S., Christensen, M., Khudayberdiev, S., Leuschner, P.F., Busch, C.J., Kane, C.*, et al.* (2009). A functional screen implicates microRNA-138-dependent regulation of the depalmitoylation enzyme APT1 in dendritic spine morphogenesis. Nat Cell Biol *11*, 705-716.

Siekevitz, P. (1985). The postsynaptic density: a possible role in long-lasting effects in the central nervous system. Proc Natl Acad Sci U S A *82*, 3494-3498.

Simons, S.B., Escobedo, Y., Yasuda, R., and Dudek, S.M. (2009). Regional differences in hippocampal calcium handling provide a cellular mechanism for limiting plasticity. Proc Natl Acad Sci U S A *106*, 14080-14084.

Sorensen, J.B., Nagy, G., Varoqueaux, F., Nehring, R.B., Brose, N., Wilson, M.C., and Neher, E. (2003). Differential control of the releasable vesicle pools by SNAP-25 splice variants and SNAP-23. Cell *114*, 75-86.

Sorra, K.E., Mishra, A., Kirov, S.A., and Harris, K.M. (2006). Dense core vesicles resemble active-zone transport vesicles and are diminished following synaptogenesis in mature hippocampal slices. Neuroscience *141*, 2097-2106.

Soykan, T., Maritzen, T., and Haucke, V. (2016). Modes and mechanisms of synaptic vesicle recycling. Curr Opin Neurobiol *39*, 17-23.

Speese, S.D., Trotta, N., Rodesch, C.K., Aravamudan, B., and Broadie, K. (2003). The ubiquitin proteasome system acutely regulates presynaptic protein turnover and synaptic efficacy. Curr Biol *13*, 899-910.

Srinivas, K.V., Buss, E.W., Sun, Q., Santoro, B., Takahashi, H., Nicholson, D.A., and Siegelbaum, S.A. (2017). The Dendrites of CA2 and CA1 Pyramidal Neurons Differentially Regulate Information Flow in the Cortico-Hippocampal Circuit. J Neurosci *37*, 3276-3293.

Stavraka, C., and Blagden, S. (2015). The La-Related Proteins, a Family with Connections to Cancer. Biomolecules *5*, 2701-2722.

Steffan, J.S., Agrawal, N., Pallos, J., Rockabrand, E., Trotman, L.C., Slepko, N., Illes, K., Lukacsovich, T., Zhu, Y.Z., Cattaneo, E.*, et al.* (2004). SUMO modification of Huntingtin and Huntington's disease pathology. Science *304*, 100-104.

Steiner, P., Higley, M.J., Xu, W., Czervionke, B.L., Malenka, R.C., and Sabatini, B.L. (2008). Destabilization of the postsynaptic density by PSD-95 serine 73 phosphorylation inhibits spine growth and synaptic plasticity. Neuron *60*, 788-802.

Stone, M.C., Roegiers, F., and Rolls, M.M. (2008). Microtubules have opposite orientation in axons and dendrites of Drosophila neurons. Mol Biol Cell *19*, 4122-4129.

Sudhof, T.C. (2012). The presynaptic active zone. Neuron *75*, 11-25.

Sudhof, T.C. (2013). Neurotransmitter release: the last millisecond in the life of a synaptic vesicle. Neuron *80*, 675-690.
Sugawara, T., Hisatsune, C., Miyamoto, H., Ogawa, N., and Mikoshiba, K. (2017). Regulation of spinogenesis in mature Purkinje cells via mGluR/PKC-mediated phosphorylation of CaMKIIbeta. Proc Natl Acad Sci U S A *114*, E5256-E5265.

Sun, H., Lu, L., Zuo, Y., Wang, Y., Jiao, Y., Zeng, W.Z., Huang, C., Zhu, M.X., Zamponi, G.W., Zhou, T.*, et al.* (2014). Kainate receptor activation induces glycine receptor endocytosis through PKC deSUMOylation. Nat Commun *5*, 4980.

Sun, J., Zhu, G., Liu, Y., Standley, S., Ji, A., Tunuguntla, R., Wang, Y., Claus, C., Luo, Y., Baudry, M.*, et al.* (2015). UBE3A Regulates Synaptic Plasticity and Learning and Memory by Controlling SK2 Channel Endocytosis. Cell Rep *12*, 449-461.

Swanson, L.W., Newman, E., Araque, A., and Dubinsky, J.M. (2017). The Beautiful Brain: The Drawings of Santiago Ramon Y Cajal (Abrams Books).

Tai, D.J., Liu, Y.C., Hsu, W.L., Ma, Y.L., Cheng, S.J., Liu, S.Y., and Lee, E.H. (2016). MeCP2 SUMOylation rescues Mecp2-mutant-induced behavioural deficits in a mouse model of Rett syndrome. Nat Commun *7*, 10552.

Tang, L.T., Craig, T.J., and Henley, J.M. (2015). SUMOylation of synapsin Ia maintains synaptic vesicle availability and is reduced in an autism mutation. Nat Commun *6*, 7728.

Tang, Z., El Far, O., Betz, H., and Scheschonka, A. (2005). Pias1 interaction and sumoylation of metabotropic glutamate receptor 8. J Biol Chem *280*, 38153-38159.

Tingley, W.G., Ehlers, M.D., Kameyama, K., Doherty, C., Ptak, J.B., Riley, C.T., and Huganir, R.L. (1997). Characterization of protein kinase A and protein kinase C phosphorylation of the N-methyl-D-aspartate receptor NR1 subunit using phosphorylation site-specific antibodies. J Biol Chem *272*, 5157-5166.

Tirard, M., Hsiao, H.H., Nikolov, M., Urlaub, H., Melchior, F., and Brose, N. (2012). In vivo localization and identification of SUMOylated proteins in the brain of His6-HA-SUMO1 knock-in mice. Proc Natl Acad Sci U S A *109*, 21122-21127.

Tonegawa, S., Tsien, J.Z., McHugh, T.J., Huerta, P., Blum, K.I., and Wilson, M.A. (1996). Hippocampal CA1-region-restricted knockout of NMDAR1 gene disrupts synaptic plasticity, place fields, and spatial learning. Cold Spring Harb Symp Quant Biol *61*, 225-238.

Topinka, J.R., and Bredt, D.S. (1998). N-terminal palmitoylation of PSD-95 regulates association with cell membranes and interaction with K+ channel Kv1.4. Neuron *20*, 125-134.

Tsien, J.Z., Huerta, P.T., and Tonegawa, S. (1996). The essential role of hippocampal CA1 NMDA receptor-dependent synaptic plasticity in spatial memory. Cell *87*, 1327-1338.

Um, J.W., and Chung, K.C. (2006). Functional modulation of parkin through physical interaction with SUMO-1. J Neurosci Res *84*, 1543-1554.

Van Hoesen, G.W., Hyman, B.T., and Damasio, A.R. (1991). Entorhinal cortex pathology in Alzheimer's disease. Hippocampus *1*, 1-8.
van Niekerk, E.A., Willis, D.E., Chang, J.H., Reumann, K., Heise, T., and Twiss, J.L. (2007). Sumoylation in axons triggers retrograde transport of the RNA-binding protein La. Proc Natl Acad Sci U S A *104*, 12913-12918.

Vasquez, R.J., Howell, B., Yvon, A.M., Wadsworth, P., and Cassimeris, L. (1997). Nanomolar concentrations of nocodazole alter microtubule dynamic instability in vivo and in vitro. Mol Biol Cell *8*, 973-985.

Vellano, C.P., Lee, S.E., Dudek, S.M., and Hepler, J.R. (2011). RGS14 at the interface of hippocampal signaling and synaptic plasticity. Trends Pharmacol Sci *32*, 666-674.

Verstegen, A.M., Tagliatti, E., Lignani, G., Marte, A., Stolero, T., Atias, M., Corradi, A., Valtorta, F., Gitler, D., Onofri, F.*, et al.* (2014). Phosphorylation of synapsin I by cyclin-dependent kinase-5 sets the ratio between the resting and recycling pools of synaptic vesicles at hippocampal synapses. J Neurosci *34*, 7266-7280.

Vyklicky, V., Korinek, M., Smejkalova, T., Balik, A., Krausova, B., Kaniakova, M., Lichnerova, K., Cerny, J., Krusek, J., Dittert, I.*, et al.* (2014). Structure, function, and pharmacology of NMDA receptor channels. Physiol Res *63 Suppl 1*, S191-203.

Wagner, W., Brenowitz, S.D., and Hammer, J.A., 3rd (2011). Myosin-Va transports the endoplasmic reticulum into the dendritic spines of Purkinje neurons. Nat Cell Biol *13*, 40-48.

Waites, C.L., Leal-Ortiz, S.A., Andlauer, T.F., Sigrist, S.J., and Garner, C.C. (2011). Piccolo regulates the dynamic assembly of presynaptic F-actin. J Neurosci *31*, 14250-14263.

Wang, C.C., Held, R.G., Chang, S.C., Yang, L., Delpire, E., Ghosh, A., and Hall, B.J. (2011). A critical role for GluN2B-containing NMDA receptors in cortical development and function. Neuron *72*, 789-805.

Wang, C.C., Held, R.G., and Hall, B.J. (2013). SynGAP regulates protein synthesis and homeostatic synaptic plasticity in developing cortical networks. PLoS One *8*, e83941.

Wang, Y.T., Yu, X.M., and Salter, M.W. (1996). Ca(2+)-independent reduction of N-methyl-D-aspartate channel activity by protein tyrosine phosphatase. Proc Natl Acad Sci U S A *93*, 1721-1725.

Wang, Z., Edwards, J.G., Riley, N., Provance, D.W., Jr., Karcher, R., Li, X.D., Davison, I.G., Ikebe, M., Mercer, J.A., Kauer, J.A.*, et al.* (2008). Myosin Vb mobilizes recycling endosomes and AMPA receptors for postsynaptic plasticity. Cell *135*, 535-548.

Watanabe, S. (2015). Slow or fast? A tale of synaptic vesicle recycling. Science *350*, 46-47.

Watanabe, Y., Katayama, N., Takeuchi, K., Togano, T., Itoh, R., Sato, M., Yamazaki, M., Abe, M., Sato, T., Oda, K.*, et al.* (2013). Point mutation in syntaxin-1A causes abnormal vesicle recycling, behaviors, and short term plasticity. J Biol Chem *288*, 34906-34919.

Watson, J.F., Ho, H., and Greger, I.H. (2017). Synaptic transmission and plasticity require AMPA receptor anchoring via its N-terminal domain. Elife *6*.

Weeraratna, A.T., Kalehua, A., Deleon, I., Bertak, D., Maher, G., Wade, M.S., Lustig, A., Becker, K.G., Wood, W., 3rd, Walker, D.G.*, et al.* (2007). Alterations in immunological and neurological gene expression patterns in Alzheimer's disease tissues. Exp Cell Res *313*, 450-461.

Wegner, A.M., Nebhan, C.A., Hu, L., Majumdar, D., Meier, K.M., Weaver, A.M., and Webb, D.J. (2008). N-wasp and the arp2/3 complex are critical regulators of actin in the development of dendritic spines and synapses. J Biol Chem *283*, 15912-15920.

Wheeler, D.G., Groth, R.D., Ma, H., Barrett, C.F., Owen, S.F., Safa, P., and Tsien, R.W. (2012). Ca(V)1 and Ca(V)2 channels engage distinct modes of Ca(2+) signaling to control CREB-dependent gene expression. Cell *149*, 1112-1124.

Wilhelm, B.G., Mandad, S., Truckenbrodt, S., Krohnert, K., Schafer, C., Rammner, B., Koo, S.J., Classen, G.A., Krauss, M., Haucke, V.*, et al.* (2014). Composition of isolated synaptic boutons reveals the amounts of vesicle trafficking proteins. Science *344*, 1023-1028.

Wilkinson, K.A., and Henley, J.M. (2011). Analysis of metabotropic glutamate receptor 7 as a potential substrate for SUMOylation. Neurosci Lett *491*, 181-186.

Wilkinson, K.A., Martin, S., Tyagarajan, S.K., Arancio, O., Craig, T.J., Guo, C., Fraser, P.E., Goldstein, S.A.N., and Henley, J.M. (2017). Commentary: Analysis of SUMO1-conjugation at synapses. Front Cell Neurosci *11*, 345.

Wilkinson, K.A., Nishimune, A., and Henley, J.M. (2008). Analysis of SUMO-1 modification of neuronal proteins containing consensus SUMOylation motifs. Neurosci Lett *436*, 239-244.

Willeumier, K., Pulst, S.M., and Schweizer, F.E. (2006). Proteasome inhibition triggers activity-dependent increase in the size of the recycling vesicle pool in cultured hippocampal neurons. J Neurosci *26*, 11333-11341.

Woolfrey, K.M., and Dell'Acqua, M.L. (2015). Coordination of Protein Phosphorylation and Dephosphorylation in Synaptic Plasticity. J Biol Chem *290*, 28604-28612.

Woolfrey, K.M., O'Leary, H., Goodell, D.J., Robertson, H.R., Horne, E.A., Coultrap, S.J., Dell'Acqua, M.L., and Bayer, K.U. (2017). CaMKII regulates the de-palmitoylation and synaptic removal of AKAP79/150 to mediate structural LTD. J Biol Chem.

Wu, Q., Sun, M., Bernard, L.P., and Zhang, H. (2017). Postsynaptic density 95 (PSD-95) serine 561 phosphorylation regulates a conformational switch and bidirectional dendritic spine structural plasticity. J Biol Chem *292*, 16150-16160.

Wu, Y.E., Huo, L., Maeder, C.I., Feng, W., and Shen, K. (2013). The balance between capture and dissociation of presynaptic proteins controls the spatial distribution of synapses. Neuron *78*, 994-1011.

Yagensky, O., Kalantary Dehaghi, T., and Chua, J.J. (2016). The Roles of Microtubule-Based Transport at Presynaptic Nerve Terminals. Front Synaptic Neurosci *8*, 3.

Yano, H., Ninan, I., Zhang, H., Milner, T.A., Arancio, O., and Chao, M.V. (2006). BDNF-mediated neurotransmission relies upon a myosin VI motor complex. Nat Neurosci *9*, 1009-1018.

Yates, K.E., Korbel, G.A., Shtutman, M., Roninson, I.B., and DiMaio, D. (2008). Repression of the SUMO-specific protease Senp1 induces p53-dependent premature senescence in normal human fibroblasts. Aging Cell *7*, 609-621.

Yau, K.W., Schatzle, P., Tortosa, E., Pages, S., Holtmaat, A., Kapitein, L.C., and Hoogenraad, C.C. (2016). Dendrites In Vitro and In Vivo Contain Microtubules of Opposite Polarity and Axon Formation Correlates with Uniform Plus-End-Out Microtubule Orientation. J Neurosci *36*, 1071-1085.

Yu, L., Ji, W., Zhang, H., Renda, M.J., He, Y., Lin, S., Cheng, E.C., Chen, H., Krause, D.S., and Min, W. (2010). SENP1-mediated GATA1 deSUMOylation is critical for definitive erythropoiesis. J Exp Med *207*, 1183-1195.

Zhang, W., and Benson, D.L. (2001). Stages of synapse development defined by dependence on F-actin. J Neurosci *21*, 5169-5181.

Zhang, W., and Benson, D.L. (2002). Developmentally regulated changes in cellular compartmentation and synaptic distribution of actin in hippocampal neurons. J Neurosci Res *69*, 427-436.

Zhang, Y.Q., and Sarge, K.D. (2008). Sumoylation of amyloid precursor protein negatively regulates Abeta aggregate levels. Biochem Biophys Res Commun *374*, 673-678.

Zhao, J.P., and Constantine-Paton, M. (2007). NR2A-/- mice lack long-term potentiation but retain NMDA receptor and L-type Ca2+ channel-dependent long-term depression in the juvenile superior colliculus. J Neurosci *27*, 13649-13654.

Zhou, P., Pang, Z.P., Yang, X., Zhang, Y., Rosenmund, C., Bacaj, T., and Sudhof, T.C. (2013). Syntaxin-1 N-peptide and Habc-domain perform distinct essential functions in synaptic vesicle fusion. EMBO J *32*, 159-171.

Zhou, Q., Homma, K.J., and Poo, M.M. (2004). Shrinkage of dendritic spines associated with long-term depression of hippocampal synapses. Neuron *44*, 749-757.

Zhu, J.J., Esteban, J.A., Hayashi, Y., and Malinow, R. (2000). Postnatal synaptic potentiation: delivery of GluR4-containing AMPA receptors by spontaneous activity. Nat Neurosci *3*, 1098-1106.

Zhu, J.J., Qin, Y., Zhao, M., Van Aelst, L., and Malinow, R. (2002). Ras and Rap control AMPA receptor trafficking during synaptic plasticity. Cell *110*, 443-455.

Zhu, Q.J., Xu, Y., Du, C.P., and Hou, X.Y. (2012). SUMOylation of the kainate receptor subunit GluK2 contributes to the activation of the MLK3-JNK3 pathway following kainate stimulation. FEBS Lett *586*, 1259-1264.

Zimmermann, J., Trimbuch, T., and Rosenmund, C. (2014). Synaptobrevin 1 mediates vesicle priming and evoked release in a subpopulation of hippocampal neurons. J Neurophysiol *112*, 1559-1565.

Zuberi, S.M., Eunson, L.H., Spauschus, A., De Silva, R., Tolmie, J., Wood, N.W., McWilliam, R.C., Stephenson, J.B., Kullmann, D.M., and Hanna, M.G. (1999). A novel mutation in the human voltage-gated potassium channel gene (Kv1.1) associates with episodic ataxia type 1 and sometimes with partial epilepsy. Brain *122 (Pt 5)*, 817-825.